

NATIONAL AERONAUTICS AND SPACE ADMINISTRATION

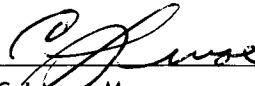
*Technical Memorandum 33-280*

*Proceedings of the Workshop on Voltage Breakdown  
in Electronic Equipment at Low Air Pressures*

*held at Jet Propulsion Laboratory, August 18-20, 1965*

*Edited by  
Earle R. Bunker, Jr.*

Approved by:

  
C. Levee, Manager  
Electromechanical Engineering  
Support Section

JET PROPULSION LABORATORY  
CALIFORNIA INSTITUTE OF TECHNOLOGY  
PASADENA, CALIFORNIA

December 15, 1966

Technical Memorandum 33-280

Copyright © 1967  
Jet Propulsion Laboratory  
California Institute of Technology

Prepared Under Contract No. NAS 7-100  
National Aeronautics & Space Administration



PRECEDING PAGE BLANK NOT FILMED.  
CONTENTS

Foreword . . . . .	vii
Earle R. Bunker, Jr.	
List of Participants . . . . .	xi
Welcoming Remarks . . . . .	xvii
Andrew Edwards	
1. Voltage Breakdown Problems at Low Air Pressures Encountered in the Mariner IV Spacecraft . . . . .	1 ✓
Earle R. Bunker, Jr.	
2. High Voltage Breakdown Problems in Goddard Scientific Satellites . . . . .	23 ✓
Harry W. Street	
3. Corona Induced Failures on Nimbus A During Ground Testing . . . . .	37 ✓
S. Charp	
4. High-Voltage Considerations for the Detector Assembly Used in the Goddard Experimental Package . . . . .	45 ✓
Peter Pokalsky	
5. Electrical Breakdown Mechanisms Affecting Space Systems . . . . .	53 ✓
Edwards F. Vance and John Chown	
6. High-Voltage Effects in Satellite-borne Spectrometers . . . . .	81 ✓
E. M. Reeves	
7. Design and Test of a High-Voltage Power Supply for Satellite Applications . . . . .	97 ✓
F. Clauss, G. Dallimore, and D. Tashjian	
8. Construction of Power Supplies for Operation in the Critical Region . . . . .	111 ✓
J. P. Clark	
9. The Generation of Potential Differences at Stage Separation . . . . .	119 ✓
J. W. Haffner	
10. Current Anomalies at Separation . . . . .	127 ✓
W. R. Abbott	
11. Booster and Spacecraft Electrostatic Phenomena - Causes, Effects, and prevention . . . . .	137 ✓
W. Coleman and R. Reeves	
12. Electrostatic Potential Sensors for Use on the NASA Scout Evaluation Vehicle S131R . . . . .	163 ✓
N. F. Bolling and R. L. Clark	

## CONTENTS (contd)

13.	Planetary Breakdown Studies in the Avco/RAD High-Voltage Breakdown Laboratory . . . . .	193	✓
	W. B. Haigh		
14.	Theoretical Study of Microwave Breakdown with Application to Space Vehicles . . . . .	207	✓
	R. Fante		
15.	High-Altitude Breakdown Prediction . . . . .	223	✓
	G. A. Bakalyar		
16.	Antenna Voltage Breakdown in Planetary Atmospheres . . . . .	233	✓
	W. K. Kinkead		
17.	Solution of a Breakdown Problem at Partial Pressures in the Apollo LEM Transceiver . . . . .	257	✓
	S. B. Newton		
18.	Voltage Breakdown in an Exploding Bridge Wire System . . . . .	263	✓
	W. H. Brown		
19.	Some Aspects of Breakdown and Corona Problems in the Critical-Pressure Range . . . . .	267	✓
	L. J. Frisco and W. T. Starr		
20.	Electrical Discharges at Altitudes Between 70,000 and 250,000 ft . . . . .	275	✓
	W. G. Dunbar		
21.	Critical Altitudes for Radio Frequency Breakdown . . . . .	289	✓
	W. J. Linder		
22.	Microwave Voltage Breakdown at Critical Pressures . . . . .	299	✓
	T. Breeden		
23.	Voltage Breakdown Investigation in the Advanced Packaging Technology Group at Jet Propulsion Laboratory . . . . .	311	✓
	Earle R. Bunker, Jr.		
24.	The Materials Aspect of Corona and Arcing Phenomena . . . . .	333	✓
	Robert Boundy		
25.	The Pressure Profile of a Rocket Experiment and Methods of Reducing the Gas Load . . . . .	347	✓
	N. McIlwraith		
26.	Gemini Transponder Degassing Problems . . . . .	367	✓
	C. L. Brock and B. H. Vester		
27.	Diffusion of Gases in Polymeric Foams . . . . .	381	✓
	E. F. Cuddihy and J. Moacanin		

## CONTENTS (contd)

28.	Prevention of High-Voltage Breakdown in Ion Propulsion Systems . . . . .	399 ✓
	G. A. Work	
29.	Prevention of High-Voltage Breakdown in Ion Propulsion Systems . . . . .	409 ✓
	R. Dunaetz	
30.	Measurement of Corona Discharge Behavior at Low Pressure and Vacuum . . . . .	423 ✓
	T. W. Dakin and C. N. Works	
31.	Prevention of Dielectric Failures in Spacecraft . . . . .	441 ✓
	E. C. McKannan	
32.	Problems Encountered Using Connector Separation for Opening Low-Voltage Circuits . . . . .	445 ✓
	J. R. Goudy	
33.	Safety Control in Space Environmental Chambers . . . . .	455 ✓
	E. A. Jackson	
34.	High-Voltage Power Supply Design for Operation in the Critical- Gas-Pressure Regions and at Low Temperatures (-55°C) . . . . .	467 ✓
	Aldus C. Myers, Jr.	
35.	A High-Voltage Problem Encountered in the Design of the Star Tracker Used on the Orbiting Astronomical Observatory . . . . .	485 ✓
	James J. Collins	
36.	Solutions to Poisson's Equation and Their Application to Voltage Breakdown Problems . . . . .	491 ✓
	Glenn E. Hagen	
	Concluding Remarks . . . . .	501
	Earle R. Bunker, Jr.	
	Closing Remarks . . . . .	503
	Andrew Edwards	

## FOREWORD

Problems of voltage breakdown in spacecraft electronic equipment operating in a region of low air pressure, where the dielectric strength drops from the sea level value of 75 kv to a few hundred volts per inch, became more and more of concern as the numbers and complexities of U. S. spacecraft increased. The approximate limits of this critical pressure region (arbitrarily defined as that region in which the dielectric strength is less than 20% of the sea level value in terms of Earth altitude) are 60,000 to 310,000 ft. Originally, the problem of operating spacecraft electronic equipment in the critical region was not considered significant by many designers because spacecraft systems employing high voltages usually are not required to be functional until the hard vacuum of space is reached, which has a very high dielectric strength. In other words, the problem could be neatly circumvented by including a timer or similar device that would energize the high-voltage circuits after the critical region was passed. However, hard experience has shown that inadvertent turnon of the high voltage while the spacecraft was passing through this critical region, the pressure lag in inadequately vented high-voltage enclosures after hard vacuum was reached, or failures of vacuum equipment or personnel during tests with full power on-all contributed to catastrophic failures in spacecraft electronic equipment. The problem is now given further emphasis for Mars soft landers, as it is estimated that the pressure of the atmosphere of Mars is probably equivalent to 110,000-ft Earth altitude, right in the critical region. Assuming a similar gaseous mixture as air on Earth, high-voltage electronic equipment in the soft lander would thus be required to operate in a gaseous environment of minimum dielectric strength.

Literature searches revealed that, prior to Sputnik, voltage breakdown in the critical region had been treated analytically, but very little equipment design and packaging technology was available. Since this appeared to be a problem area which could

rapidly become of critical importance, NASA Headquarters in June 1965, sent a TWX to all NASA and other government facilities and government contractors, requesting participation in a workshop symposium at JPL in August 1965. Releases were also made to the technical press to reach those not on the TWX distribution list.

The Workshop was designated "Voltage Breakdown in Electronic Equipment at Low Air Pressures." The response to the request could not be anticipated so a tentative 2-1/2-day meeting time was planned. The response was surprisingly large and very gratifying to NASA and JPL. Three full days and one evening were occupied with papers presented by various government organizations and private contractors.

To minimize the work of the participants and possibly obtain more last minute information (and still retain, as far as was possible, an informal, "give and take" atmosphere), formal papers were not requested. In order to preserve the information presented, and produce an accurate proceedings the following steps were taken. A stenographic transcript and a tape recording were made of each presentation and compared, so as to ensure complete accuracy in the written transcript. After each transcript was reviewed for technical inconsistencies, a manuscript was prepared in which grammatical corrections were made, without (we hope) losing the spontaneity of the presentation. These edited manuscripts were read over at JPL for possible technical discrepancies, then submitted to the authors for their review and approval. Copies of the slides and pictures shown by the authors were obtained and placed in the text. Many times authors would point out items of interest on their slides; an attempt has been made to incorporate, where possible, these references on the illustrations.

It is hoped by all concerned with the organization of the workshop and the preparation of these Proceedings that the thirty-six papers here will prove to be of interest and of use to those concerned with the engineering and design of high-voltage

spacecraft electronic equipment required to operate or pass through the critical air pressure region, and thus save critical time by anticipating possible failure modes. It is recognized of course, that these Proceedings are only a beginning---much further work is required before the voltage breakdown problems now before us, and those yet in the future, are solved successfully.

Earle R. Bunker, Jr.

LIST OF PARTICIPANTS

(\* indicates authors of papers included in Proceedings)

Samuel J. Ailor NASA Langley Research Center	Thomas Breeden RCA/Astro Electronics Division
Augustino Albanese Aerospace Corp.	*Chelsey L. Brock Westinghouse Electric Corp., Aerospace Division
Carl D. Alberts General Electric Co., High Voltage Laboratory	*William H. Brown NASA Manned Spacecraft Center
Dennis L. Backus Grumman Aircraft Engineering Corp.	J. M. Bulloch NASA Lewis Research Center
*George A. Bakalyar AVCO Corp., Research and Advanced Development Division	*Earle Bunker Jet Propulsion Laboratory
Charles C. Bates Johns Hopkins University	John Cabot Jet Propulsion Laboratory
John F. Baxter The Martin Co.	*Solomon Charp General Electric Co., Missile and Space Div.
James A. Bergey Los Alamos Scientific Laboratory	*John B. Chown Stanford Research Institute
James R. Bickel McDonnell Aircraft Corp., Space and Missile Engineering Div.	*J. Peter Clark Consolidated Avionics
Lynn W. Biwer General Electric Co., Missile and Space Division	*Ray L. Clark LTV Aerospace Corp., Astronautics Div.
Robert Blakeley Jet Propulsion Laboratory	Arthur C. Clarke NASA
James E. Blue Texas Instruments	*William J. Coleman North American Aviation, Inc., Science and Information Systems Division
*N. F. Bolling LTV Aerospace Corp., Astronautics Div.	Herbert W. Cooper U. S. Naval Research Laboratory
*Robert Boundy Jet Propulsion Laboratory	W. "Bud" R. Dagle Ball Bros. Research Corp.
Elmo C. Bruner, Jr. University of Colorado	*Thomas W. Dakin Westinghouse Electric Corp., Research and Development Center

LIST OF PARTICIPANTS (contd)

John J. Davis Electro-Optical Systems, Inc.	*James W. Haffner North American Aviation, Inc., Science and Information Systems Division
Timothy A. Day Aerojet General Corp.	Glenn E. Hagen Chrysler Corp., Space Division
Lewis G. Despain Jet Propulsion Laboratory	*William B. Haigh AVCO Corp., Research and Advanced Development Div.
Charles R. Detwiler U.S. Naval Research Laboratory	Richard E. Halpern NASA Headquarters
Earl Dieckman Jet Propulsion Laboratory	William Harby Harvard College Observatory
*Robert A. Dunaetz Hughes Aircraft Co., Research and Development Div.	Bill Hawersaat NASA Lewis Research Center
*William G. Dunbar The Boeing Co., Space Division	Nathan L. Hazen Harvard College Observatory
Gerald R. Dunn Space General Corp.	Richard M. Hollis The Martin Co.
Andrew Edwards NASA Headquarters	Carl Holzbauer TRW Inc.
*Ronald L. Fante AVCO Corp., Research and Advanced Development Div.	Raymond Hotchkiss U.S. Naval Research Laboratory
Donald F. Fowler TMC Research, Inc.	Stanley R. Hurst General Electric Co., Missile and Space Division
*Louis J. Frisco General Electric Co., Research and Development Center	*Eugene A. Jackson RCA/Astro Electronics
Paul J. Goldsmith Jet Propulsion Laboratory	Homer B. James Westinghouse Electric Corp., Aerospace Division
*Joseph R. Goudy NASA Langley Research Center	Eugene Jesse NASA Ames Pioneer Spacecraft
Boyce Gregg Raytheon, Space and Information Systems Div.	



LIST OF PARTICIPANTS (contd)

Julius Jodele Jet Propulsion Laboratory	Robert Mayne Jet Propulsion Laboratory
Donald S. Johnson, Jr. Ball Bros. Research Corp.	W. Keith McCoy Sandia Corp.
Wayne E. Johnston General Electric Co., Missile and Space Division	John A. McElligott Grumman Aircraft Engineering Corp.
*Wilson K. Kinkead General Electric Co., Missile and Space Division	*Nicholas McIlwraith NASA Goddard Space Flight Center
Don Laffert Sylvania Electronic Systems - East	*Eugene C. McKannan NASA Manned Spacecraft Center
Herman E. La Gow NASA Goddard Space Flight Center	Thomas R. McPherron McDonnell Aircraft Corp., Space and Missiles Engineering Division
Robert O. Lewis The Boeing Co.	Irwin B. Mayer AF Systems Command, HQ Space Systems Div.
*William J. Linder The Boeing Co., Aerospace Div.	Paul A. Michaels Bendix Corp., Research Laboratory Div.
Louis Lippitt Lockheed Missiles and Space Co.	James E. Milligan NASA Goddard Space Flight Center
Paul R. Little TRW Inc.	*J. Moacanin Jet Propulsion Laboratory
Billy B. Louder Douglas MSSD	Paul Molmud TRW Inc.
Paul Lukas TRW Inc.	*Aldus C. Myers, Jr. Electro-Mechanical Research, Sarasota Division
Robert A. Majka University of Rochester, Cosmic Ray Research Group	*Joseph E. Nanevicz Stanford Research Institute
Lewis E. Massie Ryan Aeronautical Co., Space Division	*Silvanus B. Newton Motorola, Inc., Military Electronics Div./Western Center
Preston T. Maxwell NASA Nuclear Systems and Space Power	

LIST OF PARTICIPANTS (contd)

Fred L. Niemann NASA Electronics Research Center	Robert A. Risse RCA Camden
Vuk Peric American Machine and Foundry, Alexandria Division	Curtis Rowe University of California, Lawrence Radiation Laboratory
Lawrence W. Petty ITT Cannon Electric	Bernard L. Sater NASA Lewis Research Center
Wallace Pierce Jet Propulsion Laboratory	Sam Sabaroff Hughes Aircraft Co. , Space Systems Division
George R. Pisarczyk AF Systems Command, HQ Space Systems Div.	Rudy Salcedo TRW Inc.
*Peter A. Pokalsky Kollsman Instrument Corp.	Eliot R. Schildkraut Harvard College Observatory
Royal B. Price North American Aviation, Inc. , Science and Information Systems Division	John R. Scull Jet Propulsion Laboratory
Stan A. Pryga North American Aviation, Inc. , Science and Information Systems Division	John C. Shabeck Raytheon Co. , Space and Information Systems Div.
Peter Ramirez, Jr. Electro-Optical Systems, Inc.	Russell K. Sherburne NASA Office of Space Science and Applications
Roger Ratliff NASA Goddard Space Flight Center	Richard Sicol Jet Propulsion Laboratory
*Edmond M. Reeves Harvard College Observatory	Ronald L. Snyder National Center for Atmospheric Research, Balloon Flight Facility
Richard A. Reeves North American Aviation, Inc. , Science and Information Systems Division	Toivo A. Somer Bendix Corp.
Jesse C. Rehberg Sandia Corp.	Douglas Spreng Jet Propulsion Laboratory
J. R. Reiss NASA Lewis Research Center	C. E. Spurlin NASA Lewis Research Center
Martin M. Reynolds Ball Bros. Research Corp.	Udo J. Strasilla Harvard College Observatory

LIST OF PARTICIPANTS (contd)

*Harry W. Street NASA Goddard Space Flight Center	Alan Watson Ion Physics Corp.
*David R. Tashjian Lockheed Missiles and Space Co.	Allen G. Weygand Bellcomm, Inc.
Joseph C. Thornwall NASA Goddard Space Flight Center	Elden C. Whipple, Jr. NASA Goddard Space Flight Center
Alan Titan Kollsman Instrument Corp.	Richard A. White NASA Goddard Space Flight Center
Robert L. Trent NASA Electronics Research Center	Donald I. Wilbur Hughes Aircraft Co.
William T. Trevaskis Aerospace Corp.	Michael R. Williams Hughes Aircraft Co.
Theofolus P. Tsacoumis NASA Headquarters	William R. Wilson ITT Federal Labs
Richard C. Turner Consolidated Avionics	Richard T. Woo Jet Propulsion Laboratory
*Edward F. Vance Stanford Research Institute	*George A. Work Hughes Research Laboratories
Glenn Vescelus Jet Propulsion Laboratory	Andrew G. Young Jet Propulsion Laboratory
Larry J. Waller (Reporter) Electronic News	Kenneth R. Zimmerman Pacific Scientific

### WELCOMING REMARKS

Andrew Edwards  
Workshop Chairman  
National Aeronautics and Space Administration  
Washington, D.C.

We at NASA, with JPL, have sponsored a number of workshops on key topics, mostly from our experiences with the Mariner Program. The Mariner team has participated in these workshops and we think they have been quite successful.

This workshop has been set up to emphasize informality. We can't very well have a roundtable discussion with this many people, but I do want to stress that we would like to hear your views on all of these topics.

The voltage breakdown topic, I think, is probably the most important one we've covered in these workshops, if the experience in Mariner is any indication. Mariner had some nasty surprises for us; they were overcome, but at a certain price. For example, one experiment could not be carried because of voltage breakdown problems. And, perhaps a final surprise after the encounter with Mars, it now looks like the Martian surface pressure is in the middle of the corona region; so, anything that is going to explore the surface of Mars will not only have to survive this corona region, but operate in it. Exploration of other planets will probably bring out some very interesting ramifications of voltage breakdown as we get into some of the more exotic atmospheres.

# 1. VOLTAGE BREAKDOWN PROBLEMS AT LOW AIR PRESSURES ENCOUNTERED IN THE MARINER IV SPACECRAFT

Earle R. Bunker, Jr.  
Jet Propulsion Laboratory  
Pasadena, California

At JPL, we are interested in voltage breakdown phenomena that require air or some other gas as a transport medium.

Last October, MIT had a symposium on "Insulation of High Voltages in Vacuum;" but they're talking about real vacuum,  $10^{-5}$  mm or harder. The initial breakdown in such a vacuum is a surface effect. There is no air, molecules, or anything to provide a conducting path for an arc across the gap. Also, we are really not going to concern ourselves with breakdown of a solid dielectric, where the electrons are torn out of the atoms and a conducting path is formed. A lot of work has been done on this at other symposiums.

The pressure range we are concerned with, in terms of Earth altitude, is about 60,000 to 310,000 ft. The types of voltage breakdown at sea level are shown in Fig. 1-1. If we start out at 0 v we have, as we increase the voltage, a linear increase of current (or ohms law) region from A to B - because there are free electrons in everything, scattered around in the air by various ionization processes. The plateau, from B to C, is the Townsend current or just free electron current. The curve seems flat because all the available electrons are being used.

As the voltage is increased further (Fig. 1-1 has a logarithmic current scale), enough energy is imparted to the free electrons to enable them to strike some gas molecules and cause ionization, which results in a rapid rise of current as shown from C to D. Depending on the conditions, this rapid rise of current can culminate in an arc shown as a dashed curve F' that is a complete breakdown between the electrodes, or the current may have a plateau that we call corona (which is a partial breakdown). As the voltage is increased further to E, the arc finally forms. As the pressure is reduced, equivalent to higher altitudes, it is increasingly difficult to distinguish between a corona and an arc.

Of course, everybody has heard of Paschen's law. It was discovered experimentally in 1889 and verified theoretically 20 yr later by Townsend; it is shown in Fig. 1-2. The three curves of Fig. 1-2 show the relationship between the breakdown voltage and the product of the pressure,  $P$ , times the separation,  $\delta$ , between two parallel plates. For any given  $P\delta$  product there is a breakdown potential, where an arc occurs. For

example, air at room pressure breaks down at about 75 kv, which would be a  $P\delta$  product of about 19,000 (Fig. 1-2c). Then, as we come down and either decrease separation or decrease the pressure, we follow an approximate linear curve. This  $P\delta$  is in mm Hg times mm of separation.

Then, as we go further down, the breakdown is still linear until we come to the curve of Fig. 1-2a, which is the so-called Paschen minimum. This is the most mis-used curve or misused term in the business.

There are those who use Paschen's curve for discharges between points or for other configurations. I have seen in literature that someone came out with Paschen's curve for a printed circuit board. If you want to be a purist, there are only three conditions under which Paschen's law holds:

1. There must be a uniform field. This rules out points or anything but parallel infinite planes.
2. Spacing of the two plates is large compared with the mean-free path of the gas molecules.
3. There are no space charge effects in the gap. This, of course, is not true at low pressures.

So, if we don't worry about these conditions, then we can call it a Paschen-shaped curve. However, for uniform field conditions, there is only one curve relating voltage breakdown as a function of the pressure-spacing product, or  $P\delta$ .

Now, as a matter of interest, for dealing with complex geometries or non-uniform fields, Fig. 1-3 shows the law of similitude. The law says we can take any system configuration and, if we increase all the dimensions by a factor of  $K$  and divide the pressure by the same factor, the breakdown voltage will be the same. This law is very handy when dealing with complex geometry.

For about 80 yr or longer, corona breakdown has been studied but no one can agree on a definition of corona.

As contrasted to an arc, corona is considered as a partial breakdown. Some definitions say it must have dissimilar electrodes, but that isn't true. You can have two similar electrodes and still have a partial breakdown.

Most of the work has been done at 60 cycles because of the power engineers. They're worried about corona because kilowatt hours are being dissipated in the air that people are not paying for, besides interfering with their television sets; so the

power people have been doing much work on it. However, they think they're working with high altitude when they go up to 10,000 ft, so that doesn't help us too much. They talk about the corona onset voltage, which means the voltage where corona starts, and the offset voltage, which is the voltage at which the corona extinguishes.

There is commercial equipment available that attempts to measure the energy in the corona. As I mentioned, corona interferes with radio equipment. Usually it's a type of radio frequency noise, but if we go down in pressure we find that this is not necessarily true. We can have dc corona and no noise. I have been able to prove this in the laboratory. The main manifestation when we think of corona is a blue haze, the crackling, the smell of ozone, and some noise. Again, this is not true at low pressures.

But part of the problem in making corona measurements is that there are so many variables such as the electrode configuration and spacing. People talk about corona breakdown voltages but they always say, "Well, it depends on the conditions. It depends on the electrodes. It depends on this. It depends on that," never really pinning it down; no quantitative definition.

I have defined corona as  $1 \mu\text{a}$  of current. I have been getting reports that say you can have corona at smaller currents now,  $0.3 \mu\text{a}$ . So I may have to revise my value. But, the point is that there is corona; we have sufficient difficulty measuring it.

Another problem in measuring corona is the constituents of the gases. This Paschen's minimum in Fig. 1-2a occurs at about 330 v. What this figure shows is that any voltage under 330 v would not arc over, regardless of air pressure, electrodes, or anything else. This was my understanding, but some later papers might show we have to worry about lower voltages.

One very great problem missed by quite a few researchers is the problem of mercury contamination. In pumping down a big bell jar with a mercury manometer or a McLeod gage, there will be some mercury vapor left unless it is very carefully trapped out. The mercury vapor will cause breakdown at a much lower voltage and the only way it can be eliminated is by chemically cleaning it; washing it out.

The frequency of the applied voltage is important; as the frequency increases, the breakdown occurs at a lower voltage.

The waveform is important. The type of insulation on the electrodes is important, whether outgassing, or whether there are creepage paths.

One thing a lot of people miss is the cleanliness of electrodes. If you touch the electrode, the oil from your fingers will increase the breakdown average in that area. You have to be very clean; almost clean-room clean.

Another problem is the source of free electrons. Before corona or an arc will form, one free electron must be in the gap. Without this, there will be no breakdown. You have to have a source of free electrons, like a radioactive source or an ultra-violet source. This makes the breakdown voltage more even, instead of erratic.

Some power reports point out that corona on the outside of insulation doesn't matter; you can live with it.

In space equipment we don't feel we can tolerate corona because it can jam or block some very sensitive receivers nearby. It also causes gradual erosion of dielectrics.

At sea level the corona effect is a high impedance effect. With 270 v and 1  $\mu$ a of current flowing there are 270 meg between the terminals, so this could be called a high impedance; when an arc occurs, it is a low impedance and current is limited only by the power supply voltage and impedance.

At lower pressure, the number of molecules gets fewer, the corona-to-arcing transition point, as shown by the step in the curve of Fig. 1-1, becomes less and less - in fact, an arc may occur with only 1  $\mu$ a of current. So, it is difficult to tell if it is corona or arcing. Arcing is a complete breakdown, as we have said, and at dc you can have a glow discharge. The dc glow discharge at various pressures is shown in Fig. 1-4.

This figure is actually a long tube, not a uniform field. At 100 mm there is the familiar spark; about 20 mm a glow, a glow discharge begins; and at 5 mm a conventional glow discharge occurs where there is the red anode glow, the negative glow, and the Crookes dark space. This is sort of highly idealized. You normally don't see this too often in your test equipment because of fluctuations, differences in conditions; but the blue glow of the cathode and the red glow of the anode are very distinctive; in my other paper I have some pictures of this at low pressures.

As the pressure is further reduced, say to 0.1 mm, the anode glow reduces as the dark spaces become much larger until you finally go off the bottom end of the Paschen-type curve (where the vacuum becomes a good insulator) with no breakdown.



Figure 1-5 shows the effect of illuminating the gap, starting with a threshold voltage,  $V_s$ , and then applying a  $\Delta V$  over this voltage; with the gap unilluminated, the time of breakdown is shown. If a 20% overvoltage is applied, we have something like  $10^{-4}$  sec breakdown. Using a 10%  $\Delta V$ , it takes nearly 1 sec. Any  $\Delta V$  less than 10% will take longer for breakdown. If we use an ultraviolet or radioactive source for illumination (which breaks down much quicker, on the order of microseconds) then Fig 1-5 applies.

Figure 1-6 shows some of the effects of this time for breakdown. If a pulse (Fig. 1-6a) we're applying as  $\Delta V_1$  is greater than threshold  $V_s$  and we have a relatively long pulse (long compared to that time  $\tau$ ), it will break down every time. As we shorten the width of our pulse, we'll reach a point A at time  $\tau_1$ , at which there is only intermittent breakdown. Now we can again get breakdown if we increase the amplitude of our pulse to  $\Delta V_2$ . Then we can decrease the width to, say,  $\tau_2$ , before we get intermittent or no breakdown.

On a wave shape (such as Fig. 1-6b) the voltage can build up past the threshold and after the maximum is reached, then it starts to break down depending on the length of time and the overvoltage applied. Waveform effect is very clear in Fig. 1-6b.

The ac voltage breakdown (Fig. 1-7) has a typical sine wave going above the threshold for a period of time,  $t$ , on the first cycle. Depending on how great this amplitude is above the threshold, a breakdown may occur immediately when

$$\frac{nt}{\tau} = 1$$

where

$n$  = number of cycles

$t$  = length of time above the threshold

$\tau$  = breakdown time from Fig. 1-5

Then breakdown may occur after several cycles.

We have been neglecting decay, recombination, or lifetime of the charges floating around. If you wait long between voltage peaks, then all the electrons will disappear and the breakdown conditions will be the same as shown in Fig. 1-6.

In concluding the general discussion, we will just make one mention of the phenomenon known as an electronegative gas.

There are certain gases, such as oxygen and sulfur hexafluoride, that apparently have an affinity for the free electrons. So, if there is a free electron in the gas, this gas molecule grabs hold of it and doesn't allow it to be in the gap to cause a breakdown. With these gases we can have actually higher dielectric strength or higher breakdown potential than, say, air or most other gases.

This has sort of been a real quick brushover of voltage breakdown at altitudes and the problems that may be encountered. Now I would like to discuss the problems we had with Mariner.

The Mariner spacecraft has the primary mission of making scientific measurements near Venus and Mars, and a secondary mission of making various science measurements en route to these planets. It was designed to operate in the high vacuum of space with the design requirements that the high-voltage equipment would not be turned on until after it passed through the critical 60,000 to 310,000-ft region above the Earth. This was done and, as we know, it was successful; but it seems like the reliability of vacuum testing systems are several orders of magnitude poorer, including the human operators.

At one time or another because of some failure of vacuum equipment, most subsystems of the Mariner (also one complete spacecraft, in fact) were exposed to operation in the critical region with full power on, with unfortunate results.

I was called in to suggest quick fixes so this exposed operation wouldn't happen again. This meant we had to improve the reliability of vacuum testing systems. This was not foreseen in the original specifications and wasn't required. We didn't have to worry about it. But I understand that the other companies have had this problem, too; somebody turning the wrong knob. It doesn't take much pressure leaking into a chamber to bring it into the critical region, then everything lights up like a Christmas tree, and a certain amount of rework and retesting is required (which is rather expensive).

Mainly, we had to drill holes in the subsystem containers (they go through the critical region) to let the air out. Equipment is always designed with close tolerances. Covers are machined to fit snugly; this creates an inside cavity that can entrap the air. Sixteen hours later, when you turn the subsystem on, that cavity is

still in the critical region even though many hours have passed since the spacecraft entered the high-vacuum region. Flow of air at low pressure is very slow because it is actually a diffusion process rather than a pressure flow process.

Figure 1-8 shows the trapped radiation detector, which has four sensing tubes. It is mounted on a box with a tightly fitting lid.

Figure 1-9 shows the interior of this box with quite a bit of space inside. The high-voltage part was foamed. We were afraid this cavity would cause a problem. In fact, this test showed it would leak out too slowly to be past the critical region by the time it was turned on, so we ended up drilling a couple of 1/8-in.-diameter holes in the lid over the cavity; the test showed it worked pretty well.

Figure 1-10 shows the ion chamber with a Geiger-Mueller tube. This was one of the first breakdowns; the tube operates at 975 v. It had to be shock-mounted inside the metal tube, and the construction is such that the end opposite from where the leads come out has a tip on it.

The tip end was used to mold the room-temperature vulcanizing rubber cup. Two holes were punched in and pushed on to the end with the leads, as shown in Fig. 1-11. The tight seals around the wire and tube enclosed a pocket of gas. After 30 hr of test in vacuum, the Geiger-Mueller tube started giving many erratic readings. When it was taken apart, the rubber had been burnt by arcing between the terminals, causing a high-resistance shunt. Apparently, the air had leaked down to the critical region, causing the arc. Because time was short, we cut grooves in that plug so the air could bleed off rapidly to reduce the pressure below the critical region before the instrument was turned on.

Figure 1-12 shows what happens when a bare printed circuit board with voltages above 270 v is operated in the critical region. Two major arcs are visible.

Coating all the components and terminals with a good heavy coating (as shown in Fig. 1-13) removed any contact with the air; when we put it back in the vacuum chamber it worked fine.

The ultraviolet photometer shown in Fig. 1-14 was a rather complicated device, operating at 2800 v. I believe this was the first one we had trouble with. It has power supplies in these side compartments. One of these supplies had almost 2800 v on two terminals. A 1/2-in. layer was foamed in place over these terminals and then covered with Solithane to seal it. After about 70 hr of operation it arced

over. The investigation concluded that the material put on over the foam tended to seal the gas in the foam so it leaked out very slowly, finally going through the critical region causing arc over and destroying the power supply. This was blamed on the outgassing of the foam and sort of gave foam a black eye on all high-voltage work at JPL.

They went through quite a program to correct this. First the foam was removed. Then the connections on the printed circuit board were shortened to get a greater spacing between the 2800-v terminals. A layer of 1/8-in. thick solid Stycast 1095 was applied. Besides that, RF chokes were put in to prevent interference with the radio system in the spacecraft if this did arc over. This was sort of a backup. It went through test and passed successfully.

Another high-voltage supply problem was rather unusual. This instrument was to work during the many months of flying and all of these instruments on the spacecraft are designed to save every speck of power they can. The power supply was a multiplier type; multiplied, I think, ten times to 2800 v dc.

Now, people who design power supplies always put in a bleeder resistor. This is standard practice. The question came up "Why do we have this bleeder resistor? Let's leave the bleeder off because all it's doing is dissipating power that we need for some other application." So the bleeder resistor was left off because, in the actual flight, it wouldn't be missed. In testing, however, leaving the bleeder resistor off caused trouble, because they would set it on the bench, test it and the capacitors would charge up (there's nothing to discharge then except their own leakage, so they sit there charged). Then the unit was put in the vacuum chamber and pumped down. When the critical region was reached, the capacitors discharged and damaged the system; so they ended up putting the bleeder system back in to discharge the capacitors for testing.

Figure 1-15 shows the Canopus tracker, which has a 12-stage photomultiplier tube, and its input circuitry. There is nothing wrong with it. It worked fine except when it went through this inadvertent chamber depressurization of the whole spacecraft, the Canopus tracker went out and for a very interesting reason that may not be apparent to the designer.

In Fig. 1-16 the 1800 v, the high voltage, is applied to the point shown (which goes to two resistors). One resistor goes to the twelfth dynode which becomes about 1500 v. The other resistor is the load resistor for the anode of the photomultiplier.

The signal is coupled by a high-voltage capacitor to the base of the input transistor, which is nearly ground potential. Under normal conditions this works fine; except in the critical pressure region an arc formed from one of the high-voltage terminals to the bare input terminal, which burned out the transistor. Obviously if it is never exposed to operation in the critical region it would be all right. What would have been better, and what we're watching now, is to locate the input a distance from the high voltage so if it's going to arc over it will arc over to a ground bus or ground plane somewhere and not hit the input of the transistor. This was found out in a vacuum test after the one that failed in the chamber.

There was also a voltage breakdown in the high-voltage transformer because of too much voltage between turns. The secondary, being scramble- or random-wound, happened either to have two turns adjacent with half the secondary turns in between, or the turn half-way through happened to be near the ground, which resulted in breakdown. Whether it was caused by a winding problem or an air bubble in the encapsulation material was not known because we couldn't take it apart.

The radio system had a problem with its traveling-wave tube. Figure 1-17 is a cutaway section of this tube. The 2-mil Teflon sheet is all that separates the grounded RF connector from this reflector, which operates at 800 v. Initially, it is 1200 v until the tube warms up. There are 800 v across less than a 0.015-in. gap, with the 2-mil Teflon against a sharp point.

The metal-to-ceramic solder seal also has a sharp edge against the Teflon. The tubes would operate for a while, then would arc over with results shown in Fig. 1-18 (the RF connector is at the bottom). The high voltage punctured the Teflon, arced through the foam, and destroyed some very expensive tubes. It required some redesign by the vendor to reduce the sharp point, increase the spacing, and improve the encapsulation technique.

Figure 1-19 shows the plasma probe. There is a very fine screen across the opening. This screen has 8 kv dc with  $\pm 2$  kv ac applied to it. Charged particles are attracted to the screen, but pass through and hit the collectors on the bottom. But the connectors were breaking down. These were connectors sealed with O-rings, but trapped air was slowly leaking out and passing into the critical region when the plasma probe was turned on, so we suggested boring holes in the connectors.

On the side opposite to the high-voltage input, there was a test jack covered by a removable room-temperature vulcanizing rubber plug. This plug was removed to enable insertion of a test probe to measure the voltage on the screen. When the plug was replaced it would trap about  $1/4 \text{ cm}^2$  of air in there, which eventually leaked out into the critical region and would arc over.

Now, in the loss of vacuum in the big chamber with the complete Mariner spacecraft, we had arcing between the screens (which discolored them). I don't know whether this affected the calibration of the instrument but it caused flakes of insulation material to stick to the screen and darkened it.

We obviously couldn't embed the screen because it has to be exposed to the vacuum. Here we suggested using something like a spark gap to take the arcing, rather than the screen.

At JPL we are beginning to feel that all spacecraft equipment, even though it's not required to operate in the critical region, should be designed and exposed to such environment so it can operate there without damage, just to take care of errors or failures of the vacuum system.

Not much extra effort is needed to make this equipment corona free. Just more consideration, but it doesn't add too much (if any) weight, as some of the examples shown here and it would improve the reliability. Then we should have a design review of all systems over 250 v, for possible failure in the critical region.

#### OPEN DISCUSSION

MR. LUKAS: You mentioned that you have created corona without its being observed in the form of noise. How do you confirm the corona; by ozone production?

MR. BUNKER: No. We are able to see the corona when the eye gets dark-adapted. It does not show up on the scope. It's a dc positive point corona. My other paper covers the work I've been doing with corona. We have found a way now to measure it in terms of microamperes.

MR. JACKSON: I have a comment more than a question, actually. You are speaking of minimums of 300 and 250 v. In radio, before the advent of solid state, we used the VR service tubes for regulators: VR-150, VR-105, VR-90, and VR-75. This tube is working at 75 v and its theory of operation demands a corona,

a glow discharge to operate. I have seen those discharges as low as 50 v. I'm told they could occur in a 24-v power supply. Personally, I've never seen it; 50 v I have seen. You have to go quite a way down in voltage before you say, "Well, this is too low a voltage to worry about."

MR. BUNKER: Well, I don't want you to give the impression that anything under 250 v is safe. This was true in air.

I've read reports where the experimenter has gotten as low as 8 v which would horrify me, but it was done under rather special conditions using mercury vapor. We used 250 v as a dividing line for a high-voltage specification that I've been preparing. Maybe this is too high, I don't know.

MR. PERIC: The neon tubes that were mentioned, I think you do go to special efforts to make them discharge at those low voltages (like gases, treatment of cathode, and possibly some radioactive material inside the neon tubes). It's possible to have discharges at those low voltages but under special circumstances, I would say.

MR. MEYERS: I think Dr. Covine's book, Gaseous Conductors, would throw a great deal of light on some of these problems. Have you used that or have some information?

MR. BUNKER: No. I am not familiar with that book.

MR. MEYERS: Dr. Covine's Gaseous Conductors, by McGraw-Hill, covers many of these topics very well and is very well referenced.

MR. BUNKER: Good. We will check that. Speaking of books, we had a new book by Dr. Loeb, Electrical Coronas, Their Basic Physical Mechanisms, dated 1965, added to our library. Rather interesting book and brings up to date the work that has been done and it does go down in low pressure. However, it is quite heavily mathematical and not directly applicable to practical construction of equipment, which is what we are trying to cover in this symposium workshop.

MR. EDWARDS: Excuse me. I thought maybe it would be worth mentioning that a number of these things you've talked about weren't discovered until we got into a complete spacecraft and in the large chamber environment. In other words,

in the subsystem test we failed to pick up some of these problems. Maybe you could comment on that.

MR. BUNKER: For other considerations, all the exposed conductors, such as on printed circuit boards, are normally covered with an insulating covering or conformal coating. Insulation of exposed conductors is mandatory because, apparently, as the equipment flies through space with zero gravity you can have space junk, which is usually conducting, fall across the conductors and short something out.

At our five-story space chamber at JPL we had a flight model operating at full power under high-vacuum conditions. Some failures in the pumping systems occurred that were thought impossible, but the pressure in the chamber was raised to the critical pressure region besides spraying oil all over the spacecraft. Arcing and corona occurred in several subsystems, causing some damage.

Some voltage breakdown tests on various subsystems were made but this idea of something breaking down after quite a few hours was not expected. For example, how fast does gas diffuse through foam?

CHAIRMAN EDWARDS: Well, what I had in mind was not so much the breakdown in the chamber, but that it did take days and, perhaps once, a couple of weeks to find these problems under normal operation in the chamber. We did not find the difficulty in the subsystem test, which theoretically is supposed to qualify pieces of equipment before you get so far along that everything is put together in the large chamber as a final test cycle.

MR. BUNKER: This is true. The spacecraft approval tests last for weeks, even months, under vacuum conditions. But subsystems tests are shorter, because of schedule requirements. Failures may not show up in these shorter subsystems tests, but may show up in the longer approval tests.

MR. BROWN: I'll be different and ask a question where everyone else is adding comments.

A term that I've recently come across, the term "multipactor" in a Hughes report. They call it a new term; I had not heard it before and I wonder if this is the same thing as simulated and described by you. I wonder if you could add any light on that?



MR. BUNKER: I can add very little on it; I have some reports on it, but as I understand the multipactor (or the multipacting breakdown) is an RF, or microwave breakdown and can occur in a pure or high vacuum. It does not need air or other gas as a transport medium. There were some papers submitted on multipacting and we said, "No. This is in the high-vacuum region." We feel that this has to be covered elsewhere or has been covered at MIT. Very little is known about multipacting breakdown I guess. Hughes is doing a lot of work on it. Now, you can have antenna breakdown in the critical region at microwaves. This is a corona and high-voltage arcing problem but not multipactor breakdown as I understand it.

VOICE: I wonder if I might add that the multipacting can occur at some frequencies within altitudes of your region.

MR. BUNKER: Is this a multipacting breakdown or is it a breakdown of the air at that point?

VOICE: Well, I think it is a transition apparently started by multipact mechanism. But perhaps, after that, maintained in the presence of a gas, but it does seem to sort of set an asymptote that may appear at around 300,000 or 400,000 ft at some frequencies.

MR. WILLIAMS: The multipactor is a resonance form of radio frequencies; it doesn't exactly cause damage or much trouble itself, but it can cause out-gassing from surfaces, foam, and things that allow the pressure to rise and corona to occur. That's where multipactor comes from.

MR. BUNKER: I also understand that multipacting, when it occurs inside a wave guide, changes the impedance drastically and can possibly damage the transmitting tube with the high standing wave ratio existing there because of that arcing.

MR. SHEPHERD: Multipacting, as this gentleman just said, is a resonance phenomena and can occur between two plates, at radio frequencies as well as at microwave frequencies, and it results from the multiplication of secondary electrons as these pass back and forth between the two plates.

MR. HAWERSAAT: I would just like to comment on your plan to design for all pressures.

As we are moving into (or hope to be moving into) ion propulsion and other types of plasmas, voltage breakdown gets more critical because when you run in a vacuum tank you're filling a whole tank with a dilute plasma; voltage breakdown is going to get very important in these programs, so I think you start to talk about voltage breakdowns in the 50-, 100-v region, things like this. You're definitely not talking 250 or 300 v.

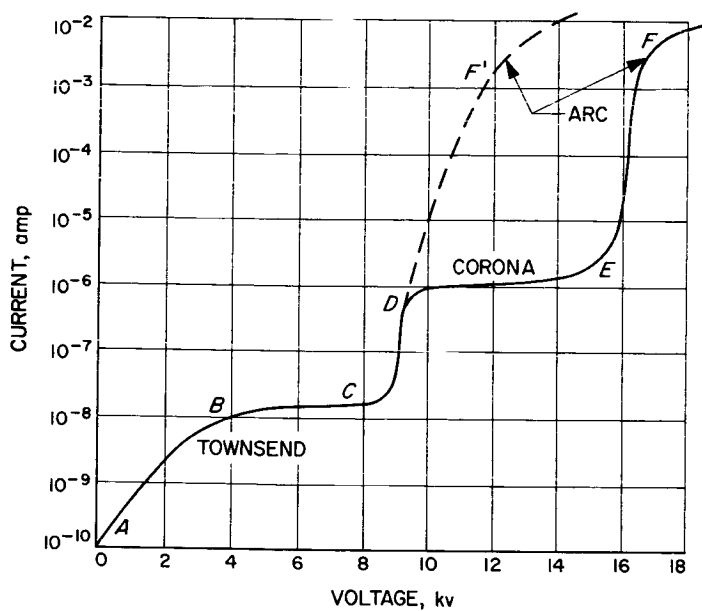


Fig. 1-1. Current vs voltage, various types of voltage breakdown in air at sea level pressure

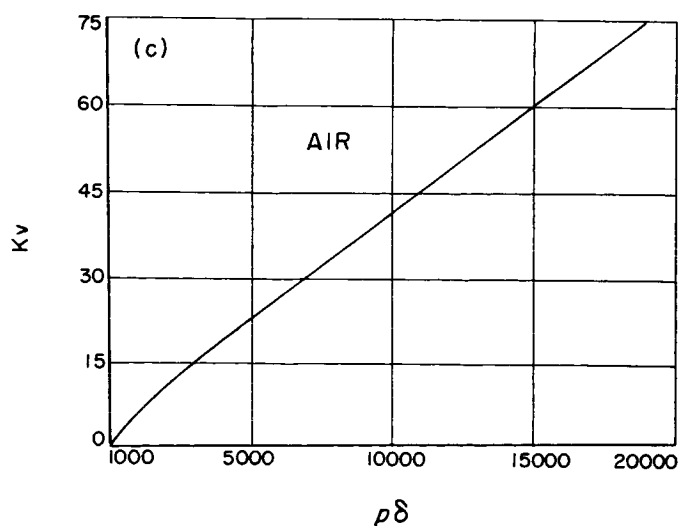
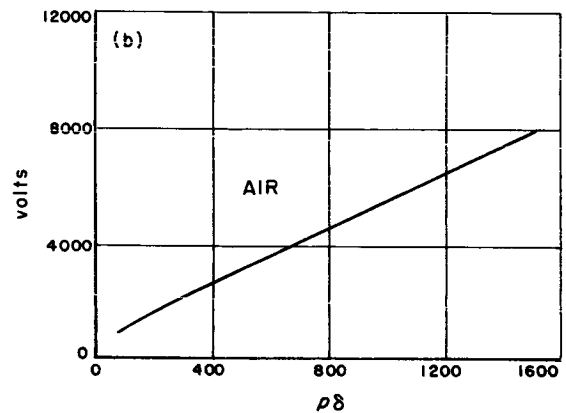
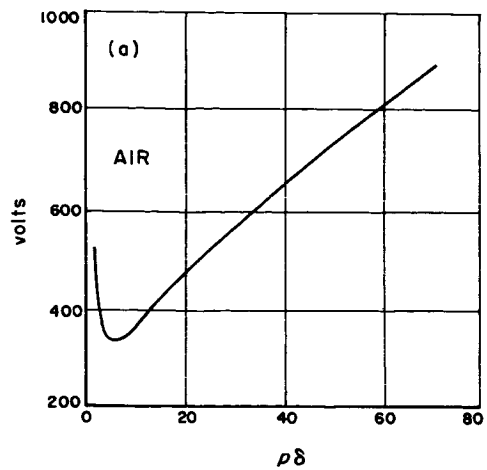


Fig. 1-2. Arcing voltage vs  $p\delta$ , product of pressure and separation of parallel plates

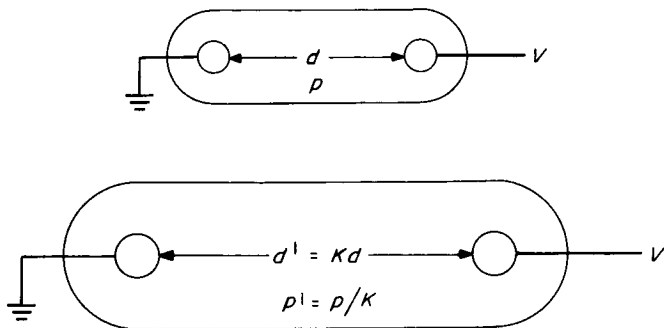


Fig. I-3. Law of similitude

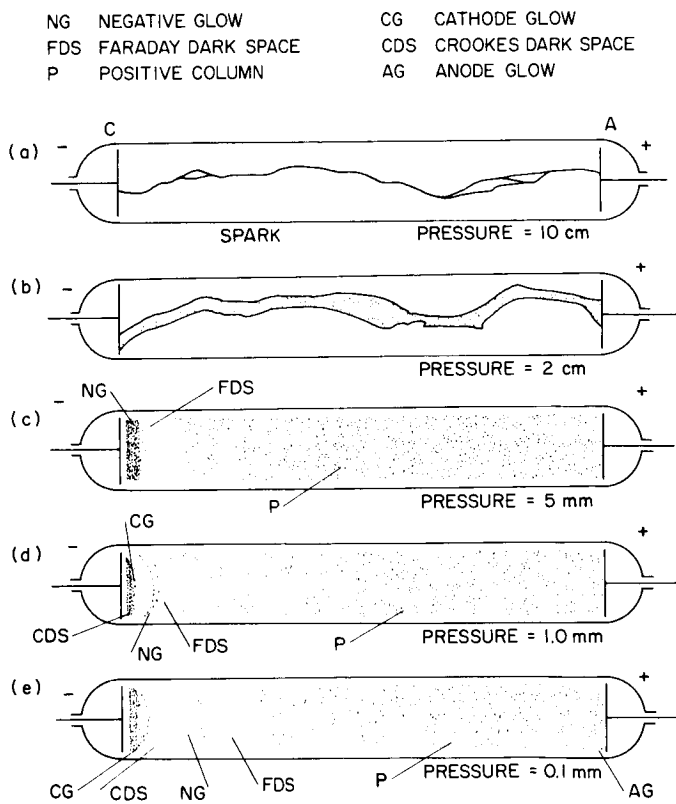


Fig. I-4. Appearance of DC arc at various air pressures

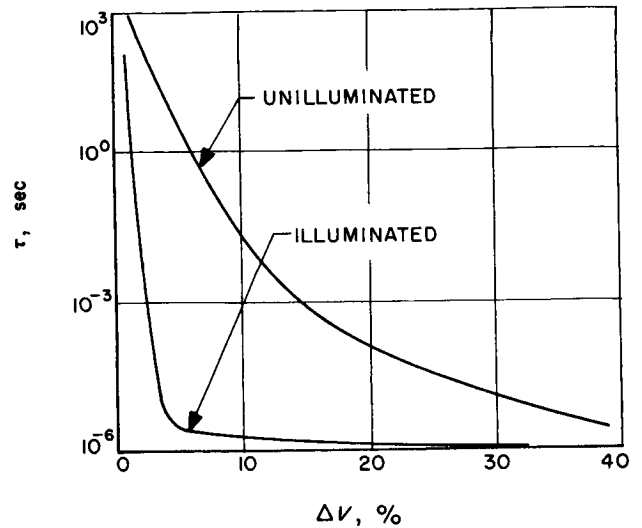
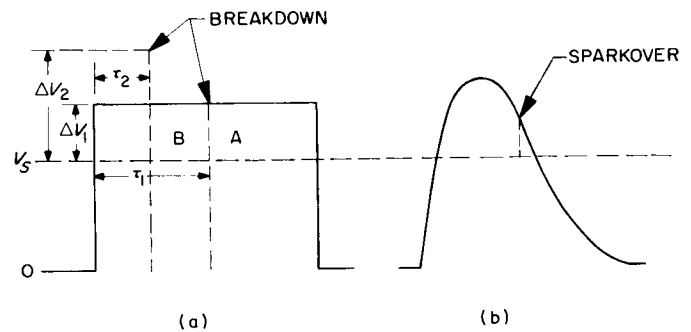
Fig. I-5. Breakdown time  $\tau$  vs overvoltage  $\Delta V$  for illuminated and unilluminated gaps

Fig. I-6. Waveform effects on time for voltage breakdown, square wave and pulse

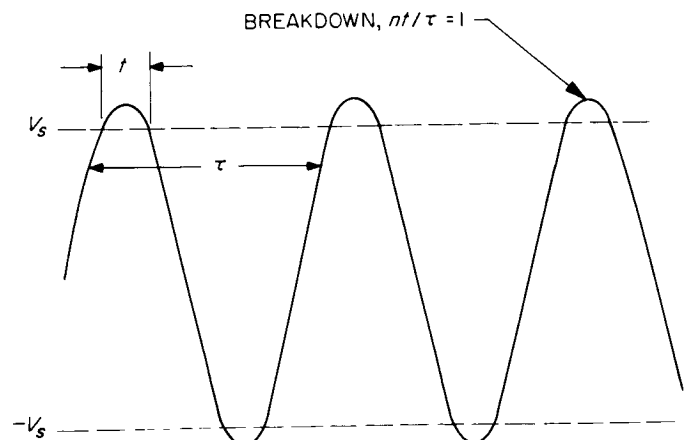


Fig. I-7. Waveform effect, AC voltage breakdown

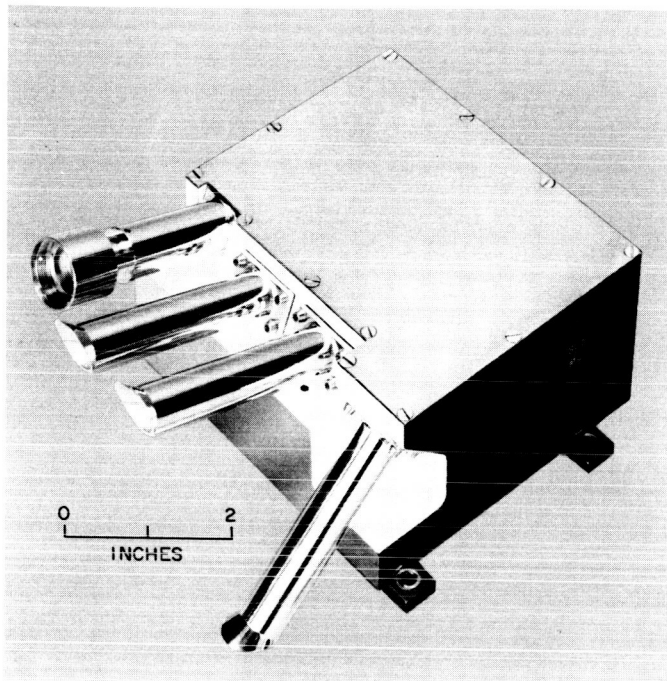


Fig. I-8. Trapped radiation detector

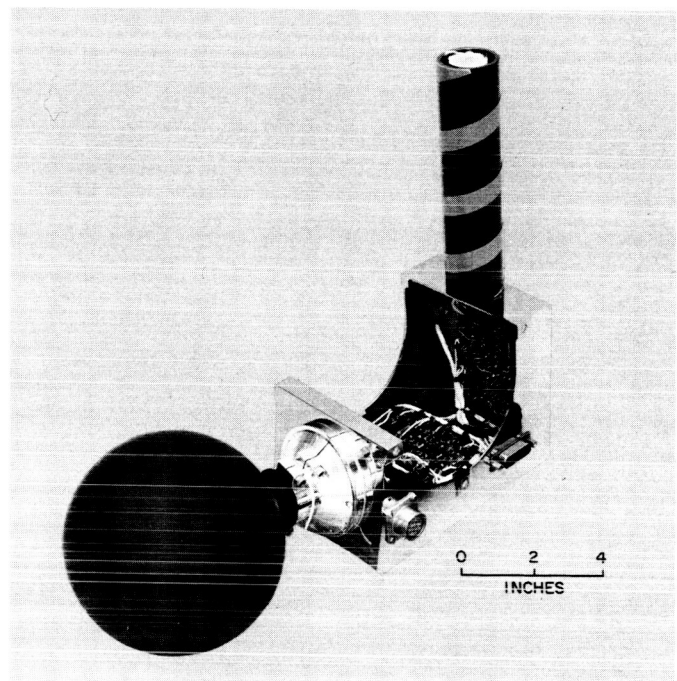


Fig. I-10. Ion chamber and GM tube

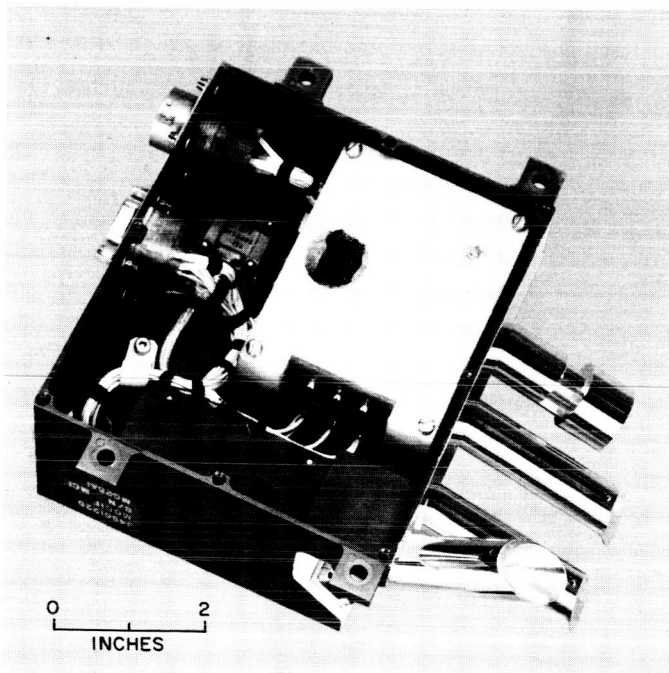


Fig. I-9. Trapped radiation detector, bottom cover removed

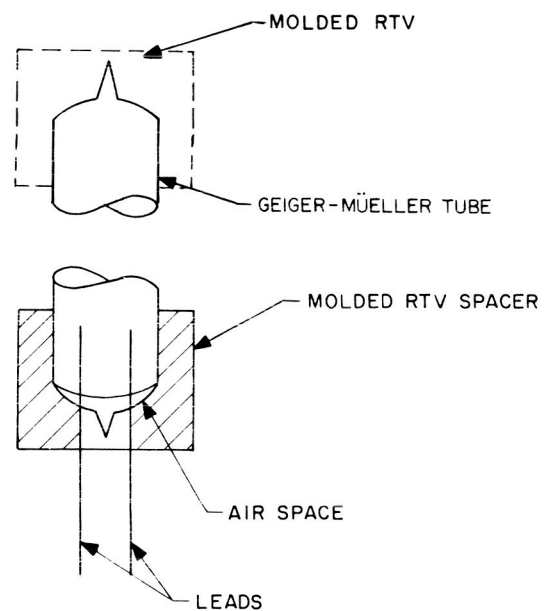


Fig. I-11. Molded RTV spacer showing air space

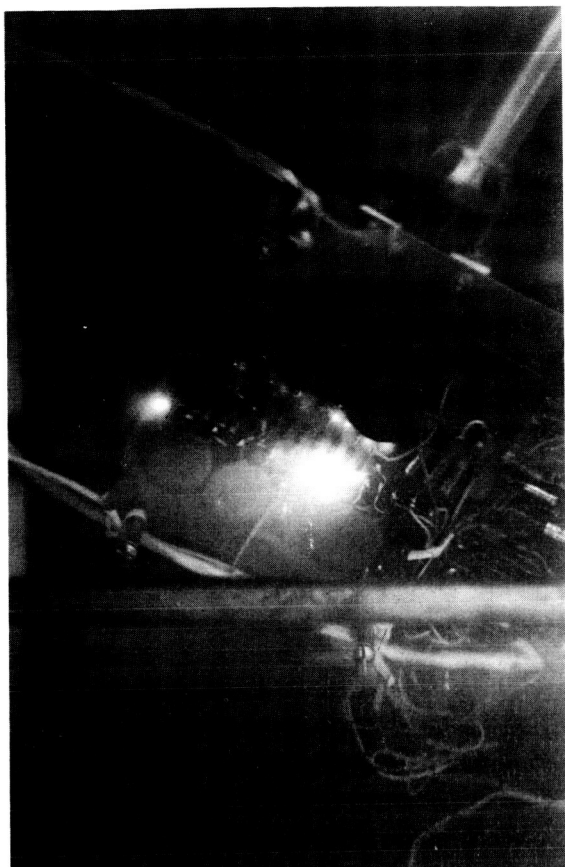


Fig. I-12. Circuit board arcing in critical region

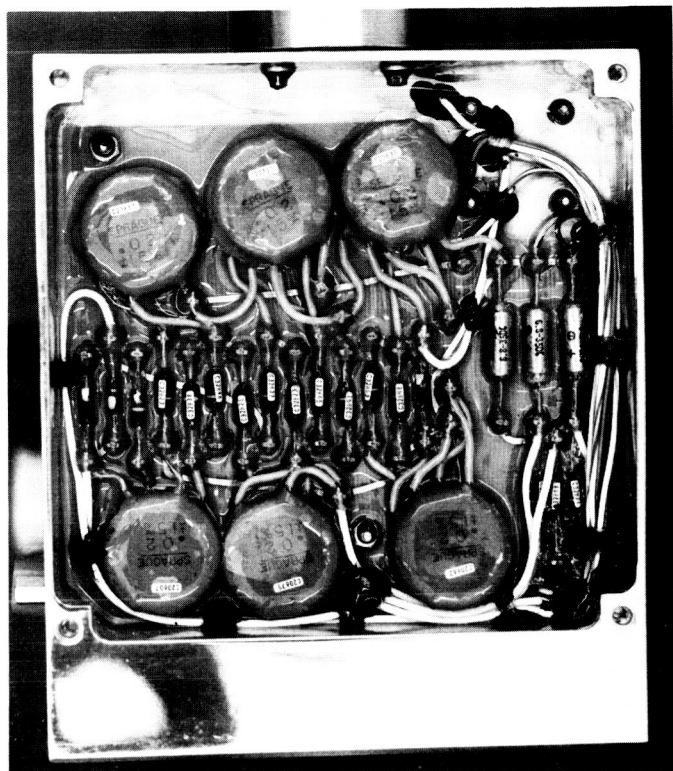


Fig. I-13. Conformal coating of circuit board to inhibit arcing

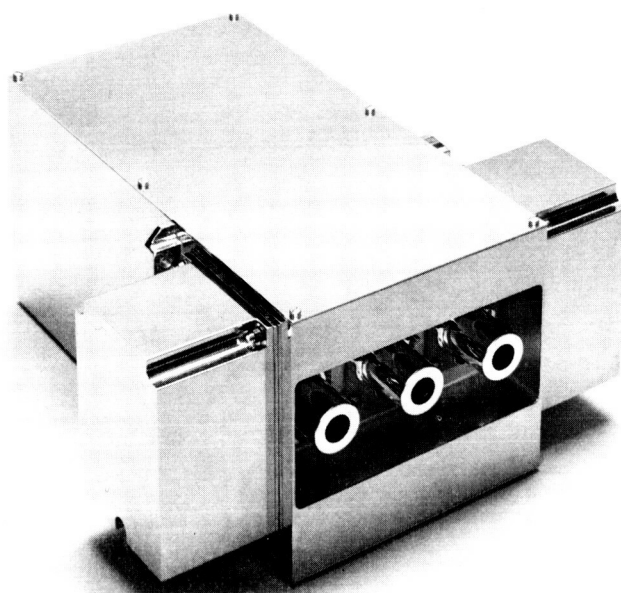


Fig. I-14. Ultraviolet Photometer

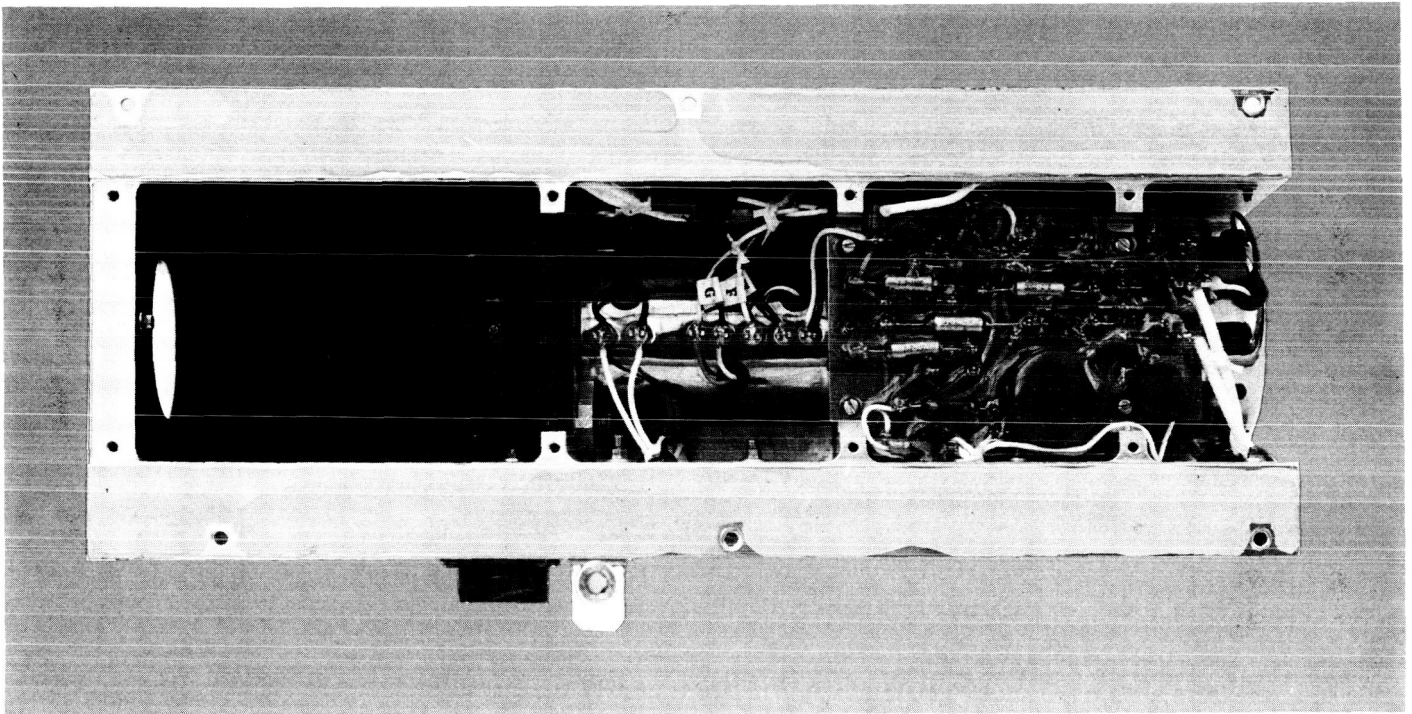


Fig. I-15. Canopus tracker with panel removed

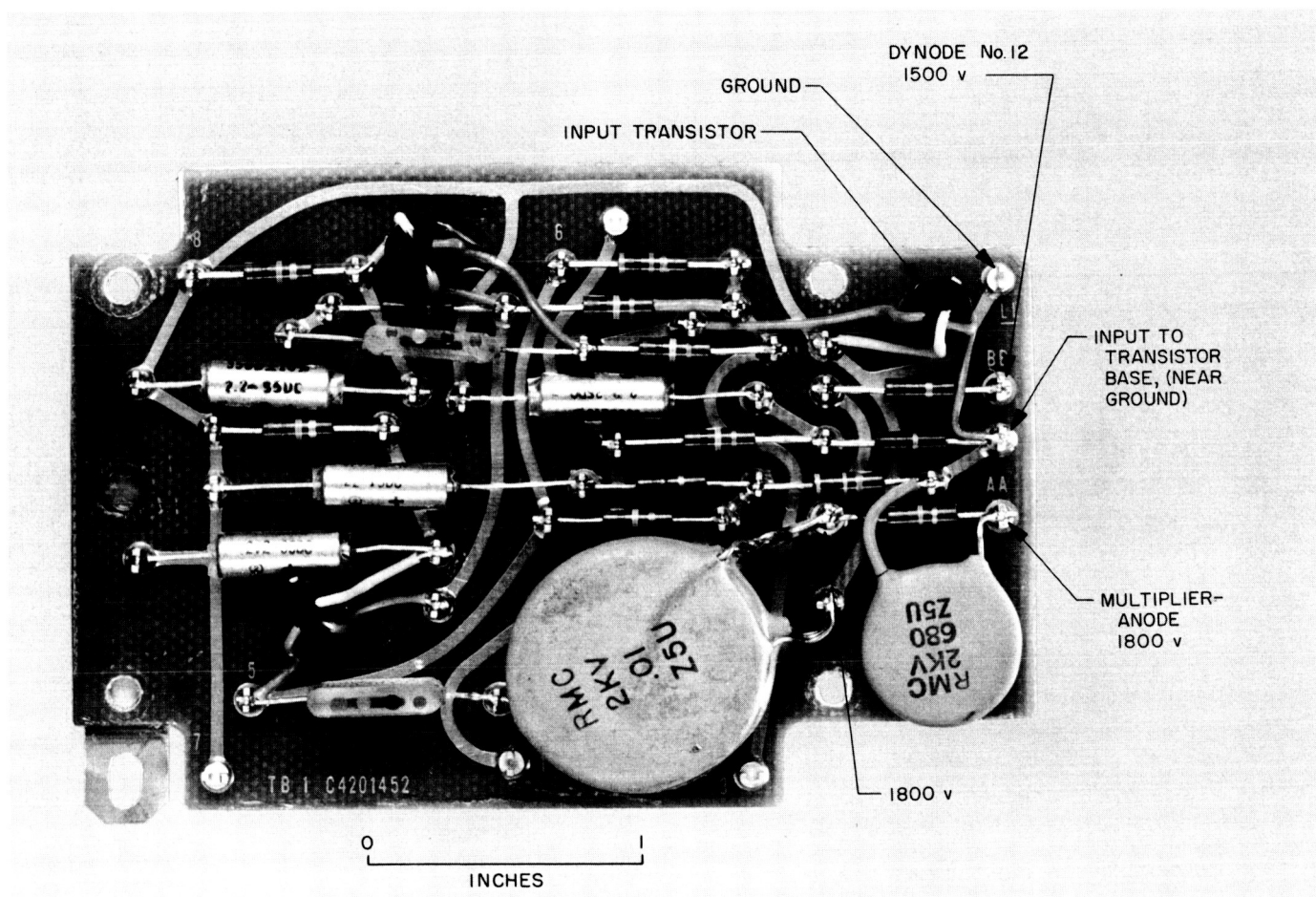


Fig. I-16. Canopus tracker high-voltage circuit board



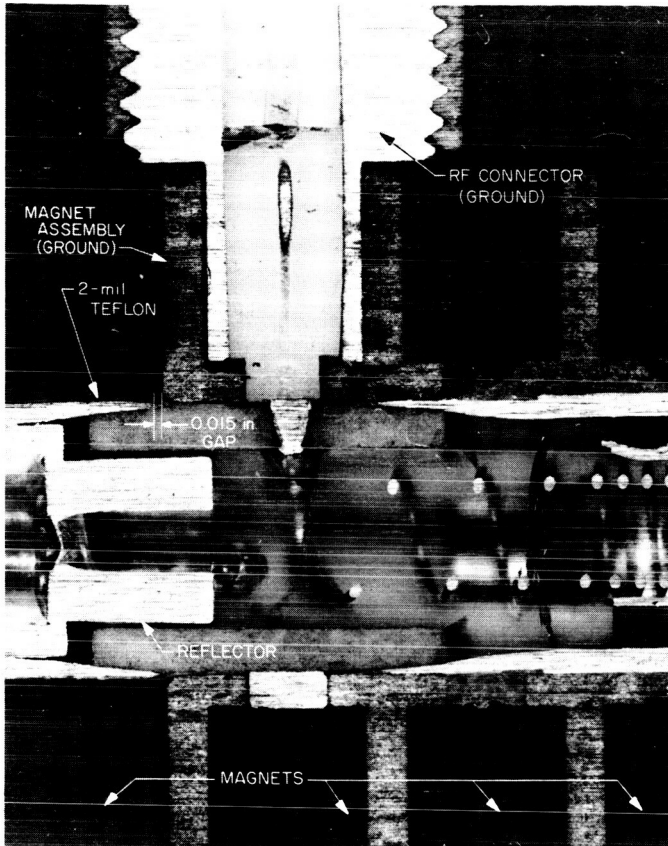


Fig. I-17. Travelling wave tube, cut-away view



Fig. I-18. Effect of dielectric failure, travelling wave tube

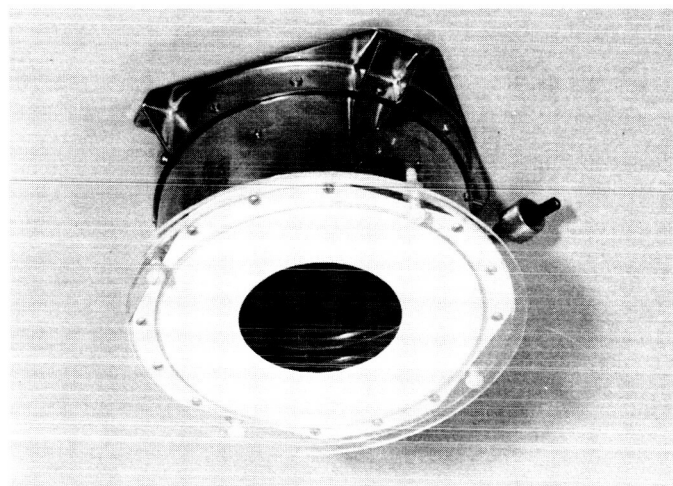


Fig. I-19. Plasma probe

N 68-26877

## 2. HIGH-VOLTAGE BREAKDOWN PROBLEMS IN GODDARD SCIENTIFIC SATELLITES

Harry W. Street  
Goddard Space Flight Center  
Greenbelt, Maryland

My talk is based on a report that we are preparing at Goddard. The report is prepared by a committee. Its members are Mr. Joseph C. Boyle, Dr. E. Maier, Mr. K. F. Plitt, Mr. C. E. Thienel, and Mr. A. F. Block. This is just an ad hoc committee set up to look into this high-voltage problem.

We have assembled a typical collection of problems in the report. I don't think we have covered all the problems that we encountered at Goddard, but I think it's enough to show the types of problems we have been having. The purpose of the report is two-fold: (1) to disseminate information so designers will not repeat some of the old mistakes and (2) to serve as an instrument, if you like, so our management can look into the practical problem of constructing equipment using high voltages to operate in the space environment.

Some of the problems that I'm going to discuss now may be treated in more detail in later papers; so, if there's some duplication, please forgive us.

The Nimbus spacecraft system was designed to operate at atmospheric pressure and in vacuum, but not in the transition region where ionization of air occurs at low electrical stress. The operation at atmospheric pressure, of course, is desirable to test the equipment and you would certainly like to have your equipment operable at atmospheric pressure, particularly for a prelaunch check.

This spacecraft has 1000, 500, and 300-v power supplies, and lines running from the power supply units to the camera system.

Initially, failures were encountered during thermal-vacuum testing, the first complete failure was after 13 days in vacuum at  $10^{-6}$  mm Hg. No damage was apparent in the camera systems, but failures occurred in the telemetry multicoder. Once, the cameras were turned on by mistake when the pressure was in the corona region, and the same components failed, showing that the failures occurring in the TV test were because of transients caused by the high-voltage discharge. It wasn't originally suspected that the failures were caused by high-voltage discharges but this was the tip-off, I think, that gave us the lead to what happened. It was

determined that the high-voltage breakdown was occurring in connectors and wiring harnesses. Examination afterward showed no damage in the power supplies, etc., themselves.

Originally, shielded polyolefin insulated wire (rated 600 v) was used and connection made at each end of the cable through Cannon type DM connectors, except for one high-voltage pulse line carrying a 4000- to 6000-v, 12  $\mu$ sec pulse. This line was wired up with RG/A880 coaxial cable using Cannon connectors that are standard for that cable. These high-voltage connectors were modified to vent entrapped gas. Cannon DM connectors were potted to the harness with polyurethane that, originally, was not deaerated. A silicone rubber washer was inserted between the DM connector halves to prevent shorts that were expected because of cadmium plating whisker growth. This turned out to be a mistake, though, because it trapped air in the connector. The equipment side of the connectors was not potted, but soldered joints between leads and connector pins were covered with Thermofit sleeving (Ray Chem irradiated polyolefin).

Teflon insulated wire (Tensolite 800 v/mil) was used in the equipment modules and the circuitry was assembled on fiberglass boards, with heavy components cemented to the board with epoxy cement. The boards were prepared for potting with Resiweld primers mixed in equal volumes, and then conformal coated with Solithane. I think we found that the use of primers is often desirable to ensure that the potting materials will stick to the surfaces; at least partly to avoid the problem of potting pulling away from surfaces during thermal cycling and leaving voids that can cause trouble. All materials were vacuum deaerated, and this seemed to help considerably.

Examination of the wiring harness after some failures showed that just arc over, or discharges, had occurred in voids in the potting of the connectors to the wiring harness, and this left high-resistant shorts. The trouble was corrected by running high-voltage lines separate from the other wiring, and using silicone-rubber-insulated cables with wire braid shielding. The shielding was covered by segmented Teflon sleeving. To bypass troublesome connectors, the ends of the cable were connected directly to the circuit board terminals, which were not potted. To facilitate handling, one in-line coaxial high-voltage connector was inserted in each cable. These connectors were modified for in-line use, and were vented; all rubber

gaskets were omitted to avoid entrapment of air or other gas. After these modifications, no further problems were encountered.

Now, the OSO II (actually OSO II-B) spacecraft gave us some real trouble. This is an example of problems that did not show up in the thermal vacuum testing (quite extensive thermal vacuum testing). I'm not saying we didn't have problems during thermal vacuum, but these were corrected and everything appeared to be okay; but when the spacecraft was placed in orbit, we had quite a number of failures and failures from the point of experiments.

The spectroheliograph experiment allows light from a small area of the Sun to enter through a 1-in.-square opening, and is focussed by concave mirror on to a grating. Light dispersed by the grating impinges on a slit that allows the desired wavelength band to enter an open strip-type photomultiplier. About 2000 v was supplied to the terminals of the photomultiplier from a power supply unit. The high-voltage power supply was completely potted with a high-density epoxy compound. This is Armstrong C-7, I believe. But the high-voltage output is on an open terminal with solder lugs on the outside of the package. Insulated wires are run from these terminals to open terminals in the photomultiplier assembly. The soldered joints are covered with epoxy potting compound. It was not expected that breakdown would occur in vacuums better than  $10^{-4}$  torr, but this was confirmed by tests in thermal vacuum chambers.

When the experiment was turned on after 21 hr in orbit, however, there were immediate indications of high-voltage breakdown, and the shift register on one of the pointed experiments that read out the count on the photomultiplier was damaged so that it first showed an "all zero" count and a few seconds later changed over to an "all ones" count and continued putting out "all ones" thereafter. From this has been deduced that failures occurred in the signal handling circuits. You can more or less pin it down to certain specific failures that would cause this kind of behavior.

Another spectroheliograph experiment on the same spacecraft, which also uses open photomultipliers (these are different, these are the little tubular ones), has given indications of arcing in space also. This experiment uses Channeltrons. In both instances, the cathode end of the multiplier is at a high negative potential with respect to the framework, what you might call the ground potential in the spacecraft, and it is believed that one cause of the breakdowns may be the presence of positive ions that get attracted to these negative surfaces. In vacuum chamber tests of

equipment using this type of detector, it has been seen that positive ions generated by vacuum gages will trigger discharges. It is recommended that these multipliers be used with the negative side of the supply grounded, (if feasible). This essentially has been done on the next OSO that we hope to fly soon. When we put it in orbit, maybe we will find out.

It is believed high-voltage breakdown may be occurring in other experiments in the spacecraft because periodic loss of synchronization of the subcommutators in the telemetry system are being observed. Some, if not all, of these are probably caused by the pulses generated by high-voltage discharges. Some of the slips actually have been seen to coincide with other indications of arcing in the output of the experiment, such as high counts from the photomultipliers when they should be giving a low count.

Going back to the OSO I spacecraft, that's the orbiting solar observatory, it has been reported that arcing occurred after 11 days in orbit and continued for one full orbit; but, when the spacecraft went into the shadow after this orbit and the equipment was turned off, the problem did not recur when it was turned on again at the next spacecraft sunrise. So, apparently, here it cleaned up, probably because of outgassing.

The Explorer series of satellites are smaller scientific satellites that do not have command systems or timers to turn the experiments on after achieving orbit and, therefore, must be designed to live through the minimum breakdown voltage pressure region, we hope without arcing. But what we require, of course, is that they survive; there may be some slight arcing during this time but, if it does no permanent damage, it really doesn't matter.

During pumpdown of the S-51 spacecraft in the vacuum chamber, arcing occurred at the interface connection board of the X-ray experiment. The high-voltage lead was then run directly from the high-voltage supply to the X-ray sensors. Arcing then occurred at the ends of this lead at the high-voltage card and the sensors. Records show that the high-voltage circuit on the card was conformal coated with synthetic rubber, probably room temperature vulcanizing (RTV). Foam potting (Ecco foam, 8 to 10 lb/ft<sup>3</sup>; this is a fairly dense foam) was then applied over the circuit and lead ends and also over the lead terminals at the sensors. This reduced, but did not stop, the arcing (at the sensor terminals) during the critical pressure; but it was found that arcing stopped and normal operation was restored when a good

vacuum was attained. So here we had a condition where the spacecraft could live through the low-pressure region without any permanent damage. The experiment performed satisfactorily in orbit. I might note that in these spacecraft everything is turned on at launch, so everything has to live through the transition pressure.

The S-52 is a closely related spacecraft. A connector in a high-voltage lead (2000 v) gave trouble during thermal vacuum tests because of entrapped gas. The problem was corrected by drilling a vent hole in the connector shell to provide an escape path for the gas.

Some problems were also encountered in the photomultiplier units; these were attributed to inadequate potting. The unit was repotted with Silastic RTV 503, using a primer on the metal surfaces to ensure adhesion, and the potting material was vacuum deaerated to remove air bubbles; no further trouble was encountered. This type of potting compound doesn't adhere to many surfaces very satisfactorily unless the proper primer is used, but has proved to be very effective when properly applied.

The S-6 spacecraft is a completely pressurized spacecraft. The spacecraft was built in the form of a stainless steel sphere and the whole spacecraft is pressurized at about atmospheric pressure. It was originally intended to fill it with argon gas, but difficulties with high-voltage breakdown in argon occurred. We had 5000 v applied to a "redhead" gage and we couldn't avoid breakdown with various attempts to cover the connection with potting material, etc. Several attempts at potting the connections with foam plastic, epoxy, and silicones were made before breakdown was eliminated; it was eliminated by a combination of not using argon, we pressurized it with nitrogen instead, and improving the potting coating techniques using silicone rubber RTV 731.

Now, we've had two breakdowns at radio frequencies that have been attributed to this multipactor mechanism we heard about a little earlier. One was in the OAO spacecraft during thermal vacuum tests. A 400 Mc transmitter exhibited breakdown within an output filter that has fairly high-Q resonant circuits; this has been attributed to the multipactor type mechanism. This problem was eliminated by pressurizing the container in which the filter was housed. This is an effective cure but it's sometimes a problem to maintain pressure for a long time, and pressurizing itself is quite a problem.

The other breakdown was the OGO spacecraft. We had a similar problem in a diplexer that had a fairly high-Q resonant circuit, an ambient pressure less than

$5 \times 10^{-5}$  mm Hg, and a power output of 2 to 3 w. We had problems in the high-Q resonant trap. It was found, however, that we could do without the high-Q resonant trap and still meet the requirements for the spacecraft; so the trap was eliminated and we got rid of the problem.

The theory of the multipactor mechanism has been treated by Hughes Aircraft Company in their report, which was referred to earlier, I think. It is a final report on contract NAS 5-3916 by Hughes Aircraft Company, dated April 1965. The title of the report is "The Study of the Multipactor Breakdown in Space Electronics Systems."

At high radio frequencies another breakdown mechanism occurs besides the low frequency or dc breakdown mechanism; this has been seen to occur at low voltages and lower pressures. In fact, it seems to occur over quite a wide pressure range starting from, perhaps, about  $10^{-3}$  and going down to  $10^{-7}$ , possibly even lower. But, with the advances and the techniques for developing higher powered transmitting equipment for spacecraft application, there is a need for better understanding of the cause, effects, and methods for "designing out" this problem.

Too frequently the problem has been overlooked or a quick fix injected that may have either corrected the cause or masked the effect. This is often completely overlooked in the design of equipment until discovered in the late thermal vacuum test phases of a spacecraft. It may not be discovered until catastrophically too late if tests are not conducted at all pressures. Sometimes it appears that the pressure at which this phenomenon occurs may be quite critical and it depends on a combination, apparently, of the pressure and geometry, the frequency and the voltage stress. If all these factors are right (or should I say "wrong"), you will get breakdown. So, it is important that this problem is considered during the early phases of design and adequate thermal vacuum tests are carried out on the subsystems before integration into the spacecraft. If we discover this problem in the final thermal vacuum tests of the whole spacecraft, it's too late to make any major changes.

I'd like to cover some of the recommendations we are also putting in this report, some recommendations based on experience to date (which we hope will assist experimenters and designers of high-voltage equipment, and at least avoid some of the errors that have been made before) and give them some guide lines with which to proceed.

There's usually more than one right way to do a job and, also, a multitude of wrong ways. The following remarks are mainly based on the experiences of the

Goddard Space Flight Center, which shows some of the pitfalls to be avoided and suggests methods of approach to lead to the successful operation of high-voltage equipment in the space environment.

The approach will depend on whether the equipment is required to survive being turned on when the ambient pressure is in the range of the minimum voltage breakdown or whether it will be turned on only after injection into orbit. It is usually desirable to be able to operate high-voltage power supplies in an atmospheric pressure to check the proper operation before launch.

To be able to operate under all ambient conditions, it is necessary to encase all conductors in suitable insulating material. This can either be solid potting or a liquid or gaseous dielectric enclosed in a hermetically sealed container. Sealed containers with fluid dielectric are not frequently used in scientific spacecraft because of increased volume and weight, and the problem of ensuring a good hermetic seal that will endure for 1 yr or more (which is usually our goal; a minimum life of at least 1 yr in scientific satellites). Solid potting has been used with moderate success, but great care is necessary to eliminate voids in the potting material because corona discharge is likely to develop in voids that are close to high-voltage conductors. Sometimes voids or a cracking of the potting material cause delayed failures after the equipment has been in a vacuum for a considerable length of time (days or weeks) because of leakage or diffusion of gas from them.

They also have the phenomenon of treeing or branching, which results in a delayed failure when the insulation gradually breaks down and a conducting path is gradually formed. Sometimes it can start with minute cracks in solid potting material, and progresses along these cracks and finally breaks down from high-voltage terminal to ground.

If the equipment is not required to operate in the critical pressure region (generally in the range between  $10^{-2}$  to  $10^2$  mm Hg), it may be better to leave components exposed and provide adequate venting of the enclosure to allow the pressure to drop rapidly to a low value.

Usually it is necessary to use some form of potting to mechanically anchor components to withstand vibration during launch. Conformal coating of a compound by dipping, or painting, has been used successfully. Here, as in solid potting, it is essential to avoid bubbles of entrapped air or other gas (especially next to conductors), and vacuum degassing of a potting compound is necessary. The use of foam potting of



high-voltage equipment is not recommended. We have gotten out of trouble in some last minute fixes by using high density foams and sometimes these seem to avoid major breakdowns that result in catastrophic failures; but, in general, we feel that the use of foam potting is not desirable in high-voltage equipment. One method of construction that has been fairly successful is to first conformal coat the equipment with possibly an epoxy and then, if we use foam potting on top of this, we seem to keep out of trouble.

Occasional corona or spark discharges do not permanently damage the high-voltage equipment itself, but may often result in serious interference with the operation of other equipment in the spacecraft. The orbiting solar observatory is a good example of this. We've had quite a bit of interference with the encoding system causing subcommutators to step at random and getting out of synchronization. The filter-capacitors of high-voltage power supplies store much energy, which is suddenly released when the sparkover occurs. Only part of this energy is dissipated as heat in the spark, while the remainder is propagated away from the site of the spark as a steep wave front or impulse on all neighboring conductors. Energy can be transferred to other circuits by direct ionic conduction or by inductive and capacitive coupling. Frequently, there seems to be enough energy transferred to induce transistor failures in equipment that is not associated with the high-voltage equipment at all.

Now, I would like to mention a problem that I have not included in my report, because we really haven't made up our minds what the problem is. We have had a number of failures of some high-voltage power supplies ranging from 2000 to 5000 v. These power supplies have a series type regulator on the input because they have to operate over a wide range of input voltages. The regulator is followed by a converter and high-voltage rectifier. A number of these power supplies have shown failures in the regulator section, the transistors and the amplifier of the regulator, and the high-voltage part of the power supply is generally found to be okay after the failure occurs and after the failure analysis is conducted. I believe, personally, that arc overs are occurring in the experiment fed by the power supply, and the output side of the power supply and energy pulses are feeding back to the power line feeding the power supply; and this is causing these transistor failures.

So, it seems to be important to isolate, if possible, the high-voltage circuitry from all low-voltage circuitry. This is a subject of some of our recommendations that I will read now from the report.

High-voltage power supplies should be designed to have current limiting characteristics so no components are overloaded in the event of corona or sparkover of the output. Current limiting resistors should be used, if possible, between the output filter capacitors and the loads to limit discharge current in the event of a sparkover.

Equipment should be packaged so that all the high-voltage wiring is isolated or shielded from other circuits, to avoid transfer of energy. The best approach is to apply the principles of radio frequency shielding, and encase the entire circuit in a conducting envelope. The low-voltage power leads (including ground returns), which sometimes are overlooked, entering the envelope should have effective radio frequency filters to prevent propagation of impulses generated inside the enclosure. When the high-voltage power supply is enclosed in a separate container from the experiment sensor that it supplies, the cable between the two should be a coaxial shielded cable and the shield should be electrically bonded to both enclosures. This is applying a principle of RF shielding and, if connectors must be used in the cable, arrangements should be made to maintain continuity of the shielding through the connector. It is recommended that the connectors in high-voltage leads be avoided, if possible; however, it isn't always possible and we have to build the equipment, then integrate it into the spacecraft and sometimes it is just absolutely essential to use some kind of connectors unless it is possible to wire in the high-voltage connections after assembling the spacecraft. Here again we have another problem. If we have a failure, and we have to install the spare or backup unit, this makes the problem rather difficult to do in the field.

Adequate venting of enclosures should be provided to prevent buildup of pressure during outgassing of materials.

Precautions should be taken to avoid entry of ionized particles or electrons from the environment and, also, ultraviolet light that will eject electrons from surfaces. Any electric fields that may extend from openings in the enclosure will attract ions of one polarity; suitable shielding grids and ion traps should be provided. This results from our experiences on the orbiting solar observatory.

We had, I think, more than a week of thermal vacuum testing on some of the experiments and their performance in the thermal vacuum tests was satisfactory; but when they were turned on after 21 hr in orbit, we had all kinds of problems that are definitely caused by arc overs in the high-voltage department. So, there is a

difference between the environment in orbit and that in the thermal vacuum chamber. We don't know all the answers yet, but it's obvious that there is something that wasn't taken into account in the thermal vacuum tests.

#### OPEN DISCUSSION

MR. CABOT: On the Nimbus spacecraft where you observed failure during testing on the telemetry multicoder, was the electronics of that system potted within a semi-rigid polyurethane foam and did the failure occur within the foam or on the printed circuit board?

MR. STREET: I don't know personally. I'm not familiar with all the details of the Nimbus construction. I'm not on the Nimbus project. Maybe somebody else here could answer that.

I don't think the failures of the transistors were related to the method of packaging the low-voltage equipment. I think they were probably caused by high-energy pulses propagated along conductors, which were generated in the high-voltage department, and arc overs occurred.

The sudden discharge of a capacitor releases quite a lot of energy in a single pulse, this sets up damped oscillatory waveforms in all nearby conductors and these propagated as, if you like, RF waves down the conductors; we believe this is what's damaging the transistors.

MR. HAWERSAAT: When you're talking of venting these and allowing openings and then shielding these openings to prevent ions or electrons from coming through, what techniques are you using; fine mesh or something, or some other approach?

MR. STREET: Well, at the moment I don't know whether we're in a position to specify any particular techniques. We are hoping that by distributing this report and making the whole problem of high-voltage breakdown better known that a study will be set up to look into these things. Then we hope we will be able to develop some standard practices for taking care of these problems.

I think possibly, as you suggest, a fine mesh might be one solution.

VOICE: When will this report be available?

MR. STREET: It should be ready a month from now. This is probably the most informal type of report that we issue as a Goddard report. It's the type of report that merely reflects the opinion of the authors and has the blessing of management so they can get it out relatively quick. It went for final typing a couple of days ago and I hesitate to say it will be out before a month from now.

VOICE: What would the title be?

MR. STREET: The title will be "High-Voltage Breakdown Problems in Goddard Scientific Satellites."

MR. MILLIGAN: Could I make a comment on this screen thing here?

We've been flying meshes, screens, and rings, things of this sort, for protecting high-voltage equipment in rockets and satellites for several years (I guess it's about 5 yr, something of that sort); we find almost anything you want to fly works, which is about what you'd anticipate.

Rings will work, fine meshes will work, things of this sort. One thing the people ought to be aware of is you can fly extremely efficient ion traps at even 100 v or so, something of this sort; so you do have to protect equipment anyway from 100 v up to 20, 25 kilovolts, which is the highest we're anticipating flying, at least now.

But there really are no serious problems here. Putting the screening on is very good. You just have to be sure you put on the right polarity.

MR. STREET: Now, the point is to make designers aware that there is a problem. If they think about it, they generally figure out the solution.

MR. McCoy: We had a high-voltage connector problem in which we vented the connector early but didn't try to seal it. Yet, when we first turned on the high voltage, we had some partial breakdown that only happened during turnon; then it would go away suggesting, perhaps, there are some molecules glued to the insulators that somehow could excite it and leave the connector when you have a small arc. Did you have this problem?

MR. STREET: I think this may be related to another problem. In coaxial cables there are always some voids within the stranded conductors and there's some gas trapped in there that slowly leaks out through the ends of the cable and, of course, this goes directly into the connector. This may be the problem. We

haven't been able to pinpoint these problems, to be this specific, to say that it is caused by this. But it may be caused by this kind of thing.

DR. DAKIN: Because we're going to be talking about discharges here for the next three days, I would like to suggest that we clarify our terminology a little bit. You used a term "arc." An arc has a very distinctive characteristic to discharge people. It has a negative voltage current characteristic. In other words, when you raise the current, the voltage goes down and it's concerned with the copious emission of electrons from the cathode.

Now, I think that many of these discharges that occur in the critical pressure region are, really, not arcs.

In a paper I presented about 2 yr ago I showed you can draw much current in the glow discharge type of regime without actually developing an arc and the current is somewhat limited by the voltage drop in the glow discharge; but this is not so true for the arc. An arc would be a much more damaging type of discharge and would draw much higher currents. Furthermore, there are probably two types of corona discharges that we should discriminate; one of these is the pulse type behavior where you get pulses occurring intermittently, or regularly, and the other type in which you have a plasma occurring when the current will flow in sort of a pulseless manner. You can't detect any pulses with a pulse detector circuit.

I'm just suggesting that we clarify our terminology in this way.

MR. STREET: You are absolutely right. I know we throw around a lot of these terms very loosely and I think the term "corona" has been the favorite one used to describe all of these problems, but not all the problems are strictly corona discharge.

I think, as you pointed out, an arc generally requires a pretty husky power supply to actually sustain an arc discharge. Maybe we should call them sparks. This is a very nice general term and describes a sudden discharge.

MR. CABOT: I have a comment. I might mention that polyurethane foam is a hyposcopic material that contains much moisture and, when used within a sealed package during experimental testing, the relative humidity within that package often increases to as high as 80% or better within the package itself because of the release of moisture (because the material acts as a sponge that

will come to equilibrium with whatever atmospheric conditions exist around it).

I just thought I might mention that one point.

MR. MYERS: You mentioned that foams are out and this other gentleman mentioned the discharges of polyurethane foams. Because foams do have some very desirable properties as far as adhesion to other things and elasticity, I'm wondering if there aren't some foams (perhaps epoxy foam) that can still be considered before foams are completely eliminated as a packaging material. I would hate to see foams totally eliminated, because they do have some advantages. I wonder if someone could comment on that or if a paper is being presented on this?

MR. CABOT: Certain polyurethane foams have been eliminated quite early, and that is the freon-blown type of foam. Most of the foams that are used now are carbon dioxide-blown, which is the cause of the foam or the bubbles.

Now, this carbon dioxide will diffuse out of the foam itself with the moisture that may come out of the system in blowing the foam. Some of the other synthetic foams, where you have a closed bubble or structure, eliminate this problem because they're not subject to as much moisture absorption as the polyurethane foams would be.

MR. STREET: Would you expect the cells in these foams to hold and maintain a pressure for a long time in vacuum?

MR. CABOT: The cell structure, when subjected to moisture conditions of high humidity, will actually collapse if the temperature is raised at the same time the moisture is raised; then you get a collapse of cell structure, and breakage of the cell structure itself, and outgassing from the bubble structure.

MR. STREET: I think we probably have to assume that any foam will eventually get completely outgassed in the vacuum, isn't that true?

MR. CABOT: Yes. There tends to be an equilibrium process that's reached where the gas leaves the bubble and the surrounding ambient gases tend to enter the bubble structure itself.

MR. STREET: Would we eventually have a condition with a fairly good vacuum in the bubbles?

MR. CABOT: Well, I don't know if it would reach a vacuum or not. The bubble structure needs some gas to support it. If the temperature is raised and the cell walls become very weak, then the bubble can collapse.

There's very much moisture within the foam itself and it's like a sponge; it would just pick up moisture from the air. If you are in a high-humidity laboratory, or region, the foam itself will have much moisture (about 2% by weight, which is appreciable because the foam is a very light material).

MR. STREET: Although we are not recommending foams, we have used high-density foams successfully in some high-voltage equipment and spacecraft; they have flown and performed successfully in orbit.

MR. MICHAELS: I believe the problem here is that if the foams are used in space you will get a pressure equilibrium between the inside of the foam and the outside environment that will be close to zero pressure; the foam will outgas. They are permeable to gas medium inside the pores; this will go out and you will go through the critical phase region where discharges will take place and, when using foams at normal pressures, what you say is quite true. You will exchange moisture, carbon dioxide, oxygen, nitrogen, etc. But it's in space, I think, that we have been concerned with here; and under those conditions you will end up with zero pressure.

**N 68-26878**3. CORONA INDUCED FAILURES ON NIMBUS A DURING GROUND TESTING\*

S. Charp  
General Electric Company  
Spacecraft Department  
Philadelphia, Pennsylvania

I would like to define what I'm going to talk about. The corona I am referring to is essentially a soft electrical discharge which is prevented from becoming an arc either by geometry or by the presence of solid insulation barriers. Basically, corona is developed only if a number of conditions exist.

In particular, the first condition is a high electric field strength. I emphasize this because of some of the questions already raised. Electric potential level is not necessarily the main criteria. The main criteria is the field strength and this pertains to the question of why it is possible or not possible to use a foam insulation after you've already reduced the field strength. Not mentioned was conformal coating over terminals.

The second condition is a gas must be present. The gas must be present because, after all, the phenomenon is developed by electrons leaving an electrode and then creating a secondary emission with the particles of gas in the region. The particles of gas ionize and, if there is high enough energy level, then corona will exist. The corona, of course, will show up in a number of ways as was mentioned earlier. Some of these are meaningful for observation and testing spacecraft, and others are not particularly meaningful.

While it is true corona can be seen, observation makes sense only if you can see the corona; if the corona exists on the external surfaces. This is a most unusual situation during system testing of a spacecraft; when you have electronic equipment inside a spacecraft you never see corona, so I think we can say this method of detection is not very pertinent.

We have audible noise under some circumstances. Again, this is not meaningful. It's meaningful, perhaps, in a power system or in a laboratory demonstration of some kind; but, again, it is not applicable to systems testing of spacecraft. Smell

---

\*Nimbus A is now identified as Nimbus I; Nimbus C is now in orbit, identified as Nimbus II.



is in the same category; ozone is created because of electronic disassociation, which can be detected in a laboratory but not under system testing. We are then left with two other means of detecting corona. One is electrical noise and the other is a failure of a piece of hardware. The failure of a piece of hardware leads to some thinking. We are faced with the problem of trying to separate assumptions about what could have happened and observations about what did happen.

I think this is enough introduction to the Nimbus problem. In the latter part of 1963, during the time the prototype spacecraft and the first flight spacecraft were being developed and fabricated, we had a series of unusual problems. We found several low-energy transistors in the multocoder failed. Although we tried, we never could determine the cause of those failures. The failures of the multocoder transistors were attributed to corona problems.

This tagging of that set of failures did not occur at the time the failures were observed. The tagging of failures in the multocoder occurred long after the observations which we actually did make and we were rid of our corona problem. We did understand something occurred in the system (during system testing) which caused the transistors to fail. Some sort of correlation existed, associated with the high-voltage systems that are part of the two camera systems carried on Nimbus A.

During system test (not in the vacuum chamber) we had failure of a high-voltage connector. When that failure occurred the usual failure analysis was made. The failure was attributed to a void in the encapsulation material of the connector.

The most important failure (and one which gave rise to a substantial test evaluation program) occurred inadvertently because of human failure and misdirection.

The prototype spacecraft and the flight spacecraft were being tested simultaneously. One spacecraft was in the large space simulation chamber; the second spacecraft was in a preparation area nearby. The time scales of the two spacecraft were to have been off-set so that one spacecraft was to operate 12 hours ahead of the other spacecraft; this is clock time with respect to the clock on Nimbus A.

Unfortunately, full directions were not followed. The clocks in the two spacecraft were set by two separate test crews to the same clock time instead of 12 hours apart as directed. You can imagine what happened. The prototype spacecraft was commanded on, its camera systems were turned on, and testing proceeded on schedule. The flight spacecraft with its command receiver on, however, was in the

vacuum chamber being pumped down. Because of the time coincidence, its cameras were turned on just when the pressure in the space simulation chamber was in the corona region. The camera systems failed.

It took a short time (not minutes, but, let's say, half a day or a day) to finally realize what had happened. The first thought was the flight spacecraft had a major problem. It wasn't until the work program on the prototype spacecraft was correlated with that of the flight spacecraft that we recognized the inadvertent turn on of the flight spacecraft's cameras.

Now, what was done about it? We examined the equipment, of course. Transistor circuits in the camera electronics were found to have failed. No simultaneous failures occurred in the multocoder.

The phenomenon was random-like. Prediction could not be made, with any degree of certainty, of the effects of high-voltage spikes or corona spikes which would propagate through the power lines, enter and affect low-voltage systems or low-energy systems.

A substantial failure analysis program was undertaken in two areas; critically examined were (1) all harnessing and all connectors, (2) the routing and design of leads and circuits in the high-voltage camera electronic systems, for the first time from a systems point of view, from a hardware point of view, and from a component point of view.

The latter was a responsibility of the camera supplier. Representatives from the General Electric Company, Goddard Space Flight Center, and the supplier of the cameras met and "right across the table" dismantled the covers of the camera electronics, critically looked at the ways wires were routed, and looked at wire insulation. As a result: wire routings were changed; connectors in the inside and at the wall of the camera electronics case were eliminated or changed, and insulation on some wires was changed. The changes were made by the supplier, based on the recommendations of an afternoon's roundtable review and discussion.

With respect to the former, two test programs were started within the General Electric Company, one for connectors and the second for wires and harnessing. The results of this effort also led to redesigns with no subsequent failures.

The most used type connector on the Nimbus spacecraft (this was Nimbus A and we are using the same connector on Nimbus C, the present spacecraft being assembled) is the DME-9 type Cannon connector.

The connector in the high-voltage section of the cameras was considered a problem because of a previous failure traced to voids in a potting compound and because in this particular connector, which carried the high voltages, 1000 v to the camera tube in the automatic video camera system and 600 v in the automatic picture transmission system, the high-voltage leads and pins were not separate from the low-voltage leads and pins.

Unfortunately, during the initial system design, distribution of high voltage was treated the same as low-voltage. No apparent attempt had been made in the design to physically separate, by selected location of pins in the connector, high-voltage leads from low-voltage leads. This was rectified.

In considering methods for eliminating corona, two interesting points were encountered, one of which I will return to later.

A number of tests were made which showed breakdown can be avoided by loading a connector with grease. This method for eliminating corona, however, presents problems because grease can trap air. This was not a very good solution.

But, more important, we discovered performance data, published or privately quoted by manufacturers, especially the voltage rating of connectors, have no actual bearing on their performance in a space environment. Connectors are designed, tested, and standardized mainly for aircraft use. Connectors are not designed for spacecraft use. If you examine the specifications for connectors (the manufacturer's specifications, the manufacturer's test programs, test results) you do not find them to be derived or basically intended for applications under very high-vacuum conditions. If a particular connector is planned to be used in a spacecraft, and if data are not available regarding the performance of this particular type in a simulated space environment, then plan to undertake your own expensive test and qualification program.

The second area of concern was the subject of wires and harnessing. Unfortunately, the wire that was used on the 1000 v line was a 600 v-rated wire, having irradiated polyolefin insulation.

This is, of course, completely underrated for the application; unfortunately three years after the design this was found to be true. Again, a design faux pas had occurred.

An identical unmodified harness was fabricated and tested in a space chamber. It did not break down at 2000 v. The original harnesses also were tested in a vacuum chamber and did not break down. Confidence was not established, however, because the original failure had occurred. New harnesses were built with 3000 v-rated wire; the way in which the leads were dispersed in the harness was controlled. The new harnesses were subjected to testing in a space chamber using a dc power supply instead of an ac power supply. They lasted for 15 hours in the chamber, again exhibiting breakdown at 2000 v. Why should a harness made with 3000 v-rated wire break down at 2000 v?

In consultation with representatives from the General Electric Company, Insulated Wire Department, Research Laboratory and Advanced Technology Laboratories we concluded the basic cause of voltage breakdown of wires, used under high-voltage conditions, is entrapped air; as we've heard so many times today. This is a phenomenon very well known to wire manufacturers, especially the larger manufacturers who produce high-voltage wires. So it appeared as though we were "rediscovering the wheel;" methods for eliminating the problem were examined.

If you examine the construction of high-voltage wire, for example, that used on neon signs, you frequently will find a little ring of a carbonaceous material next to the wire. This serves two purposes: (1) it provides a medium for a very high cohesion of the insulation to the wire, eliminating entrapped air, (2) it provides a slow reduction of electric field strength, ie, lower voltage gradient, so the tendency for the formation of corona is reduced.

Based on the resulting recommendations and a review of the types of high-voltage wires commercially available, new harnesses and new leads using silicone rubber were built. All corona problems were eliminated.

Simultaneously the use of silicone rubber pads between the two mating parts of a connector were eliminated because the pads entrapped air. Further it was discovered the pads were not stored in clean conditions. Handling of pads with bare fingers left oils and dirt on their surfaces, which lead to a potential source of voltage breakdown. Hence these were eliminated. Aeration holes were provided in connectors and in all containers which housed high-voltage electronic circuits.

The failures noted earlier led to an interest in developing a simple method for detecting corona. We wanted to detect potential corona failures during the next series of tests, while the spacecraft was to be in the environmental chamber. A radio receiver was used to detect corona. In particular, the receiver used was an NF 105, Field Intensity Meter, an extremely sensitive device. A simple loop antenna was mounted on the spacecraft near the camera electronic systems, resulting in a very good method for detecting corona. Since then we have been using this method for all tests; it's a very sensitive one. Subsequent to its introduction the same method was used during testing of the flight spacecraft and during the launch countdown. The method is now used by the camera supplier during his environmental testing of the camera electronics as a component.

The method is particularly useful because not only can corona be detected but all the spacecraft functions can be monitored. By looking at the different and unique frequencies floating on the ground leads (not by using an antenna but by direct connection to ground return leads) we can see which systems are energized.

I would like to close with one thought. If you ever look at the women's page of a 1965 newspaper and look at a 1945 or 1925 newspaper, you will find the same subjects are covered. There is a section on cooking, on how to clean the house, how to handle the baby, etc. I sometimes wonder if many of our high voltage problems are created because we have forgotten or never have learned how to read the literature on high voltage and corona phenomena.

## OPEN DISCUSSION

MR. CABOT: While it is possible, on connectors, to protect the wire side of the connector against corona, how do you handle the pin side that goes through another connector?

MR. CHARP: There's nothing that we can do about it. I say "we" as a user; the connector is a connector. You buy it. Now, what can you do; what precautions can you take? The insulation material we have been specifying on the Cannon connectors is diallyl phthalate. In the high-voltage system we do not now run the high-voltage lead in the same harness with the low-voltage leads. During the redesign of the electronic containers, the high-voltage leads were made separate; they were brought out through the case as pigtails. So, in essence, we eliminated the camera electronics problem by changing the wiring method.

Where a connector is used on the high-voltage line, the 1000 v line, it now is a ferrule type in-line connector. As a user there really is nothing that you can do about a connector from the pin side. You can only reduce its effectiveness, for example, by using a silicone pad, as we had originally intended, to eliminate the metallic whisker growth we thought would occur. But this doesn't occur to any extent to be bothersome.

With respect to the wire end, the cable end of the connector, we did try vacuum potting; this raised many fabrication problems. The connector's solder ends have to be primed. The epoxy and encapsulant is then applied with a vacuum process, creating the question of how to detect the voids. We tried several methods including X-rays. Unfortunately, they do not produce sufficient density difference in the film to serve as a good detector of voids for the types of connectors or for the types of potting compounds which we use.

Another off-shoot of our problem was the development of standards for wiring and harness design, which we use now for designing all harnesses.

I could describe various methods for improving the design of high-voltage systems, but you could do this for yourself if you read the literature.

High-voltage problems occurred when radio companies were making transmitters for airplanes 30 years ago and the problems haven't changed. It is only the people who have changed: the solutions haven't changed.

VOICE: Have you ever thought of using ultrasonics to detect flaws in the material in connection with this problem?

MR. CHARP: We use sonic methods for detecting the quality of honeycomb systems, for example, honeycomb panels. This is a standard technique. We do not use this type of testing for connectors.

VOICE: You said you have been using the loop-type field strength meter to detect RF noise as a result of corona discharge. Have you ever tried measuring the electric vector as compared with a magnetic vector in a loop?

MR. CHARP: No, measuring with a loop is just a very convenient way of picking up a signal. We made the simplest kind of loop that would closely approximate the 50 ohm impedance of the measuring system.

Incidentally, you could use the system (and we have used it) to detect potential ground failures during vacuum thermal testing in the component because you should, and do, pick up a little bit of static if you have intermittent grounds.

CHAIRMAN EDWARDS: It is a good point about reinventing the wheel. The wheels seem to be getting more costly as we go on and, although we are getting smarter, the mistakes do seem to cost more than ever.

#### 4. HIGH VOLTAGE CONSIDERATIONS FOR THE DETECTOR ASSEMBLY USED IN THE GODDARD EXPERIMENTAL PACKAGE

Peter Pokalsky  
Kollsman Instrument Corporation  
Syosset, New York

The detector assemblies used in the Goddard experimental package (GEP) are ultraviolet photon counters. Six assemblies are mounted side by side in the focus of the spectrometer section of the GEP. Actually, there are nine 3000-v supplies, and six 25-kv supplies. Light entering the GEP is separated according to the wavelength and directed to the detectors by the spectrometer section. Figure 4-1 shows the detector assembly.

We have a photomultiplier power supply and a power supply ladder that is mounted on the rear of the chassis, the oscillator for the ladder is in front. Connections are made right from the oscillator to the ladder. Connections are open and the junction is vented to prevent any accumulation of gas under changes in pressure.

Light falling on the window of the detector ejects electrons from the cathode on the underside of the window. The ejected electrons are then accelerated and focused by a series of rings maintained at progressively higher positive potentials. An artist's concept is shown in Fig. 4-2. Here you could see the window, accelerating rings, scintillation crystal, and dynodes of the photomultiplier. At the end of their travel, the electrons strike a fluorescent screen with an energy of 25 kev causing a burst of light to be emitted from the screen onto the cathode of the photomultiplier.

The photomultiplier output is processed, by the signal conditioning electronics portion of the detector assembly, to provide a standard pulse as an output for every photon that goes through the detector's window and ejects an electron. So, we're working with very low light level and we can't have any corona that we've been talking about or we'd be counting corona.

We use 2500 v as photomultiplier excitation and 25 kv as the screen or anode potential for the image intensifier portion of the detector assembly. Excitation for the rings is taken from a voltage divider across the 25 kv. The divider current is 1 $\mu$ a and six rings are used. So, with a divider current of 1 $\mu$ a you can't talk about corona as we did before. We could talk about 1% of this and it would still make trouble.



Failure of the dielectric can cause the power supplies to have a reduced output because of the increased loading. It can also affect the ratio of the outputs of the voltage divider, those outputs necessary for proper operation. The light comparable to the level under study can be generated by any currents that flow in the dielectric materials. Changes in dielectric materials because of stray currents can cause catastrophic failure. More likely chemical effects that happen in voltage fields cause dielectric deterioration.

Besides being impractical, from a design standpoint, to obtain 25 KV by rectifying corresponding ac potential, the problem of insulating such a system would be very difficult. Any solid insulation has a dielectric constant greater than one and, in an ac field, the voltage distributes according to the capacitive reactance. For the most part there are losses. Placing an insulator into this field increases the gradient across any gaseous dielectric present. To insulate ac requires that the space between conductors be completely filled. Any voids that contain or can accumulate a gas, depending on size and location, can reduce the insulating qualities to unacceptable levels.

In dc fields, the voltage gradients are determined by their resistances and we can use thin film such as Mylar. When used in an atmosphere of gas, the dielectric film will charge up to the supply potential and reduce the voltage gradient in the gas to a low value.

So, when you first turn on, you will get currents until the film is charged up, then you'll have essentially no field. You can feel this 25 kv by holding a ground plane near the power supply.

It's an advantage to keep the ac voltages as low as the circuit requirements will permit. A ratio of 1:10 to 1:20 with respect to the dc voltage level seems practical from our experience. For the intensifier power supply, 1400 v rms is stepped up to 25 kv dc.

After consideration of the space limitations and performance requirements, we decided to make the photomultiplier power supply a complete single unit, and make the intensifier power supply in two parts: an oscillator remote from the intensifier tube and a capacitor-rectifier network in direct contact with the tube.

The photomultiplier power supply is a 750 v peak-to-peak square wave generator followed by a two-stage Cockroft-Walton voltage multiplier network. The

secondary of the output transformer is progressively wound on an insulated toroid, then the transformer is vacuum impregnated. The circuit performed satisfactorily in the air and, after an in-process test, it's vacuum potted in a metal container. Potting material is gravity fed into the container while the unit is maintained in the vacuum. The circuitry is placed in a mold under a bell jar, and everything is pumped out. Before this we pump or degas the potting material and it's fed in through a connection.

The intensifier oscillator is a class C sine wave oscillator. The high-voltage winding of the output transformer is layer wound with Mylar interlayer insulation. The windings are vacuum impregnated before being incorporated into the oscillator circuit. After in-process testing, the oscillator is mounted in the metal enclosure and potted. A void-free encapsulation is ensured by first pumping out the air, then filling with Emerson and Cumings 2651MM under 50 lb of positive pressure. Figure 4-3 shows the intensifier oscillator.

The voltage multiplier is fabricated and mounted to the intensifier tube in three steps. The capacitors used are the processed mica dielectric type. After interconnection, the capacitor assembly is placed in a closed mold, the air is pumped out and the mold is filled with Emerson and Cumings 2651MM under 50 lb of pressure. After curing, the capacitor assembly is x-rayed. Figure 4-4 shows one of the capacitors x-rayed. The circles show the voids.

In the second step, the diodes, resistors, and high-voltage bushings are added. These bushings are used to reduce the gradient in the potting material and let us pre-test by just mating the tube and ladder together. It shields small springs that are used as contacts. Otherwise they just spray all over the place. The assembly is then potted under pressure in a mold that conforms to the intensifier tube.

This mold provides a recess that is filled under pressure when the voltage multiplier is mated to the intensifier tube. Here, the potting compound is RTV 601. Electrical connection is made through springs mounted on the inside of the bushings. Figure 4-5 shows the multiplier network after encapsulation: note the recess and contacts. This portion of the detector assembly is covered with a two-ply Mylar jacket formed to the outside dimensions of the assembly.

While there are general rules for handling high voltages, each application requires careful consideration. For power supplies that are to be used in space, particular attention must be paid to the construction of the circuit components. Today I've heard a few people say this is really where they have problems. You buy

something and it is a big unknown even though there is a specification. You don't know what's inside; you don't know how fast it's going to leak out and this is our problem, too.

We went to the processed mica capacitors because these are open capacitors. There's no container at all. They're painted with an epoxy coating when we get them and we bake them out before we pot them.

Unvented enclosures, even though potted, will leak until the critical pressure is reached and cause failure of the unit.

Resistors for high voltages are not generally available and attempts to use the resistors that do exist complicates the high-voltage problem.

In general, increased knowledge of the characteristics of components and materials, together with concise specification of these characteristics, will go a long way in solving our high-voltage problem.

#### OPEN DISCUSSION

MR. MILLIGAN: I want to bring up one possible problem with extremely high voltages in potting.

Over the years we have used silicone potting compounds for protecting high-voltage tubes (glass tubes, things of this sort). Normally, until within the last couple years or so, we only used this type of potting compound for voltages up to about 2000v.

We had to pot devices with 25 kv on the tubes and we ran into what may be a potentially very serious long-life problem for silicone potting compounds. After a few thousand hours of operation, three tubes leaked a very small amount of fluid from the potting compound and the tubes immediately went into corona and destroyed themselves.

We discovered (after talking to some physical chemists) that most silicone potting compounds trap free oxygen while they're being cured and, apparently, the bond was broken, the silicone went to the oxygen, we had a breakdown in the potting compound, and this induced breakdown in the system.

If you are dealing with extremely high voltages to the order of, let's say, 20 kv and above, it's something you're going to have to worry about. We don't

now have a solution, we've just got our fingers crossed. But it's something that could kill you even in a space application, even under high-vacuum conditions.

We do not see this around a couple of kilovolts, only at very high voltages.

MR. TASHJIAN: I have one comment about the silicone deterioration with high voltage problem.

We've seen this same thing. We've seen it at about 2 kv and, in general, it is caused by inadequate cure. If you double your cure cycle over what is recommended by the manufacturer, you'll probably find the problem will go away.

MR. MULLIGAN: It didn't help.

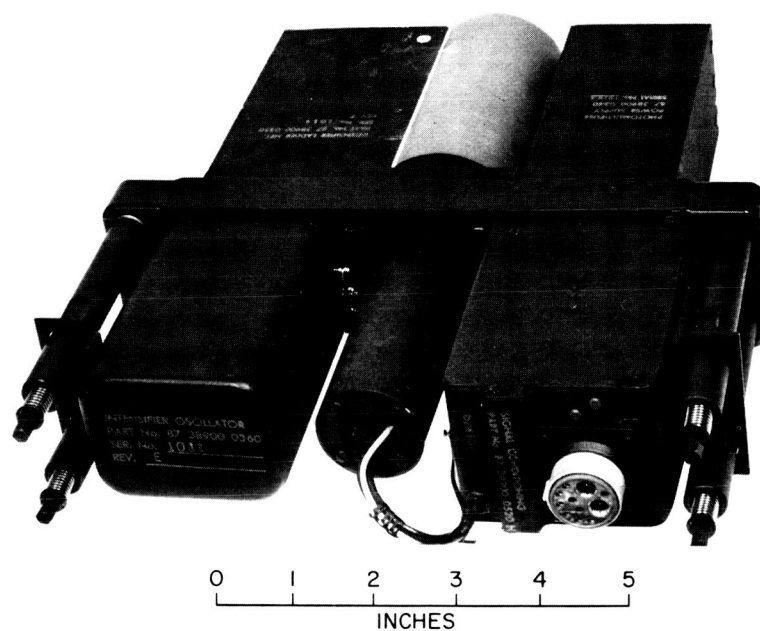


Fig. 4-1. Detector assembly

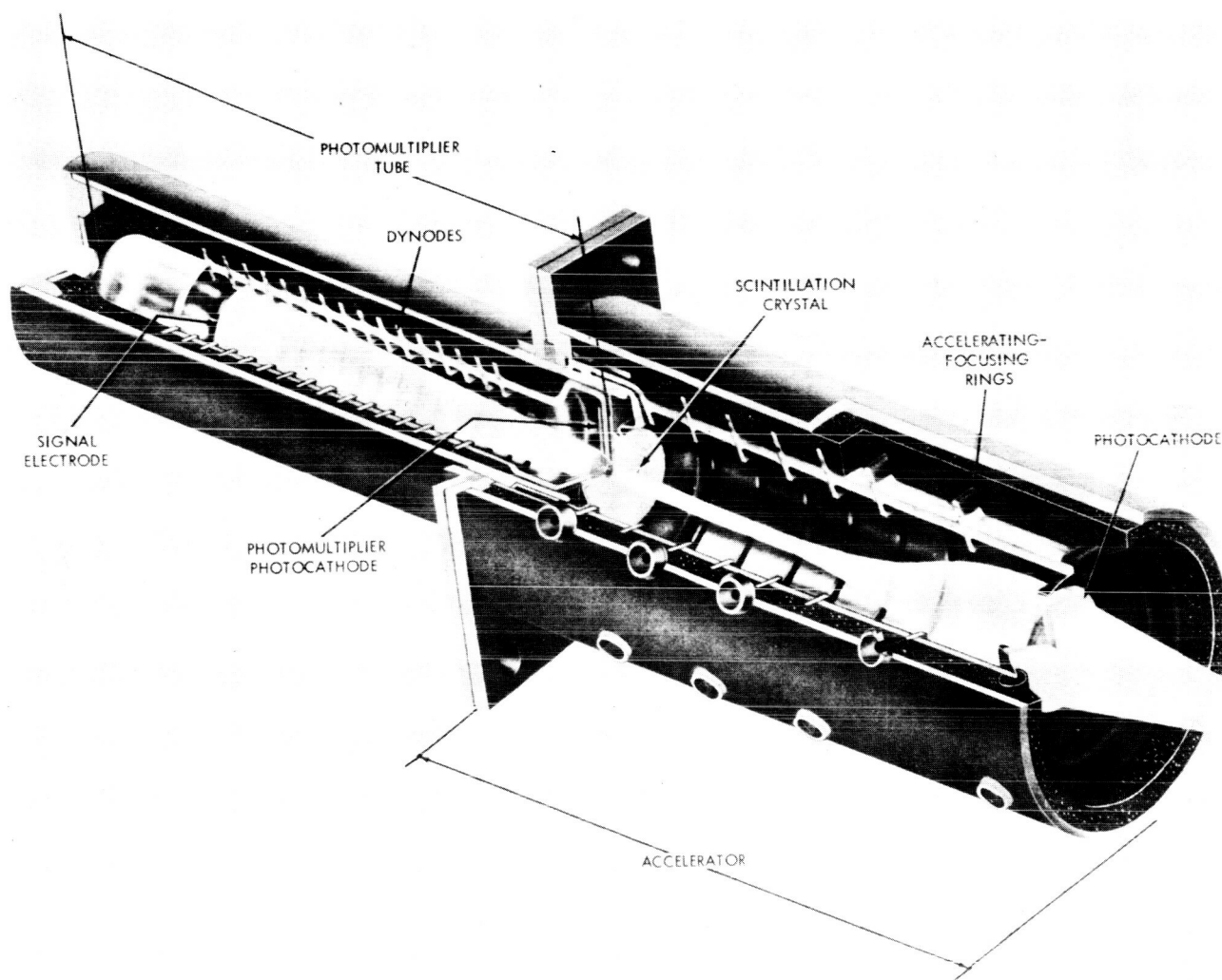


Fig. 4-2. Artist's view of detector

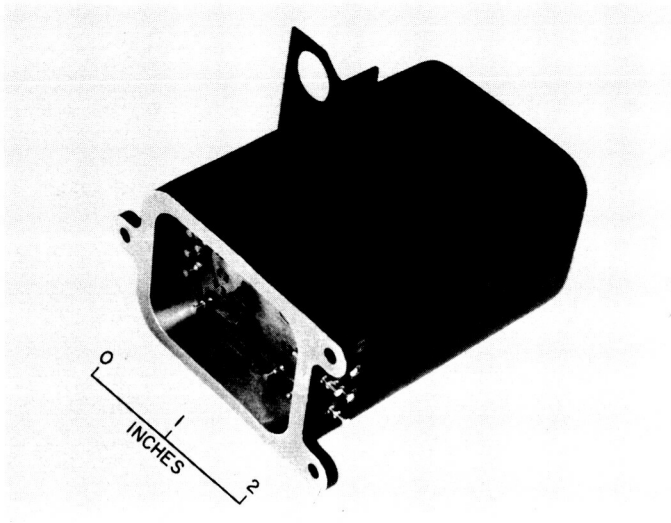


Fig. 4-3. Intensifier oscillator

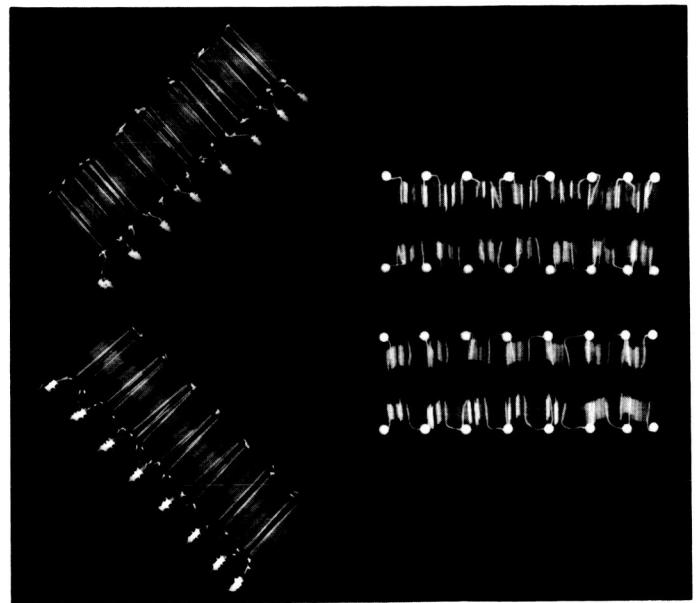


Fig. 4-4. X-ray of capacitor

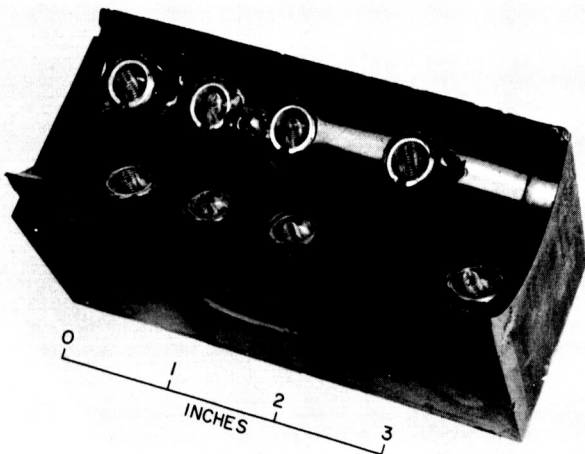


Fig. 4-5. Multiplier network after encapsulation

N 68-26880

5. ELECTRICAL BREAKDOWN MECHANISMS  
AFFECTING SPACE SYSTEMS

Edward F. Vance  
John Chown  
Stanford Research Institute  
Menlo Park, California

Four general subjects are covered: (1) electrostatic problems related to vehicle charging; (2) low-voltage arc discharges associated with high power and low voltage DC systems in plasma environments; (3) multipactor discharge (here will be demonstrated that this is not a phenomenon that is too far removed from the minimum breakdown pressure regime); and (4) breakdown as a gaseous discharge or glow discharge.

Vehicle Charging -- Edward Vance

The vehicle charging phenomenon is a vehicle-created phenomenon. The vehicle can become charged by a number of processes during launch or at satellite altitudes. The principal charging mechanisms that I'm concerned with are precipitation charging and engine charging.

Precipitation charging refers to frictional charging as the vehicle flies through clouds, ice crystals, dust, or other particulate matter.

A vehicle flying through a cloud of precipitation particles will intercept the particles. The particle will contact the surface of the vehicle. You have a frictional charging effect, the particle is then deflected off and carried away by the wind stream (I'm talking about a low altitude phenomenon here) and the vehicle is left with the charge, generally a negative charge for ice crystals and metal vehicles such as aircraft and missiles.

Figure 5-1 shows the intercepting area of the aircraft is generally (at least at subsonic speeds) somewhat smaller than the projected frontal area of the aircraft, because many of the particles are deflected around the vehicle by the wind stream.

Some probability curves of encountering charging are shown in Fig. 5-2. These are taken on a 707-type aircraft at altitudes below 40,000 ft and, as you can see, the charging rate to this aircraft traveling at 600 mph can be as high as 10 ma.



You can juggle velocities in effective areas, etc., and come up with numbers for the charging rate to missile systems or rocket systems in the lower atmosphere. This, of course, is an effect primarily associated with the lower atmosphere where you do have particulate matter in the form of cirrus clouds and ice crystals.

So much for precipitation charging other than to say that precipitation charging can (using this charging rate and the capacitance of the vehicle, which may be 1000 pf or less), charge the vehicle to extremely high voltages and the voltage is generally limited by some process such as a corona discharge from the surface of the vehicle or recirculation of ions from the engine exhaust.

The other major vehicle charging mechanism is the engine itself, and I think it's safe to say that the processes involved are not well understood. There are about half a dozen processes that can produce charging in the engines. These include diffusion of electrons in the combustion chamber to the walls, thermionic emission, photoelectric emission -- triboelectric charging from solid particles being ejected and striking the nozzle, fuel flow in liquid rockets, contact ionization, and possibly some others.

We have a great deal of experience with vehicle charging on aircraft and very little on rockets. There is a great lack of information on vehicle potentials -- attained by rocket vehicles.

We have put field meters on two Nike Cajon rockets which were fired -- the last one was fired from Wallops Island a couple months ago -- and the indication from these rocket firings is that the engine charging does charge the vehicle to several tens of kilovolts, twenty or thirty kilovolts, but it does not charge to exceedingly high potentials, that is to the order of hundreds of kilovolts that we ordinarily encounter on aircraft.

We should mention here that the manner of interpreting the field meter reading on rocket shot is of some importance in determining what really is the potential of the vehicle. In our last shot we had a synchronous detector on our field meter which would discriminate between current drifting into the field meter and true field, and it turns out that this clarifies some of the things that have happened at higher altitudes in previous experiments. Without synchronous detection the field meter will collect at higher altitudes and will provide a misleading indication of the potential of the vehicle. You may think the vehicle potential is several hundred thousand volts when it is actually less than a thousand volts potential.

The effects of this high potential though are generally two: (1) it produces RF noise in systems and (2) if not controlled properly the static charges on the vehicle can fire electroexplosive devices.

I'll very quickly run through some of the noise characteristics. I don't think I'll dwell on the electroexplosive end of the game.

Figure 5-3 shows the form of the corona pulse which is produced at low altitudes, say, 40,000 ft or below, by a corona discharge from an extremity of a charged vehicle.

You'll notice this has a very fast rise time (the rise time shown in Fig. 5-3 is limited by the oscilloscope response) and an exponential decay. This produces considerable RF noise at frequencies well into the HF range.

Figure 5-4 shows the spectrum of the corona discharge noise. As you can see this spectrum is fairly flat at low frequencies, flat out to around 1 Mc, then it begins to drop off in the 10 Mc range.

Two curves are shown, one for 30,000 ft and one for 10,000 ft. The 30,000-ft curve has a larger low frequency noise content because of the corona pulses, the Trichel pulses, are somewhat slower in rise and decay time at a higher altitude where pressure is lower.

The pulse rep rate we have measured for corona discharge off of a sheared edge of a sheet with 100  $\mu$ a of DC current being discharged, is about  $10^5$  pulses/sec., and this of course also affects the spectrum here slightly.

A second form of interference occurs if an insulating surface becomes charged by precipitation particles. The charge cannot flow off to the rest of the vehicle, so it builds up to a very high potential on the plastic surface and eventually a streamer discharge or a spark discharge occurs over the surface to the metal structure surrounding the surface. The form of pulse produced by a streamer discharge over a plastic surface is illustrated in Fig. 5-5. These are very energetic pulses, but the repetition rate is relatively low. The third noise mechanism is applicable to systems which may be coupled to activity occurring outside of a plastic surface, and this is -- particle impact noise.

In this mechanism the neutral particle strikes the plastic surface and acquires a charge. From then on it is a moving charged particle. Thus a step-fronted current pulse as is illustrated in Fig. 5-6 is produced as the particle acquires charge

potential and an upper threshold potential, and anywhere between the discharge can occur.

Figure 5-8 shows RF breakdown voltage as a function of pressure in the vicinity of the minimum breakdown potential. The right-hand portion of the curve is the conventional gas breakdown curve. Normally you would expect the breakdown voltage to go up as the pressure went below the minimum at a rather rapid rate because the sparsity of the molecules in the gas, but in an RF discharge we observed that it doesn't go up. The breakdown voltage becomes flat and out in the low-pressure region we have true multipactor discharges.

Figure 5-9 shows the region of multipactor discharge when we have DC bias between the plates as well as RF voltage. These are both normalized to a factor which involves the electron charge to mass ratio and frequency and gap widths.

The solid curves are theoretical curves based on a rather idealized theory. The points are experimental points that we have measured in the laboratory, and you'll note that as you increase the bias the RF breakdown voltage initially goes down. You will also notice that the experimental region is considerably larger than the theoretical region based on an idealized theory.

You will also notice a peculiar shaped region at large DC bias values. This is a result of a one-sided multipactor discharge mode which occurs only in the presence of DC bias and in this case the electron does not go all the way across the gap and impact and produce secondaries and come back as it does in the normal two-sided modes. In the one-sided mode the electron is emitted from one electrode, and pulled out by the RF field against the DC field. The RF field then reverses and the electron is driven back to the same electrodes from which it was emitted with sufficient energy to produce secondary emission.

Figure 5-10 shows the DC bias voltage and RF breakdown voltage where one-sided multipactor discharge will occur. This is for the same general gap which is about a 2-in. or 5-cm gap. Uniform field is used again. The lower curve is for 34.9 Mc. The upper curve was for a higher frequency. The region over which the discharge will occur in this case increases with frequency. That's not necessarily always the case, however.

Figure 5-11 shows some data we have taken on coaxial geometries where we have a solid outer conductor and a solid inner conductor, and the discharge is

and the charged particle moves away. This is also a source of electromagnetic interference.

I have a short film that shows this effect rather dramatically. We installed some regular type "N" RF connectors in a vacuum chamber and pumped it down to a pressure of about  $10 \mu$  of Hg, and produced a plasma in the region with an RF discharge. The RF discharge served only to produce the plasma. We applied a negative bias to the center pin of these connectors from 28- or 36-v storage battery sources, so that we had a high current source and we've created an arc. Figure 5-7 shows the result of an arc discharge produced by low voltage in a plasma environment. Molten metal spewed out of the connector is visible on the bell-jar base near the connector.

#### Low Voltage Arc

If a metal such as aluminum or stainless steel, or practically any other metal that will form an oxide film, is immersed in a plasma environment and a DC voltage is applied to it, little scintillations or flashes will be observed on the surface of the metal. This apparently is the result of the voltage between the base metal and the plasma all appearing across the oxide film. With a very thin film and only 10 or 20 v across this film, extremely high field strengths are produced within the film. As a result the film breaks down in a manner similar to the breakdown of a capacitor. The film is shorted and a certain region around the point of breakdown is discharged. In the process of this breakdown a cathode hot spot is produced which can trigger an arc discharge.

It turns out that you can trigger these arc discharges at rather low voltages. We have produced arcs at voltages as low as 28 v DC in a plasma environment, and you do have to have the plasma environment to produce the arc.

#### Multipactor discharges

The multipactor mechanism, as has already been pointed out, is a secondary emission discharge mechanism. The electrons are produced by secondary emission from the electrodes rather than by collision processes occurring within the gas as in a conventional glow discharge.

The electron must travel in synchronism with the RF field; therefore it is a frequency and gap-length dependent discharge. Because of this a lower threshold

occurring between the inner and outer conductor. Again we have plotted RF breakdown voltage along the ordinate and DC bias voltage along the abscissa. We decreased the size of the center conductor, while the outer conductor remained the same size. The discharge occurs anywhere within the contour.

We have also looked at what multipactor breakdown will do to an antenna of the discone type. In Fig. 5-12 we have the results for a cone driven against a ground plane. We also again applied bias to see what bias would do to the discharge. In this case we are using an ambient ionization produced by a little auxiliary discharge at a different frequency.

These curves were compiled using about 40 Mc as the frequency with which we were driving the antenna to produce breakdown and these curves are for various cone angles. A 180-deg cone angle is, of course, parallel planes. When we got down to much below 120-deg cone angle, we were unable to produce breakdown with the power we had available (approximately 75 w).

It appears that multipactor breakdown is primarily of concern in high-Q circuits. I think this was where someone this morning had noted that they had observed it.

One other characteristic in multipactor discharge is that all of the power is dissipated in the electrodes. There's none dissipated in the gas as there is in a normal glow discharge so that all the heating takes place in the electrodes and as a result you can heat electrodes in a multipactor discharge sufficiently to melt some soft solder junctions even though the power absorbed by the discharge itself may not be of much concern as far as, say, a radio transmitter operation would be concerned.

#### Gas Discharge Breakdown -- John Chown

I'm going to consider the breakdown mechanism at relatively high pressure and speak mainly about gas discharge breakdown. This case is different than the other phenomenon that we have been considering this morning in that it is the breakdown of the gas itself which is brought on by accelerating the electrons in the RF field. They sustained collisions and became out of phase with the RF field so that they gain enough energy after successive collisions to have an ionizing collision with a

neutral molecule. In this way the plasma density starts to grow exponentially and when the RF field reaches the proper value, a discharge is sustained.

There is a visible glow involved and the electron temperature is quite high being several electrovolts. RF energy is dissipated in the medium.

I will briefly go over some of the things that occur when you sustain a gas discharge, mainly from the antenna aspect. However, certainly these sorts of things can clearly happen in a coaxial geometry or in voids in dielectrics. There the problem is even worse probably because if it dissipates enough heat locally it can actually char and produce considerable heating.

$$\frac{\nu_i}{P} = \underbrace{\frac{\nu_a}{P} + \frac{DP}{(P\Lambda)^2}}_{\text{CW}} + \underbrace{\frac{\ln\left(\frac{n_\tau}{n_0}\right)}{P\tau}}_{\text{PULSE EFFECT}} \quad (5-1)$$

Equation (5-1) presents the continuity equation normalized with pressure (P). The left side of the equation is the production rate of electrons and the right side indicates the loss mechanisms. When they are equal, or the production rate slightly greater, a discharge is sustained. The first term on the left side of the equation takes into account the attachment loss and the second term the loss of the electrons to the reaction by diffusing out of the high field region and no longer available to the reaction. This becomes a principal loss mechanism at the lower pressure. This covers the cw breakdown case. In other words the RF power is applied and it stays on. If you're dealing with pulse power then the last term in Fig. 5-12 is used which suggests that we now have to take a certain amount of time  $\tau$ , for the pulse to be applied before the reaction can carry on to the point where the discharge occurs.

Figure 5-13 indicates the essential features of gas discharge breakdown. Plotted in Fig. 5-13 is the normalized parameter of the pressure times the wave length as a function of the power; the field squared. When you start at high pressure and decrease it the field required to produce a discharge starts to decrease. It reaches a minimum, the value of which is dependent on the diffusion loss rate. The  $\Lambda$  values in Fig. 5-13 are for different characteristic diffusion lengths which depend upon the field geometry and indicate the rate electrons are lost due to diffusion away

from the high field region. The breakdown power level then starts to increase again; the power required starts to go up because of the increased diffusion losses and also because of the efficiency of the RF coupling.

Shown in Fig. 5-14 is an X-band end fire aperture under breakdown conditions to indicate the appearance of the glow discharge. The pressure is around 10 mm Hg for the left-hand photo. The intense glow is at the feed end of the aperture. As the pressure is decreased the glow becomes more diffused and striations appear as shown in the right hand photo of Fig. 5-13. The light areas along the edge are actually just the small gap between the metal ground plane and the dielectric.

In Fig. 5-15 there is a plot for two different power levels and at two different pressures for the X-band end fire array. The solid line in Fig. 5-15 is the antenna without a discharge over the surface. The next two curves are for breakdown conditions at 5 mm Hg pressure and the peak powers of 5 and 25 kw. The average power, the integrated value over the pulse length is plotted on the output scale. As one can see when the discharge occurs, the amount of power that is transmitted decreases. Also, the shape of the pattern changes rather drastically.

Examination of Fig. 5-15 indicates that the side lobe levels for both power settings are comparable, even though they lost 7 or 8 db for the case of the 5 kw and 12 to 13 db and 25 kw in the power radiated in the main lobe. Another effect of the breakdown is that when the discharge occurs normally the impedance is changed. It doesn't necessarily go up. It depends upon the matching circuitry of the antenna, the antenna type, the power level, and the pressure. However, generally after you increase the power so far it certainly tends to end up in a worse condition if you're initially matched fairly well.

In pulse systems one may encounter additional trouble because if the antenna aperture is several wave lengths in extent, it is possible to have pulse shapes which now vary as a function of antenna look angle as shown in Fig. 5-16. In Fig. 5-17 the pulse is applied at zero time, and remains unbroken until about a half a  $\mu$ sec. At that point the discharge occurred in the pulse, and then the radiated power varied.

The pulses radiated right around the main lobe show a significant decrease at breakdown but off to the side one finds that the pulse shapes vary radically as the function of the look angle, and they also don't appear to have reached a steady state, even after 2  $\mu$ sec. The pulse shapes will vary with the pressure and the power applied.

The effects described above take place as one increases the field in the vicinity of the antenna to the point where the discharge occurs. Another thing that happens normally at the pressure ranges of interest here is that the vehicle is moving and consequently it may be moving into an ionized region (the ionosphere) or if moving fast enough into a planetary atmosphere, it can be creating electrons by the aerodynamic heating of the medium and breakdown can occur at lower power levels.

A plasma layer adjacent to an antenna attenuates the transmitted signal and, at the same time, modifies the antenna impedance, radiation-pattern characteristics. The plasma can also cause additional losses by interacting with the normally reactive near zone fields of the antenna. The low-signal-level effects are distinguished from the high-signal-level or breakdown effects since they occur while the plasma still behaves in a linear fashion; i.e., the phenomena are independent of power level in this regime. The antenna characteristics begin to be affected as the plasma density is such that the plasma frequency  $\omega_p$  approaches  $\omega$ , the operating angular frequency. That ratio of  $\omega_p$  to  $\omega$  where measurable effects appear, depends upon the extent of the plasma and the effective collision frequency.

At high altitudes, the important parameter determining the minimum breakdown field strength is the diffusion coefficient for electrons; this coefficient is radically altered if the air is already ionized, in which case the diffusion becomes ambipolar. Under this condition, the velocities of electron diffusion away from the high field region are so reduced that the probability is increased of their gaining ionizing energy through successive accelerations and collisions and, consequently the breakdown field strength is reduced.

As an example of the effect of a plasma on antenna performance we can consider the results of some laboratory experiments.

Measurements were made on a slot antenna subjected to a thin plasma layer created by a low-pressure flame. Data were obtained at several different collision and plasma frequencies. The L-band slot antenna used in the tests is shown in the low-pressure vessel (Fig. 5-17). The slot-backing cavity was filled with Teflon and a thin alumina window was used as a pressure seal. A thin plasma layer of thickness  $d$  was produced over the slot surface using a potassium-seeded ethylene-oxygen flame. The carbon burning chamber and the thin slit through which the thermally ionized gas passes are visible below the antenna. The plasma thickness was such that  $d \ll \lambda$  -- a condition similar to that of the plasmas existing about slender



re-entry bodies. Visible also in the low-pressure chamber is a movable, unbalanced ion probe, used to obtain the plasma-density profiles.

Figure 5-18 presents the power required for breakdown as a function of collision frequency  $\nu$ . The top curve indicates the breakdown power level for free diffusion and the lower curve for ambipolar diffusion. In the breakdown process, the diffusion loss mechanism dominates below the minimum breakdown power point.

In Fig. 5-19, the power radiated normal to the L-band slot antenna is given for various ratios of  $\omega_p/\omega$ . The collision frequency corresponds to the minimum power handling point in Fig. 5-18. Where high fields are present and breakdown considerations are important, the plasma becomes nonlinear in the sense that as the power delivered to the antenna is increased, the characteristics of the medium are altered. As can be seen in Fig. 5-19, when the plasma is such that  $\omega_p \ll \omega$  and the electron loss is by free diffusion, the change in the plasma is abrupt and the power radiated typically decreases by an order of magnitude. When  $\omega_p \leq \omega$  and the diffusion is ambipolar, the decrease in the radiated power is only a few decibels, since the initial breakdown level has now decreased. In the case where  $\omega_p > \omega$ , the transition to the nonlinear plasma condition is gradual, with no abrupt change in signal level.

As the power is increased (Fig. 5-19) beyond the breakdown level, the additional power is absorbed in the plasma, which grows in extent and density and the radiated power remains essentially constant. Figure 5-20 which is the plasma-density profile normal to the slot obtained with the probe, indicates this point clearly. Even though the ambient electron density levels differ by an order of magnitude, once the RF power is applied and breakdown occurs, the density profiles are essentially the same. It can thus be seen that for thin plasmas, which are considered here, once breakdown exists, the power radiated is essentially independent of the initial conditions and the low-signal-level attenuation as well.

In Fig. 5-21 radiated signal data for the same L-band antenna (Fig. 5-18) was taken where a plasma jet provided the ambient density. In this case the elevated temperature air which is heated by a 14-Mc transmitter is provided rather than hydrocarbon flame by-products. It turns out that the production rate of electrons in the flame by-products were essentially the same as the hot air. The plasma jet yields essentially the same results but inasmuch as no gas was being burned we were able to actually run considerably lower in pressure. As before, the power radiated increased and then remained constant after breakdown, up to the point where the

pressure for the minimum in the breakdown curve occurred at about 800  $\mu$ . At lower pressures as you increase the power after you have sustained breakdown, the radiated power started to decrease.

As shown, the breakdown thresholds are as one would predict them. The way the radiated power behaves after breakdown is a function of pressure as well; however, predicting its behavior is much more complicated.

The idea of using the plasma jet has several attractive aspects for people who are interested in the problems occurring when one reenters planetary atmospheres. This is one facility in which you can actually take a variety of gases and heat them in an electrodeless discharge, so that they can be dealt with at high temperatures without worrying about contamination from electrodes. The shock tube, of course, is another facility which can be extremely valuable in planetary reentry studies.

For an example of how one can inhibit breakdown let us consider a dipole antenna. A dipole using a DC bias can be made to either attract the electrons into the dipole and capture them or repel the electrons so that you can increase the diffusion loss. Of course, one can envision the fact that you can only carry biasing so far because as the bias is increased a DC discharge will eventually occur.

The other obvious one for aperture antennas is to spread the power over a larger aperture and decrease the maximum field. This technique again has its attendant problems. The principle one is being able to control the phase and the amplitude distribution as you start to increase the aperture size. Where an ambient plasma is provided over the surface due to the environment itself, difficulty will be experienced in maintaining pattern control because of the phase and amplitude distortion produced by the varying plasma conditions.

The other technique to increase power-handling capability is one in which you try to modify the environment. Injection of various materials to attach out electrons, or to reduce the local gas temperature by the injection of water, for example. These sorts of things are being done experimentally and have been considered for some time. If one has a lot of latitude, clearly body shaping to modify the environment is an important one to consider. Normally, however, the people who design antennas never have anything to say about the shape.

## OPEN DISCUSSION

MR. KINKEAD: I wonder if I could ask Mr. Vance if he would be able to give us any idea on what happens in this transition region and multipactor region as you go to higher frequencies. I suppose this being a NASA-sponsored symposium we're particularly interested in S-bands perhaps, and I see your data is down on the megacycle region where most of the prior data in this area has been taken. I've seen some data of X-band where this multipactor discharge didn't become evident down below critical pressure taken by, I think, Lockheed people. I wonder if you could fill us in, perhaps, with what you expect might happen in the intermediate region between, say, HF and X-band.

DR. VANCE: Because it's a frequency gap-width dependent discharge, the region where the discharge will occur pressurewise depends on the gap and the frequency. The higher in frequency you go, the shorter the gap has to be.

On the particular slide that I showed, your transition from the gas discharge to multipactor discharge is near the minimum multipactor discharge gap-width-frequency domain also. And this was at about 40 Mc.

If you go up to X-band 10 g Mc, your gap widths become exceedingly small. You don't encounter gap width of that size too often in X-band plumbing or antennas or this sort of thing.

You do encounter them occasionally in X-band tubes, Klystrons, or magnetrons, and the discharge can detune cavities. They are a problem. In fact, this is where multipactor has been the main problem up until very recently.

MR. KINKEAD: One other aspect is that higher order modes seem to also be able to be formed. I expect that even for relatively big X-band gaps they might be a problem.

DR. VANCE: That's true. I mentioned only two modes, the one-sided mode and the half cycle mode in which the electron crosses the gap in a half cycle. The electron can cross the gap in any odd number of half cycles which allows you to get the multipactor discharge in a larger gap and this is in fact the principle of one microwave device which uses multipactor as a switching device but the highest frequency I've worked with is about 1 gc and there the gap is

only a few millimeters and at these frequencies you have to be rather careful in designing your apparatus to get the right sort of gap to produce the multiplier.

MR. MOLMUD: I'd like to hear some more about your Wallops Island measurements.

DR. VANCE: We haven't reduced all that data yet. We have had two field meter experiments. One was made in a manner of a few weeks when we found out that the payload and the weight in space would be available for it and we made it up in that amount of time and we didn't use a synchronous detector, so we were not able to distinguish an ion drift current to the field meter and a true electric field on the surface of the rocket.

In that experiment we observed what appeared to be high fields or high ion currents at altitudes above about 60 km. If we had interpreted these field meter readings as true field strengths, this would have indicated that the rocket was of the order of 200 or 300 kv in potential.

On the last Nike Cajun occasion that was fired at Wallops Island a couple of months ago, we had considerably more time to design the experiment. We did use a field meter with a synchronous detector so we could distinguish between ion currents and true electric field on the surface of the rocket.

In that experiment we observed something like 20 or 30 kv vehicle potential during launch -- that's during the Nike motor burning which is at very low altitude and burns for only about 3 sec.

During Cajun burning we observed a fairly low potential. I think it was of the order of a kv or a few kv.

At about 60 km we observed ion currents.

Now on this rocket experiment, the field meter was sort of a piggyback thing. The main experiment was an antenna breakdown experiment and at about 60 km a VHF or VHF antenna breakdown experiment was entering the minimum breakdown voltage regime and the antenna was breaking down. Each time the antenna broke down we observed the currents on the current channels of the field meter but we did not observe any high potentials above about 40,000 or 50,000 ft. No high potentials in the D region or above. In fact, I think we can state that the vehicle potential was less than 5 kv in that altitude regime.

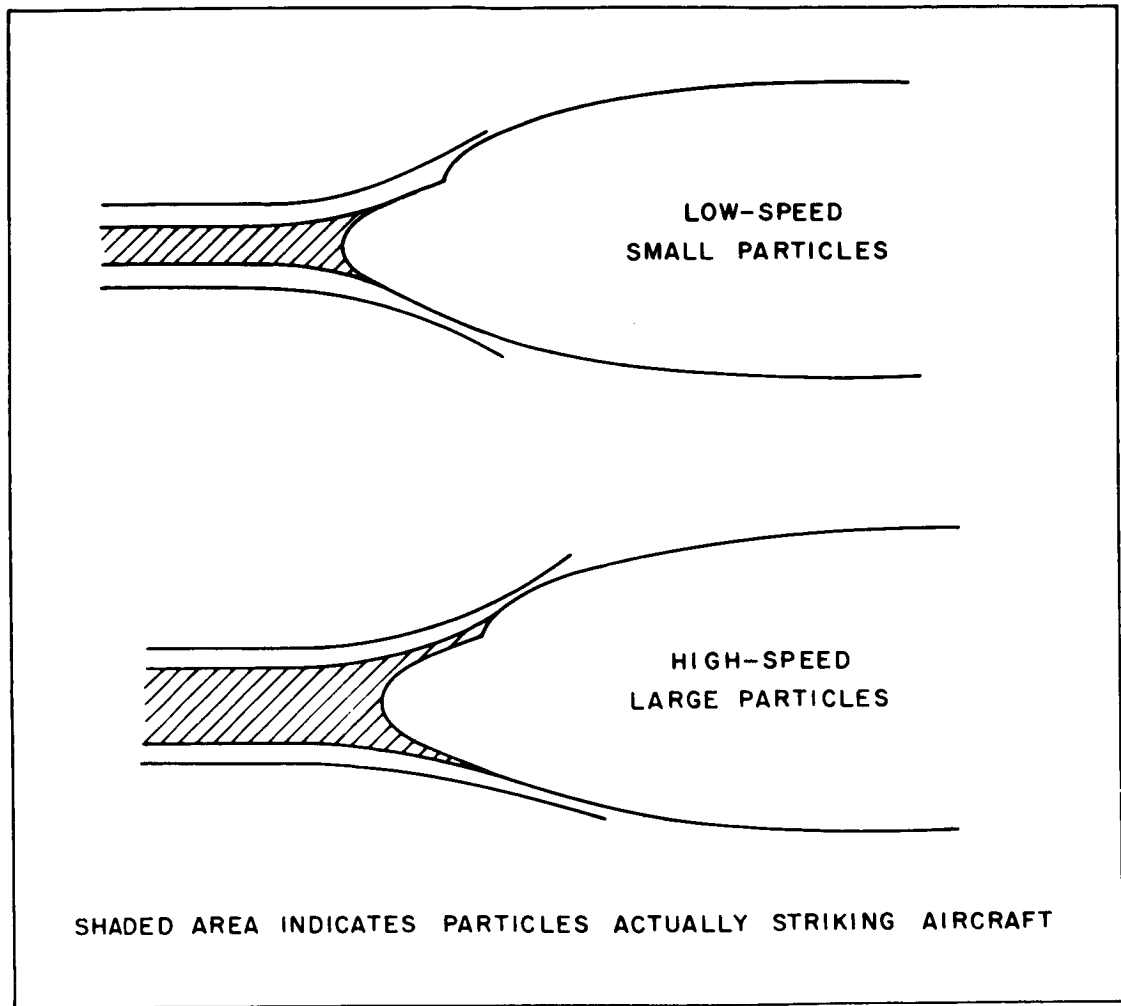


Fig. 5-1. Column of particles intercepted by a subsonic aircraft

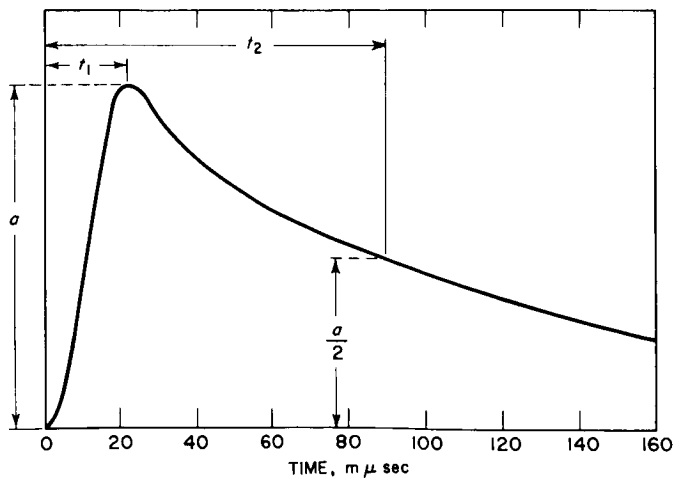


Fig. 5-2. Probability of encountering a given charging rate on a 707 Aircraft

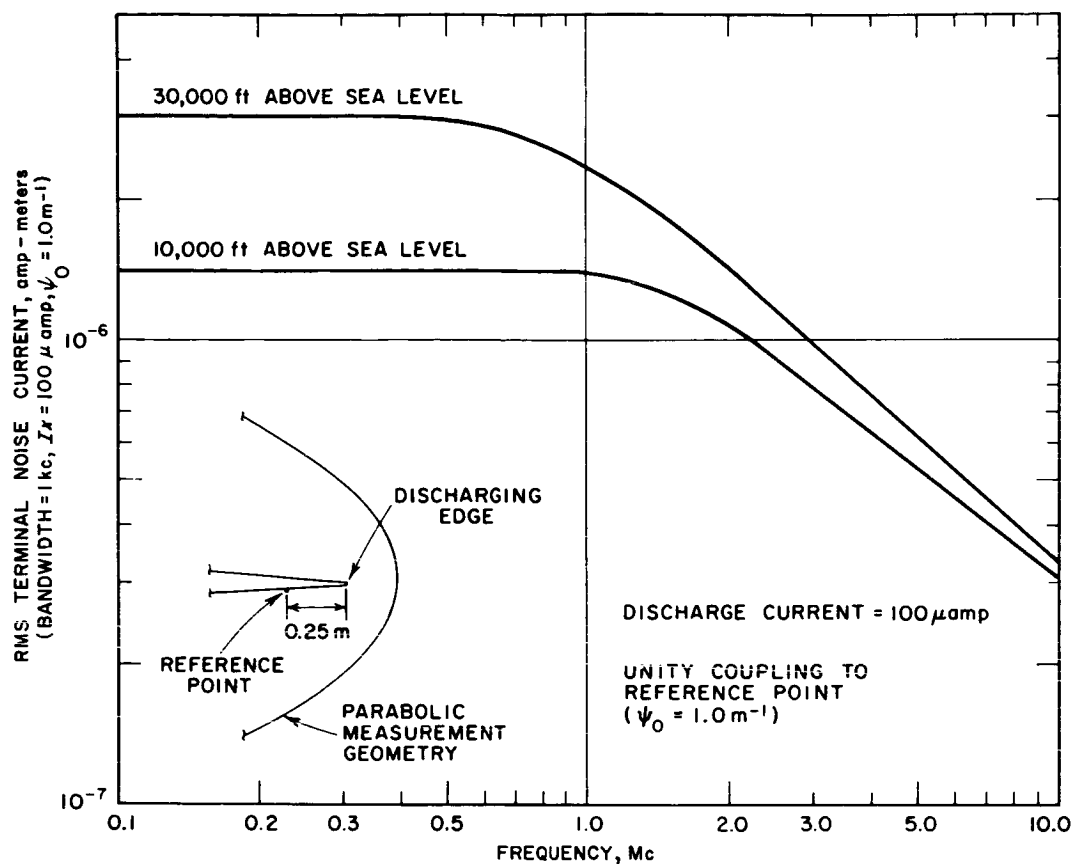


Fig. 5-3. The form of an individual pulse produced by a corona discharge

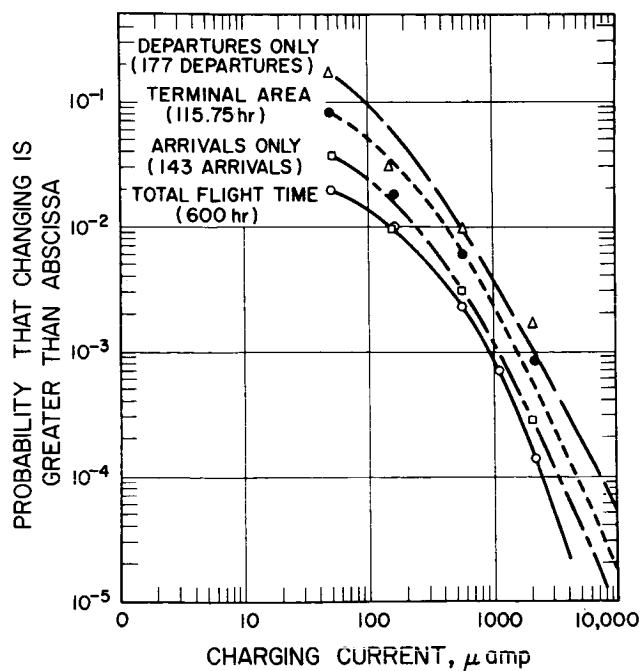


Fig. 5-4. The spectrum of corona discharge noise

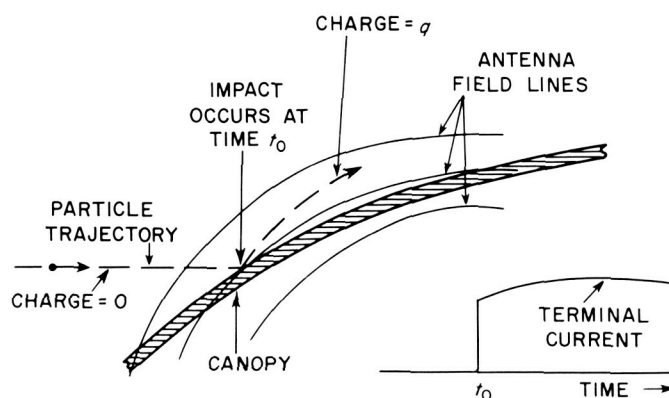


Fig. 5-5. Pulse produced by a streamer discharge over a plastic surface

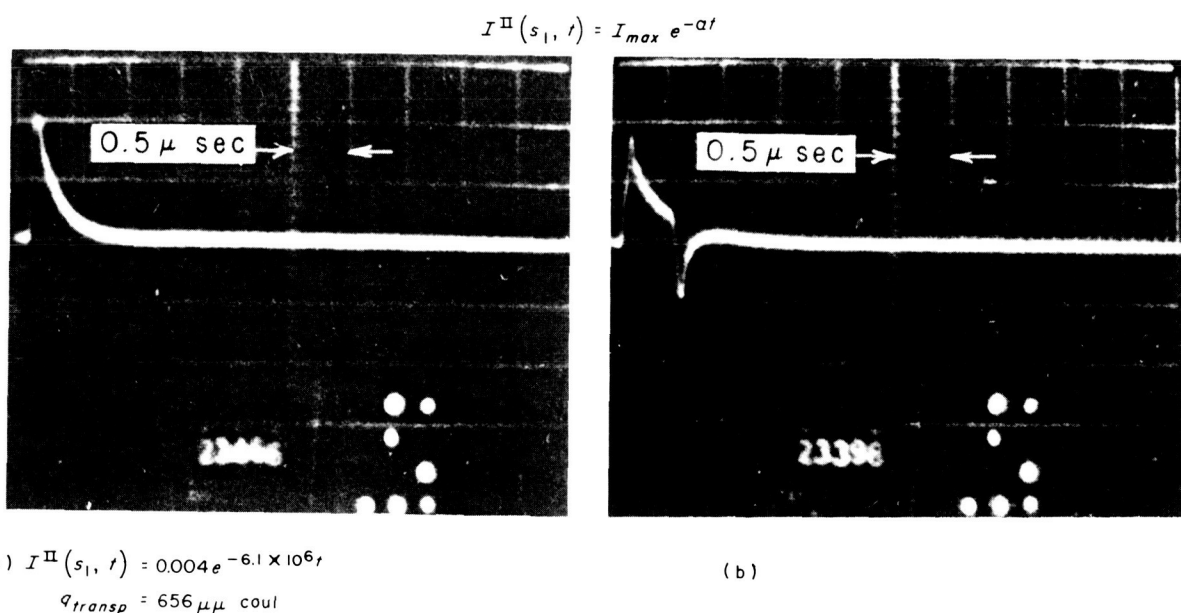


Fig. 5-6. Arc discharge produced by low-voltage in a plasma environment

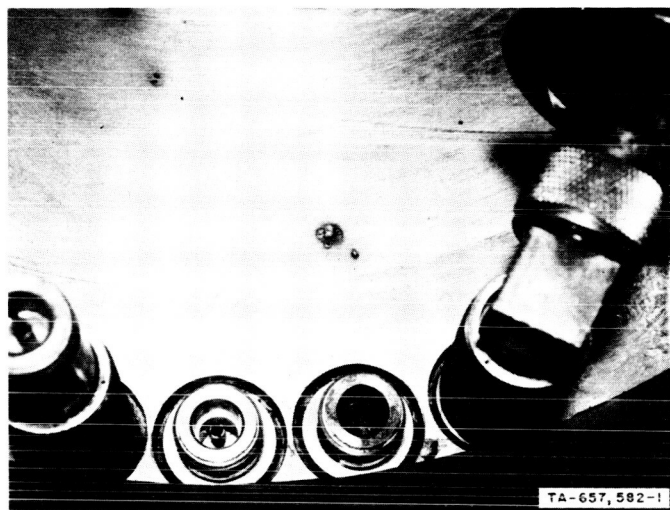


Fig. 5-7. RF connector damaged by low-voltage arc

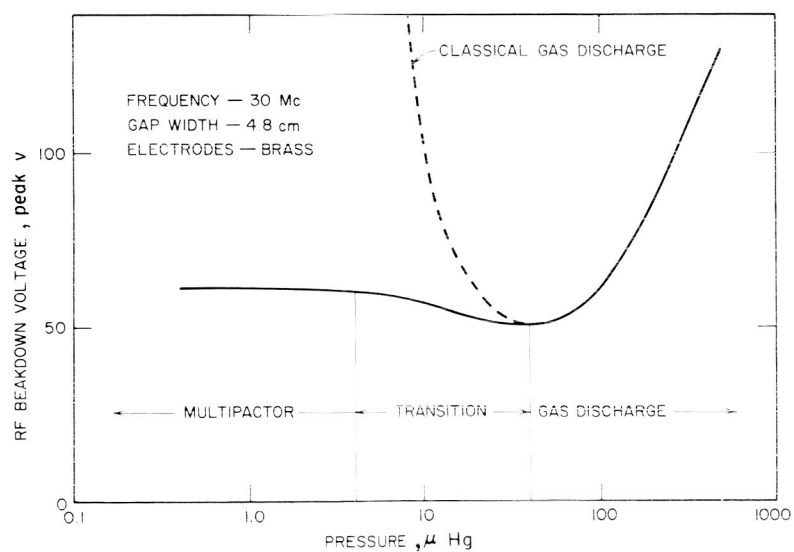


Fig. 5-8. Voltage for initiation of RF breakdown as a function of pressure



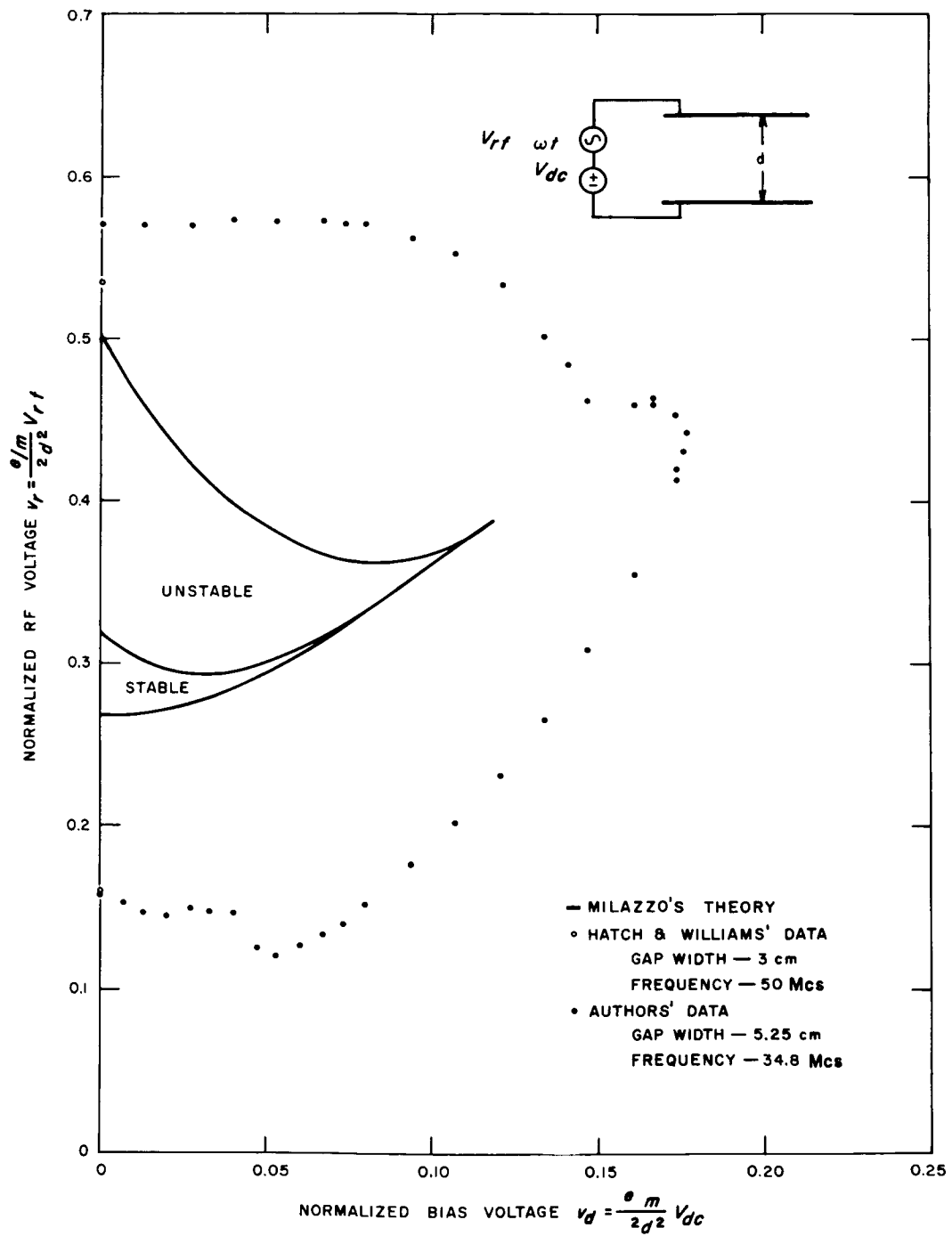


Fig. 5-9. The region of multipactor discharge in the presence of DC bias

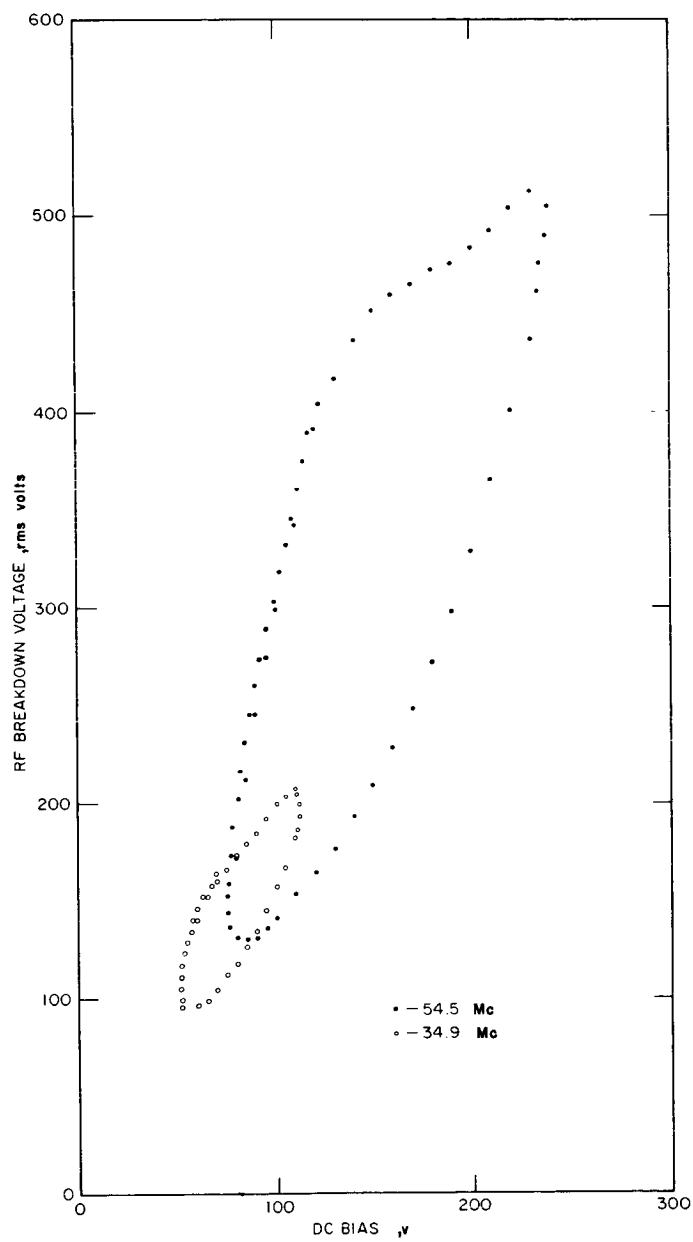


Fig. 5-10. Regions of one-sided multipactor discharge

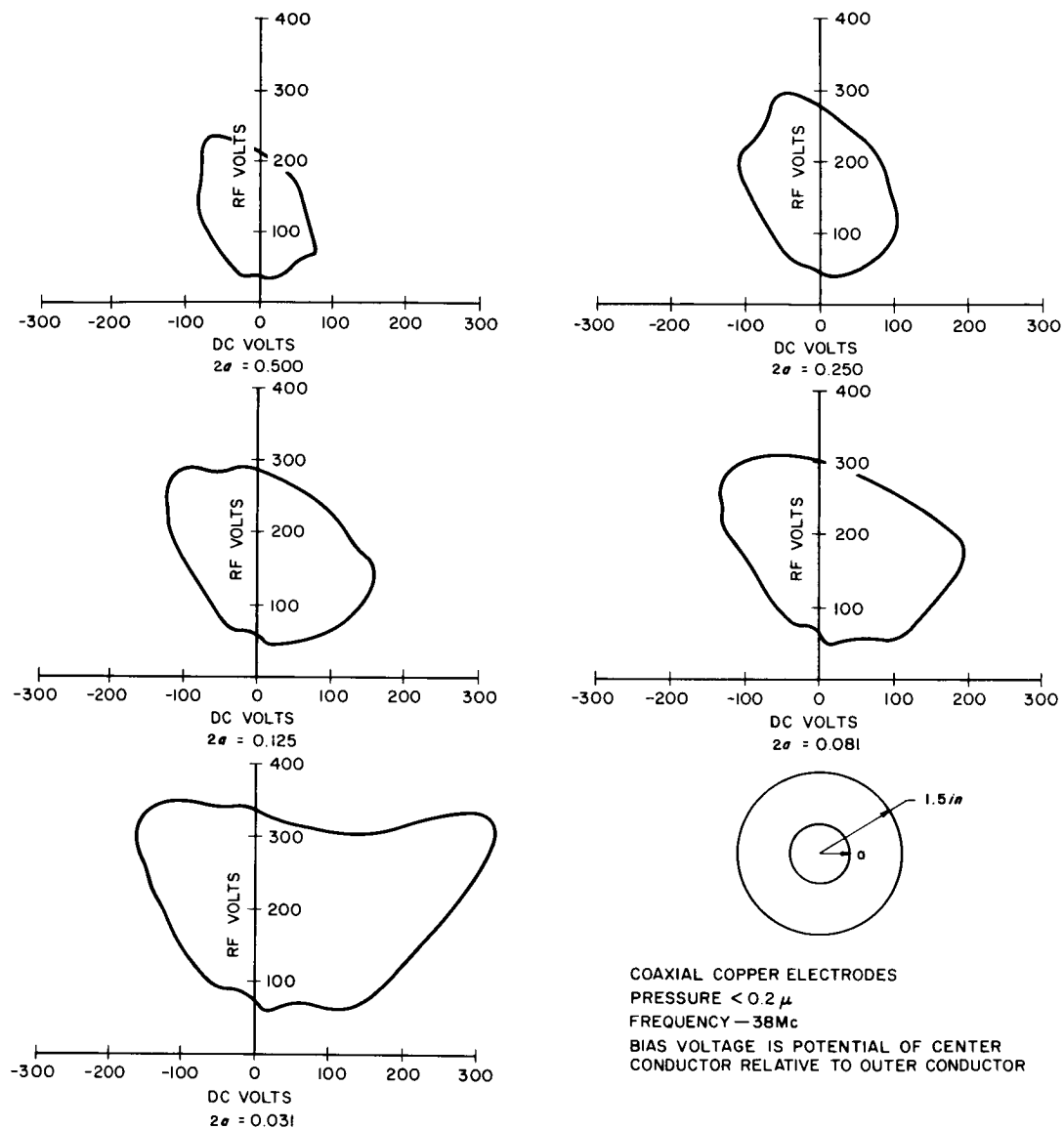


Fig. 5-11. Regions of multipactor discharge in a coaxial geometry

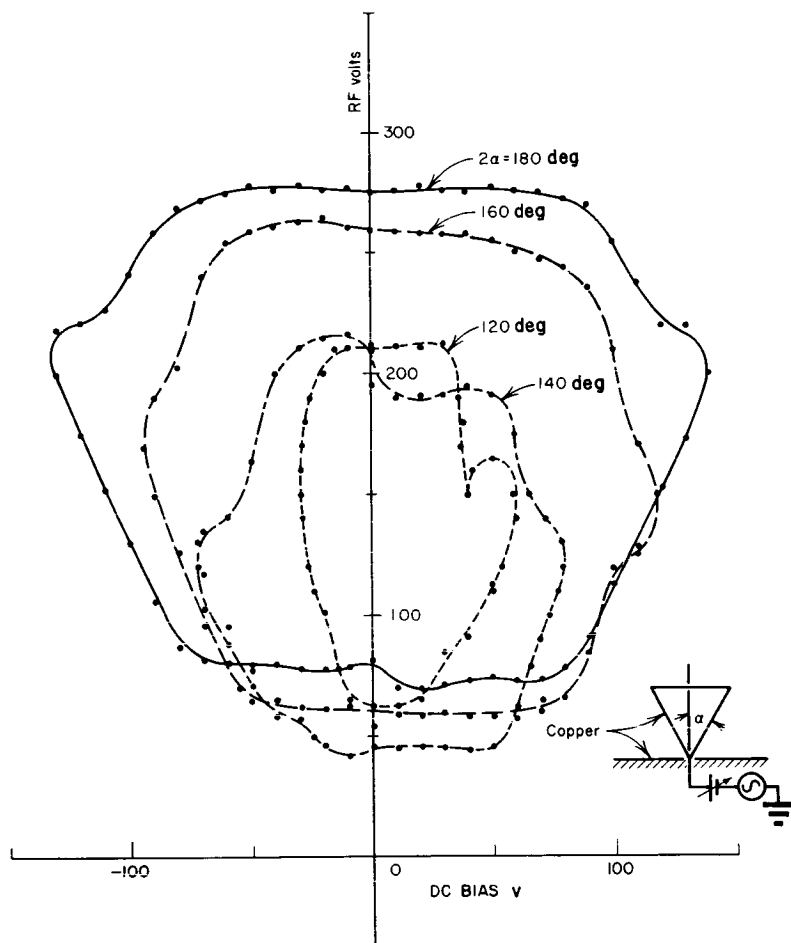


Fig. 5-12. Regions of multipactor discharge on a disc-cone configuration

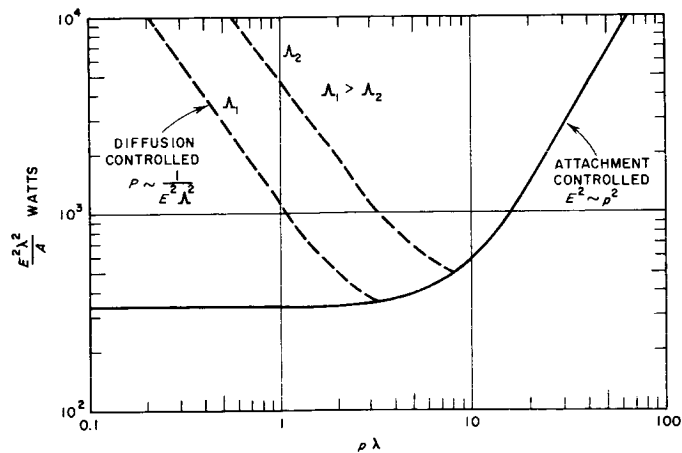


Fig. 5-13. Normalized breakdown characteristics

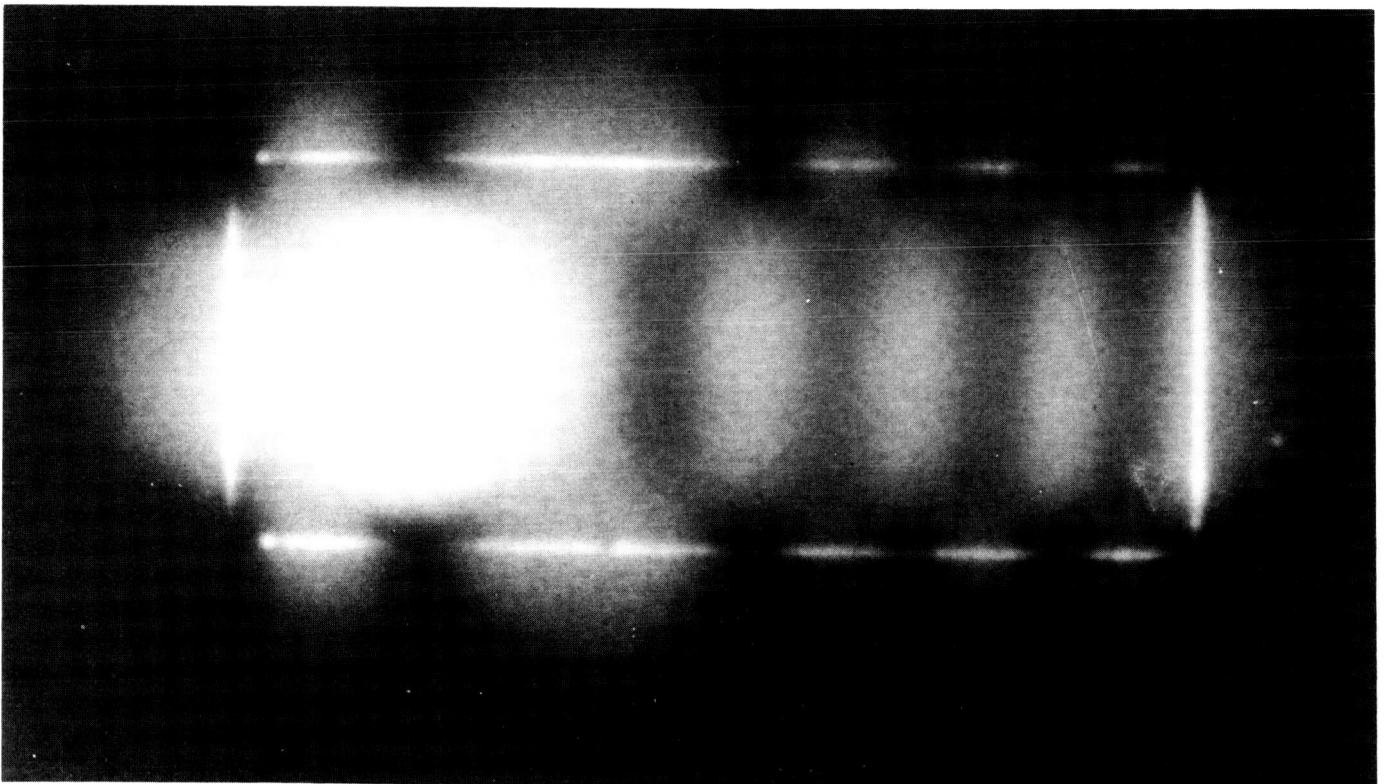
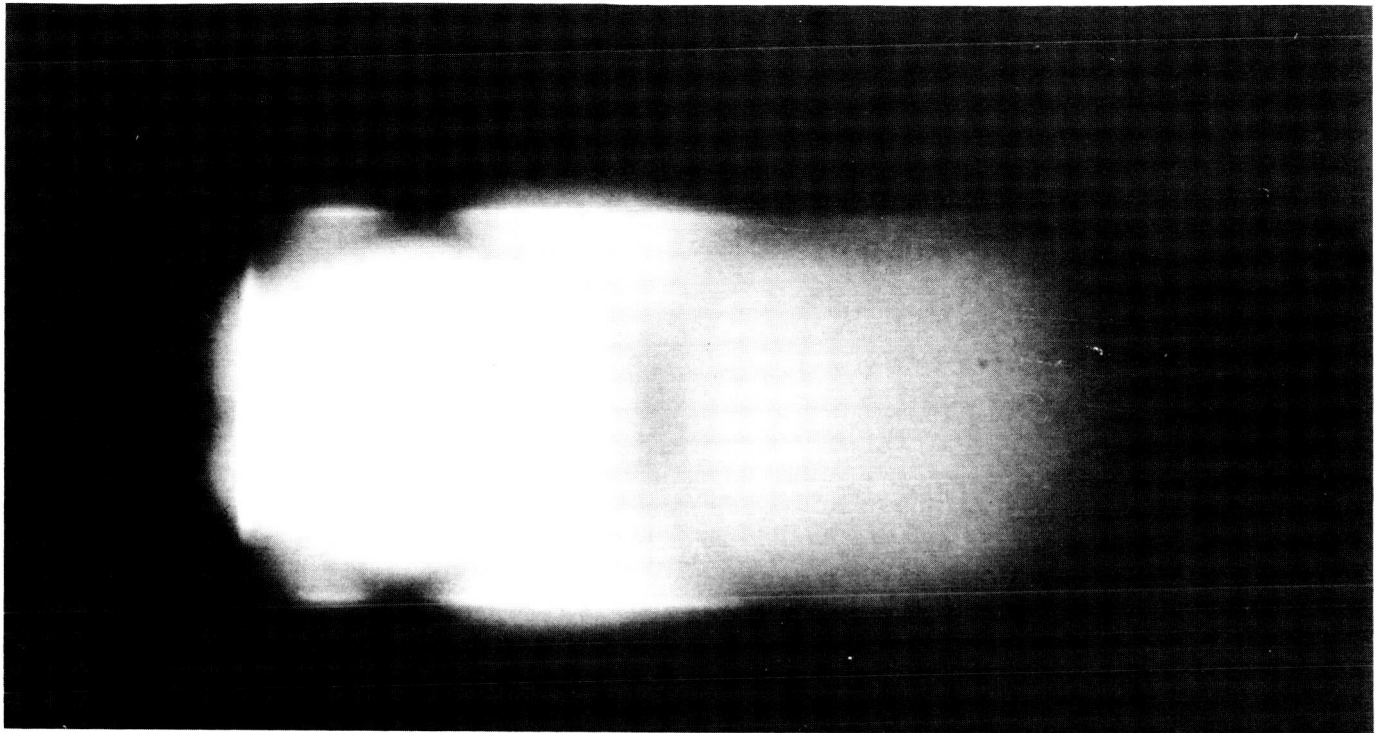


Fig. 5-14. X-band end-fire array under breakdown conditions

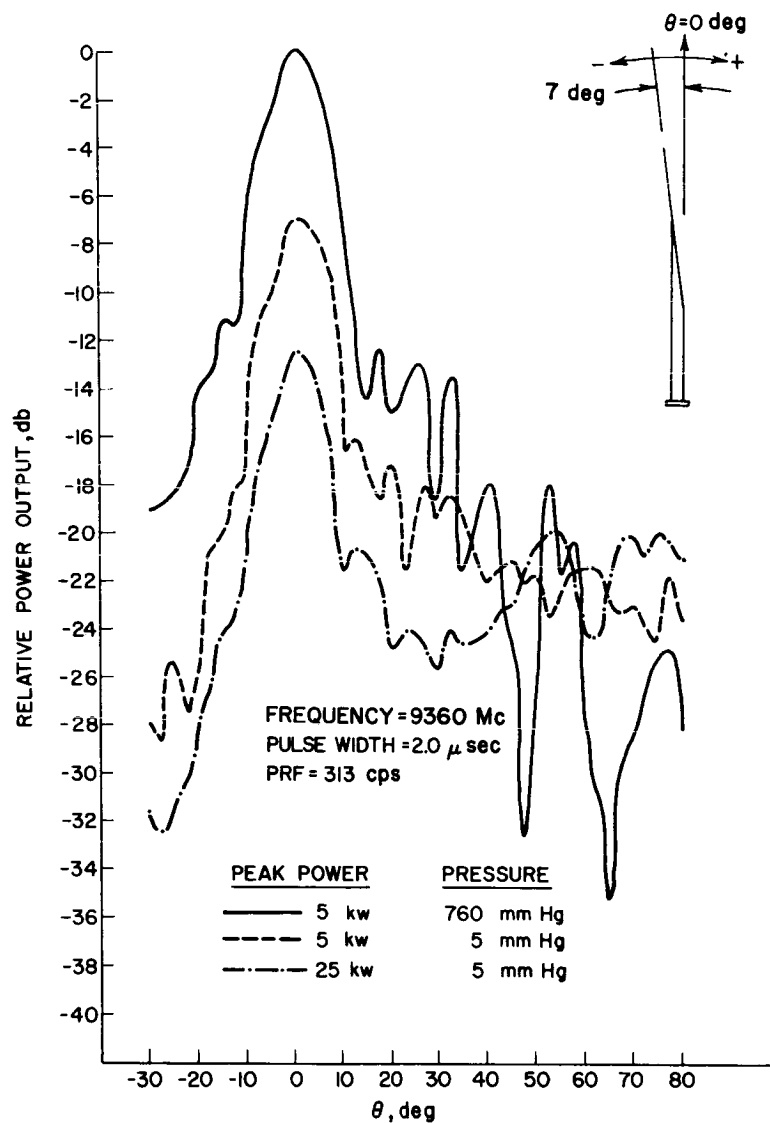


Fig. 5-15. Radiation patterns of end-fire X-band antenna under breakdown conditions

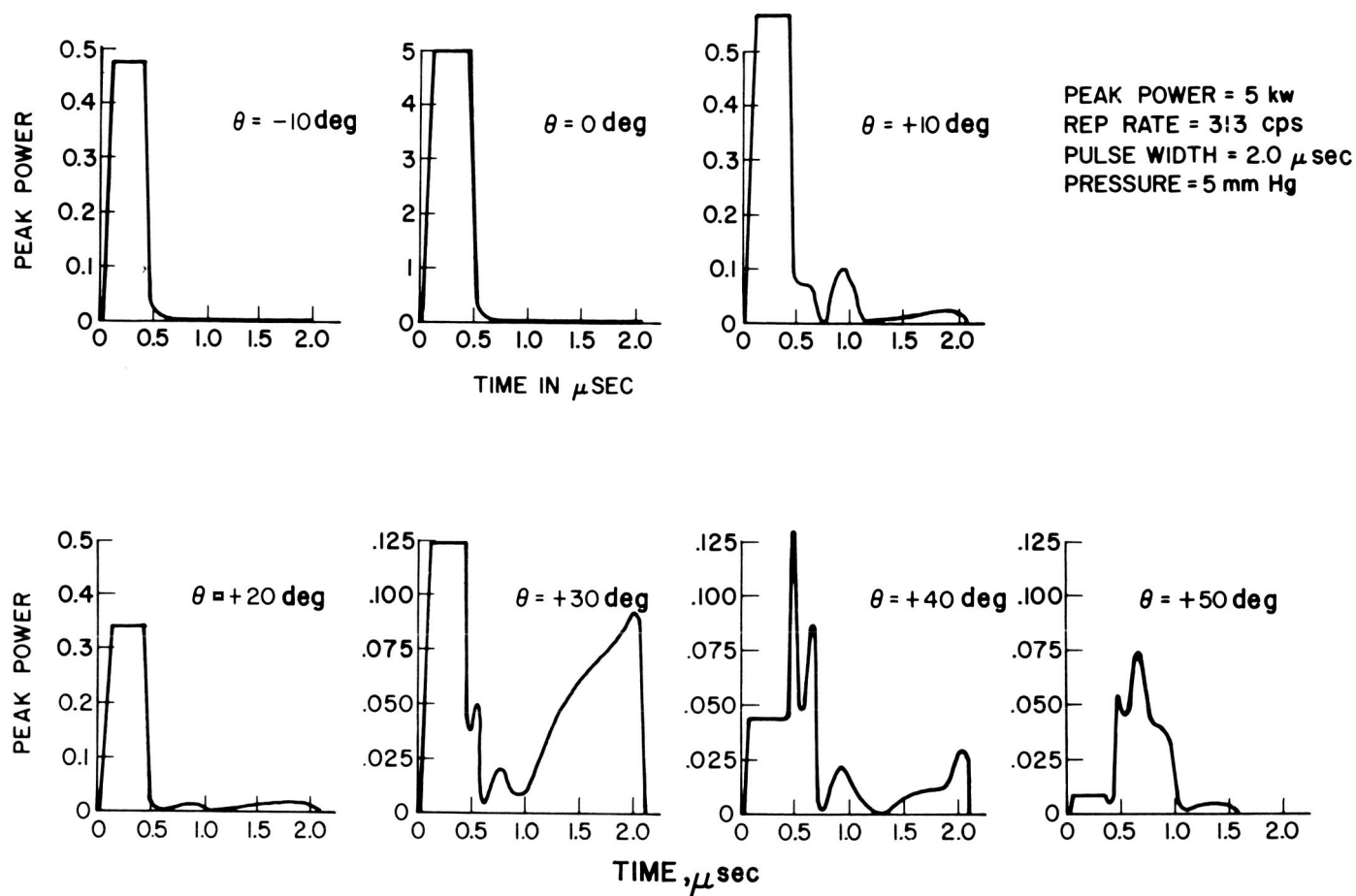


Fig. 5-16. Effect of breakdown on pulse shape

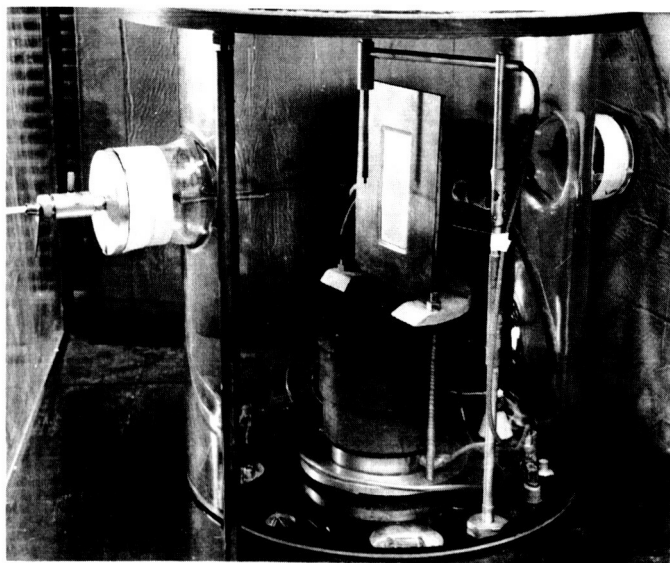


Fig. 5-17. Experimental setup

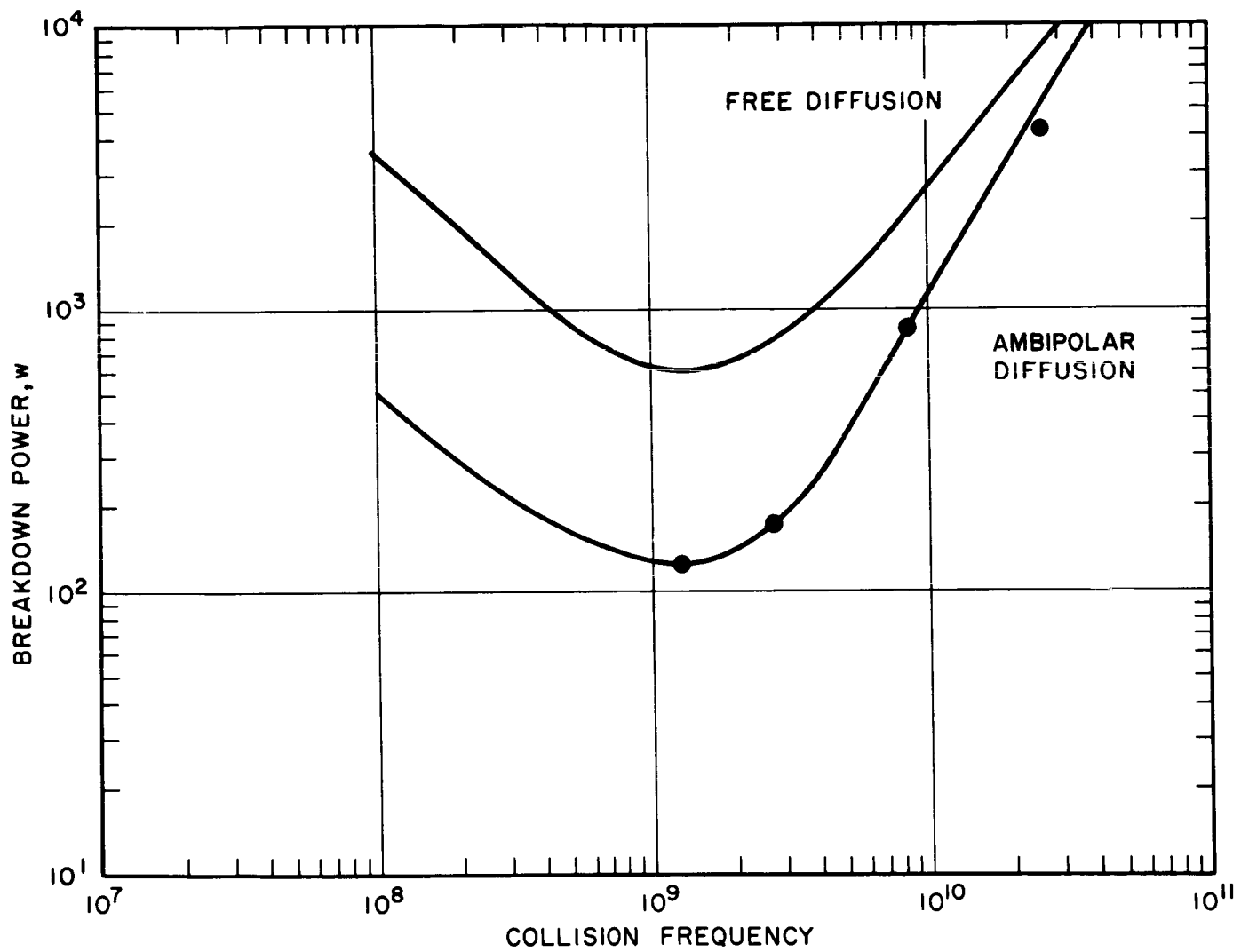


Fig. 5-18. Breakdown characteristics of 2-in. L-band slot antenna



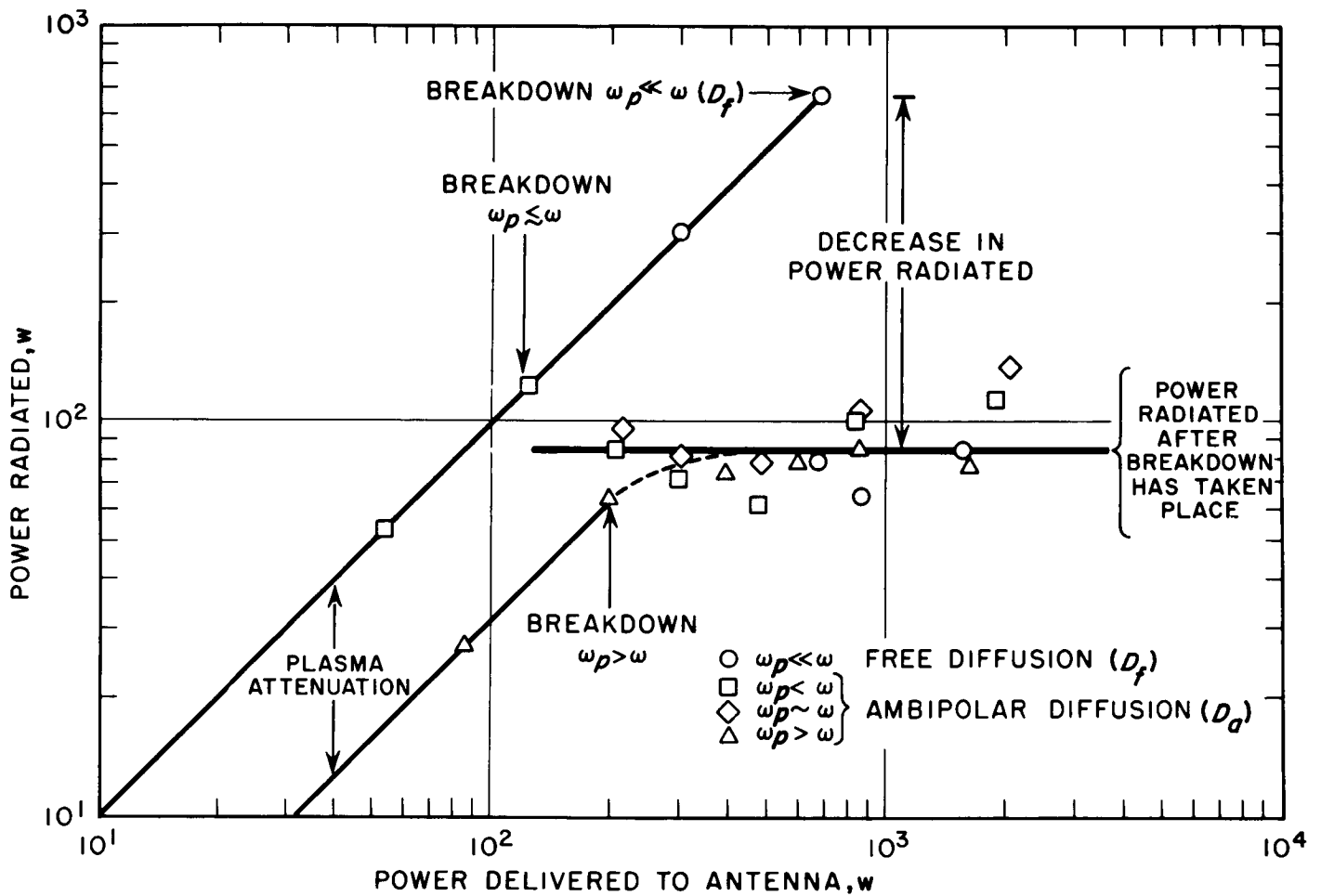


Fig. 5-19. Power radiated normal to an L-band slot antenna

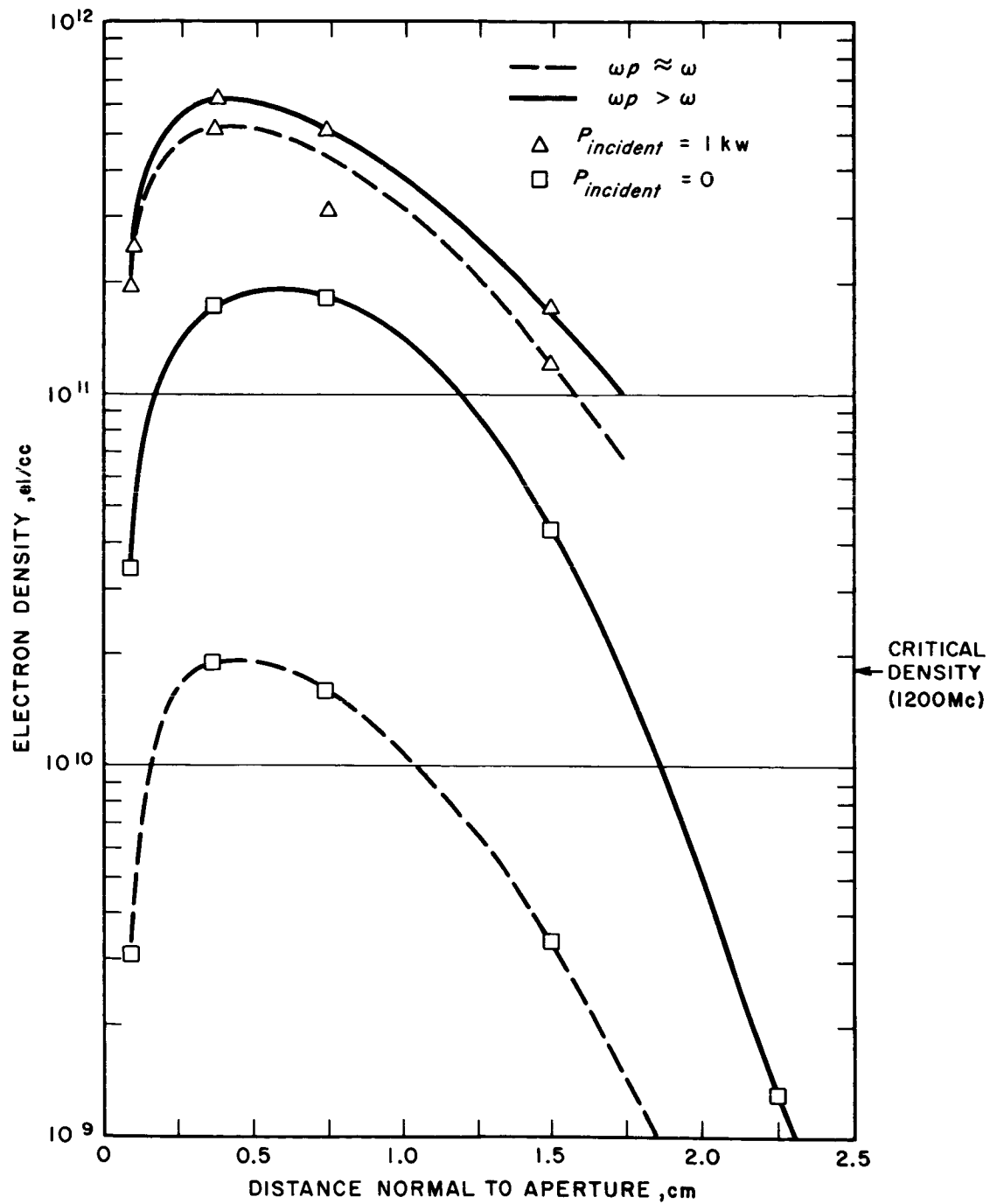


Fig. 5-20. Effect of RF field on plasma density over L-band slot

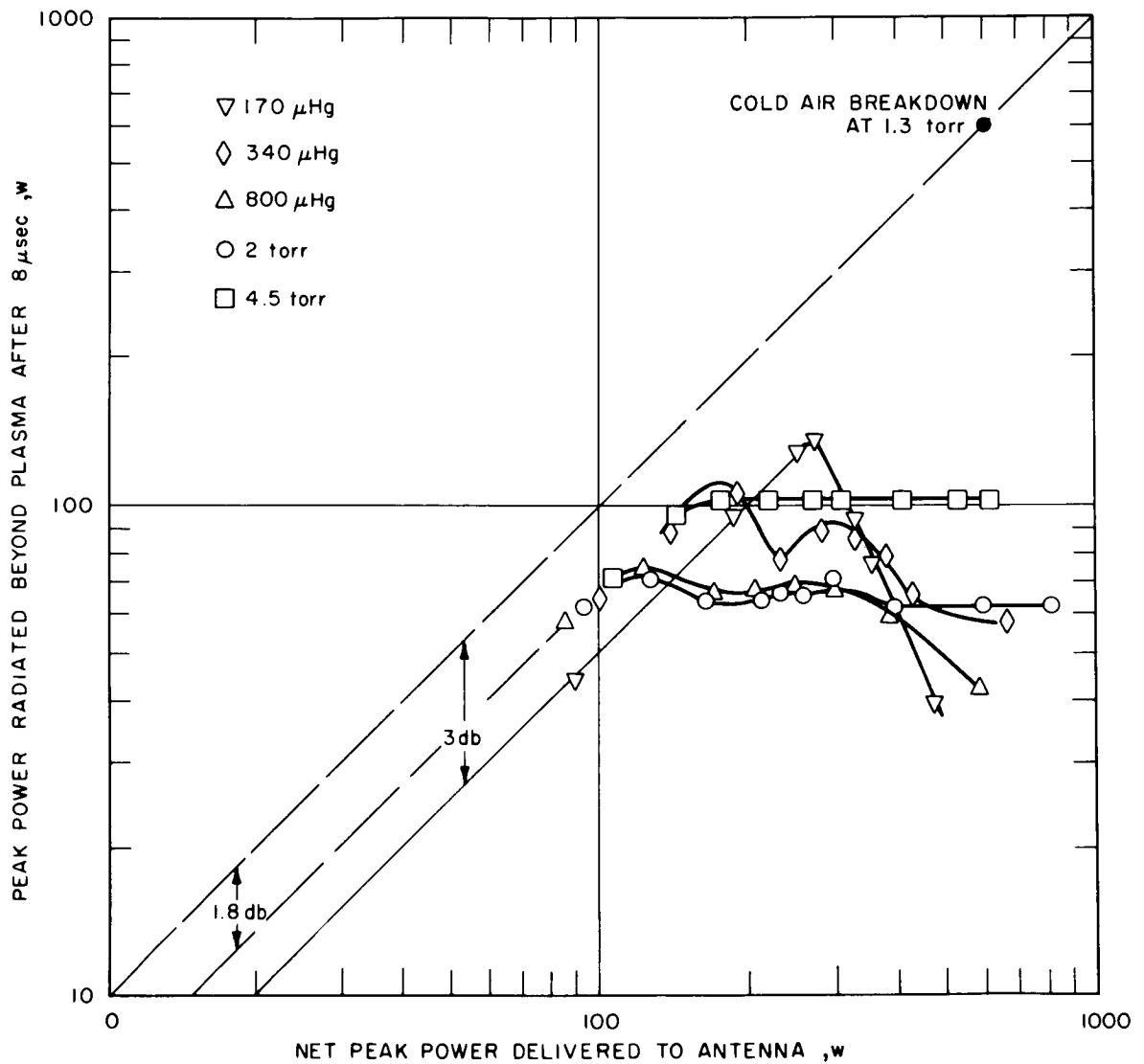


Fig. 5-21. Power radiated normal to L-band slot antenna

## 6. HIGH-VOLTAGE EFFECTS IN SATELLITE-BORNE SPECTROMETERS

E. M. Reeves  
Harvard College Observatory

It was mentioned this morning in one of the other papers that a significant amount of difficulty had been experienced with the Orbiting Solar Observatory experiments. I'd like to spend a few minutes this afternoon describing particularly the experiences of the Harvard Observatory, which has an experiment consisting of a scanning spectroheliometer, the purpose of which is to measure the incident energy from the solar disc in the wavelength region between 500 to 1,500 Å.

Figure 6-1 shows that the spacecraft used for the OSO is a rotating wheel which has on its top a segment containing solar cells that remains pointed toward the Sun and carries two instruments side by side in the sail portion of the spacecraft. The experiments are tilted up and down within the semicircular wheel and sail is driven in azimuth against the wheel segment to maintain an orientation to the center of the solar disc to better than one minute of arc.

Figure 6-2 is a photograph of the Harvard instrument removed from the spacecraft. The instrument is covered with a gold-plated dust cover for thermal balance considerations. The eyes which control the orientation to the solar vector clamp on to the experiment as shown. Optical alignment is carried out perpendicular to that plane. The entrance aperture of the experiment is shown with a plexiglass cover.

The rear portion of the experiment is shown in Fig. 6-3. The instrument necessarily has to be without windows because in the wavelength region from 500 to 1,500 Å, there are no transparent materials. Outgassing is a problem. The instrument was provided with a large pumping port at the back of the instrument. Our approach has been to use an optically dense baffle with two screens. Some of the detail of the screen can be seen in the figure. It is a 90% transition etched screen of about 1/4-in. spacing with  $\pm 19$  v between the two screens, which are insulated from the main body of the spectrometer.

The instrument consists primarily of a spectrometer. The entrance aperture, or optic axis, is along the length of the instrument. The Sun's radiation enters through a 1- or 2-cm<sup>2</sup> aperture again screened with two screens; this aperture also serves as a pumping port. The light passes down the length of the spectrometer onto

a platinum-coated mirror, which focuses the Sun's image. The Sun's image is of the order of a few millimeters. In the center is placed a  $100\mu^2$  entrance slit that selects the light from the central portion of the solar disc of about 1 to 2 arc min and allows that radiation to enter onto a concaved diffraction grating ruled in gold, which in turn images the dispersed radiation on the exit slit, behind which is a detector. The zero-order, or specular reflection, is imaged to a visible light detector.

Figure 6-4 shows the forward end of the instrument. You can see the entrance aperture; the grating is moved by a stepping motor gear chain and lever mechanism. A Johnson-Onaka mounting rotates the grating about a point off the Roland circle. There is a snout (not shown in Fig. 6-5) which limits the field of view of the photomultiplier so that it only sees the diffraction grating. Shown in Fig. 6-5 is the mirror, the entrance aperture, the exit aperture, and the third zero-order slit. Some of the electronics are contained in separate boxes.

The electronic systems of the experiment need only concern us in this discussion because we are only interested in high voltage effects. The detection system consists of an open-structured photomultiplier with crossed electric and magnetic fields (produced by the Bendix Corporation primarily for mass spectrometer application). The photomultiplier is accompanied by an impedance-matching preamplifier, a moderate gain wide-band amplifier, and a 10-Mc binary counter shift register combination. The high-voltage power supply, which runs the photomultiplier, was of a commercial manufacture integrated into the experiment during final assembly. The high-voltage terminals were porcelain leadthrough insulators exposed to the interior of the instrument. High voltage was conducted from the power supply to the photomultiplier through high-voltage wire of ample insulation. Short leads from the voltage divider network provide the various voltages required at different parts of the photomultiplier from the one high-voltage supply. Those leads were of low-voltage hookup wire, and no attempt was made to assure smooth corona-free surfaces. The power supply was highly regulated and protected against overload current. The photomultiplier, which is seen inverted in Fig. 6-5, was operated with a grounded anode (i. e. , the photocathode was at high negative potential), which would tend to attract positive ions into the region of the photomultiplier.

The main structure of the spectrometer was provided with optically dense pumping ports which were screened at  $\pm 19$  v. The electrical harness (which connected the various electronic boxes) was constructed from individual insulated wires bound together and shielded with braided wire. The shield was insulated from the case of the spectrometer and was connected to signal ground through capacitors. All the electronics were contained in solid metal cans filled with epoxy. An attempt was made to minimize outgassing regions within the instrument because arcing had been observed on previous rocket flights carried out to test the OSO-B instrument.

The Harvard instrument suffered a failure soon after turnon in orbit because of high-voltage breakdown. (Notice how I used "breakdown" rather than "arc" or "spark" or "corona," because the exact mechanism is a bit hard to pin down.) This breakdown occurred after 24 hr in orbit, so I think it's germane to discuss briefly the prelaunch qualification program which was used to test the instrument to qualify it before flight.

All electronics were qualified in a prescribed fashion including shock, vibration, excessive temperature soaks and fluctuations, and thermal vacuum. All electronic systems and subsystems unquestionably survived all such tests. Since high-voltage difficulty had been experienced on a previous rocket flight, a series of tests were carried out to determine the immunity to this effect. Care was taken to minimize regions of trapped gas and to provide adequate pumping area to the vacuum environment. Additionally, the instrument was qualified in a fully operational mode in a large vacuum tank provided with an ultraviolet light source. During the course of these tests the instrument was energized many times. Each time we took the precaution of pumping to  $10^{-5}$  torr and leaving it at that pressure for 1 hr before applying the high voltage. In no case was a high-voltage problem ever observed either through the digital link from the photomultiplier or in a current monitor in the analog channel, which was a monitor for the primary current to the high voltage power supply. To test the instrument operation in a large photon flux, the instrument was subjected in the vacuum tank to as large a Lyman  $\alpha$  flux as we could generate with a microwave discharge. The total flux entering the system in the 1215 Å hydrogen line was approximately the same as could be expected in orbit. There was no indication again of any difficulty due to photoemission on surfaces or photoionization of residual gas inside the tank at a vacuum of  $10^{-5}$  torr. One would expect that the vacuum to be expected in orbit at 300 miles is of the order of  $10^{-9}$  torr.

A very similar rocket instrument, at one stage, was operated in a normal vacuum region, followed by an increasing pressure environment. High-voltage breakdown was not observed until the pressure had risen well into the  $10^{-3}$  torr region. This pressure region was, of course, some 2 orders of magnitude above the normal operating pressure for the laboratory and approximately 6 orders of magnitude above that to be expected in a 300-mile orbit. Hence, in our opinion the instrument had been adequately tested for the environment in which it was expected to operate. The instrument was incorporated along with the other experiments into the observatory at the prime contractor's office and given a long-duration thermal vacuum test at high and low temperatures. It was in thermal vacuum continuously for over a week. It was put in a vacuum tank as a completed observatory at least several times. However, to further ensure the success of the mission, it was decided to allow the instrument to remain in orbit for approximately 24 hr before commanding the high-voltage to the detection system. These precautions proved to be inadequate.

The instrument was energized from Fort Myers, with real-time observation of the data at Cape Kennedy and also at Goddard Space Flight Center. The instrument was on for approximately 110 sec during which two failures occurred in the detection system. After this time the "off" command was executed. Although a detailed analysis of the exact failure mode is not possible with the incomplete data we obtained, a failure mode is suggested, which we feel adequately explains the observations.

The instrument was turned on in a slow wavelength scanning mode. In this mode the normal low background of several counts during the gate time of 40 millisecc was observed, accompanied by a grating reference position bit and several very high count words. Experience had shown that these high count words were indicative of a high-voltage breakdown, which also causes an extra step to the grating drive mechanism. After some 28 data words were transmitted (one data word being approximately 160 millisecc) the reference bit disappeared prematurely. The number of high-voltage breakdowns (observed as high count rates) was consistent with the number of extra steps in the grating drive system.

The following 46 data words contained the normal background count, accompanied by intermittent spikes from the high-voltage breakdown. The data format then suddenly changed to complete zeros, followed by 41 words and later by a change to all "ones." The change to all "ones" occurred during the serial readout of the  $2^6$  binary bit. The  $2^5$  to  $2^0$  and all subsequent transmitted bits are read into the telemetry as

"ones." The 16-bit binary counter is combined with a shift register. A count from the photomultiplier detection system is stored in the flipflops of the counter, which then become shift registers and the 16 bits are read out serially into the telemetry system starting with the highest order bit. We observed the failure as  $2^6$  was being read out. Failures in the last shift register stage can occur according to an analysis of the circuit in two discreet modes, in which either zeros or ones will be read out. All indications were that the output shift register failed twice in one or both of these modes.

High-voltage breakdown in the experiment appears to be accompanied by a slip in spacecraft sail data subcommutator, which samples analog data voltages throughout the spacecraft. Slippage in the subcommutator, excess current drawn in the primary of the high-voltage power supply, an intermittent high data count followed by failure of the output shift register stage, all point to a high-voltage breakdown as the cause of the instrument failure. Presumably a transient pickup on one of the lines of the electrical harness, arising from one of the high-voltage breakdowns, was responsible for a failure of the transistors in the output stage of the shift register. The experiment was commanded off for approximately 3 mo while the remainder of the experimenters on board were using their instruments, at which time it was decided to reenergize the Harvard instrument. The instrument was off from approximately February 14 to May 11, and when energized again on May 11, there was no further indication of high-voltage breakdown, nor has any been observed since that date.

Following the failure of the instrument in orbit, a series of tests were carried out on the flight's spare instrument in an attempt to determine the cause of the high-voltage breakdown. One of the possible causes of the high-voltage breakdown would be insufficient pumping of the instrument in the space environment, possibly through excessive outgassing, although this would not really be consistent with our laboratory tests on the experiment, on the one hand, nor with the thermal vacuum tests of the completed observatory, on the other. The flight spare was placed in a thermal vacuum facility in our own laboratory with pressure gages inside and outside the instrument. At  $10^{-9}$  torr in the chamber there was approximately one decade of pressure differential across the interface. It may, therefore, be safely assumed that gases evolved in the experiment causing a pressure differential of one decade could not be responsible solely for the difficulty observed.



One suggested cause for the production of the ionization necessary to produce such high voltage breakdown is the production of ions or electrons inside the instrument through photoionization of residual gas by the extreme ultraviolet radiation of the Sun. Twice in the 10 days immediately following the first turnon after launch (February 4, 1965), the instrument was energized as the spacecraft came into sunrise, but before orientation with the solar vector had been achieved. The intense ultraviolet radiation would then not enter the entrance aperture of the experiment. No significant diminution of the high-voltage breakdown frequency could be observed. These tests are consistent with the prelaunch laboratory test (in which we also tried to produce photo-ions within the instrument) and do not indicate that photoionization of residual gas was the primary culprit.

The high-voltage circuit of the flight spare was purposely arced in the laboratory at atmospheric pressure, first with a mechanical spark gap, and then with the photomultiplier itself with reduced mechanical tolerances to check the radiative coupling of the breakdown of the transients into the lines of the harness. After careful investigation it was discovered that nearly all of the lines of the instrument received transients of several hundred volts at tens of nanoseconds duration. At lower pressures ( $10^{-5}$  or better), the wavefronts could be even sharper due to the lower ionization time associated with discharges in high vacuum. Although extensive arcing of this type was observed to produce transients more than adequate to destroy transistors, no failures could be produced in the flight spare instrument after many hours of arcing tests, let alone after the 12 sec the instrument had been in orbit. Although this test is somewhat inconclusive, it does illustrate that if such an arcing test had been incorporated into the prelaunch testing program, all modules would have passed the test successfully. I think, though, that in spite of this negative test result such a phenomenon is almost certainly responsible for the failure of the shift register stages.

A detailed inspection of the disassembled flight spare photomultiplier revealed that particles had adhered to various parts of the structure during storage and testing period. These particles remained even after ultrasonic cleaning and were presumably due to the magnetic fields associated with the Bendix photomultiplier. There is some evidence to indicate that such contamination can enter the instrument through the dry nitrogen purge gas which was used to prevent just this problem. The reduced tolerances produced by the contamination would certainly be responsible for such an observed failure, but again would require that the particle causing the difficulty either

burn off, evaporate, or somehow fall off between the last arcing observed on February 14, and the turnon again on May 11th. For in the 15 complete activated 90-min orbits between May 11 and July 8, no high-voltage breakdown could be observed, either as slips in the spacecraft's subcommutator, or as excess current drawn in the primary of the high-voltage power supply, the normal binary data link being completely unusable.

The high-voltage problem exhibited by the Harvard instrument was by no means unique on the OSO-B2 spacecraft. The majority of other experimenters also suffered difficulty and premature failure, presumably owing to this problem.

If the results from the prelaunch and postlaunch tests are valid, there does not seem to be a consistent explanation for the failure within the Harvard instrument. It is also difficult to understand how the evaluation tests of the other experimenters seemingly also failed to provide an adequate explanation, or why no indication about outgassing or other problems was evident from the thermal vacuum tests of the completed observatory.

It is possible that ions from some source either within or without the spacecraft were responsible for this difficulty. One suggested source of ions is the low natural concentration of ions at this altitude swept into the entrance aperture of the experiment when the spectrometer comes into sunlight and the velocity vector is aligned with the solar vector. This would certainly cause a great enhancement of the ion concentration inside the instrument and could cause a high-voltage breakdown. This mechanism should, however, present a rather constant difficulty, and we don't understand if this is the true mechanism, how the instrument would either become less susceptible to the ion flux, or why the ion flux would go away. The absence of high-voltage breakdowns after many weeks in orbit does not seem to be consistent with this explanation.

An additional difficulty might arise from normal spacecraft outgassing or leakage from the spacecraft or experimenter gas supplies, particularly the OSO-B2 flight. The gases would certainly be ionized by the ultraviolet radiation (a condition not evaluated in the thermal vacuum test) and would tend to disappear with time.

A report describing the Harvard instrument and the details of the failure and test programs is currently being prepared. But, needless to say, a completely satisfactory explanation for the high-voltage difficulty on the OSO-B2 satellite is just not available.

Since no one cause of the high-voltage difficulty can be located, we are of necessity, following a shotgun approach for prevention. A considerable improvement in all phases of the engineering has been implemented. Briefly, these approaches include the following:

1. A reduction of the outgassing through elimination of further potential trapped gas pockets and the placing of the electrical harness (a bound group of wires and a potential source of outgassing) in a separately pumped compartment as much as possible.
2. The photomultiplier itself has been redesigned with improved insulation. It will be enclosed in a separate box magnetically and electrostatically shielded, and assembled under degaussed conditions and white room laminar flow, and will be operated with a grounded cathode to eliminate any possible attraction of positive ions through the exit slit of the spectrometer.
3. An exhaustive effort has also been implemented to select only fully qualified and aged components for all of the electronic units within the instrument, and to provide for as much filtering of transients from the lines of the harness as is consistent with the sound redundancy requirements. All units will again be tested for operation under arcing conditions without deterioration of performance. Every effort will be made to have a system pass through the corona region without harm to any of the systems. Some of our preliminary tests indicate that this can certainly be achieved.
4. The entire experiment will be assembled under laminar flow conditions to ensure cleanliness. The nitrogen purge gas line which was used to obtain a stable atmosphere within the instrument will be electrostatically and magnetically filtered to remove dust and any magnetic particles which come through the purge line from the nitrogen gas bottles.
5. The high-voltage power supply used for the OSO-D instrument will be self-limiting to reduce the power that may be dissipated in arcing conditions.

The prototype for the OSO-D instrument incorporating most of the above changes, as well as many additional changes, is now nearly complete, and testing has begun on the evaluation test program. Assembly of the flight instrument will begin

shortly, and launch of the OSO-D is expected some time next summer. We will then hopefully have achieved a formula on what to do in order to overcome the high-voltage problem.

#### OPEN DISCUSSION

MR. JACKSON: I have a comment, I think, or perhaps a question. The problem you present is very interesting in this breakdown. A couple of things occur. One, I think you brought out one of them that one of the other experiments could have contributed a small atmosphere around your satellite for a period of time which could have bothered you as well as other experiments. The other thing that occurs to me is this: In your testing which was very, very thorough, I think did you try to simulate your soft x-ray; that is, below the vacuum ultraviolet, you were actually measuring the high energy particles in the soft, and perhaps even cosmic, ray region?

DR. REEVES: No. We did energize the instrument over the wavelength region down to 500 Å. We were illuminating the instrument with a gas discharge light source off a grazing incidence, off axis probably at 80°. We would normally have expected to have illuminated with no radiation lower than approximately 100 Å, and we probably did not produce in any quantity radiation much below 300 Å.

MR. JACKSON: In other words, I was thinking that maybe the subvacuum ultraviolet--the soft x-ray stuff--may have been bothering some insulation, ionizing enough to bother you.

DR. REEVES: That would just go away.

MR. JACKSON: Well, perhaps whatever it was that was being ionized was eventually destroyed.

DR. REEVES: Yes. But in the test made in the few days following turnon in which we turned the thing on when it was not pointing towards the solar vector, arcing was still observed. In this case, if the flux is coming from the Sun, it would not then have been passing into the instrument.

MR. JACKSON: First, I don't think it necessarily has to come from the Sun. Secondly, I think we have found that some of the stuff from the Sun--the soft x-rays and so forth--may be bordering on the vacuum ultraviolet and follow a magnetic field path, which is not a direct vector from the actual body of the Sun.

DR. REEVES: Yes.

MR. JACKSON: The other thing I had to make was more or less a suggestion.

DR. REEVES: May I interrupt just one second to ask you a question on this?

MR. JACKSON: Yes.

DR. REEVES: How would you go about producing such a simulation?

MR. JACKSON: A Hinteregger gas discharge source; that strikes me as being the apparent one.

DR. REEVES: Yes. Or presumably a Weissler-type capacitor charge.

MR. JACKSON: Well, a continuous gas flow source is the regular one I've used and it seems to be pretty good. You can get anything out of it you want depending on what you put into it, what kind of gas you flow through it from hydrogen through the inert gases. The other thing was more a suggestion I've found quite useful. One of your worries seems to be this purity of the nitrogen you have in your flushing through and so forth. One way I've found of getting very pure nitrogen very cheaply without having any trouble is to use the nitrogen as a liquid. Get yourself a little bottle of liquid nitrogen, let it gassify, and use it. You know it's pure. You know it's dust free. You know it's got nothing in it. It can't have.

DR. REEVES: In fact, this technique was used at the prime contractor's facility. We did not use it at our facility for no good reason; we didn't appreciate the problem.

I might mention that one of the main problems we have has nothing to do with high voltage, and that is the outgassing from some of the materials used to encapsulate electronics. The effect of these materials as they outgas is very much a problem because it destroys reflectivity of optical surfaces in this vacuum ultraviolet radiation region. Any material which outgases enough so that a mass loss can be measured, is coating optical surfaces with practically a measurably thick layer; and monomolecular layers are more than adequate to cause a strong decrease in reflectivity particularly when these layers are then exposed to extreme ultraviolet radiation. I'm sure many of you here will have your electronic systems used in conjunction with optical systems, and I would be interested if anybody here has any comments on this problem.

MR. CHARP: There are a couple of questions and comments I'd like to make. In the case of the Nimbus spacecraft during thermal vacuum testing, we did instrument the interior of the spacecraft and found that we had a pressure differential of slightly over a decade between the chamber pressure and inside the spacecraft, so your comment about finding this is not unusual.

DR. REEVES: May I ask here, what sort of ratio your pumping aperture was, in comparison with the volume being evacuated?

MR. CHARP: I believe that our pumping aperture was about 40 in. in diameter. This is a 39-ft space chamber, and I believe we have two apertures on that chamber.

The next item I wanted to ask was, who is fabricating the instrument?

DR. REEVES: We are.

MR. CHARP: Then presumably you have white rooms when you commented that you're going to fabricate this instrument in a clean room? Do you mean an industrial white room?

DR. REEVES: The instrument I have been describing was assembled only under rather standard laboratory conditions because there was no indication that there was any difficulty arising from contamination. The instrument which I spoke about, the OSO-D instrument, will be assembled again in the same laboratory only using laminar flow benches. All assembly will be done in this kind of environment, not a white-room type of environment.

MR. CHARP: Did I hear you mention that the instrument is going to be magnetically cleaned?

DR. REEVES: The instrument contains a magnetic structured photomultiplier which will be contained in a magnetic and electrostatically shielded box. The instrument itself is not magnetized and I couldn't tell you what the residual magnetic field is outside the region of the photomultiplier, but it's rather low.

MR. CHARP: With respect to your last question about outgassing and its effect on optical surfaces, this is a problem with which we have been concerned and are continually concerned on Nimbus. During the design of Nimbus A, we simulated the optical paths and the outgassing paths from many of our potential sources of outgassing to the optical surfaces, and these are essentially straight line paths. They also are very intimately related to the temperatures that

would be encountered on the optical surfaces because the outgassing products will tend to deposit on the colder surfaces. We carried out extensive tests under thermal vacuum conditions and determined as a result of these that there was not a problem of loss of optical transmission to worry about. We undertake very much the same kind of testing every time we may undertake to use a new material. Unless you have essentially a straight line path to the optical surface, I don't think that there is a particular problem, at least insofar as optical surfaces for cameras are concerned.

DR. REEVES: This is very strongly wavelength-dependent, and the problem becomes much more difficult as you get below 2,000 Å. In the instrument we had a monitor mirror which we removed from the instrument frequently and took back to our laboratory for reflectivity measurements. We could find a change in reflectivity with time. Sometimes this could be removed by cleaning with ordinary solvents, indicating it was an oil of some kind and then after a few cleanings of the optical surfaces it just wouldn't recover. We started a rather broad program to measure reflectivities in the 300 to 1,500 wavelength angstrom region and the effect on reflectivity from outgassing from plastics and the common materials inside any normal experiment. There is some indication from published work on NASA that there is a deposition from black anodized aluminum surfaces on optics and on all our instruments; all our cans are black-anodized. This has been observed under ultra-high vacuum conditions. I was told the other day that Goddard has begun to implement a program to start measuring the effect of various materials on reflectivity at the one wavelength of the Lyman- $\alpha$  line.

MR. SOMER: What is the turnon time for the high-voltage power supplies to the magnetic multiplier?

DR. REEVES: I really don't know. Would you know, Mr. Schildkraut?

MR. SCHILDKRAUT: The primary power supply is energized instantaneously. It's a relay controlled by the Ball Brothers satellite central power control system. The output of the high voltage rises approximately 50% in 1 sec, and from there on it is a RC-charging; so I would say that it's completely up to the voltage, 2,000 v in 3 sec.

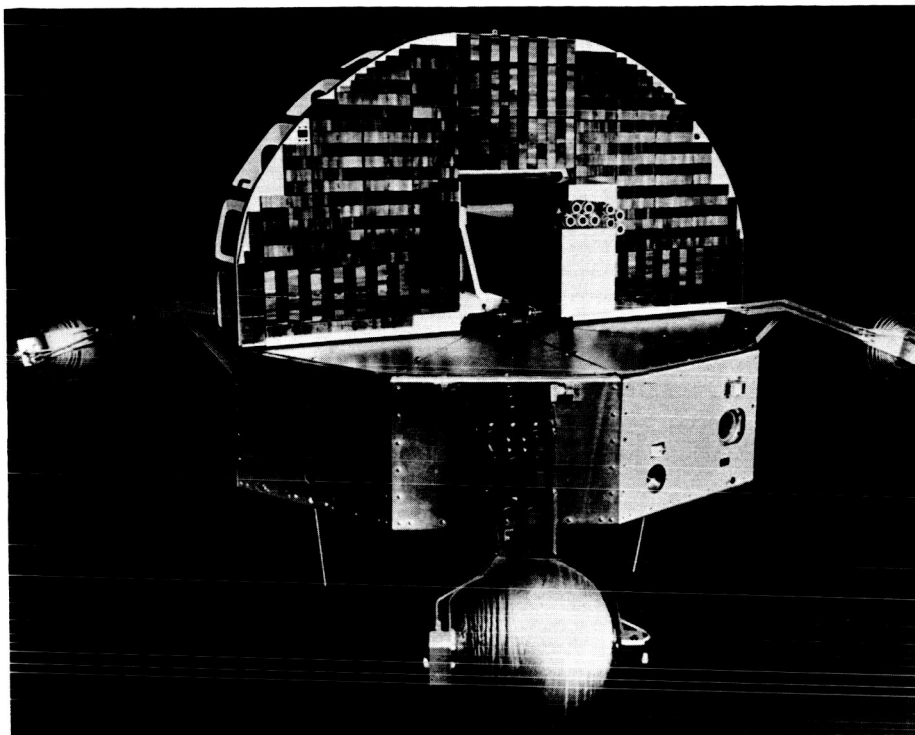


Fig. 6-1. Orbiting Solar Observatory

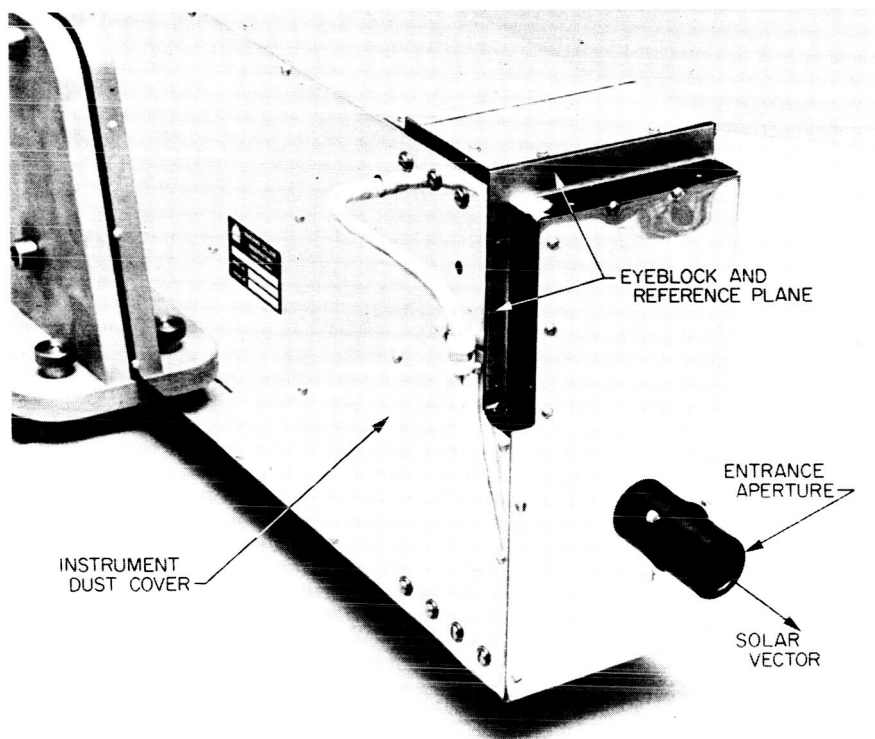


Fig. 6-2. Front view of Harvard instrument



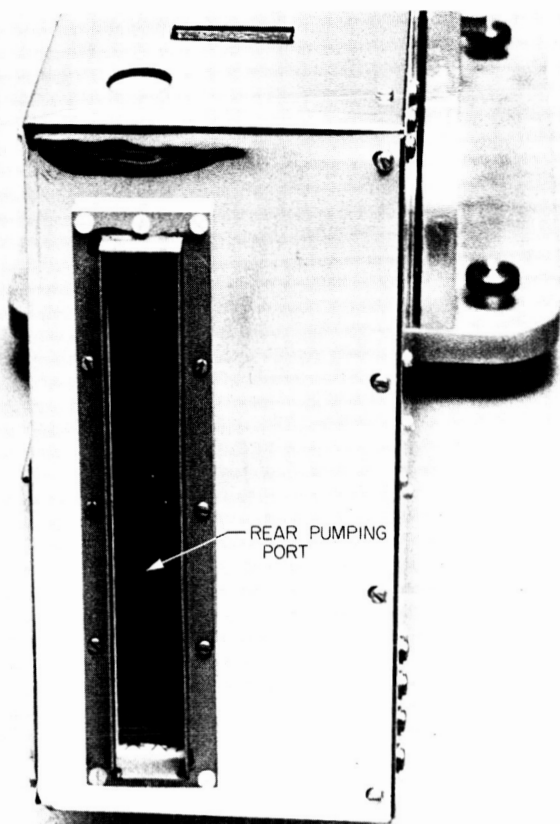


Fig. 6-3. Rear view of Harvard instrument

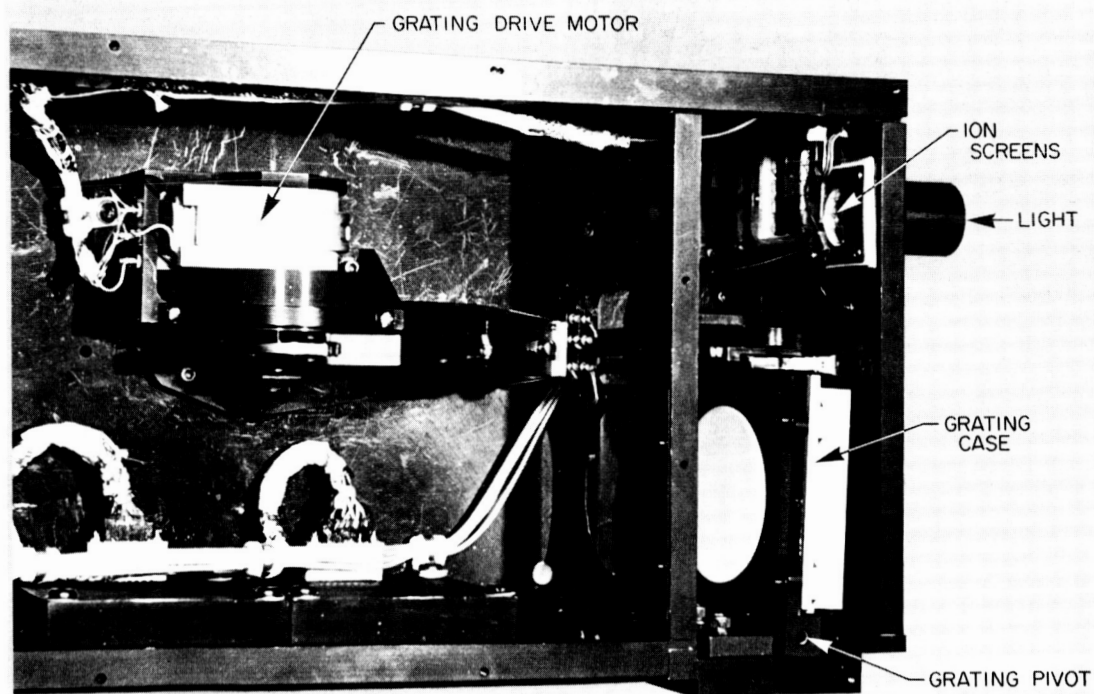


Fig. 6-4. Instrument interior - forward end

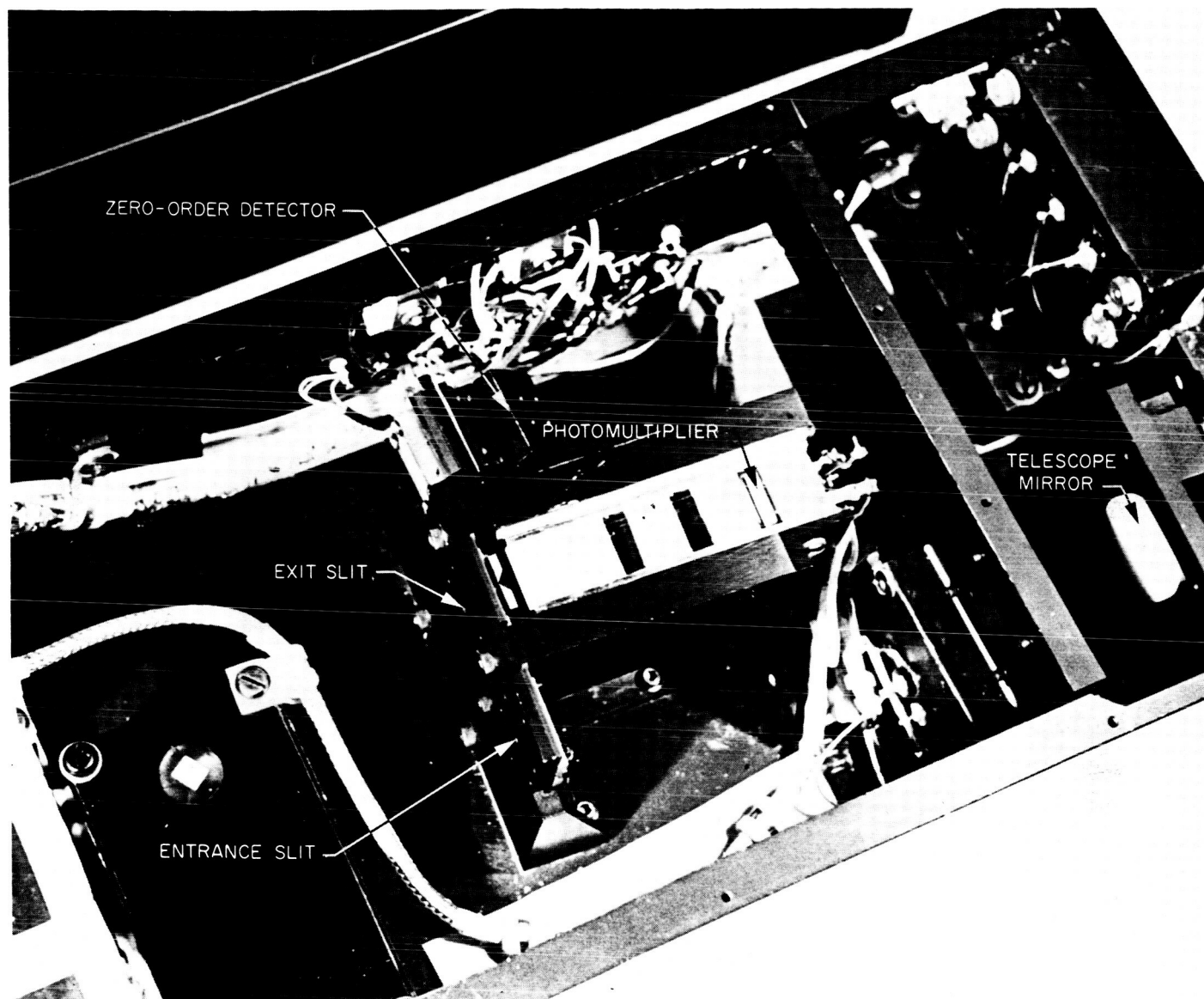


Fig. 6-5. Instrument interior - aft end

## 7. DESIGN AND TEST OF A HIGH-VOLTAGE POWER SUPPLY FOR SATELLITE APPLICATION

F. Clauss, G. Dallimore, D. Tashjian  
Lockheed Missiles and Space Company  
Sunnyvale, California  
(Presented by D. Tashjian)

During the past year, Lockheed had occasion to fly a satellite payload that required a high-voltage power supply of more than 1,000 v. The character of the payload was such that operation was not required until after orbital altitude was reached; not, in fact, until several orbital passes at about 150 n. mi. This fact suggested the possibility that we could assume that the pressure within the payload and the power supply would be below the critical region. There were some thoughts that perhaps a decade of pressure difference between the real world outside and the power supplies within might be representative. In order to make some determination of just what this pressure might be, we did a bit of searching in our own files and came up with the answer that we really didn't know. There was an appallingly small amount of data that would indicate just what the pressure would be within a payload box as compared to the standard ARDC atmosphere at 150 n. mi. Nevertheless, we then looked at the possibility of assuming that the ARDC atmosphere would hold within the payload boxes and considered various means of insulation for high-voltage protection.

We might well have elected to vent, as many of the people that have talked before me here have suggested. We might have used a pressurized container. We might have used immersion in a dielectric fluid which is, after all, a special case of pressurization, or we might have elected to pot the apparatus. Because of the difficulty of determining exactly the outgassing rates should we elect to vent, we decided to conduct a few simple laboratory simulation experiments.

We constructed a chamber which we have shown in Fig. 7-1 consisting of a piece of steel pipe with a welded cap and a welded flange at the opposite end with vacuum gages inserted so that we could read pressures from about  $10^{-1}$  mm Hg on down below the critical region, using the ion gage for the lower region. The cover plate was fitted with a threaded hole such that we could insert orifices of various sizes and thus simulate various size vent holes. Figure 7-2 shows the cover plate as it was constructed. The hole is threaded and is about 1 in. in diameter. This was the largest vent hole used. We also tried tests with 1/4- and 1/16-in. holes.

Within the compartment, we placed a circuit board (Fig. 7-3) that had a number of resistors. We could heat this board to typically high temperatures to simulate the outgassing of electronic components as power was turned on. Admittedly the circuitry density here does not approach the packing density we were going to get within our boxes, but it did provide a controlled means of determining outgassing rates. Each time we ran a test, we replaced the circuit board with a fresh one. We wanted one that was typically contaminated with water vapor, people dirt, etc., although we did make some efforts to clean it before we inserted it in the chamber. We did not deliberately smear it with lab dirt, but we did use a fresh board for each of the tests. We also ran tests both with the board bare and with conformal coatings applied to it.

Figure 7-4 shows the kind of results we obtained from these outgassing tests when the chamber was placed in a 30-in. bell jar. We pumped down fairly rapidly and then we applied heat. The result was bursts of outgassing which raised the pressure quite a bit. I don't argue that these curves are illustrative of what you would have in typical electronic boxes; these curves represent only a very special case. They represent only one class of materials; they represent only a certain ratio of surface and volume to the outgassing orifice. What we really think they show is that it is difficult to vent and that one must really work if one is going to be sure that when the power is turned on the pressure doesn't rise to a dangerous area because of outgassing.

As a result of these experiments we decided fairly early that we would not vent, or at least that we would not depend on venting as a primary means of high-voltage protection. We also decided that we would not pressurize, because of the added weight of pressure vessels, the problems of measuring what the pressure is inside the box at liftoff, and the leak rate of the box. The problems associated with dielectric fluids, which have already been mentioned, led us to the conclusion that we would pot the assembly. We did make some attempts to use oil-filled components. By oil-filled components, I mean an oil-filled capacitor in a rectangular box that has an oil or dielectric fluid in it and a capacitor connected by leads to a high-voltage bushing. The definition alone illustrates the pyramiding problems that one can encounter in this method. With us, the first thing that happened was that as we took the device to higher altitude in the lab chamber, the sides of the box expanded even though there was a bellows to take care of thermal expansion of the oil. This expansion reduced the pressure on the oil, and the capacitor flashed over internally. To fix this, we added reinforcing ribs to the outside of the box and a spring behind the

bellows to maintain tension. It worked but was heavy and crude. I should add that we did not fly this device in the power supply. However, it is illustrative of the kind of problems encountered with oil-filled components.

The method finally selected, as I said, was to encapsulate, or pot, all the high-voltage circuitry and to test the assembly through ascent. We were going to test through ascent, and what we did was to conduct extensive testing at  $10^{-1}$  and  $10^{-2}$  mm Hg to assure that any unexpected outgassing or inadvertent turn-on would not ruin the system. When I say extensive testing, I mean that, in addition to the developmental and confidence testing on the subassemblies and on the boxes themselves, the acceptance test and the qualification test required that the boxes operate for something like 25 times the normal life cycle at pressures of  $10^{-1}$  and  $10^{-2}$  torr. The entire system was placed in a chamber and operated for four times the total mission, which we felt was sufficient to ensure operation.

Unfortunately, the decision to pot the assembly was not made until some little time had passed and design decisions had been fairly well crystallized. The insulation materials and wires had already been selected. Therefore we had to conduct some quite extensive tests to determine the compatibility between the candidate potting compounds and the materials and metallic finishes that had already been selected. Some problems arose because silicone wire had been selected. Silicone wire is great from the standpoint of high-temperature operation, but it's a substance to which potting compounds don't adhere. There's really only one thing that will stick to silicone wire and that's more silicone; and then you are faced with the problem of priming metal surfaces. There were some small places where we used Teflon wire, and we had the problem of sticking potting compounds to Teflon. We conducted a number of compatibility tests and in some cases altered the basic insulation material in the box so that it would be compatible with potting compounds.

It isn't within the scope of this talk to dwell on potting problems, but I'd like to mention a few of them because I think they bring out the fact that this path that is not without its thorns. For instance, you might have poor bond due to improper surface preparation, insufficient cleaning, roughening, or priming too much or too little. This primer is a snare and a delusion. You can put too much primer on and then the compound won't stick. You may have potting voids due to short pot life of the compound, inadequate degassing of a compound, or faulty pouring techniques (it's very easy to develop potting cracks at thermal stress lines), or you may have

insufficient curing of the cast material. The typical problem of this kind involved a failure of the potting at the top of the high-voltage capacitor bushing as shown in Fig. 7-5. Beneath the piece of potting compound is the high-voltage capacitor (that had originally been an oil-filled component) and sticking out of it was a porcelain bushing. After some few hours of operation we had a flashover traced to a glazed surface on the bushing. We corrected this problem by lightly sandblasting the bushing surface and repotting. I mention these things because I think they're the sort of problems that one gets into. It is possible to solve the problem with potting materials. It is possible to write procedures so that only moderately skilled personnel can produce units one after the other and have them all work. I think we've proved that point.

I would like to illustrate another problem that has already been touched on today. That is the problem of corona. Figure 7-6 is not nearly so spectacular as some we saw earlier today, but here is a unit which was really glowing. As people say, it lit up like a Christmas tree. In this case merely sealing the high voltage so that it doesn't break down is not necessarily sufficient. The corona did not interfere with the operation in any way. It didn't really argue very well for the life of the unit, and there was possibility of EMI problems, i. e., interference with other payload functions. But more certainly, we were courting disaster for the ultimate failure of the insulation due to corona degradation, the local heating, chemical changes, and the like. Each class of insulating material will respond differently to this corona degradation. Any test for life expectancy would be a long and time-consuming process, so we elected to get rid of the corona. This seemed easier. To do it we decided to cover with a metallic shield all exposed surfaces where there was any evidence of corona or where analysis showed that we might get such corona. We used rigid metal boxes where possible. In cases in which we wanted flexibility on wires, we used Belden braid potted to the base insulation material of the wire. We might well have bought such shielded wire, but we already had the wire. The program was marching along and time was going so, we merely made our own shielded wire.

Another view of the unit is shown in Fig. 7-7, which may also serve to illustrate some other points. The places where we had the most trouble in the development of this unit were largely at the connections, that is, where a wire terminated on a component. There was no problem in the middle of wires, nor within the components themselves. But where there was a termination of a wire such as at the top of the shielded cans, we had problems. The whole channel shown in the figure was ultimately filled with an epoxy and potted solid rather than just with a small conformal

coating around the area. The same was true of other areas. The low-voltage circuitry was also given conformal coating. In this way we were able to assure ourselves that we had a unit with good integrity. The unit was successfully flown. I might also point out that the total weight of this unit was 58 lb. of which slightly less than 4 lb was potting compound. Since we obviously derived some mechanical support from some of this potting, it's not likely that the whole 7% increase in weight was chargeable to the potting solution. In addition, we vented the unit. We had some openings in it so that there would be no real collection of the gases evolved as the unit was turned on and heat was generated. We operated the power supply and its associated payload in orbit successfully for the entire normal 5-day life of the vehicle.

I think one additional comment may be of interest. We wanted to know just what the pressure would be within the payload rack and boxes. We therefore flew some gages selected for their range for diagnostic purposes in case we should have a failure. We didn't really want to explore what the ARDC atmosphere might be. What we wanted to explore was whether a failure could possibly be caused by operating in the critical pressure region. Four thermocouple gages (reading in the region from  $10^{-1}$  to  $10^{-3}$  mm) were installed in the vehicle. Two of these were outside the boxes but within the enclosed 5-ft-diameter by 4-ft-long payload rack. Two of them were inserted into the boxes, each one of which had about 2 in.<sup>2</sup> of vent hole. The total rack was vented by means of about 60 in.<sup>2</sup> of hole where horizon sensor doors had been removed. Results from the gages showed they tracked the predicted ARDC atmosphere very closely. They bottomed out at  $10^{-3}$  mm and never read on-scale again. The results seem to indicate that we were conservative in our design and that we might have well gotten by with venting only. On the other hand, from the comments that I've heard today about problems involved in venting as the sole method of voltage protection, I think had we to do it over again we would still use potting.

#### OPEN DISCUSSION

MR. MYERS: What temperatures did you test to qualification?

DR. TASHJIAN: The standard specifications we used for qualification testing carried us to 165°F ambient. In the case of this particular box there was a 5 or 10°F temperature rise within the box itself. Now, the curves I had for the outgassing experiments did carry us to 175 and 220°F, as you may have noticed.

MR. MYERS: How about your lower temperatures?

DR. TASHJIAN: Our lower temperature was -30°F, and this range of qualification limits was far beyond the temperatures experienced during the mission. But, it is usually the case that the qualification limits are broader than the expected temperatures.

MR. MAJKA: You mentioned that you had silicone- and Teflon-coated wires. What did you finally do to make the potting compound adhere?

DR. TASHJIAN: We got rid of them. However, I might add that there are solutions to both of these problems. We had other boxes in which we couldn't get rid of these materials. What we did in the case of the silicone wire was to use RTV-type compounds (503 and 511) and take the penalties where it had to adhere to adjacent materials. In the case of Teflon we used a fluorine dip etch. When this is done carefully, one can get fairly good adhesion to the Teflon wire with materials such as RTV and certain epoxies. We ran extensive pull tests in making beads of the potting compound against wires and looked over many suggested materials for getting adhesion to Teflon wire. The fluorine type was the method finally selected.

DR. DAKIN: I'm wondering if, in the case of this sheathing, you didn't just cover up the corona rather than eliminate it.

DR. TASHJIAN: Perhaps I didn't make it clear. We actually bonded the Belden braid to the base insulation of the wire so that there was no air included. If we had merely pulled the braid over the wire and left an air gap in there, we might well have just covered the corona up. But we actually dipped the whole assembly--the wire, its insulation, base insulation, and braid--in a potting compound, pulled vacuum on it, and let it cure so that there was no air trapped in it at all.

DR. DAKIN: However, if you hadn't done this, if the pressure had been low enough in this space, it might still have been all right. With the small spacings at intermediate pressures, your threshold voltage is quite a bit higher.

DR. TASHJIAN: Our theory was that we just didn't know what the pressure was going to be. Therefore wherever possible we eliminated the possibility of voids.



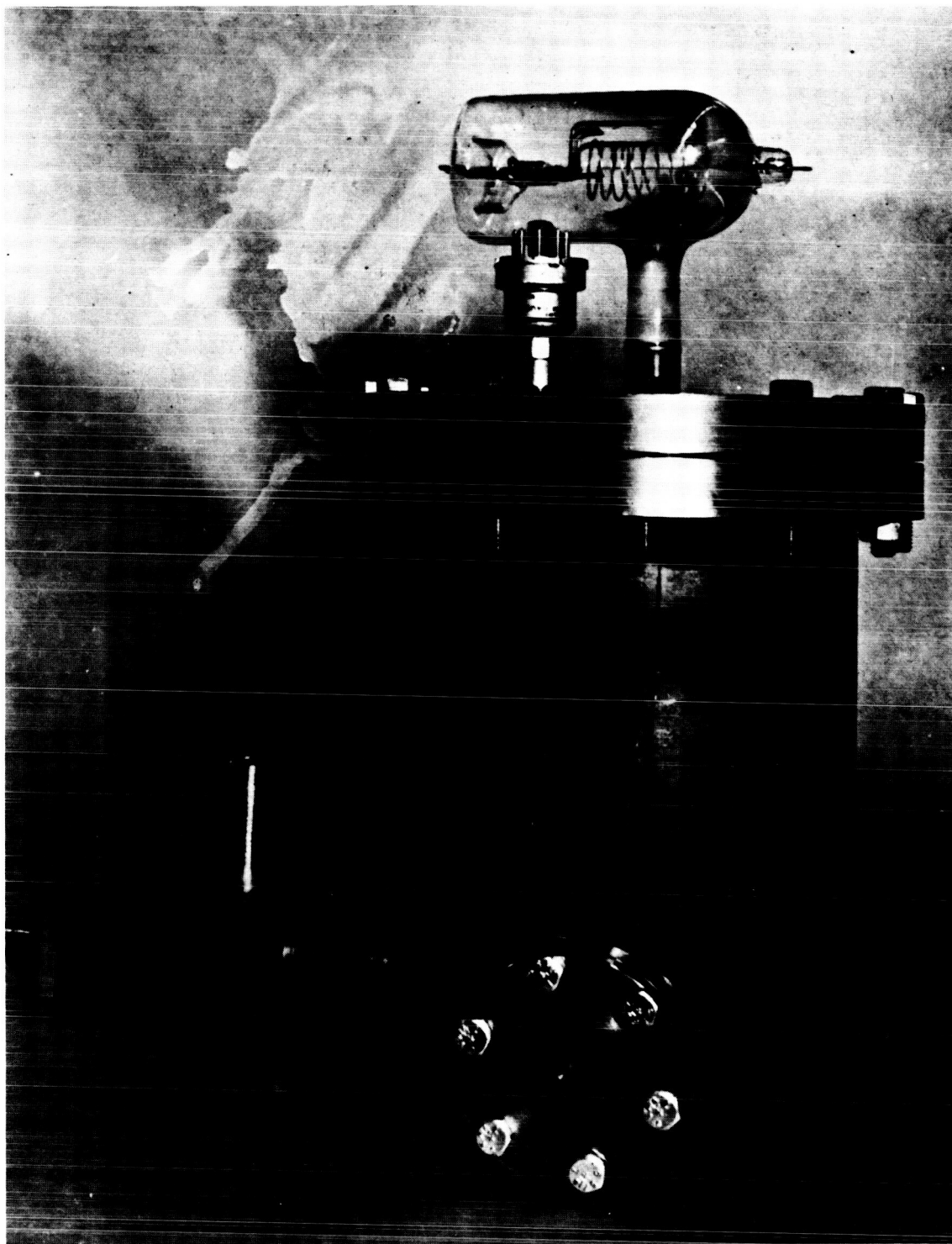


Fig. 7-1. Test chamber



Fig. 7-2. Test chamber head

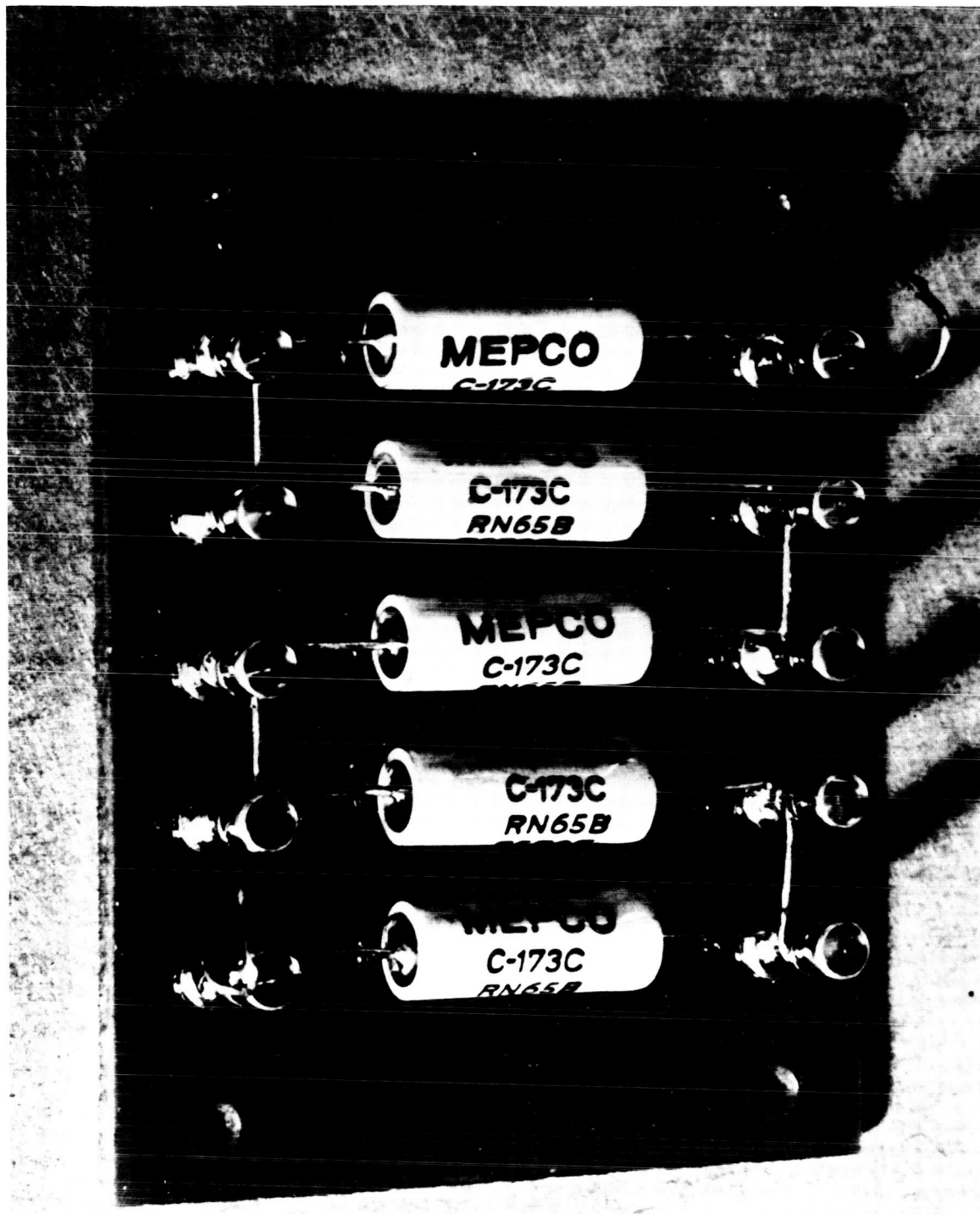


Fig. 7-3. Test specimen

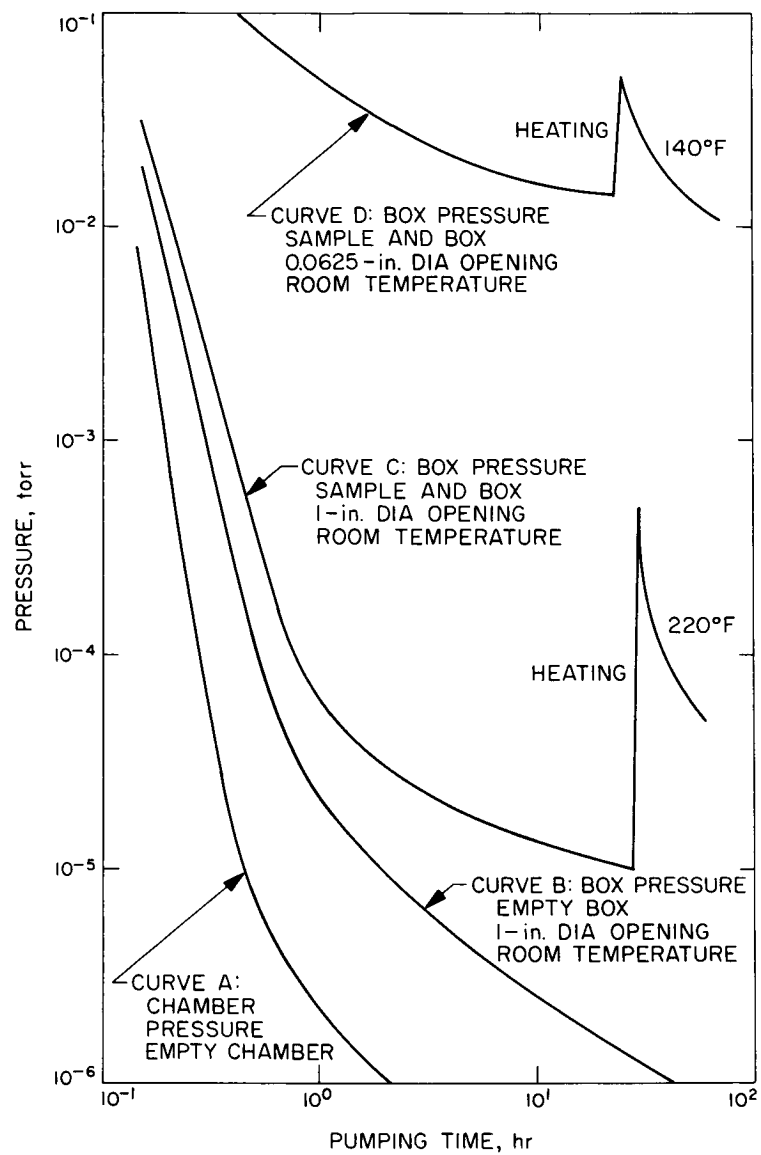


Fig. 7-4. Test specimen outgassing

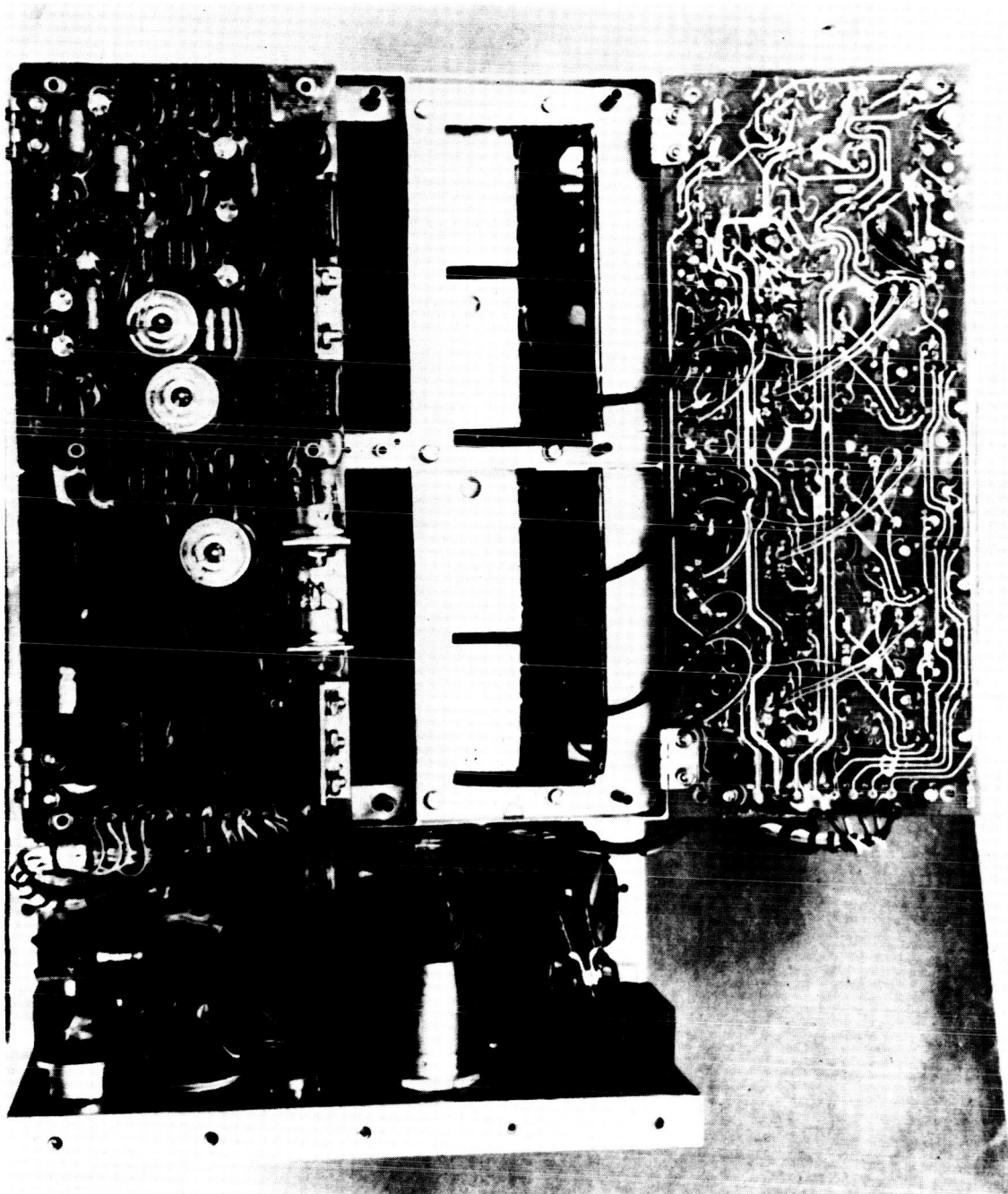


Fig. 7-5. Power supply and high-voltage bushing



Fig. 7-6. Power supply corona

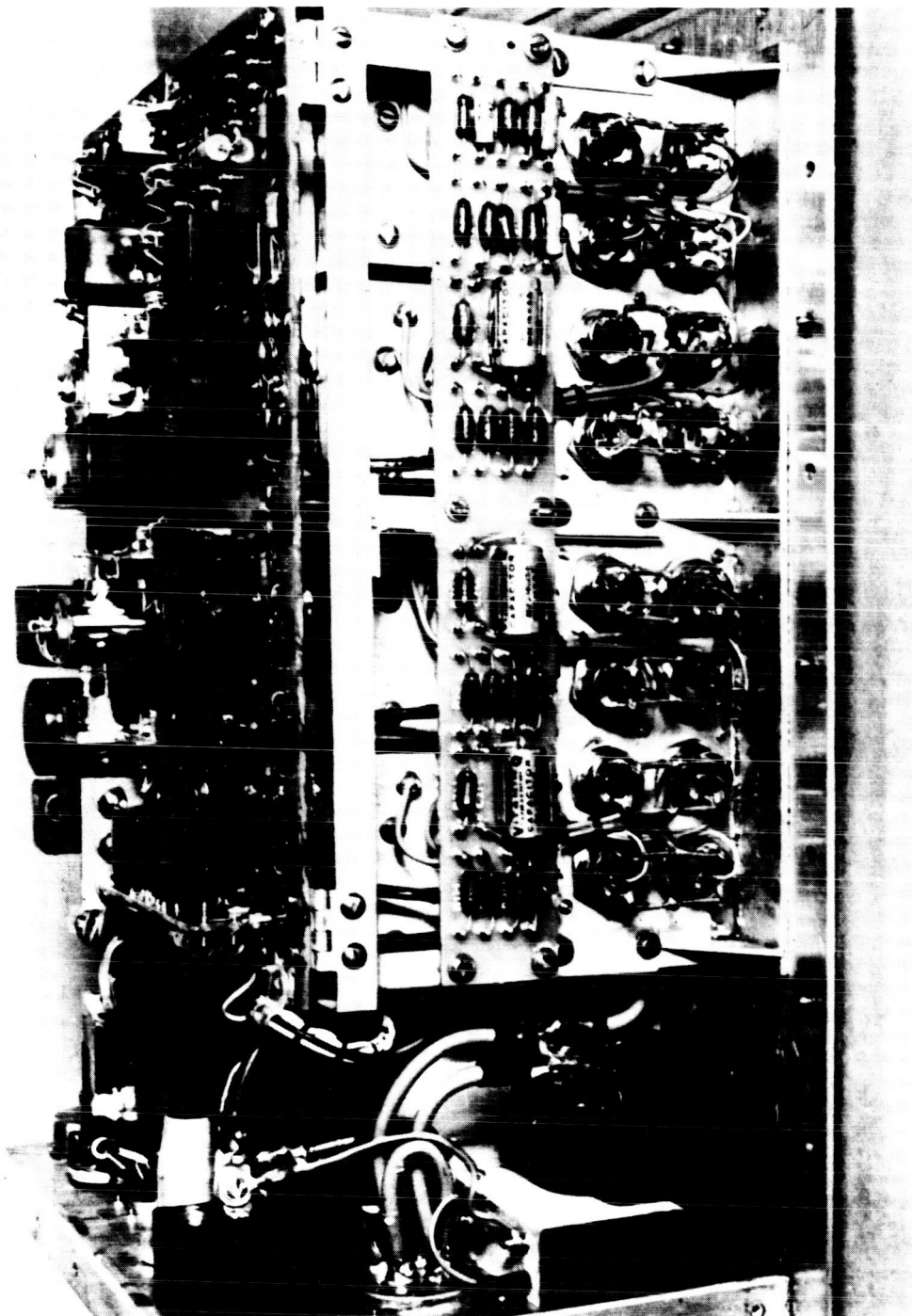


Fig. 7-7. Power supply - side view

8. CONSTRUCTION OF POWER SUPPLIES FOR  
OPERATION IN THE CRITICAL REGION

J. P. Clark  
Consolidated Avionics  
Westbury, New York

I don't know whether it's better to start off one of these affairs or finish it up. If you start it off you are likely to say something which will be very wrong according to somebody else a little later on; and if you finish up, somebody has stolen all of your thunder. I'm kind of in the middle here and there are a few things I'd like to second as we go along.

The difficulty of utilizing high voltage in equipment that must be operational between sea level and outer space is well known. We refer to the number of experiments which have been degraded because of this problem. Failures of this type are divided into two groups: temporary and permanent. The temporary failures are usually an arc or corona (and I apologize for use of the terms) condition that loads the supply when the partial pressures are encountered and heals or corrects itself when outer space conditions are encountered. The problem with this, of course, is that you often get coupling to other circuits when these arcs take place. I would hazard a guess that perhaps 20% of supplies that we've manufactured have been lost because of this one cause. We don't lose very many of them any more because we've learned a few things about protecting the sensitive resistors. Usually what we do is put a simple RC on the base of the transistor that may have a line going beside high voltages. This technique will generally, although not always, reduce the level of the arc, or energy, that goes into the transistor thereby protecting it. Of course, this method cannot be used when you have high-frequency energy going into the transistor. The permanent failure results when the arc or corona damages some sensitive part of the equipment by electric or thermal overload. Consolidated Avionics has designed hundreds of supplies capable of continuous corona without damage. As a matter of fact, we run each one of these through the bad region a number of times to make sure it can stand it. Sometimes arcing is permitted if you don't mind losing the data and taking a chance on hurting other circuits.

Consolidated Avionics considers corona to be divided into two groups, namely corona in gas (which is what most of the discussion today has been about) and corona in solids. Corona in solids, of course, is something that will come up for immediate



argument. However, we have observed a phenomenon which looks electrically like corona that will occur in a solid. I think somebody here mentioned degradation of silastic upon exposure to high voltages. In the past we have potted material, transformers, and the like, in clear potting materials, turned off all the lights, put high voltage on it, and observed; and then you can see two types of corona. The first type is a glow that looks electrically like the type of corona which we've been talking about here. The other type is little sparks which have a much lower period and much higher amplitude and roughly the same energy content. Temperature is a strong factor in this phenomenon: the higher the temperature, the more it occurs and the larger its amplitude. We've never had a catastrophic failure in these solid corona conditions. However, the tests were not run to their logical conclusion of corona breakdown, because the materials we were using--polyurethane--certainly did not lend themselves to this type of application. Incidentally, I should note that the voltages involved were in the range of 25-30 kv. We did not observe this problem with lower voltages of 2,000 to 5,000 v, and we have never had difficulty that we could trace in that lower range.

One of the things you can do to defeat corona in solids is by putting shields around the points that have a lower voltage. I think somebody mentioned putting carbon around the wire as they do in neon signs. The main thing is that if you can decrease stress--electrical stress in volts per mil--around the wire or around the point, the problem will be largely eliminated. I might also offer at this point a technique to use with troublesome silicone rubber wire. You can do two things. One, which has already been mentioned, is to pot a shield on top of the wire to eliminate the corona that occurs between the shield and the wire. The other method goes further than this, and can be best used on short lengths of silicone wire (which quite often is all that you need). The method is to pull the wire out of the center conductor (out of the silicone wire), and put this in an evacuated-type container with silicone rubber and force the rubber into the wire, and then before it is cured pull it back into the original wire. This must always be done under a vacuum and in very clean circumstances. If you do this you can eliminate most of the air pockets that occur inside the silicone rubber wire. Secondly, I offer that you can pot silicone wire. You have to be very careful with the priming, cleaning, etc. I think we have successfully potted the various types of silicone wire which are commercially available today and with voltages as high as 30,000 v on the 1/4-in. -wire.

One of the most common techniques used today for high voltages is one that we use involving silicone rubber of various types. We've had good luck with practically all the different types of rubber. I'll only lightly touch on one of the problems we have had because it's going to be the subject of a paper later on, and I don't want to upset the apple cart. It involves the problem of moisture in the rubber during the potting process. I'll simply say that one must be extremely careful with the amount of water that gets into this material when you're handling it and while it's curing. All our potting is done under vacuum conditions. I think somebody has already said you take the mold, put it in the bell jar, evacuate the jar; if necessary, you can bake the components. Some components will outgas for a long time if they are not baked. This should be determined before you get to the potting process, of course. You allow previously evacuated and outgassed rubber to flow into the molds. This must be done under carefully involved conditions in which you do not allow bubbles to exist. If you get bubbles there's only one thing to do and that's to pull it out and start all over again. Therefore, it must be done where you can see what's going on. The technician must be very careful. I might add that we have tried the method of putting pressure on the system after the rubber or other potting material is in there. The problem that we can't solve is what is the right gas to use to pressurize the system afterwards? Since we haven't been able to come up with a good answer, we prefer to use a straight vacuum system. I might also add that we have used polyurethanes, and we find them to be unsatisfactory because they pick up too much water. We've found water to be one of our biggest problems.

With respect to cleaning before potting, we have used successive boilings in alcohol rather successfully on most applications. Now, some parts can't take this, obviously you can't do it. After boiling, the unit must be immediately placed in the vacuum system and nobody must handle it. If you put your hand on even a piece of this high-voltage equipment, the probability of its enduring the environment is slight. If it does not occur immediately, it will eventually, because there appear to be various types of migrations which are not fully understood; but if the unit is not antiseptically clean you're going to have trouble either in the adhesion of the potting or perhaps in the generation of gas with temperature later on, or perhaps just an out and out void where you will get an arc.

The high voltages require another technique in most cases. The most obvious solution is to control the environment with the use of oil or with one of the liquid gas systems. This solution is a good one if weight is not a big factor, or if the period to

be endured is a short one. Oil is heavy, and the problems of leaks in thermal expansion have already been indicated. If your neighbors find out you're using one of these systems, they will usually scream to high heavens; undoubtedly there must be a better solution. One of the solutions that is used in voltages approaching 100 kv is to seal it in glass as in the case of a tube. I hasten to add that we have not built a system at the 100-kv level; however, we have done some investigation in this area. This approach--sealing in glass--is not a bad idea if you have a real good glass blower working for you. It does have some advantages. It's really not too heavy if you compare it with the oil and gas solutions that some people have used. In addition, if you break your seal after you get it out in outer space, you really haven't hurt anything. In fact, some people indicate that if they used this technique they would like to break the seal intentionally to ensure that they do have a good system when it gets in "the big bell jar" of space. I might point out that if you should consider using the vacuum solution that you must be very careful of the components you put into it because you have now sealed your environment, and if you stick in a capacitor that exhibits an outgassing of its own, particularly when it gets warm, you're in trouble. This brings us to the general subject of potting, either selective or mass potting.

For higher voltages the use of the hard material is more satisfactory. This statement reflects our experience with solid corona (which you may or may not accept as a phenomenon, but we feel it is there). In general, the harder the material, the less the corona. If you used glass or something as hard, I think you could be quite safe in saying corona did not exist. We have used stycast materials with some success. As an example we have a 2,000-v power supply which is intended for use with geiger tubes or in photomultiplier applications; it is  $\pm 1/4\%$  line load, and temperature, and it is comparable from sea level to any pressure that you care to use it at. Members of this family of power supplies are flown on very nearly all the shots that have been made on the East coast. We've flown hundreds of these in rocket shots where the area of interest was perhaps right in the corona region. If you use the hard materials, and something goes wrong, you've got to dig in there and fix it if you choose to do so. This has led us to a method in which we use selective potting of just the high-voltage components--usually highly miniaturized--and we pot them in a very hard material in which we have considerable confidence. The remaining low-voltage components are usually covered with a selective coat of rubber. We avoid the foams whenever possible because there is no way to predict how long the outgassing of a foam will take. We use foam when we are not concerned with the

power supply from the point of view of corona or arcing because of partial pressures. But if the experiment doesn't work, it isn't always easy to determine exactly what the problem was. We would much rather have it work the first time.

I'll pass on to another problem that we have had involving the simple extension of power supplies to combine in them an instrument with a photomultiplier tube or a similar detecting device. We have built quite a number for different applications, and we ran into a problem that others possibly have noticed. I don't have a very good explanation for it, but it might be useful for you to be on guard in case you have a similar application. The problem is a photomultiplier tube probably encased in a can, perhaps looking at a crystal of some sort where the light level is very low and you're concerned with dark current in the tube. You test the unit and discover it doesn't work properly; the dark current is too high and/or you see sporadic pulses which you may immediately attribute to corona or breakdown in your potting material. We have found that there is a phenomenon that occurs on the face of phototubes (and probably other detecting-type devices) wherein a particle is accelerated and perhaps collides with another particle and generates a small amount of light; it does this because a lot of the phototubes are operated with the high voltage near the aperture that is exposed to the environment.

The high voltage accelerates the particle and some phenomenon (which I will not try to explain at this point) generates light at the face of the tube. This problem very nearly scotched a program that we had until somebody came up with the idea of placing grids along the face of the tube and operating them at ground potential with a thin coating of clear rubber attaching the grid to the tube. This method was satisfactory for some applications but not for others. A second solution involved using a piece of glass slightly coated with a metal (so the transmission was not heavily impaired). This glass was then operated at the ground potential isolating the free particles in front of the tube from the high potential on the tube. The solution to this, of course, is to turn the tube the opposite way so that the glass near the tube is operated at a low potential. This solution has telemetry implications, and a lot of people don't like to do it.

All the supplies we build have to pass through multiple tests involving operation from the ground to the outer space environment, as near as we can simulate it. We've developed a small bell jar which is completely instrumented for high-voltage applications and allows us to get in and out of the box in about 5 min. With respect

to corona testing, we use a combination of two methods. For the high-voltage power supplies we monitor the voltage and the output of the power supply through a large capacitor. If the voltage jumps around, we conclude we have corona and report the component.

The other test (used with other devices) is a capacitance probe placed near the unit, usually with the scope on very high gain. When no problems appear on the scope, we do not have a corona problem. To date, we have not been able to trace any corona problems to a supply tested by this technique. It is relatively simple and easy to use.

The major point I'd like to make is that in the potting of high-voltage units for the partial pressure areas, I think the key is in the plastics lab where the technician handles the materials. I again will defer on this humidity aspect to the paper to be presented here later, because we came to the conclusions simultaneously and independently, but we've compared notes and find we agree on the problem.

#### OPEN DISCUSSION

MR. SCHILDKRAUT: I have a question on your rigid potting in high voltage-sections of your supplies. During cure, most of these rigid epoxies go from exothermic cycle where they give off a good deal of heat, but when launched, they go through subthermal extremes. Have you had any trouble with components cracking because they were rigidly encapsulated without a conformal dip of some soft compound?

MR. CLARK: We have used conformal dips when we anticipated this problem. With some of the new components that we're using--particularly some microdiodes and some of the better capacitors--this has not been a problem. We have a unit coming out that's about two-thirds of this size which has essentially the same characteristics, and there's no conformal coating in that at all. It's all solid. It is 70 gram, by the way, so it's small and doesn't weigh much.

VOICE: What's the lowest temperature you test that to?

MR. CLARK: Most of the shots, as everyone well knows, get down around  $-30^{\circ}\text{C}$ ; we have built units as low as  $-85^{\circ}\text{C}$ .

VOICE: Using that hard pot?

MR. CLARK: No. We don't use hard pot over that kind of range. You've got to use something with a lot of plasticizer there.

MR. BUNKER: This is a passing comment. It has nothing to do with this symposium. One of the other projects I'm working on is measuring the compressive stresses of rigid epoxies on components, and they get rather high. We've squashed some diodes so it does exist.

MR. THORNWALL: When you say microdiode do you actually mean this unit-construction-diode there?

MR. CLARK: They're little bead-type diodes manufactured by PSI and two or three other companies.

MR. MYERS: Are some of the materials listed on your paper specifically by number?

MR. CLARK: No, but if you're interested in that specifically, we'll supply the information.

N 68-26884

## 9. THE GENERATION OF POTENTIAL DIFFERENCES AT STAGE SEPARATION

J. W. Haffner  
Space and Information Systems Division  
North American Aviation, Inc.  
Downey, California

I imagine you have all noticed that the altitude range at which we seem to get these anomalies just happens to be the same altitude range during which first-stage separation of a launch vehicle often occurs. The work I'm going to describe to you this evening pertains to some simple experiments we have carried out in the laboratory pertaining to this first-stage vehicle separation. The result of a fair amount of work which has been done at North American (and which Mr. Coleman will be talking about in more detail later) indicates that launch vehicles under most conditions will probably charge to fairly high voltages. Data received from telemetry links and other sources indicate that a fair number of anomalous occurrences take place at stage separation. Therefore, we wanted to do some experiments to determine if by any chance there could be a potential difference generated between the two stages of the vehicle as it separates. We plan further experiments in which we want to investigate what may occur at the reduced pressures that exist at these altitudes. Let me briefly describe the experiments and the results we obtained. It may appear to be merely sophomore physics, but at the same time it was a little unexpected unless you really think about the effect.

In Fig. 9-1 are shown schematically the three geometries we investigated. These are basically cardboard and Reynolds Wrap models, configuration A being the one which includes a cone. The reason it's shaped that way is that we used the first thing we could get our hands on, namely a funnel and a wood screw, and we made a cylinder out of cardboard with Reynolds Wrap. The ends are covered to represent closed bodies. They are suspended on strings from the ceiling of the laboratory. Configuration B is essentially the same as configuration A except that the cone is replaced with a cylinder. The dimensions in inches are shown in the figure. Configuration C involves two identical cylinders. Theoretically we expected to get the greatest effect with configuration A, a less effect with configuration B, and zero effect with configuration C; and this is what it turned out to be.

The electrical circuit which involved these cone and cylinder configurations is shown in Fig. 9-2. The square labelled V represents an electrostatic voltmeter;

the circle labelled V is a typical moving-coil voltmeter. The effects to be described took place only when the electrostatic voltmeter was in the circuit and the other two switches were open. The point here is that you have to have an extremely high-impedance-measuring circuit because even though we may be talking about very large potentials, we're talking about extremely small charges. The entire Saturn V launch complex, for example, is going to have a capacitance of less than  $10^{-8}$  f. In fact, if you think about it, the Earth has a capacitance of less than 0.1 f. It doesn't take much in the way of a charge to give rather high potentials. Resistances even in the megohm range are sufficient to kill the effect that we were interested in measuring.

The first thing we wanted to do, since we are talking about such small amounts of charge, was to make certain that the potentials we expected to measure when we separate the cone and cylinder were not due to the unequal leakage of charge from these two bodies. In order to do this, we did the following: (1) We charged the two bodies while they were in contact, (2) kept the high-voltage lead on one of the bodies, (3) separated the two bodies approximately 2 in. and held them there with the power supply keeping one body charged at the set voltage, and (4) observed the rate at which the charge would leak off the other body. The results of this portion of the experiment are shown in Fig. 9-3. Plotted on the vertical axis is the difference in potential (in kv) vs time (in sec).

We go from zero to 1.2 kv in zero to 40 sec. We charge the two bodies initially to 20,000 v and, as I described before, separate them, and measure the potential difference as the charge leaked off one body as the other body is held at the 20 kv of the power supply. We did this experiment first with the cone being held at 20 kv. The figure shows the data we got at the cylinder. The significance lies in the fact that it takes over 30 sec for the 20 kv on either body to drop down to 19 kv. This result says that we had a fair amount of time to do the experiment in and that if we did measure potentials appreciably larger than this we could attribute it to the changing geometry of the situation and not to the unequal leakage of charge.

Having convinced ourselves that the experiment was feasible we proceeded as follows: (1) We recharged the two bodies while they were in contact, (2) removed the high voltage lead, thus effectively isolating the bodies, (3) separated the bodies a given distance, and (4) measured the potential difference between the two bodies as a function of time. The data for configuration A (cone and large cylinder), is shown in Fig. 9-4. As you can see, as time goes on the potential difference drops down.



Extrapolating back to zero time, we get a potential difference, which is a function of stage separation. The 2-in. data is anomalous. We repeated the experiment and got the same thing. We think that the unequal leakage of charge may be the factor causing us trouble. But if you make a crossplot, you will see that 2-in. separation at zero time will give a value of the order of 0.3 kv; 4 in. will give better than 0.8 kv, 6 in. better than 1 kv, 8 in. better than 1.4 kv, etc. All these experiments, I should mention, involved initially charging the body to 20 kv.

The corresponding data for configuration B (large cylinder and small cylinder), are shown in Fig. 9-5. We see a similar effect; however, the potentials measured are smaller. I don't have any explanation at this moment for the fact that the slopes of the lines did not all come out the same. As a matter of fact, we didn't make any tremendous attempt at curve fitting. We just plotted the data obtained as the points, and since they didn't disagree violently with straight lines, we arbitrarily drew straight lines.

The experiment has been repeated qualitatively a number of times, and it has been observed that as you separate the two bodies the potential does build up. You can change the potential cyclically by changing the distance between the two bodies in the same way. We did one interesting experiment again just on a qualitative basis. It involved removing the cone away from the cylinder in configuration A, reversing the cone, and then bringing it back to the cylinder. When we did this we detected (audibly) a small spark. What this really says is, that, there will be a potential difference between two bodies at stage separation, assuming these two bodies have different sizes and shapes (i.e., different geometries). Since these measurements were taken at atmospheric sea level pressure, we did not detect any electrical discharges -- corona, arcs, or any other kind.

The next experiments we plan will involve similar experiments in the reduced pressures which one experiences at altitudes. We don't know for certain whether there will or will not be any sort of discharge at that time. However, we have shown that if you attempt to rendezvous, you want to make very certain that the two rendezvousing bodies are at the same electrical potential. A number of factors (which Mr. Coleman will explain later) will make these bodies tend to be at different potentials. Obviously when two bodies of different potentials rendezvous, you're going to have trouble.

That's the sum and substance of the material I had to present. It's mostly, as I said, sophomore physics, but it's sophomore physics with perhaps an unexpected twist that does have application to rocket separation at these critical altitudes.

## OPEN DISCUSSION

VOICE: What happened to configuration C?

DR. HAFFNER: Configuration C gave us essentially zero voltage. The data we recorded was all less than 0.3 kv. Because of the nonlinear scale it's very difficult to separate 0.3 kv from 0 kv. The two models in configuration C were identical only in the sense that they had the same diameters and the same lengths. Because they were made out of Reynolds Wrap, we couldn't guarantee all the individual crinkles were identical. But the data we obtained indicated that we get essentially zero potential difference for configuration C.

VOICE: Was the experimental error then 0.3 kv?

DR. HAFFNER: For the low voltages, yes. We could read, for example, 0.5 kv to better than, say, 200 or 300 v because the scales expanded tremendously. But when it came to reading 0.5 kv, we could tell it wasn't 0.3 kv but we couldn't tell it wasn't 0.4 kv, for example. The error was on the order of 0.3 kv at the low-voltage range and had dropped to, perhaps, 0.1 kv at the high range.

MR. STREET: What was the capacitance of the electrostatic voltmeters? Probably considerably larger than the capacitance of the bodies that you're measuring, actually.

DR. HAFFNER: I don't have a direct answer to that. I would not think it would be that much larger because the vanes, although closer together, are much smaller in area. We did not measure the capacitance of the voltmeter or of the two bodies, so I can't really answer directly.

MR. STREET: The effect of the voltmeters capacitance would be to reduce the voltage that you observed below what you would have gotten if it hadn't been connected to the system. Isn't that correct?

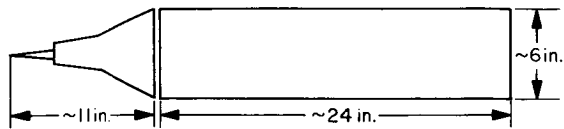
DR. HAFFNER: I believe that is right. We haven't really thought about it. The first experiments, the ones I am describing, were, as I say, of a very semiquantitative nature, to see if the effects we expected would show up. We plan more

detailed experiments, and I think that the point you raised is a very good one. We plan to measure the capacitances of the voltmeter and of our own models to see what effects this may have.

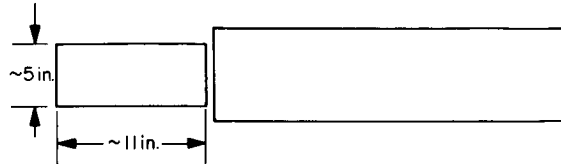
DR. VANCE: It seems to me that you've omitted a scale factor if you're talking in terms of a scale model here and comparing this to what you would get on an actual missile or rocket during staging. This is a twentieth-scale model that you're working with. You might have only one-twentieth of that voltage between the parts or you would have this same voltage at twenty times the spacing between stages on a full-scale vehicle.

DR. HAFFNER: Your point is well taken. To begin with, these models were not scale models of anything. They were just simply two geometries that we put together in the laboratory. The potentials applied were not necessarily representative of what we expect on the vehicle. I agree, though, that what you're interested in is the potential difference you observed as a function of the initial potential on the bodies and that perhaps this difference is a function of the separation distance in terms, say, of the body diameters. So the effects we observed at 2 in. would be expected to occur correspondingly maybe 20 or 30 times the distances for the full-sized vehicles. In other words, I'm not saying you're going to get this percentage change at 2 in. separation in the big vehicles. We found that we essentially got maximum effects when we got to, say, a half a dozen vehicle diameters.

CONFIGURATION A



CONFIGURATION B



CONFIGURATION C



Fig. 9-2. Schematic showing electrical circuits used (same for all three configurations tested)

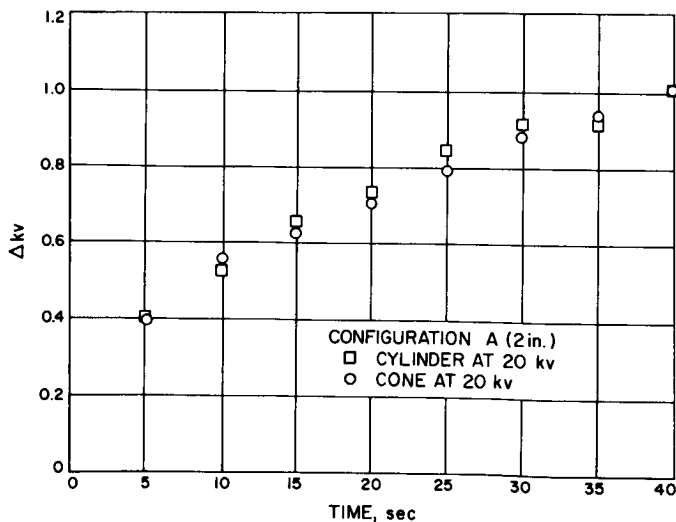
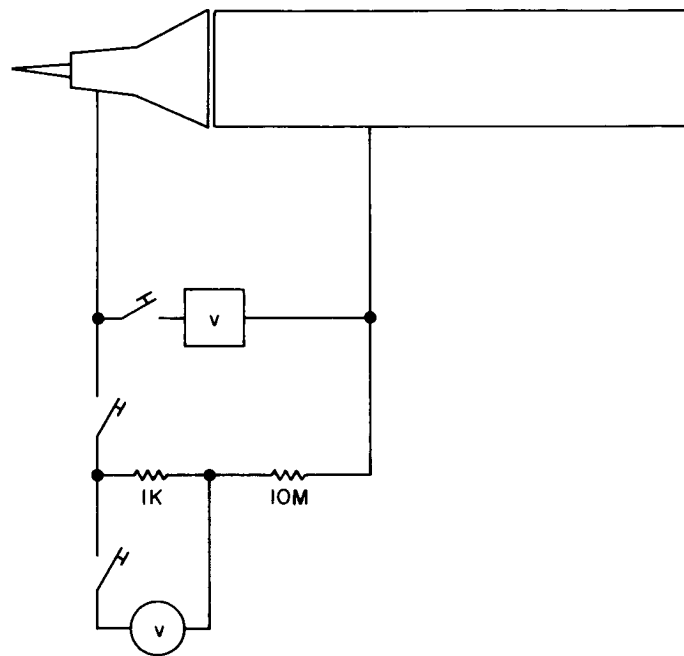


Fig. 9-3. Graph showing rate of charge leakage from isolated bodies

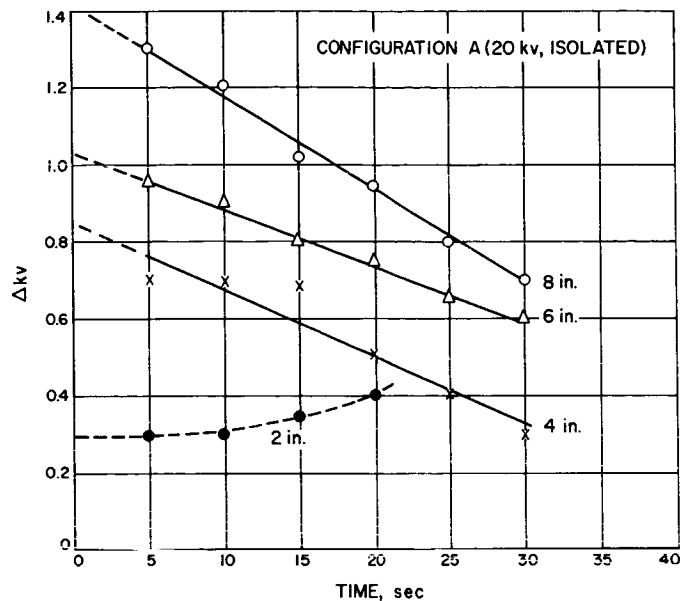


Fig. 9-4. Graph showing potential difference between the cone and the cylinder of configuration A

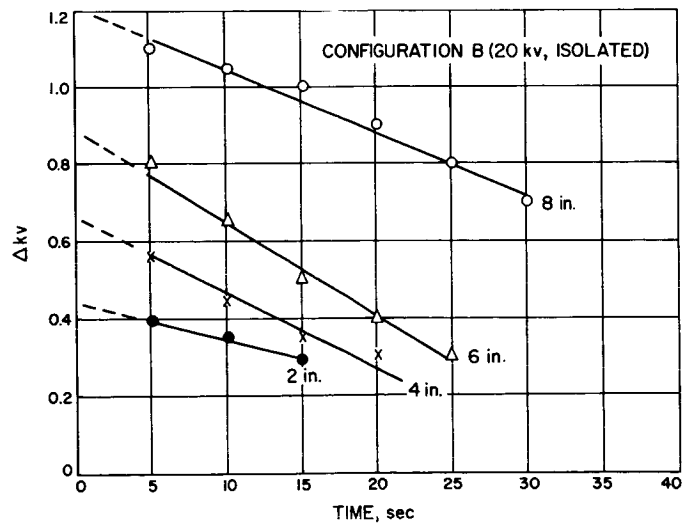


Fig. 9-5. Graph showing potential difference between the large and the small cylinders of configuration B

N 68-26885

## 10. CURRENT ANOMALIES AT SEPARATION

W. R. Abbott  
Lockheed Missiles and Space Company  
Sunnyvale, California

(Presented by D. Tashjian of Lockheed)

We're going to talk about a type of anomaly at separation which is, we think, explained in quite a different fashion than in the preceding paper. It is a mechanism that was discussed very briefly by Dr. Vance earlier.

For several years the Agena program has been plagued by an occasional short circuit occurring at or near the time of separation from the booster. All these short circuits involved very large current flows, some of which have stopped as mysteriously as they started. Others have burnt out circuitry such as to impede or prevent completion of the mission.

All such anomalies are potentially catastrophic, and therefore it is essential that they be understood and prevented. As it turned out, all these occurred in the spring of the year on two successive years. However, we weren't able to find any particular effect that was oriented towards the spring of the year that might bear on this. We therefore sought other explanations.

Figure 10-1 shows the approximate current-time histories for the short period under consideration. The tops of the curves are flat-topped because of telemetry limitations, making it impossible to determine actual current-time variations, but you can see by the ordinates that the currents involved were indeed very large. It should be pointed out first that in the normal sequence of operation the booster final burnout is denoted as VECO. Shortly after this time the Agena is cut free by an explosive charge that cuts it loose from the booster adapter. Retro rockets then start and back down the booster. The Agena is then allowed to slide out of the booster adapter. The burning time of these retro rockets is from 0.5 to 1 sec and typically about 0.8 sec. This 0.8-sec is, I think, a significant number. At about 0.5 sec from the separation event, an electrical plug that connects the booster to the Agena pulls away, thus cutting off all electrical connections to the booster and the booster adapter. When the Agena is completely free of the booster adapter, switches turn on the pneumatics, typically at about 2-1/2 sec from the separation event.

A glance at Fig. 10-1 shows several striking facts. Seven of the nine anomalies shown started exactly at separation or as near as was possible to tell from telemetry. Three of these anomalies stop with the pull-away plug separation, indicating that a short was on the booster side of the pull-away plug and opened at this time. The anomalies on two of the vehicles stopped at approximately the end of the retro fire. The second peak on one of them was probably due to a brief touching to ground of a wire which had pushed loose during the first anomaly.

Table 10-1 presents these and some other characteristics. The first column shows the separation altitude for all except the first vehicle listed, and in this case the value was unknown. It will be noted that with the exception of one at 56.4 miles, all these anomalies occurred with separations of 52.5 miles or lower. One vehicle had a short on the 400-cps, 3-phase power, one on the -28 v regulated, one on the +28 v unregulated, and the others on the 28-v pyro supply (which is an independent supply), with some current returns to the vehicle frame and some to the pyro bus. There doesn't seem to be any discernible pattern between the point of return and other functions. While the nine anomalies listed may not represent faults resulting from a common cause, it is quite clear that seven of these have much in common and should be considered together. It is significant to emphasize the fact that all of these problems occurred with separation at low altitudes. There have been many flights with separations above 52.5 miles as well as many in that neighborhood and below 52.5 miles. It seems significant that above these altitudes (with one exception at 56.4 miles), there have been no current anomalies at separation in any flight. Thus, in looking for a common cause, it is very desirable to look for an altitude-dependent effect.

Another phenomenon that appears to be altitude-dependent is that of the loss of telemetry data. Upon occasion at the separation command, the telemetry signal strength drops so low that no data are received. The signal strength recovers after a period of time.

Figure 10-2 plots the duration of the data loss as a function of separation altitude. The small arrows point to those occurrences of separation anomalies. It should be noted that there is essentially always a data loss below 53.5 miles. Above 53 miles there is less often a data loss, and above some 60 miles there is never a data loss. I think these numbers are significant.

The characteristics shown in Fig. 10-3 are typical signal strength readings for flights at various altitudes. The upper record shows a flight at which separation occurred at 48-1/2 miles. The data was somewhat noisy. But nevertheless it is typical that over this limited period of time there was a substantial data loss. The second record from the top shows that the data loss was a minimum. It is noted, however, in this case (as in the preceding one) that the signal strength disturbances endure for about 0.8 sec. You remember this was the duration of the retro firing.

At 58-1/2 nautical miles the record shows some slight signal strength fluctuations for about the same duration as before, but not large enough to produce any loss of data. The bottom record (68 nautical miles) shows no significant signal strength loss at all, the variations before and after separation being of about the same type. The correspondence of the duration of signal strength fluctuations with the duration of retro rocket burning strongly suggests a connection. It is postulated that the loss is due to the attenuation caused by the transmission of the signal through the plasma in the retro rocket plume. Lack of time correlation in signal strength and data losses at various receiving stations leads to the conclusion that the transmitter continued its operation.

The altitude-dependency is a result of the rocket plume increasing in size as the ambient pressure decreases at higher altitudes. Thus even with a fixed amount of ionization in the combustion chamber, the plasma density decreases with increasing altitude. Radio frequency attenuation produced by a plasma is a result of the interaction of the electrons in the plasma with the rf field being transmitted. These electrons absorb energy from the field and then reradiate it. There are two cases to consider. Whenever an electron, which is at a higher energy level as a result of receiving energy from the field, undergoes collision with an ion or a neutral atom before it has a chance to reradiate energy, the rf energy is lost. This form of attenuation is due to particle interaction. The average number of such collisions undergone by an electron every second is known as the collision frequency, and at the altitudes of interest the collision frequency is of the order of 100,000 collisions/sec. Since this frequency is substantially below the telemetry frequency, it is felt that attenuation due to this phenomenon is not of any very great importance.

The other source of attenuation is that which occurs when the frequency is below the Langmuir resonant frequency of the plasma. Roughly, this frequency is that at which the inductive reactance caused by the lag of electron velocity behind the field



resonates with the displacement current which leads the field. In a given plasma below the Langmuir resonance, an rf field attenuates exponentially with distance. Above the resonance it is transmitted without attenuation except that due to particle interaction, but with a phase different from that which is produced in free space. Using the known telemetry frequency and the observed attenuations, ion and electron densities to produce these attenuations have been calculated. Densities of the order of  $10^9$  to  $10^{10}$  electrons/cm<sup>3</sup> are adequate to explain the observed attenuation. These are the densities after the rocket exhaust is expanded to a distance of about 20 to 25 ft toward the telemetry antenna.

The induction of arcs by the introduction of a plasma in the interelectrode space is a subject of a fairly sparse but reasonably definitive literature. However, the literature does not indicate any lower limits on voltage as compared with ion density. Therefore, some experiments have been performed at Lockheed to determine these numbers. I might add that the experiments we conducted are quite similar to those described by Dr. Vance.

Electrodes spaced some 3 mm apart were immersed in plasmas of varying densities, and the voltage required to produce an arc was determined. It was found that with a magnesium thorium cathode (magnesium thorium is the material of which the structure of the Agena is largely made), arcs could be produced at voltages as low as 26 v with ion densities of  $10^9$ /cm<sup>3</sup> or less. With a copper cathode the required density is less than  $10^{10}$ /cm<sup>3</sup>.

Let me reiterate the explanation we have for this phenomenon. A thin coating or inclusion of some nonconductive material is required on the surface of the cathode. When a field is applied, positive ions are attracted to the cathode, and some will stick to the inclusions. As the surface ion density builds up on the inclusion, the electric field through the inclusion increases. When this reaches a value of  $10^6$  or  $10^7$  v/cm, the underlying metal can emit electrons by the phenomenon of field emission. The energy stored in the capacitance (of which the inclusion is the dielectric) is then dissipated in the dielectric itself, producing vaporization and ionization and forming the site of a potential arc. This will be happening in many centers over the surface (much as Dr. Vance's movie showed), and thus if other conditions are right, one or more sparks will occur which will then transform into an arc if circuit conditions are appropriate. Studies at the Lockheed Propulsion Company have shown that in general the positive ion density in a rocket exhaust is from 100 to 10,000 times

the electron density; this is because the impurities in the exhaust contain chlorine which very easily attaches itself to an electron, and thus the positive ion density will be considerably greater than the electron density even though the positive and negative ion densities themselves will be approximately equal in any plasma. The electron density has been shown to be of the order of  $10^9/\text{cm}^3$ , and since positive ion densities of this order of magnitude have been shown to be sufficient to induce arcs in 28-v circuits, it would appear that the connection between the retro rocket exhaust and the current anomalies has been established.

At the time that we had these anomalies, we did a number of things to correct them. We made several changes in the way we routed wires. Among other things, we took the precaution of plugging the hole through which the igniter wires passed through the booster adapter. This hole was just below the booster adapter, and therefore it was a possible place where the rocket plume could enter into the booster adapter area where the aft rack of the Agena was lodged and where the short circuits were occurring. Since plugging the hole, we have had no further anomalies. I don't contend that there might not have been one of these other changes that assisted in correcting the problem, but we believe that this explanation is reasonable because since the hole has been plugged the anomalies have not returned even though we have had a springtime.

#### OPEN DISCUSSION

MR. HAWERSAAT: I have a comment on this. Dr. Vance's pictures earlier in the day basically remind us that when you run ions you get almost an identical picture. If you do get trouble it looks like his, but in the CERT I test program in which we were running a spacecraft test in a big vacuum tank with a new plasma, we found potentials as high as 60 v in several tests. Perhaps three or four times out of one hundred tests we did start a plasma discharge across this 56-v contact, and when the thing was examined after the tank was opened we didn't have the 56-v pin. This happened several times. As a precaution (not only for flight but also for testing), we had a cover that snapped over the fly-weight. It was vented but it did snap over to protect the plasma from getting in. This might be considered a solution on spacecraft, too.

MR. DAY: Do you have information on the frequency response of the signal strength measurements you showed in one of the charts? And where in the receiver the signal strength was measured?

DR. TASHJIAN: This is the standard TM band that we are using here--the VHF band. Does that answer your question?

MR. DAY: No. I'm wondering about the frequency response of the signal strength measurement.

DR. TASHJIAN: These signal strength measurements are represented as the readout of the TM, and since this is commutated, I don't think I can specifically answer that question.

VOICE: Was he referring to the subcarrier frequency response of your TM?

MR. DAY: No. I'm not. I'm wondering how accurately the displaced traces represent what was actually happening to signal strength.

VOICE: I have a comment. Quite a few of the records on the Atlas vehicle were similar, and that record is quite common, not at all unusual. I think the analysis is quite correct because many of our records act closely akin to what you would expect to find in the TM and on a FMFM telemetry system, which I am not sure you had on your Agena.

DR. TASHJIAN: That is right. FMFM.

VOICE: I think the maximum bandpass is 20% or higher. It depends on whether you have an analog signal channel there or not. I expect that you did, and as such, it probably would be a maximum of 20% deviation.

DR. TASHJIAN: As far as the recorder itself is concerned, I am certain that it's 100 cps, or something like this because there's no effort made to record at a higher rate.

VOICE: I am thinking more of the circuitry that comes before the recorder; typically these things aren't any better than about 10 cps because of the signal strength, and sometimes you have anomalies never detected on signal strength record, for example.

DR. TASHJIAN: That could well be.

VOICE: There again a phenomenon is observed, whether it be decommmed or whether it be a straight signal on your AGC loop on your receiver or pick-up, it very definitely represents AGC of what you see, and the 200 Mc band (which I suspect you are in) is more predominantly corrected by the type of thing you're describing. I believe that even though your retros are canted at about 30 deg, you still get the plasma.

DR. TASHJIAN: There are two phenomena we're talking about here. One is the loss of signal strength and the other is the possible injection of plasma into the Agena.

VOICE: I'm referring to both.

DR. TASHJIAN: In the one case, of course, the hole that we're interested in is close to the retro rockets, and in the other case the antenna is some 20 or 25 ft forward but it is included in the plume. No question about that.

MR. GOUDY: What kind of connector were you separating?

DR. TASHJIAN: You mean the pull-aways?

MR. GOUDY: Right. The pull-away.

DR. TASHJIAN: I don't believe I can answer that question.

DR. GOUDY: Friday I'm giving a talk on something in this area. We ran across some very interesting things on separating these connectors, possibly opening circuits with them, which is basically what you were describing doing here.

DR. TASHJIAN: Remember that there were three of these short circuits that went away when the pull-away opened. They were presumably on the downward side of the booster. The other anomalies remained and were associated with circuitry, which was not disturbed by the pull-away at all. They were powered by the vehicle battery and the vehicle pyro battery.

MR. GOUDY: What I was thinking of, though, was a possible short circuit, and then when you opened your connector you were breaking a pretty high current with your connector separation.

DR. TASHJIAN: Not really. The currents that are broken by this pull-away connector are merely some relay actuators and do not involve very high currents at all. As a matter of fact, they were not associated with the circuits in which we had the arcs.

MR. GOUDY: I thought you mentioned the circuits opening up. You had a short circuit and the circuits opened up after connector separation.

DR. TASHJIAN: There were nine anomalies listed there. Three of these just disappeared when the pull-away plug opened. The balance of them remained with us; in some cases they stopped after the retro firing stopped, and in some cases they remained there until the battery used itself up or there was a burnout.

Table 10-1. Current anomalies

Separation altitude, miles	Anomaly start at separation	Anomaly stop at pull-away plug	Anomaly stop at end of retro	Current return to structure	Current return to bus
--	x <sup>a</sup>				
52.5	x	x			x
51.7	x	x			x
48.5				x	
56.4	x		x		x
52.0	x	x		x	
51.5	(b)			x	
51.2	x		x		x
52.5	x <sup>c</sup>			x	

<sup>a</sup>400 cps, 3 phase.

<sup>b</sup>-28 v regulated.

<sup>c</sup>+28 v unregulated

All others +28 v Pyro.

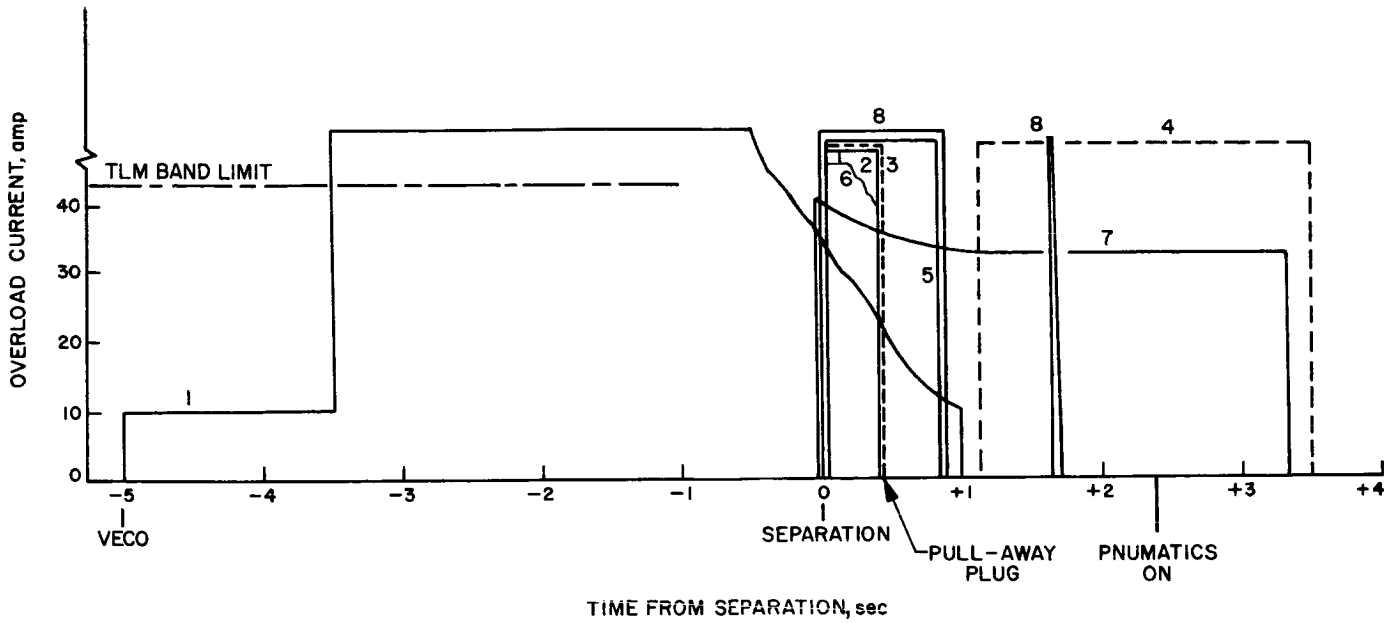


Fig. 10-1. Shorts at separation

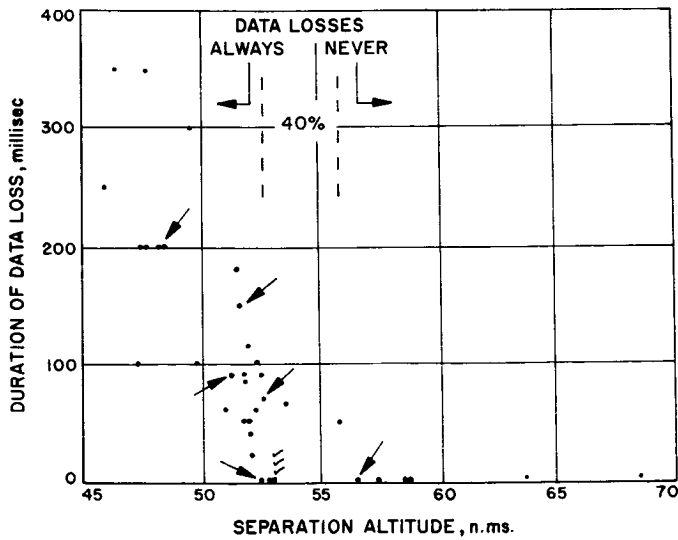


Fig. 10-2. Correlation of separation altitude with loss of data

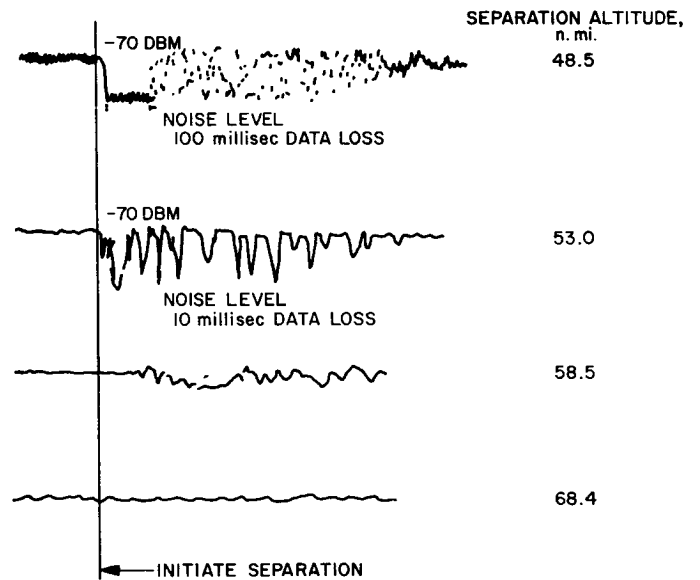


Fig. 10-3. Signal strength data from selected flights

11. BOOSTER AND SPACECRAFT ELECTROSTATIC  
PHENOMENA - CAUSES, EFFECTS,  
AND PREVENTION

W. Coleman and R. Reeves  
Space and Information Systems  
North American Aviation, Inc.  
Downey, California

(Presented by W. Coleman)

I certainly enjoyed the program this morning. I have particularly enjoyed the buildup and the direction, one might say, of a good detective story. We began this morning by being concerned with high-voltage discharges that take place in gaseous media, namely the corona avalanche type of discharge. We listened to many fine papers which told us how a gaseous atmosphere could be realized by means of outgassing. And then Dr. Reeves of Harvard gave a splendid presentation in which we began to recognize a mysterious suspect that we could not really pin down. Then we began to follow Dr. Reeves' effort to nail the suspect, to identify him, and so forth. Just now we learned that sometimes the criminal apparently strikes only in the springtime. So we find that we have quite a challenging case to solve here. It is our intention to complicate the matter still further by introducing yet another suspect and also to suggest that there may be multiple crimes, not just one crime and one criminal.

I will make some reference to Dr. Haffner's presentation as we begin to develop our presentation, but first I would like to summarize our presentation right now. First of all, it is our intent to describe for you the various means whereby space vehicles, boosters, and spacecraft may become charged to high voltages. Secondly, we wish to describe to you the effects of high voltage on the vehicles. We will be returning to the sophomore physics many times and dwelling on elementary aspects of high voltage to make sure that we get our ideas across to you, because we believe it is important that you consider them. Then we will talk about these effects, and say something about the possible means whereby the bad effects can be prevented.

We at North American Aviation Space and Information Systems Division have been studying electrostatic phenomena in connection with spacecraft and space vehicles for about 2-1/2 yr. Our interest is what you would expect from people who are concerned with the Apollo mission. There will be many significant events throughout the course of that mission where electrostatic phenomena could reasonably be expected to provide problems for us. Beginning with the boost phase we must pass through

the critical pressure regime. Then we must have separation events. We must have various rendezvous maneuvers and transposition maneuvers in the vicinity of the Moon. Finally, we must put a man on the Moon. This man, of course, will have to walk about the surface of the Moon in some sort of a space boot, and in all probability he will be shuffling about the surface of the Moon with these plastic boots in some sort of a dust. And the analogy, of course, is one of us walking across a carpet, or perhaps a man being caught in a sandstorm on the desert.

The astronaut could well become charged up to a pretty high potential of the order of 10 kv, and when he returns and touches the LEM, he may get a pretty damaging electrical shock. And, of course, assuming that all of these hazards are survived, we still have to get the astronauts back to Earth. Once more they go through various docking maneuvers, with the possibility of a discharge at every one. Finally we have to make the reentry, and once again we have to face the triboelectric effects of the atmosphere on reentry, which have fortunately in the past been successfully carried out. Let me just say that something like the Saturn V launch configuration is indeed a flying bomb. We have many electroexplosive devices, and a recent study by Dr. Vance's SRI has shown that electroexplosive devices may indeed be inadvertently set off by electrostatic discharges. So you can see immediately why we have seen fit to devote 2-1/2 yr of effort to the study of electrostatic phenomena and its effect on space vehicles.

I believe Table 1 will summarize our phase I work. We began work in December 1962 and continued phase I for a little over 1 yr, until February 1964. The purpose of that work was to come up with a general definition of the scope of the problem for the Apollo mission. We also wanted to make a detailed study of internal charging mechanisms. Dr. Vance said earlier that it is well known that aircraft will charge up just by passing through the atmosphere, and he also said (and we certainly agree with him) that while one may expect rocket engines to contribute to the charging situation, very little is known about the mechanisms. Therefore, as a part of our phase I effort, we wanted to make a detailed study of internal charging mechanisms. As a result of the phase I effort we did indeed evaluate the internal sources for all the Saturn V stages. We came up with a little computer program because one has to try to keep track of the ions in the exhaust and keep track of space-charge phenomena, as well as the kinetic force of the gases which tends to remove the charges from the rocket. Finally we made predictions of maximum charge accumulation as a result of engine operation.



Let me emphasize that all of this was done with pencil and paper, and no one can say for sure that problems will exist on such large boosters going by the results that we have achieved. So I will not tell you the numbers that we came up with for fear of misleading you into thinking there definitely will be problems on these large boosters. But I will say they were quite high. Having seen these theoretical numbers, we decided to continue into a phase II study to see what the discharging mechanisms might be.

We set out in our phase II investigation (see Table 2) to make a detailed study of the effects and consequences of high voltage on isolated space vehicles. This means, of course, that we did not consider the rendezvous with the phase II work, not to any great detail, at least. We also wanted to identify the damage mechanisms whereby high voltage could hurt us, and finally, to get an idea of how serious the electrostatic phenomena problem might be for large launch vehicles and spacecraft.

We got some results in our phase II work. We identified what appears to us to be the most critical phase of the Apollo mission. That phase is the first phase, which is from the launch pad until shortly after first-stage separation. It so happens that separation is just about in the middle of the critical pressure regime. We indeed predicted some harmful effects as being possible, and we uncovered some clues to a suspect which previously had not been a suspect, namely the separation phenomena which Dr. Haffner has described to you. Other phases and rendezvous maneuvers were judged to be relatively safe. Finally we came up with a program which we are now following, to do experimental analyses of the effects we predicted.

It is well known that aircraft flying through the atmosphere can become charged to very high voltages in the absence of discharging means. For example, we know that something like the DC-8 aircraft could charge up to perhaps 200 or 300 kv of potential just by passing through regions in which there are atmospheric particles. We also know that jet aircraft may be charged to a lesser extent just by operating the engines, so it stands to reason that something almost as big as the Empire State Building or the Washington Monument, namely the Saturn V, with engines much larger than jet airliner engines, could throw sufficient charge out the back such that the engine charging mechanism would predominate over the atmospheric charging mechanisms. We took a real good look at the engine charging mechanisms. Dr. Vance this morning actually told you what most of the mechanisms were, but in our

Table 1. Work accomplished to date (Phase I)  
(Dec 1962 - Feb 1964)

Nature of effort	Results
<ul style="list-style-type: none"><li>● General definition of scope of problem</li><li>● Detailed study of internal charging mechanisms</li></ul>	<ul style="list-style-type: none"><li>● Evaluation of internal sources for all stages</li><li>● Formulation of "ITRACK" computer program</li><li>● Prediction of maximum charge accumulation ~ internal sources</li></ul>

Table 2. Work accomplished to date (Phase II)  
(April 1964 - Oct 1964)

Nature of effort	Results
<ul style="list-style-type: none"> <li>● Detailed study of effects and consequences ~isolated vehicles</li> <li>● Identify damage mechanisms</li> <li>● Assess seriousness of problem</li> <li>● Recommend preventive measures</li> </ul>	<ul style="list-style-type: none"> <li>● Most critical mission phase identified</li> <li>● Harmful effects predicted</li> <li>● Unsuspected separation phenomenon uncovered</li> <li>● Other phases and rendezvous maneuvers judged to be safe</li> <li>● Program to develop suitable preventive measures formulated</li> </ul>

work we evaluated these mechanisms, and to our surprise it appears that the photoelectric emission is predominant in the engine.

Table 3 goes over the possible internal charging mechanisms one by one. Incidentally, when we speak of internal charging mechanisms, let's confine our attention to the engine because it is the source of all the appreciable internal charging. First, there is thermionic emission which is well known to us, and may take place within the engine. Secondly, there is triboelectricity, because we have things flowing, gases, liquids, etc.; things being sprayed about in the engines. Then we have photoelectric emission well in the ultraviolet regime. We must remember that these photons strike the inner walls of the engine. Unless you have a fiberglass nozzle or possibly a fiberglass combustion chamber, you may expect that electrons will be emitted from the inner walls of the engine. Finally you have combustion products; that is you'll have plasma particles as constituents of the rocket exhaust. There are other charging mechanisms as well. On the outside we have atmospheric triboelectricity, which is well known and fairly well understood. Thermionic emission, since outer surfaces get hot due to the engines. Interaction with environmental charges is actually a discharging mechanism (as we will see later). We also have photoelectric effects resulting from photons coming from the Sun and striking the exterior of the vehicle.

I have spoken with many people regarding the engine charging mechanisms. One man that I spoke with said that he had listened to about a half dozen people and consequently he had heard a half dozen different mechanisms for engine charging. So let me say now that what we say about photoelectric emission is just the results of our pencil and paper study, and it is only for your consideration that we give you the results now. There are other mechanisms which other people favor. As a matter of fact, I have heard it said that it is impossible for the photoelectric emission to be effective. What is the photoelectric emission mechanism? We have energetic photons striking the inner walls of the engine, and we have electrons being ejected to mingle with the exhaust products. It so happens that electrons have a strong affinity for some of the particles which are constituents of the exhaust. So immediately we don't have tiny electrons, but we have massive negative ions formed; and these ions then are driven out of the exhaust by the kinetic energy of the rest of the exhaust fluid. I explained this to another person -- a very competent scientist. He said this is ridiculous. He said that everybody knows that an exhaust is really a plasma and that a plasma can't support an electric field, so where is the electromotive force

Table 3. Engine charging mechanisms

<ul style="list-style-type: none"> <li>● Thermionic emission</li> <li>● Triboelectricity               <ul style="list-style-type: none"> <li>Flowing gases</li> <li>Flowing liquids</li> </ul> </li> </ul>	<ul style="list-style-type: none"> <li>● Photoelectric emission</li> <li>● Combustion products               <ul style="list-style-type: none"> <li>OH<sup>-</sup> and + ions</li> <li>Electrons</li> </ul> </li> </ul>
Other charging mechanisms	
<ul style="list-style-type: none"> <li>● Atmospheric triboelectricity</li> <li>● Thermionic emission</li> <li>● Interaction with environmental charges:               <ul style="list-style-type: none"> <li>Ionosphere, Radiation belts, Solar winds</li> </ul> </li> <li>● Photoelectric effect</li> </ul>	

Table 4. Discharging mechanisms

Atmosphere: Corona and spark breakdown  Ionosphere: Collisions with environmental charges (ions and electrons)		
	Charging currents	Discharging currents
Sep 1st - 61.7 km	2.52 amp	$4 \times 10^{-3}$ amp
Sep 2nd - 183.1 km	0.15 amp	51.0 amp
Van Allen belts Environmental charges (negligible discharge rates)  Solar wind Ionized gas from Sun		

coming from to remove your so-called negative ions? I'm sure this man had heard of the van de Graff generator and the various gaseous MHD power-producing devices. Yet he didn't know where the electromotive force was coming from. What is an electromotive force? It is pretty clear that an electromotive force is any force whereby charges can be given a motion, and in this case we don't need an electric field. We need only something to remove the negative ion out of the engine and this something is the kinetic energy provided by the rests of the exhaust particles. Clearly it is conceivable that any negative ions produced in the exhaust can be driven out of the nozzle leaving behind a net charge, even though a frightfully large number of uncharged particles as well as plasma particles may accompany them.

From our pencil and paper study we therefore say that engine charging on large liquid rockets would result in a positive charge being left behind on the vehicle. We also recognized the fact that there would soon be an equilibrium condition reached where all of the charges wouldn't go on forever. Some of them being pushed out would tend to turn around and come back by the simple laws of electrostatic attraction. We also know that in the lower atmosphere there are innumerable neutral atmospheric particles which would tend to impede the return of the ionized particles that went out the back and are now trying to get back in. Nevertheless, quite a few of them would get back, and at equilibrium we would expect to see a recirculating current. Suppose of them got back and none of them escaped to infinity. You will still get a net charge on the vehicle because they are not all on the vehicle; some are on the way out and on the way back. We believe it is possible for a very large rocket to charge up possibly in excess of a million volts net.

Having talked about charging mechanisms, we now have to turn our attention to mechanisms that prevent us from attaining an infinite voltage buildup. Table 4 presents information about discharging mechanisms. Quite a bit was said this morning about corona discharge. I've been working with corona devices for something like 6 yr now. I've seen quite a few discharges. In fact, I've seen a discharge that probably none of you have seen, called the adjection discharge. It is sort of a souped-up corona discharge that you get when you add fluid kinetic energy to the energy of the ionizing field in the vicinity of a point. It is not a glow discharge. It is not an abnormal glow discharge because it is cold, and it's perhaps 10 or 15 times the power level that you would get from a normal discharge. Corona discharge to me really means the breaking down of a gas by the avalanche process. Of course, you have to have an electron to start it. But there are always electrons about. They're being

made available all the time. You have an electron which is accelerated in a very strong field (it is the field which is important, by the way, and which is dependent on the geometry) then you get this avalanche effect. If the anode that initiated the discharge is charged positively all your avalanche electrons will go into the anode leaving behind a big pulse of ions, which gives rise to the space charge effect. This is what corona is to me. Corona plays a very important part in the discharging of booster vehicles in the lower atmosphere because actually it is the only means in the atmosphere that prevents the buildup of large potentials. Were it not for corona breakdown in the lower atmosphere one could build up many millions of volts on a very large rocket vehicle. The geometry of the vehicle would cause breakdown long before you reach 100 million volts. Therefore in the atmosphere we have to depend on corona to discharge.

Once we get into the ionosphere, we get into a regime of pretty good environmental charges. If the vehicle is charged positive, it selects negative particles to discharge itself, and vice versa. Eventually it would reach an equilibrium voltage in the upper ionosphere of about 10 or 20 v, which is not significant, but let us not forget that some of these vehicles are not bright and shiny conductors. Some of them have insulation practically all over their surfaces, because we have to have ablative paint, various heat shields and plastic covers, and so forth. Let's be careful when we start computing the discharging time of an insulated vehicle. It may not discharge on the order of milliseconds. But in general, a large rocket vehicle once it gets to the upper reaches of the atmosphere, the discharging capability of the ionosphere (and further out, the solar wind) will more than offset any charging which the engine can provide. You can readily see why we say that the most dangerous phase of a large launch vehicle mission is probably from the launch pad until just after the first separation, before it gets to the region of the higher environmental charges.

We have discussed what can act to charge up a large launch vehicle, and we saw that the engine probably can charge a large rocket like the Saturn V to much higher voltages than the atmosphere alone. We also saw that extremely large, or ultrahigh voltages are prevented by the breakdown of the atmosphere in the nature of corona discharge. It would appear that corona is our friend because it prevents us from getting very high voltages. On the inside of the craft, however, corona is not your friend because it interferes with the subsystems. You're liable to have breakdowns between the high-voltage and low-voltage components of the electronic



subsystems. On the outside it would appear to be a friend. But let us not forget that a corona discharge is very, very noisy from an rf standpoint. If we provide a discharging system to work in the lower atmosphere (just as we have discharge systems for aircraft), we have to be careful to locate the discharge systems away from antennas, etc., to prevent unwanted coupling.

Dr. Vance also mentioned this morning the possibility of a streamer breakdown. A streamer breakdown is a one-time expenditure of stored energy from a nonconducting surface to a conducting surface, and sometimes it can be pretty energetic. For example, there is a documented case of a B-29 in World War II returning from a raid over Japan. Apparently the pilot flew through a thunder storm or something and the aircraft became charged to very high voltages. Unfortunately there was a difference in the potential of the windshield and the surrounding structure of the aircraft. We have the stage set for a streamer-type discharge from the windshield to the skin, or maybe it was the other way around. The discharge did happen because the windshield was not properly bonded, and the resulting streamer-type discharge was so energetic that it broke the windshield and blinded the pilot. Other previously unexplained B-29 accidents--the planes that didn't come back--were subsequently attributed to this triboelectric-induced streamer type of discharge. We can also get streamers on large rockets from an insulated surface to the rest of the frame. You get a very energetic noise pulse out of a streamer discharge, but also one could get structural damage in thin areas, but only in thin areas.

Figure 11-1 presents a recapitulation of some of the salient facts about corona breakdown as it is presently understood. A vehicle that has the tendency to become charged will become charged, whether by passing through the atmosphere, by engine charging, or what have you. As this vehicle goes through the atmosphere it will reach an equilibrium condition in which the discharge rate equals the charging rate. This equilibrium condition is a function of many things. It is a function of pressure, speed, mean free path in the corona process, how fast the space charge is being removed, and so forth. And also equilibrium condition is certainly a very strong function of vehicle geometry. We will reach an equilibrium condition when the discharge rate equals the charging rate. But it turns out that something with a very strong field, like a sewing needle, for example, will reach an equilibrium potential long before a DC-8 without a discharging system

attached to it. For example, we know that something like a little needle will begin to corona at just 5 or 10 kv. This fact is why similar things are placed at the extremities of an aircraft to discharge it. You see, when you put a lot of sharp points at the extremities where corona would naturally tend to occur, we tend to lower the equilibrium voltage of the vehicle. This effect, in essence, is what the discharge system for aircraft consists of. That thing on the right of Fig. 11-1 is not really the Washington Monument. It is supposedly the Saturn V launch vehicle, and we have a little lightning bolt in the middle which is supposed to represent the streamer--a one-time discharge of stored energy type of a breakdown--and we notice that corona would tend to occur about all edges, about all extremities, and particular about those that have sharp points.

Another thing about corona discharge is that it is a strong radio interference generator. Figure 11-2 shows the manner in which RFI emanates from discharges; in this case an interstage discharge taking place at separation may be coupled into a black box. These relationships are well known, and there's no need to spend a lot of time describing them to you.

Figure 11-3 shows why one should not let the vehicles charge up to very high voltages. At the top we have two geometrical figures. The one on the left has a sharp point; the one on the right has a blunt point. Both of these objects are presumed to be charged up to say, an equilibrium threshold condition where they are just starting to corona. The one on the left, having the sharpest point, by the ordinary laws of electrostatics would tend to have an extremely high field concentrated at the point. The one on the right would not have such a strong field at its point because it has a very large (relatively speaking) radius of curvature at the point. Therefore, the blunt point would have to be placed at a much higher voltage before it would reach the corona threshold than would the one on the left. Consequently, if we take a look at the discharge current pulses from these two points at the moment when they're both at their threshold voltages, we find that the amplitude of the sharp point is considerably less than the amplitude of the blunt point. This effect is something that you have to associate with the properties of a corona discharge. Now, what does it mean to us? On the bottom we have a squaring amplifier with a clock pulse output. I believe the sine wave at the top represents the trigger level. The corona noise pulses appear as spikes on the wave form, and at the bottom are ordinary clock pulses. Considering the corona signal which emanates from the blunt point, because of the higher amplitude we find that we have sufficient noise pulses superimposed on the sine wave to afford

an extra clock pulse. This is not something we dreamed up. This is something that actually happened. So you see, if you let the body charge up to a high voltage before it begins to discharge to the atmosphere, you get very strong noise problems as a result of the corona RFI. If you don't let it reach high voltages by installing, for example, a discharge system, then the noise pulses are relatively insignificant.

Back in the 1930s there was a lot of work being done by the best brains in physics on gaseous discharges. Someone mentioned earlier the works of Cobine and Loeb. These books are just chock-full of data from the 1930s. Everybody was interested in gaseous discharges, fascinating high voltages. Then along came nuclear physics, and all the best brains turned their attention to what they thought was much more fascinating than high voltage. If you do a literature search you won't find much of any significance beyond the 1930s. In fact, most of the stuff dates around the 1830s or the 1530s. For example, if you're interested in the triboelectric series and you want to determine what the effects of flying a rocket through a dust storm will be, you want relative dielectric constants and so forth. What you're going to find are cat's fur, amber, lodestone, and things of that nature. So you see, there's a lot of work which has to be done in the field of high-voltage research. As a matter of fact, it was interesting to notice the empirical nature of most of the discussions this morning. Here we are sitting around exchanging recipes, mind you, for potting compounds; how long do you cook this one, and so forth. So there's quite a bit of work to be done.

We believe we have uncovered a suspect. Dr. Haffner has shown that if you have a conducting body and if it becomes charged up and is isolated, then no matter how it becomes charged up, the point is this: Separate the two bodies in an asymmetrical fashion, in other words, cut it at any other place except that particular point at which the resulting bodies would have equal capacitance. If the body is cut in almost any way, there will be developed a potential difference between the two separated parts. By studying the results of Dr. Haffner's various configurations, we discover something else significant. This potential difference will be greater, the greater the dissimilarity between the bodies. For example, if I were to take the Saturn V launch vehicle and just cut off the launch escape tower, I would have the worst situation of all according to that theory. But if I cut it somewhere above the S1C stage, there may be practically no potential difference generated. We must remember that separation takes place in a very short time, usually by linear shaped charges (LSC). There is not much time for the charges throughout the entire stack

to realign themselves to the new locations or positions demanded by the new geometrical and electrical configuration resulting from stage separation.

So you cut the body. You don't have one body, but rather two bodies. You don't have one capacitance; you have two capacitances that are mutual capacitances. As they begin to pull apart the mutual capacitance part of it will change. I'm not going to repeat the little that's known about charge distribution and electrostatically-charged bodies. I'll just say one thing. Most of the charge is in the point; that is where the charge density is greatest. The part on the bottom that got cut off doesn't have enough charge. It gets complicated. If you count the charges before and after the separation and compare the capacitances of the bodies, you'll find that there has to be a potential difference and that this potential difference is a function of many things. For example, the LSC explosion may afford a conducting path between the two vehicles. If you don't have an appreciable plasma, you have sharp edges; you have dangling umbilical cords; you have all sorts of possibilities. Sometimes you have gas coming down which can become ionized by the field that may exist between two separated bodies.

We are not saying that this happens. We are saying that it may be happening. A lot of things have been happening at separation. We are saying this: There can be a potential difference; there can be an interstage discharge. So you get an interstage discharge, so what? Here's what. The vehicle frame and the skin constitute the electrical ground reference system, and these things are supposed to be nice and linear forever because this is your reference platform. Suppose you have a discharge in which you have something like even 50,000 v, practically nothing; not a million volts, just fifty thousand volts potential difference. You got a big spike going to the ground system. This spike is going to do something to some systems. Dick Reeves has conducted some experiments in which he wanted to find out what happens if he put a healthy spike, a corona spike, on a ground system. What he did was to construct a shielded and enclosed chamber; inside this chamber he placed representative RC networks. Inside the chamber he also put a little battery-powered Tektronic oscilloscope. He referenced the circuit, which was being test, to the container itself. In other words, he took a wire from the circuit and connected it to the inside of the test chamber at one point, and this was supposed to simulate grounding to the vehicle skin. Then he had just a small, screened aperture to look in at the scope to see what was happening. He then proceeded to charge this container up to, I believe, 18,000 v. He took a grounded probe and drew arcs from the enclosure, thereby

introducing something of the order of 18,000 v transients into the electric ground system. He observed that signals were introduced into his RC network as evidenced by the scope. One of the capacitors was 40 pf. For this particular configuration, I believe he got something like 10 mv extraneous signal introduced up through the ground. Mind you, this is only at 18,000 v. He also found out that the signal introduced was inversely proportional to the value of the capacitors. He did certain other things to ensure that this was not RFI. What it amounts to is that suddenly you have a generator between the ground point of your circuit and the ground itself. We at North American are planning more extensive tests of this phenomenon--conduction through the ground--and we would like you to consider it. Perhaps it may be the answer to some of the problems that are happening. As I said, there may be lots of crimes. Surely there are local crimes in the boxes themselves; there is localized breakdown; there is RFI. But now let's look at another villain. Here suddenly is the generator interposed between the ground and the grounded point of your circuit.

#### OPEN DISCUSSION

MR. MOLMUD: In your sources for charging, I did not notice the source mentioned by Ed Vance, which is the higher mobility of the electrons in the rocket exhaust that would give you a charge of the opposite polarity.

MR. COLEMAN: As I said, if I start now beginning tomorrow morning and talk to various investigators concerning engine charging mechanisms, I would be willing to wager a bet that probably for every five people you talk to you'll get probably four different predominant mechanisms. We have not considered the relatively high mobility of electrons as compared with ions in detail except in the case of the environmental charges which tend to act as a discharging mechanism. In this regard, let me say that if you have something in orbit in the region of environmental plasma, one would expect that the equilibrium potential after you have shut down the engines would be negative. It would be negative because of a greater mobility, the thermal motion of the electrons. You would tend to get more negative particles striking the craft over a period of time.

MR. MOLMUD: You also have the photoelectric effect working there, as a matter of fact.

MR. COLEMAN: Yes, you do. You do have the photoelectric effect working there, but our studies have indicated that it is relatively insignificant.

MR. MOLMUD: How do you account for that? The temperature of the Sun is higher than the temperature of the combustion chamber.

MR. COLEMAN: Yes.

MR. MOLMUD: So the UV content is higher.

MR. COLEMAN: But now in the case of photoelectrical effects from the Sun, we have to remember that the electrons are trying to leave the exterior of the craft, and therefore we have to take into consideration such things as electromotive force. Remember that in the case of the internal photoelectric effect we had plenty of electromotive force with all that gas rushing out to push the ion out because the electron inside the engine has an affinity for certain of the molecules, and it becomes quickly a big negative ion, big enough to be pushed out by the exhaust gases. On the exterior surface if you have a UV photon striking the surface and causing the surface to emit a photon, any charge as a result of a series of such events, the net charge of the exterior of the vehicle, would tend to pull the electron back in. You don't have the same electromotive force on the outside as you have on the inside.

MR. MOLMUD: I have a rebuttal to that. For the interior, when you have a photoelectric effect--and a photoelectric effect will occur in the interior--you're going to produce (if that's the only effect occurring) a net excess of negative charge in the interior. In the exhaust you will have a net excess of negative charge. Therefore you will have a radial electric field which will tend to drive the electrons back out. You have to take into account the current that may be running because of such fields. Those currents will tend to drive electrons back onto the surface of the wall. The rocket exhaust is very conductive at those temperatures at which you are invoking the photoelectric effect because it's only when you have high temperatures that you have a large amount of UV. You have to take into account all the currents that are flowing radially in the rocket exhaust. There is the current due to the electric field. There is the current due to the photoelectric effect, which is in the opposite direction. And there is the current due to diffusion caused by the higher mobility of the electron. All these have to be taken into account in order to figure out what is the net excess of charge coming out and what is its sign. I wonder whether you did that.

MR. COLEMAN: We did, and they were considered. And if you'll see me after the meeting, I'll be very happy to give you a North American report number that describes in great detail how we went about evaluating all the various mechanisms.

MR. BROWN: Mr. Coleman, can I join your force here to say that you must have taken these into account. If I can, maybe I'll add a little authenticity to what you say. On the eve of a launch coming off tomorrow you possibly will have noted, I believe, in the June issue of Electronics (published by McGraw-Hill) a list of experiments on the Gemini program. Have you been in contact with this program to that extent?

MR. COLEMAN: Yes, I have.

MR. BROWN: I think it is June; I'm not sure. At least it lists a whole raft of experiments there. There is one that was listed that has been flown once. I don't feel that I should give actual numbers, but nevertheless, you're in the ballpark. To the best of my knowledge, the figure you dispensed as to the charged vehicle is very closely akin to what has so far been resolved. More than that, I'd rather not say. However, this charge was there as measured on the experiment and did not go away for some time, as had been figured by some other calculations. Others have calculated as you have and have come up with something of the same nature. There's another company that did this work on a solid fuel and actually made some experiments to confirm somewhat the same results that you have; they found that some of the phenomena that hasn't been really explained yet involving the ionosphere may or may not have contributed to some other charges that were apparently prevalent. This is yet to be derived, and we have to have one more flight before we can evolve some more data.

At the Saturn launch recently some instrumentation was available to instrument lightning gradients. One of these Saturns took off and pegged the meters; as I recall, this instrument registers 15 kv at full scale. This happened on a Saturn launch and it also happened on one of the Titan launches that was supporting the Gemini. So the vehicle does dispense, I presume, a charged water particle as they have in the flame bucket. In the case of Saturn, I recall, the charge that was registered on this instrumentation (and it was confirmed that the instrumentation was working properly, at least to detect lightning gradients) did not relieve itself for 2 or 3 hr thereafter. It held in the

area there for some time. That was rather interesting. I suspect this was the prelude to the experiments that were going on to actually measure some of the vehicle charges you're speaking of.

Another company made a little further analysis in this area and ended up with a solid rocket firing which they confirmed did have a charge and was at the opposite polarity from what you'd expect from a liquid engine. This particular experiment was being performed to substantiate the problem they thought they had with instrumentation. To get rid of this charge, they ended up by putting some discharge mechanisms--sharp edges and things of this nature--rather than having the corona prevalent. They wanted to discharge this thing with a point source that would let it leak off. This apparently solved the problem from what I can recall of the report. I think we're on the right track if we can just find out how to apply it on vehicles, and I think we're working on that.

MR. COLEMAN: Thank you. In the past, quite a few measurements have been made on smaller rockets, quite small solid rockets in most cases, but now we need information from the real big boosters. Steps are now being taken within NASA to make such measurements. I am aware of the tests you referred to, both at MSC and MSFC and, I believe the subject of the next presentation is just that, namely, measurements of relatively large boosters for electrostatic effects.

Let me say again that you really can't hold me to anything I said tonight because I believe I suitably qualified everything, but that is the way it looks.

MR. LEWIS: I'd like to ask a question about the Saturn. Did the Saturn have static dissipators on it at the time these measurements were made?

MR. BROWN: Was that directed to me?

MR. LEWIS: Yes.

MR. BROWN: I don't know the Saturn vehicle too well. However, as far as I know there were not any dissipators. The information I gave you there on the charge was measured by a ground instrumentation system that was made by some company in Denver. They had two measurements. One was nothing more than a simple probe in the air that was a construction of a probe with a high resistance and a microammeter across and a DC amplifier to amplify the charge.

The other was more of an elaborate instrument; the full scale on this instrument was something like 15 kv, and this was pegged at the time of takeoff.



I don't believe there were any dischargers or discharge mechanisms on the Saturn. However, I don't have the information of what happened in flight. This was a matter of the engines themselves spewing out the flame and, in so doing, moving particles. And this charge was imparted to the water vapor, or whatever else; it might have been dust. The charged particles were the things that were measured there.

MR. LEWIS: Was this insulated? Was this a vehicle on a high stand?

MR. BROWN: This was a vehicle that was launched from Cape Kennedy. This was the Saturn launch, I'm speaking about, and a Titan launch. Instrumentation was fixed in the blockhouse and intended to instrument for lightning, of which they measure the field gradient.

VOICE: Were they measuring field gradient due to the launch?

MR. BROWN: They were measuring a field gradient wherever it may have come from, and it was there as measured by the instruments.

VOICE: Was there a field gradient before the launch?

MR. BROWN: Negative. They don't launch in lightning, as a rule.

VOICE: There is usually a field gradient anytime, anywhere and it varies.

MR. BROWN: Having watched one of these meters, it departs very little from the normal, and I've watched some lightning. As a matter of fact, I might say that just recently a man was killed by lightning down there. I happened to be watching one of these meters during that lightning storm and prior to it there was no indication that there was any field in the area until the storm moved over the area. And this time it didn't go quite that high when we were looking at the instrument. This was another instrument, not at the blockhouse.

VOICE: Now for a rather cool day, would you have 15 kv per meter?

MR. BROWN: No more than that. The instrument, as I recall, is calibrated  $\pm 15$  kv max scale at which time you can set an alarm; it would go off, and you can also get a reading that will give you a strip chart to show it, and it pegged. I didn't see the one that pegged on the launch, but I have it from a good source because I know the instrumentation man quite well.

VOICE: Was this plus or minus direction?

MR. BROWN: I don't know.

VOICE: I wondered if they could determine the polarity during the launch.

MR. BROWN: I didn't have that information. I just don't know.

DR. VANCE: Could I comment on this?

What you have there, I think, is an electric field meter mounted on the ground, and it measures the atmospheric electric field which is normally 100 v per meter. If lightning is imminent, the field strength at the surface of the ground will go to 10 kv per meter or higher. What you're measuring with this meter, I think, is the charge on the exhaust gas that is expelled down through the launch pad and deflected about. It drifts out in the vicinity so you do have a charged gas or dust cloud in the air. This will cause a deflection on the field strength meter. It doesn't necessarily say too much about the potential of the rocket vehicle. We have performed a similar experiment at SRI. Some of our people (I personally wasn't involved) placed a similar electric field meter at the end of the San Francisco Airport runway and monitored the charged exhaust gases expelled by the jet aircraft during takeoff. Here you have a similar effect. You have a charged gas which hangs in the air for quite a while because the collision frequency is very high and the mobility of ions is fairly low, so it takes quite a while for this charge to be attracted down to ground and neutralized. I don't think that you can conclude from this measurement that the vehicle is charged or not charged. The charge you see may be picked up as a result of the gas flowing through deflectors at the launch pad. It may be a charge that is ejected from the combustion chamber.

MR. BROWN: May I say that I did intend to give three sources and three bits of information that I may have run together. The bit about the lightning field gradient meter was thrown in for good measure to show you that you do get some good charge from these engines from the practical standpoint, rather than the theoretical. Another bit of information was the fact that the company that made these measurements, or rather detected an instrumentation anomaly, had theoretically supposed this was a problem of vehicle charge. The company ran some measurements on a solid fuel motor, measured the charge on this small scale motor, and determined that, yes, they did have a problem. They took corrective measures by adding some sharp spines and things of this nature to discharge it. As I recall, this corrected the problem they thought they had, and apparently this would be a confirmation of that. That's the second bit. The other one is the fact that the

Gemini program does have a program to make a measurement of an electrostatic field. So far I can say that from what I know the results have confirmed what Mr. Coleman has stated, at least from the measurements from the spacecraft end at the time of separation.

I'm not saying that the vehicle had the charge, but there were no engines being fired on the spacecraft at that time, and on top of that, they didn't have the magnitude of engines that could fire to give that kind of charge. Secondly, this charge didn't last. It lasted longer than theoretically had been calculated by some other calculations, as a matter of fact, quite long. But it did drain off, and then they had some other readings which they tried to confirm by later measurements which we hope tomorrow may give us some other ideas.

DR. VANCE: This discharge will hang around for quite a while in the air.

MR. BROWN: Some calculations say no.

VOICE: What charge are you talking about?

MR. BROWN: I'm talking about the one on the vehicle that is there at the time of separation.

VOICE: Is that in the ionosphere or above?

MR. BROWN: This is at the time of orbit insertion, and this is the nature of 100 miles.

VOICE: It is quite startling to hear that last remark.

MR. BROWN: Well, I don't have the information. I have not seen the data myself but I am in the area where I get word of mouth as good as anybody could get it.

MR. LEWIS: I would like to make one more comment in regard to these static dissipators that have been mentioned. To really get good noise reduction you need more than just a fine point. The fine point, as Mr. Coleman has pointed out, will give you some reduction. Our experiments indicate that a needle point will give you about 6 db of noise reduction over a discharge off a fairly smooth edge, such as the training edge of a DC-8. In order to get more noise reduction, you need to do a little bit more than merely put a point on. We have developed techniques for getting as much as 60 db of noise attenuation, and these techniques are used in static eliminators you see on aircraft. The primary source of noise reduction is not the fine point.

VOICE: It's a peculiarity of the design--not a peculiarity really--but is in the design of the discharger. These dischargers are rods about 6 in. long, and they have a conductive or a slightly conductive coating on them of about 20 megohms of resistance between the base of the discharger which connects to the aircraft and the needle point where the discharge occurs. If you plot noise produced in, say, a receiving antenna on the aircraft or missile as a function of distance along this rod, you'll find that it goes down as you go out along the rod and about an inch or so from the end you reach a minimum of coupling; and then as you go on out toward the end there is an increase in the coupling. These tungsten needles are placed at this point of minimum noise coupling. It has to do with the geometry of the rf fields about this discharger rod and with the orientation of the discharge relative to the rf fields that would be reproduced by the antenna if it were driven as a transmitter. It's a fairly involved electromagnetic coupling theorem or reciprocity theorem involved.

DR. WHIPPLE: I'd like to clarify some of the comments that were made about the Gemini IV experiment in which it was claimed that the results of the experiment are evidence for these high potentials. This experiment was an electric field experiment, and if you'll remember Dr. Vance's comments on the rotating shutter type of field mill, this instrument is very susceptible to currents from the plasma. You need a phase discrimination technique to separate the signal due to the field from the signal which is due to the current. The experiment on the GT-4 spacecraft did not have a phase separation technique. If you talk to the experimenters at Houston you find out that they really don't believe the high potential measurements. In addition, the input network of the sensor had a very high impedance so that any currents flowing into the stator of the field mill would build up a high potential merely across the input network which would add to the confusion and be interpreted in terms of a very high spacecraft potential. I'd like to show a little bit of data that also might help to clarify some of the effects that can occur at launch.

MR. BROWN: May I add something to this? Maybe you have the information also that this new experiment that is going to help to clarify the information from the earlier one. Are you aware of this?

DR. WHIPPLE: Yes, I am. I'd like rather not to speak for the Houston experiments since I'm not directly involved, but what they are going to do on the next shot, as I understand it, is to screen out the electric field and just look at the

currents alone to check the idea that what they were seeing was currents and not really the electric field. Now, this data here that I'm presenting is an electric field measurement made a number of years ago on the Viking rocket which is a liquid fuel rocket, and this is at takeoff. The electric field mill was right on the nose of the rocket. You can see the zero-second marker. Now, the two channels are parallel. One channel indicates the amplitude of the field and the other one is a channel that indicates both the polarity and also indicates the phase. I just want to call your attention to the top channel. To the left of the zero-second marker, in other words, before takeoff, there was a measurable electric field, and this is the normal fair weather atmospheric electric field of the order of 100 to 200 v/meter. This field is augmented by the fact that the field meter is on the tip of a very long prolate spheroid, namely the rocket, and the augmentation factor can be quite large in order of magnitude.

When takeoff occurs you can see the large excursion there in the first 2 to 3 sec. What I believe is happening is that as the rocket lifts up on the tongue of flame, the augmentation factor increases tremendously because you have a much longer conducting body, both the rocket and the flame behind it. As a result, the measured electric field is still there; the normal atmospheric fair weather field is augmented at the point of measurement, and that's the cause of the increase. As soon as this flame separates from the ground there is a redistribution of charge, and I suspect that this may be the cause of the disturbance in any other field meter in the vicinity such as the one Dr. Brown just described. When the flame does separate, there is an outflow of charge from the vehicle, and in this case apparently it's in such a direction as to reverse the charge on the rocket. At the time of separation, the net charge on the rocket would be caused by the induced charge from the atmospheric field which would be a negative surface charge on the rocket. When the flame separates, this charge is left on the rocket. Consequently, the exhaust here is in such a direction as to take off this negative charge and to charge it positive. It goes through zero at 4 sec. That's actually a reversal of polarity, as you can see from the channel below. At 5 sec it reaches a maximum, and from there on it decreases. There's another change in polarity, and from 10 sec on there is a slow decrease. By the time of 40 sec the field is down to zero. I'd like to go on about 100 sec. At about a 100 sec and after as the vehicle gets into the ionosphere, look at the bottom channel. You can see that the signal rises again starting at about 103 sec or 102 sec.

It comes up slowly and then between 110 or 115 it comes up very fast. Looking at that naively you would say again there is a large potential. However, since there was a phase separation technique which would be shown on the channel below, that signal is due to currents flowing and not due to electric field at all. And indeed later on you can show that this current or that signal is modulated by the spin of the rocket, that it is in phase as the field meter looks at the Sun. You get a signal indicating a photoemission current, in other words, a positive current to the rocket. When it is looking away from the Sun, you get the opposite polarity. We have seen the same type of thing on other rockets later and also on Explorer VIII. I just want to emphasize that you have to be very careful when you're measuring electric field. The plasma can be very misleading in its effects, and it's very easy to interpret results incorrectly.

MR. COLEMAN: Thank you, Dr. Whipple. For those of you sufficiently interested to do a literature search on rocket charging, you are in for a rare treat because you will find other results in the literature which have even more irregularities than the ones in the Viking, and consequently have some very interesting interpretations, which I'm sure may be valid. For example, some small 5-in. solid rockets were tested in various environmental conditions on the ground. They even pointed one straight up, I think. They made a special afterbody for it because they wanted to straighten out the erratic results. To their great surprise the rocket charged first positive and then negative, or maybe it was the other way around, in very erratic fashion. They decided that this charge reversal was indeed due to engine charging but that the particles resulting from the ignition process had such a physical chemistry to them as to cause the charging to go up one sign, and then when these preliminary particles were finished the main exhaust stream came out and charged the other way. But I think it changed signs again later. This thing has got to be resolved and I believe the next paper will show current steps which are being taken to resolve the problem. I might add that the SA-10 measurement on Saturn was made at the order of Dr. Von Braun himself. I don't know the results of it. They have not been released.

MR. LEWIS: I'd like to clarify one thing. The test that you're speaking of was made by the Boeing Company, and the reason that the rocket engine was pointed vertically was because it was felt that the ion gas was grounding to the ground as the engine was fired horizontally. In the vertically fired engine they obtained good results.

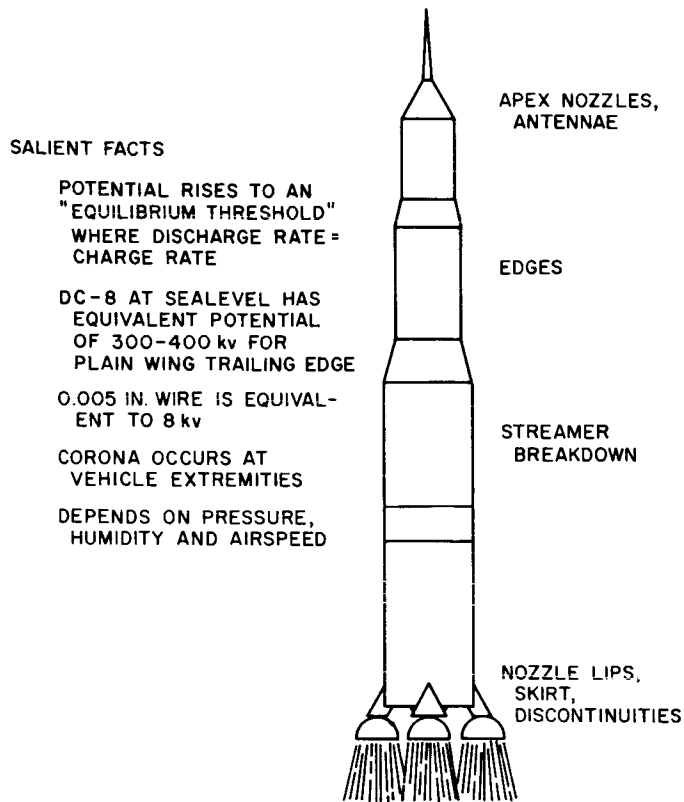


Fig. 11-1. Corona breakdown

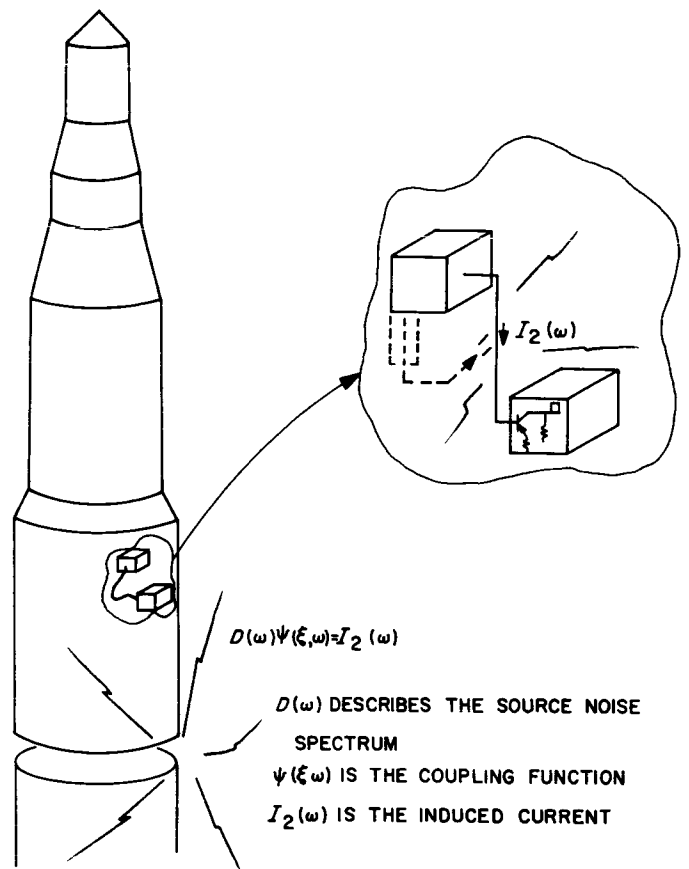


Fig. 11-2. Discharge coupling

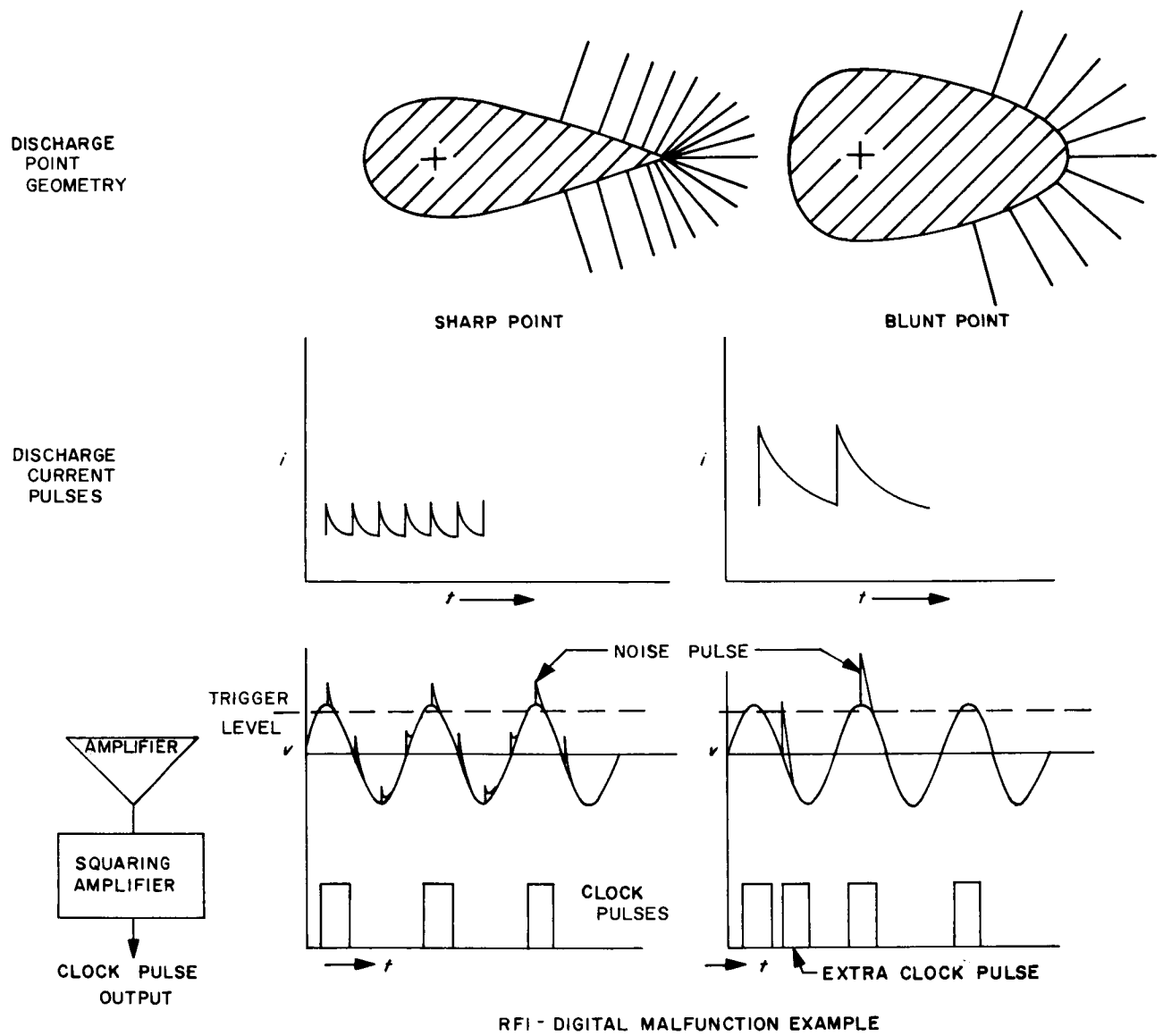


Fig. 11-3. Corona RFI effects



## 12. ELECTROSTATIC POTENTIAL SENSORS FOR USE ON THE NASA SCOUT EVALUATION VEHICLE S-131R\*

N. F. Bolling and R. L. Clark  
Astronautics Division  
LTV Aerospace Corporation  
Dallas, Texas

### ABSTRACT

Unexplained electrical disturbances have been considered as possible causes of malfunctions occurring during a few Scout launches. It is postulated that the disturbances, principally during staging operations of the boost sequence, could be due to corona effects and/or sudden discharge of electrostatic potentials. Such lightning-like transfer or redistribution of accumulated electrostatic charges may induce high-voltage steep wave front transients in low-voltage circuits, or cause arcover through ionized paths between exposed electrical connections at altitude, thus transferring firing energy into critical upstage pyrotechnic control circuits.

This paper discusses some of the basic hypotheses and theories concerning electrostatic charging mechanisms related to Scout, and the buildup of potential differences between parts of the vehicle, and describes two types of sensors developed for in-flight measurement of those voltages. Both sensors are of uniquely modified field-mill (generating voltmeter) design. One type is a low-frequency response sensor, and is used to measure steady-state or quasistatic potentials due to electrostatic charges accumulated on Fiberglas skin surfaces of the vehicle during motor-fire and coast periods. The second is a high-frequency response sensor, and is used for measurement of transient potential differences developed between upper and lower stages of the vehicle during separation. Both types operate from the 28 v dc vehicle supply and provide 0 to 5 v dc outputs for multiplexing onto the Scout vehicle telemetry system. Output of the transient potential sensor is linear with input electrostatic voltages from 500 v to 50 kv, output of the other is logarithmic for inputs from 10 v to 30 kv. To sensors of each type are used on Scout Evaluation Vehicle S-131R. Continuous data channels monitor the transient potentials developed during

---

\*This paper is a reprint of Engineering Report 000TP001 LTV Aerospace Corp., Astronautics Division. It has been edited slightly in style and format to make it consistent with the other papers in the Proceedings.

the first and second and the second and third stage separations. Commutated channels monitor the electrostatic potential differences between vehicle structure (electrical system ground) and fiberglass skin surfaces on "upper B" and "upper C" interstage sections. Basic characteristics of the units are as follows:

<u>Characteristics</u>	<u>Surface sensor</u>	<u>Transient sensor</u>
Frequency response	12.5 cps (20 ms)	100K cps (2.5 $\mu$ s)
Voltage range	10 to 30,000 v	500 to 50,000 v
Input impedance	$10^{12}$ ohms	$10^{12}$ ohms
Output	0 to 5 v dc	0 to 5 v dc, peak output signal retention 5 ms
Amplifier	Logarithmic response	Linear response

The unique characteristic of these electrostatic sensors is the enclosed sensing head permitting remote monitoring. The enclosed head maintains high input impedance, achieves ease of installation, avoids the disadvantages of a standard field mill such as ram current, photoelectric emission, vacuum lubrication, and vehicle modifications for surface installations.

This work was performed as part of the Scout Systems Engineering Program and NASA-LRC contracts NAS1-3589 and NAS1-3657. The sensors were fabricated by Rawco Instruments of Fort Worth to specifications developed by the LTV Astronautics Division of LTV Aerospace Corporation at Dallas, Texas.

## INTRODUCTION

### Background

Unexplained electrical disturbances were considered as possible causes of certain malfunctions that may have occurred during a few Scout launches. In particular, the studies and tests which were conducted in support of failure investigations subsequent to the in-flight loss of vehicle S-128R indicated the following. First, the Destruct System Safe and Arm units might be susceptible to inadvertent squib-firing in the bridgewire-to-case mode if subjected to sufficiently large dc voltages or to short duration pulses of lesser magnitude. However, the required voltages appeared to be approximately one to two orders of magnitude larger than the normal operating

voltages of the Scout vehicle (Ref. 1). Second, the Pyrotechnic Control Circuit supplies might sustain, but probably could not initiate, arcover under simulated flight conditions (Ref. 2). Third, it could be postulated that electrostatic charging during actual boost sequences might develop sufficiently high voltages to cause electrical disturbances of the required magnitudes, principally during staging operations, by corona effects and/or by sudden discharge of the electrostatic potentials (Ref. 3-10). Finally, the redistribution of accumulated electrostatic charges by lightning-like transfer or by corona-type leakage might cause arcover through ionized paths between exposed electrical connections at altitude, or induce high-voltage steep wave front transients in low-voltage circuits. Thus firing energy might be transferred into critical upstage pyrotechnic control circuits. Based on findings of the investigations, LTV Astronautics Division submitted to NASA-LRC a plan for tests and analyses to determine: (a) the probable magnitudes of electrostatic voltages and electrical energy (charge) storage capacities available during ascent and staging of the Scout vehicle, and (b) the probable threshold sensitivity of the Destruct Systems Safe and Arm units to inadvertent firing by discharge of electrostatic energy (Ref. 11). Recognizing the need for answers in this potential problem area, NASA included the installation of sensors for electrostatic charge measurements in the Scout Systems Evaluation Vehicle, SEV S-131R. Thus, rather than a formal study program of tests and analyses followed by a flight experiment, an electrostatic charge measurement experiment was established. The LTV Astronautics approach used four sensor installations — two each of one type for measurement of steady-state or quasi-static potentials due to accumulation of electrostatic charges on Fiberglas skin surfaces of the vehicle (on "upper B" and "upper C" interstage sections), during motor-fire and coast periods; and two each of a second type for measurement of transient potential differences developed between separating stages of the vehicle, during the first and second and the second and third stage separations. The basic measurement requirements and sensor performance characteristics were determined, and procurement specifications were prepared (Ref. 12 and 13). The design, development, fabrication, and installation of the required sensors were conducted as part of the LTV Scout Systems Engineering Program and NASA-LRC contracts NAS 1-3589 and NAS 1-3657.

## Charging Mechanisms

In lieu of the information which would have been obtained from the proposed study program, the required measurement ranges and sensor performance characteristics were established by technical report surveys, review of fundamental theories and laws of electrostatics, personal contacts with prior experimenters, and a qualitative study program including upper atmospheric phenomena. Only rough estimates could be made of probable charging rates, charge storage capacitances of vehicle system configurations, magnitudes of accumulated electrostatic charges, and ranges of potentials to be measured. Within the subsystems, environment and operational sequences of the Scout vehicle launchings, there appear to be several mechanisms capable of producing, storing and discharging electrical energy at significant levels. Those considered most applicable are as follows:

First, the electron diffusion (or rocket engine firing) mechanism which may produce significant charging rates. It is postulated that the electrons within the thermally ionized combustion products (plasma) of the rocket motors are more mobile and move at higher velocities than the positive ions. Hence the electrons may diffuse more rapidly to the combustion chamber walls and the less mobile positive ions may be expelled in the motor exhaust (rocket plume), so that the motor case should become negatively charged (Ref. 3). Motor cases of conductive materials may permit the electrons (negative charges) to flow to the outer surface as fast as they diffuse to the inner surface. Thus the region within the combustion chamber may be left virtually field-free and further diffusion of electrons to the walls may not be inhibited by the charge already accumulated there. By this process negative charge may continue to build up on the case during motor firing, and the electrical potential of the vehicle structure may continue to increase negatively until limited by some process such as corona discharge, recirculation of positive ions from the vehicle exhaust, or another charging mechanism. Analyses based on what appear to be reasonable assumptions show that potentials of several kilovolts might result from the engine-firing mechanism.

Second, the triboelectric (frictional or contact) charging mechanism may develop significant charging rates and potentials of either positive or negative polarity depending upon the materials involved. A material higher in the triboelectric series becomes positively charged when brought into intimate contact with and then separated from any materials below it in the series. Simultaneously the materials

which are below it become negatively charged. The phenomena involves electron transfer from one material to another by interatomic (or molecular) electrostatic forces and does not require prior "charging" of either material. Electrostatic charging by this process is widely observed in commonplace daily occurrences and has previously been the subject of many investigations in relation to charges developed on flying aircraft (Ref. 14). More recently the phenomena has also been studied in regard to electrostatic charging of missiles and payloads (Ref. 3-10). Again, analyses show that significant charging rates and potentials (many kilovolts) can be developed and, dependent upon available capacitances and environments, appreciable quantities of electrostatic charge may be accumulated.

A third charging mechanism which is considered applicable involves the sweeping-up or collection of charged particles as the Scout vehicle ascends through an "atmosphere" or "plasma" of gaseous ions, charged meteoric or volcanic dust, cirrus cloud crystals and other particles. Some studies have indicated the largest charging rates may occur during encounters with low-altitude cirrus cloud formations (Ref. 3). Again, depending on vehicle configuration (intercepting areas, radii of curvature of exposed surfaces, etc.) and on electrical characteristics of the surrounding plasma, the charging rates could be on the order of  $10^5$  pico-coulombs per second (hundreds of milliamperes), due to cirrus clouds alone.

Other charging processes that were considered included those due to photo-electric effects, plasma effects in the ionosphere, and antenna rectification. Although these processes should not be disregarded when comparing total charging rates, particularly at extreme altitudes, they are generally considered negligible at altitudes of interest to the Scout launch phase measurements (Ref. 3 and 4).

Further investigations of the most important charging processes revealed that some differences of opinion exist in the electron diffusion theory. Recent experiments, in which the charging of small solid-fuel rocket motors was measured during static firings, indicated that the motors often charged positively rather than negatively (Ref. 3). The results of a series of static firings, and also some actual flight experiments, conclusively show that, although the charge buildup is large, some charging mechanism other than electron diffusion must be active to account for the observed positive charging. Charging current measurements, of a secondary nature, were made during motor firing within a large evacuated chamber (Ref. 15 and 16). That data also indicated polarity changes in the charging processes. A possible explanation

of the positive charging may lie in the triboelectric or frictional effects as the solid particles in the combustion productions strike the nozzle walls.

### Credits and Acknowledgments

The authors wish to acknowledge the contributions and cooperation of engineering personnel in several groups (Ref. 1, 2, 11-13, and 15-20) who assisted in collection and review of technical data during the design, testing and reporting phases of this development effort. In particular, much information presented in this paper is also contained in the Ref. 20 detailed engineering report.

In addition, the approval granted, by the NASA Resident Engineering Management Office (REMO) at LTV Dallas, for presentation of this paper, does not include permission to release final results or flight data from the launch of Scout vehicle SEV S-131R on August 10, 1965. That data can be released only by the NASA-LRC Scout Project Office. It can be stated, however, that the four electrostatic potential sensors were flown on SEV S-131R and did measure voltages.

## BASIC DESIGN REQUIREMENTS

### Measurement Requirements

The electrostatic measurements on SEV S-131R were to determine electrical potentials existing during ignition and separation of the first and second and the second and third stages. Based on results of the 138R analyses, the charge mechanism studies, and consideration of interstage structures and materials, it was concluded that the measurement of electrostatic potentials due to static charge accumulation on fiberglass surfaces of "upper B" and "upper C" transitions prior to separation would provide the most useful data for determination of the potentials existing at second and third stage ignitions. These would basically consist of measurements of the relatively slow buildup of voltages due to charge accumulations on "capacitors" comprised of the internal metallic structures and components as one plate, the Fiberglass skin as dielectric, and the "conductive" outer surface of the Fiberglass as the second "plate." Such measurements would not require continuous monitoring and could be handled by conventional commutator sampling rates.

Consideration of charging mechanisms and the operational sequences during separation indicated rupture of an interstage diaphragm might result in charge buildup

of one polarity on the upper stages and simultaneous charge buildup of the opposite polarity on the separated lower stages — directly in the path of ions being discharged via the upper-stage motor plume. Voltage differences arising from these unequal (opposite polarity) charging rates might build up rapidly enough, and reach sufficiently high values to cause "lightning-like" discharges between stages. It was concluded the measurement of these transient voltages between stages would provide the most useful data of the potentials existing during separation. These would consist basically of measurements of steep wave front transients, spikes, or oscillatory voltages. They would require continuous monitoring during separations and the use of high-frequency response sensors and data channels.

### Sensor Concepts and Performance Requirements

Sensor concepts considered for the surface charge measurements included (a) electric field meters capable of sensing the electrostatic field strength produced by charges on the vehicle surface and (b) electrostatic voltmeters capable of sensing potential differences between the vehicle conductive structure and electrically isolated reference surfaces on the vehicle skin.

Sensor concepts for the separation transient measurements included (a) electrometers, or electrostatic voltmeters, and (b) "charge amplifiers." High-voltage, high-frequency, flexible cables would be required with either transient sensing device to span the gap between upper and lower stages during separation.

To further define sensor performance requirements and permit development of specific sensor hardware for SEV S-131R, these concepts were examined to determine (a) the effects of the measurement technique on the desired measurement, (b) the vehicle and subsystem modifications required for implementation of the concept, (c) the reliability, size, weight and power requirements of applicable sensor hardware, and (d) the availability and schedule compatibility of flight-qualified sensors. To avoid "bleedoff" of the electrostatic charges, both the surface measurement and the transient measurement sensors would require input impedances equal to or greater than  $10^{12}$  ohms shunted by not more than 100 pf. In addition, measurement range requirements were estimated on the basis of information obtained from the studies and test reports on missiles and spacecraft investigations (Ref. 1-16), and on preliminary measurements of the "effective" capacity of conductive coatings on outer Fiberglas surfaces (Ref. 17). The effective capacitance was found to be approximately 2 pf per square inch and the resistance to ground (vehicle

structure) was measured to be  $8 \times 10^{10}$  ohms. The resulting rough estimates of charging rates ranged from  $10^2$  to  $5 \times 10^9$  pico-coulombs per second (100 micro-microamperes to 5 milliamperes). Estimates of voltage ranges were made on the basis of available Fiberglas surface areas for application of conductive coatings to establish known capacitance with respect to internal metallic structures, and consideration of typical flight trajectory times to determine probable values of total charge that might be accumulated. Based on these calculations, estimated requirements for voltage measurements ranged from 10 v to 30 kv for the surface charge sensors. Required ranges for the separation transient sensors were determined by consideration of this estimated 10 v to 30 kv present at the time of motor ignition, the possible increase in potential because of the decreasing capacitance between separating stages, and additional charging due to motor-fire or electron diffusion charging. Only very rough estimates were obtainable from these calculations and the required range was established at approximately 50 v to 100 kv and later reduced to 500 v to 50 kv during sensor development. To permit analysis of the vehicle and subsystem modification requirements, and the reliability, size, weight and power requirements of hardware, vendors were contacted for technical data and delivery schedules on off-the-shelf and development items. Four techniques or sensor hardware concepts were considered for implementing the two measurement concepts. They were:

1. Measurement of electrostatic potential differences using "charge amplifiers" of the type developed by Endevco or Kistler for use with piezoelectric transducers.
2. Measurement of electrostatic field intensities using electric field meters of the "field mill" (generating voltmeter) type.
3. Measurement of electrostatic charging rates using electrometers of the vibrating reed type.
4. Measurement of electrostatic potential differences using electrometers of the type developed for NASA-Goddard by Applied Physics Corporation.

Evaluation of the vendor data determined that the most promising solution to the problem required further development and modification of an "electric field-mill" (generating voltmeter) type of sensor to adapt it to the particular requirements of each of the two measurement concepts (Ref. 18 and 19). Modifications to the basic design were required to provide additional voltage measurement range, compatibility



with the Scout vehicle 28 v dc power supply and the systems performance telemetry system, and a logarithmic output for increased resolution in low measurement ranges. Technical specifications for each of the two types of sensors are included as Appendix I and Appendix II of this paper.

#### Number and Location of Measurement Points

Four sensors are used to measure the electrostatic potentials during ascent and separation of the first two stages. Two surface charge measurements and two separation measurements are made as follows.

##### Surface measurements

Surface measurements are made on upper "B" section and upper "C" section. They are separate measurements and require two sensor installations and two commutated telemetry channels. Because of the symmetry of the vehicle, the electrostatic charges are considered to accumulate and distribute uniformly over the surfaces of the sections. Therefore, neither multiple sample points nor coating of the entire outer surface is required for measuring total charge buildup or net effective potential. If required, total charge and average charging rates can be calculated from measured values of capacitance of the conductive coatings.

##### Separation measurements

Separation measurements are made to determine maximum voltage amplitude between a "system ground point" in upper "B" section and lower "B" section during first and second stage separation. An identical measurement is made between upper "C" and lower "C" sections during second and third stage separation. These measurements are made with the techniques and components described, plus a special cable to maintain electrical continuity between stages until a separation distance of approximately 18 in. has been achieved. It is estimated that the stages will separate a distance of 18 in. approximately 80 to 100 millisec.

### DETAIL DESIGN CHARACTERISTICS

#### Description of Operating Principles

After a study of the system requirements and hardware availability, the sensor concept established as most practical for the electrostatic measurements was the "Electric Field-Mill" or generating voltmeter. With certain unique modifications to

the basic field-mill principle, two types of sensors were designed specifically for application on the Scout vehicle. The modifications were incorporated to overcome disadvantages associated with the use of generating voltmeters, and to eliminate excessive vehicle modifications.

The operating principles of the instruments selected are described as follows.

### Surface Measurements

The sensor for the surface measurement is a generating voltmeter modified to overcome the disadvantages associated with flush mounting. A normally configured generating voltmeter is a flush-mounted electric field meter consisting of a stationary electrode (stator) and a rotating electrode (rotor) and associated electronic circuitry. The rotor and stator are configured such that as the sensor views an external electric field, the stator is alternately exposed to and shielded from the field by the rotor as it rotates at some fixed angular velocity; thus, an ac signal is induced in the stator. The ac signal is amplified and then rectified to produce a dc output proportional to the electric field at the stator. To eliminate the extensive vehicle modifications necessary for flush mounting, the instrument was modified to remotely sense the surface potentials with only minor vehicle modifications. A fixed plate was built into the instrument and electrically connected to a conductive coating on the Fiberglass surface. The fixed plate is then at the same potential as the coating. The rotor is located so the stator will view the electric field between the plate and the stator as shown in Fig. 12-1. The rotor modulates the field viewed by the stator in the normal manner, and the output signal is a measure of the field produced by the fixed plate, and therefore the potential common to the fixed plate and the conductive coating. The sensor head is pressurized to prevent electrical breakdown between the electrodes at reduced pressure. As an oversimplified example, consider the fixed plate and the stator as a parallel plate capacitor. The electric field is  $E = V/d$ : where  $V$  is the potential difference between the fixed plate and the stator, and  $d$  is their relative separation. Then  $E$  is measured, and  $d$  is known, so the potential of the fixed plate and therefore of the conductive coating can be determined. In practice direct calculation of surface voltage from sensor dimensions is not precise. The rotor distorts the field, and because of the size of the electrodes, edge effects introduce significant uncertainties. However, these factors can be calibrated out of the system. Figure 12-1 is a functional diagram of the surface measurement subsystem. The sensor operates from the 28 v dc supply of the Scout vehicle and requires approximately one watt of power.

The amplifier input has a nonpolarity sensitive logarithmic response with a range from 10 to 30,000 v.

### Separation Measurements

The sensor for the separation measurement is the same as that used for the surface measurement with the rotor removed, and with the amplifier modified to provide a higher frequency response and a linear output. The separation measurements are made during the first 18 in. of separation (approximately the first 80 millisec of stage separation). Since the potential to be measured is expected to be a short duration transient, the input requires no "chopping" and the rotor has been eliminated. In evaluating the possible transients during the first 18 in., or 80 millisec of separation, it was estimated the rise time of the pulses could vary from 2 microsec to 80 millisec. Thus, the sensor should have a frequency response from near 0 cps (dc) to over 100 kc. Since this measurement was assigned to IRIG channel 12 (10.5 kc) subcarrier band in the "D" section telemetry system, and channel 12 has a frequency response of 160 cps, a pulse retention network was required to assure oscillator response to short duration transients. The pulse retention requirements were established such that 98% of the peak value of an input pulse should be retained for 5 millisec on the output. It was initially desired that the amplifier should be nonpolarity sensitive and have a logarithmic output for input voltages in the range from 50 v to 100 kv. However, to permit delivery within schedule a linear response amplifier with a maximum range of 500 v to 50 kv was used in the sensor. The power requirements are the same as those of the surface measurement.

### Sensor Installations and Mountings

As a part of the vehicle modifications required to incorporate the electrostatic potential sensors, a conductive coating was applied to the outer Fiberglas surface of "upper B" and "upper C" sections of Scout vehicle S-131R. Figure 12-2 is a diagrammatic sketch showing the location and extent of the coating on each section. The conductive coating is flame sprayed aluminum 0.003- to 0.005-in. thick. The Fiberglas surfaces were cleaned of all foreign matter prior to application of the aluminum coating, and the coated area was so designed that no vehicle ground point or rivet head was closer than 0.5 in. Since the capacitance of the coating, relative to the vehicle structure, was a design parameter for the measurement subsystem, the specific values of capacitance, resistance to vehicle ground, and the total area of the coating were measured. The values are recorded in Table 12-1.

Table 12-1. Conductive coating characteristics

Location	Total area, in. <sup>2</sup>	Capacitance to ground, pfd	Resistance to ground, ohms
"B" section	250	157	$8 \times 10^{10}$
"C" section	180	90	$8 \times 10^{10}$

The values of capacitance are necessary to provide calibration data for the determination of average charging rates and total accumulated charge.

The electrical connections from the conductive coating to the sensor units for the surface measurements, and the connections between stages for the separation measurements are provided by high voltage coaxial cables. The design parameters of the required cable, both electrical and mechanical, were special due to the unique application for which it was intended. It was initially desired that the cable be rated at 100 kv-dc, and possess a capacitance (conductor to shield) of 25 pfd per ft or less, and a minimum insulation resistance of  $10^{13}$  ohms per 1000 ft. The mechanical construction requirements for the cable were that the overall OD be 1/2 in. or less, and that it be flexible enough to bend in a 1.5-in. radius. In addition, it must withstand a temperature of 4000°F for 80 millisec. Several major cable manufacturers were contacted but none would comply with the desired requirement from existing cable. Special orders with the long lead time of delivery could not be considered. From a thorough survey of existing cables, two types were obtained. Extensive laboratory tests were conducted on the two cables and the cable selected for use on this experiment was Amphenol RG-87-A/U. Although the cable did not meet all the requirements, it was considered the best compromise and acceptable for use on the experiment. The results of the laboratory tests and the compromises are reviewed below:

1. The cable was tested for 85,000 v instead of 100 kv dc. Repeated voltage breakdown tests revealed that the breakdown point was between 85 and 93 kv. Although it was estimated that a range of 100 kv would be desirable, the cable and other sensor design constraints suggested that the maximum voltage be reduced to 50,000 v. This is not considered to be restrictive in the conduct of the experiment in SEV 131R.

2. The capacitance of the selected cable was 29 pfd per ft, rather than the 25 originally specified. Cable capacitance appears as a parallel network in the case of the surface measurement and can be accounted for in the final calibration of the instruments. This small variation, therefore, was considered acceptable.
3. Insulation resistance measured  $3 \times 10^{13}$  ohms per 1000 ft at  $25^{\circ}\text{C}$ , and  $1 \times 10^{13}$  ohms per 1000 ft at  $170^{\circ}\text{F}$ . This value is within specification for the selected cable. Other cables tested with insulations other than teflon showed unusable characteristics at elevated temperatures.
4. The overall diameter of the RG-87 was 0.425 in. and it was also found to meet the flexibility requirements.
5. Tests indicated that the ability of the cable to withstand  $4000^{\circ}\text{F}$  for 80 millisec was a minor problem. Other tests were conducted in the Materials Laboratory to determine the optimum technique for installation of the cable for the separation measurement. Details of the final installation of the 18-in. separation lanyard are available on engineering drawings (Appendix III). Figure 12-3 is a block diagram of the entire Electrostatic Measurement Sensors system.

### Telemetry Requirements

The 0-5 v dc output of the electrostatic sensors modulates a standard IRIG, FM, Subcarrier Oscillator. Therefore, no intermediate signal conditioning is necessary to incorporate the Electrostatic Measurements subsystem directly into the performance telemetry system of the Scout vehicle. Two commutated data channels are assigned to the two surface measurements and one continuous channel is assigned to the two separation measurements. The separation measurements are multiplexed on the 10.5 kc SCO of the "D" section T/M system. A 2.5-sec time delay relay is activated at second stage ignition to switch from the "B" section separation measurement to "C" section measurement approximately 2.5 sec after first and second stage separation. Use of a much higher frequency response channel would have been more desirable for the separation measurement, but the pulse retention characteristic of the sensor amplifier assures peak amplitude measurement of short duration transients.

## SENSOR FABRICATION

The fabrication of the electrostatic sensors, and the design and fabrication of the associated electronics, was performed by Rawco Instruments, Inc., at Fort Worth, Texas. Procurement and Acceptance Test Specifications were developed by LTV Astronautics. Selection, procurement, and testing of the high voltage cable was an LTV responsibility. These input cables were supplied to Rawco for installation and testing in the sensor assemblies.

## Electrostatic Potential Sensor

The electrostatic potential sensor, or surface charge sensor, is designated by Rawco, as Model SD-5L. The instrument case is constructed of 7075-T6 Aluminum, with an overall length of 4.84 in. and a diameter of 2 in. (see Fig. 12-4). The logarithmic amplifier developed for this sensor provides for a range of 10 to 30,000 v with an accuracy of 5% per logarithmic decade under all environmental conditions. This 3.3 decade range amplifier uses field effect transistors in a two stage amplifier circuit with negative feedback. The first instrument was assembled and ready for checkout approximately 30 days after go-ahead. During acceptance testing of the first sensor, it was found that the output would not return to zero after a large voltage had been impressed on the input. Investigation of this problem revealed a residual charge was being held on the teflon walls of the rotor cavity. Further analysis and testing showed the walls of the cavity should be a good conductor rather than a nonconductor. Redesign of the cavity walls was accomplished and the residual charge problem was eliminated. Later, when the unit was being subjected to high voltage input levels, the input cable broke down between the inner conductor and the shield. Close examination of the cable revealed the breakdown occurred at a dark spot in the teflon insulation. Investigation revealed that foreign matter created the dark areas in the teflon and caused the breakdown, which varied from one batch of cable to another. Other pieces of cable, from different sources, were procured and tested and the variation in breakdown voltage was found to be quite wide. As a result, each section of cable to be used on an instrument was first cut and then tested to a voltage level of 150% of the rated voltage of the instrument. The sections of cable for the surface sensors were tested to 45,000 v, those for the transient sensors were tested to 85,000 v. This eliminated the cable breakdown problem and the first unit was then acceptance tested and passed all functional and environmental tests. While the postenvironment calibration was

being completed, an arcover or voltage breakdown occurred inside the instrument as the 30,000-v point was being recorded. Investigation revealed that the unit, pressurized to 150 psi with dry nitrogen, was marginal for potential arcover, and, if any microscopic particles were deposited on the input plate, thus forming a point source, the electric field intensity at that point would be increased sufficiently to cause voltage breakdown. To solve this problem, carbon dioxide was added to the dry nitrogen in a mixture of one part to three. The  $\text{CO}_2$  acts as a collector of free electrons and prevents the formation of ions which permit the arcover to occur. Adding the  $\text{CO}_2$  to the gas mixture, and increasing the initial pressure to 200 psi, eliminated the possibility of internal voltage breakdown even when the internal case pressure was dropped to 150 psi. Repeated tests were performed on the instrument prior to installation of the new amplifier and it was established that 45,000 v would not cause internal breakdown with the case pressure as low as 140 psi. Following the installation of a new amplifier module in the first surface sensor, the instrument was again subjected to acceptance testing. All tests were completed and the instrument accepted and delivered to LTV. Figure 12-5 is a photograph of the first unit. A total of three units have been delivered and two were installed on SEV S-131R.

#### Transient Electrical Potential Sensor

This sensor, also referred to as the separation measurement sensor, is designated Model CA-1L by Rawco. The instrument case material is 7075-T6 Aluminum, with an overall length of 3.84 in. and a diameter of 2 in. (see Fig. 12-6). The sensor responds to positive or negative going pulses, in a range from 500 to 50,000 v, with rise times varying from 2 microsec to 80 millisec. The delay time of the pulse or pulses may also vary in the same range. The sensor therefore tracks the rise time of any particular pulse, and retains the peak amplitude for at least 2 millisec. This required signal conditioning ahead of the logarithmic amplifier. To achieve the proper signal conditioning, several techniques were conceived, bread boarded, and tested. They used transformers, full wave rectifiers, choppers, split amplifiers and various combinations of these. Combinations tested as possible solutions to the problem included (1) a full wave bridge into a differential amplifier, and then to the log amplifier, (2) an emitter follower to a transformer to the log amplifier, (3) a transformer coupled bridge to the log amplifier, and (4) two separate log amplifiers. None of these proved satisfactory, and, on the basis of an engineering review of the measurement requirements, and in recognition of the critical schedule requirements

for the program, the logarithmic amplifier was eliminated and a linear amplifier used. This decision was also based on the fact that the already developed signal conditioning circuit was, in fact, a linear amplifier which had been tested and was completely acceptable for use in the transient sensor. The only compromise introduced by the decision to use a linear amplifier, rather than logarithmic, was the reduced resolution at the low end of the measurement range. Following the decision to use a linear amplifier, the only difficulties encountered in the testing and calibration of the transient sensors were in the test equipment. Switching high voltages to produce varying pulses to the instrument required the use of a high voltage vacuum tube switch, and therefore the test equipment setup became quite complex. The two flight sensors were delivered to LTV after vehicle S131-R had been shipped to the field and final installation and system tests were therefore performed at Wallops Island, Virginia. Figure 12-7 is a photograph of the transient sensor. Figure 12-8 shows both types of sensors for comparison of physical configurations.

## FINAL INSTALLATION AND CHECKOUT

### Electrostatic Potential Sensors

Installation of the surface sensors, on the vehicle, was a relatively simple procedure, required no major modifications to "standard" configurations, and was accomplished at LTV Dallas during predelivery checkout of SEV S-131R. The sensors were attached to the vehicle, inside the tunnel sections on upper "B" and "C" sections. Interconnecting cables were then routed to the conductive coatings and connected in the final flight configuration. Checkout of the sensors consisted of applying known voltages to the measurement subsystem between the conductive coating and vehicle ground. The output of the sensors was monitored through the T/M system by the RF link and compared with the original calibration data. This installation and checkout was accomplished with no difficulty. The only restriction imposed on the checkout and flight of the surface sensors was in regard to the final internal pressurization at 200 psi prior to flight. For this purpose, a special pressurization kit was fabricated, filled to 200 psi with the proper mixture of nitrogen and carbon dioxide, and supplied to the field for use during the final prelaunch checkout.



## Transient Electrical Potential Sensors

Because the transient sensors were not received at LTV until after Scout SEV S-131R had been shipped to Wallops Island, those installation were accomplished at the launch site. GSE field equipment was used for the installation and checkout except that the necessary high-voltage test equipment was hand-carried to the field from LTV Dallas for the final system tests. The installation of the sensors and complete system tests were accomplished with very little difficulty. Although installation of the cable for the separation measurement was quite unique and somewhat time consuming, the planned procedure was completed with no unexpected difficulties.

## Installation Photographs

Figure 12-9 is a photograph of the "B" section installations showing the sensors installed in the tunnel (the tunnel cover was removed for this photograph). Figure 12-10 shows additional details of sensor mounting, cabling and cable routing — in particular the method of permitting the cable to "feedout" during separation is clearly shown. The "C" section installations are shown in Fig. 12-11.

## CONCLUSIONS AND RECOMMENDATIONS

### Conclusions

Although not fully understood or firmly established theoretically, it appears there may be mechanisms within the subsystems, environment and operational sequences of the Scout vehicle which can produce, store and discharge electrostatic energy at levels that are dangerous to mission success. The redistribution of accumulated electrostatic charges by corona discharge or lightning-like transfer may cause arcover through ionized paths at altitude or induce steep wave front, high-voltage transients in low-voltage circuits, thus transferring firing energy into critical pyrotechnic control circuits. To obtain flight data for further evaluation of these theories two uniquely configured electrostatic voltage sensors have been developed and installed on Scout vehicle S-131R to experimentally measure potential differences between parts of the vehicle during the launch trajectory, including staging. No known measurements of this type have previously been made on launch vehicles. Consequently, the estimated measurement magnitudes and the dynamic characteristics which have been postulated may not be observed. However, the information

obtained in the development of the sensors and that expected from the launch experiment should add significantly to the limited information available in this field.

The electrostatic sensors developed for this experiment are of the basic Field-Mill type, but uniquely modified in such a way as to permit remote sensing of potentials due to electrostatic charging of the vehicle. Because of the differences in the characteristics of the two potentials to be measured, two types of sensors were developed, (a) a low frequency response unit, and (b) a high frequency type. Both sensors are polarity insensitive. They will be used for in-flight measurements of (a) the electrical potential between the skin surface and the conducting inner structure of the upper "B" and "C" transition sections, and (b) the electrical potential between the first stage and second stage during separation. The latter measurement will also be made as the second and third stages separate.

#### Recommendations

Should the need for further experiments of this nature arise, it is recommended that polarity discrimination be incorporated on both the surface sensors and the separation sensors, that individual outputs be provided for each polarity, and that the signals be monitored continuously on separate SCO channels.

It is also recommended that the separation measurements be assigned to much higher frequency response channels, thereby eliminating the need for pulse retention. This would allow monitoring, not only the peak amplitude of the voltage buildup, but also the complete wave shape including the discharge characteristics.

It is further recommended that the data gathered from this experiment be correlated with theory by means of a formal technical study, since continued effort in the field of electrostatic sensor design and application may yield valuable data on possible hazards created by electrostatic charging of launch vehicles and spacecraft.

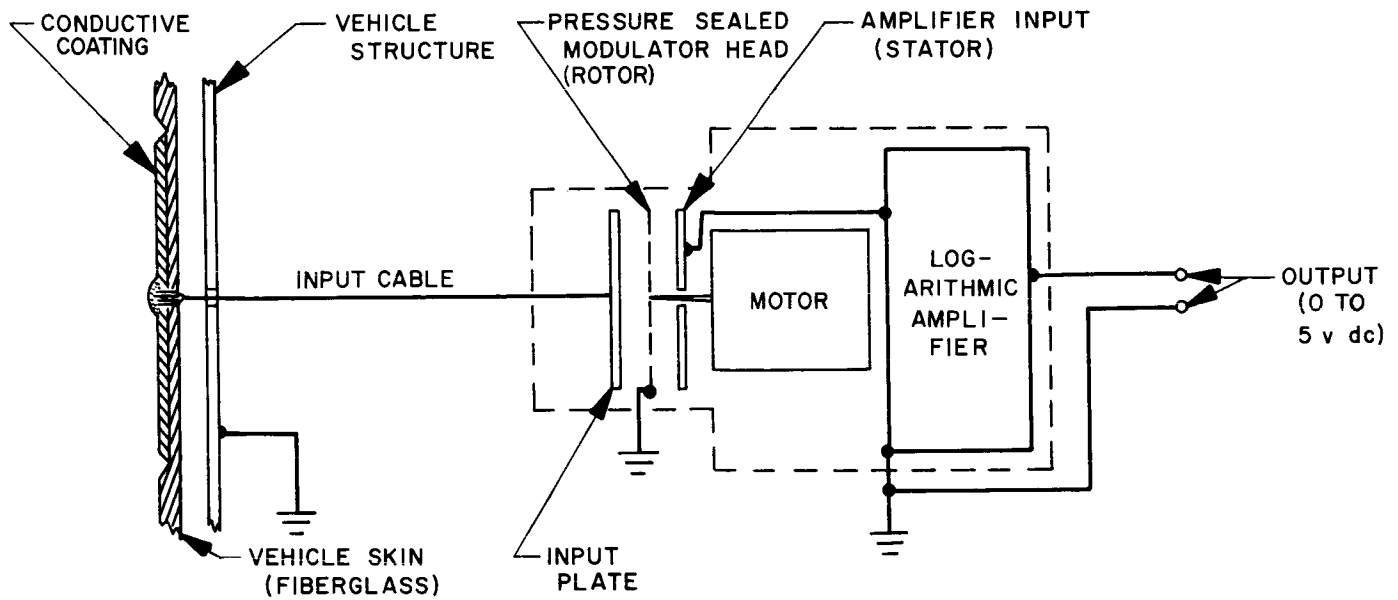


Fig. 12-1. Functional diagram of electrostatic potential sensor

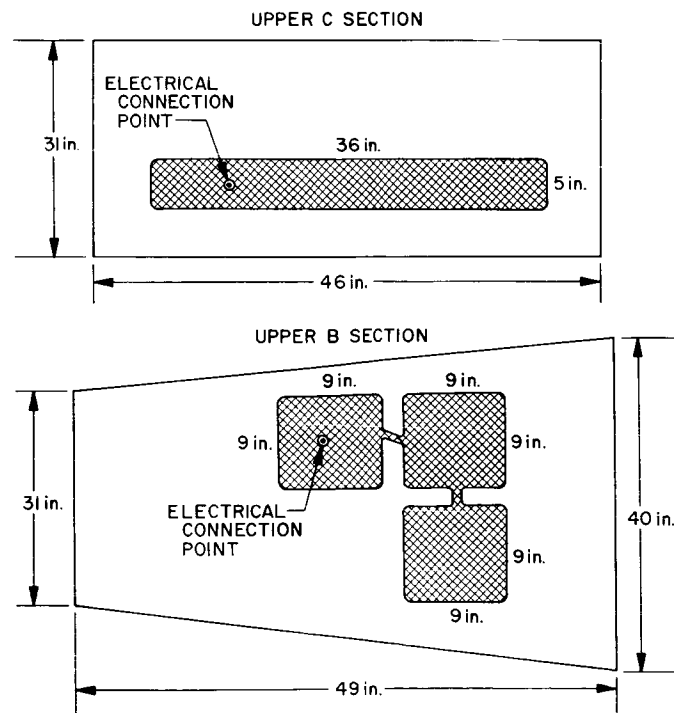


Fig. 12-2. Conductive coating layout

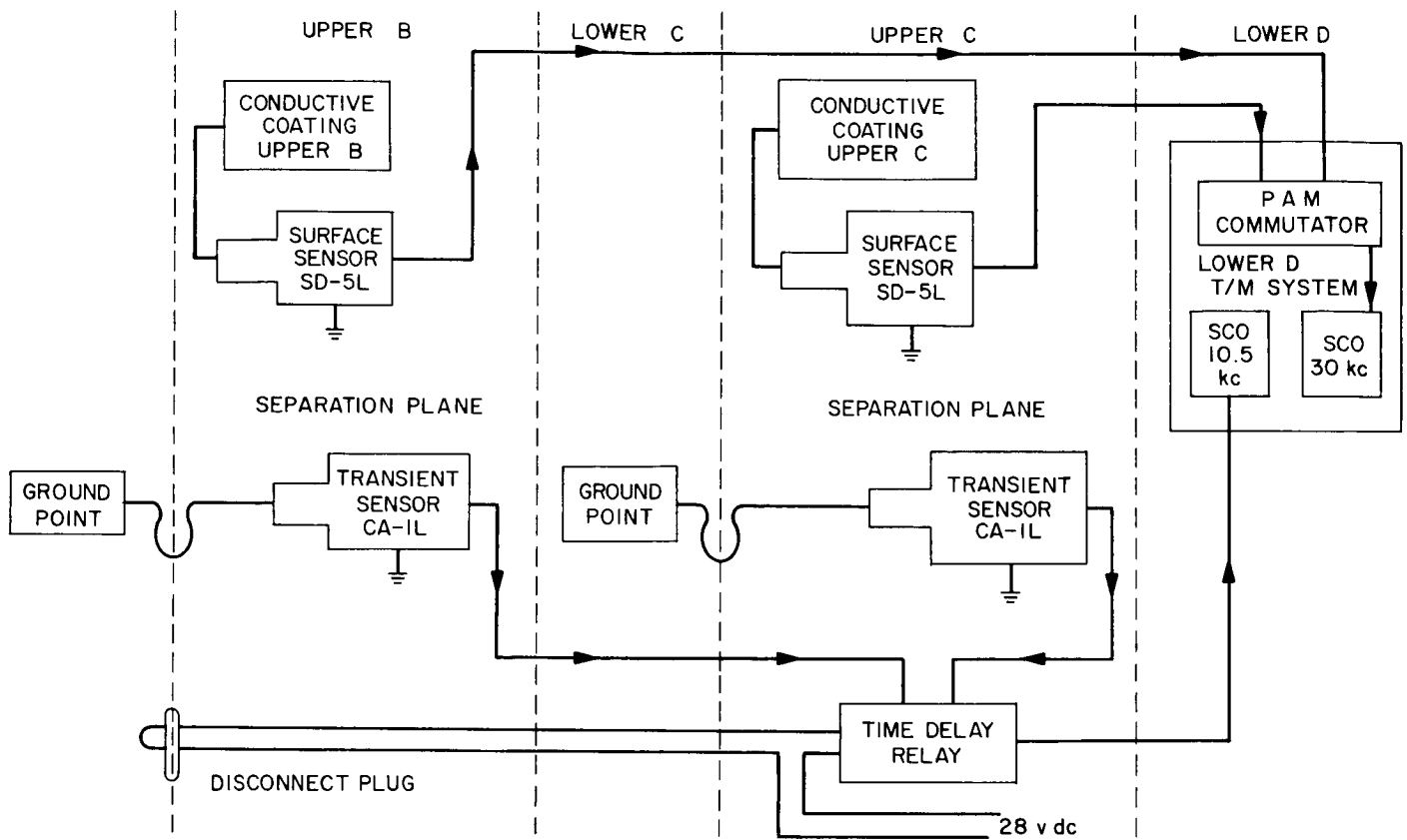


Figure 12-3. Block diagram of electrostatic measurement sensors

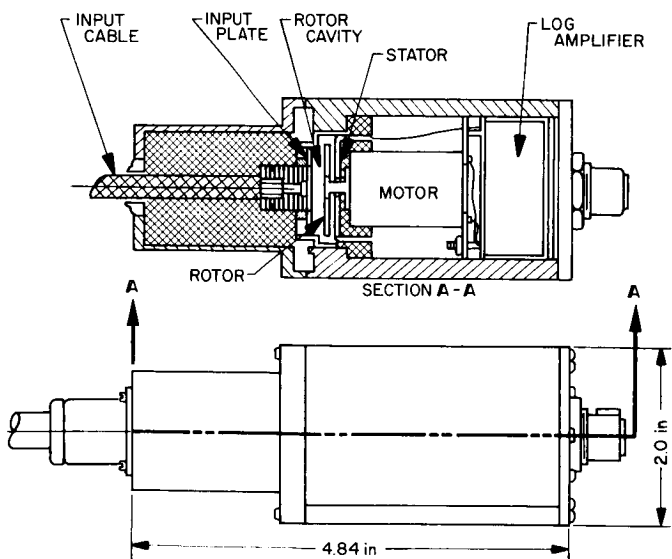


Fig. 12-4. Cross section and outline of electrostatic potential sensor

0 1  
INCHES



Fig. 12-5. Electrostatic potential sensor

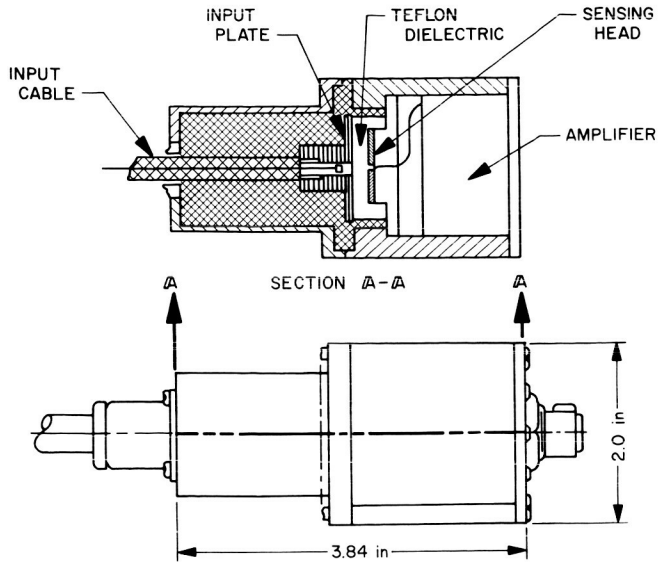


Fig. 12-6. Cross section and outline of transient electrical potential sensor

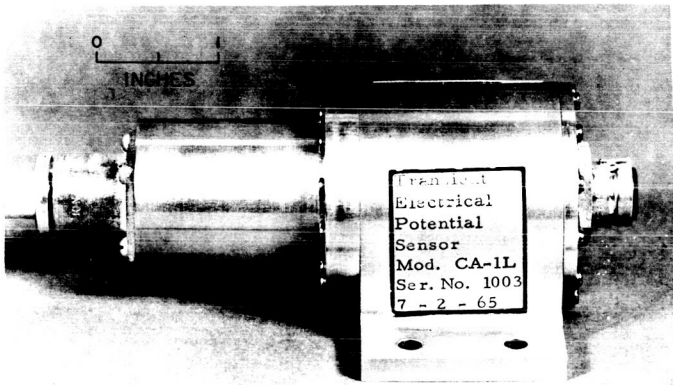


Fig. 12-7. Transient electrical potential sensor

Fig. 12-10. Details of "B" section electrostatic sensor installations

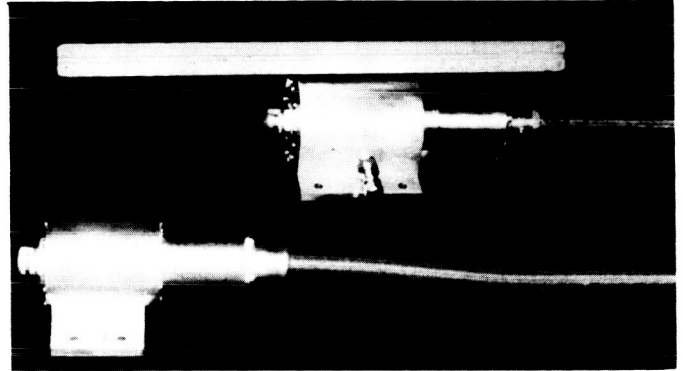


Fig. 12-8. Electrostatic potential sensors for use on NASA Scout Vehicle S-131R

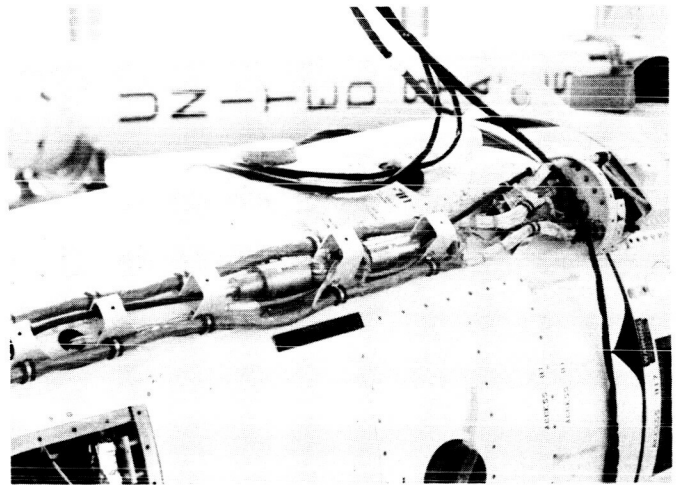
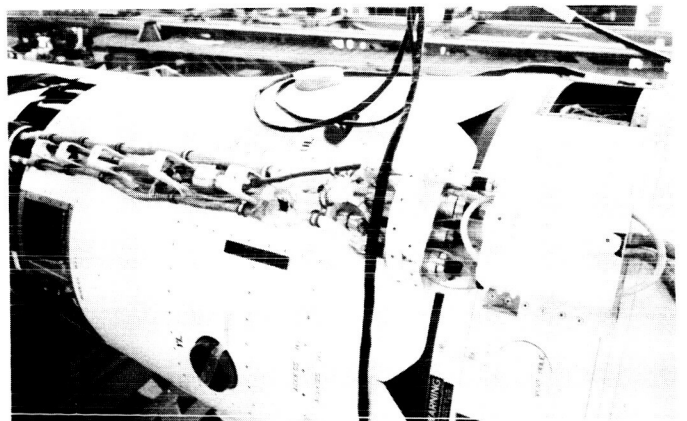


Fig. 12-9. Electrostatic sensor installations - "B" section



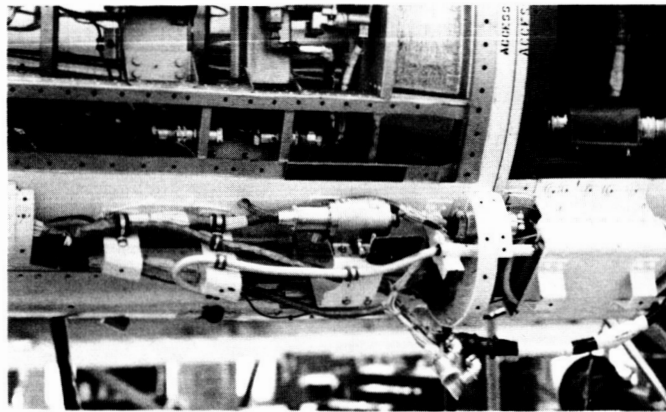


Fig. 12-11. Electrostatic sensor installations - "C" section

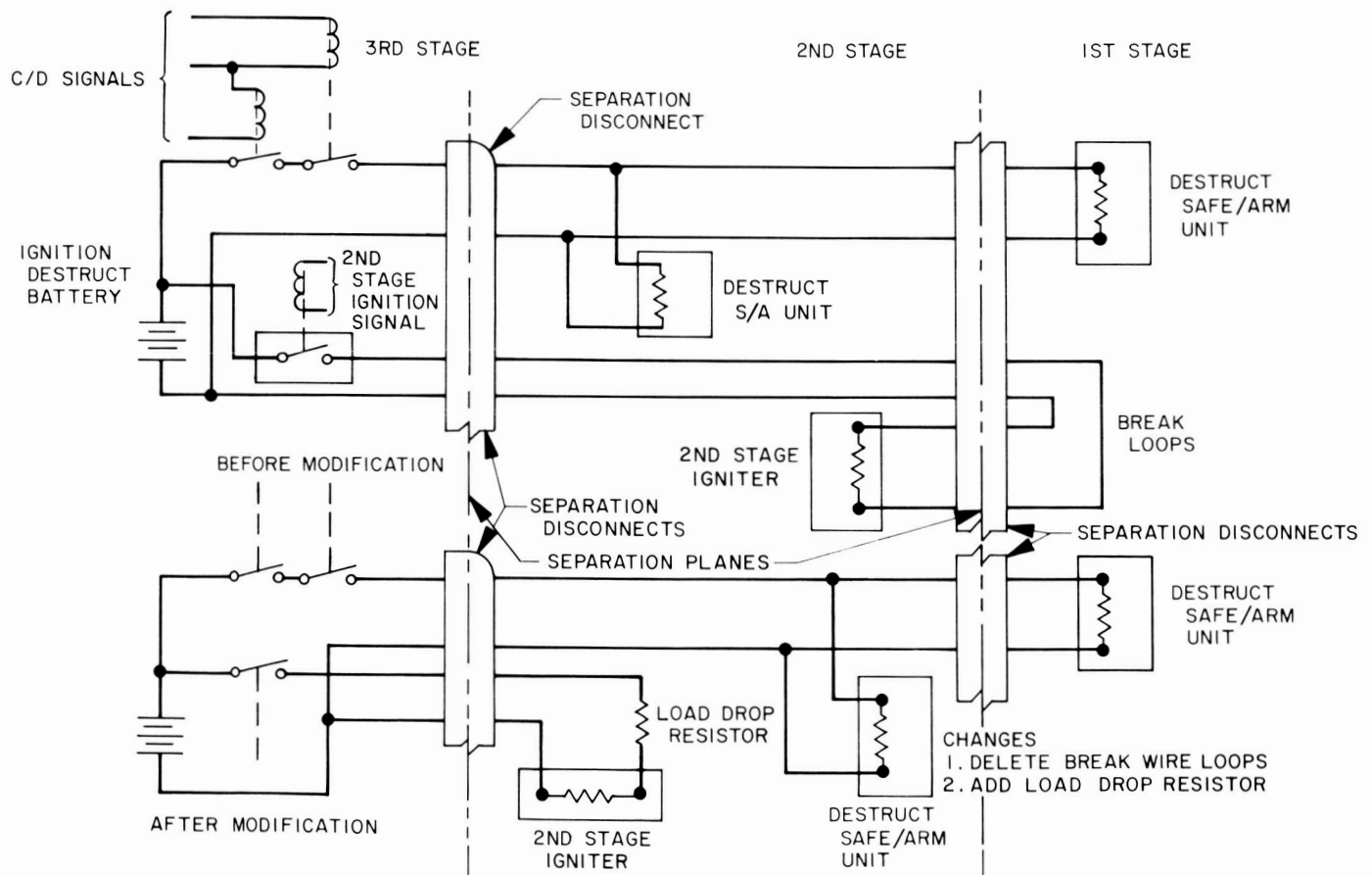


Fig. 12-12. Simplified circuit arrangement - Scout second stage ignition - destruct system

# REFERENCES

1. Private Communication with Messrs. Harold Meese and Louis Nees, and Dr. Seville Chapman, Cornell Aeronautical Laboratories, Buffalo, New York.
2. Private Communication with Mr. J. R. Goudy, NASA Langley Research Center, via Messrs. A. Gustaferrero and J. C. Gowdey, NASA Resident Engineering Management Office, LTV, Dallas, Texas.
3. Vance, E. F., Seely, L. B., and Nanevich, J. E., "Effects of Vehicle Electrification on Apollo Electro-Explosive Devices," Contract NAS9-3154, SRI Project 5101, NASA, Manned Spacecraft Center, Houston, Texas, December, 1964.
4. Chown, J. B., and Kennan, M. G., Study of the Effects of Environmental Conditions on the Breakdown of Antennas at Low Pressures on a Supersonic Vehicle, Final Report, SRI Project 2879, Contract AF19 (604)-5483, Stanford Research Institute, Menlo Park, California (September 1961).
5. Axtell, J. C., "Preliminary Minuteman Electrostatic Charge Studies," Model No. WS-133A, Contract AF04 (647)-580, The Boeing Company, Seattle, Washington (1963).
6. Rasque, D. E., and Smith, W. J., of Autonetics, "Electrostatic Phenomena on Minuteman Missile," Transactions of the Eighth Symposium on Ballistic Missile and Space Technology (Secret), Volume VI, 18 October 1963.
7. Stanley, A. L., "Electrostatic Charge Experiment," Gemini Electronics Design Note No. 411-133P-175, McDonnell Aircraft Corporation, 14 December 1964.
8. Hinners, K. A., and Brown, D. A., Gemini Electrical Potential Analysis, LMSC-A014291, Lockheed Missiles and Space Company, Dept. 58-71, 22 January 1963.
9. Krupen, Philip, Measuring the Electrical Charge on a Missile in Flight, No. 69,690, Defense Documentation Center, August 1960.
10. Whittaker, D. A., Electrostatic Characteristics of a Thor Nose Cone, No. 69,735, Defense Documentation Center, February 1962.
11. Memo 3-15000/4L3976, dated 8 October 1964: LTV Astronautics Division, Dallas, Texas Subject: Electrostatic Discharge Investigation, Vehicle 128R.
12. LTV Specification 304-518, "Transient Electrical Potential Sensor" (Cf. LTV Spec. 309-115).
13. LTV Specification 304-519, "Electrostatic Potential Sensor" (Cf. LTV Spec. 309-116).

14. Pilie, R. J., Ford, James W., and Chapman, Seville, A Study of Instrument Errors in the Measurement of Electrostatic Fields and the Design of a New Electric Field Meter, Cornell Aeronautical Laboratory, Report No. RM-824-P-4, 21 February 1955.
15. Private Communication with Mr. J. C. Goudy, NASA Langley Research Center, via Messrs A. Gustaferro and J. R. Gowdey, NASA Resident Engineering Management Office, LTV, Dallas, Texas.
16. Gowdey, J. R., of Langley Research Center, "Problems Encountered Using Connector Separation for Opening Low Voltage Circuits," Workshop on Voltage Breakdown in Electronic Equipment at Low Air Pressures, Jet Propulsion Laboratory, August 18, 19, and 20, 1965.
17. Design Information Release, 23-DIR-3-54200/4-18, "Electrostatic Measurement Sensors, SEV S-131R, Capacitance of Conductive Coatings on Fiberglass," "Upper B" and "Upper C" Transition Sections," LTV Astronautics Division, 22 December 1964.
18. Design Information Release, 23-DIR-3-54200/4-15, "Electrostatic Measurement Sensors, Scout Vehicle SEV S-131R," LTV Astronautics Division, 8 December 1964.
19. Design Information Release, 23-DIR-3-54200/4-19, "Electrostatic Measurement Sensors, Scout Vehicle SEV S-131R, Final Design Information," LTV Astronautics Division, 28 December 1964.
20. Edens, D. L., and Greer, P. E., Development of Electrostatic Sensors for Scout Systems Evaluation Vehicle SEV S-131R, Report No. 23.233, LTV Astronautics Division, Dallas, Texas, 30 July 1965.



## APPENDIX I

TECHNICAL SPECIFICATIONS FOR THE ELECTROSTATIC  
POTENTIAL SENSORA. Electrical

Input voltage	28 v dc $\pm 10\%$
Input power	1 w or less
Output	Output shall be 0 to 5 v dc. Limited to $\pm 5-1/2$ v maximum. Limiting circuit shall not affect the accuracy of the system. Output impedance shall be 5000 ohms or less. Single ended
Amplifier	Logarithmic response type
Input	Input signal to be capacitively coupled to amplifier through a pressure-sealed modulator head. Input impedance shall not be less than $10^{12}$ ohms
Input cable	Input cable shall be furnished by LTV

B. Performance

Detection limit	10 v minimum
Range	10 to 30,000 v logarithmic response
Response	20 millisec response time; 98% of step input
Drift	Less than 1 mv/day at constant temperature
Accuracy	5% of logarithmic decade
Filtering	Unit shall be filtered to eliminate radio frequency interference

## APPENDIX II

TECHNICAL SPECIFICATIONS FOR THE TRANSIENT  
ELECTRICAL POTENTIAL SENSORA. Performance

Detection limit	500 v minimum
Range	500 to 50,000 v
Response	Minimum response of 100 kc
Drift	Less than 1.0 mv/day at constant temperature
Accuracy	1.5% of full scale
Filtering	Sensor shall be filtered to eliminate radio frequency interference

B. Electrical

Input voltage	28 v dc $\pm 10\%$
Input power	1 w or less
Amplifier	Linear response type
Output	Unbalanced output to be 0 to 5 v dc. Limited to 5-1/2 v maximum. Limiting circuit shall not affect the accuracy of the system. Output signal retention of 98% of peak input signal for 2 milli-sec minimum. Output impedance shall be 5000 ohms or less
High voltage input terminal	Constructed to operate at 85,000 v
Input impedance	The input impedance shall be not less than $10^{-12}$ ohms

## APPENDIX III

PERTINENT DOCUMENTS - ELECTROSTATIC POTENTIAL  
SENSORS FOR SEV S-131R

<u>LTV No.</u>	<u>Description of Document</u>
23-003143	Spec. Control Drwg. - Transient Electrical Potential Sensor.
23-003144	Spec. Control Drwg. - Electrostatic Potential Sensor.
23-003167	Design Drwg. - Conductive Coating, Upper "B" Section.
23-003168	Design Drwg. - Conductive Coating, Upper "C" Section.
23-003169	Installation Drwg. - Electrostatic Sensors - Upper "B" Section.
23-003170	Installation Drwg. - Electrostatic Sensors - Upper "C" Section.
304-518	Procurement Spec. - Transient Electrical Potential Sensor - (See also Deviation Spec. 309-115).
304-519	Procurement Spec. - Electrostatic Potential Sensor - (See also Deviation Spec. 309-116).
SEI-0916	Checkout of Conductive Coating, Electrical Characteristics.
SEI-9857	Acceptance Test Procedure, SEV, "D" T/M - (See Procedures 1 and 2).
SEI-0856	Transition "D" Telemetry System Checkout, SEV - (See Task W).

## APPENDIX IV

IGNITION VOLTAGE BREAKDOWN ASPECTS  
AND MODIFICATIONS

After malfunctions were experienced on two Scout vehicle flights in which second stage ignition pressure decayed to zero pressure within 100 to 300 milliseconds coincident with unexplained high levels of lateral and longitudinal accelerations, a comprehensive investigation consisting of circuit analysis and testing was undertaken. One of the possible failure modes investigated was that of arcover in exposed electrical junctions and altitude.

In the Scout system, stage separation is obtained by breaking a mechanical diaphragm, which couples the stages, by the blast of the upstage motor. The interstage electrical disconnects are of the lanyard pull type and located just forward of the separation plane in a tunnel. The circuits in the connectors are active (not dead-faced) at all times and protected after separation by a spring loaded fiberglass door. The interstage circuits are separated so that guidance, pyrotechnic, and ground control wiring are in separate connectors. Figure 12-10 shows the arrangement of a typical separation plane relative to disconnects.

Figure 12-12 shows a simplified circuit arrangement of the second stage Ignition-Destruct circuit interface for the original and modified design. Note that in the original design a jumper loop is provided in the interstage disconnect plug to clear any high level currents that might occur in the second stage igniter circuit due to squib shorting after initiation. It is further noted that the command destruct tie-line between stages and the second stage ignition circuit wiring share the same first stage separation disconnect and that the ignition and command and destruct pyrotechnic circuits are powered by the same battery allowing a common return circuit.

It was hypothesized that a possible failure mode was arcover between the ignition and destruct squib circuit at the interstage connector at reduced pressures and perhaps greatly accelerated by ionization produced by the motor exhaust. Analysis of the circuit and test data showed that post-fire shorting currents on the order of 12 amps could be present at a voltage level of approximately 20 v. Past experience shows that arcing or corona is to a large degree based on the current that is being broke, voltage, and pressure level. In other words, breaking a circuit carrying a

large current may tend to generate its own ionized path and might be accelerated in an environment of lower pressure and heavily ionized motor flame.

Based on this observation coupled with evidence of a hot separation, or fast motor pressure buildup, from telemetry data, it was theorized that hot gases may have transversed the connector bulkhead just prior to door closure to generate a low resistance ionized path between critical circuit pins in the connector.

Tests were conducted by NASA Langley Research Center (Ref. 15 and 16) to determine if under simulated flight conditions arcover would take place. It is understood that results of those tests show arcover never occurred at system levels but was obtained at somewhat higher levels under other than simulated circuit conditions. It was further noted that the only arcover experienced was under the conditions of fast pumpdown to simulate vehicle ascent to staging altitude.

Based on the unknowns of space environment, its effect on arcover, and the inability to recreate the exhaust plasma in test coupled with the fact that arcover was obtained at only slightly higher voltage levels, it was decided to eliminate the probability of this malfunction by removing the second stage ignition wire from interstage disconnect.

Figure 12-12 shows a simplified circuit of the second stage ignition-destruct arrangement after modification. To protect the basic ignition batteries from possible high post-fire shorting currents in the second stage igniter circuit, limiting resistors were added to the circuit. Subsequent to incorporation, no further flight malfunctions have been experienced.

In summary, ionized arcover paths can be generated at exposed electrical connections at reduced pressures and low voltages, and might be accelerated by motor flame plasma and internally produced ions. Although it was not possible to produce the hypothesized flight failure mode at system conditions, the phenomena is considered significant enough to warrant preventive design in rocket electrical systems where rapid ascent to a low-pressure staging altitude is experienced.

13. PLANETARY BREAKDOWN STUDIES  
IN THE AVCO/RAD HIGH-VOLTAGE  
BREAKDOWN LABORATORY

W. B. Haigh  
Research and Advanced Development Division  
Avco Corporation  
Wilmington, Massachusetts

I would like to talk a little about RAD's background in breakdown. (RAD is Research and Advanced Development Division of Avco.) We have been working mainly on reentry, and over the years we have flown several hundred 10- to 20-w antennas in the VHF telemetry band and several-kilowatt antennas in the 5-Gc range. At the moment we're working on antennas of slightly higher power, of the order of 200 to 400 kw. This is average power and extends from the very, very low VHF up to the top end of the X-band.

About 2 to 2-1/2 yr ago we began thinking about getting off the Earth and into the atmospheres of Mars and Venus, and we started to consider breakdown in these different atmospheres. A small company-sponsored research project was set up with very optimistic goals; we wanted to be able to predict breakdown of any antenna in any atmosphere. It might sound a little naive, but at least it was a very ambitious goal. Now, to predict breakdown requires knowledge of the near-field structure of an antenna (which is generally unknown and generally uncalculable thus limiting investigation to simple types such as slots and dipoles). Also we must know something about the parameters of the constituent gases of the atmosphere in which we're working.

Our reasoning was this: We can calculate a breakdown curve (field strength vs pressure) for one or two single constituent gases, such as nitrogen, which is non-attaching and well behaved. This fact is well known. We can also take an antenna and measure a breakdown curve of power into the antenna vs pressure for practically any gas we wish. Our approach was to take these two things, put them together, and relate the power going into the antenna to an effective breakdown  $|E|$ . This  $|E|$  effective then takes into account the near-field structure, provides a "fudge" factor for the antenna effects on diffusion and gives a measured basis for future theoretical work.

This reasoning was the basis of our program. First we just consider nitrogen. We calculate the breakdown curve for nitrogen (i.e.,  $|E|$  field vs pressure). Then we take the antenna and run a breakdown curve of power vs pressure, again in nitrogen. Then through analysis we tie the power going into the antenna to an equivalent  $|E|$  field, as far as

the breakdown is concerned). Using this  $|E|$  field we can start grinding in the dynamic case and consider flow fields, ambient electron densities, etc. Essentially what we're doing is using theoretical work and experimental work to relate power to field strength. We can use this same method to look at the gases and determine any unknown parameters, such as elastic and inelastic cross sections.

The assumption in this method is that the  $|E|$  field we are determining is invariant with the atmosphere; that is, the  $|E|$  field of our antenna doesn't vary from, say, nitrogen to argon, or any mixture of gases. We also assume that we're looking at the field immediately before breakdown, because once breakdown occurs, things change radically.

Another thought is that perhaps we could use the same technique to determine breakdown in a plasma by looking at the ambipolar diffusion curve rather than at the initial breakdown curve. Here, there are several questions, such as radical changes in the  $|E|$  field, but perhaps this method is one avenue of attack.

About this time we had conducted an analysis; we had computer programs running, and we started getting measured data back from the lab. We looked at the nitrogen, helium, argon, carbon dioxide, and several bottles of what we call Mars gas. We took several postulated atmospheres of Mars and called them one, two, and three. When they were examined, no difference, or no appreciable difference, was found in any of them. This conclusion, of course, has been recorded by SRI. We were not looking for gross effects but rather for an analytical tool. Particularly we were looking for a procedure that would help us examine such effects as "seeding" a reentry vehicle, whereby water is squirted out the nose end so that it flows back, effects of plasma, ablation products, etc. Since we were looking for something to enhance the power-handling capabilities of an antenna and to maximize the operational performance, we weren't too disturbed by this rather negative finding. We charged ahead.

To summarize this part we're in now: we're working with theoretical and experimental approaches to determine an equivalent  $|E|$  field that can be used to relate the static measured case to the dynamic case or to the actual operational vehicle in any atmosphere.

The theoretical portion of this will be discussed next by Dr. Fante. Mr. Bakalyar will discuss the applied physical part; he did all the analytical work in that area.

Since I'm more the dabbler that plays in the lab, I'll talk a little bit about the experimental work and about the facilities we have.

Figure 13-1 shows the breakdown of a Teflon-sheathed monopole in helium. The frequency is 235 Mc and a CW power of 25 w is being used.

Figure 13-2 is the same monopole in nitrogen at a higher pressure. The power is 40 w. Figure 13-3 shows the result of dropping the pressure from the previous level. Breakdown at the antenna base shows a redistribution of the external fields because of the generated plasma. The bluer tinge of the breakdown is largely caused by the diffusion of helium into the system.

Figure 13-4 shows a sphere. (Clever photography makes the sphere look very, very large; the man is not standing in it, but behind it.) The sphere itself is just 6 ft in diameter. The background shows an RF absorber that is 2 to 3 ft thick and absorbs all the incident fields from VHF up. Around this absorber is a screen room. An arm or a probe can rotate about the sphere, and the whole structure on the inside of this sphere can also rotate, enabling us to take complete antenna field patterns. This whole apparatus is instrumented as a pattern range. The picture is a little old. At the moment the sphere is raised up to a higher level and has a 10-in. diffusion pump underneath, along with automatic valves and so forth. The lines come out on the side to the control room. Two other pumps are used in the operation, including a 350-ft<sup>3</sup> blower that works from 200 mm down to about 1  $\mu$ . Along with this equipment is a 150-ft<sup>3</sup>/min mechanical pump, which enables us to get very, very rapid pumping speeds. We can pull down to a pressure equivalent of 300,000 ft in 2 to 5 min, depending on how "dirty" the apparatus is inside the sphere. I might add here that these pumps have about two or three times the rating recommended by the pump manufacturers. Using the diffusion pump of course increases the absolute pressure considerably - to an altitude of 700,000 or 800,000 ft.

The manufacturers said we'd need about a third of the capacity we have. When we requested the money from the company, we asked for twice as much as we needed because such requests are generally cut, but this time they didn't cut the funds, so we had twice as much money, and being good people we felt obligated to spend it. So we put the extra funds into pumps, and this money turned out to be extremely well spent because of the outgassing and the dirt and oils we'd pick up inside the sphere. We certainly do not have a clean atmosphere, which essentially derates advertised pumping speeds considerably.



Other instrumentation includes high-speed cameras of 50,000 frames/min or so, Fastax cameras, and closed-circuit TV. We also have another smaller system having a pumping capacity considerably higher than the one just mentioned; it's a bell jar with a 6-in. diffusion pump. In addition, we have five temperature-humidity chambers. They're large, 10 x 10 x 24 ft, and pump up to about 200,000 ft; we use this system for high-temperature work. Lastly, we have two huge metal spheres that pump up to about a million feet; these are 10-ft cylinders about 12 ft long.

That list covers what we have been working on in the way of facilities. In our work we found (as I guess everybody else has) that you have to work extremely fast, especially in the low-pressure range, because in these ranges you have leakage through the sphere; you have diffusion through it; you have outgassing in it. So when you make an experimental run it has to be set up with people in the "ready position." You push the button on and they go; you have, maybe, 1 or 2 min to make a run before the contaminants start to affect the results.

I might add that we're looking for very, very accurate data here, not the characteristic breakdown curve, but extremely precise readings.

We also found that we just can't use air here. We have nothing against the Massachusetts air, but it seems to contain oil that varies from day to day. There is also the humidity; even working in an air-conditioned humidity-controlled lab, the change from day to day does affect readings considerably. I would imagine that in Los Angeles, with the high hydrocarbon content, it would also change very, very radically from day to day. So we pretty well exclusively use high-purity bottled nitrogen for our experiments.

The effects of contamination may be readily seen. Figure 13-2 has the characteristic red glow of nitrogen. In Fig. 13-3 the pressure has been lowered considerable and the glow has picked up a decidedly blue tinge as if helium is diffusing into the system. In time, the completely blue color of Fig. 13-1 would be seen. Differential pumping speeds also play a part here.

We found one other thing that might be mentioned here and that is the use of argon; we found it to be a nasty gas to work with but a very nice gas for trouble-shooting. We found that if an antenna or a component was going to break down at all, it would break down in argon.

To illustrate, we had some trouble on a reentry experimental vehicle for the Air Force. We were asked to look into it, and the problem was narrowed down to some little filters. These were run through the breakdown cycles and nothing happened. So we put them in an argon atmosphere, where they broke down immediately. And the nice thing about using argon is that components not only break down but they burn up. I don't know why, but it's a sort of troubleshooting by smoke test. We found that this effect also applies to antennas.

We have one antenna that has, as I said, flown several hundred reentry flights. We have this antenna working at 100 w in the lab day after day after day, and it just sits there radiating. We have broken it down many hundreds of times in air, and it breaks down and comes back and breaks down again. Then we broke it down in argon.

Figure 13-5 shows what the antenna looks like. On the top is a low-temperature heat shield. I think low temperature there is around a thousand degrees, or something like that. It has a stainless steel body and is pressurized; it will hold its pressure for many, many weeks. What we do is fill it up with nitrogen or some such gas and seal it off; this prevents any breakdown on the inside.

Figure 13-6 shows what the antenna looks like on the inside. The feed point can also be seen. This antenna is broken down with maybe 5 or 6 w, whereas if run with a heat shield on the top, it would handle in excess of 100 w without any trouble.

When we put this antenna in argon, even though we have the heat shield on top and it's sealed, breakdown will still occur. The antenna will break down right in the inside.

After the breakdown in argon, we find there is a little puncture hole as shown in Fig. 13-7. This breakdown probably occurred at 15 w, and we had a mechanical failure; it just arced right over at the sharp corner shown.

What happened on the inside is shown in Fig. 13-8. This result is typical. I think anybody who's ever built stripline has seen this kind of thing; but what is

not typical is that a sealed antenna that will handle many hundreds of watts in one atmosphere will arc with just a few watts in a different atmosphere.

I am trying to bring out the fact that there is a little more to breakdown than looking at a pretty glow on the outside; there are one or two things going on that we don't quite understand and that bear considering any time you get into the hardware design phase, where you might experience breakdown. Problems might arise if you're using an atmosphere with which you're not totally familiar.

#### OPEN DISCUSSION

MR. MOLMUD: Why does argon produce breakdown better than air? Could you explain that?

MR. HAIGH: Better? I think it depends on which side of the fence you're sitting on.

MR. MOLMUD: In an atmosphere of argon what produces the breakdown?

MR. HAIGH: Argon, I believe, has a lower ionization level. Mr. Bakalyar will be talking about this in more detail in a later paper.

MR. KINKEAD: I wonder if you could explain a little more about that last figure, in which you got feed burning up there with argon. Was that when you had argon inside the cavity or just outside?

MR. HAIGH: No. The antenna itself was still pressurized with either air or nitrogen, probably nitrogen.

MR. KINKEAD: Internally, then, there was no difference between the one test and the other, and yet when you had argon externally the feed burned up and when you had air and nitrogen externally it didn't. Is that right?

MR. HAIGH: At the start of the run there was no difference internally. This is not an isolated instance, or else I wouldn't even mention it. We've burned up six or seven antennas (which amounts to several hundred dollars). It also happens as I said, in other components such as filters.

Apparently, the argon likes to diffuse where it shouldn't diffuse, even into a high-pressure area.

- MR. KINKEAD: In other words, your feeling is the argon got inside the cavity by some strange unexplainable mechanism and caused the feed to burn up at a few watts, whereas ordinarily it would handle a hundred?
- MR. HAIGH: Yes; and I think it's something we should be a little bit familiar with especially since we do have a high argon content on Mars.
- MR. LINDER: I would like to ask if this effect is observed in impure argon? I take it this was rather pure argon.
- MR. HAIGH: Yes. We have limited our work to single constituent gases in the main so that we can control them, and in this instance it was an extremely pure atmosphere. We would let the gas enter and purge the system ten or twelve times to ensure a pure atmosphere.
- MR. McPHERRON: It doesn't seem like your results are consistent with SRI's work. They put argon in antenna breakdown tests and didn't get any difference, essentially, from air.
- MR. HAIGH: I think there's a different thing here entirely. If we broke down a monopole, we would come out with exactly the same thing; however, this is not breakdown at the interface of the antenna window and the atmosphere, but right inside at the feed point.
- MR. McPHERRON: When you used your Mars atmosphere did you put argon in or did you use carbon dioxide?
- MR. HAIGH: I think two of them had argon and one did not. As I said earlier, it was about a year ago that we ran tests on helium, nitrogen, and so forth, and we came out with results identical to SRI.
- MR. CHOWN: The tests that we (SRI) made that were just referred to are ones in which we used something of the order of 70% nitrogen and 20% CO<sub>2</sub>, and the rest was argon; so it was essentially a trace argon, and it really didn't make any difference.

To answer the question of why argon goes to a lower power level, I think for a given field value at a given pressure, you're just going to get more electrons created. The production rate is higher for a given field value as compared with air or nitrogen, as is the case here.

MR. HAIGH: I might perhaps add one thing I left out entirely. In this program we were looking at the effects; we were worried about the effects of measurements in a small enclosed volume. Although a small enclosure doesn't affect things electrically, it does have an effect insofar as diffusion is concerned. So, we made several experiments in which the electrical boundaries remained identical, but the diffusion boundaries were changed. We put a transparent plastic or glass sleeve over the top of a monopole and observed the different breakdown powers required.

We removed the monopole from the solid metal ground plane on which it was situated and put it on a mesh ground plate. The mesh plate was electrically identical with the solid plate, but physically the electrons couldn't see it, and this again made considerable difference in the power required. Moving the antenna up and down and from side to side in the test bubble also made a difference. These results had to be incorporated into our analytical work.

The point I want to make is that you can't take a one-to-one correspondence in breakdown in a small contained chamber like we have and extend it to a situation in which you have infinite diffusion, such as in an operational vehicle.

VOICE: What was the supporting insulation that seemed to be tracking there?

MR. HAIGH: The material was probably fiberglass and Teflon, if you mean on the strip that was burned up.

VOICE: Yes.

MR. HAIGH: I think it's glass-supported Teflon; it has Teflon in it. I think this is characteristic of that material.

VOICE: I see. I'm concerned, since we have done a lot of work on tracking on plastics and this might have been a problem connected with this effect, but Teflon doesn't track very easily. On the other hand, there can be a reaction between fluorine and glass that is quite energetic, and if there is a discharge, you can influence the reaction; in other words, the Teflon decomposes in fluorine, which attacks the glass, and this reaction can be a very energetic one.



Fig. 13-1. Monopole breakdown in helium, 235 Mc, 25 w

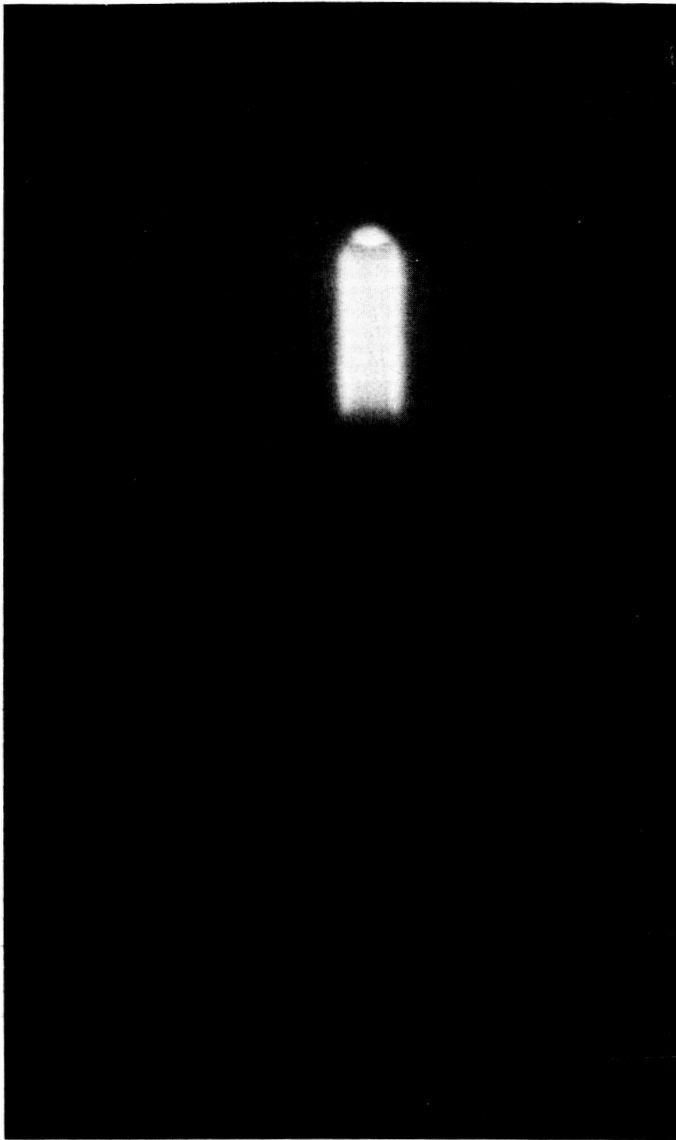


Fig. 13-2. Monopole breakdown in nitrogen, 40 w

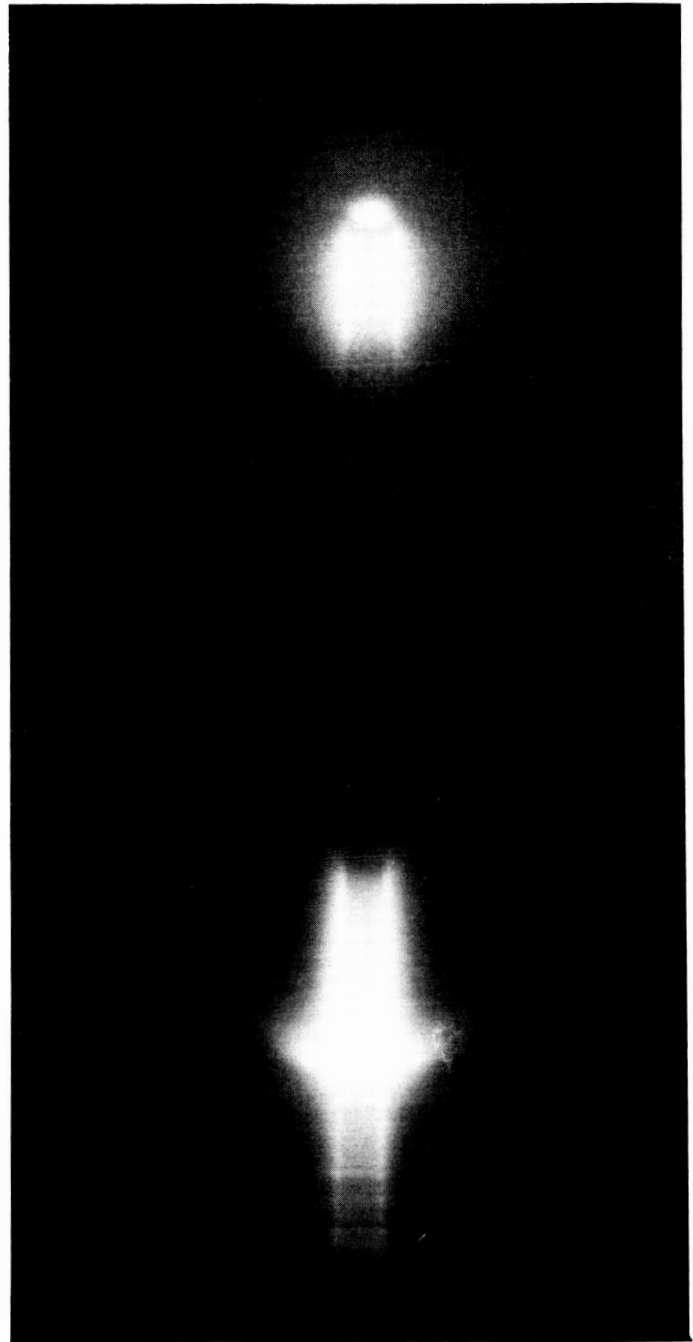


Fig. 13-3. Monopole breakdown in nitrogen, 40 w



Fig. 13-4. Avco high-altitude antenna facility



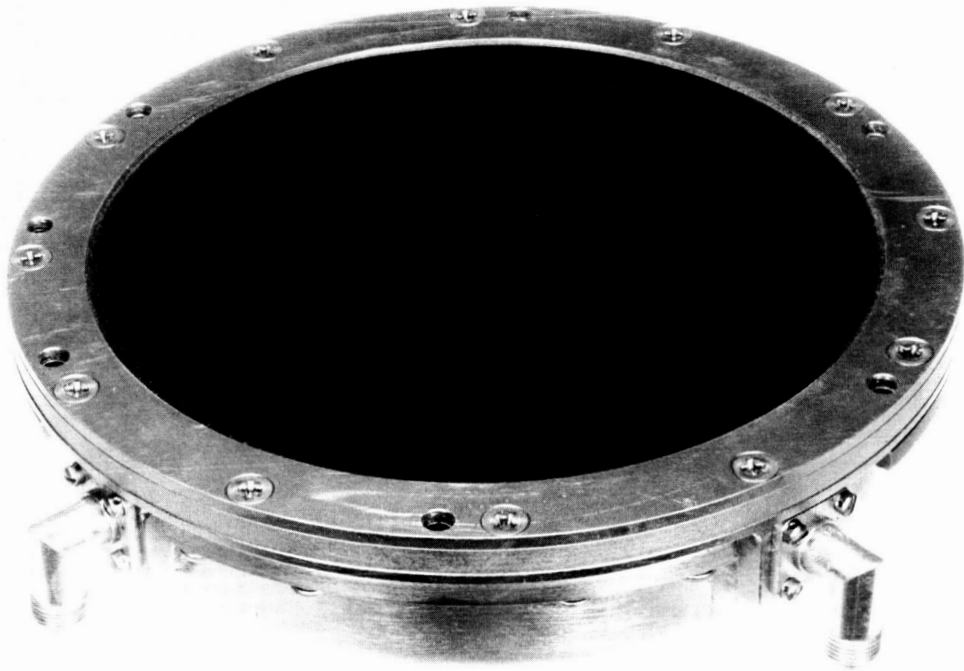


Fig. 13-5. VHF reentry antenna

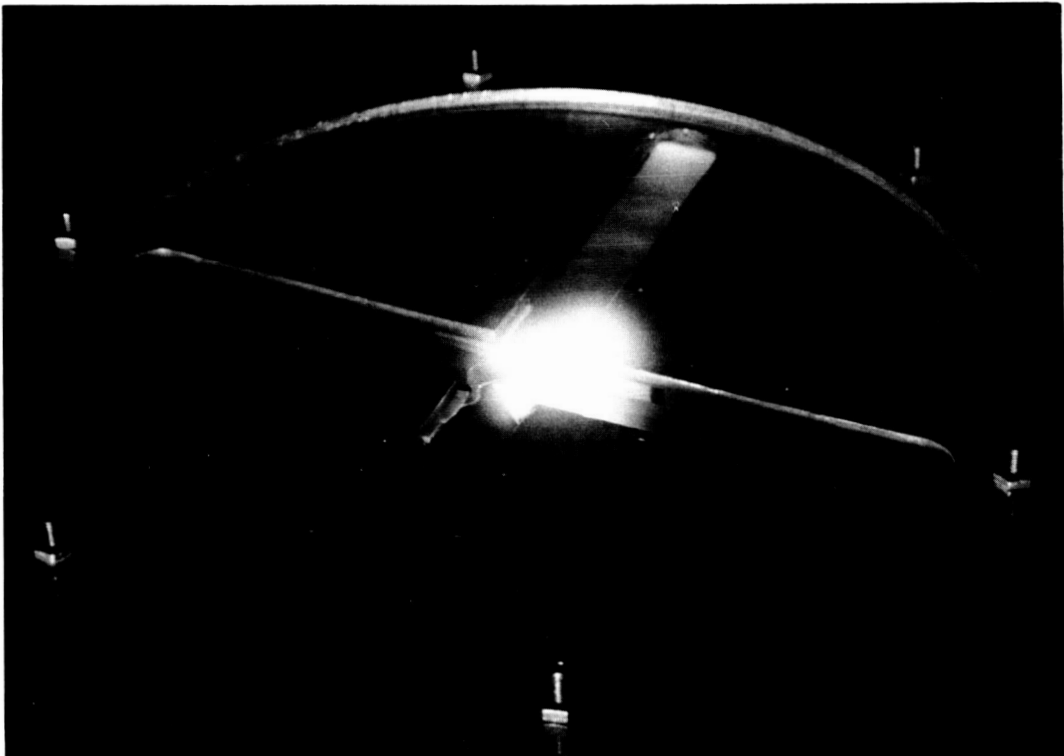


Fig. 13-6. Breakdown of VHF reentry antenna

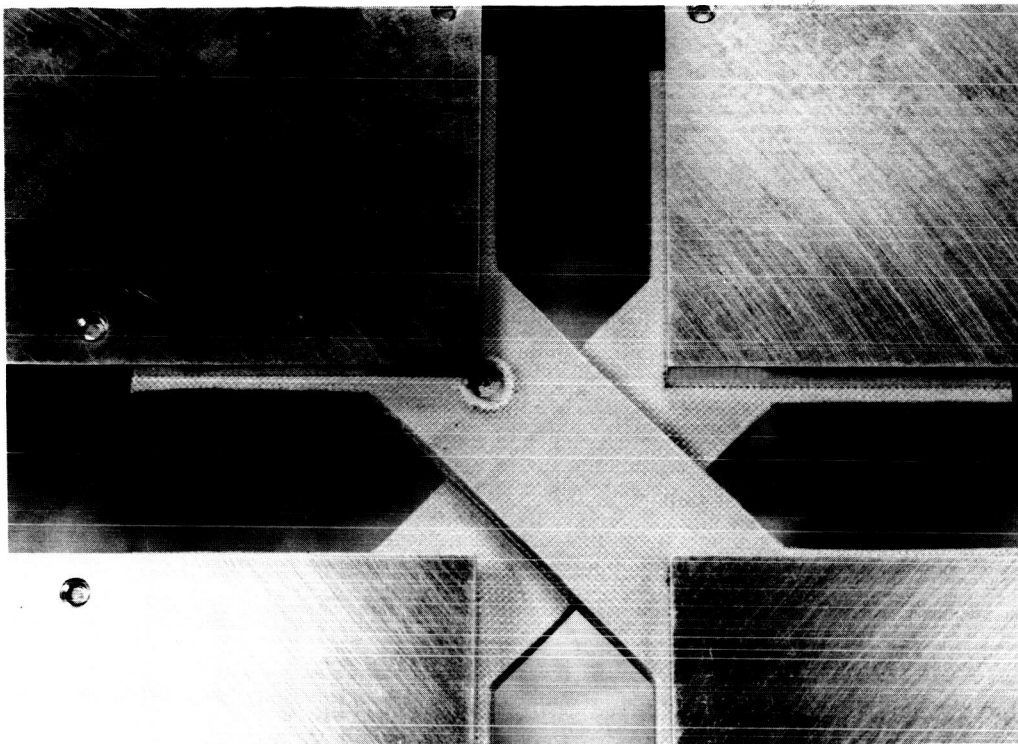


Fig. 13-7. Result of feed arcing in VHF reentry antenna

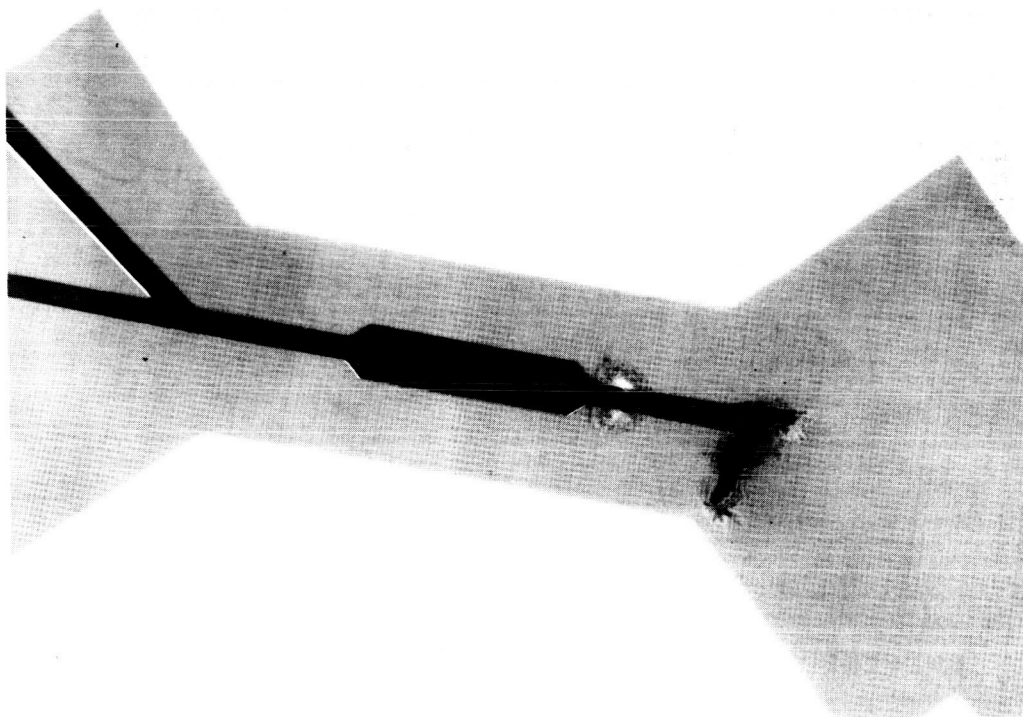


Fig. 13-8. Result of feed arcing in VHF reentry antenna

#### 14. THEORETICAL STUDY OF MICROWAVE BREAKDOWN WITH APPLICATION TO SPACE VEHICLES

R. Fante  
Research and Advanced Development Division  
Avco Corporation  
Wilmington, Massachusetts

This paper will discuss some mathematical models that will enable us to extend some laboratory results for microwave breakdown to space vehicles.

For instance, in the laboratory measurements, we must have a closed container with a finite diffusion length. We cannot handle the effects of flow velocity. We also cannot handle the effects of hot layers, although some work has been done on this. There is a variety of things that are difficult to handle in the laboratory, and it is expensive to make measurements on each space vehicle and to have complicated experiments going. Therefore, we decided it would be worthwhile to explore some rather simple mathematical models that will enable us to determine the effects on breakdown of the parameters.

There are some typical parameters that we might want to change. Ordinarily people use a single continuous wave microwave signal. But suppose you wanted to use some band of signals. How does this affect breakdown? On the effect of the flow velocity? How does this? We expect the flow velocity is going to help us increase the breakdown field strength. By how much?

We expect that diffusion layers might affect things. Hot diffusion layers adjacent to space vehicles might hurt us by changing diffusion from free to ambipolar diffusion (or not quite all the way to ambipolar but to a diffusion coefficient that is less than the free diffusion). How bad is this?

In addition, there are some nonlinear effects which have been measured by SRI. There is not a very consistent theory for these effects, and so we are going to present a very elementary theory that is valid for the high-pressure region to explain these effects.

We are going to stick to continuous wave breakdown during this talk; the extension to pulse breakdown is straightforward.

We may show later how to extend it to pulse breakdown. Let's just say that pulse breakdown is always better than a cw breakdown. That is, you have a higher breakdown field strength than the cw case, but we will consider cw because it's usually the most pessimistic case.

The first thing I would like to talk about is the effect of changing the structure of the field. In other words, ordinarily you may have a single, monochromatic cw signal. Does it do you any good to spread your frequencies over some band? Will this help you? Will it make breakdown better or worse?

The way in which the effect of the signal enters is owing to the effective field strength of microwave breakdown. The effective field is an equivalent dc field; in other words, you apply some ac field, but it is an equivalent dc field that transfers the power to the electrons.

So first we derive an expression for the effective field for any signal component:

$$E_B = E_B (Ng, E_{\text{eff}}, \text{geometry})$$

$$E_{\text{eff}} = \left[ \int_0^\infty \frac{S_E(f) df}{1 + \left(\frac{\omega}{\nu_c}\right)^2} \right]^{1/2} \quad (14-1)$$

The effective field strength for a single frequency signal is shown in Eq. (14-1). It is a familiar equation;  $\omega_0$  the frequency of the signal in radians,  $\nu_c$  the collision frequency in radians, and  $E_v$  = the rms value of the wave.

We have derived this expression (valid for any general signal) which says that it is the integral of the spectral density of the field fluctuations integrated over frequency. For a single frequency, the spectrum is just  $\delta(f - f_0)$  so that this expression reduces directly to

$$\left[ \frac{1}{1 + \left(\frac{\omega_0}{\nu_c}\right)^2} \right]^{1/2} E \quad (14-1b)$$

Now we know what the effective field is for any signal. Does it help us to spread our frequencies over some band?

$$\frac{P_0}{P_N} = \frac{1}{2} \frac{(\omega_0^2 + \nu_c^2)}{\nu_c \Delta \omega} \tan^{-1} \frac{2 \Delta \omega \nu_c}{(\nu_c^2 + \omega_0^2 - \Delta \omega^2)} \quad (14-2)$$

To derive Eq. (14-2) I assumed that I had a slot antenna and obtained the ratio of the power which could be transmitted without breakdown by a single frequency  $P_0$  to the power  $P_N$  which could be transmitted by spreading frequencies over some band,  $\Delta \omega$  about  $\omega_0$ .

Effectively we're considering a white noise signal with bandwidth  $\Delta \omega$  spread about  $\omega_0$ , and we find this a rather complicated expression for the ratio of the powers. I would like to look at several limiting cases.

$$\text{Case I} \quad \Delta \omega \sim \omega_0 \ll \nu_c, \quad \frac{P_0}{P_N} \sim 1$$

$$\text{Case II} \quad \Delta \omega \sim \omega_0 \gg \nu_c, \quad \frac{P_0}{P_N} \text{ ranges from } \frac{1}{2} \text{ to } \frac{\pi}{4} \frac{\omega_0}{\nu_c}$$

$$\text{Case III} \quad \omega_0 \sim \nu_c, \quad \frac{P_0}{P_N} \sim 1 + \frac{5}{6} \left( \frac{\Delta \omega}{\omega_0} \right)^2$$

Case I is where the bandwidth is comparable to the center frequency but much less than the collision frequency. As you might expect, in the limit of high-collision frequency everything looks like the dc field anyway. The frequency has no effect at all, and so obviously the single frequency and the noise are no different.

In Case II we suppose that the bandwidth is comparable with the signal frequency but is much greater than the collision frequency. Here we find that the ratio of the power that could be transmitted by a single frequency (that is, the power that can be transmitted by the band of noise) ranges from about 1/2 to

$$\frac{\pi}{4} \frac{\omega_0}{\nu_c}$$

which is a quantity much greater than one. As a result, you can go from a case where the noise signal is better to a case where the single frequency signal is much better.

The final case we considered is Case III, where  $\omega_0$ , the single frequency, is comparable with  $\nu_c$  and  $\Delta\omega$ . The bandwidth is small compared with  $\omega_0$ .

Microwave breakdown usually is worse at frequencies comparable with the collision frequency so this last case is a very important one. Here we find the ratio of the single frequency to the noise is

$$1 + \frac{5}{6} \left( \frac{\Delta\omega}{\omega_0} \right)^2$$

which is a quantity greater than one. That is, the single frequency is actually better in the worst case than using the band of frequencies.

We're still working on this; we're doing some variational schemes to see what sort of spectrum will give really good results. But the net result is that you don't gain anything by spreading out your signal over a whole band of frequencies.

The next thing we'd like to talk about -- now that we've talked a little bit about the effective field -- is the effect of flow velocity on breakdown and, further, the effect of not having a finite diffusion length but rather some infinite diffusion length. Can you define an equivalent diffusion length?

Figure 14-1 shows a problem we have considered of a slot antenna in an infinite flat plate with another flat plate at some distance  $L$ . We have a flow in the channel, and we would like to find out how much the flow affects breakdown, and in addition, whether there are some equivalent  $R_{\text{eff}}$  -- I've called these virtual boundaries -- where we could pretend we had an absorbing wall and call this the diffusion length. By solving the continuity equation, we will find that there is.

This model may strike some people as nonrealistic because of the the outer plate. It is somewhat nonrealistic, but for space vehicles one could think of it as the outer edge of the shock layer. It is not quite right, but for mathematical simplicity we had to do it this way.

$$v_n = \underline{v} \cdot \nabla n - \nabla^2 Dn$$

$$v = v_i - v_a \quad (14-3)$$

$$\frac{v}{D} - \left(\frac{\pi}{L}\right)^2 - \left(\frac{V}{2D}\right)^2 = \left(\frac{\pi}{R_{\text{eff}}}\right)^2$$

The continuity equation for breakdown is Eq. (14-3);  $v_n$  is equal to the rate of ionization  $v_i$  minus the rate of attachment to neutrals  $v_a$ . This has to be balanced by the flow,  $\underline{v} \cdot \nabla n$  (which is the flow outside the volume where the antenna is) minus the loss in that region due to diffusion.

You can show after a very long and hairy calculation that the breakdown condition can be put into the canonical form. When velocity is zero and  $R_{\text{eff}}$  is infinite. This is just the usual breakdown condition.

$$v_i - v_a = D \left(\frac{\pi}{L}\right)^2$$

The effect of the velocity is the term  $(V/2D)^2$ , and we find that there is some  $R_{\text{eff}}$  which we have plotted numerically that is the function of some of the parameters in the problem (see Fig. 14-2). Equation (14-3) should be borne in mind when examining Fig. 14-2. On Fig. 14-2,  $\rho$  is

$$X_0 \left[ \left(\frac{V}{2D_0}\right)^2 + \left(\frac{\bar{v}_a}{D_0}\right) + \left(\frac{\pi}{L}\right)^2 \right]^{1/2}$$

We had a problem of a plate and an antenna and we've assumed the field is uniform over  $X_0$ ; that doesn't mean the diffusion length is  $X_0$ . We have a uniform field

inside and no field outside. The diffusion coefficient in the presence of the field is  $D$ . The diffusion coefficient without a field is  $D_0$ . Outside, the diffusion is  $D_0$  and the rate of attachment outside is the field-free attachment  $\bar{v}a$ . Thus outside the field region the diffusion rate is  $D_0$ , and the attachment rate is  $\bar{v}a$ , and so forth, and  $v_i$ , of course, is zero, because there's no field out there. If you solve the equations, you can put the results in canonical form with

$$\frac{R_{\text{eff}}}{X_0}$$

given by the curves in Fig. 14-2.

People usually say when they have problems like this, "Let's take the diffusion length in this direction to be of order of the size of the antenna." Others say, "Let's take it to be a wave length because the wave length is of the order of the width of the antenna."

You can see that only in the limit of large  $\rho$  does  $R_{\text{eff}}/X_0$  actually approach 1. Large  $\rho$ , as you can see, more or less implies either a small diffusion rate outside the volume, a very large  $X_0$ , a very large  $V$ , or a very large  $\bar{V}_a$  (very large attachment rate). You can see this physically. If you have a large attachment rate outside the region, then everything that gets out there is automatically sucked up and it's just like a wall there. You can see that in general it is not correct to take the diffusion length as  $X_0$ . You can go pretty far wrong for small  $\rho$ .

To include the effects of velocity we took two different frequencies and compared the results for the breakdown field strength at 35 kMc and 300 Mc for no velocity ( $V$  equals zero), as shown in the lower curve in Fig. 14-3, and for velocity of  $10^4$  ft/sec. As you can see and as you might expect, the effects of flow velocity can raise the breakdown curve about 10 or 15% at high pressures (which corresponds to low altitudes for a space vehicle) and similarly for 300 Mc; at the low pressures (which correspond to the very high altitude), the effective velocity is outweighed by the diffusion.

The diffusion becomes very large at low pressures and you find that there is really not much difference between having a flow velocity and not having it. You can see that for 35 kMc the effects of the flow velocity pull up the worst point on the curve, maybe 1 db or so.



Figure 14-4 considers another problem found on many space vehicles: hot layer next to the vehicle where the diffusion isn't free, especially in sharp space vehicles. We find that we have a hot boundary layer, and adjacent to that, a cooler shock layer. Effectively we have the problem of two different diffusion layers.

We've considered the situation of an antenna with some  $R_{\text{effective}}$  determined by the previous effects, so there are some virtual boundaries as indicated in Fig. 14-4. There are two layers of plasma, one with diffusion constant  $D_1$  and width  $Z_0$ , and another of diffusion constant  $D_2$  and width  $L - Z_0$ . We really get the problem of breakdown in a box with two different layers,  $D_1$  and  $D_2$ . The width of the inner one is  $Z_0$  and the width of the whole thing is  $L$ .

$$\nu = D_{\text{eff}} \left[ \left( \frac{\pi}{L} \right)^2 + \left( \frac{\pi}{R} \right)^2 \right] \quad (14-4)$$

$$D_{\text{eff}} = D \left( \rho = \frac{Z_0}{L}, R/L \right)$$

The continuity equation is re-solved to get the breakdown equation again in canonical form (Eq. 14-4), where  $R_{\text{effective}}$  is already known, but now we have a  $D_{\text{effective}}$  and it is not equal to either the ambipolar diffusion coefficient or to the free diffusion coefficient. It is a function of  $D_1$  and  $D_2$ , and of the two ratios,  $Z_0/L$  and  $R/L$ , where  $R$  is the width across.

Suppose the inner layer is pure ambipolar diffusion and the outer layer is free diffusion. What kind of effective diffusion coefficient do we get? Figure 14-5 plots  $D_{\text{effective}}$  over  $D_{\text{ambipolar}}$ . The free diffusion is about 40 or 41 times the ambipolar diffusion. You can see that for very small  $Z_0$  or  $\rho = Z_0/L$ , obviously everything has to approach the free diffusion. But, what you can also see is it doesn't take a very thick  $Z_0$  ( $\rho$  can be pretty small) for the ambipolar (and the diffusion can be effectively ambipolar) to yield very low diffusion coefficient.

It has been found by Chown, Weissman, and Morita experimentally that a very thin ambipolar layer can go a long way and make things look like it is just a big thick ambipolar layer. The net conclusion you come to in general is that a little bit of ambipolar diffusion can go a long way. To show how much ambipolar diffusion can hurt you, in Fig. 14-6 I've taken a cone-cylinder space vehicle and made some

assumptions. I've assumed that on the cone the gas density is  $5\rho_\infty$ , and on the cylinder it is  $\rho_\infty/5$ . I have computed the effects for a thin ambipolar layer of free diffusion. What happens if you have a thin ambipolar layer? Theoretically you find that the thing is reduced by about 7 or 8 db.

Chown, Weissman, and Morita have done these things experimentally. They've only plotted the worst point on their curve, and they get values just slightly lower than ours. They find a difference of about 8 or 9 db.

The theory does agree pretty well and we've got good reason to believe that if you have a little bit of hot ambipolar layer next to your antenna it can cause you a lot of trouble.

Next we want to discuss the questions: When is a layer ambipolar? When do we have to worry about nonfree diffusion? What happens in this nonfree diffusion? In free diffusion, the electrons are free to diffuse; the ions are so few that they're not pulling them back. When you have sufficient space charge, however, the ions tend to pull back the electrons, and as we will see, if the Debye lengths were much larger than the scale length of your problem (the width of the layer) you find that it's really a free diffusion layer; whereas if the Debye length becomes small compared with the scale on some things, you have a problem. You're going to have ambipolar diffusion or nearly ambipolar diffusion.

Criterion for nonfree diffusion:

$$\frac{\partial f}{\partial t} + \underline{V} \cdot \frac{\partial f}{\partial \underline{X}} + \frac{e}{m} \underline{E} \cdot \frac{\partial f}{\partial \underline{V}} = J \quad (14-5)$$

$$\nabla \cdot \underline{E} = 4\pi e (n_+ - n_-)$$

Space charge term negligible if:

$$\left( \frac{L}{\lambda_D} \right)^2 = \frac{4\pi n^3 e^2}{KT (\nabla n)^2} \ll 1$$

The equation which governs the flow of electrons in the layer outside the vehicle is the Boltzmann equation (Eq. 14-5), and the continuity equation is obtained by

taking moments of this. In other words, if you multiply by  $dv$  and integrate over this, you get  $dn/dt$  plus  $V_i \text{ grad } N$  type term, and so forth.

So we have these two equations, the Boltzmann equation and the Poisson equation, and the third term in the Boltzmann equation is the term which causes the ambipolar diffusion or the nonfree diffusion. There is a space charge electric field,  $E$ , which tends to impede the diffusion of electrons. You can show by looking at all the terms in the Boltzmann equation and using the Poisson equation that the third term, which represents the change drag on electrons, will be negligible if the condition shown in Eq. (14-5) is satisfied.

Figure 14-7 presents a composite curve to include all the effects. We've taken a vehicle which has an ambipolar boundary layer at the low pressures, and a  $10^4$  ft/sec flow velocity, and compared the two curves. The solid curve represents the ordinary laboratory-type curve, where  $V$  equals 0 and  $D$  equals  $D_{\text{free}}$ . The dotted curve represents the curve of flow velocity plus an ambipolar boundary layer. I think the frequency for this is 300 Mc. You can see that now that you have a space vehicle rather than a laboratory case at high pressures (or low altitudes), this fact is going to help you; it's going to push up your laboratory curve. At the low pressures, the fact that you are on a space vehicle is going to hurt you because you're liable to get some hot layers of electrons, and that's going to push down your breakdown field curve.

Figure 14-8 considers the following mathematical problem. We said let's try to predict breakdown for some of the experimental containers that people use. This is only a limiting case. We have a flat plat (as Mr. Haigh showed you) and a bell jar surrounding it with some little monopole inside. Call the length  $r_1$ . Say that the ionization rate around the antenna drops to  $1/e$  of its value at the antenna in some value  $r_0$ . As a mathematical approximation call this  $r_0$  and say that the field strength, therefore, is constant inside  $r_0$  and zero outside, as shown in Fig. 14-8. We've actually worked out the breakdown expressions for this geometry, for any  $r_0$  and any  $r_1$ . (There are all sorts of spherical Bessel functions which I'm sure you're not interested in.) The interesting thing to do is to let  $r_1$  go to infinity so that you have the problem of the antenna diffusing into an infinite medium. This problem has never been given any consideration.

If you solve the continuity equation and take the limit of all of these Bessel functions and the limit of  $r_1$  going to infinity, you can put things in the simple form shown in Eq. (14-6).

$$\nu = D \left( \frac{\eta}{r_0} \right)^2 \quad (14-6)$$

where  $\eta = 4.5$  if absorbing boundary is at  $r_0$ .

If we had put a boundary at  $r_0$ ,  $\eta$  would be 4.5, but the fact we don't have a boundary at  $r_0$  but actually diffusing into an infinite medium, means that  $\eta$  is some smaller number. In general we have shown<sup>1</sup> that depending on the conditions  $\eta$  can vary from about 3 to 4.5.

The next problem (and the final thing we want to discuss) is the nonlinear effects on microwave breakdown. Ordinarily you have a very low electron density outside the antenna and the electrons do not reflect or attenuate the signal very much. The signal goes right through the electrons. When you have a layer with high electron density outside the antenna you find that the field that penetrates into the plasma layer depends on how many electrons there are, and vice versa, and so you get a nonlinear coupling.

We have taken a very simple problem where we have a very thin layer at high pressures so that diffusion is negligible, except in a very very thin layer near the edges of our layer. In other words, we have a layer which is small compared with a wave length and high enough pressure so that there is only a very very narrow layer where the diffusion becomes important. In Eq. (14-7) we have taken the expression given by Gould and Roberts for  $\nu_i$  and  $\nu_a$  and parameterized it. In other words, we've taken the curve and fitted it with this equation. Then we solved Maxwell's equations in conjunction with the continuity equation and arrived at the following equation.

---

<sup>1</sup>For more detail see R.L. Fante, "Mathematical Theory of Microwave Breakdown in Flowing Gases," IEEE Trans A.P., Vol AP-13, No. 5, September 1965, pp.781-788.

$$\nu_i - \nu_a = -A + BE_{in}^2$$

$$\left( -A + \frac{BE_0^2}{[1 + n^2 a^2]} \right) n - \nu_r n^2 + q = \frac{\partial n}{\partial t} \quad (14-7)$$

The interesting thing about this equation is that it predicts, at least qualitatively, the behavior that was observed by Chown, Weissman, and Morita on nonlinear microwave breakdown. They found the full linear breakdown. (We don't have any nonlinear effects.) They found that for a dense plasma layer outside, the transmitter power stays linear for a while, then instead of coming up and dropping off sharply, gradually comes up. Using our equation, we have been able to further predict this curve, which we think is pretty good.

The only other work that we know of on this is by Epstein at Aerospace. He has done it by another technique, not using the continuity equation, but just by using energy balance. Basically, he comes up with the same answer.

Unfortunately, we were not able to put numbers into our theory because the work of Chown, Weissman, and Morita was done in a different pressure regime. But, we feel that if they had done it in our pressure regime they would have found this type of result.

Basically, that is all I have to say. For those of you who are curious about these equations, perhaps I should say more about the second equation. The parameter A is determined from Gould and Roberts; so is B. Notice  $E_{in}^2$ ; this means the field inside the layer, not the field outside.

The electron density is  $n$ ;  $\nu_r$  is the recombination rate;  $q$  is the rate of generalization of electrons due to external sources like heat and so forth;  $a$  is a function of the thickness of the layer and the collision frequency, and so forth.

That is basically what we have been able to do theoretically: we're trying to get a better handle on some of the experimental results which are being published.

OPEN DISCUSSION

MR. MOLMUD: In the last problem you treated, I assume you had a one dimensional geometry and a plane wave, and you solved the wave equation for the resultant inhomogeneous plasma. A self-consistent solution for the inhomogeneous plasma using that source function.

DR. FANTE: Right.

MR. CHOWN: You mentioned the pressure range. What pressure range did you solve for?

DR. FANTE: It would have to be very high pressure because I had to neglect diffusion. The diffusion terms make the equation so complicated that you just can't solve them. So I had to take a region where the pressure was very, very high so that I could throw away the diffusion terms except in a very, very narrow layer next to the boundaries. Looking through your work it seems that you've done it at other pressures, at least in the results that we've seen.

MR. CHOWN: I was going to point out (I should have yesterday) that if you go on a little further and take the low pressure side where you can't any longer neglect the diffusion problem, then it no longer starts to level out. It has a tendency to actually turn in peaks. In other words, you predict the nonlinearity point very well by the ordinary theory, but after you've established the discharge, then it starts to decrease.

DR. FANTE: Right. You can't predict that with this theory. We can't go anywhere beyond this point because as the electron density starts to get too high, our approximations begin to fail in getting this equation.

MR. CHOWN: It would appear, that even though the discharge starts to grow, it must start to level off after a while, and indeed it does. But it goes through a few gyrations before it gets to the level.

DR. FANTE: I realize experimentally the layer has to grow, but we're forced to even keep the layer at a constant thickness. That's another restriction. In theory this is a really impossible problem. We've looked at it extensively, and we know that there's no easy way with this thing.

MR. CHOWN: Another question on this plane wave geometry: did you start off with a source or an incident plane wave?

DR. FANTE: It is an incident plane wave at minus infinity.

MR. CHOWN: So if you did have a source but metallic boundaries, then you'd have the problem of standing waves. That would be a more realistic problem but would tend to confuse the issue.

DR. FANTE: You're right. It's a more realistic problem, but I think at this stage people would be happy to do the simplest as possible problems.

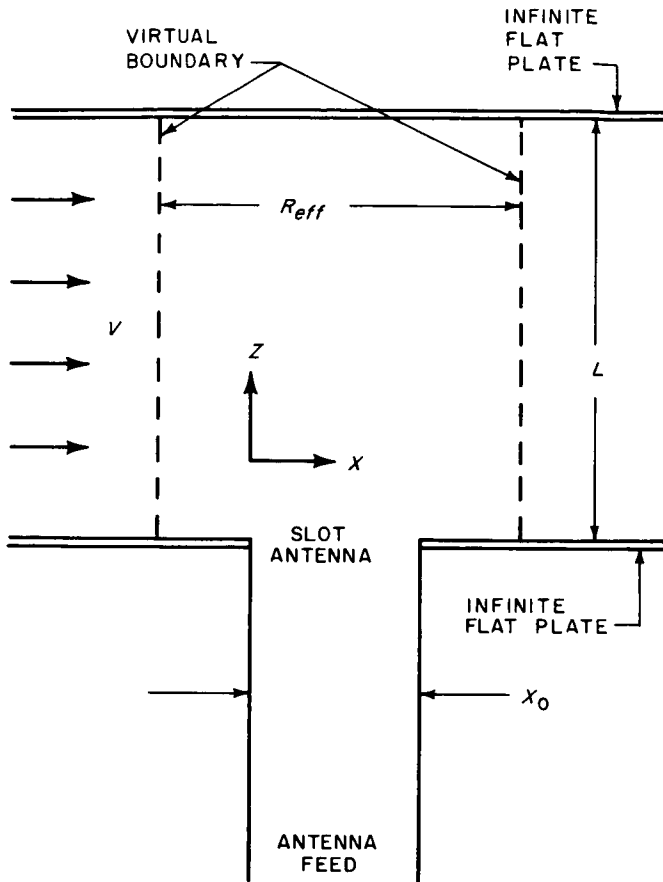


Fig. 14-1. Geometry for consideration of the effects of convection

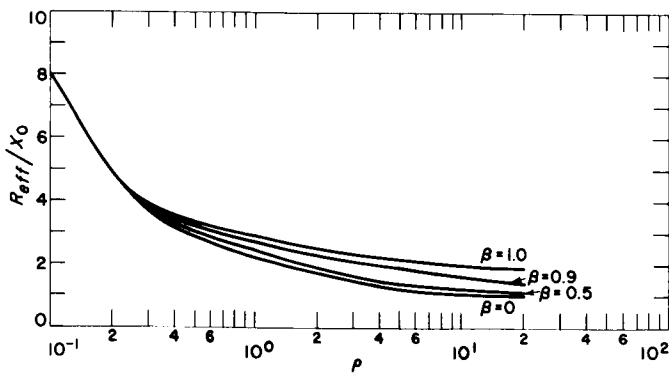


Fig. 14-2. Plot of effective diffusion length vs  $\rho$

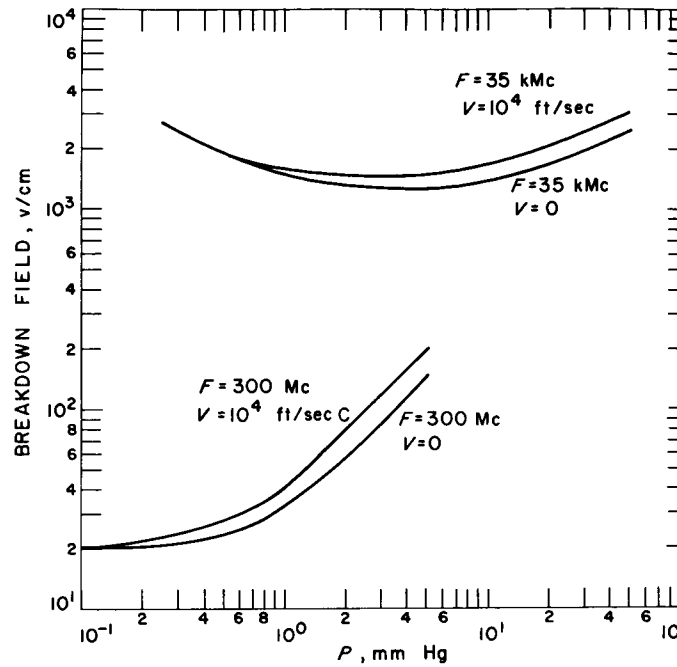


Fig. 14-3. Effect of convection on breakdown field

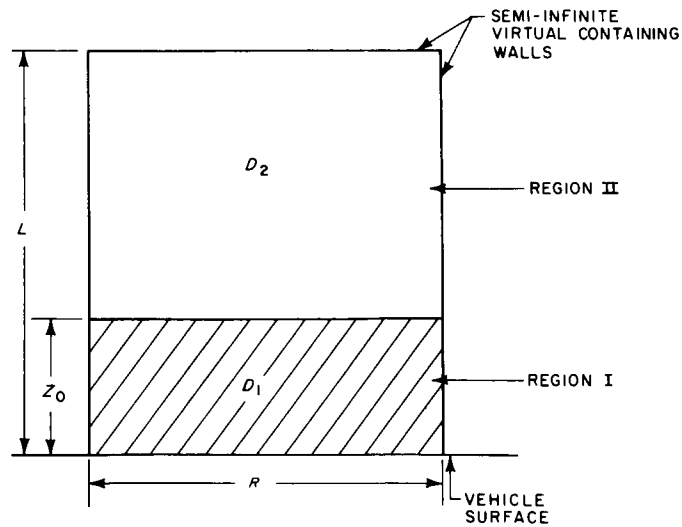


Fig. 14-4. Geometry for the consideration of the problem of two diffusion layers



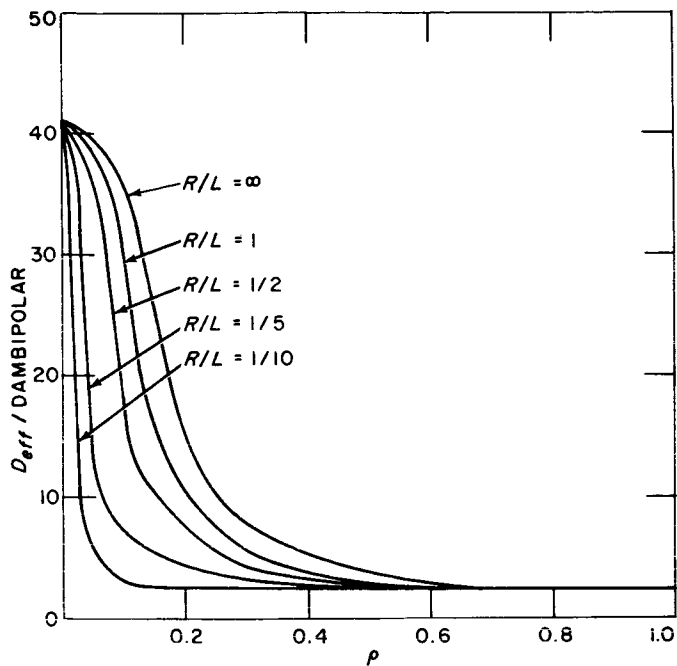


Fig. 14-5. Plot of effective diffusion constant vs  $\rho = Z_O / L$

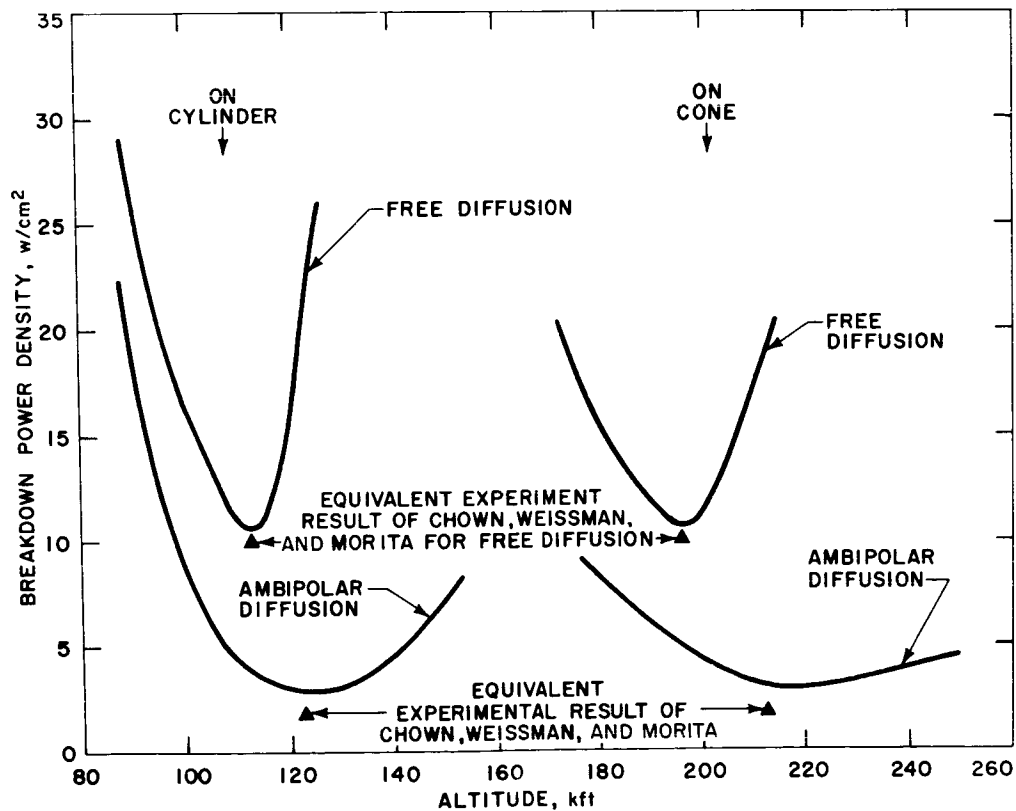


Fig. 14-6. Plot of breakdown power on cones and cylinder

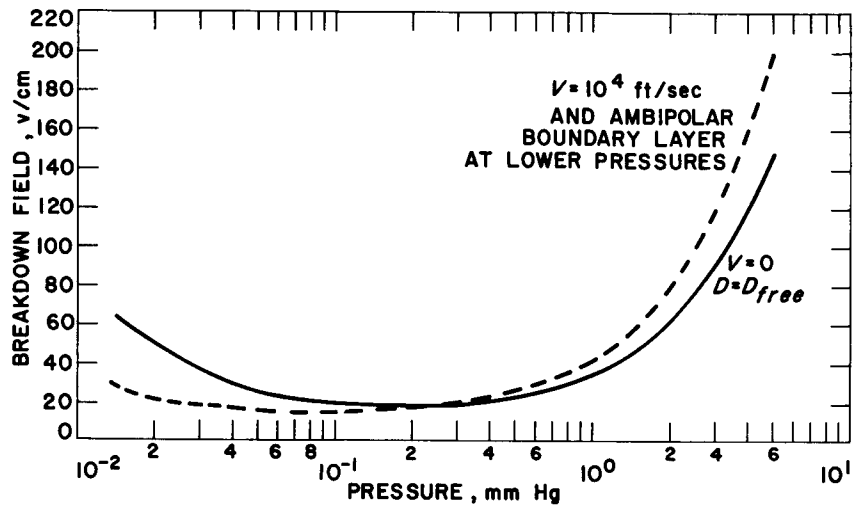


Fig. 14-7. Effect of  $V$  and ambipolar diffusion

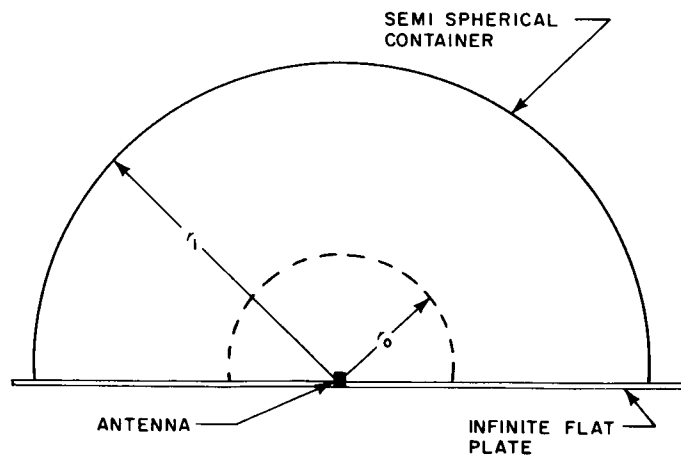


Fig. 14-8. Geometry for the solution of an antenna in a container

## 15. HIGH-ALTITUDE BREAKDOWN PREDICTION

G. A. Bakalyar  
Avco Corporation  
Avco Missile Systems Division  
Wilmington, Massachusetts

Our objective is to determine the power at the onset of breakdown when a given antenna operates in a given gaseous medium over a variety of operating conditions. To make such predictions implies that given the power into an antenna, the electric fields in the region where breakdown occurs can be calculated. Frequently this implies knowledge of field magnitudes in the near field since breakdown may occur in that region.

Secondly, it is implied that given an environment of known composition and state immersed in a known electric field, the electron number density can be determined as a function of time.

It is not practical to attempt to solve either of the two basic problems by strictly theoretical means using the minimum amount of basic fundamental data. The total problem can be reduced to a reasonable sized task, however, by the judicious use of measurement and experiment combined with theory.

Given an analysis designed to predict breakdown onset, it frequently happens that because certain data is not available or reported, the analysis cannot be fully employed. Consider the problem of calculating electron number density in a breakdown situation. This calculation can be made theoretically provided we have knowledge of a minimum number of parameters: First, those that define the composition and state of the medium (no simple task in a reentry situation); second, those parameters that define the collisional reaction characteristics of the gas components (cross sections as functions of particle energy); third, energy data (excitation and ionization potentials, etc.).

Much of the necessary data can be extracted from the literature (particle masses, ionization and exciting potentials, electron momentum transfer, and ionization cross sections). But the amount of data so available is usually incomplete (ion momentum transfer cross sections in an ambipolar situation, excitation cross sections, etc.). These considerations have determined the viewpoint we take in making antenna breakdown power prediction.

Breakdown analysis starts with the Boltzmann equation, which is operated on to yield expressions containing the zero, first, and second velocity moment of the distribution function for electrons. These provide a continuity equation for electron density (the breakdown equation), a definition of drift velocity, and an energy balance equation. All of these equations are needed to arrive at a breakdown onset calculation which is determined by the condition that  $dn/dt \geq 0$  where  $n$  is the electron density (the zero velocity moment of the distribution function). There obviously is not time to begin with the Boltzmann equation, hence only the results of the manipulations which provide continuity, drift velocity, and energy balance will be discussed. An analysis by Kihara is closely followed to obtain these expressions.

$$\nabla^2 n + \frac{(\nu_i - \nu_a)n}{D} - \frac{\beta_R n}{D} - \frac{\bar{V} \cdot \nabla n}{D} - \frac{1}{D} \frac{\partial n}{\partial t} = \frac{q}{D} \quad (1)$$

where

$$D = kT_e \mu$$

$$\nu_i = \text{ionization coefficient } \frac{1}{n} \left( \frac{dn}{dt} \right)_i$$

$$\nu_a = \text{attachment coefficient } \frac{1}{n} \left( \frac{dn}{dt} \right)_a$$

$$\beta_R = \text{recombination rate } \frac{1}{n} \left( \frac{dn}{dt} \right)_R = \nu_R n$$

$$q = \text{ambient density source}$$

$$\bar{V} = \text{relative velocity of neutrals}$$

and boundary condition  $n = 0$  on absorbing surfaces.

Equation (1) gives the continuity equation as derived from the zero moment of the Boltzmann equation after certain simplifying assumptions were made as to the nature of the distribution function for electrons. The equation is valid when  $0$  is uniform, when the mean free path is significantly less than the distance to absorbing surfaces, and for limitations on the field strength  $|\bar{E}|_{\text{rms}}$  which assures no electrons can be accelerated to absorbing boundaries in a half cycle. The coefficients  $\nu_i$  (ionization),  $\nu_a$  (attachment), and  $\nu_R$  (linearized recombination coefficient) derive from the collision integral of the Boltzmann equation. The derivation of the equation presupposes that a plasma can be represented by the behavior of a Lorentzian gas of electrons predominately in collision with neutrals. This is a reasonable assumption for high-altitude breakdown conditions (which relegates the effects of ions to a secondary role).

The diffusion coefficient  $D$  is shown to be expressed to a good approximation by

$$D = \frac{kTe\mu}{e}$$

where  $kTe$  is the average (random) energy of the electron swarm, and  $\mu$  is the mobility. In the case of free diffusion,  $\mu$  is the mobility of electrons. In the case of ambipolar diffusion when space charge effects generate a static containing  $E$  field, then  $\mu$  is the mobility of ions. This means of treating ambipolar diffusion in breakdown is dependent on ion temperature and mobility being much less than that for electrons. These are conditions which normally exist in a high-altitude breakdown situation.

Ambipolar diffusion occurs when the electron density exceeds  $10^8$  particles/cm<sup>3</sup>. Frequently, in reentry breakdown situations, the ambient level is of this order in the ionized boundary layer. Thus  $\mu$  must be represented by the  $\mu$  for ions (which ultimately requires that the momentum transfer cross section of air ions with neutrals be known). Data of this type is generally lacking in the literature. We, however, propose to obtain it by observing the extinction of breakdown of a calibrated antenna in a medium containing ions of the required type.

The fourth term of Eq. (1) is interesting, as it makes possible an estimate of the effects of a moving medium on breakdown. In Eq. (1),  $\bar{V}$  is the velocity of neutrals in the direction of the moving medium. The total effect of this component

of velocity compared to the high random velocity of electrons in an  $|\bar{E}|$  field is assumed to have negligible effect on the electron velocity distribution.

It is clear that Eq. (1) poses a linear boundary value problem if recombination is negligible (or linearizeable) over the operating range of interest with respect to  $n$ .

It is required to solve this equation for the condition  $dn/dt \geq 0$ . The coefficients can be expressed as a function of the average energy  $kTe$ . Solution of the boundary value problem thus provides the average electron energy after a time  $\tau$ . Then if from energy balance we can find how  $kTe$  varies with time given the  $|\bar{E}|_{rms}$ , we have then determined the  $|\bar{E}|_{rms}$  at breakdown. If for a given antenna, we know how  $|\bar{E}|$  varies spatially as a function of the power (antenna calibration), we can then determine the antenna breakdown power (see Fig. 15-1).

Equation (1) applied to regions in which

$$D_1 = \frac{kTe\mu}{e}$$

is nearly uniform. This essentially requires (provided we take the Maxwellian model for elastic electron - neutral encounters as proposed by Kihara) a region of uniform  $kTe_1$ , which in turn requires a region of nearly uniform  $E_1$ . Actually, to reduce the continuity equation to its simple linear form (Eq. 1) requires only that the  $\bar{V} \ln kTe$  be small, which in turn requires that  $\bar{V} \ln |\bar{E}|_{rms}$  be small in the region where breakdown occurs. Thus, as an approximation, it is reasonable to visualize a relevant - or equivalent - breakdown field which is uniform in the region of breakdown. We can assume that this field is nearly as descriptive, for breakdown purposes, as one that may have fairly high gradients. For example, in the near field of an antenna, where gradients are high, the magnitudes are also high, and

$$\bar{V} \ln |\bar{E}| = \frac{\bar{V}E}{E}$$

is quite small and hence negligible to a first- or zero-order approximation. This reasoning has led, as shown in Fig. 15-1, to an assumption of an equivalent field having the spatial distribution shown.

Further physical reasoning allows the reduction of Eq. (1) to a linear equation in the spherical coordinate  $r$ . Essentially this requires that diffusion be nearly

isotropic, and that a finite region of ionization (the breakdown region) behave much as an equivalent point diffusion source located at the center of a spherical absorbing boundary of relatively large radius. This is the geometry approximated by a breakdown test facility when antenna dimensions are fairly small compared to sphere radius. Thus in Eq. II, the coordinate  $r$  represents the distance out from the center of the breakdown region and  $b$  defines the limit to the high field ionization region. This equivalent field is appropriate to an antenna breaking down in its near field. In practice it is found that the  $E_2$  field beyond  $r = b$  can be neglected as it has small effect on breakdown calculation.

The magnitude of  $b$  which defines the limit of the near field can be estimated with sufficient precision for any antenna however exotic. Because of the point source analysis, calculated breakdown fields are not highly sensitive to  $b$  as long as  $B$  is significantly smaller than sphere radius  $r_0$ .

We say an antenna is calibrated when, in a given well-known gas - over a range of "high-altitude" pressures, we have calculated  $E_1$  and then observed breakdown powers at the pressure used in the  $E_1$  calculation. One secures thereby a plot of power vs  $E_1$  for the given antenna. Thus an experimentally derived estimate of the magnitude of the relevant or equivalent field  $E_1$  in the region of breakdown is obtained as a function of power. This calibration is valid for any mixture of gases for onset breakdown conditions.

If an antenna doesn't break down in the near field (a radome is used), then a similar but modified means of calibration is used.

As an approximation we take  $E_2 = 0$ ,  $kT_{e2} = kT_g$  where  $T_g$  is the equilibrium temperature of gases.

$$\frac{\gamma_{1i} - \gamma_{1a} - \beta_R}{D_1} = a_1^2 + \left( \frac{V_1}{2D_1} \right)^2 + \frac{\ln \frac{n_b}{n_0}}{D_1 \tau} \quad (I)$$

$$- \frac{\gamma_{2a}}{D_1} + \frac{D_2}{D_1} \left[ a_2^2 + \frac{V_1}{4D_1} \left( \frac{V_1}{D_1} + \frac{2V_2}{\frac{D_2}{D_1} D_1} \right) \right] = \frac{\ln \frac{n_b}{n_0}}{D_1 \tau} \quad (II)$$

$$\frac{J_0(a_1 b)}{a_1 b J_1(a_1 b)} = \frac{K_0(a_2 b)}{a_2 b K_1(a_2 b)} \left\{ \text{moving medium} \right. \quad (\text{III})$$

$$a_1 b \cot a_1 b = a_2 b \coth a_2 b \left( \frac{r_0}{b} - 1 \right) \simeq -a_2 b \frac{r_0}{b} \rightarrow \text{large} \quad (\text{III}')$$

$$D_1 = (kTe)_1 \mu_1 \quad D_2 = kTg\mu_2 \quad n_b = \frac{\omega_m^2}{4\pi e^2}$$

Solve Eq. I, II, III or I, II, III' for  $kTe_1$  at breakdown when  $\gamma_i$ ,  $\gamma_a$ ,  $\beta_r$ ,  $\mu$ ,  $\mu_2$  are known functions  $kTe$  ( $\tau \rightarrow \infty$  for continuous wave operation).

The solution of the continuity boundary value problem which satisfies the boundary condition  $n = 0$  on the surface of the sphere of arbitrary radius are shown in the above system of equations. The solution provides for the fundamental diffusion mode only - as this is the physically significant case. The equations reflect breakdown in a stationary medium (for which Eq. I, II, and III' apply with  $V_1 = V_2 = 0$ ).  $V_1$  and  $V_2$  are taken to be the flow velocity of neutrals in two laminar streams (separated by a distance  $b$ ). For breakdown in a moving medium Eq. I, II, and III apply. The three equations apply to pulse breakdown of width  $t = \tau$  or cw steady state when  $\tau \rightarrow \infty$ . For pulse breakdown,  $nb$  is the density associated with the plasma frequency and  $n_0$  is the ambient density.

Assuming  $E_2 = 0$ ,  $T_2 = T_g$ , then the equations represent three equations in the variables  $kTe_1$ ,  $a_1$ , and  $a_2$ , where  $kTe_1$  is the electron average energy at breakdown and  $a_1$ ,  $a_2$  are eigen value parameters (related to diffusion length) which arise when satisfying continuity conditions on  $n$  for the boundary value problem (Eq. 1).

Figure 15-2 illustrates the form of the spatial distribution of electron density for the fundamental mode and one higher order mode. A plot of Eq. III and III' are also shown ( $r_0$  is the radius of the sphere and  $b$  defines breakdown ionization region). For breakdown in a stationary medium in a gas that doesn't attach,  $a_2$  can be calculated directly from Eq. II. Since  $a_2 = 0$  for cw operations, it can be seen that  $a_1 b$  depends significantly on  $(r_0/b)$  (the curves apply to various ratios of  $r_0/b$  in the spherical boundary plot).

The topmost curve where  $a_1 b = \pi$  holds for  $r_0/b = 1$ .



The sketches of  $a_1 b$ , and  $a_2 b$  demonstrate that diffusion length differs somewhat from that which would apply if an absorbing boundary were placed at  $r = b$  ( $a_1 = \pi/b$  for this case) -- or if a purely uniform field analysis was used which includes the absorbing boundary. The experimental antenna calibration is most easily accomplished in a nonattaching gas such as nitrogen at cw operating conditions. This mode of calibration also requires the simplest theoretical calculations of  $E_1$ . Theoretically it shouldn't matter whether calibration is carried out at cw or pulsed breakdown, provided the breakdown medium is a well known gas of the simplest possible properties.

$$\bar{E}_{rms} = \left[ \frac{\left( kTe^2 - 3.12 \times 10^{-19} \left( \frac{\sum a_{\beta} \lambda_{\beta} 10^{16}}{M_B} \right) kTg \right)}{\left( \sum a_{\beta} \rho_{\beta} 10^{16} \right)} \left( \frac{3 \sum a_{\beta} \rho_{\beta} 10^{16} (W)}{\left( \sum a_{\beta} \lambda_{\beta} 10^{16} \right)} \right) \right]^{1/2} \quad (2)$$

where

$$W = \omega^2 + 93 \times 10^4 \frac{p^2}{T_g^2} \left( \sum a_{\beta} \lambda_{\beta} 10^{16} \right)^2$$

In slide V is shown the energy balance equation that derives from the second moment of the Boltzmann equation. A number of approximations are necessary to achieve this relatively simple expression. From Eq. (2), once we have solved for  $kTe_1$  from I, II, III or III', The  $E_1$  at breakdown can be calculated. The parameters  $a_{\beta}$ ,  $\lambda_{\beta}$ ,  $\rho_{\beta}$  are all assumed known constants.

- $a_{\beta}$  defines the composition of the gas, i.e.,  $a_{\beta} \rho$  is the partial pressure of component, and  $\rho$  is the total pressure.
- $\lambda_{\beta}$  is a constant parameter which allows the approximate description of momentum transfer collision of electrons or ions with the  $\beta^{th}$  neutral constituent.
- $\rho_{\beta}$  is a parameter approximately descriptive of inelastic, nearly continuous collisions of electrons with the  $\beta$  neutral. That is, the energy absorbed in an inelastic collision is small compared with the impacting electron's energy. This kind of collision takes place

when an electron impacts a polyatomic molecule (or a monatomic molecule possessing many electronic energy states closely spaced).

The analysis can provide for inelastic collisions of a different type. That is for neutrals achieving excited or metastable states of sufficiently long time duration and separated by a sizeable energy increment from all lower states. It is required, however, to estimate the number density of these excited states. They will have an ionization potential somewhat less than the neutral in its ground state, and can be treated as such. This requires the ionization cross section parameter  $\sigma_\beta$  to be known for the excited molecule. This kind of data is very hard to come by. The constant ionization parameter  $\sigma_\beta$  appears in the  $\nu_i$  of the continuity equation (i.e., Eq. 1 and I) discussed earlier. Equation (2) demonstrates, through the inelastic parameter  $\rho$ , that the breakdown field  $E_1$  is dependent on nearly continuous inelastic collisions. The average electron energy at breakdown derived from solving Eq. I, II, III, or III' is not very dependent on this type of collision. However, inelastic collisions of sizeable energy would reflect their influence through the ionization coefficient  $\nu_i$ .

$$\ln \frac{n}{n_b} = -a_1^2 \mu_D \int_0^{\tau_d} (kTe) dt - \nu_{a1} \tau_d \quad (3)$$

$$\tau_d = \frac{1}{n} - \tau$$

Using Kihara's energy balance, Eq. (3) becomes:

$$\ln \frac{n}{n_b} = -\frac{a_1^2 \mu_D}{B} \ln \left\{ -\frac{B}{A} [kTe_1] (1 - e^{A\tau_d}) + 1 \right\} - \nu_{a1} \tau_d \quad (4)$$

$$A = 2m (9.65 \times 10^2) \frac{p}{T_g} \left( \frac{\sum \alpha_\beta \lambda_\beta 10^{16}}{\mu_\beta} \right)$$

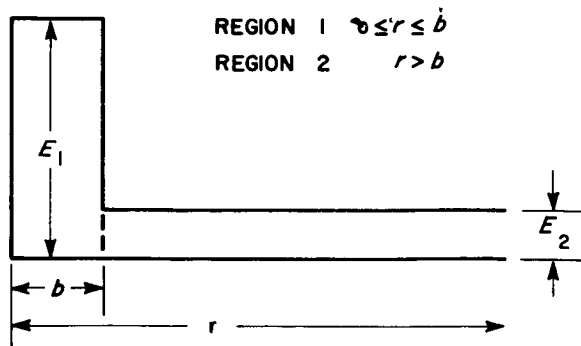
$$B = \frac{2}{m} (9.65 \times 10^2) \frac{P}{T_g} \left( \sum \alpha_\beta \rho_\beta 10^{16} \right)$$

$\alpha_1$ ,  $kTe$  determined solving Eq. I, II, III, (III').

Equations (3) and (4) show the decay of electron density from a microwave power on condition when  $n = n_b$  to the condition  $\tau_d$  seconds after power is removed. In this equation  $\alpha_1$  and  $kTe_1$  derives from the solution of Eq. I, II, III, or III' for a pulsed or cw situation when power is on.

We note that electron density in decap is dependent on the nearly continuous inelastic collisions through the parameter  $p_\beta$ . The parameter  $\tau_\beta$  which has to do with elastic (momentum transfer cross section) are usually known or deriveable from a large number of experiments reported in the literature. Equations (3) and (4) suggest therefore, that the  $\rho_\beta$  which are not usually well known data, can be derived from decay experiments, if the attachment coefficient is zero or well known.

Figure 15-3 is indicated a means to evaluate unknown  $\rho_\beta$  and  $v_{a1}$  using the same operating frequency  $\omega$  but varying pulse width  $\tau$  and repetition rate  $r$ . This requires the use of decay data in conjunction with breakdown data and the theoretical equation (Eq. 3 and 4). In particular, the attachment coefficient as a function of average energy can be evaluated over a range of  $kTe_1$ . The  $kTe_1$  is controlled by breaking down at various power on pulse widths + and repetition rates  $r$ . In the low pressure regime of breakdown, the average electron energy increases with decreasing pressure, which makes this range of data possible on a single operating frequency  $\omega$ . In the high-pressure regime, the average energy at breakdown is a slowly varying function of the pressure, hence is not as useful for evaluating unknown parameters over a wide range of average electron energy.


Fig. 15-1. Breakdown equivalent ( $\bar{E}$ )

$$b \approx 8 \ell / \lambda \quad \text{SLOTS}$$

$$b \approx \lambda / 6 \quad \text{DIPOLES, MONOPOLES}$$

MAY ESTIMATE  $b$  USING POYNTING VECTOR TH $\bar{m}$

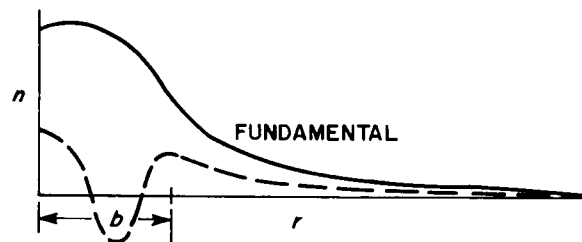
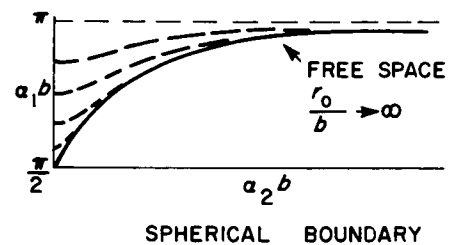
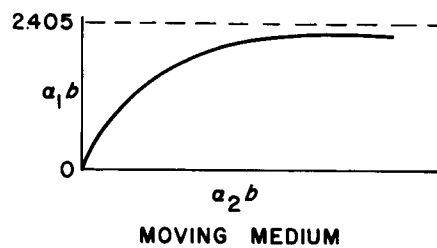
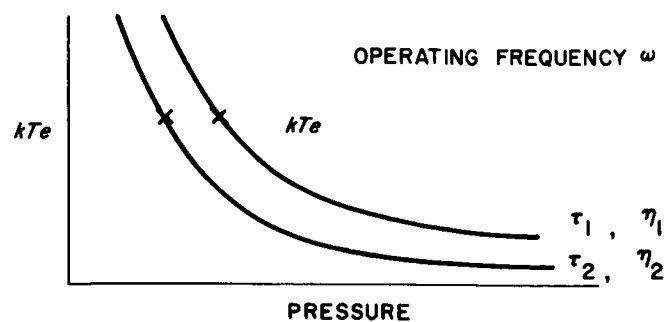


Fig. 15-2. Spatial distribution of electron density

EXPERIMENTALLY DETERMINE CRITICAL  
REPETITION FREQUENCY


Fig. 15-3. Estimate of  $\gamma_a$  and  $\rho$  as functions of  $kTe$  using decay time measurement

SOLVE TWO EQ (4) TO CALCULATE  
 $\rho$  AND  $\gamma_a$

## 16. ANTENNA VOLTAGE BREAKDOWN IN PLANETARY ATMOSPHERES

W. K. Kinkead  
General Electric Company  
Philadelphia, Penn.

## INTRODUCTION

In view of the low gas pressure expected to be found on the surface of Mars and other planets, as well as the need for substantial RF power to transmit information from such distant points back to Earth, the voltage breakdown of antennas represents a significant design problem for future planet-landing spacecraft.

This situation has led previous workers (Ref. 1) to synthesize postulated planetary atmospheres and to test a variety of antennas. These tests were aimed at establishing the relationship between non-Earth planetary atmosphere breakdown and air breakdown. Other goals were to confirm the results of scaling theory and to test a variety of antenna configurations so that design data would be readily available.

The present work was undertaken with basically the same objectives. It was desired to confirm scaling theory over the VHF-UHF range of frequencies with a variety of configurations and gas compositions. It was also desired to explore antenna breakdown conditions over a fairly wide range of gas compositions since it was recognized that present estimates of foreign planetary atmospheres were subject to many uncertainties. Most importantly, perhaps, it was desired to develop methods for improving the power-handling capability of basic antennas. Techniques for doing this were geometry optimization, use of superimposed dc fields, and use of light-weight dielectric materials.

## The Effects of Antenna Breakdown

Voltage breakdown on a typical antenna is shown in Fig. 16-1. Shown is a quarter-wave-long monopole with breakdown at its tip. As pressure decreased, the size of the breakdown area would grow. If power were increased at constant pressure the breakdown would increase in intensity and spread downward along the antenna.

A plot of the effect of this upon the transmission from the antenna is shown in Fig. 16-2. Here, power received by a distant pickup antenna is plotted vs power applied to two antennas under test in a reduced-pressure (0.300 mm) air environment.

Note that there is a hysteresis loop formed as the breakdown level is passed. This loop is associated with the space charge formed after breakdown which sets up a retarding field and serves to reduce ambipolar diffusion.

It is interesting to note that an antenna may be perfectly useful as a radiator after breakdown, but its efficiency with respect to total radiated power is drastically reduced, and apparently gets progressively worse as the operating point is raised.

The transmitted power reduction caused by breakdown usually results in an increase of VSWR or reflected power from the antenna. Sometimes, however, when an antenna or associated transmission line is somewhat mismatched initially, the breakdown may even improve the match, often to the exasperation of those trying to detect the presence of breakdown by means of an increase in reflected power.

For antennas with radiation patterns that are directive or that are formed by guided traveling waves, breakdown will usually cause a significant change in pattern. However, for the relatively small antennas considered here, patterns will not change much after breakdown occurs.

#### Quarter-Wave Monopole Tests

The instrumentation used for running the breakdown tests to be described is pictured in Fig. 16-3. The absorber used to minimize reflections (and to provide safe microwave power levels for operating personnel) can be seen surrounding the bell jar setup.

For measurements in the VHF range, a high power CW communications transmitter was used. For higher frequency, higher power measurements, a 960-Mc-long pulse transmitter was used.

The VHF transmitter was capable of producing up to 200 w CW power in the 225- to 300-Mc range. The equipment was arranged as shown in the block diagram (Fig. 16-4). The transmitter frequencies were crystal-controlled and could be digitally set in 0.1-Mc increments.

A load-isolating network was necessary between the transmitter and the variable stub to avoid burning out the transmitter with high reflected power. This device caused a 3-db reduction in the maximum power that could be delivered to a matched antenna. However, it provided 6-db isolation to the transmitter for a 100% reflection condition. The maximum VSWR seen by the transmitter was kept below

3:1, a satisfactory ratio. The stub was used to vary the power delivered to the antenna under test. In order to produce a sufficiently high and uniform background electron level inside the bell jar, four 400-microcurie polonium alpha particle sources were spaced around the inside periphery of the glass. These sources, used by other workers in the field (Ref. 2), are apparently necessary to assure uniform results. (In other words, breakdown initiation levels are not functions of random cosmic ray or local background activity when the sources are present).

The test equipment used for breakdown measurements at 960 Mc is shown in Fig. 16-5. The RF generator produced fixed frequency (960 Mc) pulses of 6-microsec length at 200 pps. A circulator was provided to isolate the generator from high reflected power.

Accurately calibrated directional couplers, attenuators, and average power meters were used to measure the incident and reflected powers. A dual-channel scope was used to display the reflected and transmitted pulses. As with the VHF tests, four 400-microcurie polonium sources were used.

The initial series of tests were carried out with various quarter-wave monopoles. The purpose of these tests was threefold:

1. To check results with those previously reported in the literature.
2. To check scaling theory over the VHF-UHF frequency range.
3. To investigate the difference in breakdown power experienced in various gases.

Typical models tested are shown in the Fig. 16-6. For the lower-frequency models, the ground plane was made so it would just fit in the bell jar. A number of legs were attached to the ground plane to provide good contact with the bell jar base plate. Initial measurements showed the breakdown power measured to be a function of both the number and height of the legs used. With relatively few legs (four) and of relatively high (6 in.) configuration, a choking effect was apparent, which resulted in high fields (and therefore low breakdown power levels) at the monopole tip. As the legs were increased in number and reduced in height, a more nearly continuous ground plane was achieved and the breakdown power measured converged to a higher value.

Scharfman and Morita (Ref. 3) have reported data on breakdown power vs pressure on a  $0.24 \lambda$  1/8-inch-diameter flat tip monopole at 240 Mc. These data,

together with an attempt to reproduce them with the experimental arrangement described above, are shown in Fig. 16-7.

The agreement is within experimental error. The difference in minimums is seen to be 1.2 db, or 31%. Also the pressures at the minimums are different by 20% or so. The differences may be attributed to instrumentation error, bell jar reflections, finite-size ground plane effects, and gas contamination.

The data reported generally represent the average of three runs. It has been found that a different breakdown power condition will result depending upon whether or not a fresh gas sample is present in the bell jar. Apparently, the presence of a discharge changes the gas composition in the bell jar sufficiently to affect the subsequent measurement at a higher or lower pressure. This effect has been observed by others, who have attributed it to the formation of oxides of nitrogen.

In order to limit the experimental work reported upon here to manageable proportions, fresh samples of gas were not introduced for each measurement. For an air atmosphere this results in reducing the observed breakdown power levels by an average of 1.0 db. This reduction may be consistently relied upon.

Scaling tests were conducted at three frequencies.

Monopoles were constructed with the lengths and diameters as shown in the following table.

Table 1. Dimension of three monopoles

Frequency of operation, Mc	Length, in.	Diameter, in.
225	12.55	0.250
300	9.45	0.187
400	7.08	0.140

Initially it was intended that only one ground plane would be used for the tests, irrespective of frequency. However, when it became apparent that the ground plane configuration was of significance, it was decided to scale the dimensions of the ground plane (including the legs) for each frequency.



The data obtained for the three stub models in an air atmosphere is shown in Fig. 16-8. Within the limits of experimental accuracy, the data confirm the results of scaling theory quite well.

The breakdown power minimums are seen to be within 0.6 db of each other. The pressures where the minimums occur should be related to each other by the frequency ratio. If the pressure of the low-frequency minimum (0.3 min) is used as a reference, the corresponding pressures for 300 and 400 Mc are 0.4 and 0.53 mm, as compared with measured minimums of 0.35 and 0.6 mm. Inasmuch as the minimums are fairly broad, the agreement shown is quite good.

In order to get a clear idea of how the various possible foreign atmosphere constituents might affect antenna power handling, the monopole tests were rerun in  $N_2$ , A, and  $CO_2$  atmospheres. An average of these data over the three frequencies used for the tests show that at the pressures corresponding to minimum power-handling capability, breakdown will result at the power listed in the following tabulation:

Atmosphere	Power, w
Air . . . . .	15.1
Argon . . . . .	7.7
$N_2$ . . . . .	14.4
$CO_2$ . . . . .	14.8

Thus, a wide difference in antenna power-handling capability among the various gases (at the same pressure) will not be evident.

With regard to mixtures of the gases tested, it is apparent that the breakdown levels will fall generally between the breakdown levels observed for the constituent gases. However, for some gas mixtures, for example argon and neon, a breakdown level even lower than that of either gas by itself may be found. However, such behavior will not be present to any significant extent for the estimated constituents of the atmospheres of, for example, Mars and Venus.

The results obtained agree reasonably well with the other experimental data available. Previous work has shown (Ref. 4 and 5) air and nitrogen to have identical (within 1%) breakdown levels at the worst pressure. This work was done in enclosed microwave cavities and involved more sophisticated experimental technique than the present work. The data derived from the monopoles shows (on the basis of "pure"

air breakdown, which would be about 1 db higher than the 15.1 w reported) a difference of 11% in power.

A difference of 5.2 db between air breakdown and argon breakdown has been reported (p. 1842, Ref. 5) for cavity measurements at 994 Mc with a diffusion length of 1.51 cm. On the basis of "pure" air, the difference measured on the monopoles in the present work was about 4 db. A pulsed measurement at 4.5 mm and S-band, with a flowing gas, shows a ratio between argon and nitrogen of 2.1 db for extinction power (p. 2077, Ref. 6). These conditions were, of course, considerably different from those for the monopoles or cavity, but would perhaps have some bearing on antenna breakdown on a vehicle during planetary landing.

Before moving to a discussion of how breakdown might be prevented on specific types of antennas, it might be noted that antenna breakdown need never be an absolutely limiting factor in antenna design. There are techniques and hardware, for example, whereby two antennas can be made to do the job of one. Thus, there is always a relationship to be established between antenna power handling and antenna weight (and/or complexity and/or size).

#### End-Loaded Monopole Tests

It is likely that any planet lander will make use of one or more cylindrical antenna elements (in a monopole, dipole, turnstile, etc., configuration). It is therefore of interest to learn how such an antenna can be made to have improved power-handling capability at low pressures. For packaging reasons, it is desirable that such an antenna not be of great length. Happily, the technique of end-loading (or "top-loading" as it is called in vertical antenna practice) both improves power handling and results in a smaller overall antenna length.

Of course, as pointed out in the literature (Ref. 1 and 3), a cylindrical antenna can be made to have increasingly higher power-handling capability as its diameter is increased. Also, by lengthening a cylindrical antenna element beyond a quarter wave length or by covering it with a dielectric sheath, it can be made to have increased power capability.

It appears, however, that the use of end-loading might result in more efficient use of weight than a dielectric sheath for an equivalent power-handling benefit. For example, our measurements have shown that a 1/4-in-diameter flat tip monopole will have a breakdown minimum of about 15 w at 225 Mc. When covered by a 1-in-diameter

Teflon sleeve, the breakdown minimum improves to about 50 w. Proper end-loading can produce better improvements than this with less weight.

In Fig. 16-9, the minimum breakdown power obtained at initiation and extinction is plotted vs end-loading disk diameter on a 6-inch-long, 1/4-in.-diameter stub at 250 Mc. The disks used were 1/16-in.-thick brass with flat, nonrounded edges.

The power data have been corrected for the VSWR for each configuration, and therefore represent "radiated" power. It is both curious and fortunate that the best power-handling capability is obtained in the configuration that results in the best match to 50 ohms. However, on the larger-diameter disks, the breakdown occurred at the base of the antenna, while on the smaller disks, the disk edges broke down. This is perhaps similar to the behavior Sharfman and Morita report on lengthened monopoles (Ref. 3).

It was felt that rounding the edges of the end-loading disks would result in distributing the electric field more evenly about the antennas and thereby produce a higher breakdown power. To test this, the models shown in Fig. 16-10 were made. These models consisted of wood covered by flame-sprayed copper. When they were tested, the only breakdown observed was at the base of the stems. When dielectric material was applied at the base (about 2-in. -diameter material was used), no breakdown could be observed at any power up to 75 w, which was the limit of the oscillator for this particular situation. These tests were run at 250 Mc in both air and argon atmospheres. The models had stem lengths of about 5 in. and average end-loading disk diameters of about 4.5 in.

Another configuration which resulted in improved power-handling capability is shown in Fig. 16-11. Here a 6-in. -long, 250-Mc monopole, with a 4-in. -diameter, end-loading disk was covered with a 6-in. -diameter, acrylic plastic plate, 1/4 in. thick. Also a fiberglass-type insulation material was arranged around the antenna stem as shown. No breakdown could be obtained on this model in air up to 75 w (the highest power attempted). In argon, breakdown could be obtained, on the top of the plastic disk, at a minimum power of 51 w at a pressure of 200  $\mu$ . The breakdown extinction point, at this pressure, was about 3 w. This was quite a reduction from any of the extinction values obtained on end-loaded monopoles without the plastic cover. Apparently, the presence of the dielectric serves to greatly inhibit the diffusion of electrons due to the high surface charge produced. It may be concluded from this experiment that the use of dielectrics in improving the breakdown levels

of antennas and microwave devices should be carried out with great care, especially if ambipolar diffusion can be established, as it might be, under certain plasma environment conditions.

#### Monopole dc Bias Test

High-frequency breakdown conditions can be changed, and generally, power-handling can be improved by the simultaneous application of a static electric field. (Use of a static magnetic field is a complicated situation, in which power handling may be improved or made worse, depending upon the geometries and field magnitudes used.)

The antenna geometry used in determining the benefits of dc Bias was the previously used 6-in. -long stub with the 4-in.- diameter end-loading plate. A frequency of 250 Mc and a pressure of 300  $\mu$  were used. The antenna was charged both positive and negative with respect to its ground plane and breakdown initiation power was measured vs voltage for air, N<sub>2</sub>, A, and CO<sub>2</sub> atmospheres. The results are shown in Fig. 16-12. Note that the improvement obtained by dc bias on a percentage basis will likely be less in a foreign atmosphere gas than in air, particularly with positive bias.

#### L-Band Tests

A series of tests were run at 960 Mc in order to provide an estimate of the power-handling problems that will likely be encountered with antennas operating on the Martian surface. It was necessary to use the higher power pulse transmitter available at this frequency in order to produce breakdown at the higher pressures used for these tests, as compared to the VHF tests.

In order to attempt to experimentally establish the relationship between the 6  $\mu$ sec pulses available and CW conditions, a scale model monopole (Fig. 16-13) was made. This antenna was a scaled version of the stubs used for the VHF tests, which were based, it will be recalled, on a 1/4-in. -diameter, 12.55-in. -long design for 225 Mc. This antenna had a breakdown power minimum of 10.5 w (peak) as compared with 15.1 w for the average of the VHF data. Because of the experimental errors involved, it would be wishful thinking to conclude that the pulse power breakdown measurements will be exactly 30% lower than for CW conditions. However, the conclusion (based on calculations of Ref. 7) that the L-band is within a 2:1 factor of CW

measurements at the worst pressure is strongly reinforced. For measurements at higher pressures, the results should very nearly approximate those obtained with CW power.

It is expected that high-gain dish antennas will someday be stationed on the Martian surface, hopefully transmitting much data back to Earth. The feeds for these antennas will be subject to power breakdown. In order to find out what power a typical dish feed might handle at the Martian surface pressure, a conical spiral (American Electronics Laboratory Model ALN 108B) was tested at 960 Mc. (Of course, a conical spiral might be more useful as a broad coverage direct radiator, but it does tend to represent present practice in space dish antenna feeds, as well.) The data shown in Table 2 were obtained.

Table 2. Breakdown of conical spiral antenna in Martian atmosphere

Pressure, mm of Hg	Breakdown peak pulse power, w			
	Air	N <sub>2</sub>	CO <sub>2</sub>	A
7.5	510	560	600	240
20.0	1150	1150	950	370

Another L-band test which dramatically illustrates the benefits possible from end-loading and use of microquartz dielectric filler is illustrated in Fig. 16-14. Here a sphere, approximately one quarter wavelength in diameter, containing a crossed dipole, or turnstile antenna is shown breaking down at about 350 w peak power (air atmosphere, worst pressure).

It appears, therefore, that very little difficulty will be involved in designing high-power dish feeds or broad beam radiators for operation from the Martian surface. This fact is especially true at the higher frequencies where resonant lengths can be used and where use of dielectric sheaths and large radii results in little weight penalty.

## Slot Antenna Tests

For some planet-landing missions — especially those making use of a relay communications link — the use of electrically small slot antennas is desirable. Electrically small implies slot length below a half wavelength and backing cavity depth less than a quarter wavelength.

A typical antenna, with an offset feed and dual capacitor tuning is shown breaking down in Fig. 16-15.

Table 3 summarizes breakdown and other data obtained on a broad range of cavity backed slot configurations. These data were taken principally at about 250 Mc. Note the considerable improvement in breakdown obtained by filling the cavity and slot aperture with dielectric. A polyurethane foam of about 8 lb/ft<sup>3</sup> density was used in most of the designs tested. A foam was used rather than a lightweight compressible filler such as microquartz insulation material because the foam provided not only breakdown enhancement but also mechanical rigidity.

A variety of dc bias configurations were tried, with the best of these showing a 3-db improvement in power-handling capability. This configuration consisted of three wires running parallel to the long dimension of the slot. Two of these were grounded to the cavity while the third, or central wire, was biased positively. At voltages above about 350 v, dc-sparking became evident and the benefit on the RF breakdown initiation level fell off.

When tested in gases other than air, the slots exhibited about the same behavior as the monopoles previously described. The results, however, were not as consistent, since a considerable problem was encountered in eliminating contamination from the gases trapped in the foam which filled the cavities under test.

## CONCLUSIONS

The following conclusions appear justified on the basis of the work reported here and on that of other workers in the field:

1. Unless foreign planetary atmospheres contain considerable portions of argon, or other rare gases — a condition that present data for the nearby planets does not support — antenna breakdown will not be significantly different than on Earth (at the same pressure).

Table 3. Electrically small slot antenna performance

Type of antenna	Size, wavelengths		Bandwidth, % (under 2:1 VSWR)	Efficiency, %	Breakdown initiation power (min.) in air, w	
	Slot	Cavity			Input	Radiated
Foam filled, capacitor tuned	0.27 x 0.04	0.28 x 0.11 x 0.024	0.36	42	9	3.8
Foam filled, capacitor tuned	0.27 x 0.04	0.28 x 0.11 x 0.044	0.52	47	24	11.3
Foam filled, capacitor tuned	0.30 x 0.05	0.32 x 0.10 x 0.083	1.47	69	34	23.4
As above, with addition of optimum dc bias configuration	0.30 x 0.05	0.32 x 0.10 x 0.083	1.47	69	56	38.6
Pressurized, distributed capacitance tuned	0.30 x 0.04	0.32 x 0.12 x 0.096	2.40	59	25	14.8
Capacitor tuned	0.21 x 0.04	0.21 x 0.08 x 0.052	0.68	50	2	1.0
As above, with addition of foam	0.21 x 0.04	0.21 x 0.08 x 0.052	0.68	50	12	6.0

2. End-loading and use of fiberglass-like dielectric materials can result in very large power-handling improvements in monopole or multipole antennas, with little increase in weight.
3. The use of dielectric sheaths on antennas should be carefully considered when ambipolar diffusion conditions can be obtained.
4. The use of dc bias for improving power handling of antennas is possibly not as effective in gases other than air for certain conditions.
5. For what appear to be reasonable power levels, typical dish feeds and broad beam antennas operating from the Martian surface can be designed to avoid breakdown with little difficulty. Lower frequency electrically small slot antennas can also be made to have adequate power-handling capability.



OPEN DISCUSSION

MR. MOLMUD: The polonium in your bell jar produces an ionized atmosphere. Do you have any idea of what the electron density is?

MR. KINKEAD: No, I don't. I calculated this at one point. I went back to the paper Mr. Chown had written in 1959, in which he had made some calculations of the low-pressure extent of the ionization field of these sources. I used a 16-in.-diameter bell jar with four 400-microcurie sources. I don't know exactly what the electron density was where the antenna was located; I'd have to calculate it.

MR. MOLMUD: The reason I ask is because some of our recent work has indicated that there might be an ionosphere on the surface of Mars, so you might get electron densities of  $10^5$  or  $10^6$ , especially under solar flare conditions. So I was wondering whether you are reproducing the Martian atmosphere inadvertently with the bell jar system.

MR. KINKEAD: Well, you're partially right. People often raise this question. They say, "Ha! You're using radioactive sources and you've got a higher electron density than you really would have in a planetary atmosphere" and very simple-mindedly without getting involved with numbers, we agree; but there are always a lot of free electrons floating around the upper atmosphere where we worry about this condition. So we are vaguely within a few orders of magnitude, perhaps simulating it, and it's partially inadvertent, partially intentional. (The basic purpose of the sources is to provide consistent, worst case, results.)

MR. MOLMUD: Another thing about the possibility of the ionosphere being at the surface of Mars; the question I have is how will that affect the dc-biasing of your antennas to prevent breakdown? In other words, you might get an excessive current drain if you're immersed in a conducting medium, so dc-biasing may not be every effective.

MR. KINKEAD: Well, it certainly isn't when there is a significant electron density present. For this and other reasons, it's not a very good technique to use the dc-biasing. Now, certainly an antenna that's re-entering is going to see a very highly conducting plasma, and dc-biasing won't do you any good for most circumstances that we can think of. The only thing I really meant to point out was that it won't perhaps do as much good as we could do with dc bias on Earth, but dc bias is seldom used even on Earth.

I think the real solution of the antenna power-handling problem is a geometry optimization. It's really spreading your field out over as big a volume as you have to in order to get the field down to as low a peak value as you think you can safely live with. I think dc-diasing, just as an opinion, is not a good solution. I think some of my tests have given me the feeling that extensive use of dielectrics is not a good suggestion because of possible weird effects you may have when you have plasmas, (either reentry or boosted flight plasma) or high ionization densities perhaps on the surface of Mars that I wasn't particularly aware of.

I realize we might have some problem in that area but not an extensive one. A figure of  $10^5$  doesn't sound like enough to provide so much dc conductivity that the field will be wiped out. Perhaps I'm wrong. It depends on the field electrode configuration, certainly.

MR. BUNKER: One comment that I got from the literature: to get a uniform field, all you need is 1 electron/ $\mu$ sec in the gap, and that's not very much.

MR. KINKEAD: We were informally talking with Mr. Chown yesterday and he indicated that when we don't have a gap and have a very small antenna with a very sharp point, you might not have one electron come by very often because of the field or the area over which the most intense field extends is very small.

Of course, with any of these antennas we have an infinitely high field over an infinitely small volume right at the sharp edge. These were flat-topped monopoles; they weren't rounded. So this is perhaps one of the difficulties where my results don't exactly match SRI's. Perhaps I've got a burr on the end of my antenna. That's just one of the many possible differences.

MR. HAIGH: I would like to make a comment. You implied that breakdown really is not too much trouble. You can spread your fields out; you can put two or three antennas on the vehicle. I just hope that none of our structures and systems people are here to hear you say this.

MR. KINKEAD: I'll have to agree with you that sometimes, as pointed out yesterday, an antenna is the last thing to be incorporated into a vehicle and it has to fit.

MR. HAIGH: Let me say this: for any vehicle you fly that has an antenna, the antenna is supposed to perform some function, have some beam with some directional properties that pretty well says what it will look like, the size of the aperture, and so forth.

- MR. KINKEAD: Since my background is antenna design, I would tend to favor somebody who could come up with a clever series of designs that could all meet the same pattern requirements but have whatever power-handling requirements needed. I think within certain limits that's possible. I think these end-loaded monopoles are one example of how it might be done. I think that all you have to do to eliminate breakdown is to put your antennas on a big enough diameter and put enough antennas around. Now, of course, this is going to make Swiss cheese of whatever vehicle you might be considering, but there's always a brute force technique available to eliminate the problem.
- MR. HAIGH: If we put antennas around and spread them out, you're going to play hob with the pattern characteristics.
- MR. KINKEAD: Oh, not at all. Not if you do it properly; just if you do it improperly.
- MR. HAIGH: We've been looking into high-power antennas for systems that would accept 200 to 400 kw on the low frequencies. If you have a small vehicle, you don't change antennas around, as such.
- MR. KINKEAD: With a small vehicle you have problems. There's no question about that. This is something that should be factored into the early vehicle design cycle rather than wait to be discovered at the end.
- MR. HAIGH: I won't belabor the point, but you are definitely limited.
- MR. KINKEAD: There are situations, no doubt; but if we think in terms of a Martian lander I don't think we have severe size limitations.
- MR. HAIGH: That is a point. You can prevent breakdown on any system; all you have to do is fly maybe a 60-ft radome around the thing and you're set. But, when you're sending vehicles out to Mars, it's a long way, and the freight cost is very very high. And the case for optimization is extremely high.
- MR. KINKEAD: That's just the point I meant to make when I indicated that by use of end-loading, or by the use of lightweight fiberglass materials, you might avoid a lot of weight. This is a mechanism we don't fully understand.

Incidentally, this material we've used and have been using for years to inhibit breakdown looks just like the insulation material in the walls of buildings. You wouldn't think it would do so much good on the basis of its mass because it really doesn't weigh very much. It doesn't change the dielectric

constant of the medium very much and it does inhibit breakdown remarkably well, especially at these VHF frequencies, and it weighs next to nothing.

REFERENCES

1. J. A. Martin and J. Chown, Study of the Breakdown Characteristics of Antennas in the Atmospheres of Mars and Venus, Final Report, JPL Contract 950380, Stanford Research Institute, Menlo Park, California (February 1963). NASA-CR-59111.
2. J. B. Chown, W. E. Scharfman, and T. Morita, "Voltage Breakdown Characteristics of Microwave Antennas," Proceedings of the IRE, Vol 47, No. 8, pp. 1331-1337, August 1959.
3. W. E. Scharfman and T. Morita, Voltage Breakdown of Antennas at High Altitudes, Stanford Research Institute, Menlo Park, California, Technical Report No. 69, SRI Project No. 2494, April 1960 (Fig. 22)
4. D. J. Rose and S. C. Brown, "Microwave Gas Discharge Breakdown in Air, Nitrogen, and Oxygen," Journal of Applied Physics, Vol. 28, No. 5, pp. 561-563, May 1957.
5. A. D. MacDonald, D. O. Gaskell, and H. N. Gitterman, "Microwave Breakdown in Air, Oxygen, and Nitrogen," Physical Review, Vol. 130, No. 5, pp. 1841-1850, June 1963.
6. W. B. Cuttingham and S. J. Buchsbaum, "Diffusion in a Microwave Plasma in the Presence of Turbulent Flow," Journal of Applied Physics, Vol. 36, No. 6, pp. 2075-2078, June 1965.
7. L. Gould and L. W. Roberts, "Breakdown of Air at Microwave Frequencies," Journal of Applied Physics, Vol. 27, pp. 1162-1170, October 1956.

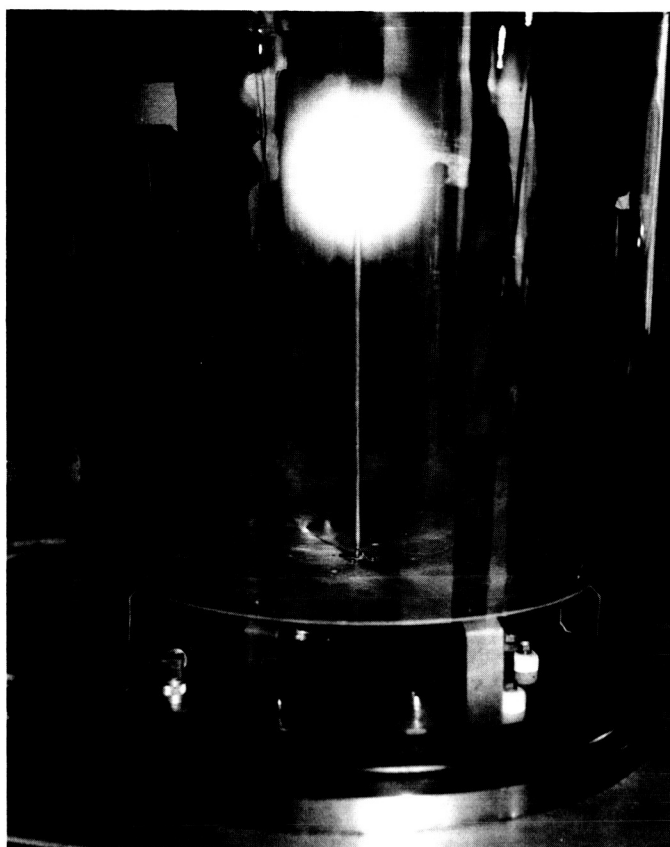


Fig. 16-1. Voltage breakdown of VHF quarter-wave monopole

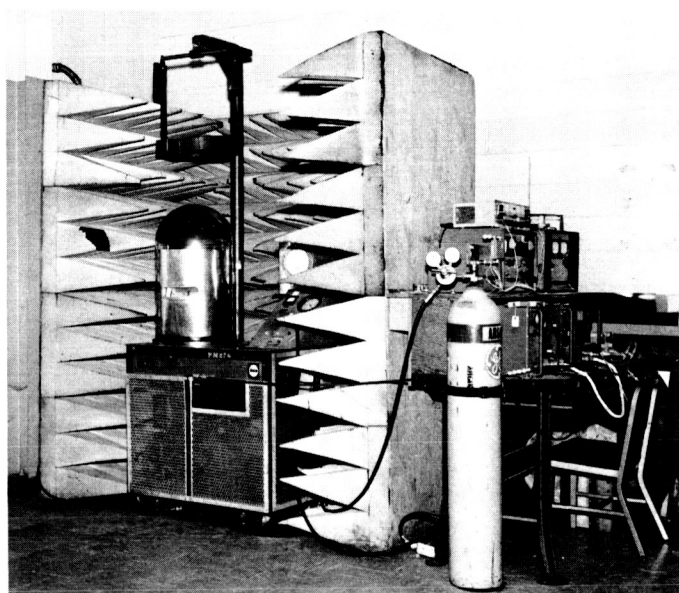


Fig. 16-3. Overall view of test equipment

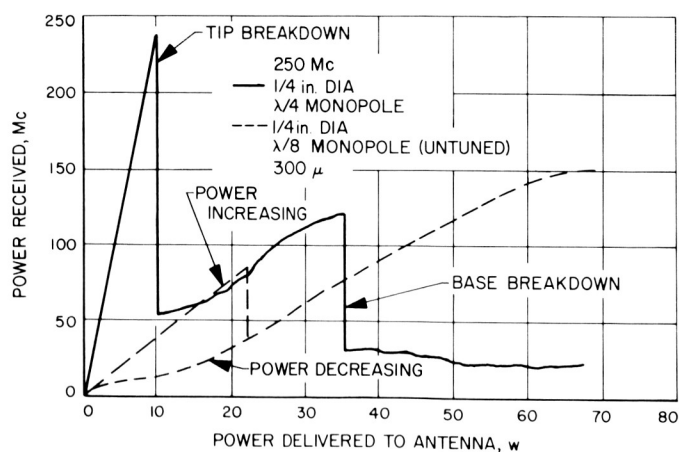


Fig. 16-2. Transmitted power vs input power,  $\lambda/4$  and  $\lambda/8$  monopoles

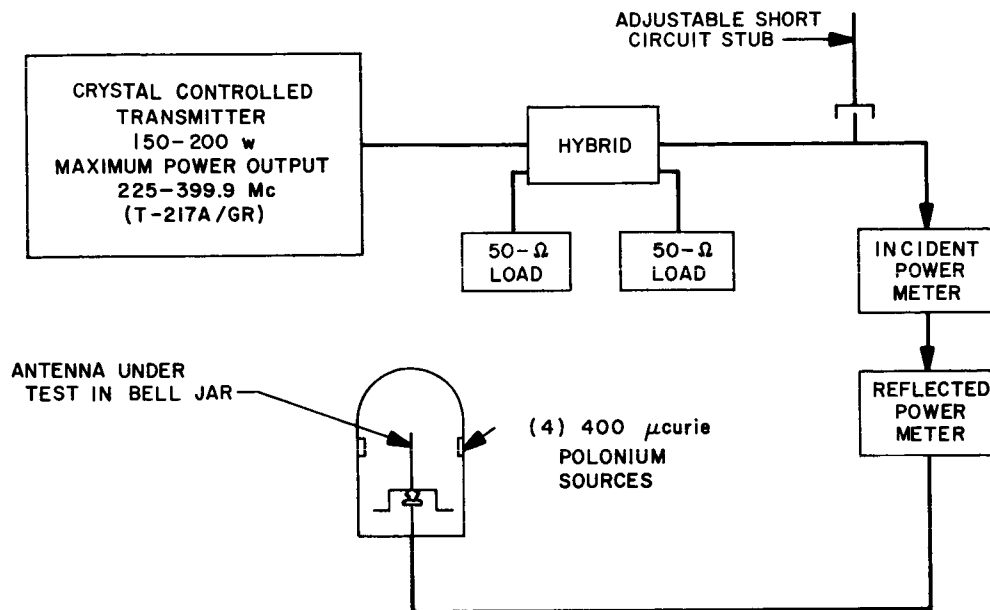


Fig. 16-4. VHF test equipment block diagram

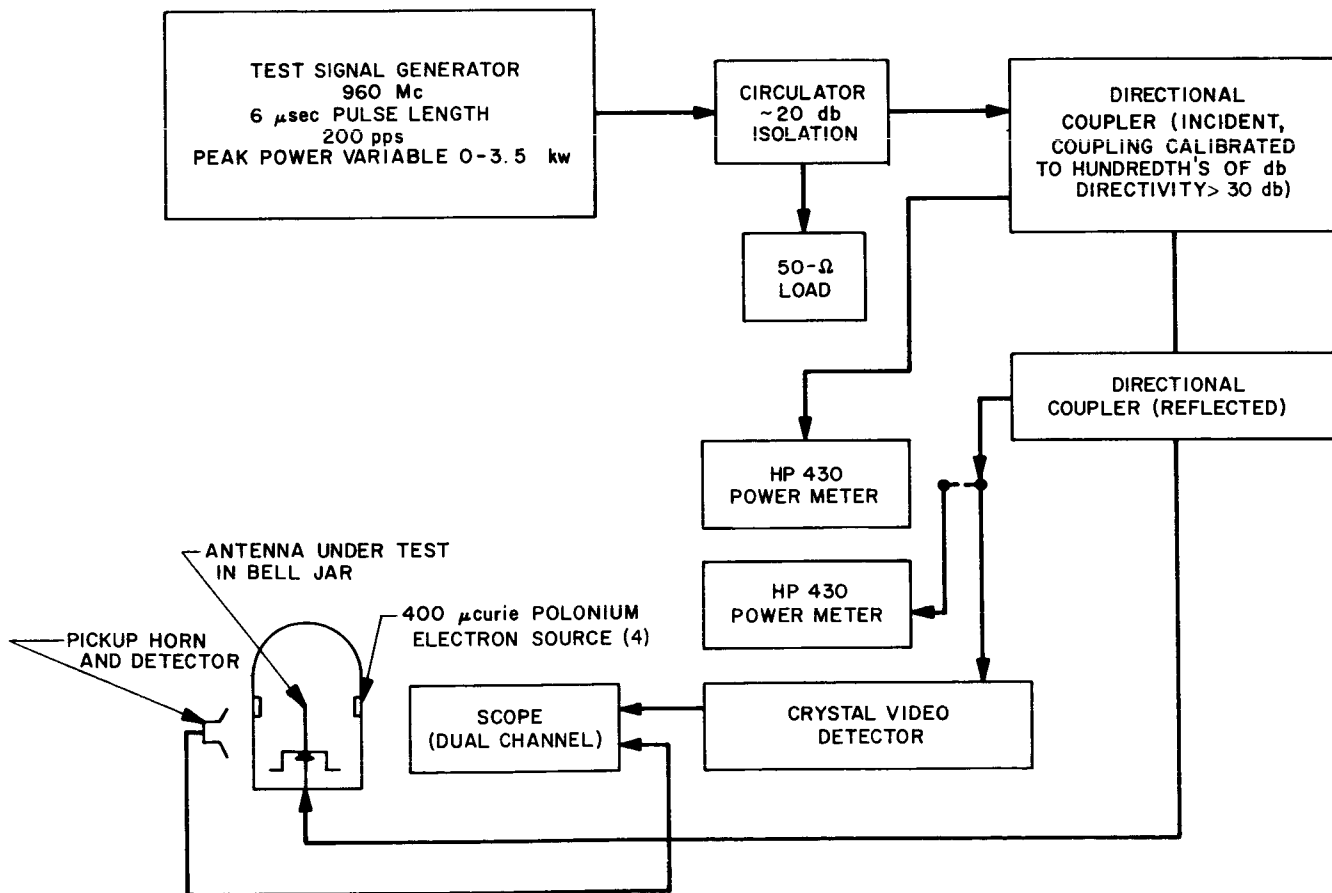


Fig. 16-5. L-band test equipment block diagram

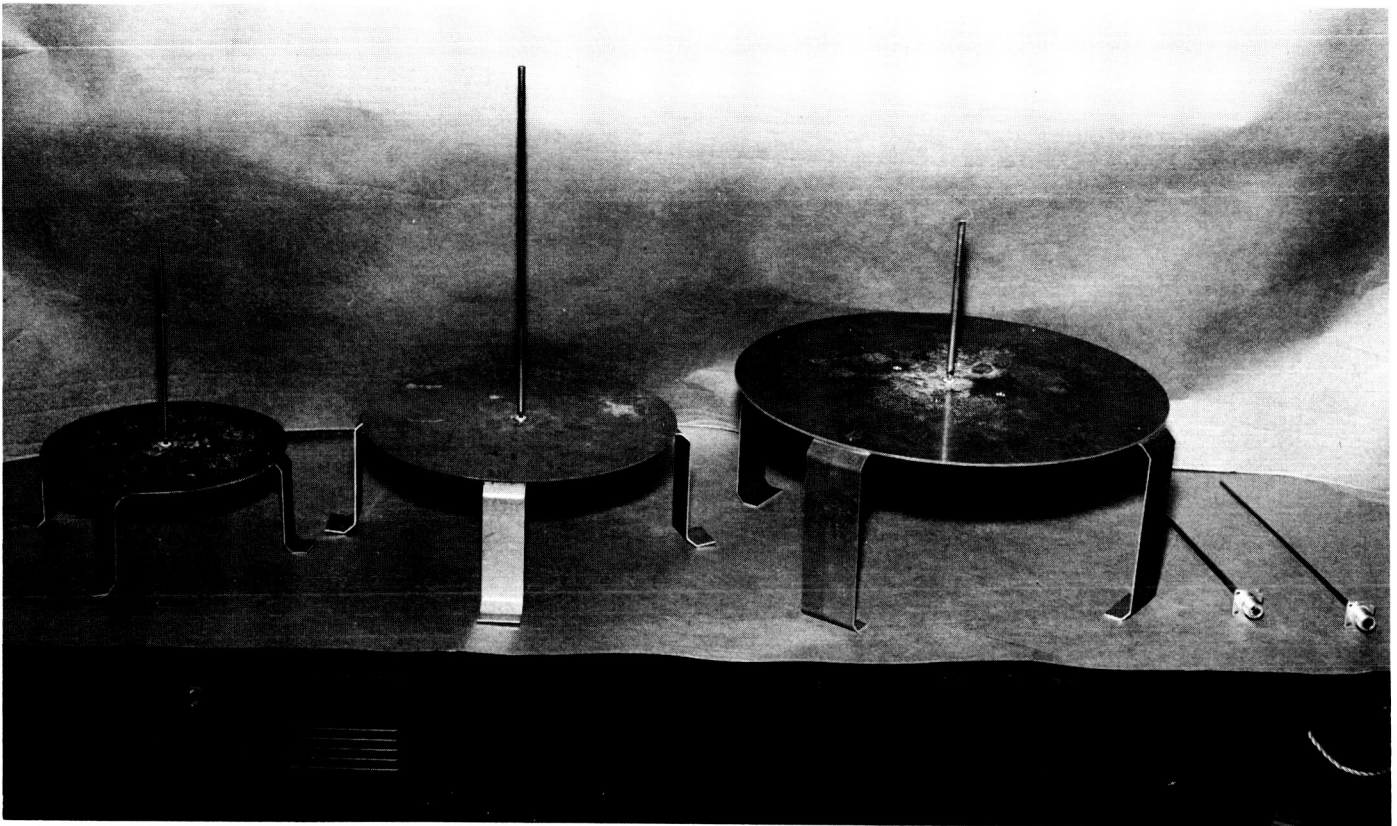


Fig. 16-6. Scaled ground planes with various stub antennas

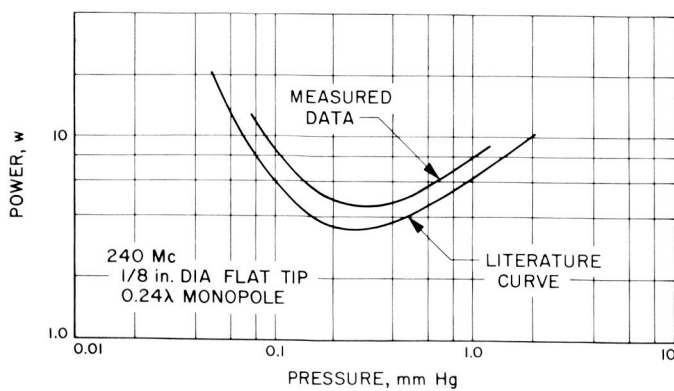


Fig. 16-7. Power to initiate break-down vs pressure

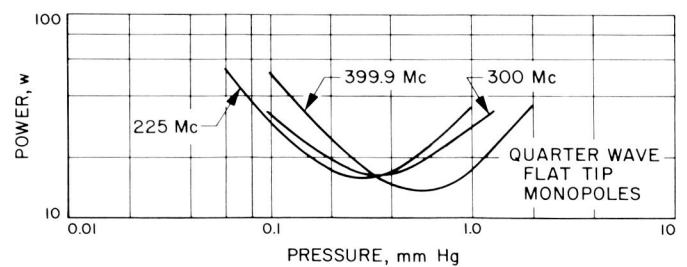


Fig. 16-8. Power to initiate break-down vs pressure, scaled monopoles



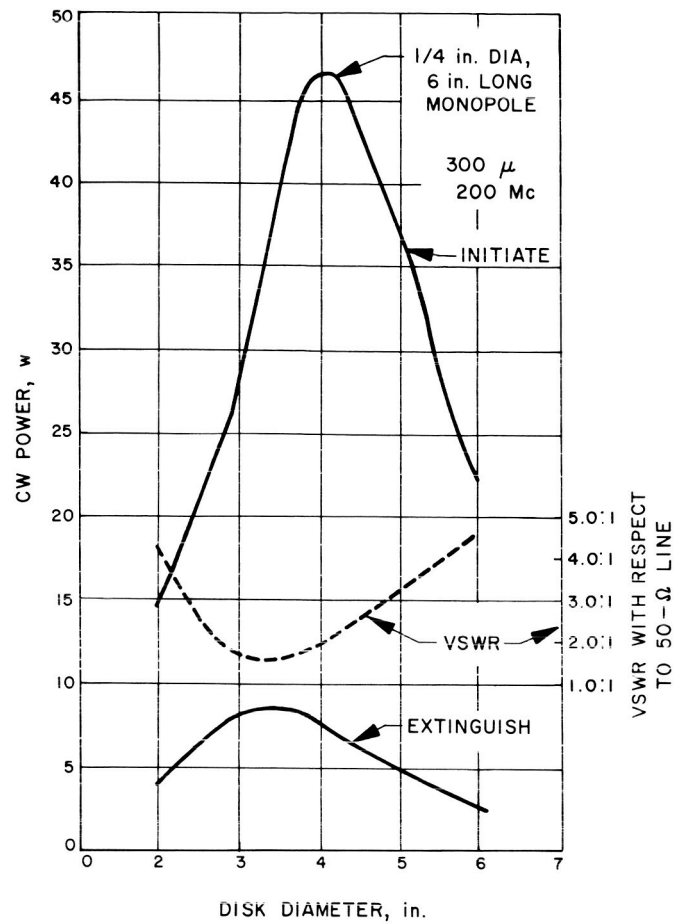


Fig. 16-9. Power to initiate breakdown, power to extinguish breakdown, and VSWR vs end-loading disk diameter

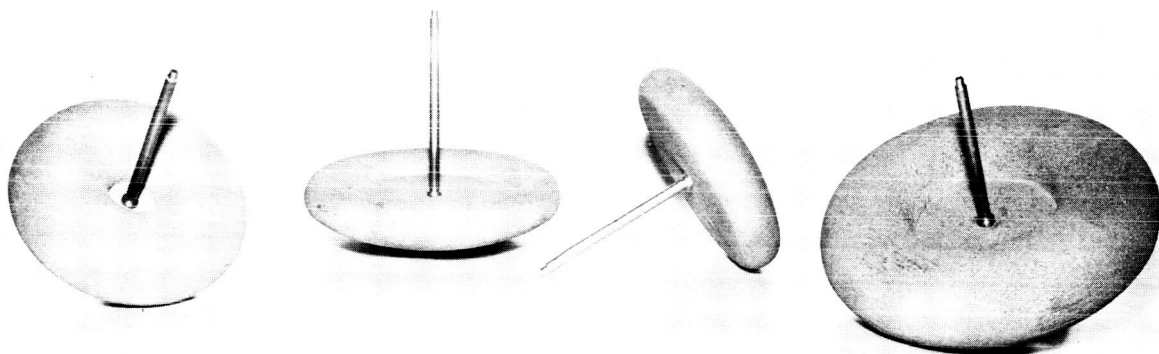


Fig. 16-10. "Mushroom" antennas, used for end-loading optimization flame sprayed copper on wood

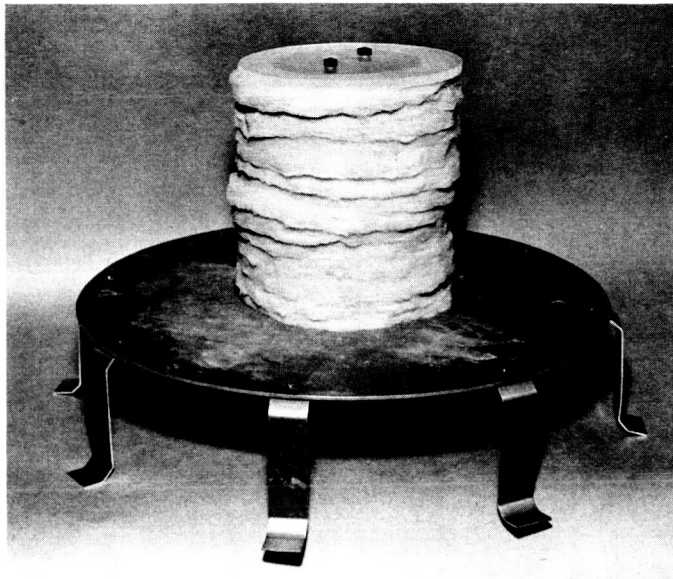


Fig. 16-11.  $\lambda/8$  end-loaded stub with plastic disk covering and "microquartz" stem dielectric

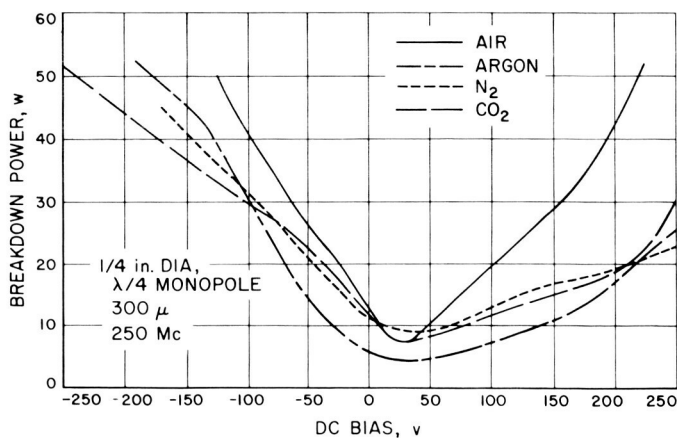


Fig. 16-12. Breakdown initiation power vs DC bias

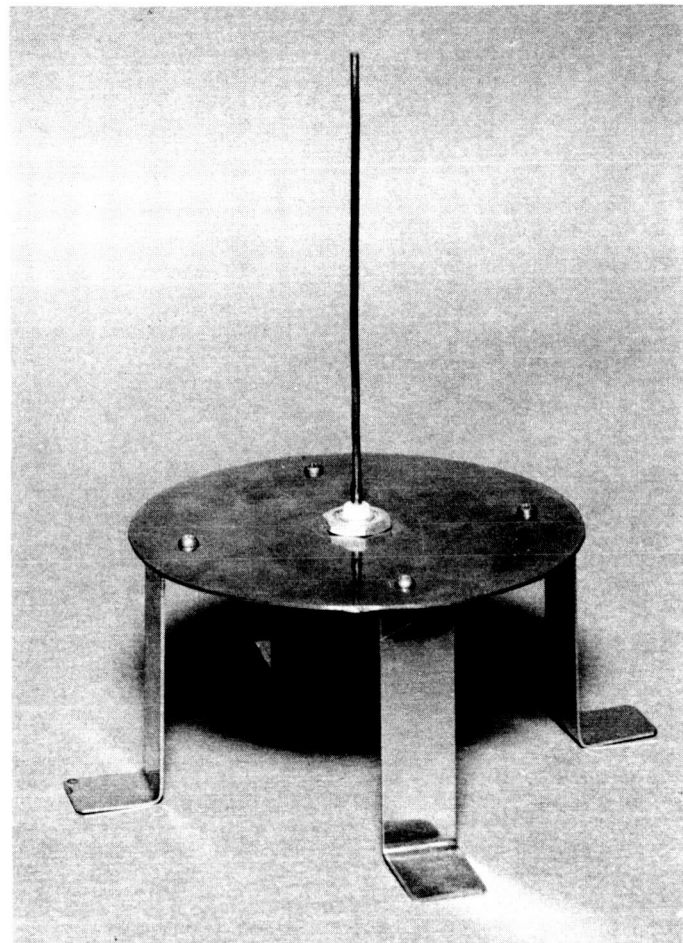


Fig. 16-13. Monopole and ground plane used for L-band tests

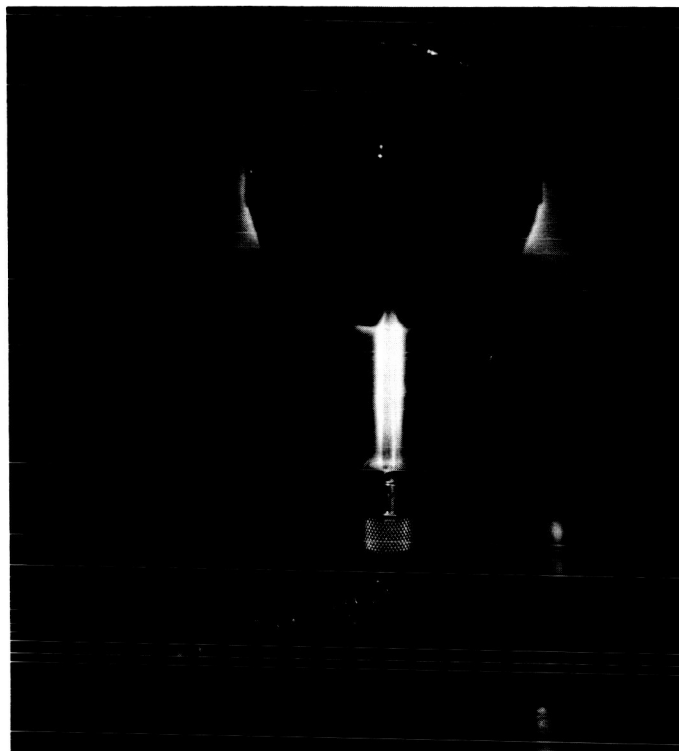


Fig. 16-14.  $\lambda/4$ -dia encapsulated turnstile antenna shown with feed line and two elements breaking down

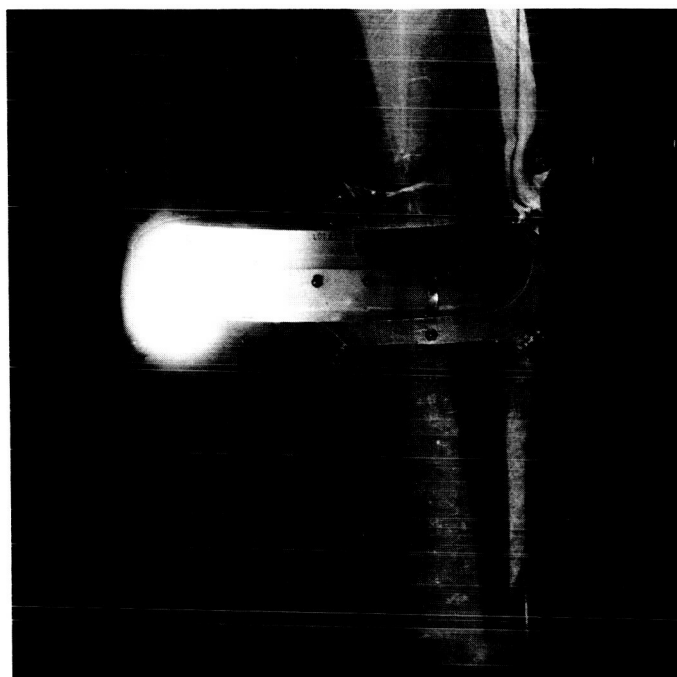


Fig. 16-15. Electrically small, VHF, unfoamed slot antenna breaking down

N 68-26892

17. SOLUTION OF A BREAKDOWN PROBLEM AT PARTIAL  
PRESSURES IN THE APOLLO LEM TRANSCEIVER

S. B. Newton  
Government Electronics Division  
Motorola, Inc.  
Scottsdale, Arizona

INTRODUCTION

This is a report of a problem encountered in the LEM transceiver during a low-pressure environment test. The problem was a loss of RF output and appeared to result from a voltage breakdown in the high-power variable reactance multiplier in the transmitter.

The symptoms observed that led to this conclusion and the actions taken are described as they occurred.

NORMAL OPERATING CONDITIONS

At this point, a brief technical description of the multiplier stage may be helpful. The multiplier stage is a 1-2-4-5 quintupler, utilizing idlers at the second and fourth harmonics of the input frequency. Input power of approximately 6.5 w is supplied at 152 Mc by transistorized power amplifiers. The nominal output at the fifth harmonic (760 Mc) is about 3.0 w. There is no dc power supplied. What dc exists is due to the rectification of the varactor.

Circuitry is composed of 1/4-in. -diameter air-core coils and JFD variable capacitors followed by a three-section helical resonator filter. Packaging is fairly dense for RF circuitry; the entire circuit plus filter is contained in 2 1/2 x 1 5/8 x 1 in. volume. A photograph of the multiplier is shown in Fig. 17-1.

SYMPTOMS OF VOLTAGE BREAKDOWN

When the transceiver was being environmentally tested at an equivalent attitude of 100,000 ft, a characteristic purple glow of corona discharge was first seen in the input section of the helical filter. It then appeared between the variable capacitors of the input network. As the pressure continued to decrease, this purple glow spread throughout the components of the multiplier.

The corona condition persisted from an equivalent altitude of from 90,000 to about 250,000 ft. Figure 17-1 shows the corona glow as it first appeared in the multiplier network. The photograph, you will notice, is a double exposure. The corona was photographed in darkness and the circuitry under normal lighting conditions.

As the pressure continued to decrease to an equivalent altitude of 350,000 ft, a second effect was noted. The output RF power dropped very rapidly to zero. However, when the input RF power was removed for 4 or 5 min. and then reapplied, operation was normal for about 30 sec. The output would then fall rapidly to zero. This cycle could be repeated as often as the input was removed and reapplied. Another symptom was noted — just as the RF output dropped to zero, the ion count in the vacuum chamber increased sharply.

### PROBABLE CAUSE OF BREAKDOWN

The corona discharge was undoubtedly due to the strong electric fields produced by the high power levels involved. This electric field intensity was estimated to be about 100 v/cm.

The cause of the power loss at extremely low pressures was subject to much speculation. Some of the suggested causes were secondary emission effects (multipacting); outgassing of the materials used in the multiplier; or, since we had a cycle-type symptom, temperature effects.

### APPROACHES TO A SOLUTION

A first approach to a solution was to coat all components with a conformal coating. After three coats of Dow Corning XR-6-2121 silicone coating were applied, the multiplier was retested and resulted in no improvement; the corona and resulting power loss was still with us. As an added item of interest it was noted that the coating did not affect electrical performance at normal pressures even at these high frequencies.

The coating was then removed, and, as a second approach, small blocks of foam were placed between the points where corona first occurred. This approach also had no effect as the discharge simply went around the blocks of foam.

A third approach was to completely fill the entire multiplier circuitry and helical resonator filter with a unicellular foam. This approach was undertaken cautiously since we didn't want the cure to be worse than the disease. Electrical performance as a multiplier still had to be maintained. Evaluation was made of three types of foam as follows:

Emerson and Cummings	FP Eccofoam
Nopco Lockfoam	BX-105C-3
Nopco Lockfoam	A-206

The basis of selection was the effect of the foam on electrical performance when used in the 760 Mc helical filter. Lockfoam A-206 proved to have the least effect when insertion loss and frequency shift were compared.

### OPERATION WITH FOAM

After foaming, the multiplier was retuned and tested in the critical pressure range where corona breakdown had previously occurred. No breakdown was evident, and subsequent tests indicated that normal operation was possible up to RF input levels of 10 w.

The effect of rapid RF output power drop was still occurring at very low pressures. Believing that it was a thermal problem because of the cycle type symptom, the multiplier was connected to a good heat sink while still in the vacuum chamber. Then pressures as low as  $5 \times 10^{-7}$  mm Hg (800, 000 ft) could be reached with no degradation in output power. This pressure was maintained for 3 days and operation was still satisfactory.

The power loss was evidently caused by extreme heating of the variable reactance semiconductor's junction. When allowed to cool by removal of the RF input, performance returned to normal until reapplication of RF power again caused the temperature to go too high. The rise in ion count was attributed to outgassing, but the outgassing itself was not deemed to be the cause of power loss.

### SUMMARY

A solution for the voltage breakdown problem in the LEM transceiver was obtained by the use of complete foam encapsulation. Electrical performance was affected to a small degree but not enough to degrade the system.

Inadequate heat dissipation was found to be the actual cause of a problem that originally appeared to be one of voltage breakdown.

An additional and distinct mechanical advantage was also gained through the use of foam. Components are now fully supported and protected against degradation due to vibration and shock.

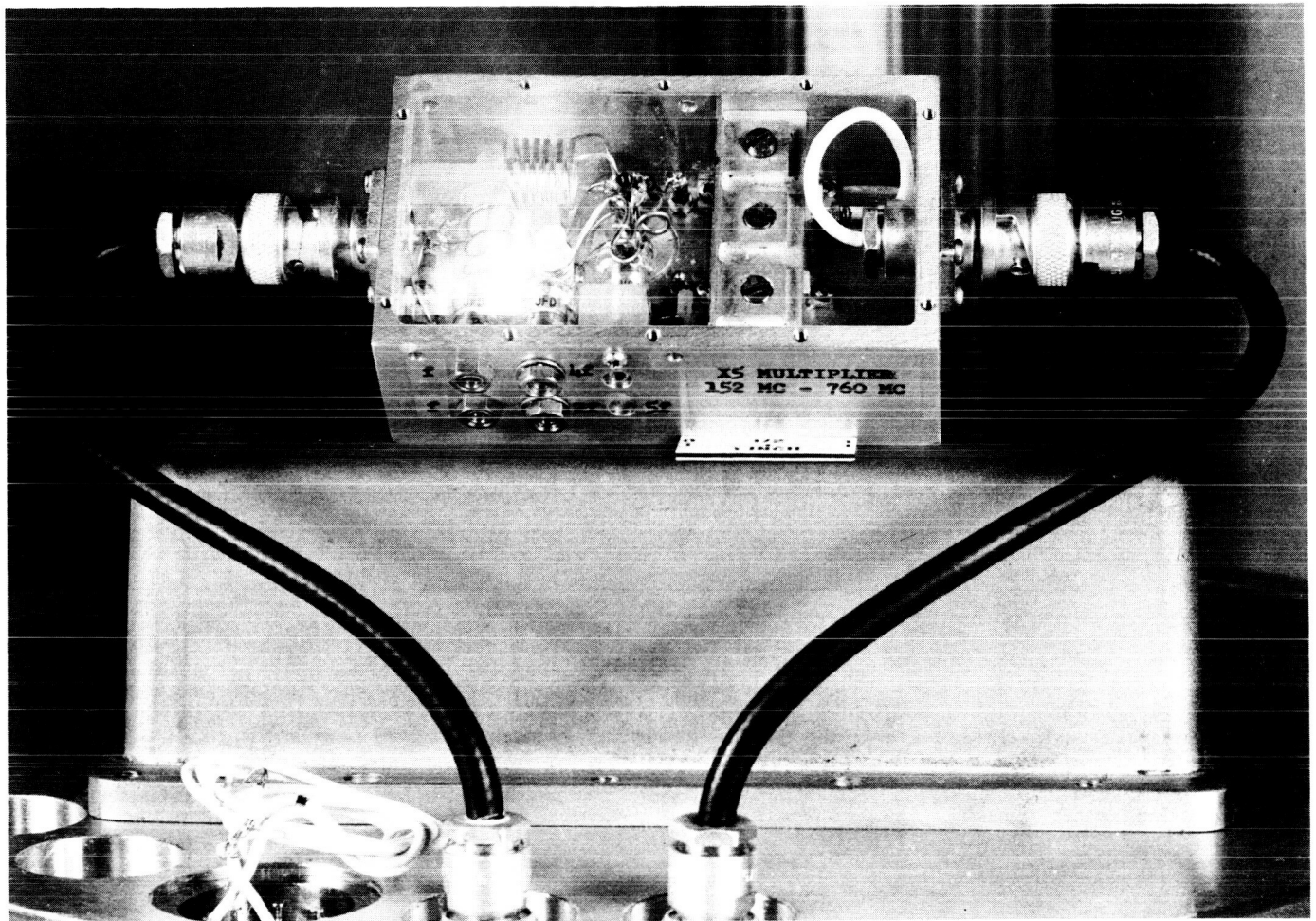


Fig. 17-1. Double-exposure photograph showing multiplier and corona glow



## 18. VOLTAGE BREAKDOWN IN AN EXPLODING BRIDGE WIRE SYSTEM

W. H. Brown  
Manned Spacecraft Center  
National Aeronautics and Space Administration  
Cape Kennedy, Florida

The exploding bridge wire (EBW) is an electronic system currently used on at least three major space boosters. The system is a method for initiating a pyrotechnic chain that departs from the classical hot wire system used for many years in the past and still used in many pyrotechnic systems.

The typical EBW system uses a low-voltage (24 v), low-current trigger system to initiate the chain reaction that results in the final pyrotechnic action. The trigger pulse acts to release an energy source in the form of a high-dc-voltage pulse of over 2,000 v, which ultimately causes a bridge wire to explode in the presence of a pyrotechnic charge. The 2,000-v source is generated by a transistorized circuit which converts 24 v dc to the 2,000 v needed in the bridge wire in the form of a short-duration pulse. A typical circuit is illustrated by Fig. 18-1.

The high-voltage pulse is transferred from the electronic packaging to the pyrotechnic detonator through a connector, P2. The connector is considered necessary so that the system may be broken and left in a safe condition before the intended use. The safe condition consists of a shorting plug connected at the detonator. This connector, in normal use, necessarily must pass high voltage without any degrading effects. A known flight failure occurred in one of the systems that used a conventional two-pin connector for this in-line connector. An immediate fix was made on the flight system by packing the connection with Dow Corning DC-4. The higher dielectric at the source of breakdown temporarily relieved the problem. The ultimate solution was a redesign of the disconnect system which would properly pass a high-voltage, short-duration pulse.

The new design was incorporated in the pyrotechnic detonator and consisted of a coaxial connector given a high-voltage rating of 2050 v. Such a detonator is made by the Dage Electric Company, Franklin, Indiana. The detonator contains the pyrotechnic charge, which is the first operation in the ordnance chain reaction. The pyrotechnic charge is detonated by the bridge wire, which explodes when the high-voltage pulse is applied to the bridge wire. In series with the center conductor between the connector and the bridge wire is a voltage breakdown gap. This gap prevents a low voltage, incapable of bridging the gap, from exploding the bridge wire.

For reference, the Dage Electric Company detonator has been described. It is known as PS-9710 modified; or the right-angle type is known as PS-9668 modified. Such a detonator has proven to be reliable when incorporated in the system for which it was intended. Figure 18-2 illustrates the connector and detonator.

The referenced high-altitude flight failure occurred at the two-pin connector used in the original system design. The failure mode was resolved to be high voltage breakdown between the two pins of the connector. A standard connector has no means of retaining pressure nor releasing pressure so that it is not known what pressure was present at the time the failure occurred.

It is the nature of the EBW firing unit that one high voltage pulse is available after the unit is armed. One 28-v-dc trigger is expected to serve to provide the high-voltage pulse for exploding the bridge wire. This output pulse from the EBW firing unit is intended to be of sufficient magnitude to jump a gap within the detonator to reach the bridge wire. The gap is evident in Fig. 18-2 as a break in the center conductor.

The coaxial connector design is very similar to a BNC coaxial connector. Such a design gives high voltage carrying capability as well as allowing good isolation from extraneous noises such as radiated radio energy. A coaxial connector carries the system wiring shield continuously through the connector.

It is intended that this information will serve to illustrate a point of failure in an otherwise safe and reliable system. A weak point need only be found and the failure mechanism understood before a cure is short in coming.

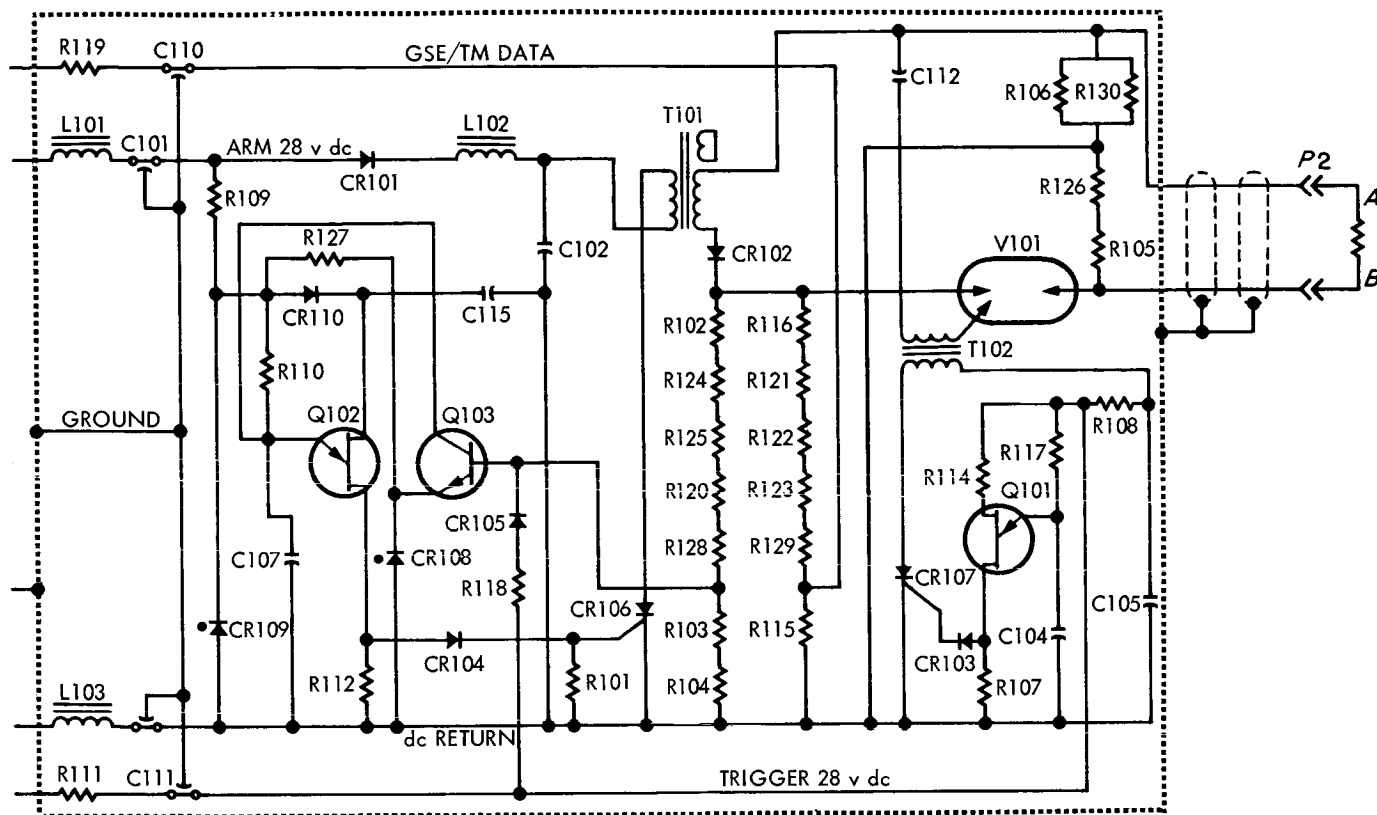


Fig. 18-1. EBW firing unit

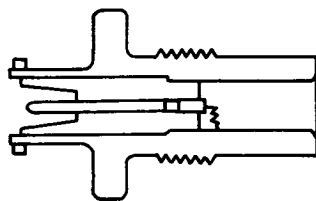


Fig. 18-2. Pyrotechnic detonator with coaxial electrical connection

19. SOME ASPECTS OF BREAKDOWN AND CORONA PROBLEMS  
IN THE CRITICAL-PRESSURE RANGE

L. J. Frisco and W. T. Starr  
Advanced Technology Laboratories  
General Electric Company  
Schenectady, New York

I would like to make a few comments relative to the breakdown problem in the critical-pressure range, and then I would like to take a few minutes to describe a program that we are currently working on at our Research and Development Center in Schenectady involving the performance of thin-wall hookup wire in the environments that might be experienced in the Apollo mission.

From the remarks and the discussion that I've heard both yesterday and today, I think that this group should be aware that such a program is underway and that it will soon (at least the first phase of it) be completed and that a rather comprehensive report will become available. I'm sure many of you are going to want to see those results.

Figure 19-1 substantiates something Earle Bunker said yesterday. He said the Paschen law or Paschen curve or Paschen minimum (terms that are sometimes not used too precisely) holds for a uniform field configuration but that with nonuniform fields we would not expect to get the same result.

Figure 19-1 shows some data taken from a paper by Wendell Starr in which he shows the comparison of the uniform field breakdown with what you would get with needle points as you do down through the critical pressure range. Of course, the needle points are much lower in the high-pressure range, and down around the minimum you actually get a phenomenon involving certain grading of the field and space charge and so forth, which can actually give you some higher voltages; then as you come up on the left-hand side of the Paschen curve the needle points fail to come back up again, and then when you get to even lower pressures (where emission takes over), the points do not behave well at all.

Mr. Bunker is quite right. You have to be careful in employing these principles so as to be aware of the field configurations you're dealing with.

Wendell Starr did rather a good job in analyzing the data that was available back in 1962, and he wrote a paper in two parts called "High Altitude Flashover and

Corona Problems," published in the May and June 1962 issues of Electrotechnology. There's no point of my going into many of the details of the paper; they have already, for the most part, been discussed here.

Now, unfortunately Mr. Starr couldn't be at this meeting. He's really our corona expert, and I'm sure he would have more to say about measurement techniques and so forth. He did tell me about a little experiment he ran that is described in Fig. 19-2, pointing up one of the anomalies in this critical-pressure region.

Figure 19-2 is a schematic, or functional diagram, of a hookup wire sample, and although it's shown as a solid conductor here, it was actually a No. 20 stranded conductor, insulated with silicone rubber about 40 mils. A conductive coating was applied to the outside of the insulation and the configuration was brought through the walls of the vacuum chamber. Then dc corona measurements were taken.

This wire had to be essentially free of corona at 2 kv dc, and it passed that test very easily. But when the pressure was reduced in the vacuum chamber, corona spikes occurred at about 1 kv at a chamber pressure of about 1/2 mm of Hg, and then they would disappear and again recur at about 5 mm when the pressure was being increased. Something was going on presumably in the region between the conductor and the insulation to give rise to corona spikes. Calculations were made, but it was concluded that it wasn't just the expansion due to the pressure of the gas in the wire. This explanation didn't seem to check out. As so often happens, just about the time that we were really getting involved with this problem, the specs were changed, resulting in the test being dropped. We never got back to the problem. This is the sort of unexpected problem that one can run into; it's another example of critical-region breakdown problems.

In some work I did at the Dielectrics Laboratory at Johns Hopkins a year or so ago (I'm a relative newcomer with the General Electric Company), we were making flashover measurements on various solid insulations in high vacuum. We found that even with the relatively low-loss materials one could get unexpected low values of flashover because dielectric heating caused localized, relatively high-pressure areas close to the surface of the specimen.

Here, again, I think we're getting into another type of breakdown in this critical PD range. The sample was a relatively small piece (1/4 x 2 3/4 in. and 1/8-in. thick) in a relatively large vacuum chamber; so when we talk about pressures, we have to be concerned with very localized pressures. It doesn't take much heating to

drive off adsorbed gases and to cause degassing from the solid material itself. In listening to some of the arguments this morning about the use of foams (particularly in the RF range), I wonder how much off gassing or outgassing is being induced by RF heating of the relatively "lossy" dielectrics that are being used. Maybe you're helping to keep the foam pumped up because each time you give it a burst of RF you're generating some gas.

The materials that have been described are relatively lossy materials, if you consider just the solid part of the structure. In the experiments in which we were making flashover measurements, we also made measurements in the RF range and at that range the thermal conditions are so severe (because the specimen is well insulated thermally, being in a high vacuum) that even the very low-loss materials would exhibit a thermal type of breakdown before we got flashover in most cases.

The program we're currently working on is oriented toward the Apollo mission and so is concerned with the behavior of thin-wall hookup wire in the 5-psi oxygen atmosphere. Although we have been talking about one critical pressure range, I think there's another critical pressure in terms of the trouble it can cause: the 5-psi pure oxygen with moisture. Of course, we're also concerned about the operation in vacuum since a good part of the wire is on the outside of the spacecraft.

What we're doing is evaluating sixteen different kinds of thin-wall hookup wires. We're working with only one wire size or conductor size (No. 20 stranded wire), and here by thin wall I mean that the insulation is 10 mils or less.

The various types of construction, or the ones you would most expect, are ML coated TFE and FEP, plain type-E teflon, various H-film constructions, so-called LEM wires, and Martin wire. Some of these have a FEP dispersion on the outside; others have a TFE dispersion. Several of them have no dispersion on the outside.

There are also three different silicone rubber constructions (a plain silicone rubber, a kynar-jacketed silicone, and an H-film kynar-wrapped silicone -- a very unusual material) and two of the irradiated modified polyolefin wires (a kynar-jacketed wire and plain IMP). I'm not supposed to mention manufacturers' names here and I'm sure that none of you know where the latter one is made; the contract number is NAS 94549 and is sponsored by the NASA Manned Spacecraft Center in Houston.

I have no intention of going into detailed results of the test we're currently running as it would take far more time than we have, and I'm not in a position to discuss these results. But I think it is worth just a few minutes to give you a general description of the program.

The first thing we do with wire that is received is to put it through an insulation resistance test in which we immerse it in water for three days. A disturbing feature is that so much of the hookup wire (even though we only ordered 1,000 ft) is coming in very small lengths, an obvious indication that even the manufacturer can't make it in long lengths (or else he's giving us his odds and ends). Even with short lengths that are apparently hand picked, very many samples are failing this initial immersing test. This gives some cause for concern: is the spec too high? or is it unrealistic? or just what is the problem? If it passes the insulation resistance test, we give it a voltage withstand test (another immersion test) at 1,600 v. Then we have an insulation resistance test after exposure to 15-psi pure oxygen at a 100% relative humidity for 15 days. This latter test is made on a cabled type of specimen (six wires wrapped around one central wire) in which the resistance between the central wire and the six outer wires is measured.

Using the same sample, we also make corona start voltage measurements and corona extinction voltage measurements; these measurements are made both at 15 and 5 psi in pure oxygen with moisture. We then measure voltage breakdown.

All the voltage breakdown measurements are made on twisted pairs (usually NEMA twisted pairs). This test doesn't really give worthwhile engineering information because the voltages are far greater than the wires would ever experience in service, but it does serve as a tool for detecting degradation during other aging tests.

Flashover testing consists of applying a voltage to the stripped end of the wire. About 1 in. of the insulation is stripped off, and then fine bare conductor (approximately 1/4-in. long) is wrapped back on the insulation. A flashover is produced between this bare wire and the end of the conductor (in an atmosphere of pure oxygen at 5 psi, wet) in order to see what effect it has on the insulation. We're interested in whether we get charring, tracking, ignition, or what have you.

We have various other tests on the physical dimensions such as outside diameter, concentricity, conductor dimension, weight per thousand ft, and stripability. Stripability, of course, is quite another problem, and we're finding that although

many of these thin-wall insulations are not difficult to strip, the difficulty is in not damaging the insulation left on the wire. In some of the breakdown tests we got some odd results that resulted from damage to insulation during the stripping operation.

Other problems include color durability, marking legibility, and compatibility with potting compounds. This latter one has led to some extremely interesting results. Here we're potting two types of samples. We age the potted twisted pair for 15 days at 15 psi of pure oxygen at 150°C, take it out of the aging, put in in water for 3 days, and then test it; and even though we're testing it in air, we've gotten fires in some cases and some pretty poor behavior in many others.

We don't have all the data yet. Although the program is only 3 months old, we already have a 259-page report on the first 8 weeks of it; we're about to finish it up in another two weeks, and much of the data is pouring in as I stand here talking. We've got about 15 people working on it, under the direction of Ken Mathes and myself.

The other type of compatibility with potting compound specimen is a pull-out type of mechanical specimen with which you're probably familiar; again, it goes through the same aging process, and then we pull it apart.

We test flexibility by using a repeated flex test, and we could stand here and talk all day about that. We don't like it too much. I think what we're really testing here are conductors rather than the insulation. We also have a cold flex, a repeated bent mandrel in which we wind from one mandrel to another mandrel and back again, and we do this at room temperature in liquid nitrogen at -196°C.

We have found in previous programs that testing in liquid nitrogen is a very sensitive means of detecting degradation. Here, again, we're not interested primarily in the behavior of the material in the liquid nitrogen because it may never see that environment. But we do find that in using this test degradation can be detected much sooner than at room temperature tests (although ultimately it will show up). It is a means of accelerating certain kinds of aging tests, and we use this as an end point in some of the aging tests where we're exposing the samples to oxygen temperature, moisture, ultraviolet, and x-ray radiation.

We also measure abrasion. The particular test we happen to be using is the NEMA repeated scrape abrasion (another subject we could talk about all day).

Blocking, that is, the wires sticking together, is another area we investigate. We're measuring cutthrough; the philosophy here is to compare the wires with the



cutthrough characteristics of something as well known as Teflon. Thermal creep is an example of a slower form of cutthrough. In regard to wicking, we use fluorescent dye solutions to determine the extent to which a solution will wick up between the insulation and the conductor.

Then, as I say, we also expose these wires to ultraviolet radiation, both in vacuum and pure oxygen. We're doing the same thing with x-ray radiation. Flammability tests are conducted at 5 psi in pure oxygen. We're doing three types of flammability tests; one to simulate a short circuit condition, in which we put a slug of current through the conductor; the second is a rather slow increase of a current in the conductor; and the third type is with external heating, using a coil around the conductor.

We're working, remember, with only one wire size, and this is an unshielded, unjacketed type of hookup wire; we have been able to get most of these wires to burn in 5 psi pure oxygen. Other wire sizes were used in just a few preliminary tests. We have gotten fires with every kind of wire, including those of the H-film constructions.

Chemical compatibility tests are conducted with some seventeen different chemicals, including the various fuels and oxidizing agents, such as fluorine and  $N_2O_4$ ; we expose wires to the chemicals and then use the flex test and the breakdown test to detect degradation. Of course, visual observations are also made.

Then we have offgassing in 5-psi oxygen. Here we are making weight-loss measurements using a quartz spring balance technique and gas analysis, determining what the products are. Then we conduct, in vacuum, volatility tests, in which we measure the products that come off and also measure weight changes.

From what I've heard here, I think that much of the work that we're doing at 5 psi is going to have to be done someday in the critical pressure range. I don't think it has been done yet. I think we're going to have to do more work in higher oxygen pressures. To my knowledge, I don't think a program this comprehensive has been conducted before. We've already seen from some of the results that one might expect different results from different wire sizes; shielded cables don't necessarily behave like a single wire, and a bundle of wires doesn't necessarily behave like a single wire.

I think there's a great deal to be done in this area, and I think some of the problems that have been discussed here might just be associated with hookup wire performance in the environments that you're exposed them to.

#### OPEN DISCUSSION

MR. BROWN: I'd like a little clarification. Did I understand you to say that you found that all the wires would support combustion? Did I understand you correctly?

MR. FRISCO: That's correct.

MR. BROWN: Even Teflon?

MR. FRISCO: Yes. With Teflon you can get a nice blue flame; the silicones too.

MR. BROWN: Well, what about polyolefin and, I believe, polyethylene?

MR. FRISCO: They're the best burners of them all. I think that is well known. As a matter of fact, we had an accident one day with a polyolefin wire during purging of the system. We accidentally lit the spark plug and the wire went up with no heat being applied to it at all. So, it's not a good actor at all in a flammability test.

MR. BROWN: Your work is being done with MSC?

MR. FRISCO: That's right.

MR. BROWN: Do they have any of your preliminary results yet?

MR. FRISCO: We sent a 259-page report to R. L. Johnson and Tony Wardell of MSC.

MR. BROWN: Okay; I know your source. I know where the information came from now.

MR. FRISCO: In fact, we were in Houston on Monday and Tuesday discussing it with them.

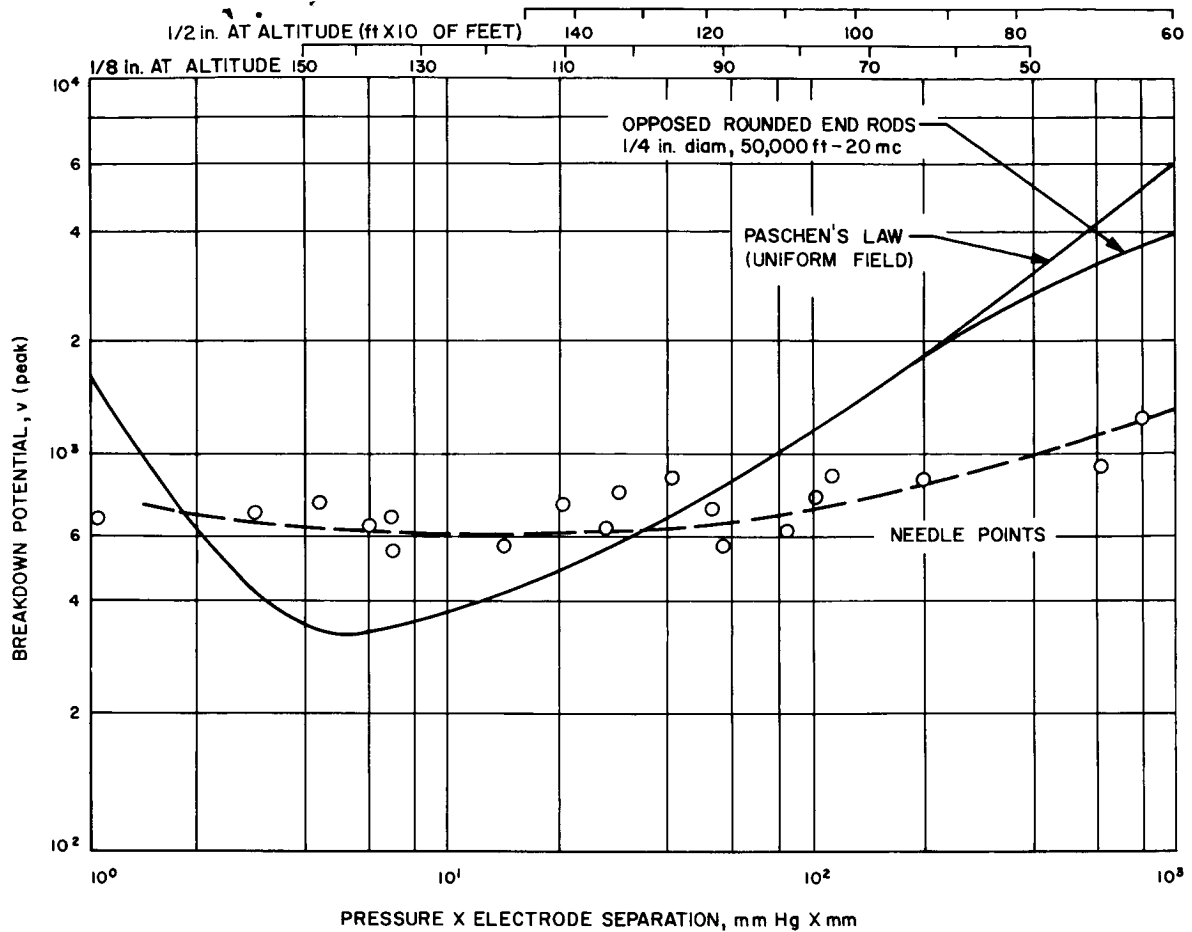


Fig. 19-1. Comparison of uniform field breakdown through critical pressure range

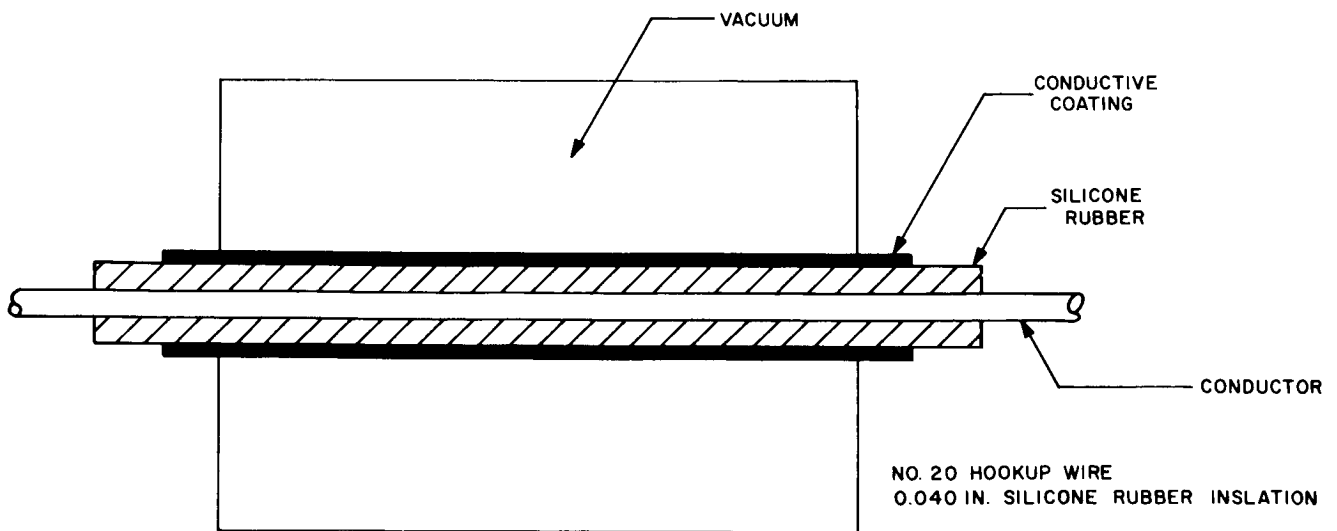


Fig. 19-2. Schematic of hookup wire sample

## 20. ELECTRICAL DISCHARGES AT ALTITUDES BETWEEN 70,000 and 250,000 FEET

William G. Dunbar  
Aerospace Group  
Space Division  
The Boeing Company  
Seattle, Washington

### ABSTRACT

Experimental measurements of electrical discharges caused by corona, glow discharges, and voltage breakdown were made under conditions encountered in aerospace vehicles operating within the 70,000- to 250,000-ft altitude range. All measurements were made in gases commonly used to pressurize spacecraft electrical and electronic compartments: nitrogen, nitrogen-oxygen mixtures, and normal atmosphere at sea-level pressure. Test results show that: (1) the onset voltage at which the electrical discharge occurred is much lower for spaced wires than for bundled or twisted wires; (2) the onset voltage between wires increases as the insulation thickness and dielectric constant are increased and decreases as the wire diameter and wire spacing are increased; and (3) the onset voltage of components depends on the type of component and its connection and installation.

### INTRODUCTION

Corona or electrical discharges within an electric power system transmit electrical interference into communication and electronic equipment, cause loss of power during the discharge time, and deteriorate insulation in the vicinity of the discharges. Spacecraft electrical system components may be subjected to intermittent electric discharges when the vehicle passes through or cruises within the 70,000- to 250,000-ft-altitude corridor. These discharges can occur whenever a potential impressed between electrodes is greater than that minimum voltage expressed by the Paschen Law curve (see Ref. 1). This law states that the breakdown voltage between two electrodes is a function of the product of the gas density times electrode spacing and decreases from ambient pressure down to a minimum, after which it again rises.

Practical methods for determining the presence of discharge require: (1) theoretical determination of the Paschen Law curve for each type of bare electrode and each type of gas used in the vehicle; (2) the determination of the Paschen Law curve for the insulated electrodes for which there is insufficient data. To meet the second requirement, experiments were undertaken to determine such curves for round, insulated conductors and for power system components that seemed to have low Paschen Law curves. Since some spacecraft use nitrogen or nitrogen-oxygen gas mixtures, rather than air, as their pressuring gas, the Paschen Law curves for nitrogen, oxygen, and nitrogen-oxygen gas mixtures were tested for their minimums between bare electrodes.

## EXPERIMENTAL MEASUREMENT PROGRAM

### Electrical Discharges

Technically, corona is an audible, luminous voltage discharge resulting from ionization of gas surrounding a conductor, around which exists a voltage gradient exceeding a certain critical value. However, the term "corona" can be used only to include those electrical discharges near sea-level pressures. "Glow discharge" and "voltage breakdown" are terms that better describe the electrical discharges at pressures below 20 mm Hg. The term "electrical discharge," rather than the three terms, "corona," "glow discharge," and "voltage breakdown," is used to avoid confusion when referring to these discharges.

### Onset Voltage Curves

The onset voltage of a test specimen as a function of gas density and spacing is shown in Fig. 20-1. The general shape of this curve, which is defined by Paschen's Law and referred to as the Paschen Law curve, has been known for many years. Paschen Law curves have been published for many gases between spaced bare metal electrodes. (See Ref. 2.) The onset voltage as a function of gas density and spacing is different for each gas and gas mixture, and is affected by the electrode material and electrode configuration.

### Detection and Measurement

Three principal methods of electrically detecting the onset voltage at which electrical discharges are initiated are described in Table 1. The method selected for electrical discharge detection measures the voltage produced across a resistor

by the discharge as shown in the table. The voltage output is then fed through a high-pass filter and a wide-band amplifier to an oscilloscope; the over-all gain of this system is 500  $\mu\text{v}$  per centimeter. This system was selected because it is simple to operate and inexpensive to install, provides consistent results, has adequate sensitivity, and is insensitive to outside interference. A schematic drawing of this system is shown in Fig. 20-2. A discussion and comparison of the other methods described is given in Ref. 2.

Table 1. Corona Detection Methods (Electrical)

Power Frequency Bridge Methods

Direct balance of bridge, wherein increased  $\tan \delta$  at higher voltages indicates power loss due to the sum of corona discharges

Observation of bridge unbalance voltage due to the corona as a Lisajou figure, where area of the figure indicates the corona power loss, if other losses are balanced out

Measurement of Voltage Produced Across a Resistor by Corona Discharge  
(Several modifications have been used.)

Resistor in series with ground lead to test specimen

1. Wide-band amplifier
2. Narrow-band amplifier

Resistor in series with coupling capacitor connected to high-voltage terminal of test specimen

1. Wide-band amplifier
2. Narrow-band amplifier (essentially like the NEMA, Radio Interference Test Method)

Measurement of Voltage Produced Across an Inductor by Corona Discharge

Inductor in series with ground lead to test specimen

1. Wide-band amplifier
2. Tuned narrow-band amplifier

Table 1 (Cont'd)

Inductor in series with coupling capacitor to test specimen

1. Wide-band amplifier
2. Tuned narrow-band amplifier

The electrical discharge onset voltage was determined by applying a 400-cps voltage to the test specimen. The voltage was set just below the expected onset voltage and then increased at a rate of 100-v/min until sustained discharges were detected. (See Ref. 3.) This test technique was performed for all specimens at several pressures and temperatures. The system was purged several times during each test to eliminate ozone and other impurities from the vacuum chamber during the tests.

Qualitative measurements were made to determine the existence of electrical discharges and the pressure and voltage at which they first appeared. A 1-mm visual display on the oscilloscope screen was found to be well below the allowed radio interference limit for the system. Several points were taken at the minimum of the Paschen Law curve, i.e., near the pressure where minimum onset voltage was detected for the spacing of the particular electrodes and gas. All the curves were drawn to include the minimum voltage data points so that the data could be used without applying safety factors. The recorded accuracy was within  $\pm 1\%$  of the calculated Paschen Law values when bare electrodes were tested.

#### Spacing, Temperature, and Pressure

At near-sea-level pressure, the onset voltage between bare electrodes is increased as the electrode spacing is increased. However, the use of spacing is not always a solution for increasing the onset voltage in unpressurized compartments of space vehicles, which travel from 20,000 to 180,000 ft or beyond. In this type of vehicle, the unpressurized electrical equipment may contain many bare electrode pairs. If each pair has a fixed spacing of 1 to 20 mm, the onset voltage of the 1-mm pair will pass through the minimum of the Paschen Law curve at a much lower altitude than will the 20-mm-spaced pair as shown in Fig. 20-3.

This implies that, in a typical spacecraft, the minimum onset voltages will occur over a wide range of altitudes. Likewise, this knowledge can be used for

checking components in an altitude chamber containing high voltage. For example, if the electric power in an altitude chamber is turned off at altitudes where the onset voltage is exceeded for the components with the closest spacings, it must be kept off until the minimum onset voltage for the components with the longest spacings has been passed.

The effect of temperature is similar to that of pressure because the gas density varies with temperature. The actual effect can be calculated by using the ideal gas law. Tests have been performed on nichrome conductors that were spaced 0.125-in. apart in air from 76 to 2000°F. The onset voltage curves had minimums of 260 v (rms) at 76°F and 230 v (rms) at 2000°F. The voltage decrease was caused partly by oxidation of the wire surface.

#### Electrode Configurations

At near-sea-level pressures, the onset voltage between bare electrodes is increased as the electrode configuration is changed from points to planes. However, the change in configuration is not a solution in space vehicles. Figure 20-4 shows that as the vehicle approaches the altitude related to the minimum onset voltage, the onset voltage will be the same regardless of the electrode configuration.

#### Pressurizing Gases

Many gases are used to pressurize electronic packages. Some gases are used primarily for their heat-transfer properties, others for their high dielectric strength, and some for a combination of weight, dielectric strength, and heat transfer.

The gases most commonly investigated have been Earth's atmosphere (air), nitrogen, oxygen-nitrogen mixtures, carbon dioxide, and helium. The onset voltage curves in air, nitrogen, nitrogen-oxygen mixtures, and carbon dioxide are shown in Fig. 20-5. These curves are of interest because a normally pressurized compartment may become depressurized because of either depletion of the gas supply or a compartment leak. It can be noted from the curves that the onset voltage, as a function of pressure and spacing, cannot be determined without having a complete Paschen Law curve for each gas or gaseous mixture. For example, if the onset voltage of pure nitrogen and pure oxygen were measured at 100,000 ft only, it would not appear that there is a considerable difference in their onset voltage at 150,000 ft.



## Insulated Wires

It is anticipated that space vehicle electric systems will require power of at least that quality defined by MIL-STD-704. This provides 115/200 v (rms) nominal and allows 190/330 v (rms) at generator ceiling excitation.

The minimum onset voltage of a wire sample is shown in Fig. 20-6. Two factors are significant. First, the insulation around a wire has increased the minimum onset voltage of wires spaced 0.25 in. apart to 320 v (rms), which is substantially above the minimum onset voltage of bare electrodes but slightly below the maximum ceiling voltage allowed on the power system. Second, twisting or closely spacing the wires again increased the minimum onset voltage to 370 v (rms). The reason the twisted wire has a greater minimum onset voltage than the spaced wire is the difference in the length of air path between the insulations.

This phenomenon is not discussed in detail; the point can be made that all tests have indicated that the minimum onset voltage of a twisted pair is always greater than that of a spaced pair, and that the minimum onset voltage difference between a twisted pair and a spaced pair is dependent on the dielectric constant of the insulation, the thickness of insulation, the wire size, and the voltage stress due to the applied potential. (See Ref. 4.) For example, a number of wires described in Table 2 were tested for onset voltage. In Fig. 20-7 the onset voltage at the minimum of the Paschen Law curve is shown for these wires and illustrates the importance of wire selection for electric system design. The main concern is to ensure that the minimum onset voltage of the wire is greater than the maximum allowed voltage on the power system.

## Connectors (see Ref. 5)

When measuring the onset voltage on electric components, consideration must be given to ensure that the minimum onset voltage of the connecting wire is at least equal to or is greater than that of the component to be tested. This was verified by performing four onset voltage tests on a 55-pin mated connector, which was tested in a simulated-high-altitude chamber. The tests were conducted with the connector shell electrically grounded and the connecting wires and unwired pins encapsulated with 0.50 in. of silicone rubber on each end of the connector.

A pair of No. 22 gage Teflon-insulated wires, spaced 0.25 in. apart, were connected to adjacent connector pins and then fed through the altitude chamber wall

Table 2. Description of wire test samples

Insulation			Wire gage	Insulation thickness, in.
Primary	Barrier	Outer Jacket		
PVC	Glass braid	Nylon	16	0.025
			10	0.036
Asbestos	Glass braid	Teflon and fiber- glass	20	0.042
			16	0.045
			12	0.052
Teflon (TFE)			22	0.022
			20	0.025
			16	0.035
Teflon (TFE)	Teflon and fiber- glass	Teflon (TFE)	20	0.030
			18	0.032
			8	0.040

to the energizing system. The second test was like the first except that the connecting wires were twisted. In the third test, one wire was disconnected from its assigned pin and then reconnected to the same assigned pin connection on the other half of the connector. The fourth test was made with the wires in the same physical position except that the connector was removed and the space filled with silicone rubber. This was to show the influence of the connector.

The onset voltage test results are shown in Fig. 20-8. The curves, drawn from the test data, show that the onset voltage of the connector was obtained in the third test. The curves of the first and second tests are similar to the spaced- and twisted-wire tests shown in Fig. 20-6. Results of the fourth test were the same as for conductors spaced 2 in. apart - the minimum spacing measured between conductors inside the altitude chamber. If insulation voids had existed between adjacent connector pins, the onset voltage would have been that of bare pins in the encapsulated gas.

## Circuit Breakers

The circuit breaker onset voltage curves of Fig. 20-9 illustrate three items: (1) when bare terminals exist, the onset voltage is the same as for bare electrodes; (2) if these terminals are potted or coated with an insulating material the onset voltage is the same as the insulated spaced wires; and (3) when the internal contacts are unpressurized, the onset voltage between contacts is the same as for bare electrodes. Thus, there are certain altitudes when circuit breakers should not be energized with voltages greater than 245 v (rms). Circuit breakers should not be installed adjacent to other circuit breakers in the spacecraft if the voltage applied to the potted terminals is greater than 245 v (rms).

## Altitude Chamber Heat Lamps

Quartz heat lamps designed for 440 v (rms) are commonly used to test samples in the laboratory. Thus, it is natural to attempt to install the heat lamps in altitude chambers when the chambers are redesigned to simulate entry environments.

Comparing 440 v (rms) with the onset voltage of bare electrodes, it is apparent that electrical discharges will occur unless special insulating techniques are used which consist of placing the electrical wiring as close to electrical ground as possible and placing neutral wires between the phase wires; thus the voltage gradient is not between phases, but between phase and neutral.

## CONCLUSIONS

Corona studies and test results recently completed at Boeing have shown that the minimum onset voltage can be raised to exceed the electric system voltage when one or more of the following design actions are taken:

1. Limit the voltage applied to the components;
2. Control the type and thickness of insulating materials;
3. Install electrical grounds when practicable;
4. Pressurize equipment when necessary;
5. Turn off electric power to equipment in the altitude range where equipment onset voltage would be exceeded.

It is also apparent that the power-system electric interference for a spaceship or altitude chamber will be within acceptable limits only after the onset voltage of each electrical component has been determined over the critical altitude range of 70,000 to 250,000 ft. In this critical altitude range, the onset voltage of spaced insulated conductors will approach that of noninsulated conductors when the ratio of insulation thickness to spacing becomes very small.

REFERENCES

1. Meek and Craggs, Electrical Breakdown of Gases, Oxford University Press, London, England, 1952.
2. T. W. Dakin and J. Lim, "Corona Measurement and Interpretation," AIEE Transactions, Vol. 76, Part 3, pp. 1059-1065, 1957.
3. C. W. Ross and E. B. Curdts, "Considerations in Specifying Corona Tests," AIEE Transactions, Vol. 75, Part 3, pp. 63-67, 1956.
4. T. W. Dakin, H. M. Philofsky, and W. C. Divens, "Effect of Electrical Discharges on Breakdown of Solid Insulations," AIEE Transactions, Vol. 73, Part 1, pp. 155-161, 1954.
5. A. L. Coats, "Performance of Electrical Connectors at High Altitude," AIEE Transactions, Vol. 79, Part 2, pp. 337-339, 1960.

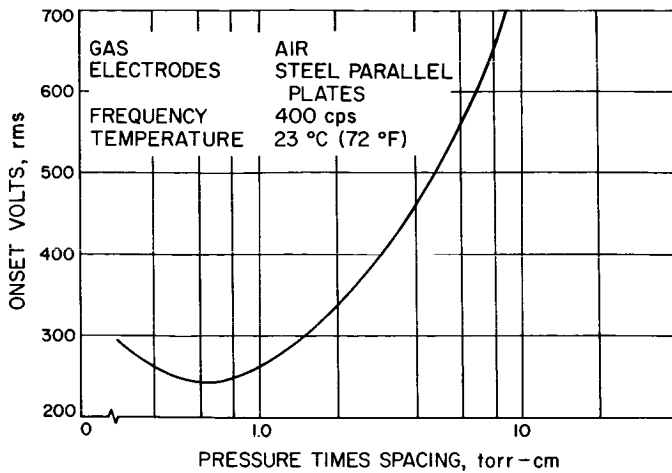


Fig. 20-1. Onset voltage vs gas density and spacing

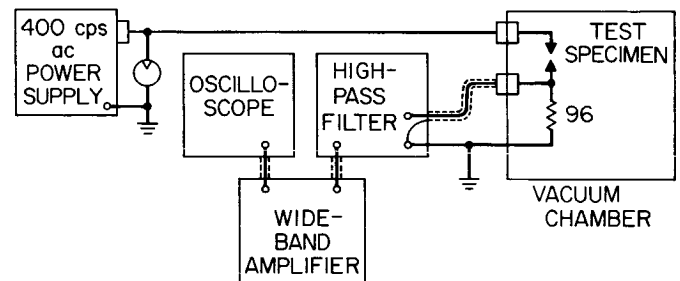


Fig. 20-2. Schematic of detection system

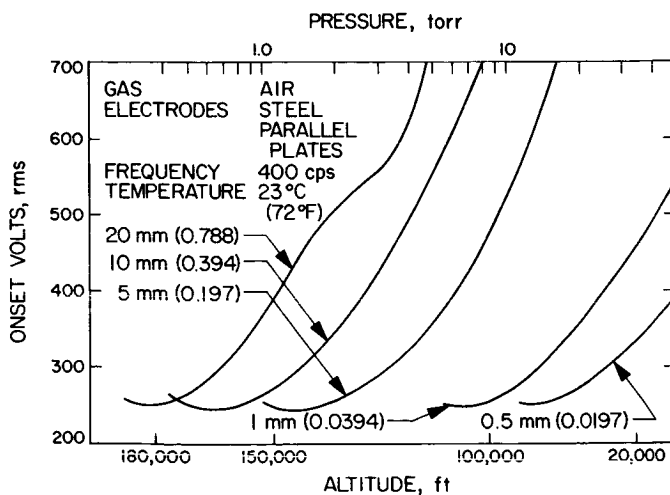


Fig. 20-3. Onset voltage vs attitude and pressure for various configurations

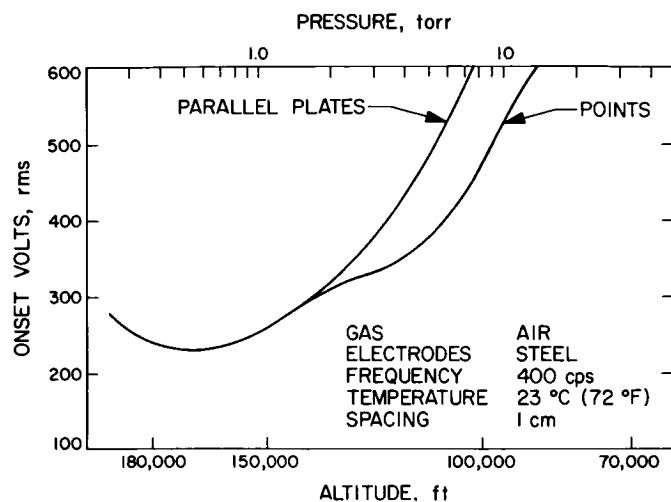


Fig. 20-4. Onset voltage vs attitude and pressure for various configurations

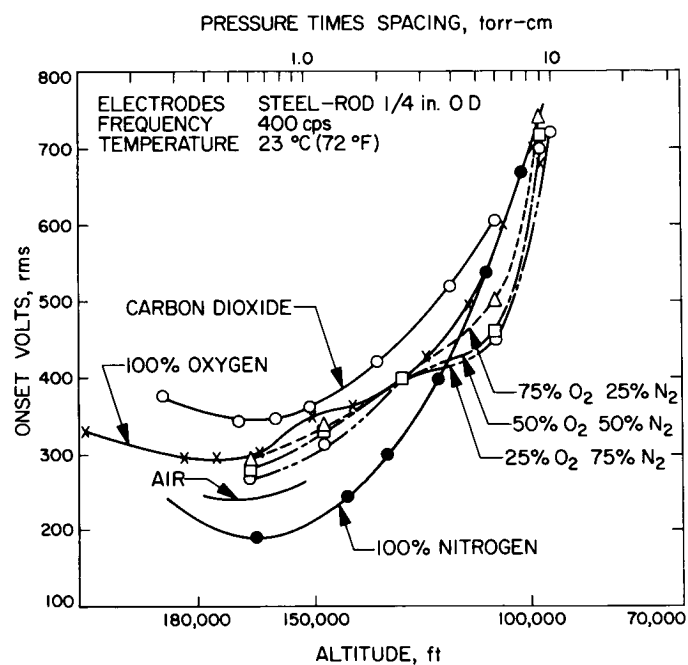


Fig. 20-5. Onset voltage vs attitude and pressure for various configurations

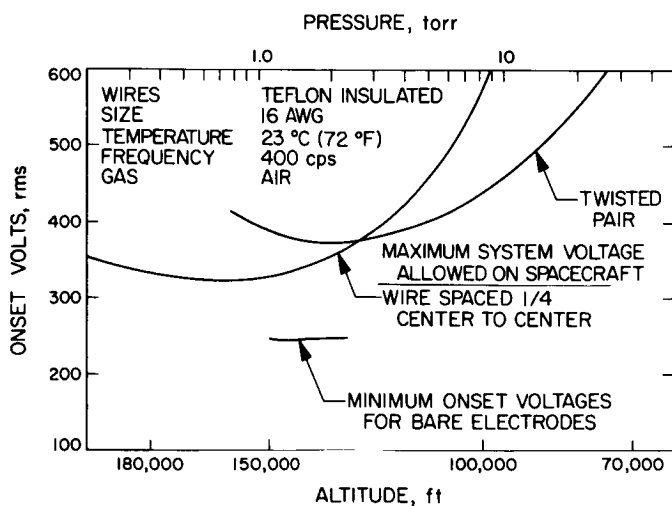


Fig. 20-6. Onset voltage vs attitude and pressure for various configurations

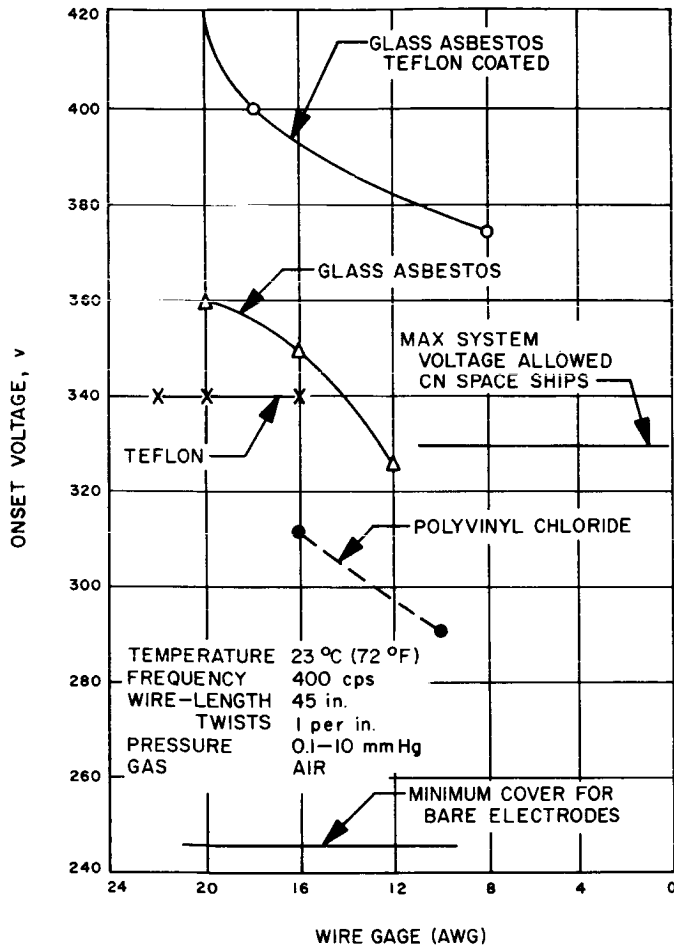


Fig. 20-7. Onset voltage vs wire gage for various electrodes

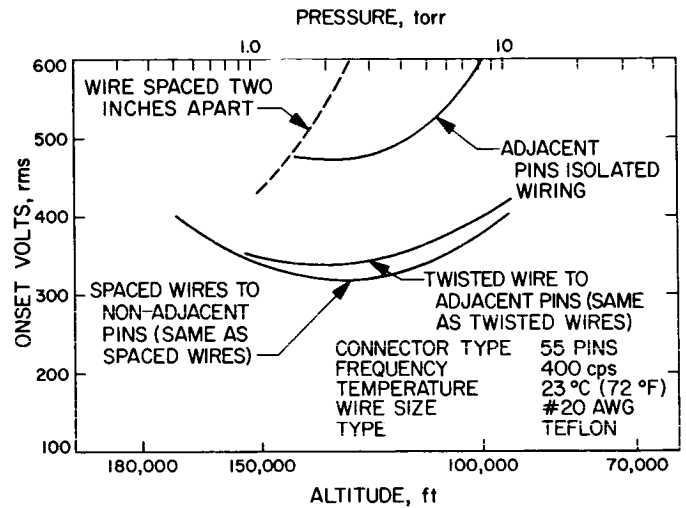


Fig. 20-8. Onset voltage vs attitude and pressure for various configurations

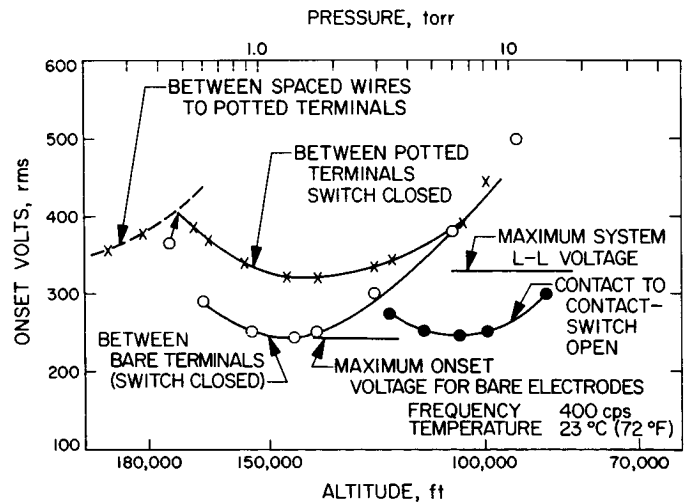


Fig. 20-9. Onset voltage vs attitude and pressure for various terminals



## 21. CRITICAL ALTITUDES FOR RADIO FREQUENCY BREAKDOWN

W. J. Linder  
Aerospace Group  
The Boeing Company  
Seattle, Washington

I have a collection of experimental data on rf breakdown which I've been comparing from the viewpoint mainly of an antenna designer. By this point in the program it may seem pretty elementary, but I think this comparison does show the variation of the critical altitude with frequency and defines this critical altitude. It covers most of the 65,000-to-310,000-ft interval of interest at frequencies between VHF and X-band.

Figure 21-1 can be described as a good argument for avoiding breakdown in antennas; one of the better arguments, I think. Glow discharges in the critical region don't appear to be very destructive of materials with the possible exception of thin films and of Teflon, but this figure shows the reflected power from a wave guide antenna vs the incident power up to and following breakdown. Since this is a pulse signal, it is accompanied by the pulse distortion and attenuation of the pulse, which has been mentioned earlier.

Figure 21-2 shows a measurement of breakdown voltage levels between copper plates. The reason I specified copper was, that at the time this was done, I was more interested in what was going on at very low pressures than in the minimum critical pressure region. This figure shows the diffusion minimum at about 200,000 ft and 0.2 mm Hg; the attachment controlled region I will show later. I think it is a fairly typical breakdown curve. The vertical line marks the approximate location of the mean-free-path limit where the mean free path and the diffusion length are equal.

The point is better shown in Fig. 21-3 in which there is a scheme for assembling a whole series of breakdown voltage measurements for each of several gaps, with pressure increasing from left to right through a minimum. These measurements are arranged according to normalized parameters, pressure times wavelength, and pressure times gap width. I think this scheme will show up much better in Fig. 21.4.

This figure is a topographical map of the surface, showing contours of constant breakdown voltage in a parallel plate gap. These are data from various sources in the literature, using various techniques. The point is that they form a consistent picture.

This scheme, by the way, is based on a presentation by S. C. Brown, who used the same picture to illustrate breakdown in hydrogen. It is based on a principle similar to Paschen's law which says that the dc breakdown voltage is a function of  $pd$ . Here the breakdown voltage is a function of  $pd$  and  $P\lambda$ . I don't mean to imply that the mechanism is the same.

We notice that the minimum which defines the minimum breakdown and critical pressure region appears at values of  $P\lambda$  between about 10 and 40 for a wide range of gap widths from less than a  $1/100$  wavelength to  $1/2$  wavelength. By the use of a standard atmosphere (the ARDC atmosphere), we show a variation of altitudes at the minimum vs frequency, and this is shown in Fig. 21-5. This figure shows altitude ( $\text{ft} \times 10^3$ ) vs frequency (in Mc). The minimum for  $P\lambda$  of 10 is shown, as is  $P\lambda$  of 40. The latter value applies to electrically very small antennas and is more useful at low frequencies; the former value is for larger antennas at higher frequencies. Up to now this calculation is based solely on parallel plane experiments from the literature. It remains to be shown if it is applicable to actual antennas. In fact, my experience has been that the limits perhaps are more often between 20 and 30 than as wide as shown here.

Figure 21-6 shows a comparison of some linear slot breakdown data taken by Worth at Lockheed some time ago. I believe one is a 1-in. slot at 227 Mc and the other, a  $1/4$ -in. slot. These slots are compared to uniform field values off the contour map. From the point of view of locating the minima and hence the critical altitude, the minima are fairly close, particularly for the larger slot. It is interesting that even the actual voltage values are rather close.

Figure 21-7 is an experiment we did some time ago with an X-band wave guide slot with a pulse signal. (The previous figure was for CW.) Our measurements in terms of power are shown. We've based some calculations on Gould and Roberts paper for the CW breakdown power and for single-pulse breakdown power. I don't believe the difference between the measured and calculated curves is significant. Aside from the difference between pulse and CW signals, there is the conductance of the slot involved, and this conductance may well be slightly in error. But, at any rate, the location of the minimum here is at 30, right in our range. For Worth's two curves, it was at 30 and 40.

Figure 21-8 presents an annular slot, electrically rather small, with a mean diameter of less than  $1/5$  wavelength. These curves show breakdown voltages rather than

power. This curve is compared to the uniform field data; the difference here, I believe, is significant. The slot was filled with a flush dielectric ring. Here the minimum appears at  $P\lambda$  between 20 and 30 in accordance with the curve for parallel plate data. The reason for building this slot was really to check out the idea of dc bias, and it certainly turned out to be successful. I remember that a rather moderate voltage of either polarity would just about flatten the curve. But, it turns out that this technique is limited to a rather small range of environments, and it doesn't appear to have been very attractive to systems designers.

A comparison of pulsed-signal breakdown in an open-ended wave guide and the same wave guide filled with a flush dielectric slug is presented in Fig. 21-9. Both are in a 4-ft ground plane underneath a 4-ft hemisphere. I attempted to fit some parallel plate data to these experimental points. This lower curve is uniform field data for the actual width of the X-band wave guide. The upper curve is a best fit to some parallel plate data for a rather smaller gap width. The adjustment indicates that the electron loss rate has been increased by the dielectric slug.

Figure 21-10 shows this same antenna in un-ionized air (curves 1, 2, 10) and breakdown levels observed in a VHF discharge at low pressure (curve 14) and a HF discharge at high pressure (3, 4, 5, 6). The decrease in breakdown threshold covers quite a range here. I think the electron densities were  $10^{11}$  or less; that is, of the order of 1/10 or less the plasma resonance density at X-band, very near  $10^{12}/\text{cm}^3$ . This observed reduction in breakdown level is consistent with the substitution of ambipolar diffusion for free diffusion.

Again, the  $P\lambda$  value at breakdown is of the order of 20 to 25. I think that verifies to some extent the location of the minimum breakdown pressure and, hence, altitude.

I might go on just to mention an experiment which we referred to earlier. Figure 21-11 shows an experimental setup of a half-wave parallel-plate resonator at 205 Mc. A half-inch plate spacing was used to conduct some breakdown experiments over a rather wide pressure range. Figure 21-12 shows the actual observed data in terms of breakdown power (I showed the breakdown voltage in an earlier figure). Shown in the figure are the attachment controlled region, the diffusion minimum at about 60 v, and the mean-free-path limit. The figure shows that we are apparently proceeding up to a vacuum asymptote; this was deliberately taken without using external ionization. I also used polonium and -- when I could not avoid it -- a colbalt 60

source in the previous measurements, but in this case we knew that when using CW in this region (0.1 mm Hg) there was very little difference with or without a source of ionization if the measurements were done slowly. And the rather wide variation observed below  $10^{-2}$  mm Hg appears to have been a real effect, perhaps connected with the transition between two types of breakdown mechanisms. As I said, our main reason for this experiment was to investigate the lower-pressure region (which is a little outside the scope of this meeting). The 310,000-ft altitude can be located on the curve, at about  $10^{-3}$  mm Hg.

I think we might close by just showing a comparison in this region as shown in Fig. 21-13. These voltages are for multipacting breakdown at a little less than  $10^{-4}$  mm Hg, which resulted in a completely dark discharge. The lines labeled "H W" represent data taken at HF by Hatch and Williams for copper and aluminum plates, for  $fd = 286$  mc-cm as in the VHF experiment. I think the comparison between VHF and HF data shows that there is a scaling rule, which can be used in calculations for similar materials. The width of the blocks in the histograms indicates our uncertainty in the calibration of the resonator. The distribution shows a real effect; it's indicative, I think, of the variation of surface conditions with outgassing. I was rather surprised to notice how much outgassing can be accomplished on solid metal plates. You can turn on a discharge and observe the vacuum gage go up, and it happens time and time again.

I could find no comparative data for brass plates. There's some anomaly here which I'm not sure I understand. The major part of these breakdown observations are grouped at comparable levels, but there is a definite second group at a rather lower level than one would expect for the initiation of the first mode breakdown. (This first-mode breakdown is denoted by the "1/2" contour of Fig. 21-14.) This lower-voltage breakdown generally occurred after several discharges initiated at a higher level.

I think I will close by saying that we appear to have for antenna breakdown in the un-ionized atmosphere, at any rate, a critical pressure region (at least a region for minimum breakdown) that extends at least from 100,000 ft for the neighborhood of X-band up to the order of 200,000 ft for VHF.

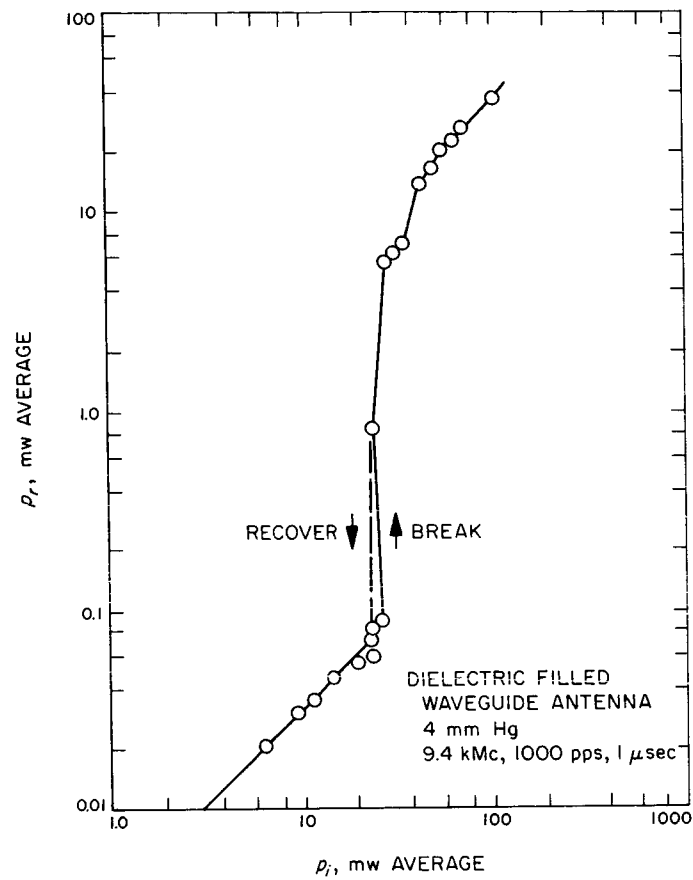


Fig. 21-1. Reflected power level before and after breakdown

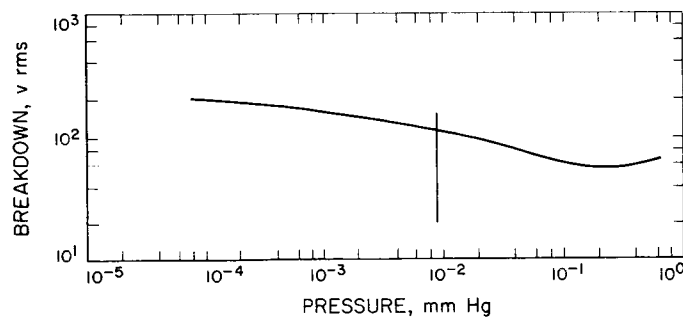


Fig. 21-2. Breakdown voltage levels between copper plates (1/2-in. spacing)

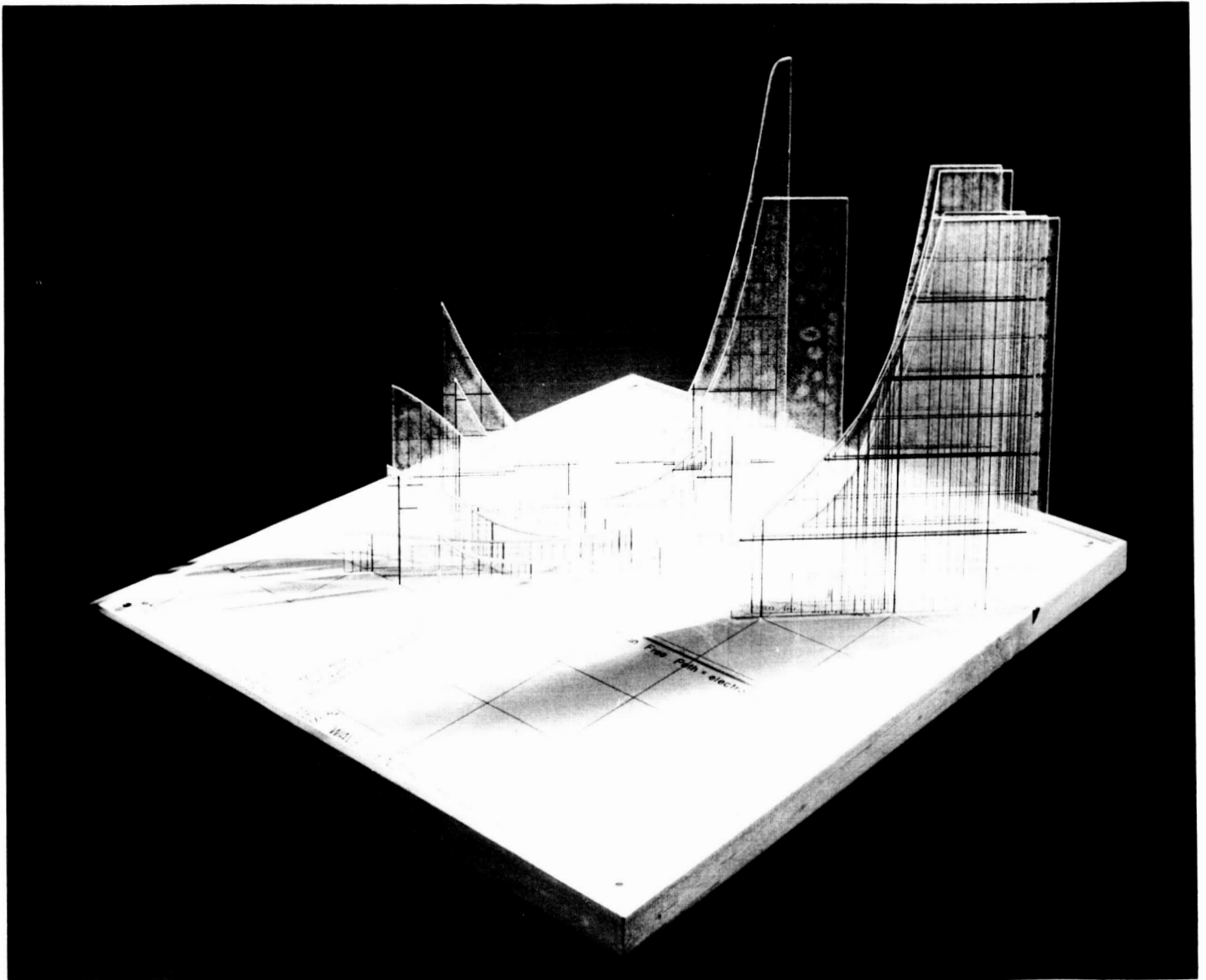


Fig. 21-3. Parallel-plane breakdown voltages

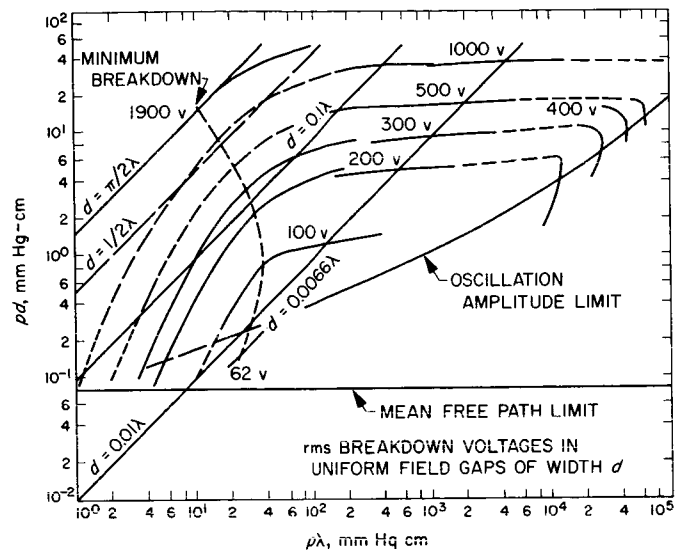


Fig. 21-4. Parallel-plane breakdown voltages

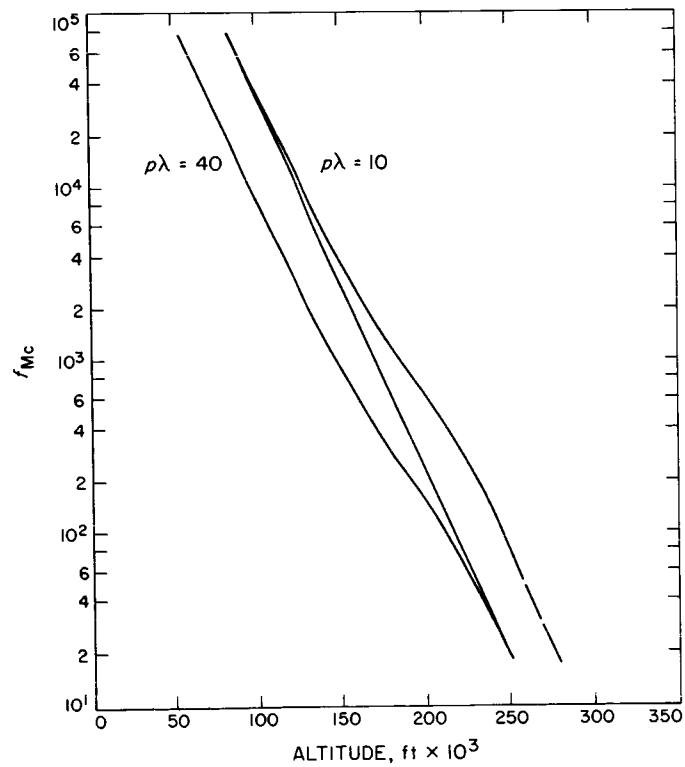


Fig. 21-5. Minimum breakdown altitude vs radio frequency

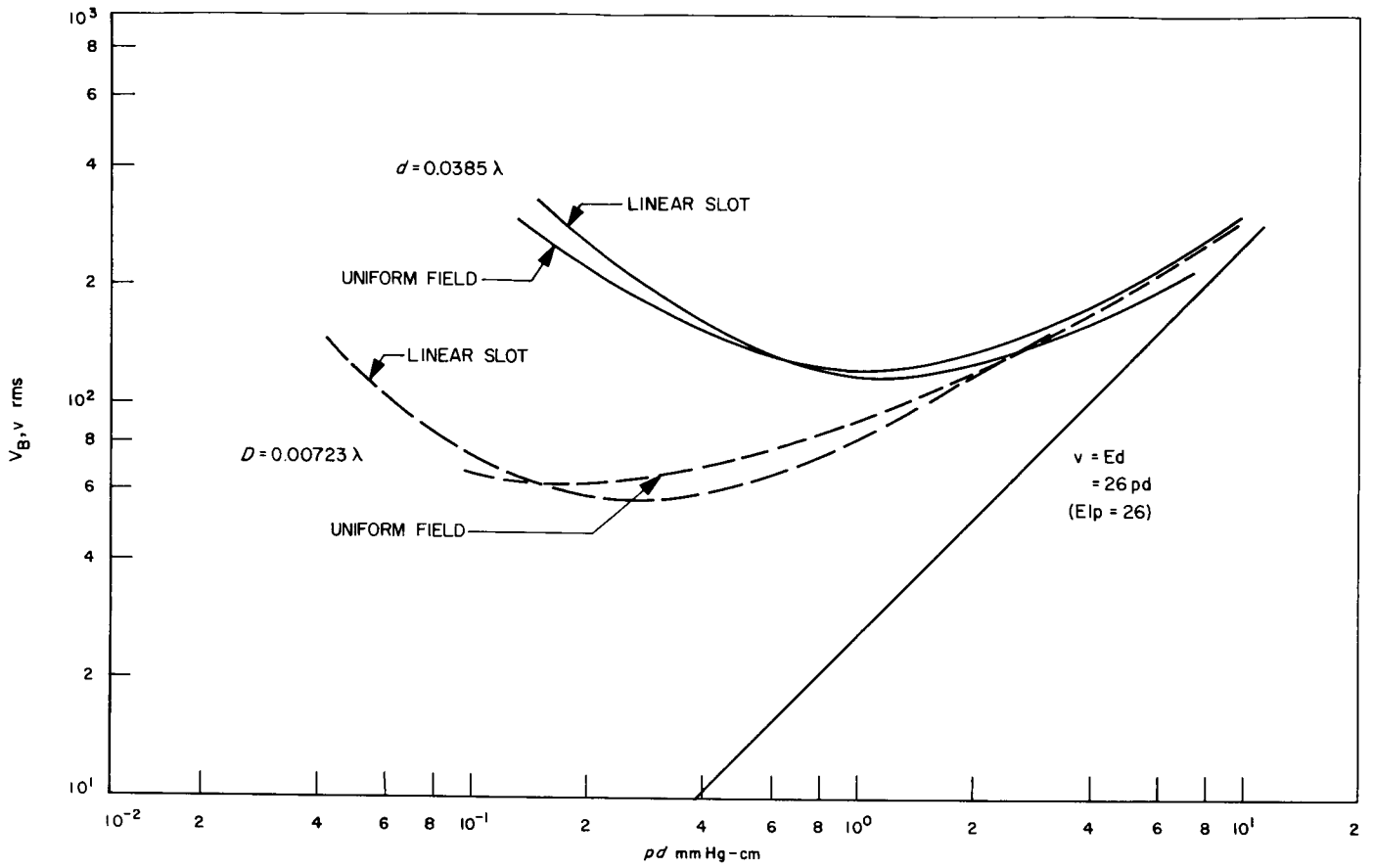


Fig. 21-6. Comparison of breakdown voltages in uniform fields and in linear slots

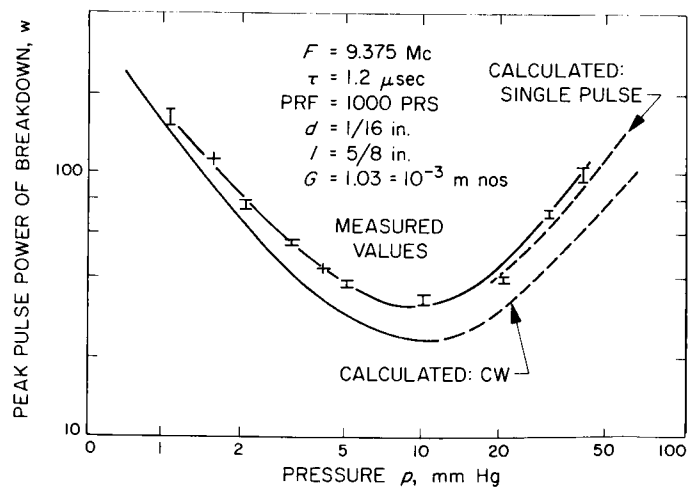


Fig. 21-7. Pulsed breakdown in X-band linear slot



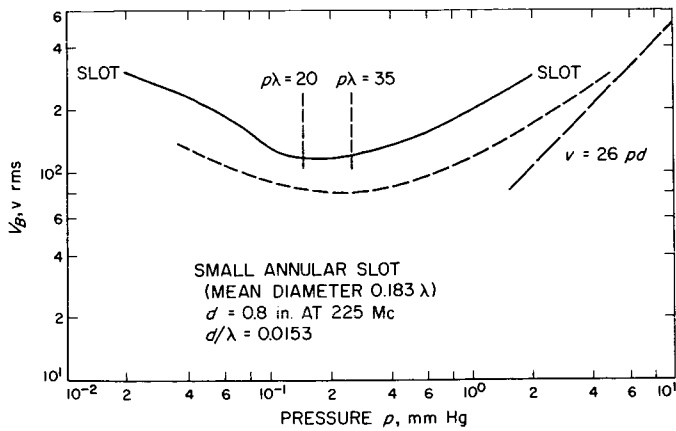


Fig. 21-8. Breakdown voltage in small annular slot

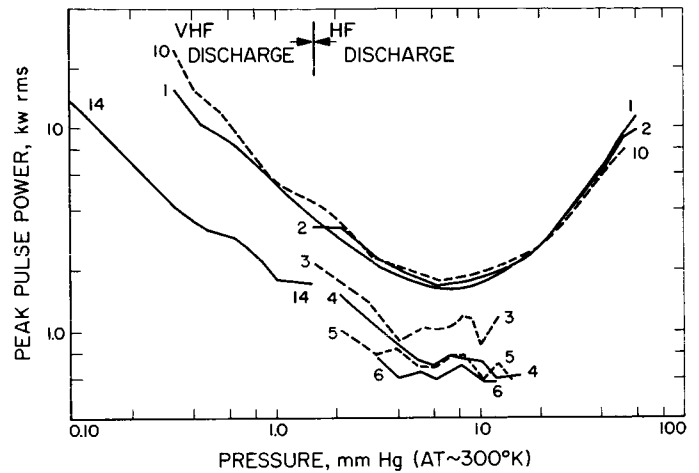


Fig. 21-10. Plasma enhanced breakdown in dielectric filled waveguide antenna

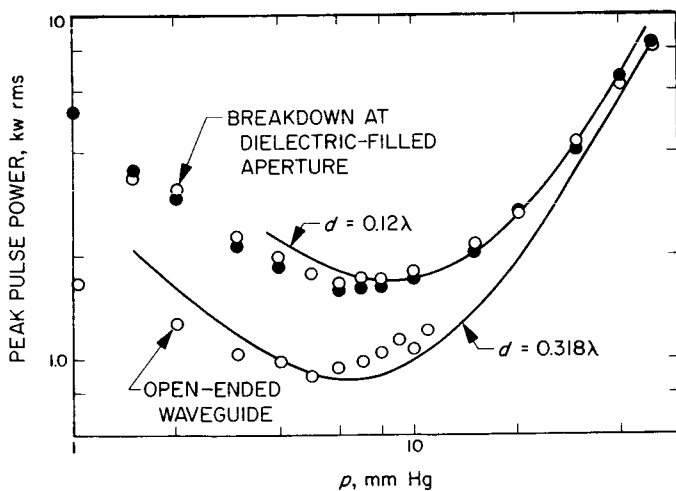


Fig. 21-9. Air breakdown in open-ended waveguide antenna

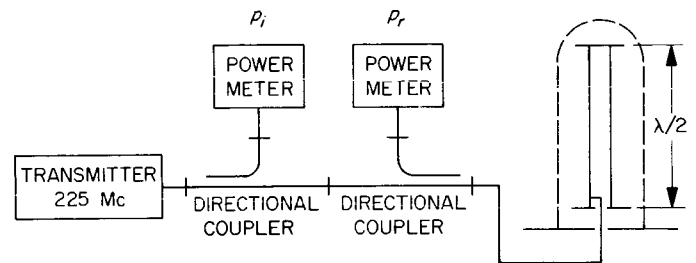


Fig. 21-11. Half-wave resonator for multipactor measurements

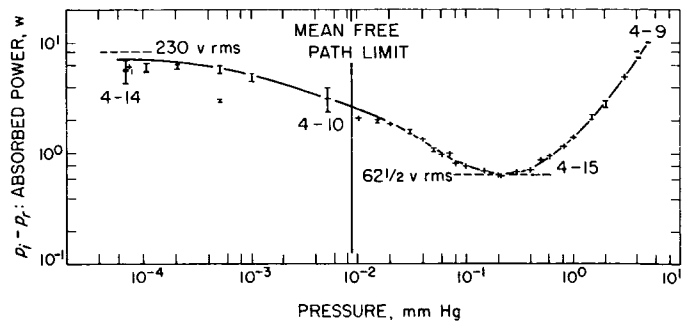
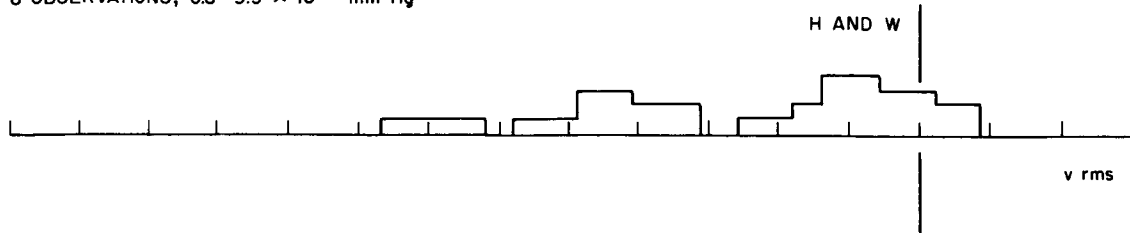
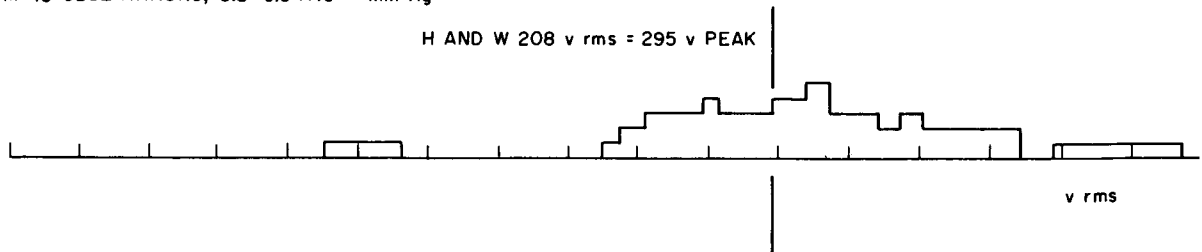


Fig. 21-12. Breakdown power levels for copper plates

COPPER: 8 OBSERVATIONS,  $6.8-9.5 \times 10^{-5}$  mm Hg



ALUMINUM: 13 OBSERVATIONS,  $6.8-9.0 \times 10^{-5}$  mm Hg



BRASS: 51 OBSERVATIONS,  $6.2-8.2 \times 10^{-5}$  mm Hg

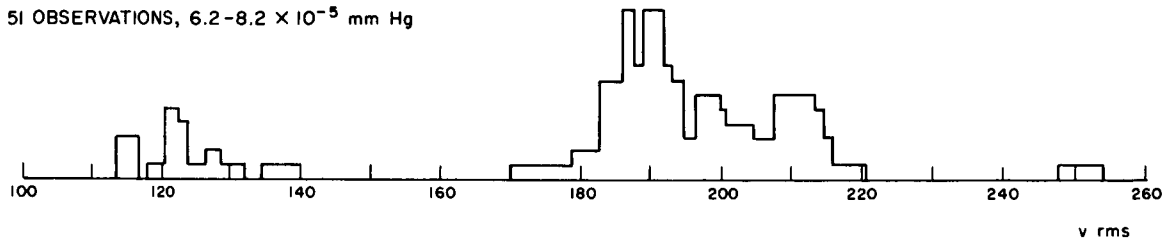


Fig. 21-13. Multipactor breakdown voltages for copper, aluminum, and brass plates

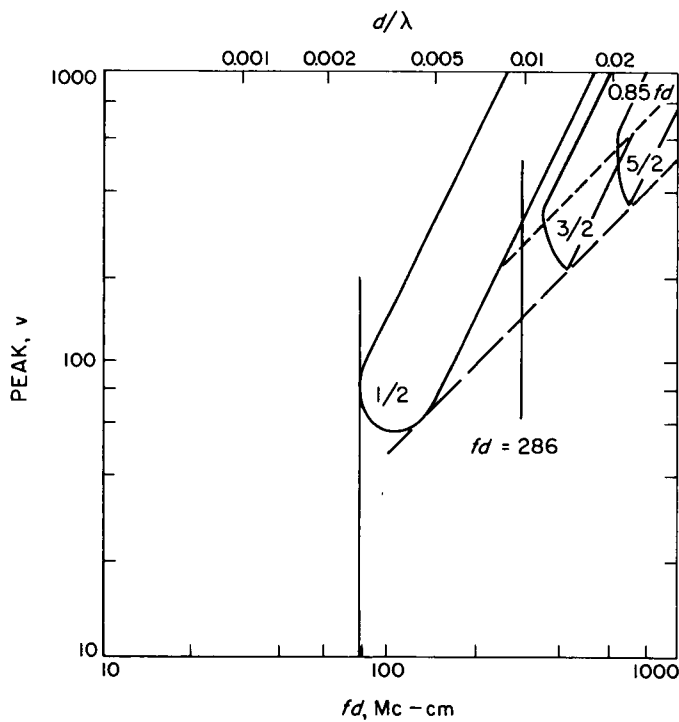


Fig. 21-14. Multipacting modes (after Hatch and Williams for aluminum electrodes)

22. MICROWAVE VOLTAGE BREAKDOWN  
AT CRITICAL PRESSURES

T. Breeden\*  
Astro-Electronics Division  
Radio Corporation of America  
Princeton, N. J.

The material I'm presenting here today comes mainly from two programs which RCA has recently experienced.

The first of these is the Ranger program and the second, the company-sponsored R&D program. Before I talk about these programs, I would like to re-emphasize some of the factors affecting the breakdowns with which we are concerned.

Table 22-1 lists phenomena known to contribute electrons to a prospective breakdown gap. At the risk of being slightly redundant, these are ionization, secondary emission, thermionic emission, photoelectric emission, and high field emission.

Table 22-1. Electron processes

Electron contributory processes

1. Ionization of free gas molecules.
2. Secondary emission through particle bombardments.
3. Thermionic emission from thermally active materials.
4. Photoelectric emission through incident radiations.
5. Highfield emission in the presence of high electric fields.

Electron removal processes

1. Attachment to neutral gas molecules.
2. Recombination with positive ions.
3. Diffusion from regions of high field strengths or breakdown areas.

On Ranger, as a result of a literature search, we narrowed down our concern to the first two, ionization and the multipacting phenomenon of secondary emission. Removal processes include attachment, recombination, and diffusion. Our in-house R&D program sought to actively enhance the diffusion-loss mechanism as a means of increasing the power-handling capabilities of microwave components. In this context, I'm using the term breakdown to denote any measurable RF power or dc voltage

---

\*Presently with the Electronics and Information Systems Division of the Fairchild-Hiller Corp.

anomaly. This definition gets us out of the question of whether or not these are bonafide arcs or corona phenomena.

That was really not our concern. Our concern was the cause for arc power and dc voltage anomalies that were experienced with the Ranger spacecraft.

Several voltage breakdowns of both types occurred in the Ranger TV and communication subsystem when it was subjected to thermal vacuum tests, and as the saying goes, we had ourselves another Christmas tree.

The dc breakdowns were taken care of by methods already outlined here in the last few days, that is, by judiciously selecting and applying encapsulating materials or rerouting high-voltage leads within the power supplies. However, the RF voltage breakdowns persisted even when there appeared to be no doubt of the good vacuum levels established in these 66-hr simulated missions.

At this point it may be well to explain just how this mission went. In the assembled TV and communication subsystem simulated missions, the subsystem was placed in an 8- or 10-ft bell jar and was allowed to soak in an established vacuum environment for 66 hr, during which time the various midcourse or cruise modes of operation were performed; these were usually all low power level operations not involving any of the TV or communications work.

At the end of the 66-hr mission, we would go into a full-power mode (the terminal maneuver in the vicinity of the Moon), which provided the RF communications link for transmitting the TV pictures back. It also may be advantageous to mention here that the frequency of the two Ranger transmitters was 960 Mc, nominally. Actually, there was 1-Mc spacing between the two transmitters, and they operated at power levels of 60-w output of the power amplifiers.

Because the two transmitters conveyed different but supplementary information, it can be said they were partially redundant. The two transmitters were attached to the single high-gain antenna through RF cabling and the coaxial hybrid ring.

At this point in the testing we apparently had voltage breakdowns existing in a very well-established vacuum environment, so we undertook a literature search to make sure we didn't reinvent the wheel, and to hopefully narrow down our concern and to yield a test program.

As indicated before, with this well-established vacuum level, we felt upon review of our symptoms that we were suffering from multipactor discharges. A

testing program utilizing the Co<sup>60</sup> isotope to create a worst-case free-electron environment was begun.

Figure 22-1 illustrates some of the hardware involved in the testing program. On the left are shown two racks containing magnetrons capable of providing continuous RF power levels from zero to approximately 190 w in the bell jar. The outputs of these two magnetrons came through two circulators in each output line to isolate potential breakdowns from the temperamental magnetrons.

We had in-line power meters for monitoring and setting up power levels through a calibrated cable system to the bell jars. We also had the HP 430's driving recorders.

We monitored both the input and output power levels of the test specimen that was being subjected to these tests. The recorder had a minimum time resolution of something of the order of several hundred msec, so to make sure that we were not experiencing breakdowns of a time duration less than this we used a crystal detector and one directional coupler together with an oscilloscope which, of course, increased the time resolution several orders of magnitude. We used Co<sup>60</sup> isotope and lead shielding with the specimen in the bell jar.

Each piece of RF equipment was taken from the spacecraft and cycled through this test setup, starting with the RF cables. Fundamentally enough, here's where we found our first problems.

Before using the particular setup shown in Fig. 22-2, we had been using type N to-N female feedthrough connectors as standard equipment in our thermal vacuum testing facility, and we found that on the vacuum side of the test chambers, the N connectors experienced sporadic breakdowns. As a result of that discovery, we changed these connectors from N to TNC feedthroughs. As was standard procedure at RCA at the time, the flight RF cables utilized TNC connectors together with RG141 cable. It was found that we were experiencing breakdowns within these cables principally in the areas of its mating dielectrics between the connector dielectric and the cable dielectric. We cycled through some frustrating attempts at solving this problem by using Dow Corning greases (DC4 and DC11, I believe). These greases, while they did eliminate the problem, did not really provide us with a good fix because we were always concerned with outgassing of these materials and the resultant coating of the optical system of Ranger; the optical experiment, as you know, was the main purpose of the mission.

Also, we could never really ensure that we had a clean grease because the grease had to be applied in wire braid areas during assembly. As a result of these disadvantages, we elected to design our own connectors; we did not want to go into the connector business, but there did not seem to be much of an alternative.

We were proceeding with a connector redesign when half way through we discovered a vendor that was marketing a connector with the characteristics we desired. One such characteristic, known as a wedge lock and located at the back of the connector, included a recessed dielectric area that facilitated an overlapping dielectric interface between the connector and cable dielectrics. Realizing that we could never eliminate voids in this mating area, we elected to control the dimensions of the area so that any voids would be near the outer conductor and in the region of the lower field strengths. These cable connector assemblies were tested in this facility with at most 8 millicuries of  $\text{Co}^{60}$  strapped right in the area of the suspected breakdowns. These cables were cycled through the test facility at power levels up to a 150 w with no anomalies noted.

The power amplifiers that were producing the 60 w at 960 Mc were cavity-tube-type amplifiers. There didn't seem to be much we could do with these devices, so we took the well-established and easy way out by submerging them in pressure vessels. And since we had a 66-hr mission, we did not have to establish a critical leak rate requirement on these pressure vessels even though we did try the best we could.

The dummy load, which was used in conjunction with the coaxial hybrid, had to dissipate a total of something like 60 w. This hybrid also experienced failures in the thermal vacuum test and again we took the well-established way out by submerging this component in the pressure vessel.

The pressure vessels were charged with dry nitrogen at about one atmosphere pressure. The hybrid ring was a device with which we experienced considerable difficulty. This device was of conventional coaxial design and had several holes drilled into it to allow outgassing. When the hybrid was operated in this test setup by itself, with the well-established capabilities in the interconnecting RF cables and feedthrough connectors, it experienced no breakdowns; it behaved very well in fact. But when it was placed on the spacecraft and run through the simulated 66-hr mission, it failed on almost every run. Such failure was very perplexing to us.

To find a way out of this predicament, we reviewed the test results we had compiled on the hybrid. These results are listed in Table 22-2.

I direct your attention to the third line of the last column, in which several breakdowns are listed. This testing sequence seems to have established that the breakdowns were a function of pumping time; that is, the breaking point seems to be somewhere between 2-1/2 and 4 hr of immersion within an established vacuum. Usually our guide rules (for the testing of subsystems or individual boxes) were to get below a  $10^{-4}$  torr vacuum and then proceed to operate once that vacuum level was established. However, the outgassing dependence is as the table seems to indicate.

At this point, we felt that our problems were not multipacting but ionization, and a quick-cycled pressure test on the hybrid revealed that it would fail well below 60 w in the vicinity of 1 torr.

We then initiated a two-pronged redesign effort utilizing the first of several possible fixes as outlined in Table 22-3.

Since we had used pressurization before (in the power amplifier and in the dummy load), we weren't going to overlook this as a possible fix for the hybrid, so we attempted to submerge the hybrid in the pressure vessels. At the same time, since the hybrid ring was a passive device, we thought the use of stripline techniques or solid dielectrics would also be a good fundamental approach.

The main question here was whether or not the stripline would hold up at the contemplated power levels of 60 w. We are mainly concerned with the junctions between the coaxial connectors and the stripline itself.

Table 22-4 illustrates one more fix that appeared to be open to us -- the application of an electric field. But, because this was a relatively new and untested method, we stayed with the two methods listed in Table 22-3. Vacuum venting has been included as a possible fix only because I'm sure it can still find its application somewhere in some boxes on some programs; but we definitely could not recommend this technique for the hybrid ring.

We could not depend upon the establishment of a good vacuum within the surrounds of the spacecraft, either because of the outgassing of the spacecraft itself when it went into the high-power mode of the terminal maneuver, or because of outgassing of the hybrid itself as it also went through the high-power terminal mode.

Table 22-2. Ranger hybrid ring test summary

Date (1963)	Co <sup>60</sup> , milli- curies	Vacuum level, torr	Pumping time, hr	Input power level (both inputs), w	Length of test, hr	Breakdowns
Oct 4	8	$5 \times 10^{-5}$	18	Up to 120	1 2/3	None
Oct 5	0	Room ambient		Up to 120	1	None
Oct 5	4	$< 10^{-4}$	2 1/2	110	2	Several*
Oct 7	4	$8 \times 10^{-5}$	4	100	2	None
Oct 8	0	$2 \times 10^{-5}$	4	100	2	None
Oct 9	0	$2 \times 10^{-5}$	40 1/2	72	2	None
Oct 10	4	$< 10^{-4}$	4	72	2	None
Oct 11	4	$5 \times 10^{-5}$	4	72	8	None
Oct 12	0	$2 \times 10^{-5}$	4	85	4	None
Oct 14	4	$3 \times 10^{-5}$	4	85	2	None
Oct 15	4	$3 \times 10^{-5}$	14	85	1	None
Oct 17	4	$3 \times 10^{-5}$	4	72	4	None
Oct 18	4	$3 \times 10^{-5}$	4	100	4	None
Oct 21	4	$2 \times 10^{-5}$	17	85	4	None

\* Largest output power drop was 0.8 db for 1 to 2 sec.



Table 22-3. Voltage breakdown elimination techniques used

Pressurization

1. Widely demonstrated technique from aircraft to spacecraft.
2. Affords opportunity of power enhancement through use of electro-negative gases.
3. Usually requires bulkier, heavier equipment with increased handling difficulties.

Solid dielectrics

1. Successfully used on Ranger at power levels of 60 w.
2. Limited application to primarily passive devices.
3. Usually lowers device efficiency.

Table 22-4. Additional voltage breakdown elimination techniques

Active controls (application of  $\vec{E}$  and  $\vec{H}$  fields)

1. Demonstrated to limited extent in laboratory.
2. Potential means of protecting entire RF systems with maximum subsystem efficiencies.

Vacuum venting

1. Not recommended because of possible space vehicle outgassing and ground handling difficulties.

We could not establish which was the actual cause, but the measured results were never in doubt.

Before the pressurization of the hybrid had progressed very far, we established that the stripline configuration would more than meet our requirements. This device was tested to a 100% overload at power levels up to about 120 w with no detectable breakdowns.

Figure 22-2 illustrates the cross section through the connector mating area of the stripline device. There are two interesting things here.

Potential breakdown existed in the connector dielectric to stripline dielectric mating area. To avoid the possible breakdowns similar to what we had experienced on the cable connector, we used the same technique that we used in the cable connector redesign effort, that is, a recessed interlocking dielectric interface. Whenever we went to this technique, our problems disappeared in connector mating areas for passive microwave devices.

Another problem area is slightly different, but I thought I might mention it. We were concerned about a certain joint at elevated power levels in vacuum. The usual method for making a connection between the connector center conductor and the stripline, was to use a third member (a piece of copper foil) to make a connection from the center conductor to the stripline center conductor; and by its nature, the solder bond would actually cover up the area we were trying to achieve a good bond in so we could never tell whether or not we indeed had a good bond. Realizing that we increased the input VSWR by introducing a reactance shunt to the ground plane -- or capacitors shunting down to the ground plane -- we elected to protrude the center conductor beyond the stripline center conductor and recess the opposite dielectric to receive the elongation of the connector center conductor. This method facilitated the inclusion of a nice solder fillet, which is idealized in Fig. 22-2 (you never get an actual fillet like that). We could get a nice solder bond with the high-temperature solder; we never experienced any difficulties in that area.

At the conclusion of this effort, the communications equipment of Ranger from the power amplifier to the output of the hybrid ring (our interface with the JPL bus) possessed the ability to operate from launch to hard vacuum. This point is important because successful operation of this communication subsystem in hard vacuum was not obtained until the equipment had the ability to operate through the launch environment, even though the mission profile did not dictate that it do so.

Figure 22-3 illustrates one interesting result of our company-sponsored work in which we try to enhance the diffusion-loss mechanism in the areas of critical pressure. We constructed a simple 3-in.-long coaxial, air dielectric, 50-ohm line section, with low VSWR (1.05:1 or less), and applied the negative-dc bias voltages to the center conductor; I think Fig. 22-3 is self-explanatory as to what the results were. Notice the zero-bias characteristic. The coaxial line section would break down somewhere around 70 w. I might note here that our problems on the hybrid were probably caused by high VSWRs near the junction areas and the areas of stepped impedance transformers (in which we would have discontinuities and high electric fields). The breakdown power levels for these other devices were lower than for this line section in which we tried to eliminate all influencing factors such as high VSWR and other factors in order to just see how much influence the negative-dc bias would have on the breakdown characteristics of the simple coaxial microwave geometry.

Notice the -10-v curve, and 20-, 30-, and 40-v curves, which indicate the approximate limit of our RF source; we did measure approximately a 4-db increase in power-handling capability of this simple air dielectric line section.

#### OPEN DISCUSSION

MR. KINKEAD: What configuration was the hybrid you originally had trouble with in the coaxial air dielectric problem? Quarter wave, coupled transmission lines?

MR. BREEDEN: Six quarter-wave lengths in diameter. A conventional rat race. It was not too conventional in some of its mechanical aspects in that it had a square annular ring, rat race portion with a square center conductor.

We realized, of course, we had concentrations of high field strengths around these square areas, so we did change the internal geometry of the rat race. We actually went through an extensive program trying to live with that particular hybrid.

We changed the internal geometry and adjusted the radii to get the right internal rat race impedance, and we also immersed the entire center conductor assembly within a Teflon bond, which did increase the power-handling capability somewhat in the isolated tests I mentioned before, but we would still have the characteristic power dropouts in the subsystem test of Ranger.

We eliminated continuous power dropouts, and we were in the area of short-duration self-quenching power dropouts with the hybrid ring. These dropouts characteristically were never greater than maybe 1 db in magnitude nor lasted longer than 1 or 2 sec. But, we couldn't live with that because we never knew just how close we were to the threshold of something catastrophic.

MR. KINKEAD: I think it might be informative to note that at exactly the same frequency I ran a long series of tests on type-N connectors with pulse systems and found I had to get well above 1-kw peak with a 6- $\mu$ sec pulse before I got breakdown.

MR. BREEDEN: Did you make any attempts to vacuum-vent these connectors, drill holes in them, or anything?

MR. KINKEAD: Just overnight sitting in the vacuum.

MR. BREEDEN: Well, we found that these things were very temperamental; you could never really depend on them. If we had a tandem connection of many microwave devices in the bell jar, we certainly would want to eliminate the possibility of having a breakdown in the air-dielectric connector. So our main intent was to establish a solid dielectric everywhere within the microwave system. Of course, that doesn't lend itself very well to the cavity power amplifier because we couldn't live with the losses in the cavity.

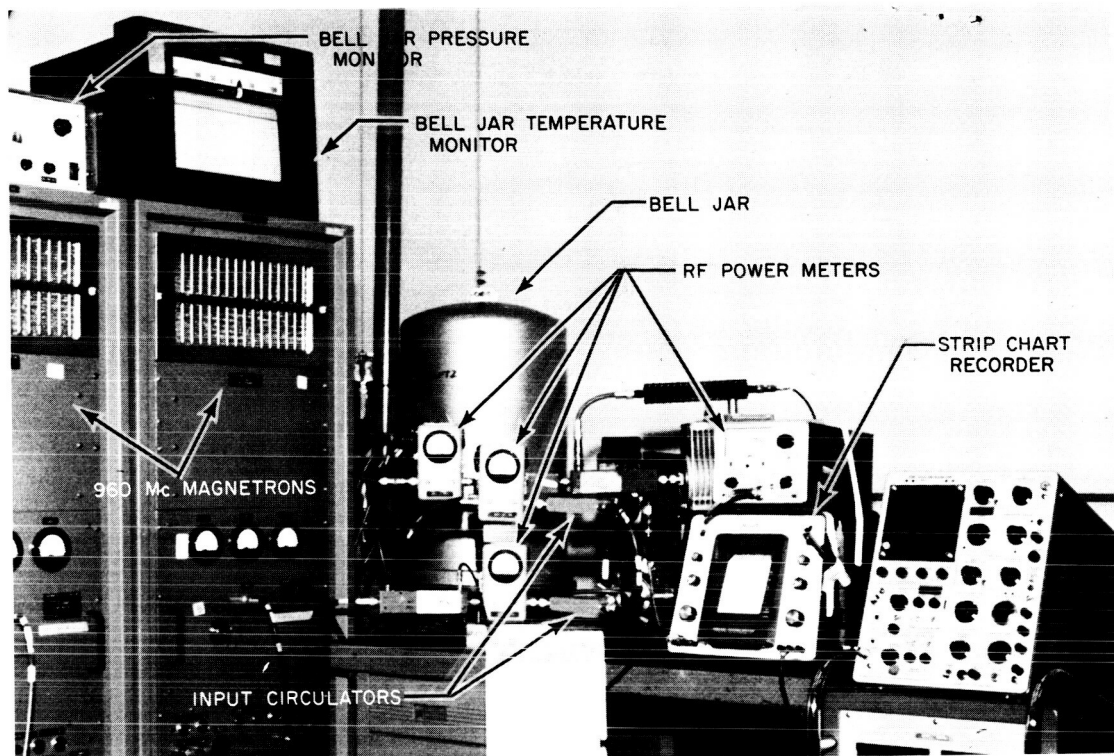


Fig. 22-1. RF voltage breakdown test facility

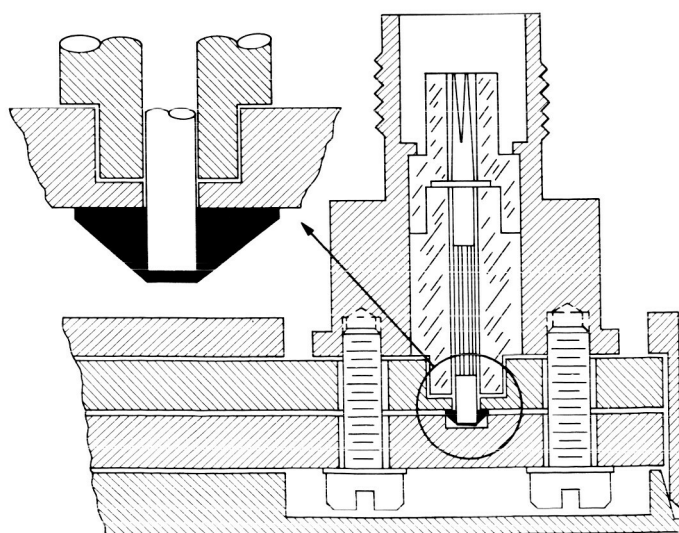


Fig. 22-2. Stripline hybrid ring cross section

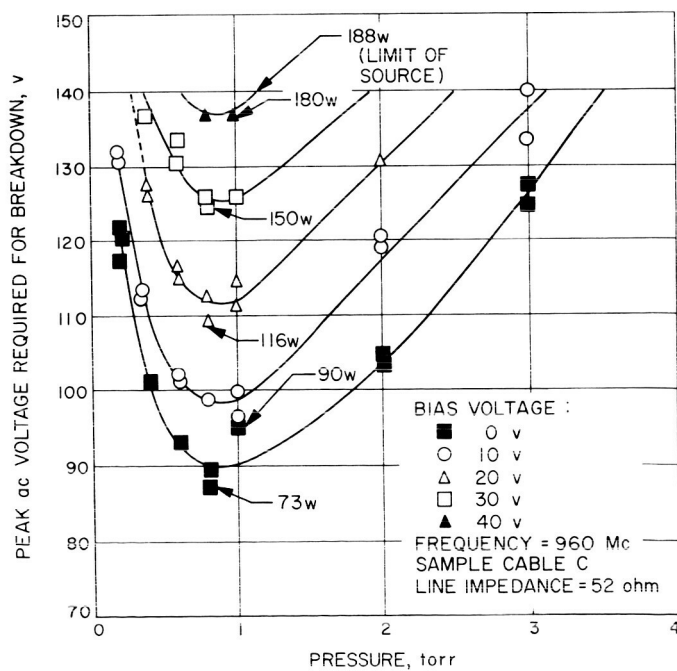


Fig. 22-3. Negative bias control of RF voltage breakdown

## 23. VOLTAGE BREAKDOWN INVESTIGATION IN THE ADVANCED PACKAGING TECHNOLOGY GROUP AT JET PROPULSION LABORATORY

Earle R. Bunker, Jr.  
Jet Propulsion Laboratory  
Pasadena, California

The high voltage work being done in Advanced Packaging Group at JPL has three objectives. The first objective was to establish parameters and techniques for high-voltage packaging through the critical pressure region and in the high-vacuum region; secondly, to improve instrumentation and established test procedures to determine if corona exists in equipment and components; thirdly, to write specifications covering design and packaging of high voltage circuitry. There was a fourth objective not included, and that was to serve on design review committees for high-voltage problems encountered in spacecraft testing in vacuum.

Since a good part of our problem is in wire, cables, and connectors, we were paying a good deal of attention to this problem. But I think we all agree that the real offender, at least for spacecraft equipment, is corona; and it just can not be tolerated. It would be nice to find a way of packaging in which we could eliminate corona, because with corona there is a gradual erosion of a dielectric and maybe an eventual arc over. The length of time it takes for corona to erode insulation to failure can not be estimated. A life test can run for a thousand hours, and maybe at a thousand and one hours it will break down, or maybe it will go for ten thousand hours.

Figure 23-1 shows an interesting curve (I think this will look familiar to Dr. Dakin), a point-to-plane distance breakdown voltage at 760 mm. Following the curve for a 3/16-in. -dia electrode at zero separation, the curve starts essentially at zero and as the separation increases we get arcing, but no corona. Apparently the corona and arcing occurs at the same time. This is reasonable, because when there is a small separation, the occurrence of a partial breakdown because of the high field generates free electrons. By the time the electrons get moving, they strike the plane (which is the ground), and therefore an arc forms. Coming up further on the curve, at about 1/2 in. at 11 kv rms, the curve divides into two, the lower is the corona onset and the upper is the arc initiation or flashover corona; in other words, the lower curve is a partial breakdown and the upper curve is a total breakdown or arcing.

You'll notice that this corona curve is relatively flat because being a partial breakdown, the position of the plane is not too critical for the voltage at which the point will break down the air dielectric. Assume a point-to-plane spacing of, say,  $3/4$  in. Increasing the applied voltage from zero will cause nothing to happen until about 11 kv, where corona will initiate. As the voltage is raised higher and higher, more and more intense corona forms until the upper curve is reached at about 20 kv where it will arcover, forming a low-impedance path.

This intersection of corona and arc curves is interesting because it tells us (at least for this geometry) that if all dimensions were kept under  $1/2$  in., corona would never occur. Then the solid dielectric between the conductors would withstand the voltage indefinitely because it would not have the insidious corona destroying the dielectric causing it to break down.

The question we were trying to answer was whether this intersection exists at low pressures. Because if it does, instead of the usual technique of routing the high-voltage lines as far away from everything as possible, the lines should be shielded or the dimensions kept under the critical distance. This possibility looked interesting, so we decided to try it.

Figure 23-2 shows the test setup inside the vacuum chamber. The high-voltage lead goes from the chamber interface to this insulating standoff mounted on a plexiglass or lucite panel. The lead terminates in an anti-corona ball with a  $3/32$ -in. - diameter stainless steel point. The plane is of highly polished stainless steel. A mechanism driven by a reversible dc motor runs the plane up and down, with a method of accurately locating the position of plane. The ultraviolet light shines down on the plane from above, which is necessary to provide the free electrons. Since the ultraviolet light is in a vacuum atmosphere in which there is no convection cooling, the UV tube is mounted on a heat exchanger with either air or water through it, from the vacuum chamber interface. We found if we ran it for no more than about 20 sec at a time, the temperature would not rise more than 10 or 15°F, so the heat exchanger was not needed. Thermocouples located on the UV tube and the motor allowed monitoring of the temperature.

Figure 23-3, just to refresh your memory, shows the difference in corona initiation with and without ultraviolet light. We found this to be true. We were

getting very erratic readings in some positions, but with the ultraviolet light, it settled right down. At very low air pressures, the ultraviolet light seemed to generate enough electrons to be read on our corona detector without the high voltage being on. This masks the corona current, if any, in that end of the pressure range.

At the same time, in conjunction with this investigation, we were developing instrumentation techniques. Essentially, there are four ways to at least measure or determine if corona is present. The first one is visual, which is all right, if it is dark enough. We had a shroud over the vacuum chamber so that dark adaptation of the eyes could be achieved. But you're never quite sure whether you're seeing things or not because if you stare in the darkness for awhile it's amazing the things you think you're seeing, so this is not too good. However, at first we were using the visual method to check the operation at our instrumentation, which was fortunate because we discovered certain conditions where dc corona would occur with no radio frequency noise being generated.

Another method detects the radio frequency noise by putting a loop in the chamber and picking up the RF noise. There always seemed to me to be a better way to do things instead of using that method. In 1929, Quinn (possibly tired of using radio frequency method) came up with a detection network for measurement of corona at power system frequencies that was rather simple, as shown in Fig. 23-4. For the purposes of tying it into an application to point-to-plane-geometry, high voltage is applied to the point; the plane is connected to the two inductances in series and then back to the ground of the power supply. The lower inductance is an iron-core type (in our case, it was a 3.3 h), and the one above was an air-core type about 2.5 mh. The capacitor to the oscilloscope was about 300  $\mu\text{mf}$  which will be of relatively high impedance to 60 cycle ac, and low impedance to corona frequencies. The trace on the oscilloscope would be a fuzz on the top or bottom peaks of the ac wave. I have designated this network for corona measurement the "series," or current, method to contrast it with another method of measuring corona using a similar network (which works entirely different) called the shunt method.

The series network is in the ground return. Low potential high voltage components are not required. The method of corona measurement called out in MIL-T 27 B, shown in Fig. 23-5, has a shunt-type corona network consisting of a high-voltage capacitor, C, which connects to the high-voltage lead. Then you have the inductor to ground with the input to the oscilloscope at the junction of C and L.



There is one serious drawback. The circuit will not distinguish between corona in the capacitor and corona in the device being tested. For moderately high voltages an oil-filled capacitor is usually used. Trying to crowd an oil-filled capacitor into some of the peanut-sized spacecraft components to keep the HV lead as short as possible to minimize corona, becomes very cumbersome if not impractical. So, for this reason I disagree with the shunt approach, preferring the series method.

An additional advantage of the series network, which was not appreciated at first, is that it enables isolation and location of corona. For example, assume that the high-voltage lead in a subsystem goes to several chassis. It would be difficult using the shunt network to determine in which chassis a corona breakdown might be taking place. On the other hand, a series network in the ground return of each chassis would indicate immediately where the corona was occurring.

This was demonstrated in my test setup at 0.1-in. spacing and  $5 \times 10^3$  mm Hg. As the voltage was raised, it was found that breakdown occurred between the point and the UV light reflector 6-in. away rather than 0.1 in. to the plane, because there just weren't enough gas molecules in the shorter gap to ionize. The corona detection network connected to the plane showed only a very slight current. I connected my corona network into the shield and reflector, and picked it up as anticipated. It gives a method of separating where the corona is occurring. This, I think, is real important in testing.

We started through to see if we could find this intersection of curves in Fig. 23-1. At about 10 mm with the point dc positive, there was no corona indication. But visually there was corona on the point. The Quinn resonance circuit method, as it is called, wasn't operating or wasn't showing any indication at those low pressures so we just stopped everything and started to make tests on the corona network and see how sensitive we could make it.

Figure 23-6 shows the modified Quinn network. The input, instead of coming directly to the junction of the inductances and coupling capacitor, goes through an NE-2 neon lamp. Neon lamp I-2 serves the same function as the film in Fig. 23-4, a gap across the inductances so in case one of these opens up, the junction point is prevented from rising to the high voltage. We found we could get, at least at the higher pressures in the critical region, a glow on I-1 which indicated corona current; when an arc occurred, I-2 would flash. These neon inductors are designated in

parentheses corona and arc, respectively. At the lower pressures this doesn't hold too well as the threshold of operation of these neon lamps is about 20  $\mu$ amp.

Using this modified Quinn network we went through these tests and some of the pictures of the point-to-plane at various pressures and polarities of dc or ac. Point-to-plane separation is 2 in. in all cases.

Figure 23-7a shows an ac arc at 10 mm. Now, some will say, "Well, you don't see a complete glow between here, so this could be corona." We found that any time there is a spot on the plane, it's an arc. This is 2-1/2 milliamp flowing, at 1,340 v. The neon lamp labeled arc was lighting up brightly. And, incidentally, there was an indication on the oscilloscope.

Figure 23-7b is corona. We ran the voltage down to 1,300 v and exposed the picture ten times as long to get this real dim glow and a very, very dim indication on I-1 neon lamp, of the order of 20  $\mu$ amp. You would have to adjust your eyes to see that. It was rather dim. But, it was a true corona.

Figure 23-7c shows a positive point arc. This has the characteristic blue cathode glow and red column. Actually this was not stable and would keep flashing. If we could get one flash, it would have a totally red glow down to the plane with a slight gap between it and the cathode glow.

Figure 23-7d shows the positive corona; a very slight glow with a very, very dim indication on the corona neon bulb, none on the scope, and none on the arc neon bulb. This was at 2.4 kv dc.

Figure 23-7e is a negative arc. The positive column up from the plane is typically red with the negative cathode glow around the point. The arc was about 2.6 kv at 7.5 milliamp to be that bright and it was fluctuating. Figure 23-7f shows again a very dim corona at 2.4 kv dc. Then we went on to one mm Hg.

Figure 23-7g shows an ac arc with red and blue layer around the point and the glow on the plane. The glow is actually about a quarter inch above the plane, with the reflection below it. It actually looks like it's floating or levitating in--I was going to say mid-air--mid-vacuum. This is 5 milliamp flowing at 680 v ac with no visible glow between.

Although appearing like corona, Fig. 23-7h is still called an arc. There is a very slight glow on the plane. With 440 v ac applied the current was approximately zero, but the corona neon lamp was lit.

Figure 23-7i shows interesting striations of a positive point arc at 600 v, 5 milliamp. The starting voltage of the arc was about 1.5 kv, and there was no corona at any time.

Figure 23-7j is a negative point, again, arcing, 5 milliamp, 520 v, and stable. It shows even a glow on the bulb around the anti-corona ball. This gives an idea of the data points and that corona does not exist at the lower pressures.

At this point we became increasingly dissatisfied with the instrumentation. We found that we could look at the point and find a glow, and yet the neon lamp wasn't lit so the corona network was modified to include a microammeter, which has a sensitivity of less than  $1/2 \mu$ amp of current. However, it can't be seen visually. We think it's there, but we can't see it, so we are in the process of rigging up a photomultiplier to see if there's corona there.

Going through the data to see if we could find our magical intersection-vs-pressure, we came up with the following curves in Fig. 23-8. Point-to-plane separates in inches, and pressure in millimeters of mercury are plotted for dc minus, dc plus and ac 60 cps. The points at the lower end are scattered because of the problem of distinguishing between corona or arcing. Although the points are somewhat scattered, I believe it shows a trend; we can say that if the dimensions are kept less than the asymptote of the particular curve then corona would never be formed. All that would be necessary would be to test the wires for breakdown voltage, and as long as it didn't arc, it would never corona, so the system should last a long while.

Another part of the high-voltage work at JPL is the method of testing components. This tentative high-voltage specification under preparation requires that components for spacecraft application be designed to operate in the critical pressure region.

I have talked to a number of you here who agree with me. I understand that in the manned spacecraft all equipment must operate in the critical region without damage. I personally feel it should be extended to nonmanned spacecraft just to protect our super-reliable equipment from super-unreliable people, if nothing else.

The next few figures show methods of testing components; the type of components determines whether ac or dc will be used for the test voltage. As you know, power people seem to have a philosophy that ac systems can be tested by applying dc to them, which is more convenient. I've never quite gone along with that because

solid dielectrics have dielectric constants, which result in a different distribution of potential under ac conditions than under dc. It is really not a valid test, at least for corona detection in high reliability equipment.

For example, Fig. 23-9 shows a generalized component to be tested by applying a voltage across the terminals. Assuming this is a capacitor, the maximum working voltage or the maximum test voltage would be applied across it. In the ground lead is a corona detection network with an oscilloscope. An auxiliary detector is a vacuum tube voltmeter, which can be used across the neon bulb and which is a little more sensitive, especially for dc. The voltage would be applied in the critical pressure region to see if corona current can be detected. This tests the corona breakdown between the two leads of the components, but sometimes there are buried studs in the potting compound, or something similar.

The unit itself may be all right, but from component to case there could be bubbles or something which could corona and cause breakdown. So, this method would give you a test in which you apply voltage to both terminals and return the case to ground if it's conducting. If it's not conducting, you merely wrap some foil around it and use a corona network, as shown, to test it. This would detect the possibility of bubbles or something that might eventually break down inside the component.

Transformers require a somewhat different technique as shown in Fig. 23-10. We've had one problem with transformers: a turn-to-turn breakdown on the same winding. To test this, voltage is applied to a winding. Let's call it the primary winding. The transformer is designed such that too much voltage at its operating frequency would damage it. We should test the turn-to-turn insulation integrity by applying a higher voltage. If at least twice operating voltage between adjacent turns is required, this could be achieved by applying twice the frequency to this winding, and doubling the voltage so that the current flowing will be essentially the same, but the induced voltage in all the windings would be twice normal. If the transformer were inside a vacuum chamber, the test in the critical region could be made.

Looking at Fig. 23-10, twice-voltage, twice-frequency is the input on the primary. A load resistor and corona detection network are in series across each secondary with a common ground. These three networks will tell in which winding, if any, there is turn-to-turn arcing or corona.

To test the insulation between windings, a test setup such as in Fig. 23-11 could be used, in which high voltage is applied to one terminal, and then the other

terminals are connected to corona detection networks. Any corona current or leakage current that flows to the other windings will show up. In addition, a connection is made to the core and also to the conducting case, if there is one, each having a corona detection network as shown. Connections to the core and case would locate a bubble between the primary and the case that normally wouldn't show in the winding-to-winding test, but it would show up on the CDN connected to the case.

We've had failures of transformers after quite a few hours of system operation. The trouble was found to be bubbles in the potting material, even though vacuum-potting procedures were used. The size of these bubbles was estimated, in some cases, to be 0.050 to 0.100 in.

With the present concept of zero defects, we have to be able to test for bubbles. We think this would work; we haven't been able to try it, but indications are that it will work. Our networks should be sensitive enough to detect voids in potting compound.

Figure 23-12 shows a possible system test using the same procedure for detection of corona during operation of a system consisting of a power supply and 3 subchassis. Corona detection networks 1 and 2 are in the ground returns of subchassis B and A, respectively. These networks will detect in which chassis corona breakdown from the high voltage lead occurs. Network 3 is in the low-voltage return of the high-voltage circuit, assuming that operation of the subsystem will not be adversely affected by the network impedance. It is assumed that operation of the subsystem under test would be adversely affected by the network impedance in the low-voltage side between subchassis B and C, consequently the shunt or high-voltage type of network is described in MIL T-27 B to measure the corona. Obviously, during system design we should allow these ground returns to be accessible to facilitate testing for corona. Also, in packaging we have to make this wire available for test, with breakout boxes, etc.

Other future work in the high-voltage project at JPL is as follows: Improvement of the corona network and design and buildup of the photomultiplier for corona detection. Other geometries such as concentric cylinders will be tested to see if the curves in Fig. 23-8 hold. We would like to set up a means of plotting out the equipotential curves for various geometries to determine where the points of maximum stress are. This can be done by using conducting paint on resistance paper.

Another area of investigation is the effects of pulses and higher frequency voltages. I have a curve in the specification which says that the breakdown voltage at 100 Mc is roughly 50% of the 60-cycle breakdown. This is a little hard to dig out of the literature, but this is what we have. We haven't had a chance to confirm it yet. We can check some points on that.

We want to be able to check out some of the proposed tests of subsystems and see if this will actually work. This is an outline of our ideas. That has been the purpose of this Workshop. All this is directed to make the spacecraft equipment designed for many months' operation with extremely high reliability; we're trying to design such equipment to be failure-proof and people-proof.

#### OPEN DISCUSSION

MR. MILLIGAN: I'm happy to see that somebody has finally decided to go ahead and test for corona with an optical detector, something like a photomultiplier. It works like a charm. You can detect tendencies for corona and things of that sort. We've been using it for 10 yr or so, and it works beautifully. You'll see corona long before you'll ever detect it electrically. And you'll detect ionization phenomena around your points and things at levels at least several orders of magnitude below the regions that you're working right now.

I'd like to say something here. It's very interesting to see people going ahead and writing out specifications for high-voltage power supplies and things of this sort. I'd say we have been flying now for about 10 yr and we have yet to have a failure. I just wonder if one is going to design himself into a real spot here by specifying something; we usually find we have to tailor the supplies. The difficulty lies in the way we hook them together with the rest of the system. If you take care of your system's problems, normally everything is all right. We just haven't had the trouble apparently other people have.

MR. BUNKER: For power supplies I think this is pretty well set. I'm thinking of some of the instrument problems in the Mariner for example, and there's been problems with Nimbus. Some of these other problems, I think, could be covered in this.

MR. FRISCO: I didn't quite follow the reasoning where you went from the configuration to a point-to-plane in a gas to a situation where you insert solid dielectric

in the gap. Point A, of course, no longer has any meaning because you don't get a breakdown of the gap. You do indeed get corona. What you're doing is designing on the basis of the dielectric strength to the solid material, and if you never knew about point A it wouldn't hurt.

MR. BUNKER: Part of this was for testing foam. If we take that region between the point and plane and completely fill it with a dielectric, whatever it is, then we essentially do not change the equipotentials or the lines of force, do we?

MR. FRISCO: No, but you won't get any corona.

MR. BUNKER: Well, that is open for discussion. As for using foams, Dr. Moacanin will cover them tomorrow. In other words, if you have a cellular structure and you have a large gap, will you get corona occurring in that foam?

MR. FRISCO: At point A, instead of getting arcing, you get corona. As soon as you insert a solid material you have an entirely different situation. Point A no longer has any meaning because you wouldn't get a breakdown of that gap. You would automatically get some corona. For instance, if you put a slab of material, a solid slab, on the point between the point and the conducting plane, point A no longer exists. You've changed the situation completely. I don't see what the data that you've obtained in the vacuum chamber at low pressure has to do with the situation in which you put a solid dielectric in there.

MR. BUNKER: The point on the plane configuration was a simple test to check out our system. Now, what I'm thinking of specifically--and I've seen it--is a high-voltage cable that has a center conductor and an outside dielectric. It's possible for that cable to glow from the corona on the outside.

MR. FRISCO: Exactly.

MR. BUNKER: Now, what I'm saying is that glow will eventually destroy that dielectric so you will get an arcover from the inside wire to the ground. Glow on the outside of that cable is undesirable and we want to get rid of it. One way we can get rid of it is by putting a ground sheath there which will eliminate ground potential at that point. Then we will not have corona.

MR. FRISCO: Right, but you can do this regardless of what the spacing is. That's what I'm getting at. What does this have to do with the spacing that's related to point A? The phenomenon you're talking about will occur at any spacing. I don't see what the relationship is between the spacing that corresponds with

point A and the spacing you're using in your example, for instance, with the cable. I think we're talking about apples and oranges. That's what I'm getting at. I don't see what we'll gain by belaboring the point.

If you were talking about high frequency or 100 Mc breakdown strength of the solid material, there's a considerable amount in the literature; for example, the work that was done at Johns Hopkins for many years.

MR. BUNKER: I have some of your reports. Essentially, the initial or main point was to test foams. We've had some problems with breakdown in foams. In fact, in the specifications I've written, I have forbidden the use of foams. This may or may not be desirable, I don't know. Based on the past experience, we thought maybe we could prove it by this system; in other words, if we could have the foam between our point and plane and run up the voltage to see if we get a corona current. We won't be able to see it visually, but if we can see it on the instrumentation, then we know it's there and eventually it will break down the foam. That may not answer the question, but that was the reason.

MR. SABAROFF: As a matter of historical interest, I used to work for a company that manufactured variable air condensers, and part of the problem was the formation of corona breakdown at high powers. By the way, I read the Johns Hopkins paper which is quite old; one of the bibles I used was a book by Peek published in 1929, and in it I finally gathered the concept of what we thought when we meant corona. That was merely the formation of an ionized layer which could be considered to be an extension of the conductor itself. Thinking in terms of the conductor itself being part of the ionized layer, you could think in terms of the radius curvature slowly changing in such a way as to finally bring the ionized layer over closer and closer to a plate or some other contact; and finally sparkover would occur.

In any event, from the point of view of the variable capacitors, I made some measurements (it's been published in Electronics, probably in 1945) in which, by making some estimates of the various plots and what-not, I arrived at the configuration which gave me minimum gradient between the two plates, and at the point of minimum gradient there was no corona - only sparkover. So the question arises now as to whether or not we can get this kind of a minimum gradient with a point and a plane. The kind of curves I finally came up with is what is called a best ratio of variable condenser thickness to spacing. I found



the best ratio to be around 2.7 or so. All the variable air condenser manufacturers in the world now use this kind of ratio based on that original article published in Electronics. The point I'm making, I suppose, is that there is a best radius of curvature for no corona and only arcover. I checked it both in ordinary air and in silicone oil.

In silicone oil you don't get corona, but you do get sparkover. At least you know that when you have this configuration, you get a minimum gradient, so that there is less heating, etc.

One interesting thing about the whole thing--and I'll conclude with this-- is that for 60 cycles, the voltage for breakdown of these two plates for minimum gradient was the same. There's no frequency effect.

VOICE: In a gas you're talking about?

MR. SABAROFF: I'm talking about a gas: thin air. There is no frequency effect, at least over the ranges I checked it to, which is about 30 Mc. And I was in the business of making hand transmitters at the time and that's where I stopped, and that's where I'll stop now.

MR. BUNKER: I have a copy of two papers which show a frequency effect on corona breakdown, and that is why we used it in the specification.

VOICE: Whether or not you get a frequency effect in a gas breakdown depends primarily on the shape of the field. If you have a highly divergent field then you're quite apt to get a frequency effect. For instance, in a coaxial configuration, you'll find Burkes, Whitehead, and Miller published data that showed you get quite a decrease in breakdown voltage from 60 cps to, say, 18 Mc.

When the frequency becomes high enough so that it's comparable to the transmitter time for ions across the gap, you have to get a frequency effect in a nonuniform situation because you build up a space charge. This depends on whether you get sparkover at the same time that you get corona at a low frequency, which indicates a uniform situation; and you would not expect to get a frequency effect in that case.

At higher frequencies the time lag between corona and complete breakdown is small because there are so many cycles involved. In a short time at least in even a highly divergent coaxial situation we were never able to see any difference between the corona start voltage and the breakdown voltage.

MR. JACKSON: I have a point to make here a little bit aside from the present discussion. This is about corona again. This corona glow occasionally is not important, as I stated before, in the sense of not utilizing much power, not wasting too much power, except perhaps for antenna work, and except for its degradation of insulation, which, of course, is a function of time. There's one other aspect that I think shouldn't be neglected. If you have a little black box and you have a corona going inside of it, you have, for intents and purposes, taken that black box and filled it with salt water. In other words, you now have a conducting media throughout the whole box. If you have a delicate network of transistor components and so forth beside the power supply that has been exhibiting corona, you will have shorted the whole system. So, I say it is like dousing the whole thing in salt water. Now arc, in that respect, is different.

An arc is a point-to-point breakdown, and will destroy the components that are arcing. But a component several inches away that's a delicate transistor network of one type or another will be totally unaffected. With corona, that delicate component would be burnt up because it would be shorted across itself.

MR. BUNKER: I agree with part of what you say. If the glow from the corona encompasses and is in contact with the parts (that is, if there is a low impedance path) it will destroy it; outside of that, it won't.

MR. JACKSON: The coronas I've seen in the region below a millimeter, that is, in the micron region, in the hundred and tens of micron region, do tend to be fairly encompassing. You'll find they fill a good volume of space.

MR. BUNKER: The question is whether it's corona or arcing. I don't know what the lower pressure limit is between corona and arcing. I always got arcing. I was tempted to take it up in the 25-ft chamber and put my rod in the middle of that thing and run up the voltage at very low pressures to see if I could get a corona out of it without it arcing.

MR. JACKSON: I've seen corona without arcing.

MR. BUNKER: Have you?

MR. JACKSON: Yes.

MR. BUNKER: I haven't been able to get it here. I'm going to have to modify this equipment.

DR. DAKIN: Since we're getting into the question of corona measurement, I should bring to your attention the fact that the IEEE has a committee that's concerned with this problem, and right now they're writing (in fact, it's in its third draft) a procedure for calibrating the circuits that are used for measuring corona. There are so many modifications of these that are in use and that are being made and sold by manufacturers. There are several in this country and one or two in Europe that I know of. There are ways of injecting standard pulse voltages to calibrate these to put them all on a common basis. A common procedure is to use a square wave or a step function pulse to calibrate the corona detection equipment. It's important to know the sensitivity of the equipment in making judgements regarding this system. I recall that in a recent paper written by a Dr. Mason of England, some potted transformers were tested and found to be corona-free. But they failed within about a month of service as a result of corona because the sensitivity of the detection was so poor that they just didn't find the corona that was causing difficulties.

The procedure whereby you use both a vacuum-tube voltmeter and an oscilloscope to measure corona is, I think, quite appropriate because the pulse-type corona can be picked up very well with an amplifier and an oscilloscope with a proper input impedance. But the glow or pulseless type of corona will not be seen by such a measuring system. Essentially a current-measuring device is needed to detect the pulseless variety of corona.

MR. BUNKER: This is right. I'm familiar with commercial equipments that show the corona pulses on top of an elliptical trace on an oscilloscope, but I don't think it would show dc, for instance. Is it possible to get the draft of that IEEE procedure that they're doing?

DR. DAKIN: Yes. I will supply it.

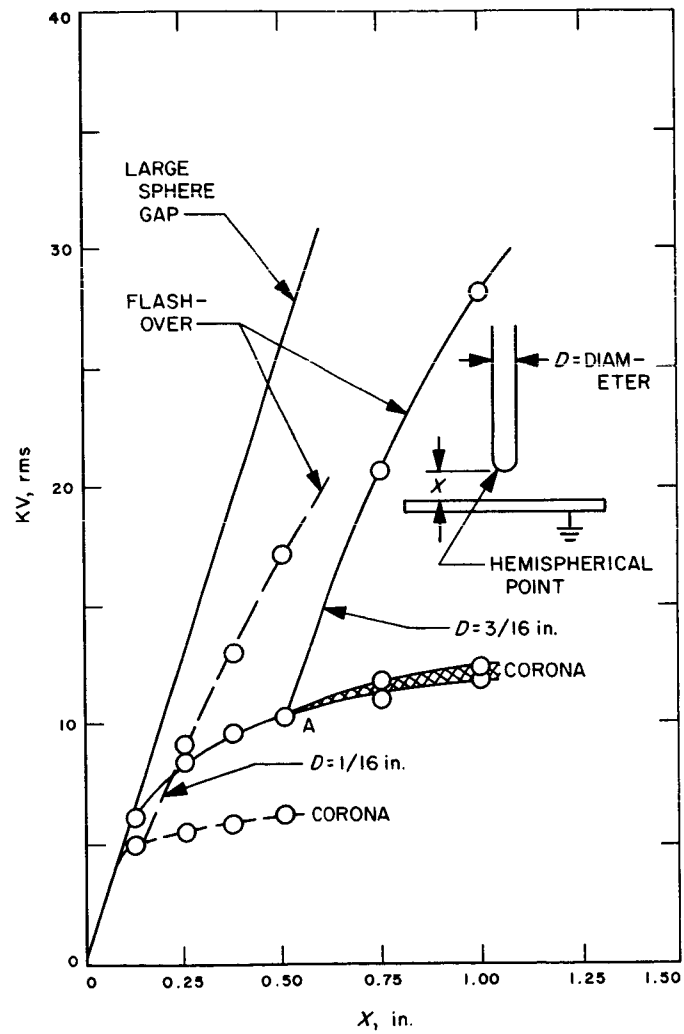


Fig. 23-1. Point-to-plane voltage breakdown characteristics

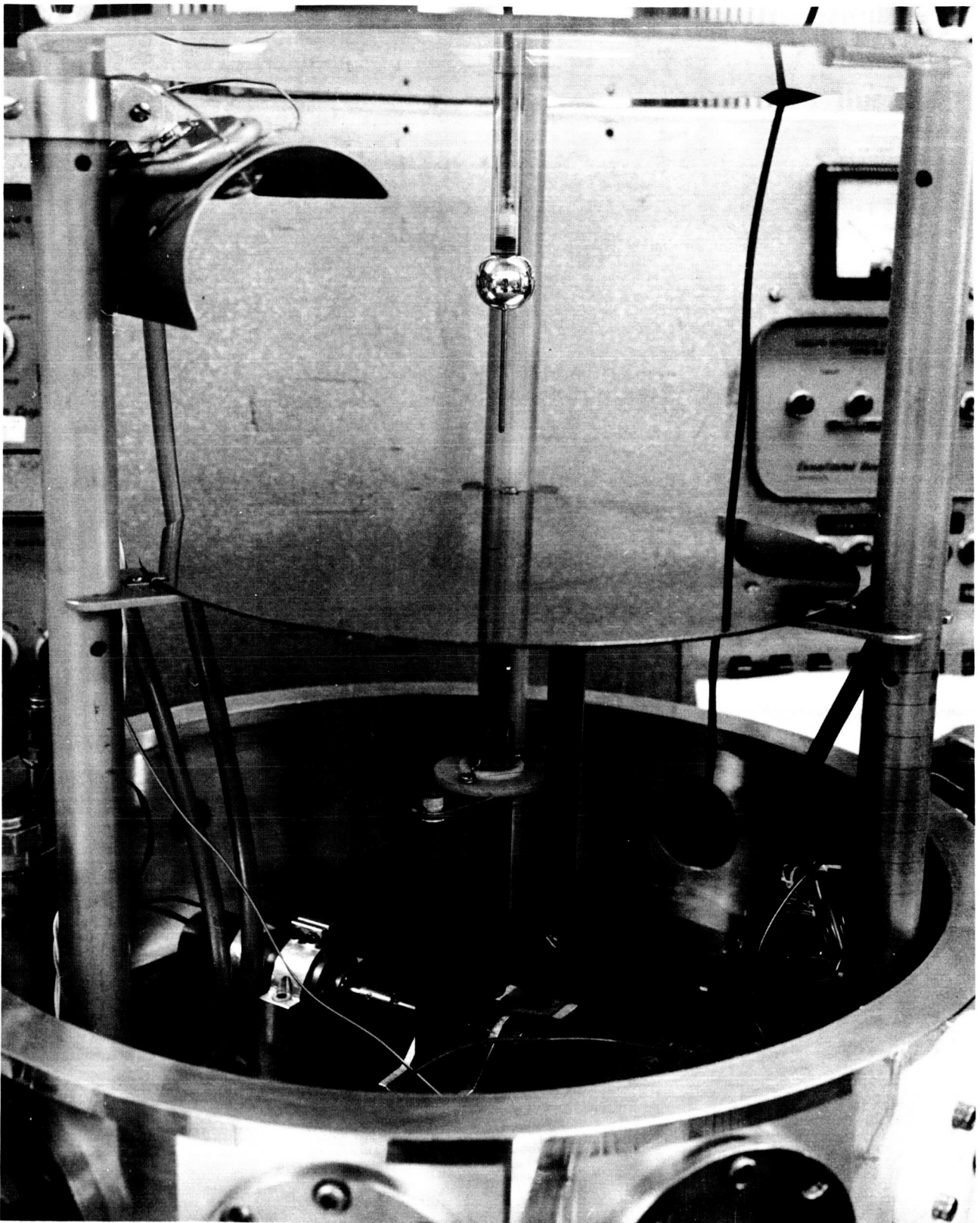


Fig. 23-2. Point-to-plane test setup in vacuum chamber

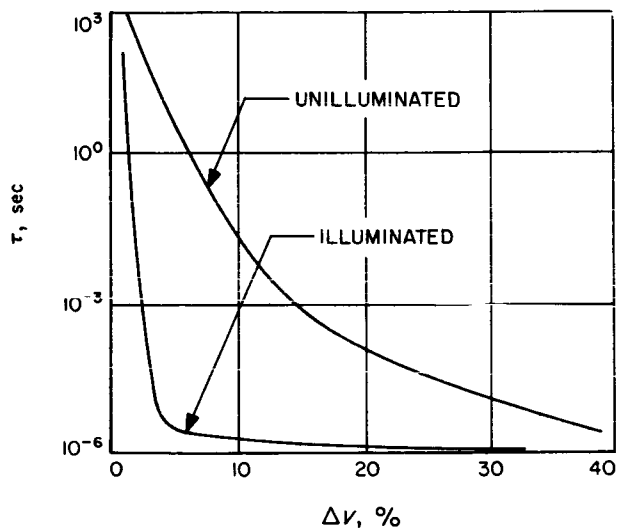


Fig. 23-3. Breakdown time  $\tau$  vs overvoltage  $\Delta V$  for illuminated and unilluminated gaps

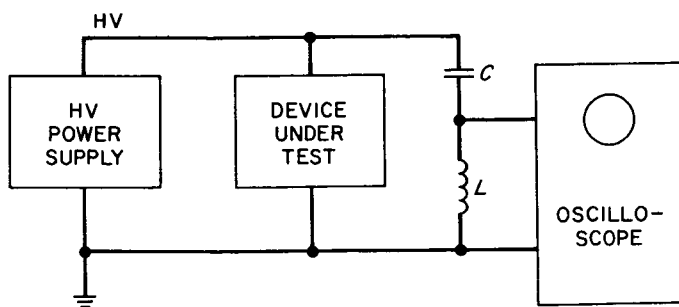


Fig. 23-4. Quinn corona detection network (series)

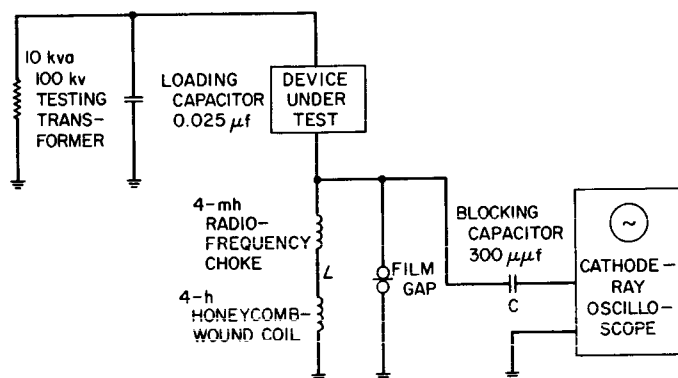


Fig. 23-5. MIL-T-27B corona detection network (shunt)

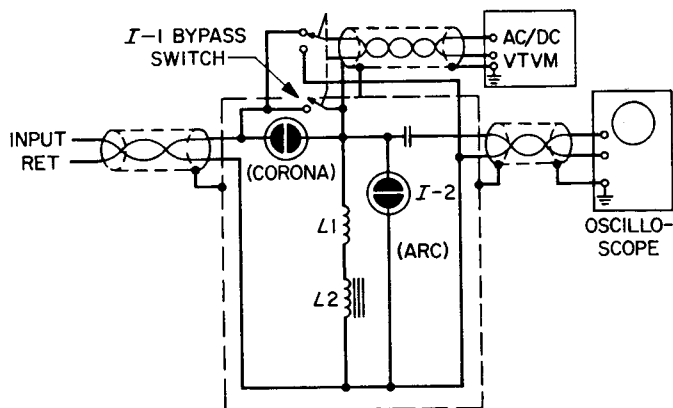
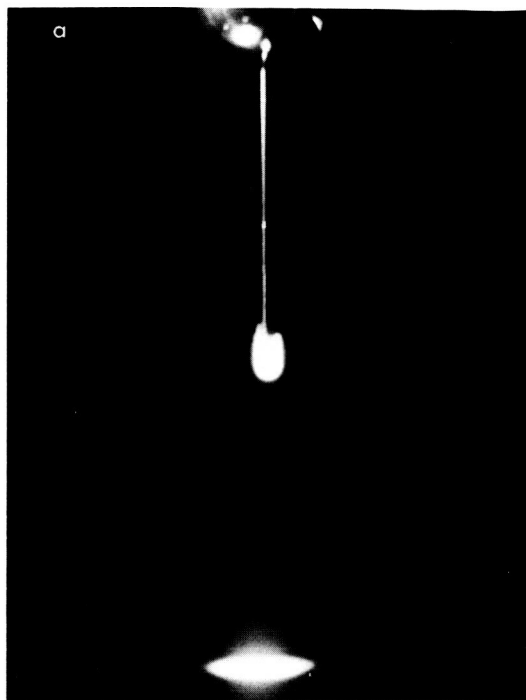
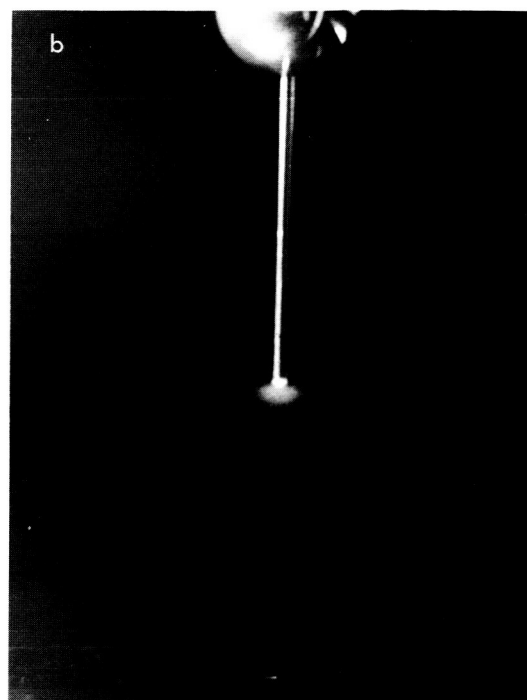


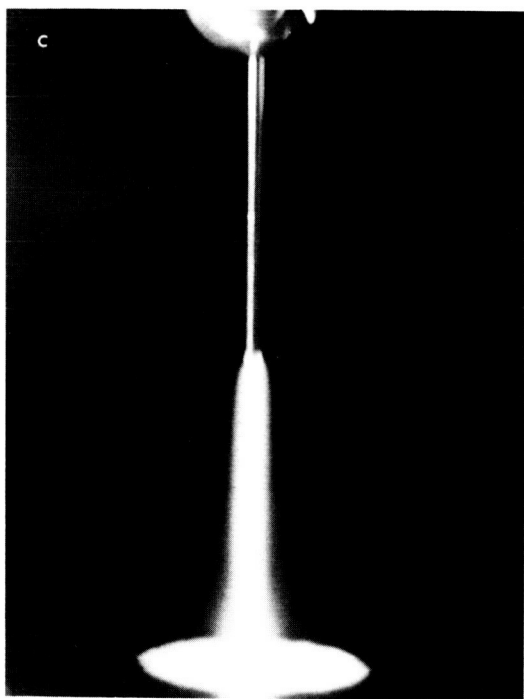
Fig. 23-6. Modified series corona detection network



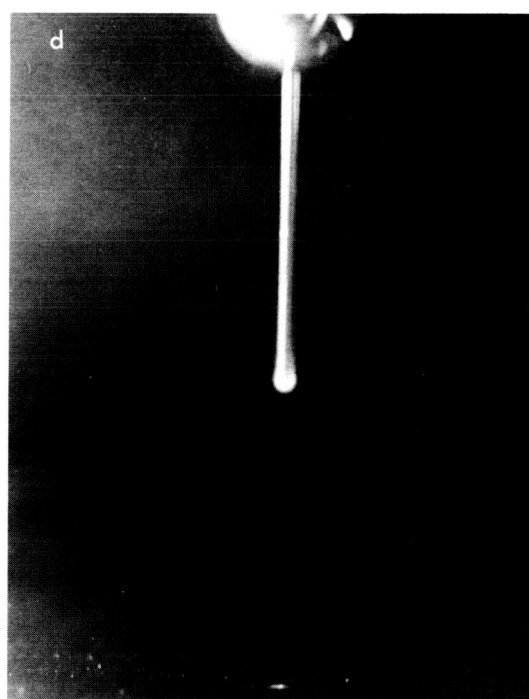
a. AC arc, 10-mm pressure



b. AC corona, 10-mm pressure

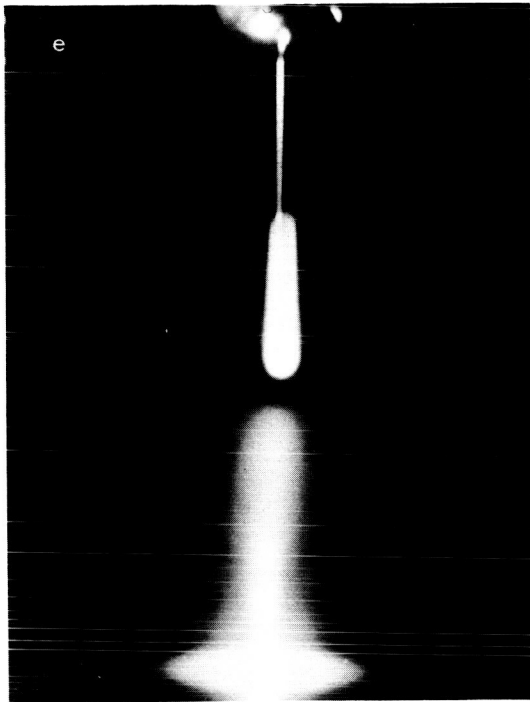


c. DC positive point arc, 10-mm pressure

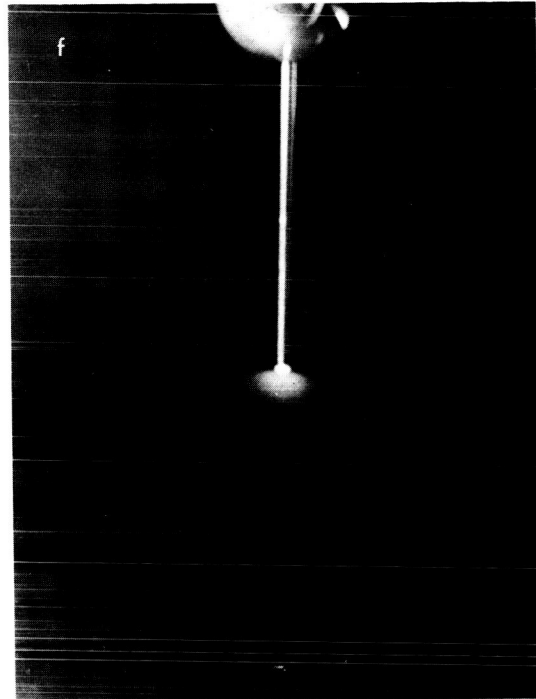


d. DC positive point corona, 10-mm pressure

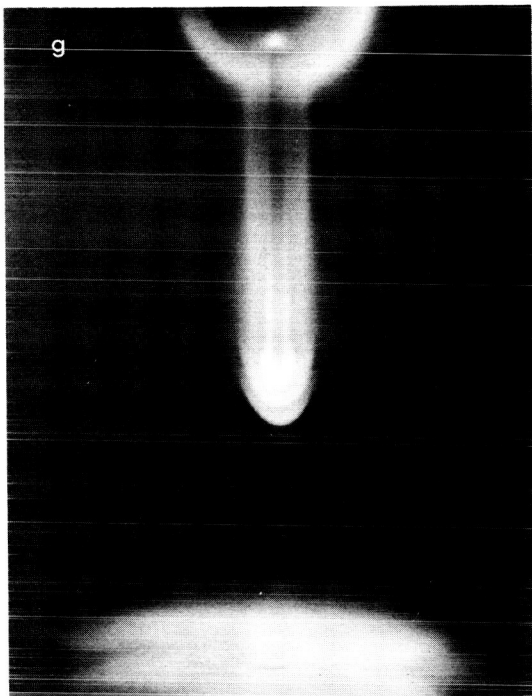
Fig. 23-7. Appearance of point-to-plane corona or arcing at various pressures in critical region



e. DC negative point arc,  
10-mm pressure



f. DC negative point arc,  
10-mm pressure



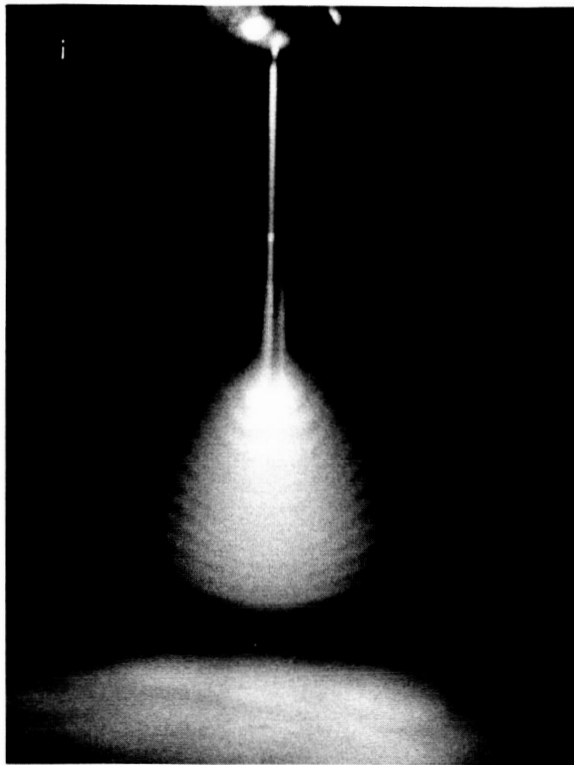
g. AC arc, 5-ma current,  
1-mm pressure



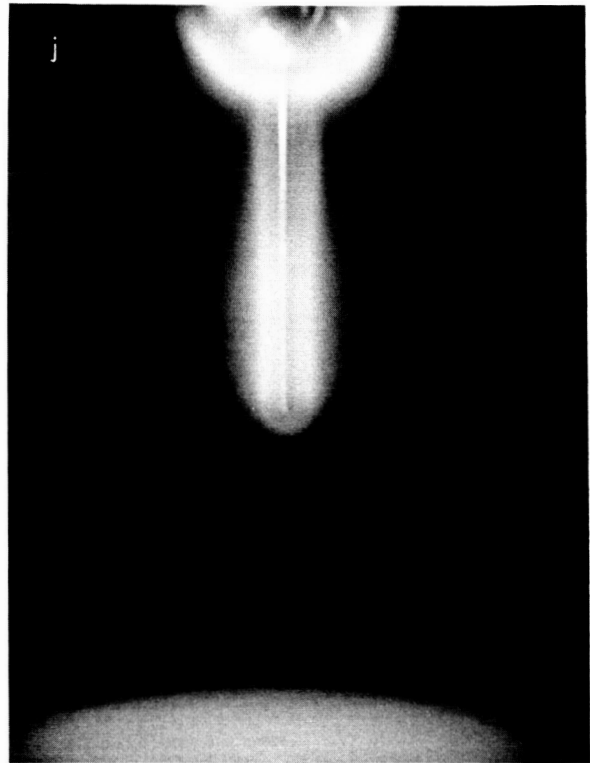
h. AC arc, low current,  
1-mm pressure

Fig. 23-7. Cont'd





i. DC positive point arc, 1-mm pressure



j. DC negative point arc, 1-mm pressure

Fig. 23-7. Cont'd

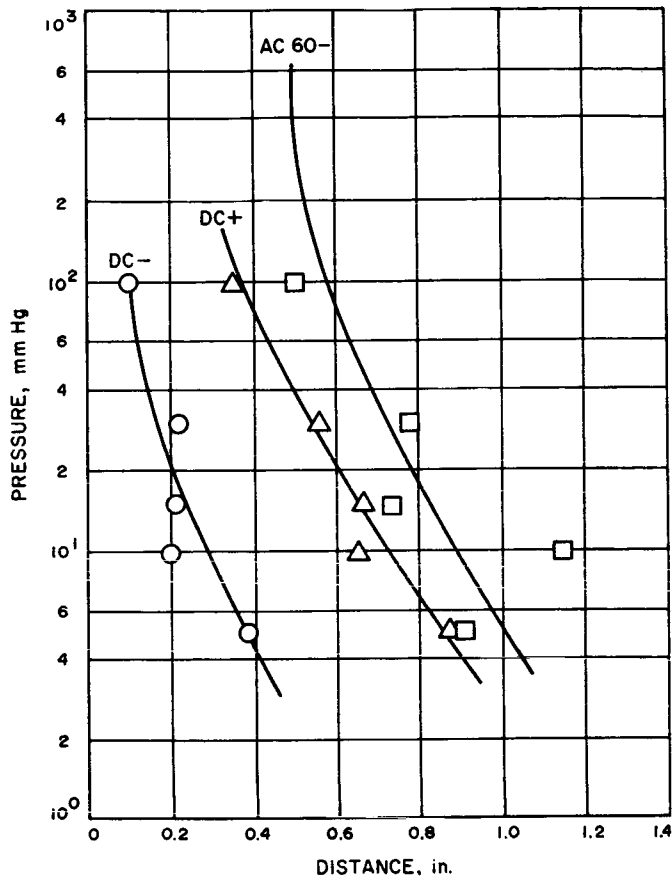


Fig. 23-8. Point-to-plane minimum distance for formation of corona

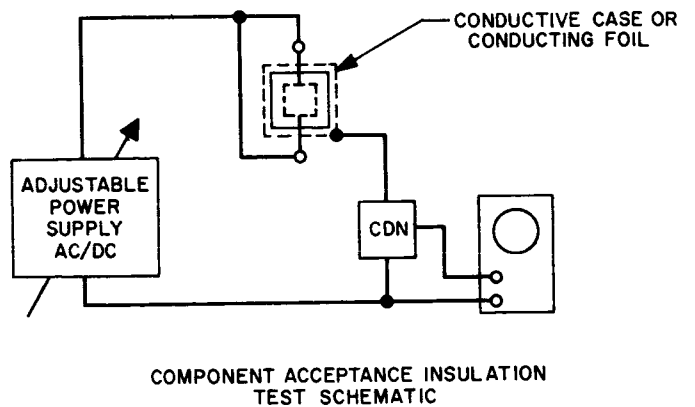
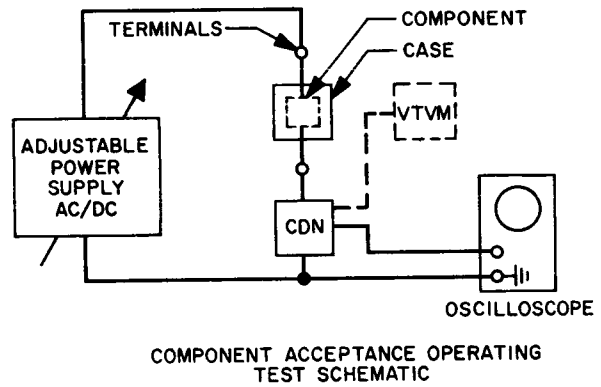


Fig. 23-9. Test of component for corona breakdown

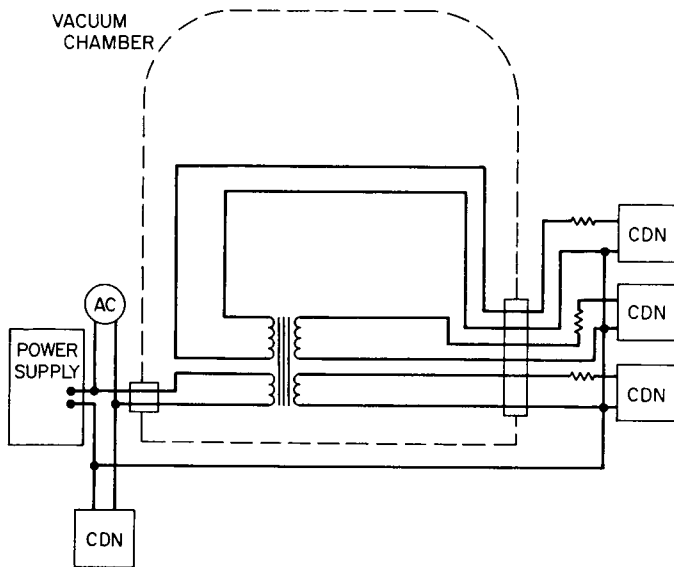


Fig. 23-10. Transformer turn-to-turn voltage test

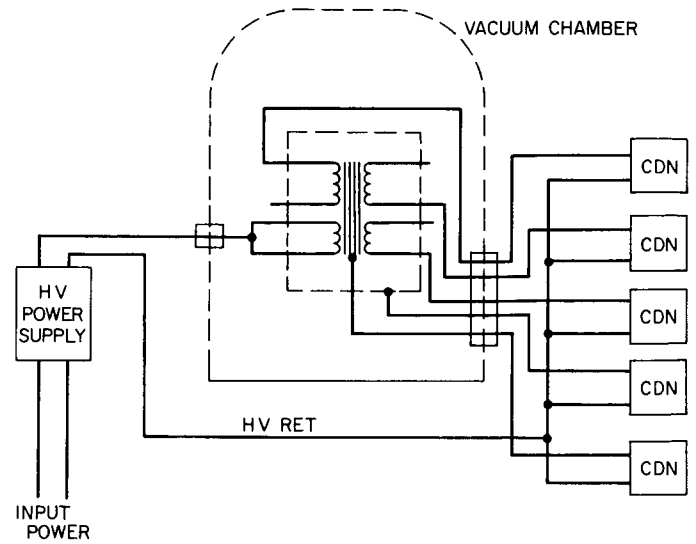


Fig. 23-11. Transformer insulation test

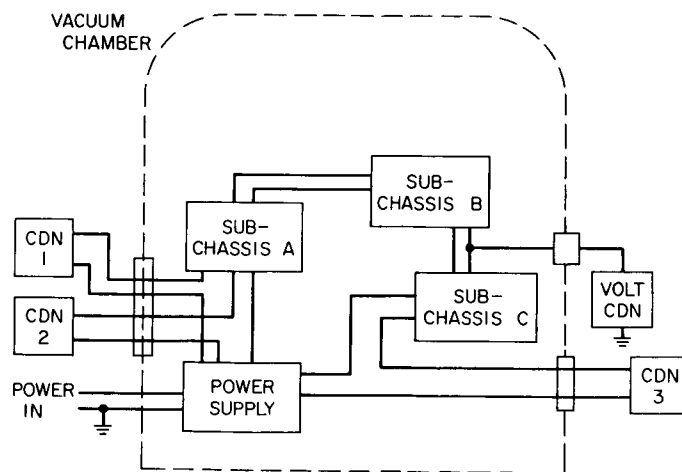


Fig. 23-12. System operation in critical region with corona detection network

N 68-26899

24. THE MATERIALS ASPECT OF CORONA  
AND ARCING PHENOMENA

Robert Boundy  
Supervisor, Materials Engineering  
Jet Propulsion Laboratory  
Pasadena, California

The apparent failure of Ranger VI due to the high-voltage arcing following an inadvertent power turnon in the critical pressure region in the Earth's atmosphere led to serious considerations of similar potential failure modes. The assumption is made that an inadvertent power turnon can be inhibited, and subsequent flights showed that it could. The following questions still had to be answered:

1. When the high voltage is turned on after 65 hr of flight, will the black boxes of the TV system be evacuated below the critical pressure of approximately  $10^{-4}$  torr?
2. During the 5-min warmup period prior to high-voltage turnon, will outgassing products raise the pressure into the critical region?
3. What is the lower limit of the critical pressure range for the various conditions that exist in the TV subsystem?

In this paper, the background of this problem and the results of an experimental program designed to answer these questions (particularly the second question) will be presented.

Briefly, the investigation program consisted of: (1) an analytical evaluation of typical systems, (2) a determination (from available data) of outgassing rates for various materials, (3) determination of materials, geometry and actual vent paths of the black boxes in the TV subsystem, and (4) an experimental program at JPL. In addition, it was intended that tests would be performed on actual high-voltage assemblies, suitably instrumented, when they were available.

The purpose of the experimental program was to determine the transient pressure rise in a typical volume with a known vent area as a result of heating samples of materials used in high-voltage units in the TV subsystem. Eleven materials were selected for testing, six of which were internal to the black boxes, while five were between the shroud and the black boxes.

Figure 24-1 shows the Ranger spacecraft. The part we are concerned with is the TV subsystem. The shroud used for thermal control and some structural support is shown removed in Fig. 24-2. This figure shows the black boxes we're concerned about, in particular the transmitter power supply which had voltages in the range of 1000-2000 v. There were electronic five units that had voltages in excess of 250 v. The polymeric materials in these high voltage units were tested in this program.

While not an intrinsic part of the materials test program, it was decided to include a pair of electrodes in the experiment; they would act as a check on the pressure gages and establish the limits of the critical pressure range for the conditions selected.

John Scannapieco of RCA-AED analyzed the transmitter power supply for voltage breakdown. Based on the known geometry and some experimental work by Wendell Starr of GE, he selected needle-point monel electrodes spaced 5 in. apart at 2,000 v, 60 cps as representative of the worst condition in the transmitter power supply, which was the worst condition in the TV assembly.

These conditions were duplicated in the materials test apparatus shown in Fig. 24-3, consisting of an 8-liter stainless steel chamber with four ports and a removable top. To one port were bolted plates with orifices of 0.040-, 0.125-, 0.250-, 0.500-, and 1.000-in. diameters. Opposite the orifice plate (not shown in Fig. 24-3) was a pyrex window for viewing corona discharge, if any. The other ports contained the needle-point electrodes that were spaced approximately 5 in. apart. The top plate contained a Pirani gage and an ionization gage as well as feedthroughs for power and thermocouples for the samples. The samples were mounted a few inches below the top plate on fiberglass-reinforced Teflon bar.

Figure 24-4 shows the test apparatus assembled in an 18 x 30-in. vacuum chamber. The vacuum chamber, like the Paschen pot (named for Paschen's law, which relates breakdown voltage with pressure and electrode spacing) was instrumented with Pirani and ionization gages as well as a Wallace and Tiernan absolute pressure gage. The 5,000-v transformer was used to supply 2,000 v, 60 cps to the electrodes.

After fabrication, the assembled test apparatus was leak-checked. In the first series of tests with the assembled unit empty, pumpdown curves were obtained for the various orifices. Then with the 0.040-in. -diameter orifice plate in place,

pressure, at which corona was first observed with 2,000 v across the electrodes spaced 5.16 in. apart was determined to be  $5.5 \times 10^{-2}$  torr.

These preliminary tests led to the selection of the 0.125-in. -diameter orifice for the major series of materials tests. Procedures for the tests were as follows:

1. Samples of materials were attached to the holder bar and connected to power and thermocouple leads.
2. The Paschen pot was then assembled in the vacuum chamber, and the power and thermocouple connections made through the feed-through collar. In addition, the vacuum gages and high-voltage connections to electrodes were completed.
3. The system was then pumped down, usually overnight, to about  $5 \times 10^{-6}$  torr in the vacuum chamber.
4. The test run began with the introduction of power to one of the samples after a stable base pressure in the Paschen pot had been reached.
5. In general, the samples were heated to about 175° F in about 15 min. The rise in pressure and temperature of the samples were recorded, as well as the pressure in the vacuum chamber (which usually remained constant).
6. After a 10-min hold at 175° F samples are allowed to cool to ambient, usually in about 30 min, and the second sample was then exposed to the same temperature-time profile.
7. After the second sample had cooled to ambient temperature, the tests were either duplicated or terminated, and new samples introduced for an overnight pumpdown.

Similar procedures were used for a second series of tests in which six materials used inside the black boxes were run with the 0.040-in. -diameter orifice.

In general, two sample configurations were used. Coatings, encapsulents, and adhesives were applied to 2 x 2 x 0.06-in. aluminum plates with thermocouples imbedded in the materials, and 5-w resistance heaters fastened to the reverse side. Rigid solid materials were also fastened to the aluminum plates while flexible materials were wound directly onto 10-w resistant heaters.

The results of the empty chamber pumpdown tests are shown in Fig. 24-5. There was no lag in pressure drop introduced by constrictions greater than 0.125-in.

diameter down to about  $10\mu$  ( $10^{-2}$  torr), about the region where a high-vacuum valve was opened. At low pressures -- approximately  $10^{-4}$  torr -- an appreciable lag between chamber and pot was noticed, especially during the first few hours of operation. However, after about six hours the pressure inside the pot matched that of the vacuum chamber for orifice diameters of 0.250, 0.500, and 1.000 in.

Figure 24-6 shows a typical pressure-time curve for one of the materials, Rayoline-N wire. The pluses are the temperature rise holding at about  $175^{\circ}\text{F}$  for approximately 10 min. The circles are the rise in pressure from the base pressure due to the sample.

Figure 24-7 shows a pressure-time curve for epoxy fiberglass, which is used rather extensively on spacecraft for circuit boards and other applications. These represent the two extremes in pressure rises.

Table 1 identifies the materials tested, the processing history, and pertinent physical data, in addition to the change in pressure ( $\Delta P$ ) due to heating the samples in the test apparatus at  $175^{\circ}\text{F}$ .

The basic bit of information obtained in the experimental apparatus was the pressure rise ( $\Delta P_1$ ) as a function of time in which a known sample of material was heated to a given temperature in a known volume with a known orifice area. This was related to the conditions in actual TV subsystem black boxes by introducing the concept of a critical area ( $A_c$ ) to correspond to a critical pressure ( $P_c$ ). Then, knowing the area of the sample used and assuming outgassing for this short period of time was a direct function of the exposed area, the following relationship was postulated:

$$A_c = \frac{P_c \times A_s}{\Delta P_1} \quad (1)$$

where

$A_c$  = critical area, in.<sup>2</sup>

$P_c$  = critical pressure, torr

$A_s$  = area of sample, in.<sup>2</sup>

$\Delta P_1$  = thermally induced pressure rise, torr

The critical pressure ( $P_c$ ) was defined as that pressure (on the lower side of Paschen's law curve) at which corona discharge first occurs. The critical area ( $A_c$ ) was defined as that area of material which, when heated to a specific temperature, will result in sufficient outgassing to attain the critical pressure. (The critical pressure for the test apparatus was  $5.5 \times 10^{-2}$  torr (55  $\mu$ ). The applied voltage was 2000 v, 60 cps across needle-point electrodes 5 in. apart.)

At no time during any of the materials tests with the 0.125-in. orifice or the 0.040-in. orifice was corona discharge observed. It should be pointed out, however, that in general the samples were smaller and the volume larger than the conditions that existed in the actual TV subsystem.

Table 2 shows the critical areas calculated as a function of temperature and volume for the 0.125-in. -diameter orifice. The first column represents the actual test data. The subsequent columns for decreasing volume and decreasing temperature are less firmly grounded. The data points ( $\Delta P$ ) for temperatures below 175°F were obtained from the experimental curves and represent very transient conditions. The change in critical area with volume rests on the fact that the pressure and volume are inversely proportional.

The first six materials shown in Table 2 are found in the TV subsystem black boxes. Under the conditions of column 1, the actual test data, the epoxy-fiberglass can be eliminated as a critical material because of its rather high value of critical area ( $A_c = 5 \times 10^4$  in.<sup>2</sup>). Stycast 1090 with curing agent 11, the RCA 688, nylon lac-ing cord, and the Armstrong A-2, which is an epoxy adhesive, can be eliminated because of the rather small quantity used, coupled with the relatively high critical area. The solithane 113/300 (which is a polyurethane coating material) cannot be eliminated because a large area is used and the critical area is relatively small (770 in.<sup>2</sup>). If the volume is reduced to 800 cc, the critical area is reduced to 77 in.<sup>2</sup>; however, if the temperature is decreased to 150°F,  $A_c$  is increased to 150 in.<sup>2</sup>.

The last five materials in Table 2 are located between the black boxes and the protective aluminum shroud. As such, they are much less critical because of apparently adequate venting around and between decks on the TV superstructure. In addition, the critical areas are relatively high under the normal test conditions which are conservative (175°F, 8 liters, 0.125-in. orifice).

It should be pointed out that a  $\Delta P$  obtained from a base pressure of  $10^{-4}$  torr is essentially equivalent to one obtained from a base pressure of  $10^{-10}$  torr because the



latter is insignificantly small. Therefore, the fact that the pressure inside the black boxes might be  $10^{-10}$  torr has no beneficial effect if the transient pressure rise is, for example,  $5 \times 10^{-3}$  torr.

To apply the concept of a critical area to the actual high-voltage units, Eq. (1) must be modified to include the effects of volume and vent area:

$$A_c = \frac{P_c \times A_s}{\Delta P_1} \times \frac{V_2}{V_1} \times \frac{C_2}{C_1} \quad (2)$$

where

$V_1$  = volume of test apparatus, in.<sup>3</sup>

$V_2$  = free volume of black box, in.<sup>3</sup>

$C_1$  = vent area of test apparatus, in.<sup>2</sup>

$C_2$  = vent area of black box, in.<sup>2</sup>

Equation (2) must be further modified to account for the three pumping modes inherent in test apparatus. The first, and intended means of egress for the gas molecules generated, is the thin-plate orifice. The 0.125-in. -diameter orifice used has a pumping speed in the molecular flow region of about 1 liter/sec. The second mode, is the ionization gage which has an inherent pumping speed of between 0.1 and 2 liter/sec depending on its life history. (A value of 1 liter/sec was used in the calculations which follow.) The third pumping mode is the ambient temperature cold wall effect of the test apparatus.

The above discussion indicates that the measured pressure rise is a function of the rate of gas evolved from the sample and the means by which it is removed from the system. To correlate the test results with the condition in various black boxes, the following expression was derived:

$$\Delta P_2 = \Delta P_1 \times \frac{F_o + F_g + F_w}{F_o + F_w \times \frac{A_2}{A_1}} = \Delta P_1 \times \frac{S}{F_o + F_w} \quad (3)$$

where

$\Delta P_2$  = pressure rise in black box, torr

$\Delta P_1$  = experimental pressure rise, torr

$F_o$  = pumping speed of the orifice, liter/sec

$F_g$  = pumping speed of the ionization gage, liter/sec

$F_w$  = pumping speed of the test apparatus cold wall,  
liter/sec

$F'_w$  = pumping speed of the black box cold wall,  
liter/sec

$S$  = rate of gas generated by sample, liter/sec

$A_2$  = internal surface area of black box, in.<sup>2</sup>

$A_1$  = internal surface area of test apparatus, in.<sup>2</sup>

Combining Eq. (2) and (3),

$$A_c = \frac{P_c}{\Delta P_1} \times A_s \times \frac{V_2}{V_1} \times \frac{C_2}{C_1} \times \frac{F_o + F'_w}{S} \quad (4)$$

Using Eq. (4), values of critical area ( $A_c$ ) for the solithane 113/300 were calculated for the high-voltage black boxes on the Ranger TV system. These values are shown in Table 3 and compared with the actual quantity of material present by a figure of merit  $Z$ .

In all cases we have a "factor of safety," of at least 10. At the time this table was put together, some of the measurements of the internal geometry of the black boxes and the actual amount of material were unknown and estimates were used.

It should be noted that the values of critical area ( $A_c$ ) presented in this table are intimately related to the original test apparatus conditions. The calculations therefore assume the 5-in. spacing of needle-point electrodes at 2,000 v, 60 cps and material temperature of 175°F for a 10-min. period. All of these conditions are conservative compared with the actual conditions in the Ranger TV system.

The value of  $Z$  represents the external boundaries of the high-voltage black boxes; that is, it assumes that the gases evolved will have ready access to the known

vent area in the box envelope. In some of the units the real geometry is more complex and the gases must follow a labyrinthine path. Because of the difficulty in handling this part of the problem analytically or by simulated tests, tests were performed on actual transmitter power supply and camera electronic units, by the JPL Electro-Mechanical Engineering Support Section to determine the pressure rise in isolated internal compartments. These tests confirm that the pressure rise was not sufficient to cause arcing.

Table 24-1. Pressure changes ( $\Delta P$ ) for various materials

Material	Cure cycle	Weight, g	Area, in. <sup>2</sup>	$\Delta P$ , torr $\times 10^4$	$\Delta P/A$ torr/in. <sup>2</sup> $\times 10^5$	Remarks
Epoxy-Fiberglass		8.2	8.0	0.1	0.1	
Solothane 113/300	16 hr R.T., 4 hr 150°F	1.4	4.0	2.6	6.5	
Stycast 1090/11	4 hr, 160°F	2.6	4.0	0.5	1.3	
RCA 688		3.7	2.5	2.7	10.8	
Nylon lacing cord		1.2	1.2	4.9	40.8	Area used for calculations (1.2 in. <sup>2</sup> ) is very conservative
Armstrong A-2/A	2 hr, 165°F	4.2	4.0	1.6	4.0	
Rayolin-N		1.3	9.2	2.5	2.7	
Thermofit type CRN		1.5	4.5	1.6	3.6	Shrunk at 300°F for 10 sec before testing
Nylon tie-wrap		1.0	2.2	4.9	22.3	
PR-1527	6 hr, 160°F	4.1	4.0	2.4	7.3	
Silicone rubber	250°F, 24 hr 10 <sup>-6</sup> torr	3.1	5.2	1.1	2.1	Cushion on TA cable clamp
Note: All the materials listed above were heated to 175°F inside the 8,000 cc corona materials test apparatus with an 1/8-in. orifice plate.						

Table 24-2. Critical areas ( $A_c$ ) as a function of temperature and volume

Material	175°F 8,000 cc $A_c$ , in. <sup>2</sup>	175°F 800 cc $A_c$ , in. <sup>2</sup>	175°F 80 cc $A_c$ , in. <sup>2</sup>	150°F 8,000 cc $A_c$ , in. <sup>2</sup>	150°F 800 cc $A_c$ , in. <sup>2</sup>	150°F 80 cc $A_c$ , in. <sup>2</sup>
Epoxy-Fiberglass	$5 \times 10^4$	$5 \times 10^3$	$5 \times 10^2$	$5 \times 10^4$	$5 \times 10^3$	$5 \times 10^2$
Solithane 113/300	$7.7 \times 10^2$	77	7.7	$1.5 \times 10^3$	$1.5 \times 10^2$	15
Stycast 1090/11	$3.8 \times 10^3$	$3.8 \times 10^2$	38	$9.5 \times 10^3$	$9.5 \times 10^2$	95
RCA 688	$4.6 \times 10^2$	46	4.6	$7.8 \times 10^2$	78	7.8
Nylon lacing cord	$1.2 \times 10^2$	12	1.2	$1.2 \times 10^2$	12	1.2
Armstrong A-2A	$1.2 \times 10^3$	$1.2 \times 10^2$	12	$2.7 \times 10^3$	$2.7 \times 10^2$	27
Rayolin-N	$1.9 \times 10^3$	$1.9 \times 10^2$	19	$3.5 \times 10^3$	$3.5 \times 10^2$	35
Thermofit type CRN	$1.4 \times 10^3$	$1.4 \times 10^2$	14	$2.4 \times 10^4$	$2.4 \times 10^3$	$2.4 \times 10^2$
Nylon tie-wrap	$2.4 \times 10^2$	24	2.4	$3.7 \times 10^2$	37	3.7
PR-1527	$6.9 \times 10^2$	69	6.9	$2.0 \times 10^3$	$2.0 \times 10^2$	20
Silicone rubber	$2.4 \times 10^3$	$2.4 \times 10^2$	24	$3.3 \times 10^3$	$3.3 \times 10^2$	33

Note: Critical area ( $A_c$ ) is defined as that area of material which, when heated to a specific temperature, will result in a rise to the critical pressure ( $P_c$ ). Critical pressure ( $P_c$ ) is defined as that pressure (on the low side of the Paschen's law curve) at which corona discharge occurs.

Orifice used was 0.125-in. diameter ( $0.012 \text{ in.}^2$ ).

Table 24-3. Critical areas ( $A_c$ ) for Ranger TV subsystem  
high voltage units

Unit	Area Solithane 113/300 $A_m$ , in <sup>2</sup>	Critical area, $A_c$ , in <sup>2</sup>	Figure of merit Z
Telemetry processor	11.7 (calc.)	244	20.8
Camera electronics	246 (calc.)	$2.5 \times 10^3$	10.1
Transmitter power supply	233 (calc.)	$3.9 \times 10^3$	16.7
Transmitter	30 (est.)	$4.6 \times 10^3$	152
IPA	30 (est.)	$4.6 \times 10^3$	152
X12 (FM Mod.)	1 (est.)	14	14
NOTE: The critical area ( $A_c$ ) is defined as the area of polymeric material which when heated to a specific temperature, will generate gas sufficient to raise the pressure into the critical region for electrical discharge. (See Eq. 4.)			

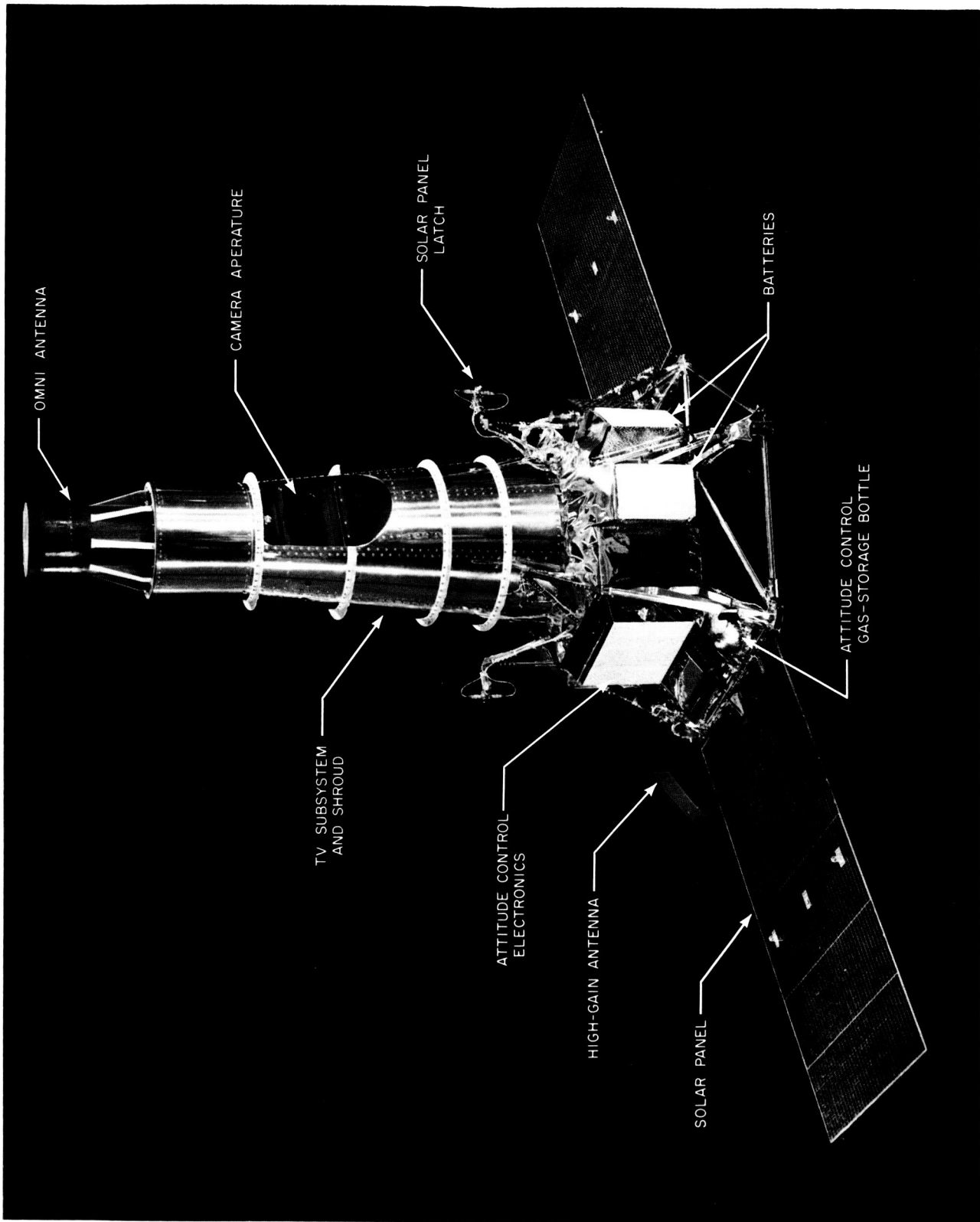


Fig. 24-1. Ranger spacecraft

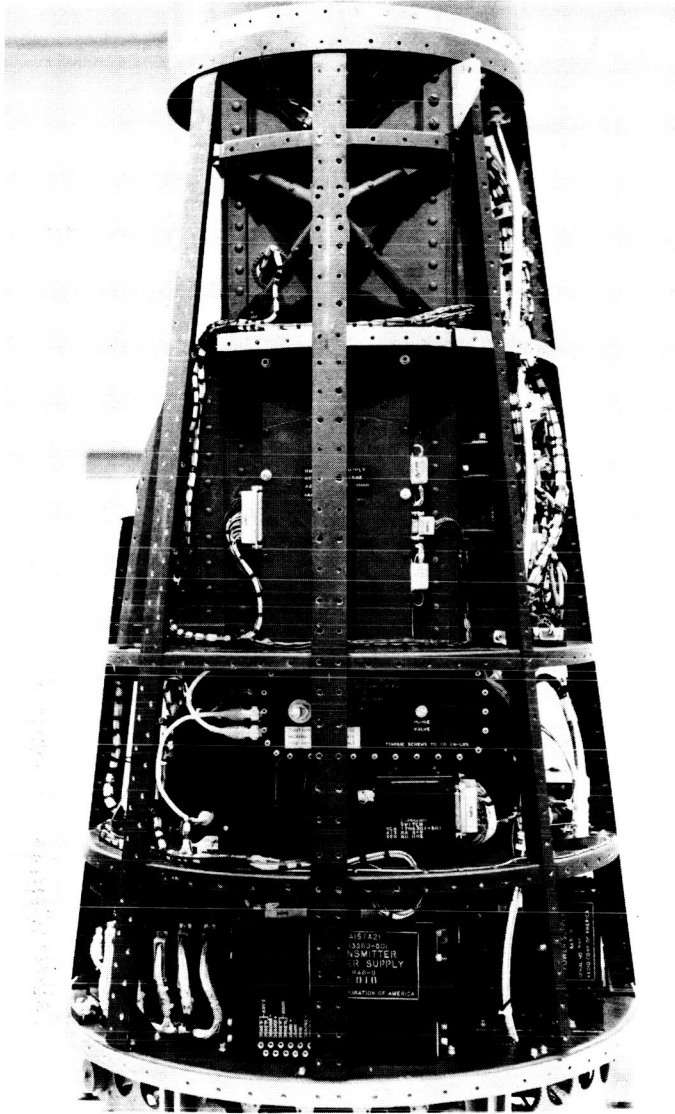


Fig. 24-2. Ranger TV subsystem with shroud removed (Note the transmitter power supply in the center of the lower deck.)

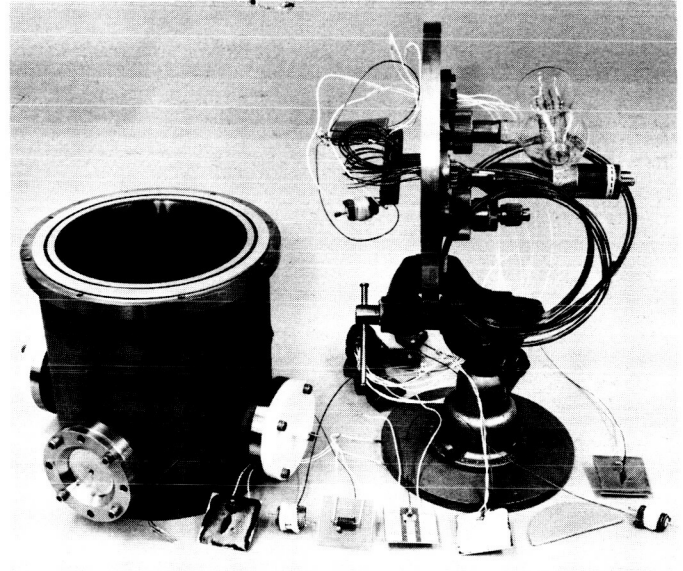


Fig. 24-3. Corona materials test apparatus

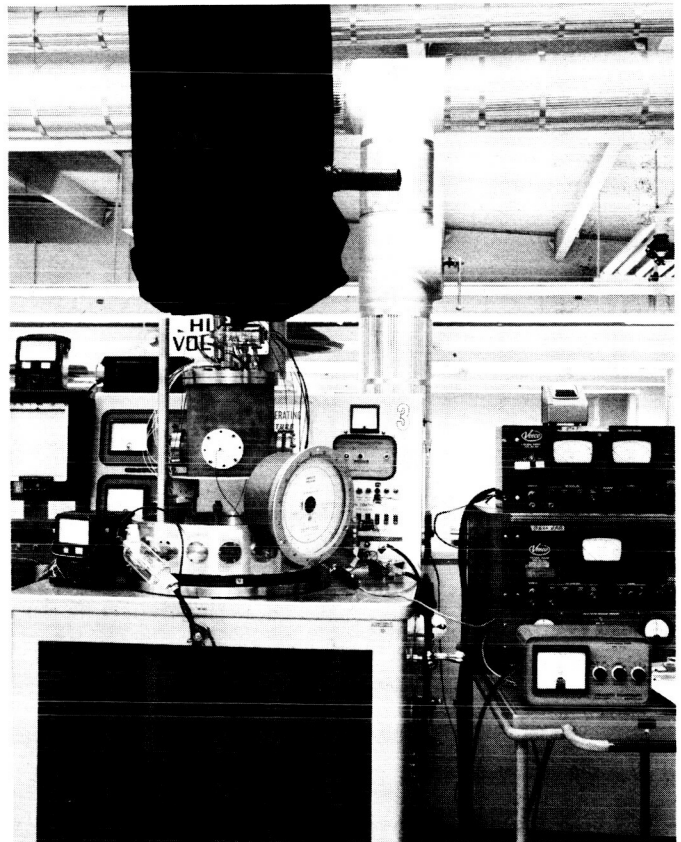


Fig. 24-4. Corona materials test apparatus assembled in vacuum chamber



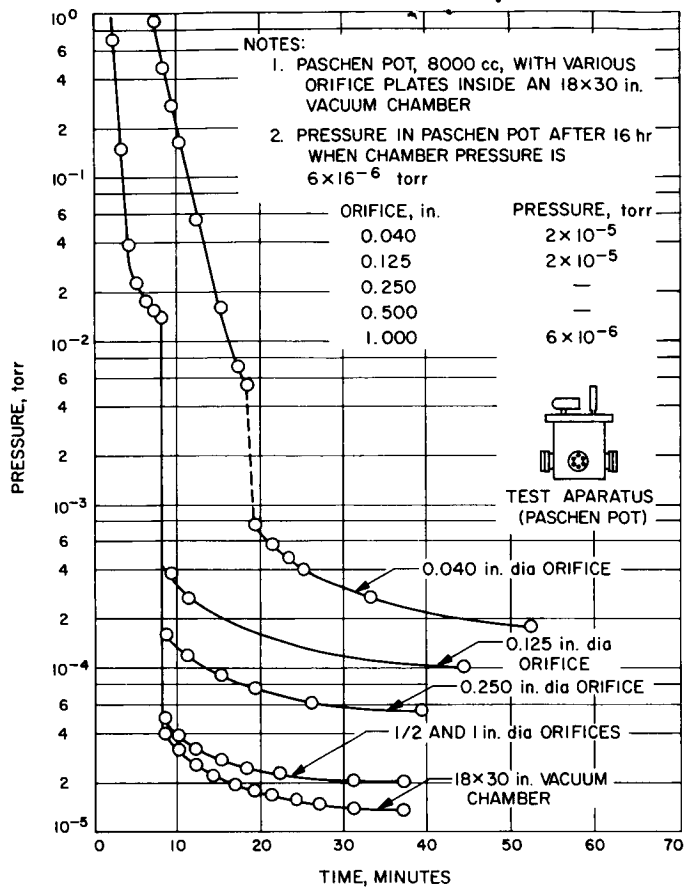


Fig. 24-5. Empty chamber pump-down curves for corona materials test apparatus

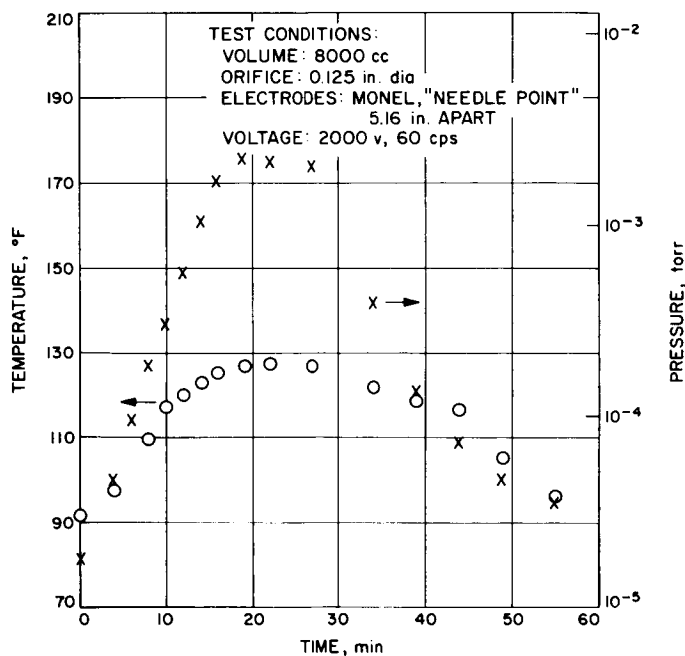


Fig. 24-6. Thermally induced pressure rise for Rayolin-N wire

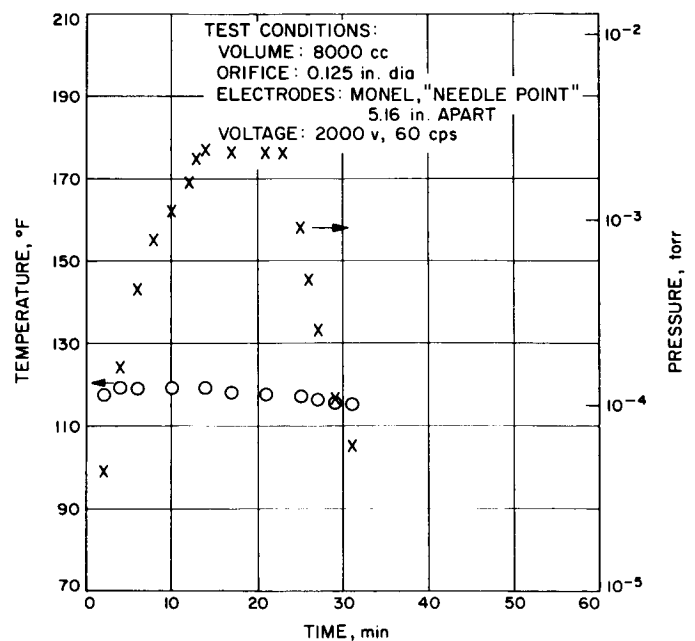


Fig. 24-7. Thermally induced pressure rise for epoxy fiber-glass

N 68-26900

25. THE PRESSURE PROFILE OF A ROCKET EXPERIMENT AND  
METHODS OF REDUCING THE GAS LOAD

N. McIlwraith  
Goddard Space Flight Center  
Greenbelt, Maryland

Since almost everything has been covered up to this point, I'm going to cut my talk quite short and discuss some results which we've obtained over the past year or so. I should like to present my discussion in three parts. First, I shall describe a plasma experiment which was developed and flown on an Argo D-4 rocket (a Javelin), which experienced difficulties with corona. Next, I shall describe the study we made and some data generated both in the laboratory and in a rocket-borne pressure gage. Lastly, I should like to sum up our present thinking regarding techniques for minimizing the gas load and to suggest avenues for further study.

A secondary emission plasma detector was flown from Wallops Island in September, 1963 on a rocket designated 8.18. Figure 25-1 shows this detector in schematic form. The essential part of this instrument is an aluminum electrode (designated K) which is maintained at a potential of -15 kv with respect to the rest of the structure. Positive particles from the ambient plasma are attracted to it, and the secondary electrons emitted are accelerated away from it, to be counted in the scintillation counter. This electrode is mounted inside a grounded aluminum can (approximately 4 in. in diameter), and any discharge between this can and the electrode interferes with the operation of the detector. It doesn't necessarily permanently damage it, but it could damage the scintillation crystal.

Figure 25-2 shows the detector in its rocket configuration. This was the first generation of plasma experiments, and there are a lot of rather obvious problems with it that we hadn't learned about yet.

Power was applied to the 15-kv supply 10 sec after nose cone ejection at an altitude of about 800,000 ft. At this time, the telemetry showed spurious counts indicating a corona discharge. Later we were able to simulate the data in the laboratory using the backup plasma detector in a bell jar at a pressure of the order of 100  $\mu$ . This corona continued past apogee where the telemetry failed. However, just before the telemetry failure we did notice a decrease in the level of corona, suggesting a lowering of pressure towards an acceptable level. One thing you have

to remember with this type of a detector having an ultrasensitive photomultiplier tube is that we're not only concerned with large arcs; only a very slight sparking or, in fact, only single electrons boiling off the electrode are enough to give us trouble. So, we're talking about a very sensitive phenomenon here.

Figure 25-3 shows the path by which gas could escape from the chamber, the chamber being up on the top. There's a slit through which gas can pass into the curved plate analyzer and along a fairly long path through two more slits and then to an area which is necessarily painted black to avoid ultraviolet and visible light reflection problems, and that in itself gives off gas, so this path turns out to be utterly inadequate.

During development of this rocket experiment the pumpout problem was considered and small pumpout holes were provided on each of the electronic packages and on the detector box. (I don't think you can see it on this figure, but there was a small hole on the upper end of the detector chamber.) These holes are of an order of 0.125 in. in diameter. Calculations using the area of the slit and holes indicated a pumpdown time of the order of 1 sec. The pressure under the nose cone was estimated to be about  $10 \mu$  at 700,000 ft. There was a delay of 10 sec before power was applied after the nose cone ejection, and about 2 sec were required for the voltage to come up. It was considered that this time would be sufficiently long. The factor which was neglected was the moisture deposited on the walls inside the analyzer. We believe the high humidity at Wallops Island was a major cause of this moisture. (I don't know whether anyone is familiar with the range, but the rocket is sitting about 40 or 50 ft from the ocean, and there's a great deal of salt spray blowing over the whole thing. We consider that this was a very large factor leading to our problems.)

Postflight analysis and launch simulation showed the pressure inside the detector chamber must have remained well above  $10^{-4}$  mm Hg, in fact, probably of the order of  $30 \mu$  for several hundred seconds after the nose-cone ejection. In the laboratory, discharges were shown to occur if the pressure in the detection chamber was above  $10 \mu$  when the high voltage was applied. The following factors were considered to contribute to the high pressure which must have occurred:

1. Outgassing of the payload, in general leading to higher than expected ambient pressure.
2. Heavy outgassing from this detector itself.

Ram pressure calculations, incidentally, at 700,000 ft (the nose cone ejection altitude) indicate the value of  $10^{-5}$  mm Hg, one order of magnitude lower than where we would expect any difficulty at all.

If the discrepancy were due to the large-scale outgassing of the whole payload, it's possible that no reasonable increase in the size of pumpout apertures would allow operation of the detector in a reasonable time. If this were the case, then an active pumped system with a breakoff mechanism would be the only way to solve this problem and the only way to fly such a detector. Figure 25-4 shows the rocket payload and the fourth stage at "spin and balance." Pressure close to the payload could conceivably be several orders of magnitude greater than the ambient pressure tables predict, since a hot case of the X-248 solid propellant motor remains with the payload after it has burned out and it's quite possible that gases are evolved both from the nozzle and from the case of the payload, which is as close as 18 in. from the payload itself.

A literature search showed that no conclusive evidence was available on the problem, and it was therefore decided to mount the pressure gage on a similar payload to establish this parameter. We shall come to that in a few minutes. But let's first consider outgassing from the detector itself. Figure 25-5 shows an experiment that was built to test the effects of pumpout ports on the plasma detector; the effect of adding two ports of relatively high conductivity, one up at the top, and one off the curved plate analyzer. These ports gave the complete structure a calculated pump-down time of a few milliseconds. A Phillips ion gage supply replaced a 15-kv power supply, the photomultiplier tube, and looked into the detection chamber. Ideally this instrument should have flown on a similar Argo D-4, but unfortunately we were unable to get the necessary payload space. So we did the next best thing, which was to place this detector in a small vacuum chamber at Goddard to simulate the decreasing pressure environment of a rocket payload after nose-cone ejection. The small chamber was connected through a quick-acting valve to a very large vacuum chamber.

Figure 25-6 is an artist's sketch of the test setup at Goddard. The experiment was sitting in the small bell jar, and we had fairly high conductivity (as high as practical, anyway) through a quick-acting valve to the very large chamber which essentially simulated the big bell jar in the sky. When the valve was opened the pressure in the small test chamber fell rapidly to the pressure of the large chamber.

The conductance between chambers was made as large as practical. The small chamber was pumped down mechanically first to  $60 \mu$ . The large chamber at the beginning of the test was  $1.3 \times 10^{-6}$  mm Hg. After opening the valve, pressure in the small chamber was monitored and recorded on a Sanborn recorder. The pressure at the end of 300 sec was of the order of  $7 \times 10^{-4}$  mm Hg, while that in the large chamber essentially remained constant. Figure 25-7 shows the results of three consecutive operations. The most interesting features of these graphs are: (1) the very rapid fall to about  $2 \mu$ , (2) the very long time to reach pressures below about  $1 \mu$ , and (3) the progressively decreasing pressure for a given time as the function of the number of cycles.

The first effect, we feel, is due to the changeover from viscous to molecular flow regime, which occurs for pressures of the order of a few microns. The second and third show the large effect of outgassing from the experiment. This point will be discussed in a few minutes when it will be shown that at least 90% of this gas load is water vapor.

In October 1964, a Phillips gage was launched from Wallops Island on a payload similar to the 8.18 (the original Argo D-4). The gage was energized during the last few minutes of the countdown and continuously through launch, ballistic flight, and to impact. Although we had telemetry problems resulting in some blank spots, since it's a slowly varying phenomena, we had no trouble in making an interpolation. The pressure throughout the flight until the gage was off scale is provided at least within a factor of two. Figure 25-8 shows the rocket payload containing the Phillips gage experiment. It's a rather typical sort of payload, and no one took any particular precautions to keep the outgassing materials to a minimum. We didn't tell any of the other experimenters specifically about our problem or what they should do. We wanted to get rather typical results. The sensing element, incidentally, is inside a cylinder,  $5/8$  in. in diameter and  $1-1/2$  in. in depth. The pressure gage is approximately 4 ft forward from the nozzle of the fourth stage, and it's about 2 ft from the front of the fourth-stage motor. And again, this is the X-248 Allegheny Ballistic Lab's motor.

Figure 25-9 shows that the pressure drops to  $10^{-4}$  mm Hg within 3 sec of the nose cone ejection, and to  $3 \times 10^{-5}$  mm Hg within about 10 sec. So that if, in fact, the plasma experiment were energized at that level, there would be no problem. This experiment seems to prove that adequate pressure differential does exist between the

inside and the outside of the payload to pump the experiment down quickly, if sufficient conductivity can be provided so that outgassing from the rest of the payload is evidently not a problem.

Shortly afterwards, a modified configuration of the plasma experiment was tested in the same pair of connected vacuum chambers that we used before.

Figure 25-10 is similar to a previous one. The modified configuration of the experiment with the two pumpout ports was similar to that used in the first vacuum test but here we got closer to the plasma detector. We put back the 15 kv power supply in place of the Phillips ion gage and used a photomultiplier to detect any corona in the chamber, leaving off the scintillator. One of the pumping ports was a 1 x 1-in. -square tube, 6 in. long, attached to the junction between the detection chamber and the electrostatic analyzer. The other was a rectangular tube,  $1/2 \times 1-1/2$  in. in cross section and about 1-1/2 in. long. So these ports are really quite high in conductivity.

Figure 25-11 shows an exploded view of the plasma detector as redesigned for rocket use. We're becoming a bit more sophisticated now and understand the problems of designing these ports. They're considered about the largest ports that can be attached to the detector and still have it function correctly. The pumpdown time is calculated to be a few milliseconds.

To simulate conditions of nose-cone ejection in rocket flight, a small vacuum chamber was evacuated to 50  $\mu$  using a mechanical pump; the pumping line closed; and the valve operated. After a number of seconds, the high voltage was applied and the photomultiplier output was monitored to detect evidence of corona. This experiment will not give conclusive results if initial conditions at the time of opening the valve to the high vacuum are not always the same. In attempting to ensure that this is the case, there is one circumstance which cannot be controlled, since it's dependent upon previous history of the apparatus, namely, outgassing of the detector itself. That outgassing is the controlling phenomenon is shown by a series of experiments summarized in Table 1. The entries in this table were made in the order in which readings were taken. The discharge in the first trial was the only one observed, even though the delay time was subsequently reduced and the pumping ports partially closed. We went first down the first column and then down the one with one port closed, starting at number three. Between each trial, the chamber was vented to atmosphere, but pumped down again after a few minutes.

Table 1. Effect of outgassing on corona discharge

Time between opening valve and switching on high voltage, sec	Both ports open	One port closed
5	discharge	--
10	no discharge	--
5	no discharge	no discharge
0	no discharge	no discharge

It is believed that time of the order of 10 hrs is required for appreciable adsorption of moisture, and that history is a dominant factor. Therefore, to establish these parameters properly, we would require several weeks (probably leaving the thing out at Wallops Island) to really do a realistic study on it. We were concerned when we mounted this program originally to answer the question about when we could turn on the high voltage and when we could operate our detector after the nose-cone was ejected.

The next step, we felt, was to isolate the offending components, since we now established that it was gas in our detector that was giving us the problem. So a complete set of components for the plasma detector and its rocket configuration was placed in a vacuum system with an analyzer on it. The analyzer was turned on at the earliest safe opportunity, which was about at the pressure of  $10^{-5}$  mm Hg. Table 2 tabulates the results of this analysis as specimen 1. A second one was taken about 1 hr later when the instrument had fully stabilized, and a third 3 hrs after that. Between 90 and 95% water vapor was found, with quantities of hydrocarbons, nitrogen, and oxygen. Many other constituents were present in appreciable amounts.

Next the experiment was removed from the vacuum chamber, disassembled, and the photomultiplier assembly alone was submitted for analysis. The results shown as specimen 2 indicate that after considerable pumping the majority of the vapors emanate from this component. This result leads us to suspect silastic potting compound, RTV-11, which was used to insulate the photomultiplier, and which was present in rather large quantity. Therefore, a third analysis was made on

Table 2. Residual gas analysis  
 Temperature 25°C,  
 Ion current = 50  $\mu$ A

	Background (relative units)	Specimen 1 (relative units)			Specimen 2 (relative units)	Specimen 3 (relative units)		
		10	10	11		13	13	13
Date: 1964 Nov.	5				12			
Hour of day	1500	1110	1400	1000	1345	0020	0400	0800
Start	.39	8.0	2.3	.40	2.5	1.8	1.0	2.6
Stop	.37	5.6	2.1	.38	2.4	1.6	1.0	.74
Mass Number: 16	123	4,900	1,260	129	810	630	340	216
17	990	47,000	12,000	1,000	810	6,300	3,300	2,100
18	3,750	100,000	45,000	3,800	30,000	22,000	12,000	7,700
27	49	570	180	39	120	56	41	32
28	650	4,900	2,310	540	990	690	460	330
29	68	660	225	48	153	70	51	39
32	32	1,080	450	120	47	67	32	23
41	74	900	300	65	213	84	68	55
43	79	750	250	57	123	63	51	42
55	48	630	216	45	120	53	41	34
57	55	680	249	51	168	63	48	39



a piece of RTV-11 alone, a cylindrical sample about 1-1/2 in. in diameter and 1/2 in. long, which was poured about 1 yr previously. The results are tabulated as specimen 3. We see that we still have substantial quantities of water vapor.

It is important to note that no attempt was made in these analyses to maintain any quantitative relationship between the material in the experiment, the photo-multiplier assembly, and the RTV sample. No conclusive evidence exists as to the relative contributions of each of these components. However, there are certainly strong indications that RTV is responsible for the larger part of the load.

Since we have now shown that RTV is an offensive component, we should make some effort to find a replacement for it. I realize that this is not conclusive evidence. I would be very glad to know of anyone else who had similar results and who perhaps has gone into it deeper than we have.

Another experiment of interest to us uses a channel electron multiplier. I notice several people talking about these Bendix devices, and we are using them. It's a windowless device which produces secondary electrons when a high potential is applied down its length. When I talk about high potential, I'm talking about 2000 or 3000 v. Mechanically, it is a segment of a thin glass tube. We're concerned with mounting this device to withstand the rocket vibration environment. Up to now, these devices have been floated in RTV in a trough cut in a phenolic block and flown successfully, apparently, by others.

Figure 25-12 shows a mockup of the channel multiplier. This is just a glass tube, and a Kel-F block into which we've mounted a second glass tube, using RTV as a potting compound. As a consequence of our outgassing studies we had several glass tubes made up, potted each in a block of Kel-F and used a different encapsulant for each block. We made about twelve samples, and each was vibrated using a range of silastics and hard epoxies. We vibrated these to fairly severe rocket specifications. We then x-rayed them, and not one of the glass tubes was found broken, even when potted with hard epoxy. Kel-F, incidentally, was used because it is a material which absorbs hardly any moisture, and we are turning more and more to using it in our experiments. It's a very good insulating material.

A spectral analysis was then made of the various samples, and some of the typical results are shown in Fig. 25-13 for the first group of silastics. Since I've used a logarithmic scale, it's not quite as dramatic as it might be, but I think you

can see that there are differences. Since water vapor is the most dominant constituent by several orders of magnitude, only that part of the spectrum is shown, water vapor and OH<sup>+</sup> being the dominant ones, although the data was taken over the entire experiment. RTV-11 shows an amplitude of about 70,000 units of water vapor, and a unit represents a partial pressure of about  $10^{-10}$  mm Hg. Therefore, we're talking in partial pressures of the order of  $7 \times 10^{-6}$  mm Hg. Sylgard 182, which is another silastic type material, is only slightly better. But if a thin layer of epoxy, Armstrong C-7, is painted over the Sylgard, the vapor is reduced by a factor of 3 or 4.

The epoxies are shown in Fig. 25-14. We took three samples, one of Epon 828 and two of Armstrong C-7. Indeed most epoxies are about the same and generally less gassy than the silastics. However, the curing process turns out to be rather an important factor. Varying the ratio of epoxy to hardener from 60-40% to 70-30% increases the gas load by a factor of 3. At this point there are a number of unanswered questions, and it's obvious that we need to seek better materials. I'll be very glad to hear of anyone else who has ideas along these lines.

#### OPEN DISCUSSION

MR. MYERS: On the samples that you tested for outgassing characteristics and measured, did you first postcure the material for, say, 100 hr in a vacuum at some elevated temperature?

MR. McILWRAITH: When we pour this epoxy we first of all mix it up and leave it in the vacuum until it's pretty well outgassed down to 10-50  $\mu$ , somewhere in that range.

MR. MYERS: That's during deaerating?

MR. McILWRAITH: Yes. Then we will pour it around the photomultiplier tube or whatever it is we're potting, and again subject it to a vacuum, and hold it in the vacuum for about 15 min, I would say. After this, we let the air in, and let it cure at either room temperature or at a slightly elevated temperature.

MR. MYERS: Is there anything done to the material after that?

MR. McILWRAITH: No.

MR. MYERS: I'm not a chemist and I'm getting into a sticky area here, but it seems to me that the major part of the outgassing will occur at the first 100 hr when it's subjected to a vacuum. If you then put it in a vacuum chamber for, say, 100 hr at as high a temperature as you dare take it, you'll get rid of these solvents, and the thing will react differently on additional exposure to vacuum.

MR. McILWRAITH: Well, I understand there's quite a bit of controversy over this because I think it's not desirable to pump too much on it because apparently what happens is that the material starts to disassociate. I'm not a chemist either. I'm not sure what goes on, but I believe that it does in fact change the nature of the material if you pull all the air out of it, or if you pull all the moisture out.

MR. MYERS: Now, this is after you've cured up the block, I mean.

MR. McILWRAITH: All right.

MR. MYERS: You've put it in an oven, you've cured it out at 65° C. The compound is cured. Now, if you take it at that point and try to make outgassing tests on it, you're bound to get a lot of gas because the first hundred hours or so there's going to be a lot of solvents coming out of it. This is what we have found and in fact Dr. Muraca of Stanford Research Institute, with whom we consulted, recommended that all pieces of iron, aluminum, and hardware that would go into a system be postcured in a vacuum at an elevated temperature to get rid of the things that are in there. Of course, as soon as you bring it out of the vacuum chamber, air, moisture, and dust are going to get back onto it, but you will have gotten rid of perhaps 80 or 90% of the outgassable materials.

MR. McILWRAITH: Yes. Well, I think there are two things. There's adsorption and absorption. I think that it's surface stuff that you will probably be pulling out. I think after it's set up properly there's probably nothing more you can do to the interior. But, in any case, that's an area we're going to have to look into some more.

MR. MYERS: Additionally, on your glass tube that you said survived shock and vibration, when encapsulated up in a hard epoxy, did you subject it to any temperature to see whether or not the coefficient of thermal expansion of the glass was of the order of 40 or 50 parts per inch?

MR. McILWRAITH: Right. We did go down to about  $-10^{\circ}\text{C}$ . We didn't go any further than that, but we had no trouble down that far and up to  $+50^{\circ}\text{C}$ .

MR. MYERS: How thick a buildup around your piece of glass was there?

MR. McILWRAITH: Let's see. The glass is about 5 mm, I believe, and probably a couple of millimeters on either side. About 2 mm on either side.

MR. MYERS: 2 mm of epoxy built up on the glass?

MR. McILWRAITH: Right.

MR. JACKSON: I'd like to make two comments. One is I believe that I'll second this business of postcuring on my own experience. The idea of preconditioning space hardware, in a vacuum is extremely important, at temperature preferably, because temperature has an enormous effect on degassing of everything--metals, epoxies, anything you want. And, it makes a big, big difference. Now, I think there's another item here that I've found favorable, and I think it's becoming more or less standard vacuum practice. You don't vent your bell jar or your chambers with air. You don't vacuum-clean your lab every time you vent your chamber. That way you pick up all the dust, all the moisture in the laboratory, and put it right back in the chamber. Instead vent with dry nitrogen--ultradry nitrogen. This isn't as expensive or complicated as it sounds. Most laboratories have a source of  $\text{LN}_2$  liquid nitrogen, for traps or anything else. Take that liquid nitrogen, let it gassify, and vent your chambers with that. This is ultradry, ultrapure nitrogen. Well, you say "Fine. I vent the chamber with that, and I have to open it to air to take the sample out." Well, that is not the same thing. Because, you see, your sample has been in the vacuum, and if you put an initial layer of gas on the sample, you have a very direct bearing on how fast that sample will degas in the future. If the first layer of air or gas touching that sample is dried nitrogen, it adheres very firmly to the surface. Then, after you take it out, you can put it in moisture at Cape Kennedy or any place you want, and you'll find that when you pump that sample next time, it will degas easily and quickly,

because that surface stuff will come off very nicely. It's the initial layer you put on that makes a big difference.

MR. McILWRAITH: Well, that's a very interesting comment, and we'll certainly look into it.

MR. DAY: I've noticed in several of the papers, including yours, that potting is a very popular technique for retaining various components in the spacecraft systems, as opposed to mechanical retention of some of the things. We've used a technique which is in a quite a different field, namely, the flight instrumentation of solid propellant rocket motors and, in particular, the Minutemen second stage. I think this technique might have some applicability in the particular instance you were talking about here. For example, the protection of the relatively fragile glass tube from vehicle vibration. What we've done is to actually wrap the components in Dacron felt to isolate them from vibration. I don't know what the outgassing properties of the Dacron felt might be, but I suspect they're probably pretty favorable for these applications. I don't propose this as a cure-all, by any means, because its applicability would be pretty limited, and it certainly wouldn't serve as a corona barrier or whatever term should be used to describe this.

MR. McILWRAITH: Well, wouldn't you have trouble with having little pockets of gas in the felt?

MR. DAY: No. It is very porous material. It would vent very readily. It would not serve as any kind of an insulation. The reason I'm bringing this up is that it would serve as a vibration damper, and it does so very effectively. We protect things like pressure transducers which are, perhaps, relatively tough items, or tough components by comparison to some of the hardware that you people have been talking about. But, they're in a pretty much more severe environment than you've been talking about, too. The kinds of things that happen during the staging sequence on a Minuteman missile are pretty dramatic. We ignite the upper stage about the same time as we separate the down stage, and the environment in the interstage compartment during staging is pretty severe. Yet these components survive it quite nicely with the technique that I'm talking about. I'm just suggesting it as a possible mechanical mounting in shock isolation technique only.

MR. McILWRAITH: Well, I'm very glad to have your comments. I think that's one of the main purposes of the workshop. And, I'm very glad to hear of any suggested techniques.

MR. HAWERSAAT: I might mention one we found, and you seemed to have found too. These fast pumpdown tanks are about the only real good way of getting data, and we found it difficult to correlate tests because of the pumpdown characteristics in the cleaning of the tanks, or cleaning the components in repeated test. But, in high-voltage applications in which you aren't going to be able to pot, I think you'll find even that vacuum storage, prior to launch, will definitely help in achieving a fast outgassing. I might also caution on potting. We've found, unfortunately, after extensive thermal cycling that we have had troubles. Maybe it doesn't even show up until after 10 thermal cycles of a potting material in a high-voltage application. And you can reach this kind of numbers fairly rapidly in your environmental testing.

MR. McILWRAITH: Yes. It would be very nice to have your payload in vacuum, but as a practical matter, particularly for the smaller sounding rockets, it is almost impossible. These things are put together in a couple of days and people jam the nose cone on, and--if you make a big fuss, they'll circulate dry nitrogen through it, and you're never quite sure how dry it is. Of course, there are periods of time when your experiment is lying around in some high humidity unairconditioned workshop. It's just a fact of life. Suddenly when you get into the more sophisticated satellite payloads, at least some of these problems disappear. But, for the smaller rockets, it's just impossible to keep your eye on the thing the whole time.

Mr. HAWERSAAT: I realize that on the Scout, but you can specify tools, like oil-free nitrogen, and things, for purging.

MR. McILWRAITH: Right.

MR. HAWERSAAT: You've got to make them aware of it. Cleanliness helps all the way through.

MR. HOTCHKISS: What was your cleaning and handling process of the channeltron in the potting process? Would you relate this, please?

- MR. McILWRAITH: I'm not sure we took many precautions on this because, first of all, we're dealing with a glass tube (the tube itself is totally encapsulated), and I think we probably didn't go to any particular trouble.
- MR. HOTCHKISS: It seems to me that the handling and the cleaning process of the channeltron is extremely important. Entrapment of grease or any foreign material in your potting compound can create an atmosphere with turn-on and turn-off in longer periods of time than in rocket flight, if you're going to go into satellite uses.
- MR. McILWRAITH: I agree with you, I think it is important. However, the data which I presented on the glass tube (on the last slide), which we potted, was to show a difference between various encapsulents. We're talking about relative data, and so we weren't really too concerned about absolute figures. We were simply looking for an encapsulating material that would be good. We found that some, in fact, were better than others. That's really all I'm able to say at the moment. I agree that, if you had a real channeltron, you would have to take precautions. Incidentally, if anyone's using the channeltrons for the first time, it's most important to keep them in oil-free vacuum systems. We use an ion vacuum pump for all our channeltron work.
- DR. REEVES: I'd like to make one comment here. I think I mentioned it to you, but some of the other people may not be aware of it. Several years ago we launched a rocket package from White Sands using the Aerobee. There is a pumping system available from NASA for the Aerobee nose cone which will evacuate the nose cone on top of the rocket for several days, if you like, before a launch. This will produce in the nose cone of the rocket a vacuum of approximately  $10^{-5}$ , and the facility exists to back-fill the nose-cone immediately prior to launch (immediately being a few seconds). Tests have been made to launch the nose cone evacuated and blow it off after it's reached several thousand feet. This, of course, is a great help to reduce the out-gassing from the system. It's also a help, if you can pump most of the products out of the package and then back-fill with dry nitrogen or with helium.

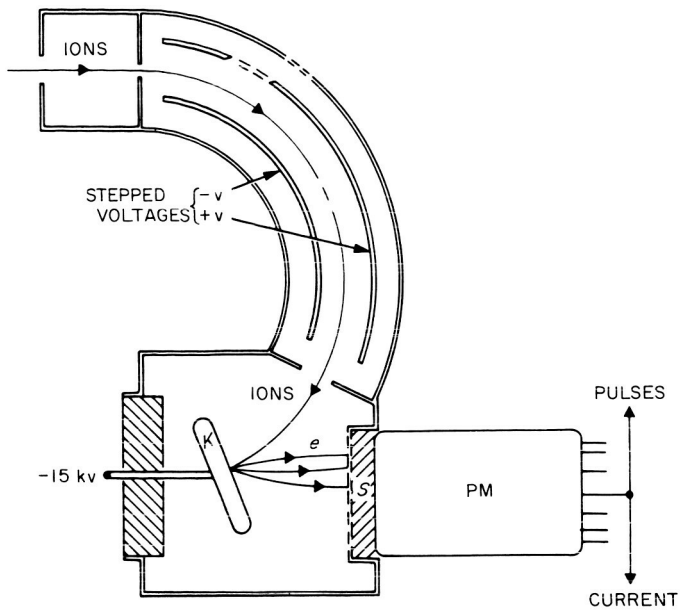


Fig. 25-1. Plasma experiment schematic

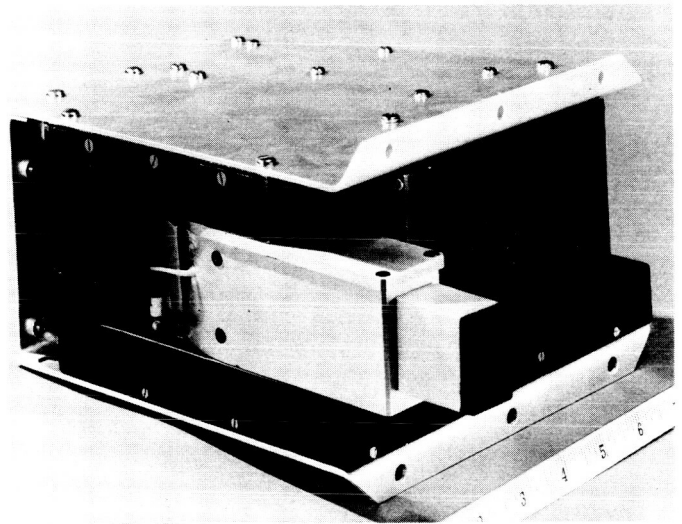


Fig. 25-2. Plasma experiment detector

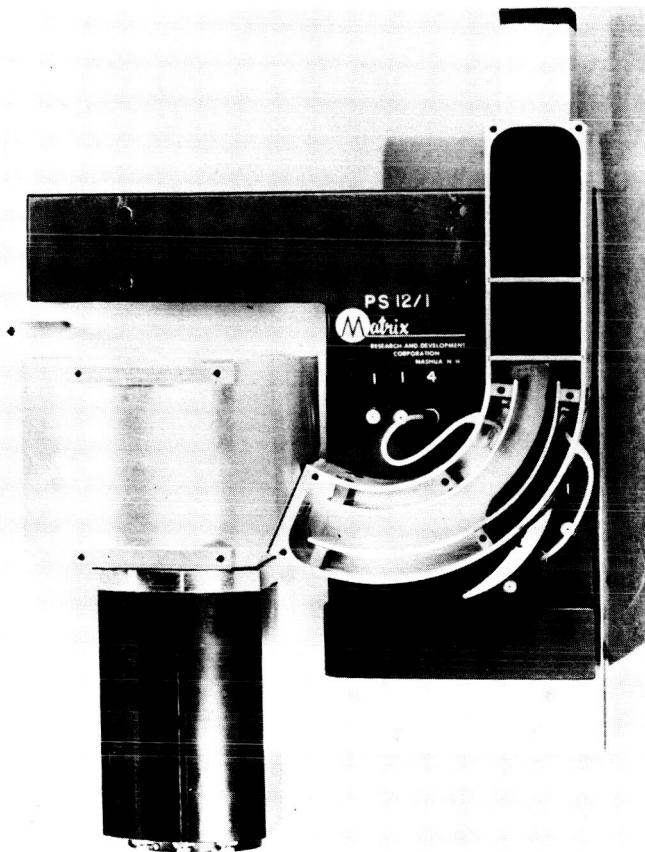


Fig. 25-3. Plasma experiment cutaway

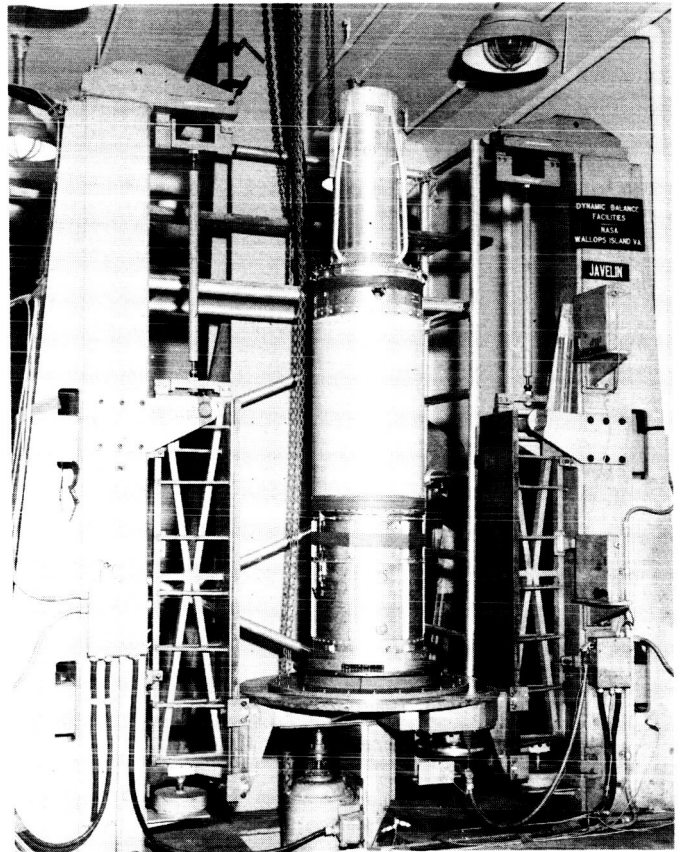


Fig. 25-4. Rocket payload at "spin and balance"



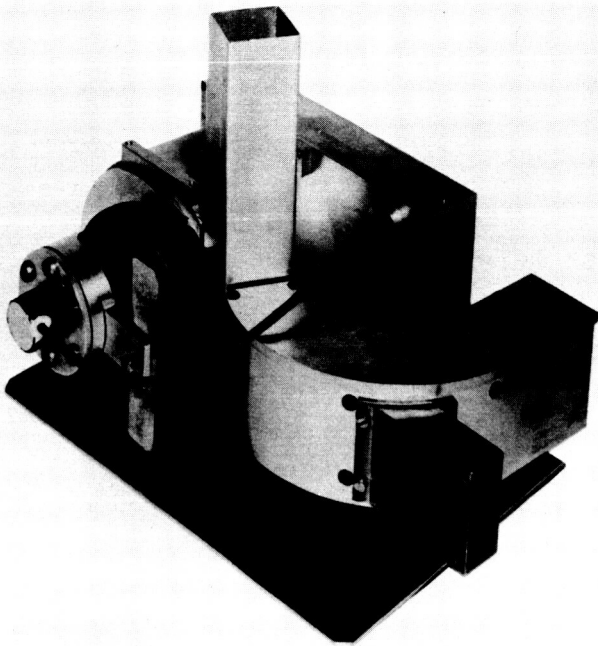


Fig. 25-5. Pressure experiment showing pumpout ports

Fig. 25-6. Test setup at Goddard

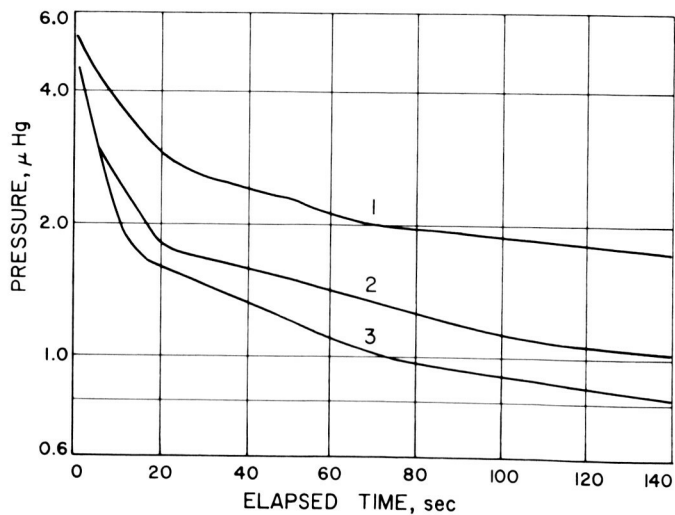
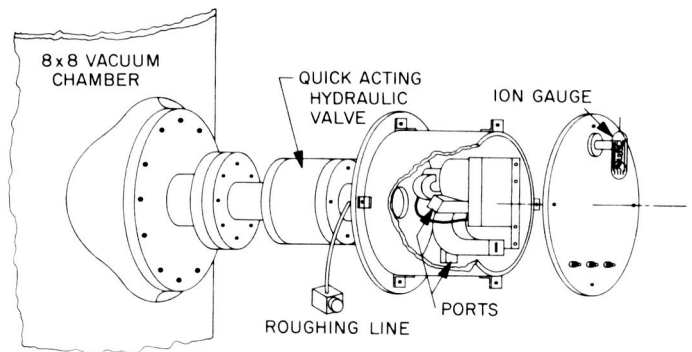


Fig. 25-7. Pressure inside plasma detector (initially at  $60\mu$ ) vs time of exposure to large chamber at  $1.3 \times 10^{-6}$  mm Hg for three consecutive runs

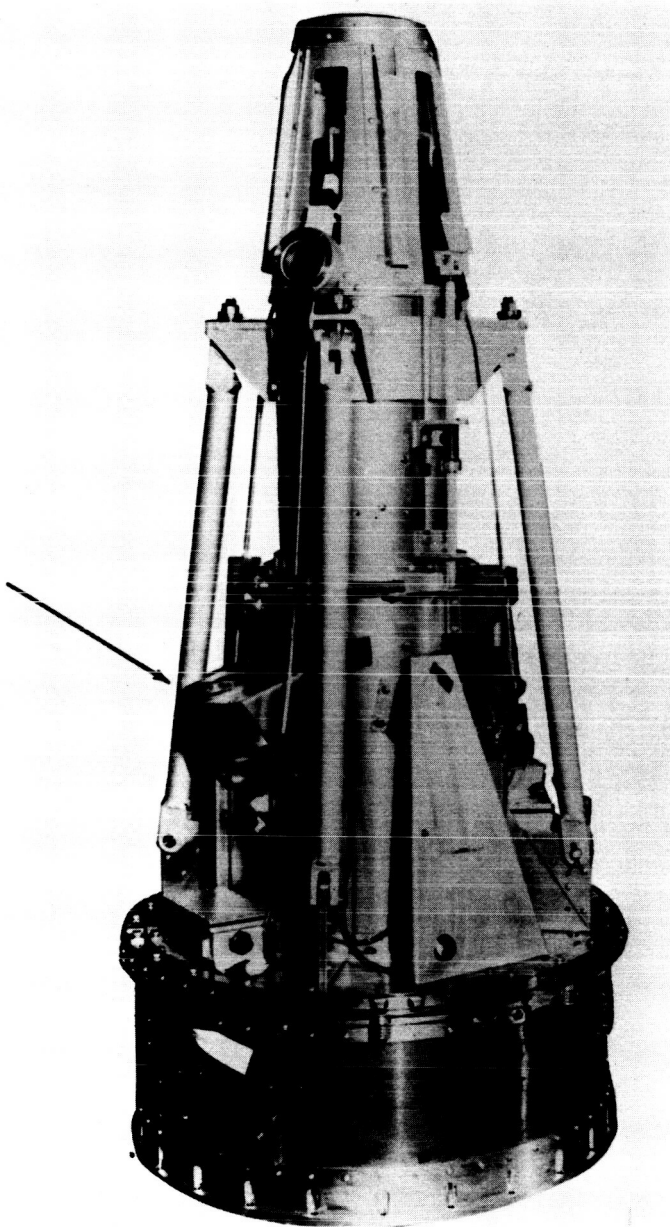


Fig. 25-8. Argo D4 payload showing pressure experiment (arrow)

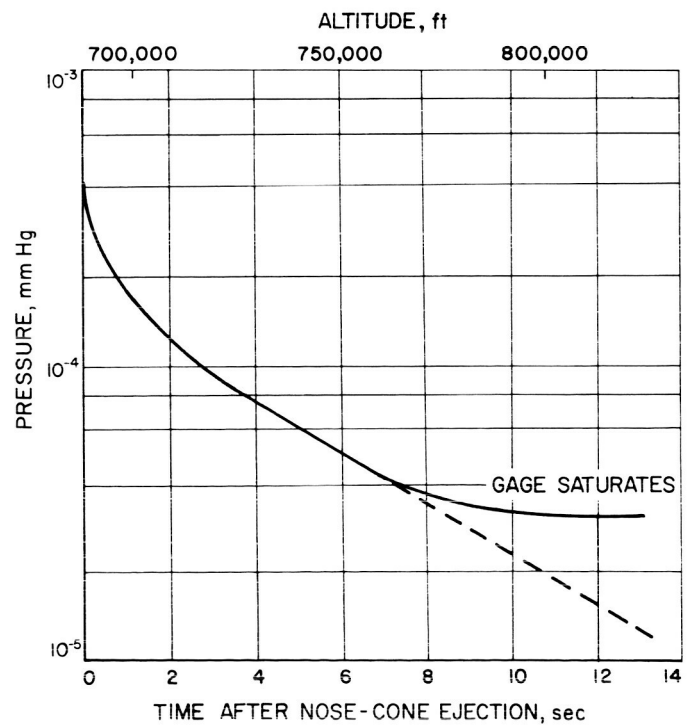


Fig. 25-9. Results of the rocket pressure experiment

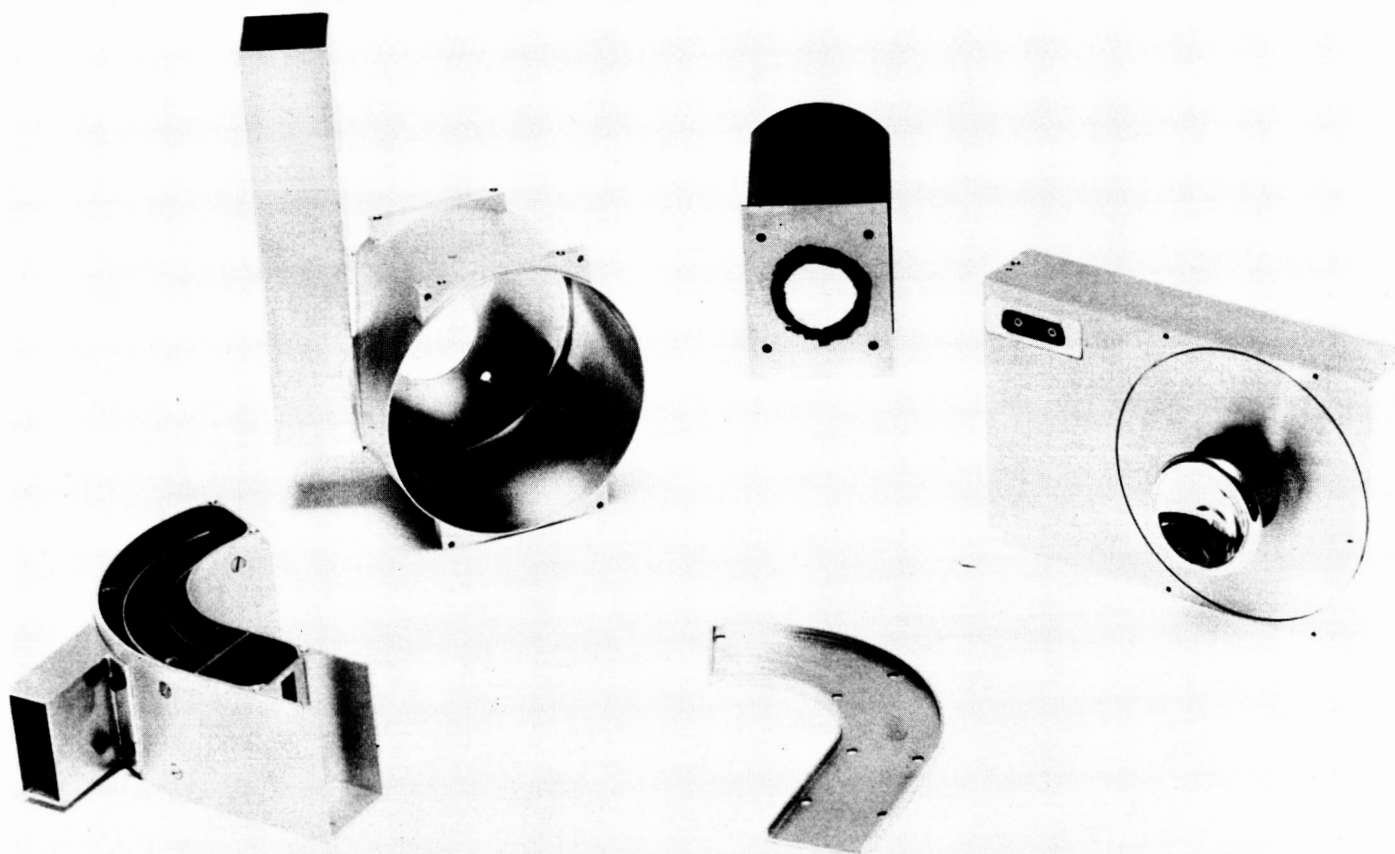


Fig. 25-10. Test setup at Goddard

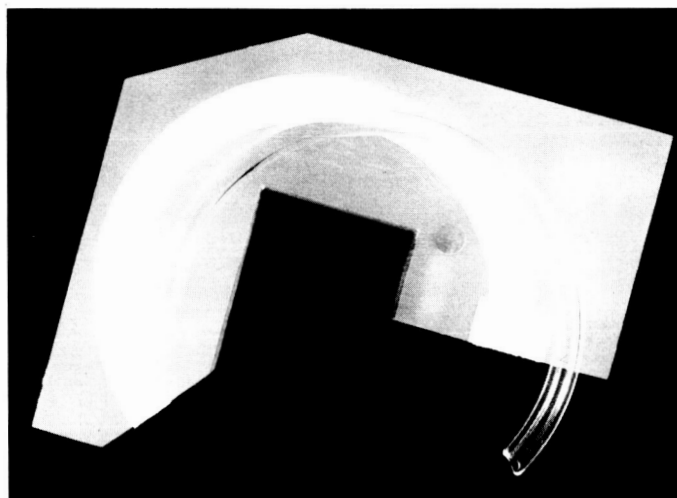


Fig. 25-11. Exploded view of improved plasma detector

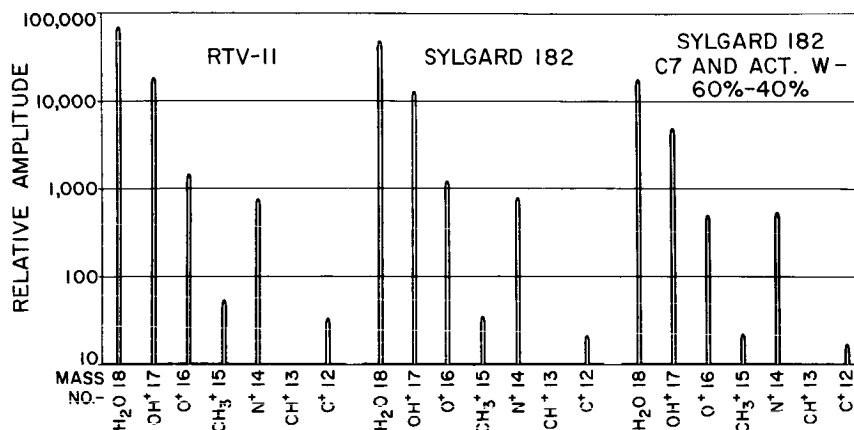


Fig. 25-12. Channel multiplier mockup

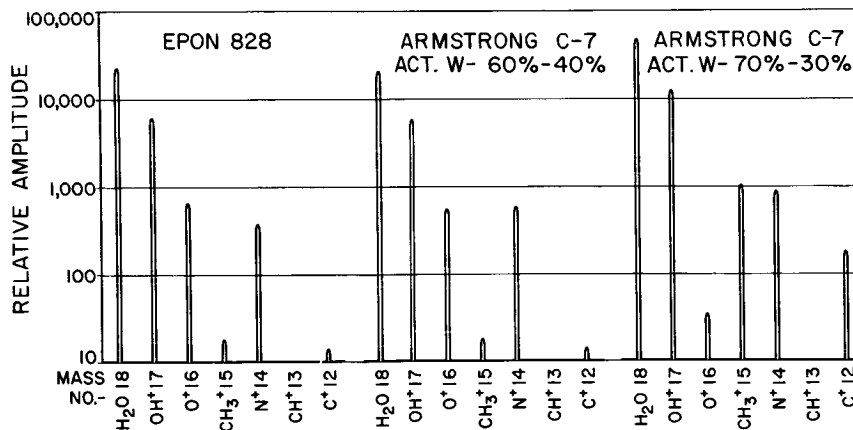


Fig. 25-13. Residual gas analysis for various silastics

## 26. GEMINI TRANSPONDER DEGASSING PROBLEMS

C. L. Brock\* and B. H. Vester  
Westinghouse Electric Corporation  
Baltimore, Maryland

(Presented by C. L. Brock)

Mr. B. H. Vester, Director of Engineering, Gemini Radar Project, is the author of the first subject of our presentation entitled "Glow Discharge Problems. Gemini Transponder". Mr. Vester was in Houston, Texas for the Gemini V mission scrubbed yesterday, and so could not be here. Therefore, I will give the first part of the paper for him.

The Gemini radar system consists of a radar unit and command link encoder on the spacecraft, and a transponder voltage preregulator and three antennas on the Agena vehicle. The command link encoder is a low-voltage foamed assembly and does not have any breakdown problem. The radar unit, because of the fact that it contains moving parts, was pressurized and hence does not encounter any discharge problems. The equipment on the Agena, however, was not pressurized, and we have had to solve a number of problems related to glow discharge phenomena. Both dc and rf voltage levels in the transponder are enough above Paschen's minimum to give problems at critical pressures. The transmitter has a peak output ranging from 1,150 to 1,400 w, carried through the system through various microwave components with characteristic impedances of 50 ohms. The high voltage used for the transmitter is 1,650 v. All other voltages in the system are well below Paschen's minimum. In order not to generate any mission constraints, it is desirable that this equipment be ready for operational use in 1 to 2 hr after launch.

Several things were done in the early design stage of the system to make it more immune to failure. For example, all the power supplies are designed to be short-circuit-proof. That is, their fault current is limited to a value such that none of the parts ratings can be exceeded under short-circuit conditions. An additional change was made later in the program such that the direct shorts across the high-voltage output to ground would not give transient fault currents, large enough to cause low power semiconductor circuits to fail because of ground coupling, cable coupling, etc. We feel it is highly desirable to design equipment that can survive

---

\* Now at The Sherman Fairchild Technology Center, Fairchild Hiller Corporation, Space Systems Division, Germantown, Maryland.

through the critical breakdown region whether or not it must operate there. This philosophy is followed in our system design.

In early vacuum tests on an engineering model of the transponder, we failed to detect the incipient glow discharge problem. In retrospect, we can see several possible reasons for this failure. First, the early parts had not completed their individual qualification test, and, in general, had not been "gunked up" with partial seals to pass humidity requirements. Another factor that undoubtedly led to not seeing the problem was that the vacuum chamber was allowed to pump down for 8 to 12 hr before attempting to operate the transponder. Incidentally, vacuum chamber pumpdown time is a serious constraint to working on and defining outgassing problems, and must be taken into account.

After we had solved our other known qualification test problems (humidity being a particular tough one to design for), a complete production-built transponder was subjected to formal qualification tests. We immediately ran into a series of problems in the thermal vacuum test, all caused by the basic glow discharge phenomena. The most serious of these problems was in the transmitter assembly itself. The transmitter is a self-excited oscillator using a ceramic planar triode mounted in a coaxial cavity. Although the plate voltage is only 1,650 v, there are rf voltages in the cavity resonator in the range of 5 to 7 kv. The transmitter not only had an initial dc breakdown, but also continued to breakdown in the rf portion after it had degassed for a few hours. In fact, this rf breakdown not only continued for hours, but for several days. The basic long-term problem in the transmitter was found to be a silicone grease, that was used for thermal conduction purposes. This grease served as a reservoir to supply continual outgassing over a long period of time (possibly for months) and the limited available vent area for outgassing allowed critical pressure to be maintained continuously inside the transmitter cavity.

We did some further investigation of high-vacuum greases and concluded that none of them would be satisfactory. There are greases rated for usage at pressures like  $10^{-12}$  torr, but even these absorbed enough volatile substances in the normal lab atmosphere to still outgas whenever a combination of temperature and vacuum was applied to it. As further investigation, we cleaned all grease from the transmitter and vacuum-baked the parts for an extended period of time to boil off any volatile substances. Even when this was done, the normal lab atmosphere over a day's span created enough contaminants in the transmitter assembly to still get

occasional discharges. In this transmitter case, the rf voltage gradients are high enough to impart considerable energy to any stray ions that are floating around. I believe there are also some field emission effects occurring that further contributed to breakdowns. The materials used in the transmitter assembly, though relatively immune to corona deterioration, still were not limited to just the small class of materials which are considered to be satisfactory for internal vacuum-tube usage. It appeared that the transmitter might have to be redesigned with vacuum-tube-acceptable materials, and even then we could not be sure that atmospheric contamination would not be absorbed to an extent to cause trouble at these high voltages. In light of this, we decided to pressurize the transmitter assembly. A seal adequate for a 2-week mission was easily obtained. To those of you who might want to solve your arcing problems by pressurization, we would like to recommend the use of O-ring seals on access holes; if applied correctly, they can give extremely low leakage rates.

The other problems encountered were in the microwave parts and antennas in the transmitter output path. With the 1,300 w or so of rf power in these parts (with 50 ohms characteristic impedances), voltages would be expected around the fringes of Paschen's minimum. With some rf "Q"-ing in the parts, however, these voltages will exceed the 270-v minimum. The rf components were not sealed, in general; however, more important, they were not intentionally vented. The breakdown observed was quite intermittent in nature, and the degassing time between different parts made to the same drawing was quite variable. In order to get positive degassing in a short period of time, these parts had vent holes added. In the case of small parts like this, vacuum pump capacity is not a limiting test factor; one can reduce environment around them to a good hard vacuum in a few minutes. This being so, we empirically determined the vent hole sizes required by testing how long the parts took to have their glow discharge clear with actual rf power applied. To get a reasonable safety margin, we used twice expected rf power on the parts where it was feasible. Though the parts are in a box which is well sealed against humidity, we decided to also design the vents such that they would still be satisfactory if the parts were exposed to Cape humidity. That is, we soaked them in a simulated worse-case Cape humidity condition, and then immediately determined their outgas time in a vacuum environment. Humidity, of course, is not the only possible contaminant. Parts may have fingerprints and other small traces of volatile contaminants inside, so we decided to also vacuum-bake all the parts prior to incorporating

them into transponders. A combination of maximum temperature and a hard vacuum will remove those volatiles which may have been introduced by the manufacturing cycle. Since the internal surfaces of the parts receive no further handling, this limits our outgassing problems to absorbed humidity. In general, we put large enough vent holes in the parts to allow them, even when humidity-laden, to clear up in 5 to 10 min after reaching hard vacuum.

The parts vented included such things as ferrite isolaters and circulators, coaxial cable connectors, antenna baluns, etc. I should mention here a problem encountered with coaxial cable that may be of interest. The cable used in the transponder was a glass cloth outer sheath, so any air around the coax outer braid will diffuse out rapidly in a vacuum. We have seen no problems with this type of cable. Breakdown problems were experienced several times, however, in the RG-9 test cables used external to the unit. These cables had well-vented connectors on them. The outer sheath, however, is of solid polyethylene, and undoubtedly there is a considerable amount of trapped air inside of it, which must leak out the ends of the cable. We haven't yet determined the exact failure mechanism, but we intend to explore this further to satisfy our curiosity as to exactly how the breakdown occurs. We suspect it is due to the trapped air finding its way out to regions in the connector where a dielectric barrier doesn't exist.

An interesting phenomenon observed on the antenna (these antennas are printed circuit spirals on a glass epoxy board) was an apparent outgassing effect caused by light illumination. An antenna was baked out at high temperature in hard vacuum until all breakdown had cleared. Then, it was allowed to cool in the vacuum jar. When the face of the antenna was then illuminated with either white light or ultra-violet light, it broke down for a short period of time and then cleared itself permanently. This was not observed with higher-level infrared illumination. Apparently, there was enough energy absorption from the frequencies in the UV end of the spectrum to cause some additional outgassing beyond what had been excited by the thermal input. This did clear itself indicating that it was an outgassing phenomena rather than energy absorption by the gases which were already there. This experiment was repeated several times with the same result.

Now that we have the components vented adequately, our problem is to vent the transponder in which they were mounted. We have previously sealed up this box to pass a very stringent operating humidity test (160°F at 95% relative humidity)



and had included an aneroid-operated exhaust valve to allow the box to vent upon insertion into orbit. We, incidentally, had chosen an aneroid valve instead of a burst diaphragm or blowout valve because of its inherent reliability; that is, its failure mode would be such as to leave the valve in an open position. It also operates on absolute pressure instead of differential pressure. With the parts well vented and a reasonable box vent, however, it still took a longer time than expected to get a satisfactory operation, even allowing for the chamber pumpdown time. We were curious about this and decided to instrument a transponder with an ion gage to actually determine what its internal pressure-time profile was. We also used several other ion gages in the vacuum chamber to be sure we knew exactly what the pressure immediately outside the box was. This precaution was necessary as there are pressure gradients in a typical vacuum chamber. The transponder gage showed that the internal pressure followed the chamber pressure quite well until the internal pressure reached about  $10^{-4}$  torr (transponder at about 110° F) where it flattened out and remained as an essentially constant value for many, many hours. This internal pressure showed a large dependence on temperature and, in fact, with 130 to 140° F the transponder temperature approached the critical breakdown region. We made some educated guesses as to what might cause this and concluded that it was probably something which covered a relatively large amount of the inside area of the box. The paint used internally appeared to be the only material whose chemistry indicated it might outgas at these pressures, and it did cover an appreciable area. To verify this, we instrumented an empty box with volume in area comparable to the transponder and containing the same size vent hole. We checked this internal pressure-time profile in the vacuum chamber with and without paint. The painted box gave almost identical results to those obtained on the transponder. This led to the obvious conclusion that we needed less paint and/or bigger vent holes to reduce this back pressure to acceptable limits. We were able to remove a large portion of the paint area and also enlarge the vent hole enough to give us internal pressure levels (under worst temperature conditions) that are at least an order of magnitude below the critical region.

(I'll cover this last phenomenon in greater detail before concluding, and offer some more widely applicable approach to the degassing problem.)

Before turning to observed data and mathematical treatment, I would like to suggest that we use slightly different terminology to describe the phenomena we

have been talking about. One possibility is "glow discharge" rather than "corona," since it is not primarily a voltage gradient problem.

I believe we can learn a lot from people who design glow discharge or TR tubes. I think you'll find they have much more useful information on our vacuum problem than the people who have concerned themselves with ground level corona problems.

The preceding was prepared by Mr. B. H. Vester, Director of Engineering, Gemini Radar, who, as I said, was in Houston yesterday for the expected Gemini V launch.

Any questions I can't answer, I'll note and ask Mr. Vester to do so. However, let me add what follows and then take all the questions at the same time.

In this section, entitled "Pressure History Prediction: Gemini Transponder," I'll offer some material on the pressure history prediction for the Gemini transponder.

The transponder of the Gemini radar system on the Agena vehicle provides an excellent example of an analytic solution to a degassing problem: That is, how does the internal pressure vary with time after launching for a package with an arbitrary vent-orifice size and containing baked out materials with their characteristic stationary rates of thermal decomposition.

During the vacuum chamber test, a longer time was required for satisfactory operation of the transponder than expected. Additional testing with an ion gage measuring the thermal pressure showed that it was decreasing to a steady value near  $10^{-4}$  torr at about  $110^{\circ}\text{F}$ , instead of approaching the vacuum chamber pressure near  $10^{-6}$  torr. The persistent pressure was observed to decrease with temperature decreases and increase with temperature increases. A model (shown in Fig. 26-1) is adopted to account for this behavior which consists of (1) a film source of volatile decomposition products in the transponder yielding a constant molal input rate at a given transponder temperature maintained by radiating heating, (2) the transponder volume, empty space confining air and vapors until they are released by expansion flow or molecular flow through the (3) orifice into the (4) vacuum chamber volume, which is shrouded with liquid nitrogen at about  $-280^{\circ}\text{F}$  and finally (5) vacuum pumps.

Figure 26-2 shows results that were obtained with a transponder with about  $0.66\text{ ft}^3$  free volume, 1-1/2-in. vent hole, and about  $6\text{ ft}^2$  of vinyl paint on the

internal surfaces. In Fig. 26-2A, as the temperature decreased from 115°F down to 40°F, the pressure decreased from  $10^{-4}$  to  $4 \times 10^{-6}$  torr. In the tests shown in Fig. 26-2B, the pressure stabilized to  $10^{-4}$  mm Hg at 110°F before we cut off the nitrogen cooling of the vacuum chamber at the end of the test. As shown in Fig. 26-2C, when provided with two vent holes instead of one, the same transponder stabilized to  $5 \times 10^{-5}$  mm Hg at 110°F. This pressure is exactly what one would predict with constant vapor production rate and molecular flow through twice the hole area (and negligible back flow from the vacuum chamber).

The results plotted in Fig. 26-3A are for empty metal boxes (which I call simulated transponders). They are geometrically similar to the real transponder. In Fig. 26-3A, the variation of pressures with temperature due to decomposition or outgassing of the vinyl chloride coating in a simulated transponder is vividly demonstrated. You note as the temperature goes up, the pressure jumps up. In Fig. 26-3B, the pressure in an empty simulated transponder almost, but not quite, follows the vacuum chamber pressure. In Fig. 26-3C, it is shown that an epoxy finish in the simulated transponder also is subject to significant thermal decomposition or outgassing, so it is possible that inadequate venting could cause voltage breakdown problems in any unpressurized system containing organic material.

As shown in Fig. 26-4, the rate of pressure decrease in the initial period of venting is proportional to the adiabatic expansion molal flow rate. Since the molal flow rate is an ungraceful function of both the transponder pressure ( $P_t$ ) and the external pressure ( $P_c$ ) derived from the familiar adiabatic flow relations for an ideal gas, integration to obtain a simple time function is impossible. Nevertheless, integration by finite differences shows that a well-vented package such as the Gemini transponder follows the external pressure very closely during the expansion flow period.

The rate of pressure decrease during the second period of venting would be proportional to the molecular flow out the orifice ( $m_m$ ) except for the stationary molal decomposition rate ( $m_f$ ) or outgassing of the vinyl coating. At steady state, the two molal rates are equal; this is the basis for experimental measurement of the decomposition, or outgassing, rate as a function of temperature. As the molal flow rate is a simple function of the internal pressure ( $P_t$ ) and external pressure ( $P_c$ ), and the molal outgassing rate ( $m_f$ ) is a function of temperature only (for fairly limited times), the integration gives a simple time function if the external pressure

( $P_c$ ) is also given as a suitable function of time. At any rate, it approaches a constant asymptotic value of pressure, for in a well-vented package after a short time the molecular flow out the vent hole is proportional to the molal decomposition rate and inversely proportional to the vent orifice area, which is as it should be.

In Fig. 26-4 we have some numerical results calculated for the Gemini transponder. The internal pressure ( $P_t$ ) is calculated with the external pressure ( $P_c$ ), varying in accordance with the mission profile. The apparent discontinuity in the curve for  $P_t$  is due to the assumption that the transition from expansion flow to molecular flow occurs exactly at  $P_c = 10^{-2}$  psf ( $4 \times 10^{-3}$  mm). Actually, both types of flow exist consistent with the variation of probability of air or vapor molecules passing through the orifice without collision with another molecule. The dashed lines for  $P_t$  through the transition region approximate the probable variation free from discontinuity. Observe that the pressure is vented down to well below  $10^{-3}$  torr within 5 min or 300 sec at 140°F or lower temperature. Therefore, it has been confirmed that the pressure will be at least an order of magnitude below the critical region.

We wondered if the breakdown voltage would be different for the typical outgassing vapors than for air. The comparative voltage breakdown data plotted in Fig. 26-5 shows that typical decomposition products free from organic materials have substantially the same extinction voltages as air. Rounded points (1/4 in.) were at positive polarity centered in 3 x 5 x 7 in. metal box painted inside except for the air tests. We don't show any temperatures for the air tests because heating wasn't required to build pressure back up in the test box.

#### OPEN DISCUSSION

VOICE: Would you explain that last curve a little bit more?

MR. BROCK: Right. The voltages were discharged according to our method of operation after breakdown had commenced. The test procedure was to evacuate the small metal box in a bell jar down to around  $10^{-6}$  torr, then heat was applied to the outside of the metal box until the pressure built up due to outgassing. This box was not sealed, but some leakage was permitted around the cover. But there were small enough openings for flow so that pressure would build up as the box was heated.

When we heated it up to a steady temperature where steady pressure was observed, we would apply voltages raising it slowly until we got breakdown as indicated by a neon bulb outside the test assembly. Then we would back off from the voltage until we no longer got indication of breakdown (called extinction voltage), and we considered it to be on the safe side for our operation. Really, the points on this curve don't have much absolute significance except that they show there's not much difference between air and the vapors of the materials we tested.

MR. BROWN: I wish to say that I'm sorry Mr. Vester isn't here because I believe he could give us some ad lib information that would be quite timely. In his absence, I want to cite an example of a problem that may possibly be of interest. Since I stood at arm's length to the problem, I'll only repeat what I know of it. I feel somewhat responsible because I didn't do something that we all neglect to do at times, and that is exchange information related to corona, and I wish to cite the example to point it out.

This example happened in St. Louis that people knew would happen; others have learned (I think JPL learned) that when you go through critical altitude you can't have things turned on. But some people were doing flight testing or altitude testing of a particular radar in St. Louis and inadvertently had the radar turned on. The results were as one would expect. They had a corona problem show up on the antenna, and, in turn, they shut down the radar and corrected the situation. But, they didn't know they were going to get corona. I feel responsible because I didn't pass on information, but I wasn't in the chain that was supposed to tell people this sort of thing. I think the responsibility is part mine, as well as others, to pass information on. I hope this meeting will do this. That's why I want to document the fact that we do have this continuing problem in exchange of information. In this case, it was confirmed that the corona was evidenced by the fact that they had a power loss as measured and a high VSWR (which was telemetered). Later it was confirmed that no damage was done to the triode. This triode wasn't damaged. As a result, they went back in and used the same radar for flight but as a result of this mismatch, the pulse width as a result of the loading shortened, which in turn caused the power to actually go down, and the voltage, of course, to go up. It wasn't a problem with the voltage going up and arcing in any way; the radar wasn't damaged as a result of it. Nevertheless, we learned a lot.

I learned that you do have to exchange information--the sort of thing we're dispensing now in this meeting--to all sources so that they do know these things and so it won't happen again. I wish to point that out very emphatically.

MR. BROCK: Now, I'm a little curious as to one thing. The radar itself is pressurized, so going through a test in which the external environment goes through the critical region shouldn't make a bit of difference.

MR. BROWN: Well, the radar itself is pressurized, but your antenna isn't. I mean, the corona developed at the antenna. Mr. Vester knew of this, and I went back through NASA-McDonnell, and also went through your local rep at the Cape to tell them what happened and why they shouldn't do it any more. But I was surprised they didn't know this was going to occur. I guess everyone else assumed too much. As a result, it did occur. The radar was not intended to be turned on during this altitude run, and in flight, of course, it will not be turned on, as you go through the critical altitude. I believe the intent of the transponder is just prior to liftoff a bathtub plug is pulled out so it will depressurize.

MR. BROCK: To exclude humidity.

MR. BROWN: Right. But they will keep it closed until just shortly before liftoff.

MR. LINDER: If I understood you right, you used the dc Paschen minimum to estimate breakdown in the rf 50-ohm line. I think this might give you a considerable overestimate in many cases.

MR. BROCK: I'm sure it would. This was just shown as something to compare with. It's really not very valid for anything.

MR. LINDER: I think although the curve is similar in shape it might very well take on different and lower values at higher frequency.

MR. BROCK: I'm sure that would be true.

VOICE: Let me give just one reference. There is a paper, "The Space Environment as a Dielectric," by A. S. Denholm, Ion Physics Corporation, Burlington, Massachusetts. He discusses where and when you can use the space vacuum and where not. This was given in the Dielectrics in Space symposium held by Westinghouse in 1963.

MR. NEWTON: Maybe I misunderstood you, but you're venting for outgassing effects and yet you're playing around with humidity. Do you do it at the same time or what do you do?

MR. BROCK: The humidity is a very short-time thing. We have cleaned the system up very well and we've found that even with the small hole and with all the paint we originally had, we could get it out in 5 to 10 min. The paint outgassing is a much more persistent thing, and went on for many hours.

VOICE: May I add a little philosophy on this? This business of venting is a very realistic situation at the Cape because we've had sealed wave guides down there--supposedly sealed--that breathe. Now, if you vent and you don't go through a temperature cycle, you don't suck back in the humidity. If you vent and the air goes out and you don't suck back in the air later due to the temperature cycle, then there appears to be no problem. At least this has been the experience in the past. We've had trouble with wave guides of that type down there.

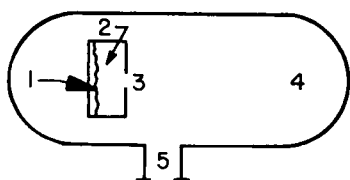


Fig. 26-1. Model for experimental measurements

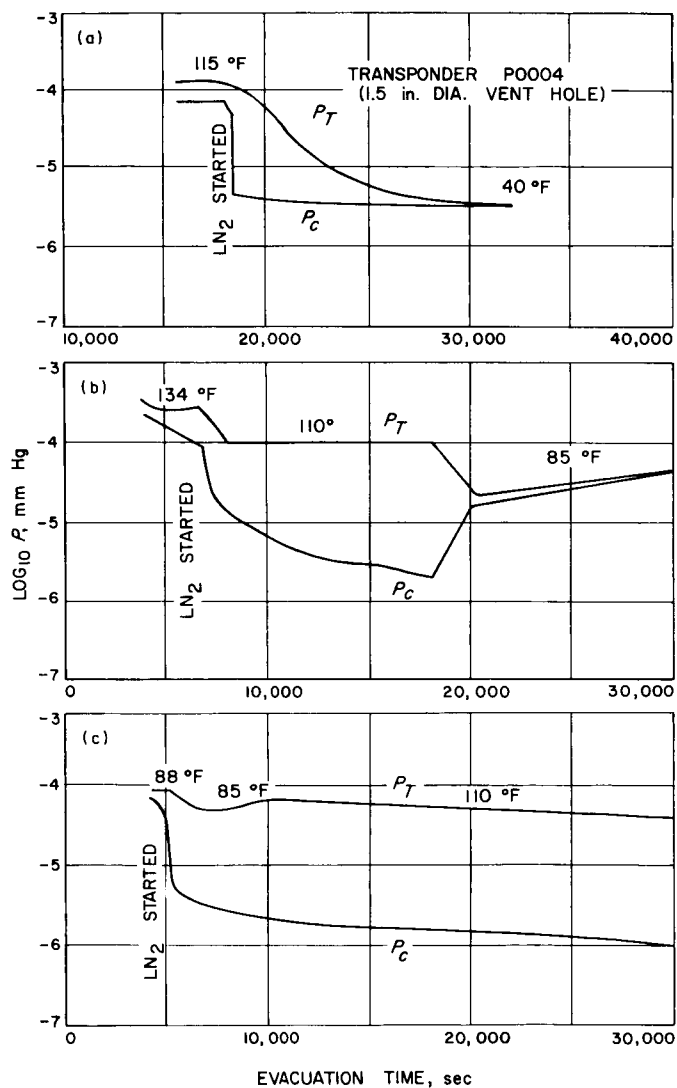


Fig. 26-2. Experimental pressures for transponder

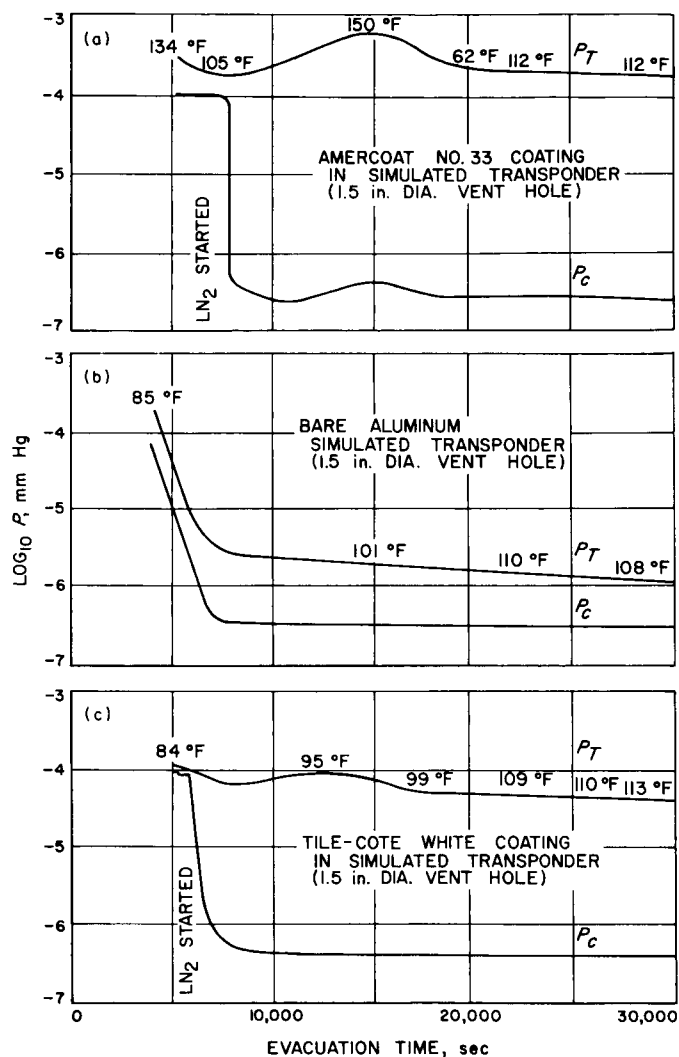


Fig. 26-3. Experimental pressures for simulated transponders



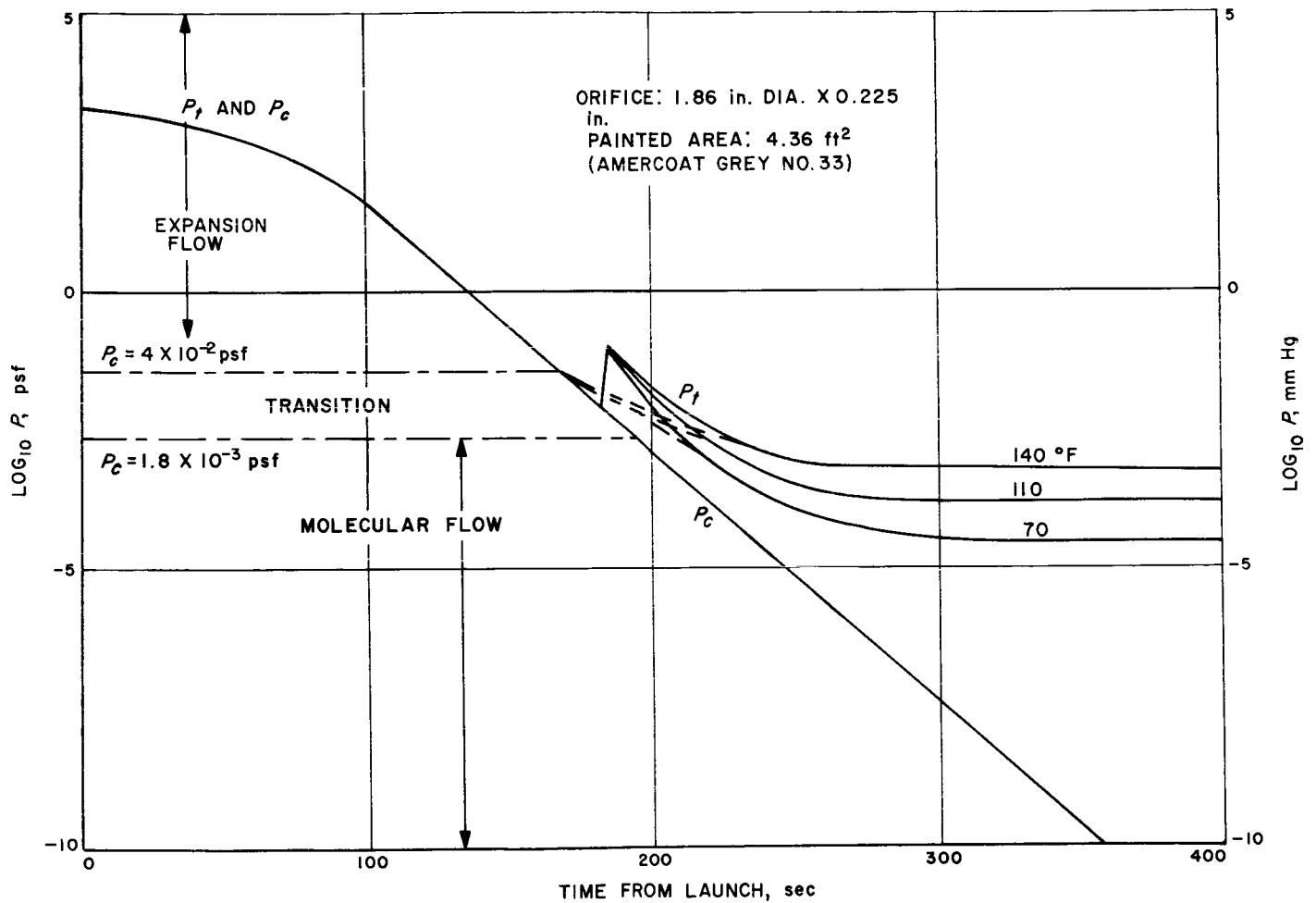


Fig. 26-4. Pressure history predictions for Gemini radar transponder

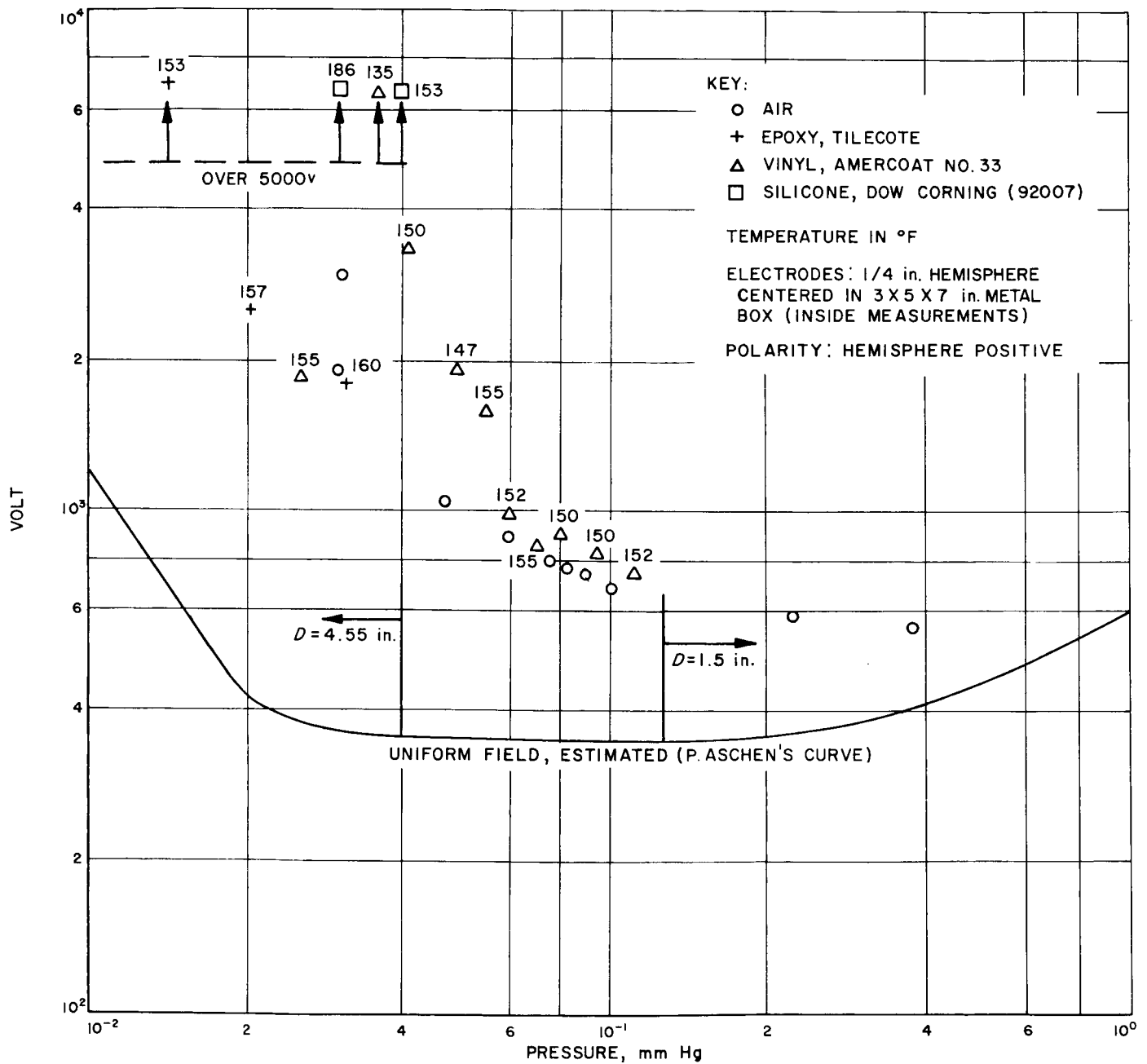


Fig. 26-5. Extinction voltages for air and vapors from heated materials

## 27. DIFFUSION OF GASES IN POLYMERIC FOAMS

E. F. Cuddihy and J. Moacanin  
Jet Propulsion Laboratory  
California Institute of Technology  
Pasadena, California

## ABSTRACT

It was found that the diffusion behavior of gases in rigid closed-cell foams could be described mathematically by conventional diffusion equations. An experimental method was developed for the determination of diffusion coefficients of gases in foams. In addition, the following equation

$$D = P_e \frac{(3RT)}{M} (\rho_0/\rho)$$

was derived which relates the diffusion coefficient to the foam density  $\rho$ , the molecular weight of the blowing gas  $M$ , and the density  $\rho_0$  and permeation constant  $P_e$  of the bulk polymer.

The applicability of the equation was tested by experimentally measuring the diffusion coefficients for low density, rigid closed-cell polyurethane foams containing  $\text{CO}_2$ .

## INTRODUCTION

Currently, there is considerable interest in the possibility of using polymeric foams as lightweight encapsulants for electronic components on spacecrafts. Very little is known, however, on the electrical breakdown behavior in foams. In this respect an important parameter is the pressure of the blowing gas within the foam cells, in particular, when the pressure lowers sufficiently to allow corona or arcing (Paschen's law) to occur between sites of high voltage. It is necessary, therefore, to be able to describe the internal pressure distribution within a foam when exposed to reduced pressure.

The purpose of this report is: (a) to demonstrate that the diffusion behavior of rigid closed-cell foams can be described by conventional diffusion theory, (b) to present a relationship which relates the diffusion constant  $D$  for a foam to its density and

the permeation constant for the bulk polymer, (c) to describe the experimental techniques for determining D and (d) to discuss experimental results on closed cell polyurethane foams.

### DIFFUSION EQUATIONS

Diffusion equations for polymeric foams were developed using as a simple, but physically reasonable model, a three-dimensional array of cubical cells having walls of uniform thickness and permeable to gases. Here, only one-dimensional diffusion is considered, although extension to the three-dimensional case is straightforward.

The general relation for the flux J at which a gas permeates through a membrane is

$$J = \frac{dw}{dt} = \frac{P_e A}{L} \Delta P \quad (1)$$

where

$\dot{w}$  = weight of gas

$P_e$  = permeation constant

A = area

L = thickness of membrane

$\Delta P$  = pressure difference across the membrane

t = time

The net flux for the nth layer of cells is given by

$$\frac{dw_n}{dt} = J_{n+1} - J_{n-1} \quad (2)$$

which, upon substituting for J, yields

$$\frac{L}{P_e A} \frac{dw_n}{dt} = P_{n+1} - 2P_n + P_{n-1} \quad (3)$$

From the perfect gas law,

$$w_n = P_n \frac{VM}{RT} \quad (4)$$

which can be substituted into Eq. (3) to yield the following differential equation:

$$\frac{LVM}{P_e ART} \frac{dp_n}{dt} = P_{n+1} - 2P_n + P_{n-1} \quad (5)$$

for the pressure  $P_n$  in the  $n$ th layer of cells.

Thus for a system of  $N$  layers, we have a set of  $N$  linear homogeneous equations. For the boundary condition that the external pressure is always zero, along with the initial condition that for zero time the pressure  $P_0$  in all layers is uniform, the following relationship is obtained:

$$\frac{P_n(t)}{P_0} = \sum_{k=1}^N a_k \left[ \sin \frac{\pi n(2k-1)}{2N+1} \right] \exp \left\{ - \left( \frac{P_e ART}{LVM} \right) \left[ 2 - 2 \cos \frac{\pi(2k-1)}{2N+1} \right] t \right\} \quad (6)$$

For the limiting case of  $N \rightarrow \infty$ , the coefficients  $a_k$  can be readily evaluated, and the solution becomes

$$\frac{P_n(t)}{P_0} = \frac{4}{\pi} \sum_{k=1}^{\infty} \frac{1}{(2k-1)} \sin \left[ \frac{\pi(2k-1)n}{2N} \right] \exp \left\{ - \left( \frac{P_e ART}{LVM} \right) \left[ \frac{\pi(2k-1)}{2N} \right]^2 t \right\} \quad (7)$$

If  $N > 20$ , values of  $a_k$  for the limiting case of  $N \rightarrow \infty$  can be used without introducing a significant error. Inasmuch as for a 1-in. thick-foam,  $N$  is of the order of a few hundred, Eq. (7) is applicable for all cases of interest. Now, if formally we consider the gas as a diffusion process in a medium characterized by a diffusion constant  $D$ , the following well-known equation is appropriate (Ref. 1 and 2):

$$\frac{P_x}{P_0} = \frac{C_x}{C_0} = \frac{4}{\pi} \sum_{k=1}^{\infty} \frac{1}{(2k-1)} \sin \left[ \frac{\pi x(2k-1)}{2a} \right] \exp \left\{ - \left[ \frac{(2k-1)\pi}{2a} \right]^2 Dt \right\} \quad (8)$$

where

$C_x$  = concentration of gas

$C_0$  = initial concentration

$a$  = thickness of solid

$x$  = distance in from exposed surface

$D$  = diffusion constant

This equation is identical to Eq. (7) only at the limit  $N \rightarrow \infty$ . But, again it will be a close enough approximation for large  $N$ . Noting that since  $n/N = x/a$ , the coefficients in both equations are identical and hence the arguments of the exponential for Eq. (7) and (8) must be equal; thus

$$\frac{D}{a^2} = \frac{P_e ART}{LVMN^2} \quad (9)$$

As  $V/A$  is the length of the side of a cell  $d$ , we substitute and rearrange Eq. (9) to get

$$D = P_e \left( \frac{RT}{M} \right) \frac{a^2}{(NL)(Nd)} \quad (10)$$

As  $a$  is the thickness of the foam and  $NL$  and  $Nd$  are the thickness of the membranes and the cells respectively, it follows that  $a = NL + Nd$ . The ratio  $a^2 / (NL) \times (Nd)$  can be readily expressed in terms of the densities of the foam  $\rho$  and the bulk polymer  $\rho_0$ . For a cube of unit dimensions, i. e.,  $a = 1$ , which contains  $N^3$  cells, the total volume of cells is  $(Nd)^3$ . This volume represents the volume fraction of voids and is therefore equal to  $(1 - \rho/\rho_0)$ . Thus  $(Nd)$  is equal to  $(1 - \rho/\rho_0)^{1/3}$  and since  $(Nd) + (NL) = 1$ ,  $(NL)$  is equal to  $1 - (1 - \rho/\rho_0)^{1/3}$ . Substituting for  $(NL)$  and  $(Nd)$  in Eq. (10) and factoring out  $\rho_0/\rho$ , the following expression is obtained:

$$D = P_e \left( \frac{RT}{M} \right) \left( \frac{\rho_0}{\rho} \right) \left[ \frac{1}{(1 - \rho/\rho_0)^{1/3}} + 1 + (1 - \rho/\rho_0)^{1/3} \right] \quad (11)$$

where

$\rho$  = density of foam

$\rho_0$  = density of membrane material

The expression

$$\left[ \frac{1}{(1 - \rho/\rho_0)^{1/3}} + 1 + (1 - \rho/\rho_0)^{1/3} \right]$$

varies slowly between 3 and 3.05 as  $\rho/\rho_0$  varies between 0 and 0.5. Since most polymer foams are of low density, this term will be taken as being equal to 3. Equation (11) can be written as

$$D = P_e \frac{(3RT)}{M} (\rho_0/\rho) \quad (12)$$

which shows that  $D$  is proportional to  $P_e$  and inversely proportional to the foam density. For a family of foams Eq. (12) can be written as

$$D = K/\rho \quad (13)$$

where  $K$  is a constant characteristic of a given polymer-gas system.

$P_e$  values are available in the literature for many systems. Recently a table was published (Table 1) which gives  $P_e$  values for a wide combination of polymers and gases.

## EXPERIMENTAL

The diffusion coefficients were determined by measuring the loss of weight under vacuum from foam samples; the blowing gas was restricted to unidirectional diffusion. The weight loss  $Q$  is given by the integrated form of Eq. (8):

$$Q = Q_\infty - \frac{8Q_\infty}{\pi^2} \sum_{k=1}^{\infty} \frac{1}{(2k-1)^2} \exp \left\{ - \left[ \frac{(2k-1)\pi}{2a} \right]^2 Dt \right\} \quad (14)$$

where  $Q_{\infty}$  is the initial weight of gas in the foam. After a sufficiently long time, all the exponential terms except the first ( $k = 1$ ) can be neglected and the equation then reduces to

$$Q = Q_{\infty} - \left( \frac{8Q_{\infty}}{\pi^2} \right) \exp \left\{ - \left[ \frac{\pi}{2a} \right]^2 Dt \right\} \quad (15)$$

or

$$\ln(Q_{\infty} - Q) = \ln \left( \frac{8Q_{\infty}}{\pi^2} \right) - \left[ \frac{\pi}{2a} \right]^2 Dt \quad (16)$$

Thus a plot of  $\ln(Q_{\infty} - Q)$  versus time will eventually become linear with a slope of  $[\pi/2a]^2 D$ , from which  $D$  can be calculated.

To obtain weight-loss data, foams of 3-in. diameter and 1-in. deep were bonded into aluminum containers, leaving the top surface exposed. The bonding agent was Eccobond 55,<sup>1</sup> a room-temperature curing epoxy.

Weight-loss data at room temperature,  $22 \pm 1^{\circ}\text{C}$ , were obtained with an Ainsworth vacuum balance unit. The balance and details of sample suspension are shown in Fig. 1 and 2.

For elevated temperatures, weight loss was measured with a Cahn RH Electro-balance, which was situated inside a vacuum unit manufactured by the Consolidated Vacuum Corporation. The sample was heated by means of a variac-controlled 250-w bulb. A temperature differential of less than one degree was maintained across the sample by means of a reflecting aluminum shroud (Fig. 3 and 4).

The following polymer foams were investigated:

1. Eccosil 5000,<sup>1</sup> a syntactic silicone foam of nominal sp. gr. 0.48, prepared by mixing together hollow silicone spheres and a silicone resin.

---

<sup>1</sup>All foams and bonding agent were supplied by Emerson and Cuming, Inc.



2. Eccofoam SH,<sup>1</sup> a nominal 8-lb/ft<sup>3</sup> polyurethane foam filled with CO<sub>2</sub> gas. This material is purchased already blown in 1-in.-thick sheet stock. Actual measured density of the sample was 7.6 lb/ft<sup>3</sup>.
3. Stycast 1090,<sup>1</sup> a syntactic epoxy foam prepared by mixing together hollow glass spheres and an epoxy resin. System cures hard with a nominal sp. gr. of 0.78.
4. Eccofoam FPH/12/2H,<sup>1</sup> a nominal 2-lb/ft<sup>3</sup> polyurethane foam filled with CO<sub>2</sub> gas. Material prepared prior to test by mixing a resin-catalyst system and allowing the combination to foam and cure. Density of sample was 2.1 lb/ft<sup>3</sup>.
5. Eccofoam FPH/12/6H,<sup>1</sup> a nominal 6-lb/ft<sup>3</sup> polyurethane foam filled with CO<sub>2</sub> gas. Material prepared prior to test by mixing a resin-catalyst system together and pouring into a mold 2-in. deep and 3 in. in diameter. Using an appropriate weight schedule, the foaming reaction would result in about half of the cured material extending above the top of the mold. Samples prepared from the top and bottom halves were found to be 4.5 and 6.4 lb/ft<sup>3</sup> respectively.

The initial weights of CO<sub>2</sub> gas ( $Q_{\infty}$ , mg) in all foams were calculated using the perfect gas law and 1 atm of pressure.

## RESULTS AND DISCUSSION

Weight-loss curves for Eccosil 5000, Eccofoam SH, and Stycast 1090 are shown in Fig. 5. The outgassing rates of these materials parallel the known order of their respective gas-permeability constants (Ref. 3). Eccosil 5000 lost 180 mg of weight in 225 hr, approximately 90 mg more than the calculated CO<sub>2</sub> content of 90 to 100 mg ( $Q_{\infty}$ ). The additional weight loss presumably results from volatile impurities or volatile components that were not consumed in the curing reaction.

The rate of weight loss for Stycast 1090 is extremely low, as only 3.5 mg out of a possible 70 mg of gas were removed under vacuum in approximately 130 hr.

This is to be expected because the  $\text{CO}_2$  gas is contained inside glass spheres of low permeability. In addition, the high density of this material results in the formation of very thick membranes between the glass spheres.

For the Eccofoam SH, the plot of  $\log (Q_\infty - Q)$  vs time shown in Fig. 6 was constructed from the weight loss data (Fig. 5) and  $Q_\infty = 184$  mg. Using Eq. (16) and the slope of the linear portion of the curve ( $t > 120$  hr), a diffusion coefficient of  $2.40 \times 10^{-6} \text{ cm}^2/\text{sec}$  at  $22^\circ\text{C}$  was calculated.

Weight loss curves at  $22^\circ\text{C}$  for three Eccofoam FPH systems of densities 2.1, 4.5, and 6.4  $\text{lb}/\text{ft}^3$  are shown in Fig. 7. Using these data, plots of  $\log (Q_\infty - Q)$  vs time were obtained (Fig. 8), and the diffusion coefficients were found to be  $6.2 \times 10^{-7} \text{ cm}^2/\text{sec}$  for the 2.1 -  $\text{lb}/\text{ft}^3$  foam,  $1.76 \times 10^{-6} \text{ cm}^2/\text{sec}$  for the 4.5- $\text{lb}/\text{ft}^3$  foam, and  $1.24 \times 10^{-6} \text{ cm}^2/\text{sec}$  for the 6.4 -  $\text{lb}/\text{ft}^3$  foam. The values used for  $Q_\infty$ , which were calculated with an assumed initial gas pressure of 1 atm, were, respectively, 203 mg, 194 mg, and 188 mg of  $\text{CO}_2$ .

From Eq. (12), the diffusion coefficient should be inversely proportional to the density. This relationship holds true for the 4.5- and 6.4- $\text{lb}/\text{ft}^3$  foams, but not for the 2.1- $\text{lb}/\text{ft}^3$  foam, which in fact has the lowest diffusion coefficient of the three. However, this is inconsistent with the faster initial outgassing rate observed for the 2.1- $\text{lb}/\text{ft}^3$  foam. This discrepancy can arise from an incorrectly chosen value of  $Q_\infty$ . Equation (14) shows that  $D$  is inversely proportional to  $Q_\infty$ . Thus a higher value of  $D$  can be obtained from the  $\log (Q_\infty - Q)$  plots by using a lower value of  $Q_\infty$ . Support for the use of a lower value of  $Q_\infty$  can be seen from Fig. 7, where the weight loss curve for the 2.1- $\text{lb}/\text{ft}^3$  foam is apparently approaching an asymptotic value of  $Q_\infty$  that is considerably less than the calculated value of  $Q_\infty$ . From Eq. (13) and the diffusion coefficients for the 4.5- and 6.4- $\text{lb}/\text{ft}^3$  foam, a value of  $3.76 \times 10^{-6} \text{ cm}^2/\text{sec}$  is predicted for the 2.1- $\text{lb}/\text{ft}^3$  foam. Using the latter value for the diffusion coefficient, and the weight loss data (Fig. 5), a trial-and-error procedure yielded a value of  $Q_\infty$  of 148 mg. Figure 9 is a plot comparing the  $\log (Q_\infty - Q)$  plots for  $Q_\infty$  values of 203 and 148 mg. Figure 10 is a normalized plot of  $Q/Q_\infty$  vs time for all three Eccofoam FPH foams, and it can now be seen that the weight loss curve for the 2.1- $\text{lb}/\text{ft}^3$  foam has assumed its expected relationship in relation to the other two foams.

It should be pointed out that extrapolation to zero time of the linear portion of plots of  $\log (Q_\infty - Q)$  vs time should intercept at a value of  $\log (8Q_\infty/\pi^2)$  (Eq. 16). Thus, if the diffusion coefficient is independent of concentration, the diffusion equa-

tions will predict the value of both  $Q_{\infty}$  and  $D$  for a given set of weight loss vs time data. It was found that for the 6.4-lb/ft<sup>3</sup> foam as well as for the Eccofoam SH the calculated values of  $Q_{\infty}$  coincided with those obtained by back-extrapolation, justifying the use of the perfect gas law to calculate  $Q_{\infty}$ .

However, extrapolation of the  $\log (Q_{\infty} - Q)$  plot for the 4.5-lb/ft<sup>3</sup> foam did not yield the calculated value of  $Q_{\infty} = 194$  mg. Inspection of the  $\log (Q_{\infty} - Q)$  plot for this foam shows that there is a greater drop in the initial portion of the curve than that observed for the 6.4-lb/ft<sup>3</sup> foam. For the 2.1-lb/ft<sup>3</sup> foam, the drop in the initial portion of the  $\log (Q_{\infty} - Q)$  curve is greater yet. This behavior is most readily attributed to a pressure dependence of the diffusion coefficient, which becomes more pronounced with decreasing foam density. If for a polymer foam the initial diffusion coefficients are higher, then the initial portion of the  $\log (Q_{\infty} - Q)$  would drop more rapidly and then after a long time, the asymptotic diffusion coefficient can be obtained from the linear portion. But because of the initial larger drop, back-extrapolation will yield a lower value of  $\log (8Q_{\infty}/\pi^2)$ , and this is observed for the 4.5- and 2.1-lb/ft<sup>3</sup> foams.

The foregoing has shown that the initial gas contents of polymer foams of densities greater than 4.5 lb/ft<sup>3</sup> can be determined from the perfect gas law. Also, there seems to be little if any dependence of the diffusion coefficient on pressure for densities greater than 6.4 lb/ft<sup>3</sup> and thus both weight loss and pressure distributions can be predicted employing a single diffusion equation and the diffusion equations for a homogeneous solid.

Using the diffusion coefficients for the 4.5- and 6.4-lb/ft<sup>3</sup> foams, it was possible to calculate the value of the constant  $K$  in Eq. (13). This equation for the Eccofoam FPH polyurethane foam is

$$D = \frac{7.9 \times 10^{-6}}{\rho}$$

where  $D$  is in units of cm<sup>2</sup>/sec and  $\rho$  in units of lb/ft<sup>3</sup>.

The permeation constant of the bulk polyurethane polymer comprising the foam material can now be calculated from Eq. (12), using the experimentally obtained diffusion coefficients. This procedure yielded a value of  $P_e$  equal to  $5.1 \times 10^{-9}$  (ccSTP) mm/sec/cm<sup>2</sup>/cm Hg.

The polyurethane foam used in the study is advertised for high-temperature applications, suggesting a high aromatic content in the polyurethane structure. Also, the material is rigid and highly cross-linked.

No permeability data were found for this type of material, but permeation constants of  $40 \times 10^{-9}$ ,  $18 \times 10^{-9}$ ,  $14 \times 10^{-9}$ ,  $12 \times 10^{-9}$  and  $7.2 \times 10^{-9}$  (cc STP) mm/sec/cm<sup>2</sup>/cm Hg were reported respectively for the polyurethane materials designated as Adiprene-L (Ref. 4), Vulcaprene (Ref. 5), Estane (Ref. 5), Vulcaprene (Table 1), and Urethane PC-6 (Ref. 4). The first three are rubbery, whereas Urethane PC-6 is leathery at room temperature, implying a higher cross-linking density, and it is therefore not surprising that Urethane PC-6 would have the lowest  $P_e$  value (Ref. 3). However, the polyurethane comprising the foam of this study is more rigid and it is observed that its permeation constant is lower than that for the Urethane PC-6.

These considerations certainly suggest that the calculated permeation constant for this present foam material is in reasonable agreement with available literature values. This result definitely supports the validity of the relationship between the diffusion constant and the foam density and the permeation constant.

#### TEMPERATURE DEPENDENCE

Outgassing rates for a 4.5-lb/ft<sup>3</sup> foam were determined at 22, 41, 61, and 81°C. The tests were conducted by first heating the samples in air to the desired temperature and then subjecting them to a vacuum. It was found, however, that the samples heated in air would lose an amount of CO<sub>2</sub> which increased with increasing temperature. It became a practice therefore to start recording the weight loss in air during heating. When the desired temperature was reached and the weight loss rate slowed significantly, vacuum was applied. The results of the tests are given in Fig. 11, which shows weight loss both in air and in vacuum with zero time taken as the point when vacuum was initiated.

The curves in Fig. 11 show a dramatic increase in the rate of gas removal with increasing temperature. The largest change occurs between 22 and 61°C. Above 61°C the changes are small. It is instructive to observe that at the higher temperatures, the weight loss asymptote appears to be the value of  $Q_\infty = 194$  mg, which was calculated from the perfect gas law. This further justifies the use of this value in determining the diffusion coefficients from plots of  $\log (Q_\infty - Q)$ . Using the same value of  $Q_\infty = 194$  mg, it is seen that this foam has lost approximately 97.5% of its

gas content in 180 hr at 61°C and higher, whereas only 57% of the gas content was lost in 180 hr at 22°C.

The diffusion coefficients obtained at the various temperatures are plotted in Fig. 12 as  $\log D$  vs  $1/T$  in °K. The general appearance of this curve is sigmoidal and indicates that the largest changes in the diffusion coefficient occur between 22 and 81°C, above and below which there appears to be only a gradual dependence of  $\log D$  on  $1/T$ .

### SUMMARY

It was found that diffusion behavior of rigid closed-cell foams under vacuum could be described mathematically by conventional diffusion theory. These equations contain only a single materials parameter  $D$ , the diffusion coefficient. Thus, to predict the diffusion behavior of a foam for given conditions it is only necessary to secure the appropriate value of  $D$ .

Using an idealized model for a foam, the following equation

$$D = \left(\frac{RT}{M}\right) P_e \left(\frac{\rho_0}{\rho}\right) \left[ \frac{1}{(1 - \rho/\rho_0)^{1/3}} + 1 + (1 - \rho/\rho_0)^{1/3} \right]$$

was obtained which relates the diffusion coefficient  $D$  to the foam density and to the permeation constant  $P_e$  and the density  $\rho_0$  of the bulk polymer. Permeation constants are available in the literature for a wide combination of polymers and gases.

The validity of this equation and the use of conventional diffusion equations was tested by measuring under vacuum weight loss of carbon dioxide from closed-cell polyurethane foams of varying densities. From these data diffusion coefficients were calculated and found to be of the order of  $10^{-6}$  to  $10^{-5}$  cm<sup>2</sup>/sec between 22 and 81°C.

Using the above equation along with the experimentally obtained values of  $D$ , a  $P_e$  of  $5.1 \times 10^{-9}$  (ccSTP) mm/sec/cm<sup>2</sup> cm Hg was calculated for the polyurethane material comprising the foam, which is in close agreement with published  $P_e$  values.

### ACKNOWLEDGMENT

The authors are indebted to Dr. Harry Lass for his assistance with the mathematical development.

REFERENCES

1. Crank, J., The Mathematics of Diffusion, Oxford University Press, 1956.
2. Barrer, R. M., Diffusion in the Through Solids, Cambridge University Press, 1941.
3. Rogers, C. E., "Permeability and Chemical Resistance," Chapter 9 in Engineering Design for Plastics, sponsored by the Society of Plastics Engineers, Inc. and edited by Eric Baer, Reinhold Publishing Corporation, 1964.
4. Major, C. J., and Kammermeyer, K., Modern Plastics, 39, No. 11, 135 (1962).
5. van Amerongen, G. J., J. Polymer Sci., 5, 307 (1950).

Table I. F and G values for permeation at 30°C

The product FG gives the permeability constant  
 $\times 10^{10}$  in cc(STP)/mm/cm<sup>2</sup>/cm Hg

Film	F Value
Saran	0.0094
"Mylar"	0.050
"Pliofilm" NO	0.080
Nylon 6	0.10
"Kel-F"	1.3
"Pliofilm" FM	1.4
"Hycar" OR 15	2.35
Polyvinyl butyral	2.5
Cellulose acetate P-912	2.8
Butyl rubber	3.12
Methyl rubber	4.8
"Vulcaprene"	4.9
Cellulose acetate (15% DBP)	5.0
"Hycar" OR 25	6.04
"Pliofilm" P4	6.2
"Perbunan"	10.6
Neoprene	11.8
Polyethylene (0.92 g/ml)	20
Buna-S	63.5
Polybutadiene	64.5
Natural rubber	80.8
Ethyl cellulose (plasticized)	84
Gas	G Value
Nitrogen	1.0
Oxygen	3.8
Hydrogen sulfide	21.9
Carbon dioxide	24.2

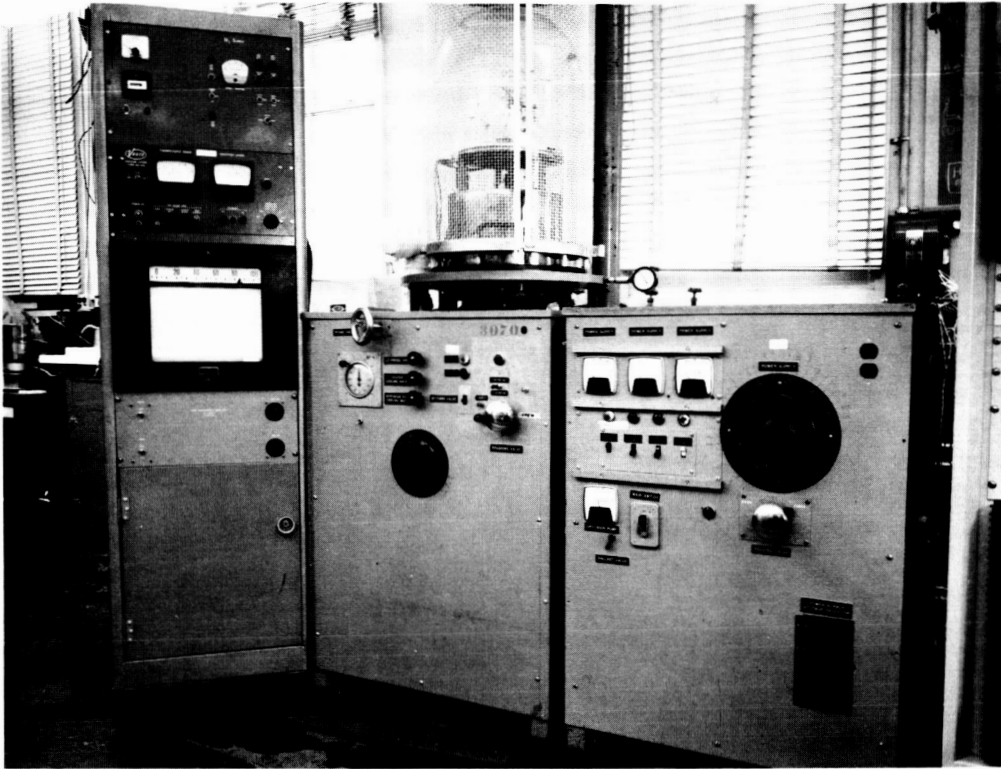


Fig. 27-1. Ainsworth vacuum balance

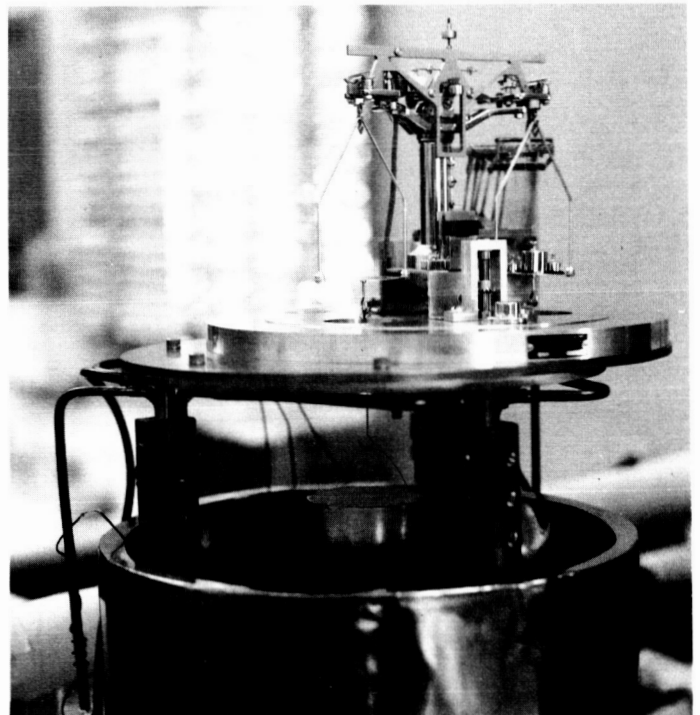


Fig. 27-2. Details of balance and sample suspension



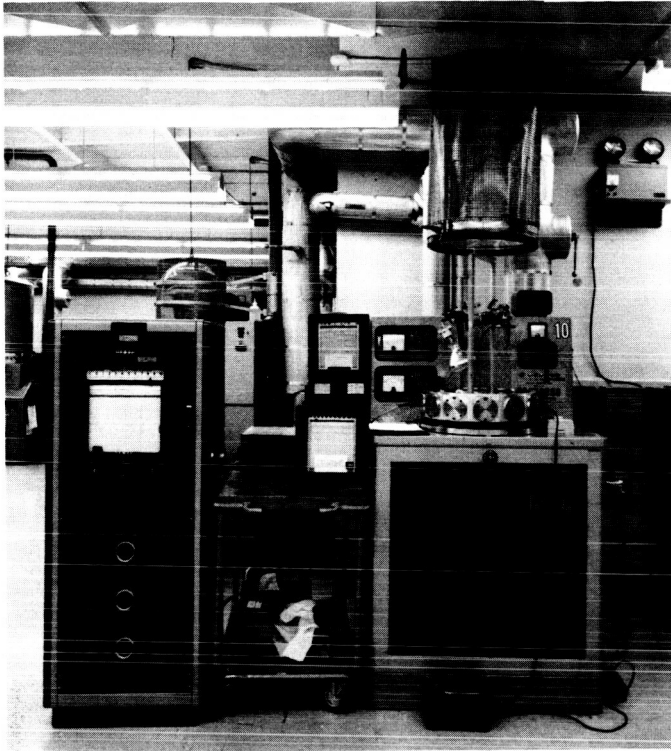


Fig. 27-3. Vacuum-balance facility for elevated temperature operations

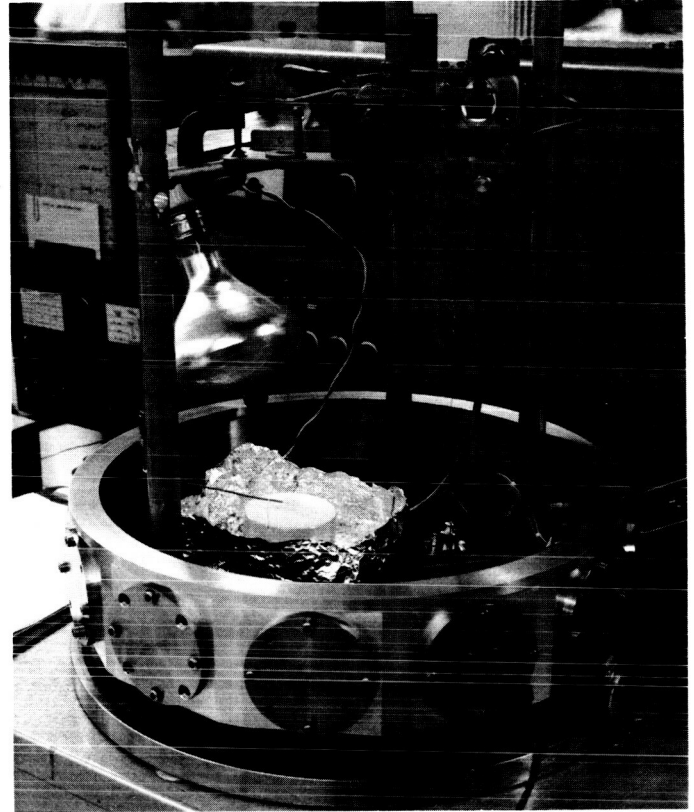


Fig. 27-4. Details of heating and balance assembly for elevated temperature operations

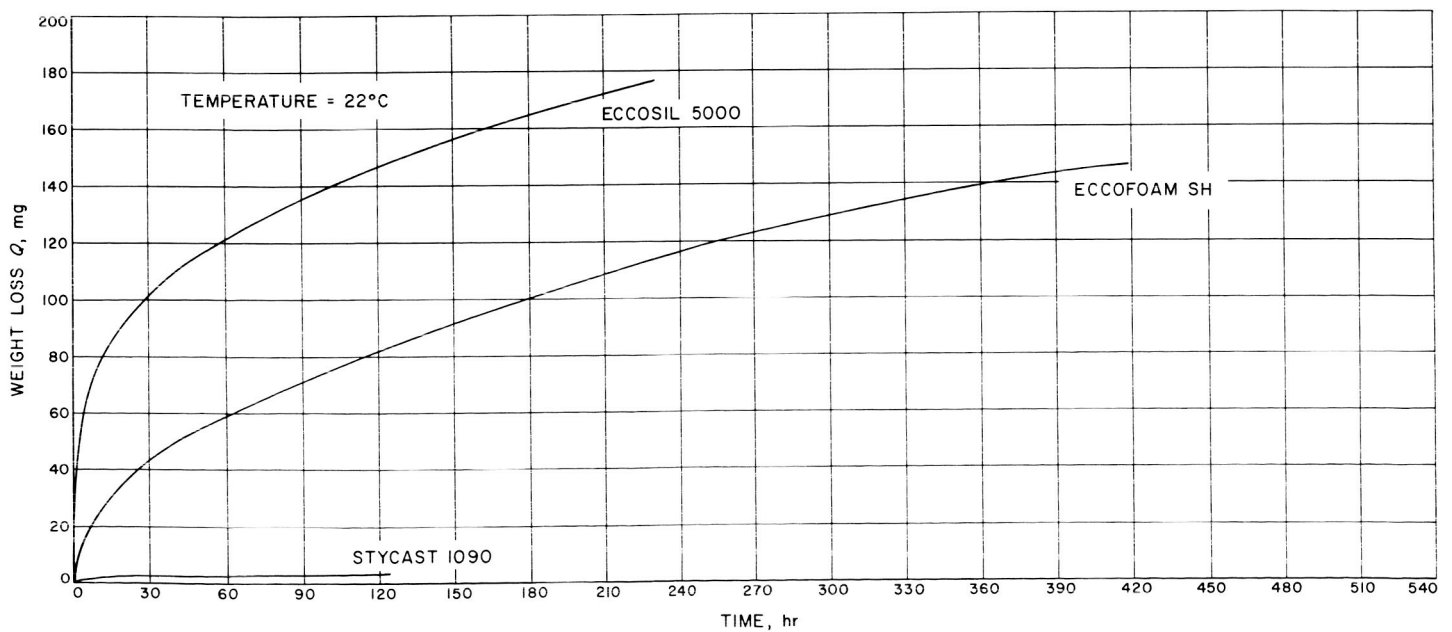
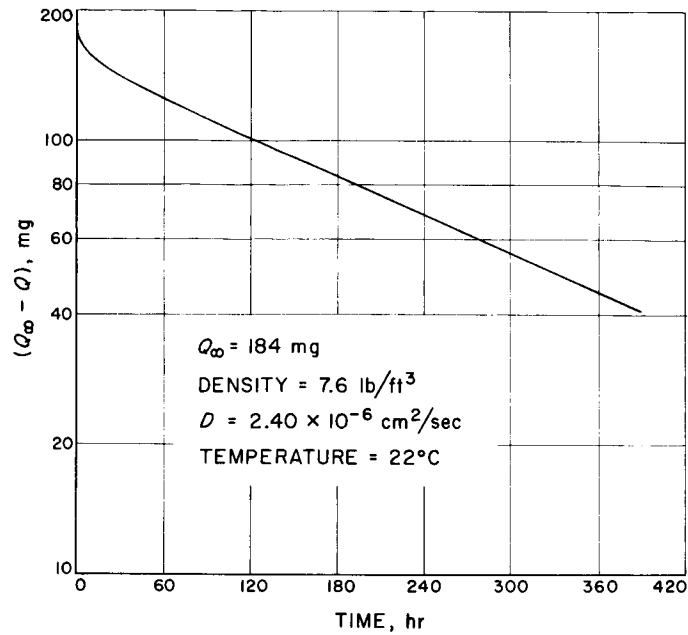
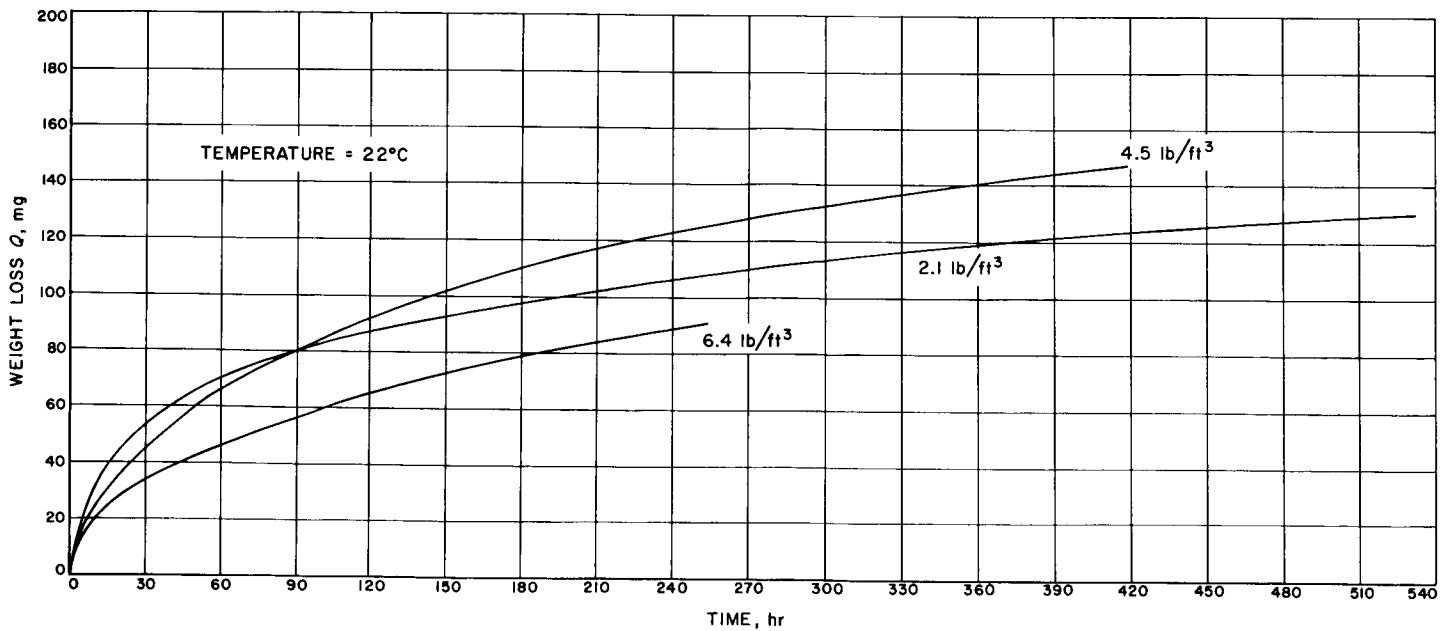


Fig. 27-5. Weight-loss curves for three polymer foams at 22°C

Fig. 27-6. Log ( $Q_{\infty} - Q$ ) vs time for Eccofoam SH at  $22^{\circ}\text{C}$ Fig. 27-7. Weight-loss curves for Eccofoam FPH foams at  $22^{\circ}\text{C}$

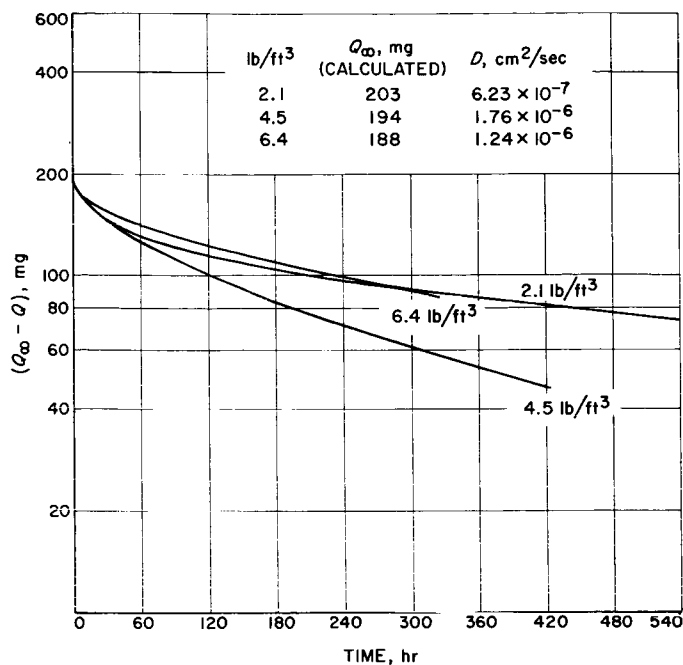


Fig. 27-8. Log ( $Q_{\infty} - Q$ ) vs time for Eccofoam FPH foams at 22°C

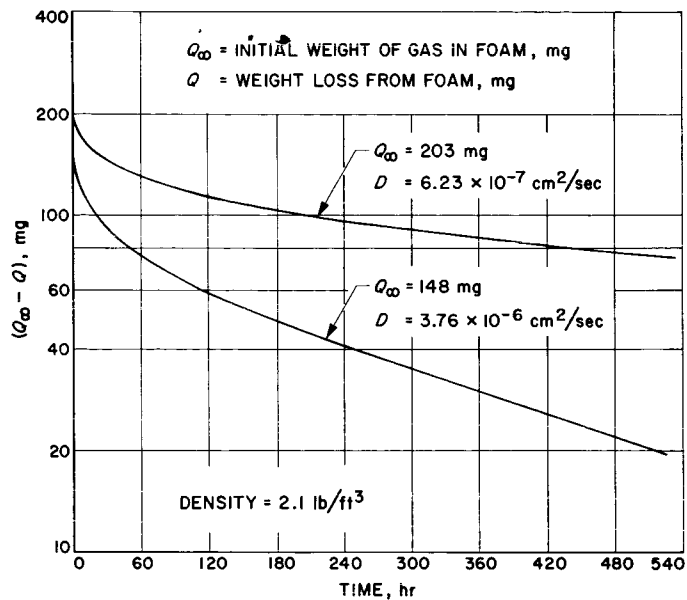


Fig. 27-9. Log. ( $Q_{\infty} - Q$ ) vs time for Eccofoam FPH/12/2H at 22°C

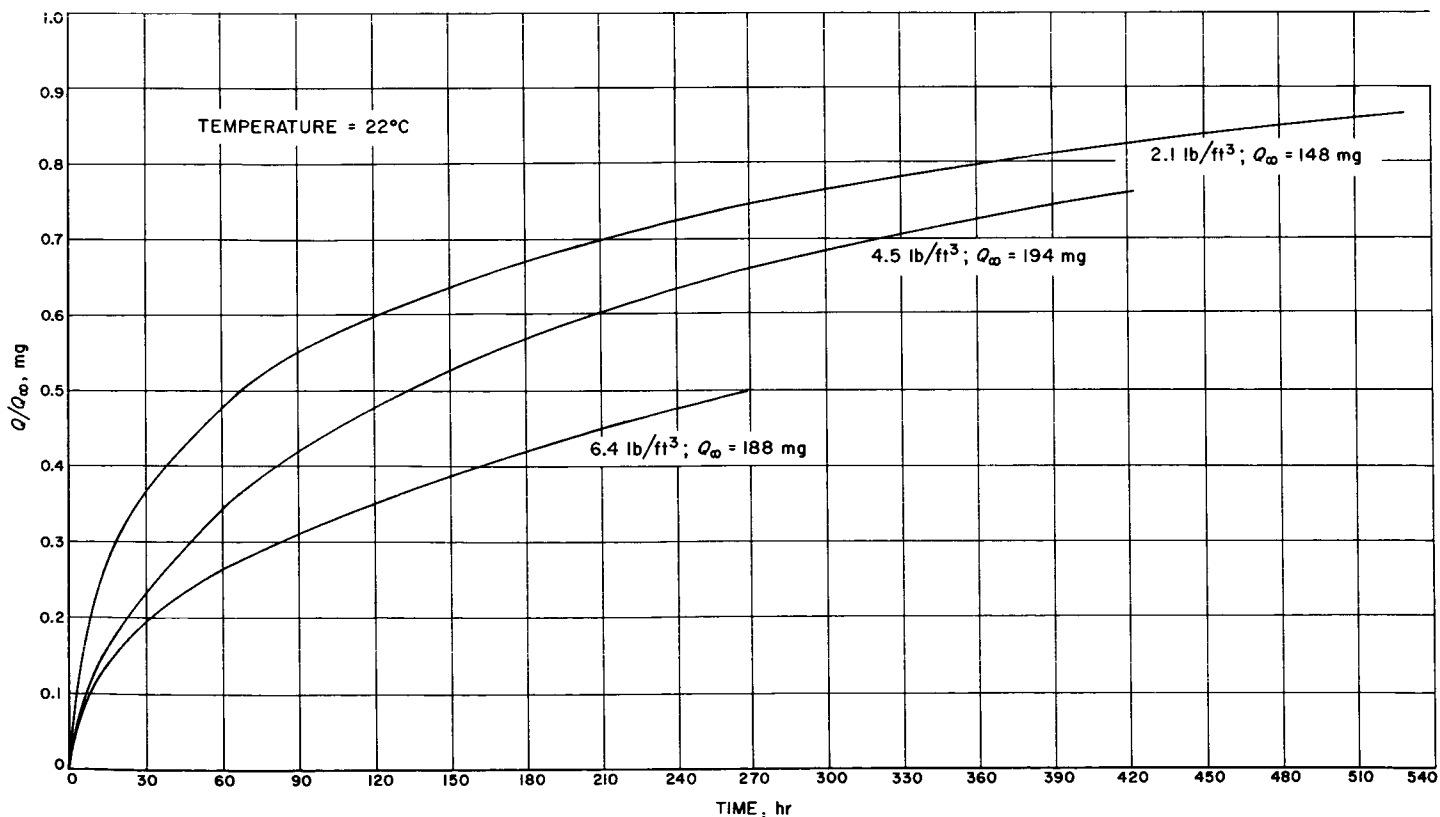


Fig. 27-10.  $Q/Q_{\infty}$  vs time for Eccofoam FPH foams at 22°C

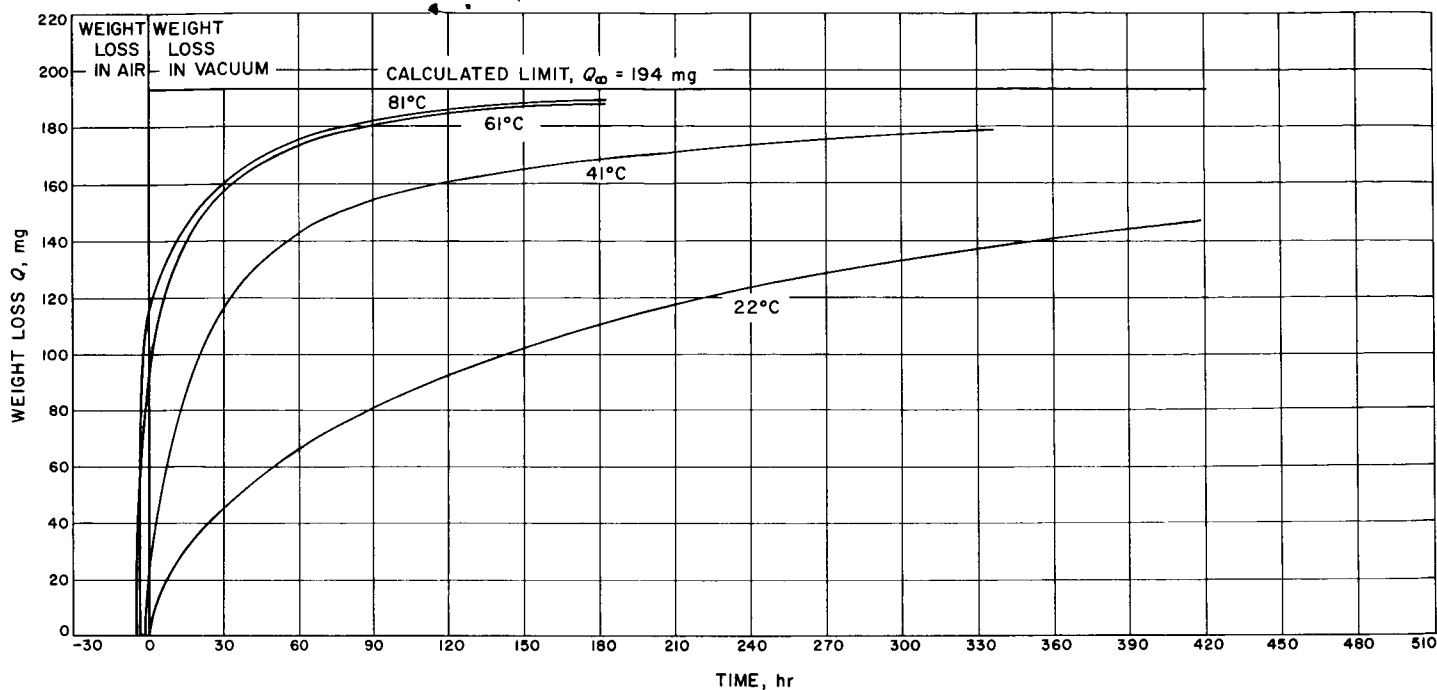


Fig. 27-11. Temperature dependence of the outgassing rate for an Eccofoam FPH/12/6H foam of density  $4.5 \text{ lb/ft}^3$

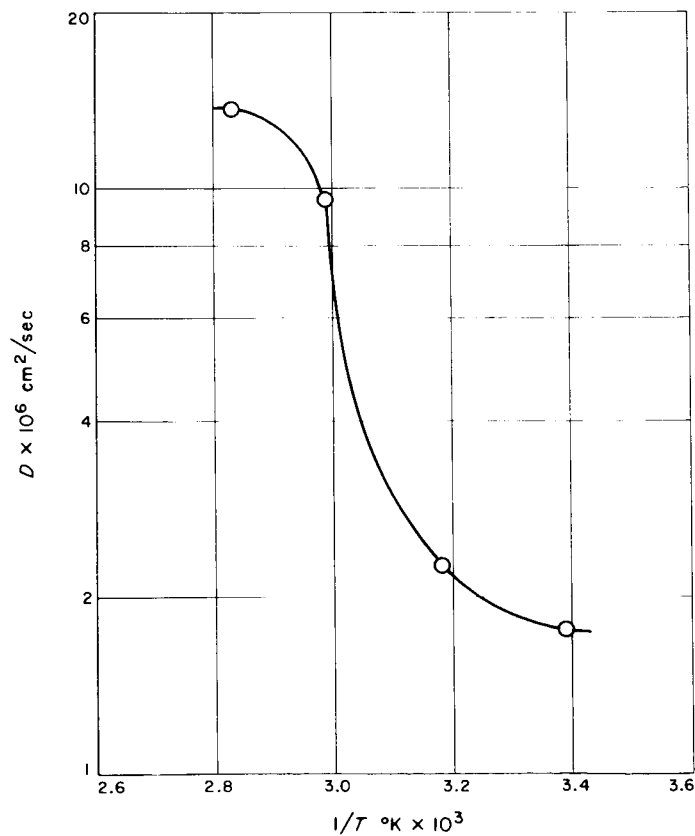


Fig. 27-12. Log  $D$  vs  $1/T \text{ } ^\circ\text{K}$  for an Eccofoam FPH/12/6H foam of density  $4.5 \text{ lb/ft}^3$

28. PREVENTION OF HIGH VOLTAGE BREAKDOWN  
IN ION PROPULSION SYSTEMS

G. A. Work  
Hughes Research Laboratories  
Malibu, California

The considerable amount of work which has gone into electrical or electric propulsion or ion rocket devices in the last few years will be of value to the space program only if we can solve the kind of problems that this workshop has been convened to discuss. The advantages of ion engines lie chiefly in their high specific impulse which is achieved by accelerating ionized material through total potentials of the order of 5 to 10 kv.

Figure 28-1 defines the problem. We have a high positive potential applied to the ion source. This provides the thrust, but to achieve high current from the ionizers in this kind of engine, we apply a high negative potential to an accel structure, to increase the perveance or emission current density. We also operate a number of auxiliary power supplies at the high positive potential--boilers, valves, ionizers, etc.--and this equipment contributes to the complexity of the high-voltage hardware. The power supplies are generally remote from the engine and are connected with high-voltage insulated wires. Occasional high-voltage arcs can occur within the engine; we have learned to live with these. The major problem is in the insulation of the power supply components, to avoid failures due to transient arcs and high voltage breakdown.

Figure 28-2 shows the hardware we flew on the NASA SERT-I flight last summer. Shown is the ion engine, sealed in a vacuum pod with a door which blew off at the test altitude. Shown in the figure are the odd-shaped elements of the power conditioning system, which were determined largely by the space left available on the payload by the time we got to it.

Figure 28-3 shows a typical box from one of these supplies. The magnetic components comprise the principal weight and volume. Ordinary electronic components were soldered in terminal boards as shown. We started out in the program feeling that the pressures on this ballistic flight were essentially indeterminate and that we could not count on a rapid transition through the Paschen minimum. Therefore we adopted a test criterion that is simple to state and simple to test, namely that all the elements of the circuits must operate at all pressures. Achieving that

goal is quite another problem. After considerable experimentation, we were able to effect adequate vacuum seals using Teflon wire etched in sodium and ammonia. It was then potted in a hard Stycast epoxy. Only by going to this combination of hard epoxy and "soft" Teflon (which was etched to make a seal) were we able to reliably achieve this all-pressure operation.

Figure 28-4 shows a power supply unit after being encapsulated with a foam material. Foaming was necessitated by vibration problems. It was a rather rough ride aboard the Scout rocket, and there were some significant amplification factors in the payload itself. Test conditions of about 80 g resulted in the loss of several solder joints, so we resorted to foam for mechanical constraint of soldered components. Foam not only solved the vibration problems, but as a dividend, we found that it also stood off the high potentials. This technique provided a backup for the etching and hard potting we did, as will be discussed by Bob Dunaetz in the following paper.

I want to discuss one major problem relating to high voltage connectors which we were not able to prevent and which caused a failure which cost us the flight. Figure 28-5 shows the simple bell jar setup in which all our pressure testing was conducted. There is nothing profound about the test setup. We go to a very simple oil seal for the high voltage conductor shown in the figure. What we're testing is a connector (shown in Fig. 28-6) for operation in the all-pressure condition. It is well to keep in mind that cables using these connectors have two ends to them, one at the power supply and the other at the ion engine.

Figure 28-6 shows high voltage connectors that we designed for this flight application. We modified Deutch connector, which had seven leads in the center in the connector. All the organic material was redesigned and modified for this application. For one thing, it had to work at a very high temperature (around 200°C), so we had diallyl phthalate pieces made for the central insulator holders. A Teflon piece with venting holes can be seen in the figure. The whole assembly was designed to provide a considerable relief or space between the Teflon piece and the glass hermetic connector into which it plugs.

Figure 28-7 shows the vent holes a little better. I believe you can see how the inner pin is relieved. These units solved the connector problem effectively and we were able to operate them at all pressures. There was some corona within them at an intermediate pressure region, but because of the rather large diameter connector pins and the metallic shells, the corona currents were limited and confined to within

the metal housing of the connectors. There was no effect on the rest of the spacecraft for the short period of their arcing during the boost vehicle ascent. Unfortunately these connectors were not flown.

Another approach to high voltage connector design was applied to this program, and it prevailed. The basic idea was to pot connectors; after removing all the pins from the shell and spacer assembly, sticking them into the mating connector, and simply potting the assembly. We did not do the potting, but we did extensive testing with units that were delivered to us in that form. The tests resulted in a number of serious failures in these units which were nevertheless used in the flight test.

Figure 28-8 shows typical connectors removed from an assembly; actually, they just were wiggled out in this case. There had been very poor adhesion to the glass. Voids were apparent within the potting material. The failures occurred at the interface of the glass and the potting. We feel that thermal cycling was a major factor in these failures.

A cross section of a connector potted in this manner is shown in Fig. 28-9. The striations are saw marks in the cutting process, but a very definite area of fractured glass can also be seen. The relative coefficients of expansion of the glass and the potting materials are in a ratio of about 7 to 1. A shoulder of the sort as seen on this figure inside the shell can retain the bulk of the potting compound so that its pressures are all exerted up against the glass face. In any such fractured area you can have extremely small interface gaps and significant gas pressures from the residual outgassing or vapor pressure of the potting material. The characteristic failure mode is an arc or glow corona that occurs between the inner and outer electrodes. Any discharge from, say, the center out to the edge results initially in a little carbonization of the potting material, and that's catastrophic. Any further current flow results in further carbonization, and it goes straight downhill from there. This, we feel, is what happened in our portion of the SERT-I flight in which a failure occurred when the high voltages were applied. We feel it could have occurred either through thermal cycling or, more likely, simple vibration stresses on the unsupported leads going out of the connector. Significant forces acting on these leads during vibration could open the interface between the glass and the potting, resulting in the kind of failure we observed. I think the principal lesson learned is that you don't take a hard potting substance and put it against another hard interface and hope to maintain your adhesion integrity at that interface. You need something that gives.

We found we had good luck with the Teflon wire and hard potting. Any potting used in conjunction with a glass assembly such as the hermetic connector should certainly be softer.

I'll yield now to Mr. Bob Dunaetz who can go into some detail on the potting techniques which were used.



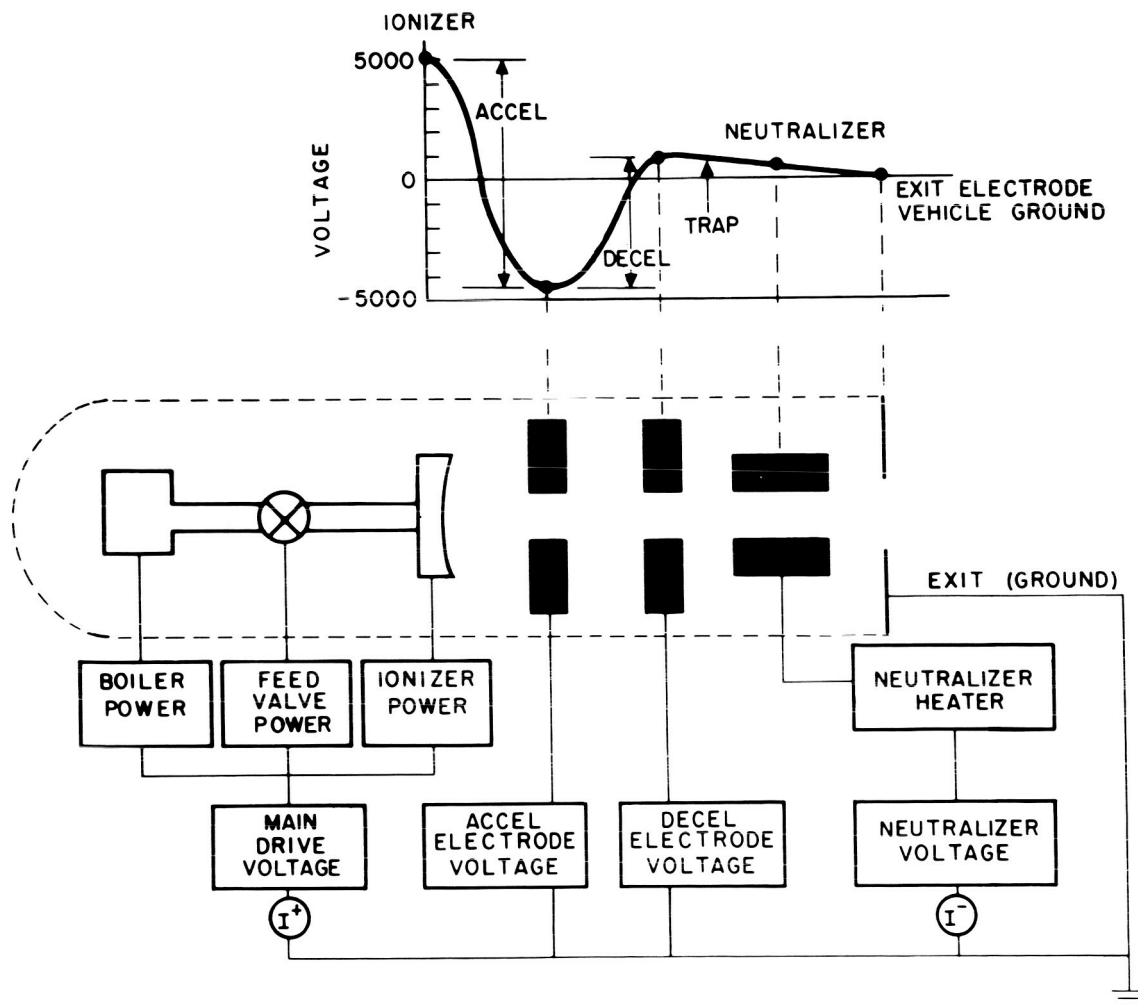


Fig. 28-1. Ion engine potential diagram

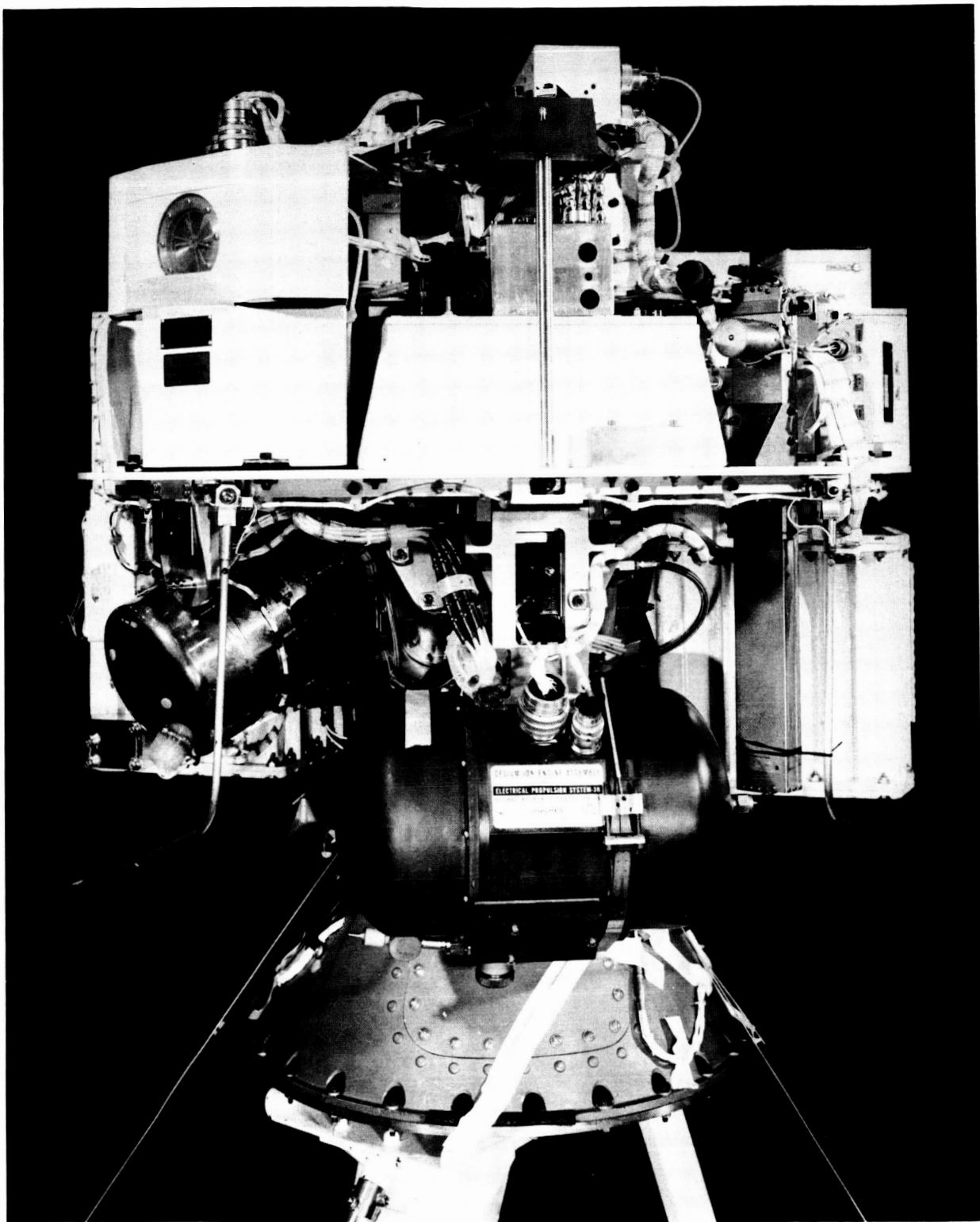


Fig. 28-2. SERT-I payload. Hughes ion engine bottom center.  
Part of power conditioning system at upper left

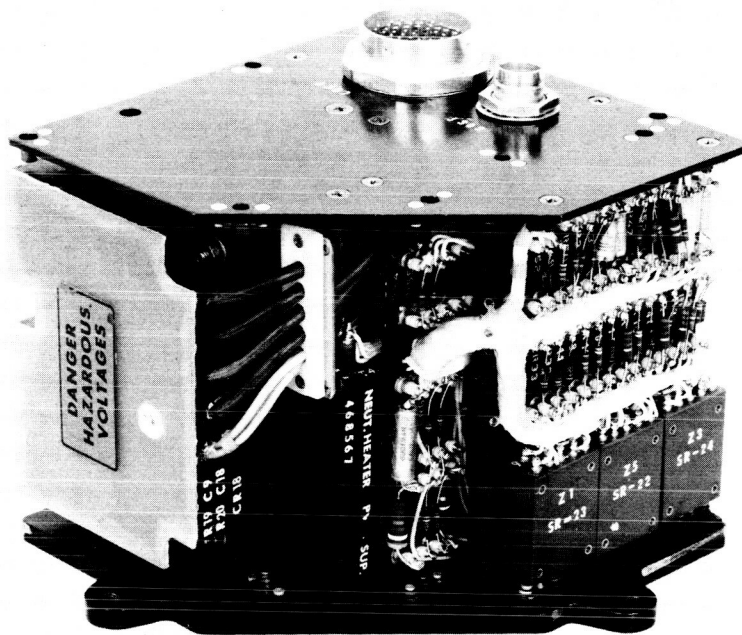


Fig. 28-3. Typical SERT-I high-voltage power supply, before foaming

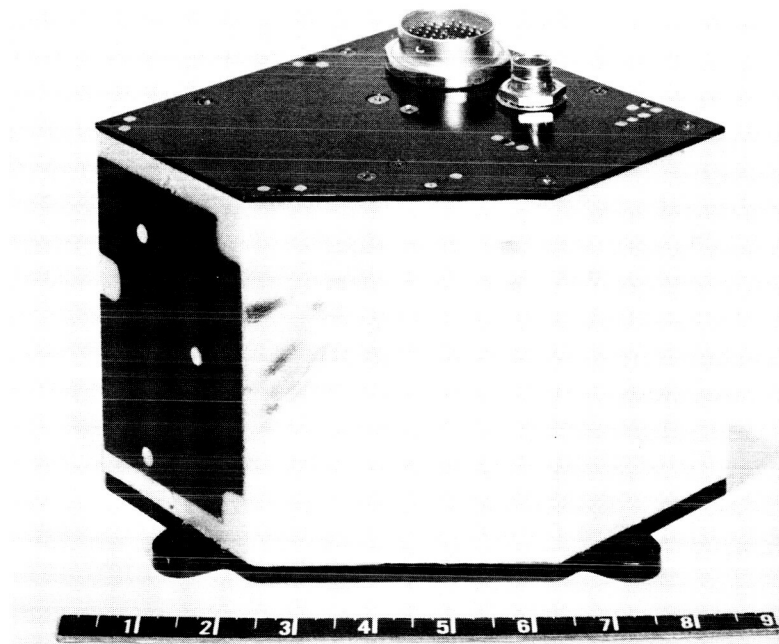


Fig. 28-4. High-voltage power supply after foaming

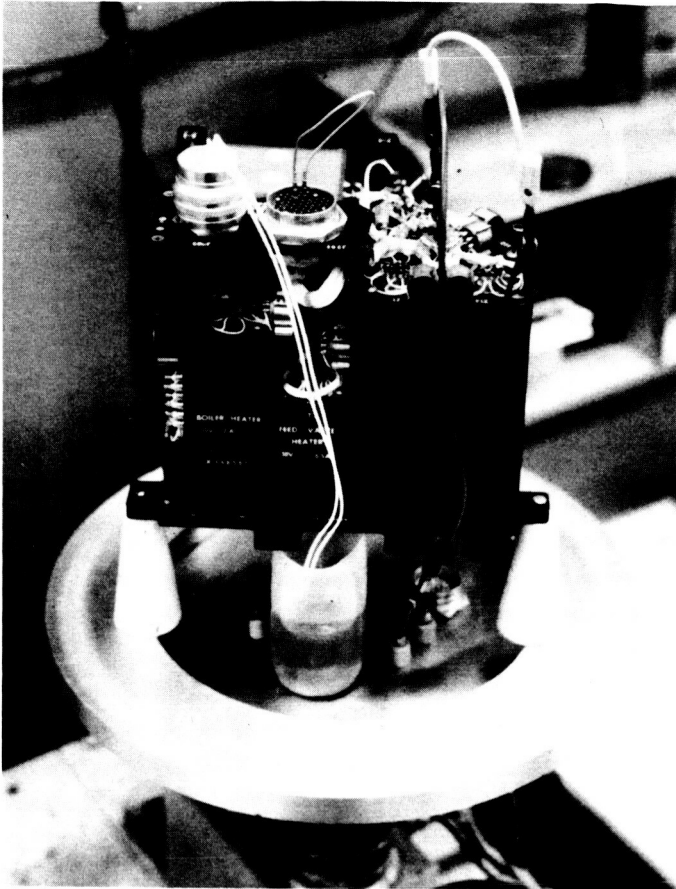


Fig. 28-5. High-voltage power supply and connector mounted for all-pressure test on bell jar stand

Fig. 28-6. Deutch connectors modified by Hughes for high-voltage vacuum operation

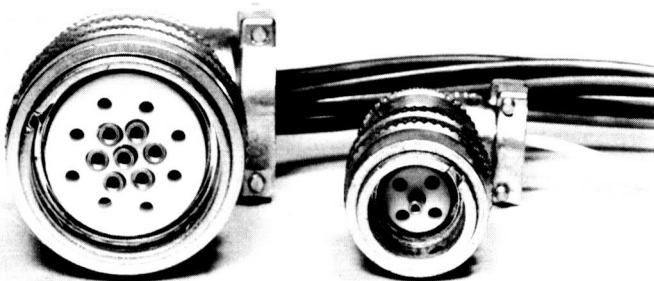
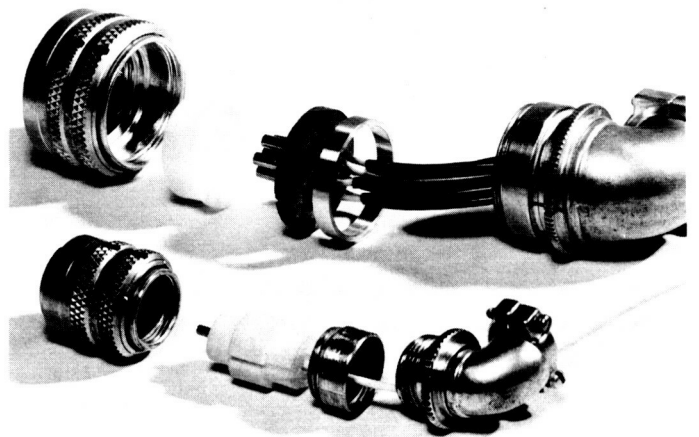


Fig. 28-7. Hughes-designed high-voltage connectors showing vent holes

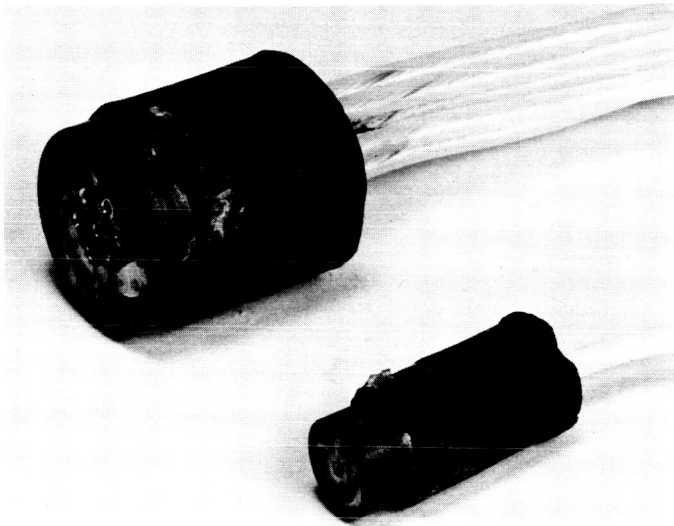


Fig. 28-8. Potted connectors after removal showing fractured glass from mating hermetic seal and extensive voids

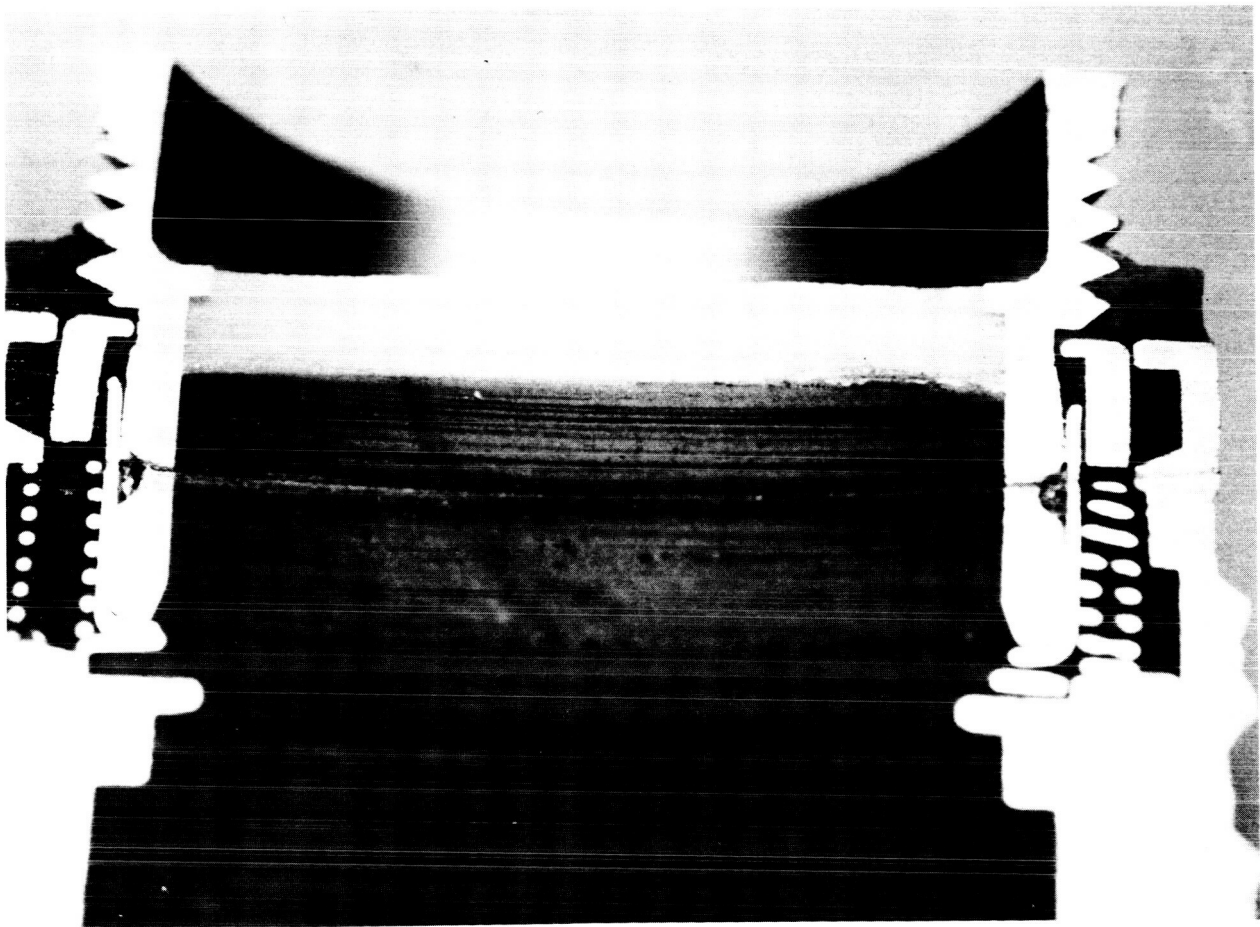


Fig. 28-9. Section of potted connector showing fractured glass at potting interface

29. PREVENTION OF HIGH VOLTAGE BREAKDOWN  
IN ION PROPULSION SYSTEMS

R. Dunaetz  
Hughes Aircraft Company  
Culver City, California

Figure 29-1 appears to be a little bit redundant of one of the other units shown in the previous presentation. The figure shows the high-voltage units (with white dots). We decided not to encapsulate this unit with foam. We used conventional methods, but as Mr. Work has pointed out, the next step was to put the entire unit in foam for mechanical protection. We found we had the added benefit of maintaining a positive atmosphere for what would be a long period of time.

Figure 29-2 is a photograph of a similar unit. Notice that some of the wires and components were fairly close to the surface. But they were fairly well supported. On this unit we used a polyurethane foam with a density of approximately 8 lb/ft<sup>3</sup>. We tried to maintain a low-density foam, and we took the position that whatever you put together you have to take apart. We tried to maintain this repairability aspect. Our problem came to be how to protect against someone accidentally digging into the foam. This problem was solved by means of having an aluminum cover on the unit, as shown in Fig. 29-3. The figure shows a dc power supply. The ac power supply is shown in Fig. 29-4. Here again, you notice there were quite a few components in somewhat of an odd shape, but the foam tied the whole problem together as well as maintaining our constant atmosphere. The dc power supply we just saw and another power unit are shown foam-encapsulated and covered in Fig. 29-5. The covers protected the units from having the integrity of the foam accidentally destroyed.

To digress a little bit, we didn't limit our foam encapsulation to the SERT I ion engine program. We saw that it had a number of advantages here and used it in a composite with conventional materials and also as a backup to maintain an atmosphere. We had also been looking at this for other programs. What I call our bird-nest network is presented in Fig. 29-6, showing one of the power supply units for our Syncom synchronous satellites. This unit operated at about 1,000 v. We have one of them that has already been operating at 22,000 miles in space for 2 yr, and this satellite maintained a constant voltage through launch. At this date, there is a second Syncom satellite that has been up for 1 yr. The type of network shown in the figure is essentially an unsupported network in a metal case and was used on our

Early Bird satellite, which has been up approximately 6 mo. now, operating at 1,500 v. Here again, the only support was furnished by the foam which filled the residual area.

What the unit looked like when we finished is shown a Fig. 29-7. The holes in the lid were put there for a purpose, primarily to let the gas escape slowly. We did not try to seal the foam hermetically. We just put the metal case on for mechanical protection; the lid was actually adhesively bonded on. This type of unit was found to be quite repairable because of the low-density foam.

Figure 29-8 shows another typical unit for the Early Bird satellite. The box shown was approximately 10 mil in wall thickness. Relief holes were not used in this unit, and you can notice that it did bulge a little bit as the gas expanded after long-term exposure to vacuum. The whole unit was put in vacuum. What I wanted to point out here was that no matter what Hughes makes, they always like to take it apart. Whether it's used again or not, it is taken apart and the defective components are replaced and refoamed.

We also examined the foam materials from the standpoint of wondering what did we have and what are the limitations. The data of Table 29-1 was performed in support of an airborne radar system for the F-111 airplane. We were looking at packaging of some of our high-voltage units. We ran through a series of tests on 8-lb-density foams. The electrode tip and gap dimensions were kept constant. The test shown was made at 400 cps. During the corona test, the breakdown occurred at 60 cps. The data is somewhat sketchy but it at least gave us a feeling for what we have or what we didn't have. This is a fairly good screening method. We had one problem when we were checking for corona. Our equipment possibly could have been better. We started developing internal corona at 18 kv, so we're not sure where the corona started with these specimens. The breakdown voltages occurred at standard conditions in room temperature and averaged 27 kv for the 1/4-in. gap.

The next column was tested at 180°F. The breakdown voltage increased considerably. This increased gas pressure was primarily due to the heating. Therefore, we had greater than 1 atmosphere within the foam. We left the foam for a short-time exposure to 7 mm Hg for 4.5 hr. We had no problem there. Everyone is concerned about foams and moistures. We did our 10-day humidity cycling, which resulted essentially in no change.

We examined other areas too. In Table 29-2 and 29-3 we have 7-lb-net foam, used with a 1/8-in. gap so that we could stress the insulation a bit more fully to see if we could detect corona with our test setup, or at least try and correlate it when it occurred, compared with the breakdown. (Figure 29-9 shows the geometry of foam failure.) In most cases, it was fairly close to where the breakdown did occur. But it's our contention that if you can detect corona with a foam-encapsulated system, it's too late. You're beyond the point of no return.

Since Hughes always likes to be able to repair equipment, we made up a number of specimens and took half of them apart and tore out one of the electrodes. By the way, this was all-imbedded-electrode type of testing. Here again, the control specimen is foamed once, and then refoamed in both cases with a 1/8- to 1/16-in. tip diameter, and 1/4-in. diameter. We experienced an increase in breakdown voltage after refoaming. This was primarily caused by a higher-density foam at the interface of the refoaming; in other words, there was more plastic material at that point. Anyway, we answered our critics in that we at least had a fairly sound dielectric joint.

From the standpoint of comparing different densities with the lower density foam after breakdown, we would have a fairly large blowout path. When the failure occurred, it tended to carbonize everything that was there and to leave a fairly large hole. As we went to higher-density foams, we used a smaller failure mode that was not quite to a hairline that you would expect with a solid dielectric; apparently this is proportional to the density of the foam. Now, this was merely run as a point of interest. We were wondering what we had. We're still not sure.

Figure 29-10 shows a typical power vacuum tank where we do quite a bit of our testing. This is not the best photograph. Most of our specimens were stacked up in this unit. The high-voltage source came in through the top, and the ground wire came out the bottom.

Figure 29-11 is a vacuum chamber with the specimens lined up within the vacuum. We had a problem in that we knew the foam was going to outgas, and it sure enough did. In some of our specimens we used uninsulated wire and electrodes. We found that with this size specimen at 10 to 12 kv, arcing would jump across from one to the other. At the time of breakdown we would have to put on our giant pumping source and get the vacuum down to  $10^{-8}$ . This is quite a feat with a foam sample, and we found it quite difficult. We had a number of these chambers going. We used different batches of foams and ended up by selecting basically two foams to test.



We were running a two-fold test. We had a constant voltage on the specimens at all times during our test period, and then we would isolate a single specimen once a month and try to break it down to see if we had reached a critical time-pressure point.

Figure 29-12 shows the results of a test we ran for 9 mo in the vacuum although results are shown only for the first 6 mo. What we were looking for at the time was a power supply for our ETS satellite to operate at 3 kv. This figure shows the constant voltage that we applied on all the specimens. This voltage did not vary a great deal, although we did lose power once (for a matter of a day the vacuum remained on but the power did not). I don't know what effect this had, but over a 9-mo. period it is difficult to maintain constant power. We couldn't establish a great trend here probably because of lack of sample size. At the end of 9 mo. a couple of them dropped off, although one of them was, I believe, high even on the seventh month, and then dropped off slightly on the eighth and ninth month. But, we felt somewhat safe in that 3 kv apparently did not have any great effect on the foam or contribute to breakdown. We monitored for corona during this time, 2 or 3 times a week.

We were concerned with how fast gas diffuses out of the unit. What we were concerned with was not particularly a weight loss. As Mr. Work, our previous speaker stated, we found that this was a somewhat difficult method. To take a block of foam and measure it in the vacuum on a quartz balance is a good procedure in itself, but you're really not sure that what is coming off is only the contained gas. It may be moisture or other contaminants that have been picked up prior to going into the vacuum. There is also a problem with lightweight foams in that crumbs constantly fall off. A crumb's weight may be significant when you're measuring in the milligram range. We also had a hard time convincing the electrical people at Hughes that weighing the specimen on a quartz balance was the way to go. They wanted something a little more visual. Essentially, we foamed some of our material around a glass tube. Figure 29-13 shows a 1/4-in. -ID glass tube. The overall block dimension was 1 3/4 in., which allowed approximately 3/4 in. from the inside of the tube to the vacuum, of which the foam was in the way. We went inside the glass tube and made sure there was no "skin" to give us any side effects. We also sanded the foam block so that we had open cells. Anyway, the outer surface had exposed open cells. We then put the tube onto a mercury manometer. The only end actually opened was opened to the foam. After this procedure, the whole unit was put into a vacuum. We

just started pumping and took readings of the cathetometer on the mercury level. We wanted to see what the pressure was inside the block of foam. We were concerned that the thing would lose its pressure within 5 days, 5 min., or what have you.

We assumed that the pressure inside the foam was 1 atmosphere, since it does come to equilibrium with ambient conditions when you foam it. We ended up with pretty much of a straight line as shown in Fig. 29-14. We tested for 200 days. We weren't sure how much longer this line would continue straight, but the program was running thin on money, so from this point we extrapolated and were able to predict a half-life for our contained atmosphere of about  $2\frac{1}{2}$  yr with this type of system. This means that somewhere along the line this thing is going to go out into an asymptote. We hope it will straighten out. The rest did not answer every question because we did have a slight gas reservoir in our manometer leg. We're aware of this, but it did give us a feeling for what we had.

At this point where the program ran out of money, I turned off the vacuum and we just let it sit there. For about 50 days I checked the cathetometer readings of the mercury level, and it climbed back up on the same straight line. I did this to make sure that we hadn't ruptured cells in the process or possibly had any other decomposition problems.

Our people are presently toying with the idea of packaging 5,000-v systems for periods of years. We're still going to have to do a lot of work in this area, of course. We still don't know our critical pressure within the vacuum. I hope that JPL people will answer that one. Here again, their foams appeared to maybe act a little differently than ours. There are many different kinds of foam. Of course, the secret is to select a foam that will maintain your atmosphere. This is what we feel we are trying to do. I noticed earlier that one of the questions was concerned with what do you do with this gas, though that goes out and contaminates the rest of the spacecraft. We're well aware of this problem at Hughes. Most of our units are encapsulated in foams, so maybe they protect themselves with their surroundings. There are a lot of ways of attacking these problems, and of course every system has its own problems. Fortunately we've been able to handle ours to date.

Table 29-1. Environmental effect on breakdown strength

Material and electrode description	Density of foam, lb/ft <sup>3</sup>	8	8	8	8
	Electrode tip diameter, in.	0.250	0.250	0.250	0.250
	Conductor to ground electrode gap, in.	0.250	0.250	0.250	0.250
Test conditions	Corona threshold voltage frequency, cps	400	400	400	400
	Breakdown voltage frequency, cps	60	60	60	60
	Environment test temperature, F°	77	180	77	77
	Environment test pressure, mm Hg	Ambient	Ambient	7 ± 2	Ambient
	Humidity conditioning prior to testing	None	None	None	MIL-STD 202 cycle
	Time in test environment	-----	4.5 hr	4.5 hr	10 days
Summary of test set results	Average corona threshold voltage rms, kv	>18.0	>18.0	>18.0	>18.0
	Average breakdown voltage rms, kv	27.0	35.8	30.2	29.4

Table 29-2. Corona threshold characteristics

Specimen* number	Corona threshold rms voltage, kv	Dielectric breakdown rms voltage, kv
1	>20.0	21.5
2	19.0	19.5
3	16.5	17.0
4	16.0	16.0
5	17.0	<u>19.0</u>
		$\bar{X} = 18.6$
*Seven lb/ft <sup>3</sup> density foam with 1/8 in. electrode gap tested at standard conditions.		

Table 29-3. Breakdown strength after refoaming, kv

1/16 in. electrode tip diameter and 1/8 in. gap		1/4 in. electrode tip diameter and 1/8 in. gap	
Control	Refoamed	Control	Refoamed
23.5	21.0	20.0	31.5
21.5	27.5	18.5	17.5
16.5	30.5	16.0	28.0
18.0	15.0	22.5	20.0
<u>12.5</u>	<u>17.0</u>	<u>23.5</u>	<u>25.0</u>
$\bar{X} = 18.4$	$\bar{X} = 22.2$	$\bar{X} = 20.1$	$\bar{X} = 24.4$

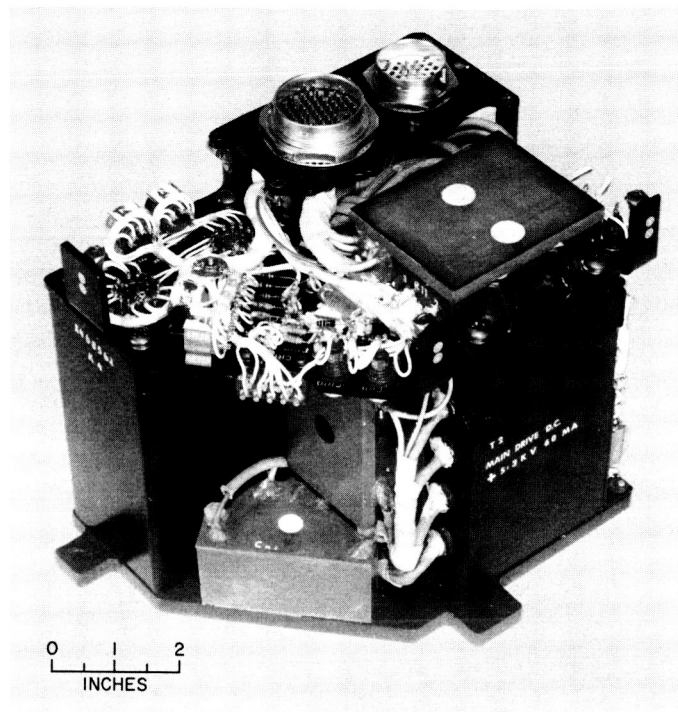


Fig. 29-1. SERT I unencapsulated high-voltage power supply

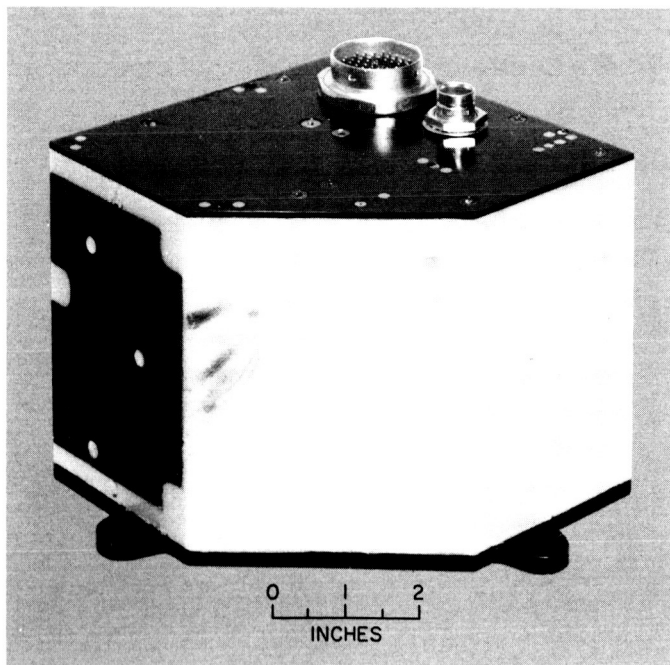


Fig. 29-2. SERT I foam-encapsulated high-voltage power supply module

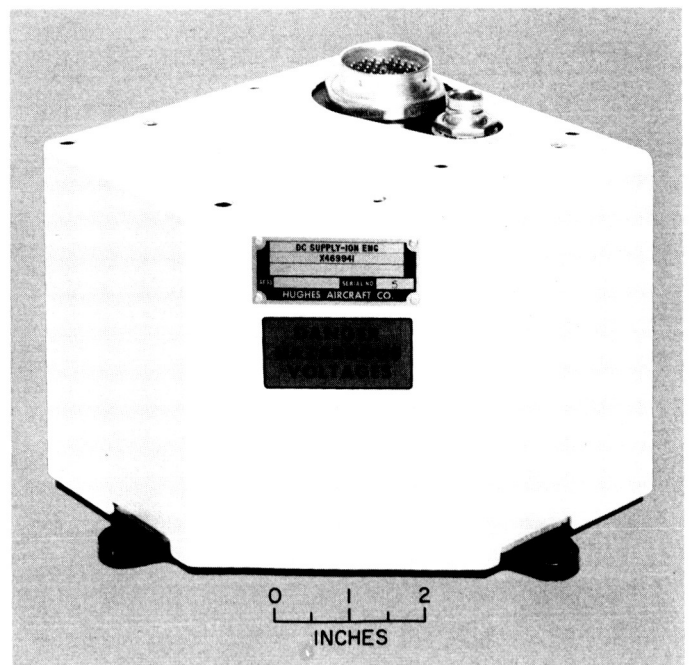


Fig. 29-3. SERT I encapsulated high-voltage power supply module with an aluminum cover



Fig. 29-4. SERT I unencapsulated AC power supply module

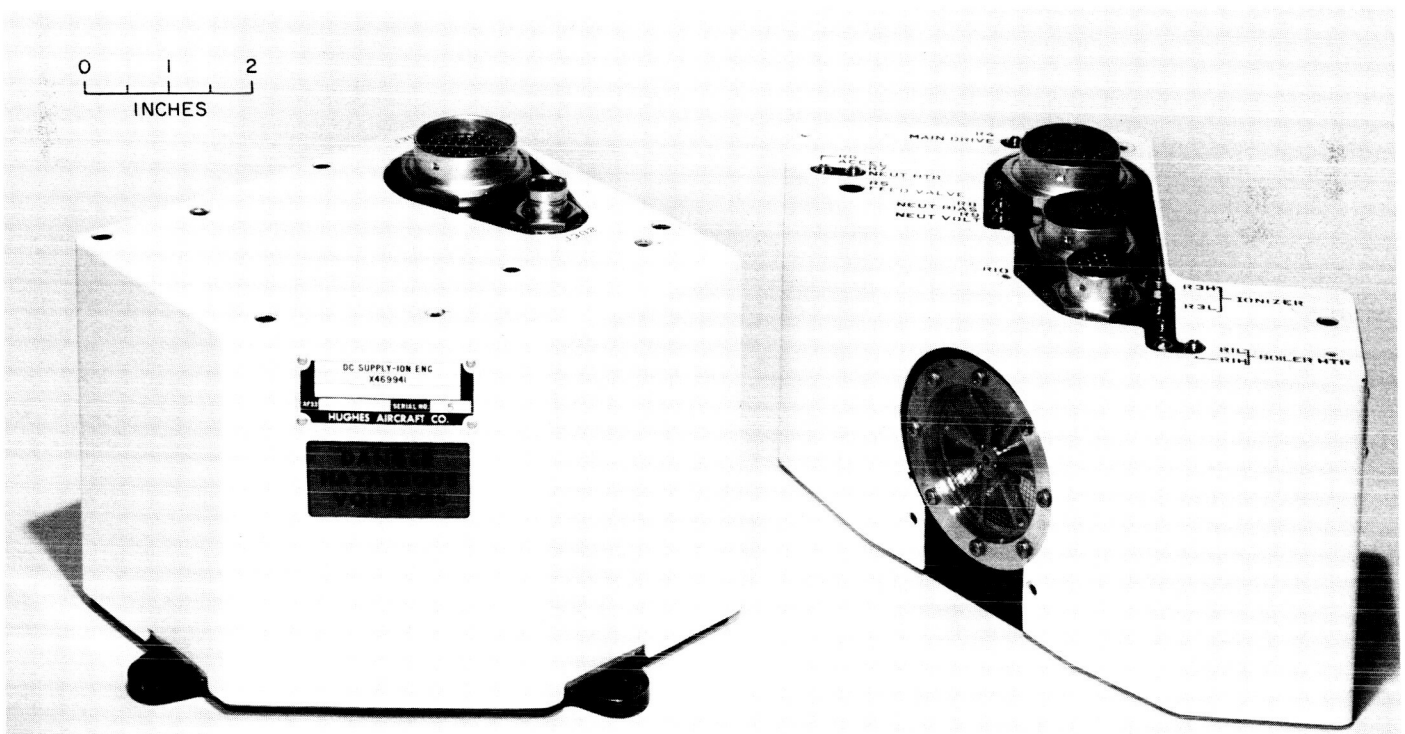


Fig. 29-5. Aluminum case covered power supply modules

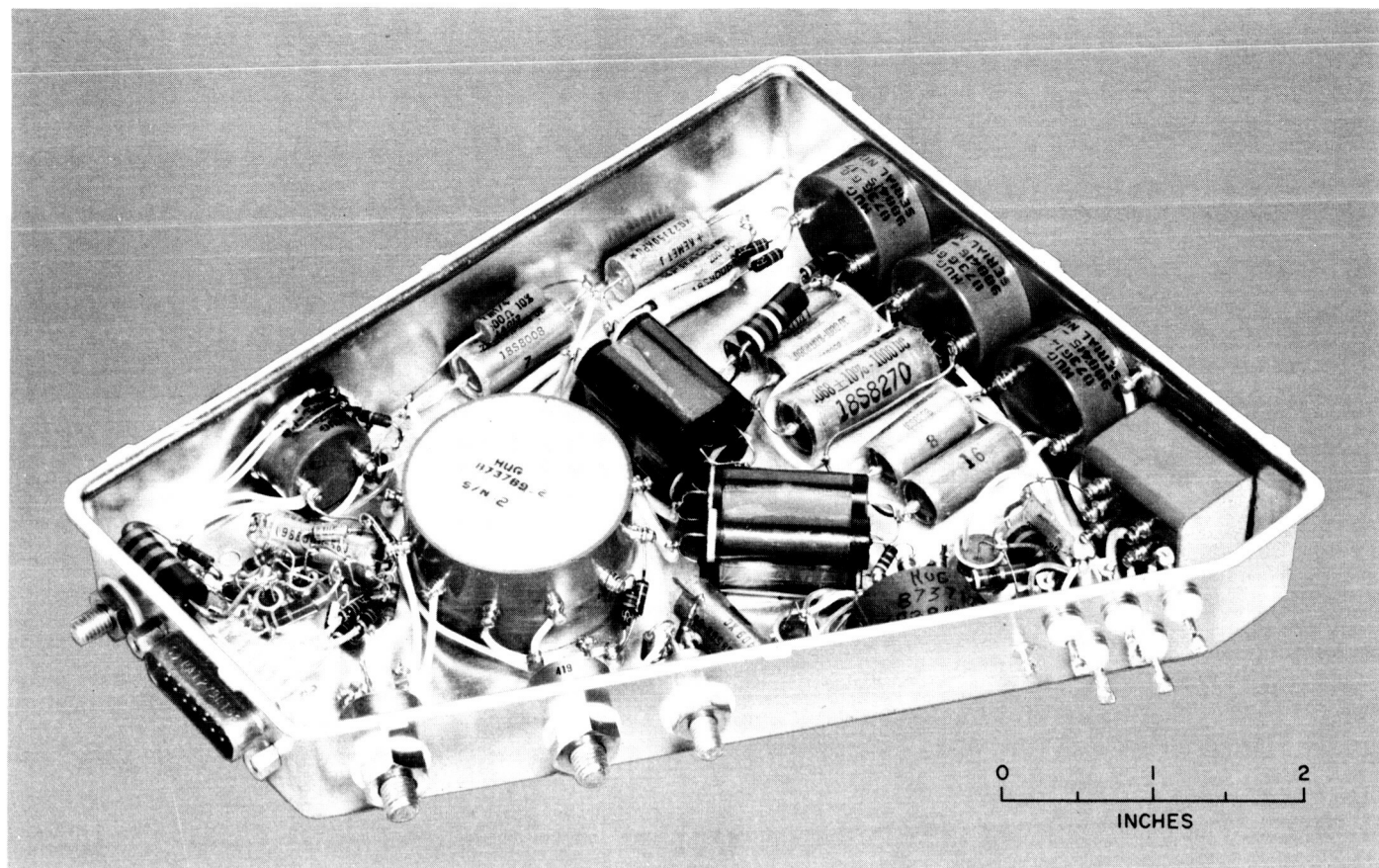


Fig. 29-6. Unencapsulated Syncom satellite power supply unit

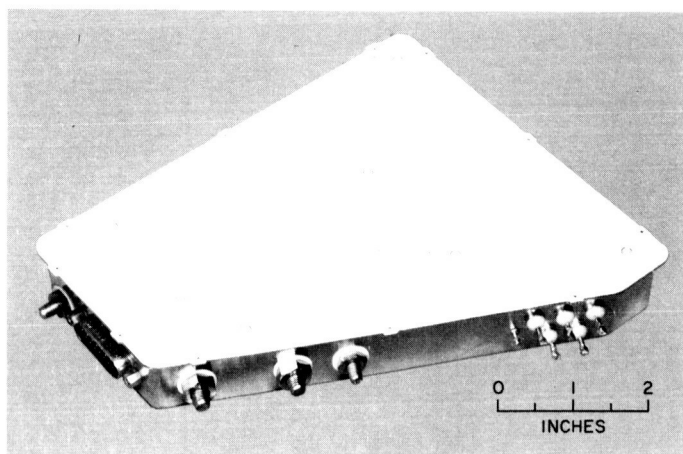


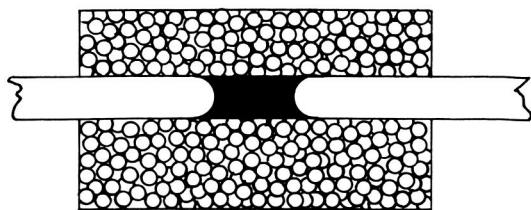
Fig. 29-7. Foam-encapsulated Syncom satellite power supply unit with aluminum cover



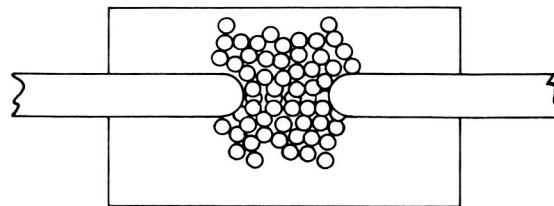


Fig. 29-8. Early Bird package with foam removed for repair of electronics





7-lb DENSITY FOAM



15-lb DENSITY FOAM

Fig. 29-9. Geometry of foam after dielectric breakdown

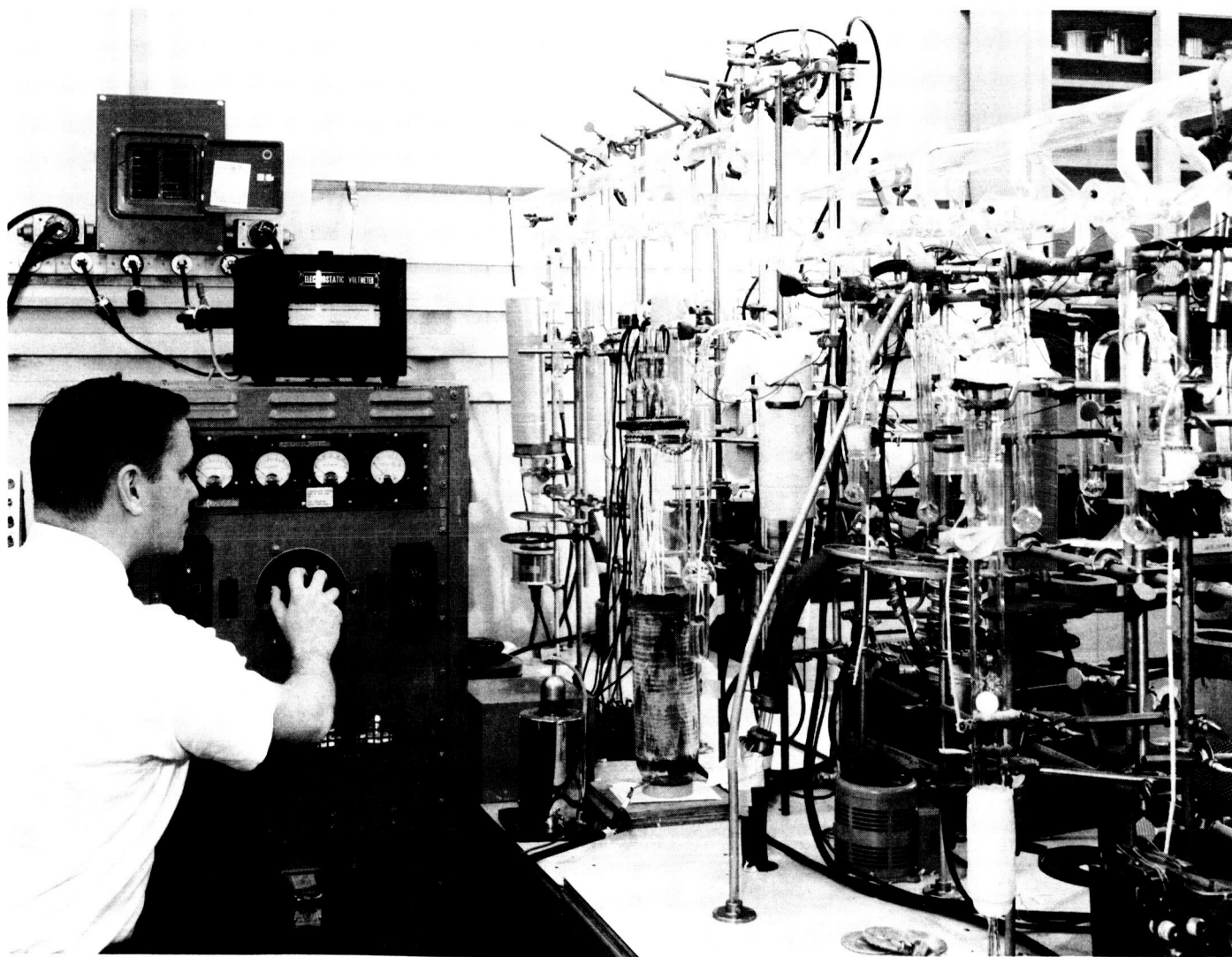


Fig. 29-10. Power supply and vacuum train

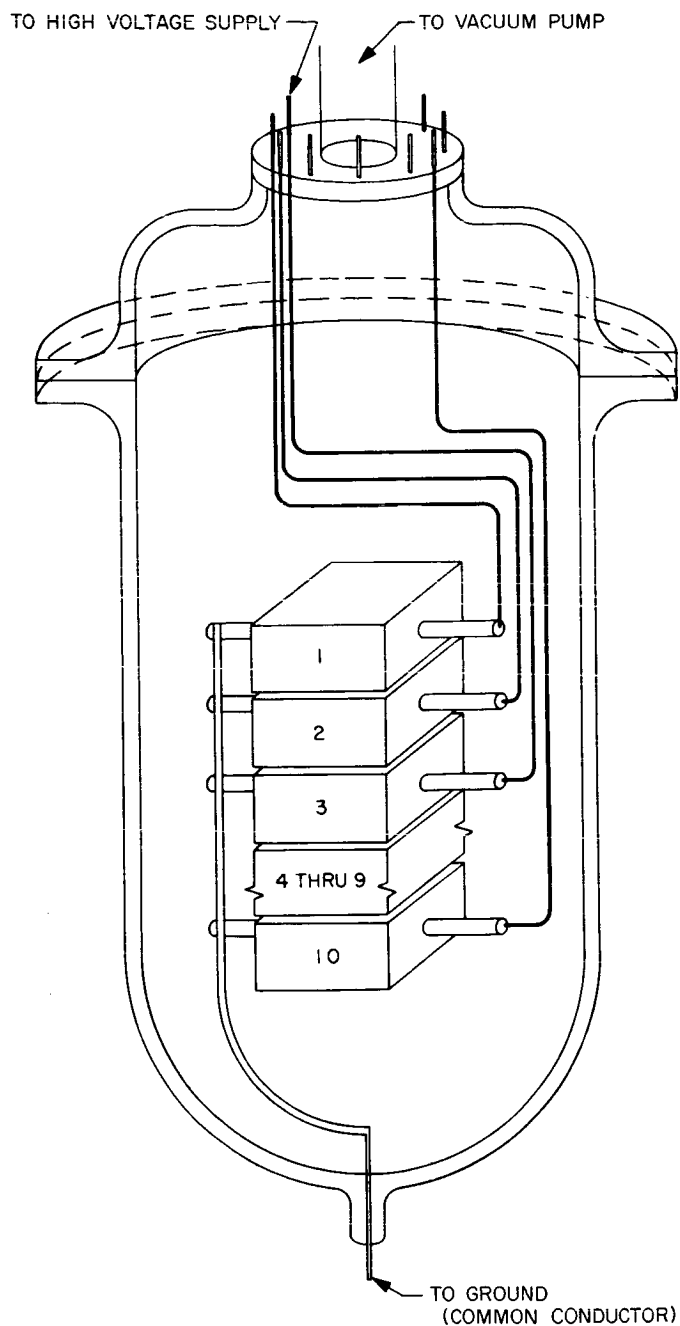
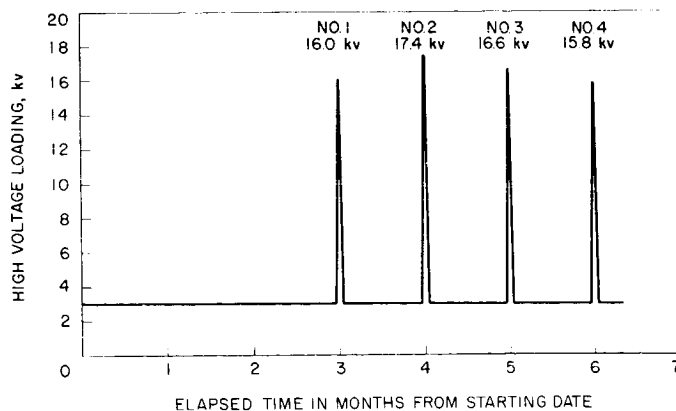


Fig. 29-11. Power supply tank

Fig. 29-12. Test of foams under high-voltage loading



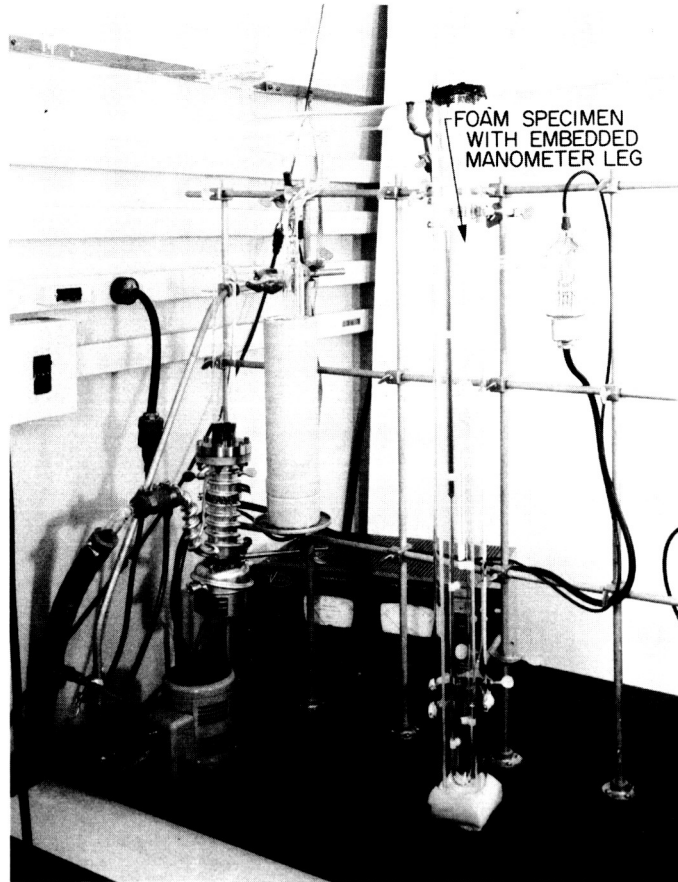


Fig. 29-13. Test equipment used to determine gas pressure within a rigid foam while in a vacuum environment

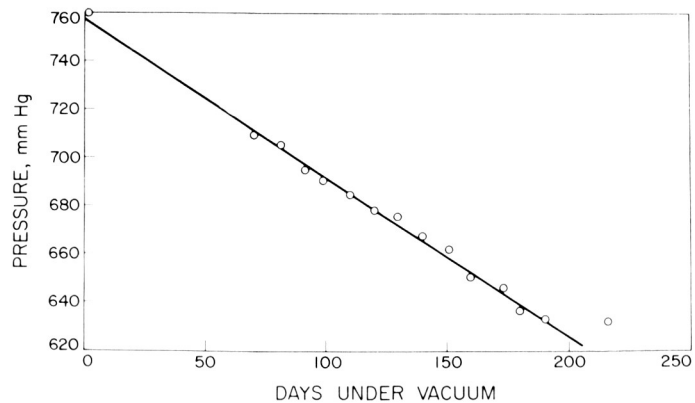


Fig. 29-14. Plot of pressure vs days under vacuum

30. MEASUREMENT OF CORONA DISCHARGE BEHAVIOR  
AT LOW PRESSURE AND VACUUM\*

T. W. Dakin and C. N. Works  
Westinghouse Research Laboratories  
Pittsburgh, Pennsylvania

## ABSTRACT

The significance of the reduced electrical strength of low-pressure air gaps near the Paschen's minimum is considered in relation to the proper operation of electrical systems in high altitude and space vehicles. Experiments are described which illustrate the occurrence and magnitude of partial discharges (corona) in air gaps between insulator and metal surfaces at low pressure and vacuum. The magnitude of the corona pulses observed with alternating voltages varied with pressure, being relatively small at atmospheric pressures and at pressures of about  $10^{-1}$  torr where glow discharges occurred; the corona pulses were considerably larger for intermediate pressures and for pressures less than  $10^{-1}$  torr. Although the pulse magnitude is low in the glow discharge region, considerable integrated charge may be transferred in this pressure region. Calculation of the pulse charge magnitudes indicated that the surface area discharged per pulse at low pressure is at least  $1/3$  to  $1/2$  of the total available area. The characteristics of corona discharges arising from direct voltages applied to low-pressure gaps are also considered.

## INTRODUCTION

While the decline in the electric breakdown voltage of air and gas gaps with decreasing pressure (Paschen's curve) to a minimum value has been recognized (Ref. 1) for more than seventy-five years, the complete significance of this effect on the proper operation of electrical systems in high altitude and space vehicles has probably been overlooked in some cases and inadequately considered in others. Many of the difficulties may have arisen from the assumption that chambers in space

---

\*This paper is a reprint of Scientific Paper 66-1B5-CORNA-P3 (Westinghouse Research Laboratories, May 19, 1966). It is being reprinted here at the request of Dr. Dakin since it contains much of the same information that he delivered at the Voltage Breakdown Conference but in a more complete form. It has been edited slightly in format and style to make it consistent with the other papers in the Proceedings.

vehicles would be evacuated through small holes by the vacuum of space more rapidly and completely than in fact they are. Reliance has been placed on good vacuum insulation when in fact low residual gas pressures probably existed as a result of outgassing of organic resin insulation components and from existing crevices.

It is appropriate to review the fact that the atmospheric pressure declines with increasing altitude to levels of 1 torr at 150,000 ft and 0.01 torr at 250,000 ft and eventually to the highest vacuum of space. At the same time the breakdown voltage of an uniform field air gap of one cm declines from about 30 kv at atmospheric pressure to a minimum of 340 v crest at 0.48 torr and then increases with lower pressure to 1500 v at 0.1 torr and a level of the order of 100 to 200 kv for 1 cm with the best vacuum (Ref. 2). It is found that the breakdown voltage of centimeter sizes gaps in proper vacuum is controlled by the metal or other surfaces and is independent of residual gas as true pressures below about  $10^{-4}$  torr.

To further review the situation: the uniform field breakdown voltage according to Paschen's curve is a function of the product of the pressure and the spacing. This is easily understood at pressures and spacings above the Paschen's minimum, but it is comprehended with more difficulty when dealing with spacings and pressures below the minimum. Paschen's curve was first obtained from experiment. It is usually obtained by measuring the breakdown voltage of a given uniform field gap as a function of pressure. These breakdown voltages when graphed as a function of the product of gap length and pressure give the well known Paschen's curve with a minimum (providing a sufficient pressure range has been covered) as illustrated in Fig. 30-1. Repetition of this experiment for gaps of various lengths yield curves that fall on the others. Papers on this subject by Paschen, Carr, Schuman, Ritz, and others may be located through Ref. 1. Paschen's relation may also be obtained analytically (Ref. 3 and 4). This also yields the principle of similar gaps extended to nonuniform fields providing the breakdown processes are a function of the ratio of field gradient to pressure. For use in nonuniform field situations, Paschen's curve should be plotted as voltage gradient vs p·d. The maximum rather than the average voltage gradient associated with a given electrode configuration should be used to estimate breakdown voltage. Therefore, it was not surprising to observe that as the pressure was reduced on a sphere gap, breakdown occurred along the sides of the spheres, then high on the supporting shanks. Thus, there is a pressure range where smaller gaps do not break down but at the same pressures, larger gaps do. At pressures approaching high vacuum, discharges will follow the longest path

possible in a chamber, avoiding nearby conductors of the opposite polarity. Thus, in larger and extended chambers, the pressure and voltage at which gas discharges can still occur, will be lower than in smaller chambers. In contrast to most sparks at higher pressure, breakdown between conductors in the pressure region in the vicinity of Paschen's minimum usually has the characteristic of a glow discharge. Glow discharges have a greater internal resistance together with a tendency to spread over a substantial volume of the chamber. Also in contrast to spark breakdown at higher pressures, the glow discharges do not instantly tend to develop into an arc between conductors with a low voltage drop, but require higher current levels to form an arc, which current levels may not be available from the circuit under consideration. In this case glow currents of many milliamps may flow, and substantial voltages be maintained, without forming an arc.

Following this background discussion of gas discharges and breakdown between metal surfaces, it is the purpose of this paper to discuss some of the characteristics of partial breakdown or discharges in low pressure systems in the vicinity of and below the Paschen's minimum. Also, the corona, or partial breakdown voltages of gaps between insulator and metal surfaces are compared with the Paschen's curve for breakdown between metal surfaces at pressure and spacing levels in the vicinity of and below the Paschen's minimum. A partial breakdown or corona discharge as considered here is one which does not bridge the gap completely. At high pressures, it is possible to have a discharge confined around points and wires, due to the divergence of or weakening of, the field away from the point or wire. The insertion of a solid insulation barrier ensures partial breakdown over a wide range of pressures.

## EXPERIMENTAL

All tests were made with 60-cycle alternating voltage, except where the use of direct voltage is noted. Several test configurations were used. Each is described in a subsequent section, together with the presentation of data obtained for this particular experimental condition. The circuits used to detect corona discharges, or partial breakdown, have been described in previous papers (Ref. 5).

Breakdown Voltages for Air Gaps Between Insulator and Metal Surfaces

Several investigators (Ref. 6) have shown that at higher pressures (about 1 atmosphere in air) the breakdown voltage between insulator surfaces is the same as between metal surfaces at the same spacing. This also has been confirmed in the authors' laboratory. There is some tendency for the discharge offset voltage at higher pressures to be a little lower than predicted for a uniform field. This has been attributed to a stress concentration by surface charges left by previous discharges on the insulation surface (Ref. 7).

In this section the corona, or partial breakdown, voltages for gaps between insulator-metal surfaces are compared with Paschen's curve for breakdown between metal surfaces at pressure and spacing levels in the vicinity of and below the Paschen's minimum. When testing below this minimum, one must be careful to devise the test cell so that the largest spacing is defined. This is completely contrary to usual breakdown voltage tests where the smallest spacing is defined and set. In the authors' case, this was accomplished as shown in the Fig. 30-1 insert by the simple expedient of using a metal base plate with a small shielded hole for evacuation and an insulating spacer including one or two O-rings with a top glass plate. This creates a large uniform flat gap. There was some edge effect which was of concern, but the test results indicate it was apparently a small factor.

The top electrode (outside the low pressure gap) was formed by a coating of silver paint 5 in. in diameter applied to the top of the glass plate. Corona could occur from the edge of this electrode, but it was determined that the threshold voltage was above any of test voltages reached for the internal low pressure gap breakdown. The corona (discharge) offset voltage is also plotted in Fig. 30-1, and follows the trend of the Paschen's curve, but is below it for  $p \cdot d$  values at and above the minimum, and somewhat above it at pressures below the minimum. The lower values above the minimum correspond to lower values previously sometimes noted at higher pressures. The cause for higher values below the minimum has not yet been decided. It appears to be a case of gap overvolting. It was conjectured that the measured curve was shifted by the  $p \cdot d$  values being in error, but this was rejected after rechecking the gaps, (measured with the O-rings compressed with vacuum in the system) and noting the good correlation of  $p \cdot d$  values falling on the same curve with quite different gap spacings.

### Nature of Low Pressure Corona Discharges

It was noted that the discharges on the positive and negative half cycle were usually fairly symmetrical in this unsymmetrical surface cell, as shown in Fig. 30-2. It was suspected that the discharges might not be always of a pulse type as is often the case at atmospheric pressure, so a higher resistance detector (1 megohm) input was used in series with the cell to detect slower current changes. As shown in Fig. 30-2a, 30-2b, and 30-2c, the discharges above the Paschen's minimum are of the pulse type. In contrast, at the minimum they indicate a glow current initiated each cycle by a small pulse. Then at lower pressures a pulse characteristic reappears.

It should be noted that there is a small opening of the synchronized 60-cycle horizontal trace in the oscillograms (Fig. 30-2) due to the cell capacitance current. (The positive crest voltage is at the right extremity.) This ellipse opening should not be confused with the glow current which shows in Fig. 30-2b at the highest voltage a loop upward in the upper right quadrant and a loop downward in the lower left quadrant. This is shown better in Fig. 30-5a.

### Pulse Charge Magnitude

The magnitude of the pulse discharges at these low pressures is of particular interest in relation both to the area of insulation affected by each discharge and the possible effect of such pulses on the operation of radio or telemetering systems, etc., in space equipment. The size of individual pulses is commonly defined in terms of their coulomb charge,  $\Delta Q$ , change at the equipment terminals. This terminal pulse charge is in turn related to the magnitude of the internal voltage drop,  $\Delta V_1$ , caused by the discharge, and to the capacitance of the insulation in series with the discharge.

The analysis of what happens when a part of gap discharges with a series capacitance barrier has been published by a number of authors (Ref. 8), but will be repeated here for clarity. Figure 30-3 illustrates the equivalent circuit.

The gas gap is illustrated as divided and represented by the parallel capacitors:  $C_{a1}$ ,  $C_{a2}$ , etc., and the series insulation for each part of the gap by  $C_{s1}$ , etc. Other parallel solid and stray capacitance within the test specimen is  $C_{pi}$  and external parallel capacitance connected to the test specimen is  $C_{pe}$ . The pulse voltage appearing across the terminals when the gap discharges is  $\Delta V_t$ .



$$\Delta V_t = \Delta V_1 \cdot \left( \frac{C_{s1}}{C_{pi} + C_{pe} + C_{s1} + \frac{(C_{st} - C_{s1})(C_{at} - C_{a1})}{(C_{st} - C_{s1}) + (C_{at} - C_{a1})}} \right) \quad (1)$$

where  $C_{st}$  is the total capacitance of the solid insulation facing the gap. It is  $C_{s1} + C_{s2} + C_{s3}$ , etc., and  $C_{at}$  is  $C_{a1} + C_{a2} + C_{a3}$ , etc.

The pulse charge is defined as the product of the pulse charge voltage at the terminals ( $\Delta V_t$ ) and all capacitance connected in parallel with the terminals.

Rearranging Eq. (1) gives:

$$\Delta Q \cong \Delta V_t \left( C_{pi} + C_{pe} + C_{s1} + \frac{(C_{st} - C_{s1})(C_{at} - C_{a1})}{(C_{st} - C_{s1}) + (C_{at} - C_{a1})} \right) \cong \Delta V_1 C_{s1} \quad (2)$$

The term within brackets is approximately equal to the specimen and parallel capacitance, if the capacitance change due to the discharge is a small fraction of this. It is assumed that this system is either isolated so far as the high-frequency pulse is concerned by chokes or the high-voltage supply capacitance is lumped into  $C_{pe}$ .

In this fairly well defined area system, Fig. 30-1, these quantities can be fairly well calculated. It is assumed that the internal voltage drop is the calculated voltage on the gas space with the corona offset voltage  $V_{co}$  applied. This gap discharge voltage is:

$$\Delta V_1 = V_{co} K_s t_a / (t_s + K_s t_a), \quad (3)$$

where  $K_s$  is the permittivity (5.0) of the glass plate,  $t_a$  is the gas gap thickness and  $t_s$  is the glass spacer thickness. From this voltage ( $\Delta V_1$ ) and  $\Delta Q$  for the discharge (as obtained by pulse injection calibration of the system) the capacitance in series with each of the discharges can be calculated:  $C_s = \Delta Q / \Delta V_1$ . This capacitance is for a fraction of the area of the glass plate covered by the upper electrode, which was 5 in. in diameter in this case. The fraction, of the electrode area calculated to have been discharged by the larger pulses noted amounts to as much as 1/3 to 1/2, of total area of this fairly sizeable area gap. In one case below the Paschen's minimum, the calculated single discharge area was about 75% of the electrode area.

There is some ambiguity about this capacitance calculation, since the measured quantity is the charge, which is the product of the capacitance in series with the discharge,  $C_s$ , and the voltage drop on the gap at the time of discharge. The maximum voltage drop possible on the gap is in the vicinity of the breakdown voltage. Possibly a small overvoltage could occur. This voltage drop could be less than the breakdown voltage, but if it were, the actual capacitance in series with the discharge would be larger (for the same  $\Delta Q$ ).

A capacitance bridge for measuring the total (integrated) corona-charge transferred each cycle was described in a previous paper (Ref. 9). The interpretation of the oscillograms produced by this method is explained very briefly to point out the significance of the oscillograms in Fig. 30-4 and 30-5. These traces are parallograms with a vertical height which is proportional to the total charge transferred during a whole cycle by integration of all discharges occurring. The width along the horizontal side is proportional to twice the discharge threshold voltage operative during the cycle, while the applied voltage is well above the discharge threshold.

Because calculations based on the integrated charge transfer per cycle from all discharges as determined from figures such as Fig. 30-4 and 30-5b give a capacitance close to that of the whole area of the plate, it seems reasonable to conclude that the gap voltage change at breakdown is equal to the breakdown voltage.

The charge values measured for the larger individual pulses bear a corresponding relation (i. e.,  $1/3$  to  $1/2$ ) to the integrated charge transferred each half cycle.

The correspondence between current and charge measurements where the glow discharge phenomenon exists is shown in Fig. 30-5a and 30-5b. Here, because of their small amplitude and almost continuous occurrence, steps of charge transfer are not observable on the charge oscillogram (Fig. 30-5b), as they are in Fig. 30-4. It should be noted that the pulse sizes (Fig. 30-5a) at p-d near the Paschen's minimum were very much smaller, being less than one tenth the total of integrated charge transfer per cycle under this condition, since so much charge was being transferred by the pulseless glow discharge.

#### Low Pressure Discharges in Fringing and Divergent Fields

It should be recognized that fringing electric fields from conductors located in a region under higher pressure or encapsulated conductors can cause discharges in

adjacent low pressure regions at quite low voltages. This is illustrated by the graph, Fig. 30-6. Electrodes were bands of wire wrapped at selected spacings around a glass tube. The pressure within the tube was reduced into the Paschen's minimum region. The corona onset and offset voltages and charge magnitudes are indicated as a function of spacing. In this case, the smaller pulses at 1 torr are probably indicative of the presence of a predominately glow discharge breakdown rather than a pulse type breakdown at this pressure. The electric field between the wire bands spreads into the low-pressure tube. This could happen at low pressures on the surface of encapsulated systems which are not shielded.

#### Discharges from Insulated Wires

In Fig. 30-7 is illustrated the decline in discharge threshold voltage for an insulated wire spaced at several spacings from a plane uncovered metal electrode. As the pressure drops to the lowest values, the discharge avoids the wire nearest the plane and spreads up to the wire near the top of the chamber. The pulse charge values shown in Fig. 30-8 for the same system indicate that a substantial fraction of the total area of the wire is brought up to ground potential by the discharge. This is estimated from the capacitance, calculated from the charge value and the corona threshold voltage. Most of the applied voltage drop prior to discharge in this system is across the low pressure gas space. Thus, the crest corona threshold values in Fig. 30-7 will be approximately the gap breakdown voltage. Incidentally, this corona discharge voltage can usually be calculated at  $p \cdot d$  values greater than Paschen's minimum especially for simple electrode geometry. For example, 2-cm spheres at 0.25-cm gap have an utilization factor (Ref. 10) of 0.92, and at a  $p \cdot d$  of 15 cm mm Hg, the uniform field breakdown is 1480 v, yielding a calculated corona onset of 1370 v. The value obtained by experiment (Ref. 11) was 1380 v.

The fraction of the total length of the wire that is discharged by each pulse may be estimated from the following data. At  $10^{-2}$  mm Hg pressure a crest voltage of 4250 v is obtained for the 10 cm gap from Fig. 30-7, and a corresponding negative pulse charge of about 18,500 picocoulombs from Fig. 30-8. The series capacitance calculates to be approximately 4.4 picofarads. The capacitance of the 9.5 cm of exposed wire is 17 picofarads (as measured in mercury) thus over 1/4 of the wire is discharged by a single pulse.

DC Discharges at Low Pressures

As at high pressures, dc corona, limited by solid barriers produces much less frequent pulses, since a discharge places a charge on the opposite surfaces of the gap, which must leak away before sufficient voltage again develops across the gap to cause a breakdown. This is illustrated by Fig. 30-9, where the discharge is created across the inside of a glass tube held internally at low pressure, and placed between metal electrodes in an oil bath to avoid external discharges. The pulses begin on a voltage rise at the discharge onset voltage. When held at a steady voltage above the onset threshold, discharges occur at intervals of 15 to 20 sec. It turns out that this time is approximately the same as the RC time constant for the capacitance of the series glass insulation under stress and the glass resistance, as it should be if the charge leaks through the glass. Also the pulse charge magnitude for this system calculates to give the right order of magnitude for the capacitance of the glass in series on the two sides. As suggested by Whitehead (Ref. 12), the relaxation time of a dielectric is the product of the dielectric constant, the resistivity in ohm-cm, and the dimensional constant  $10^{-11}/36\pi$  which yields a discharge time of the right order of magnitude. Thus a knowledge of the configuration and dimensions of the dielectric is not necessary to estimate the discharge time.

## CONCLUSION

It is shown in this paper that the corona phenomena at low pressures is in many respects an extension of that noted at higher pressures, but that glow corona with small or no pulses predominates between plane surfaces near the Paschen's minimum. In divergent fields, however, very large pulses are noted in this same region. Pulse sizes of corona in the low pressure region are often very large, indicating large areas of surface are completely discharged to the polarity of the opposing surface.

At very low pressures approaching vacuum with large chambers, the discharges take very long paths, and are observed to be intermittent during pump down, possibly due to bursts of gas evolved from materials, surfaces and crevices.

The low-pressure discharge voltage in plane gaps bounded by an insulator surface is of similar magnitude to that between metal electrodes. Maximum discharge magnitudes may be calculated approximately from a knowledge of the gap breakdown

voltages and the surface area of the insulation in series with the discharge. Also the pulse voltages occurring in the circuit due to such discharges can be estimated if the circuit capacitance at the terminal closest to the discharge is known. Such pulse voltages may be quite high, if the parallel circuit capacitance is small, and may possibly have a significant effect on control and telemetering circuits.

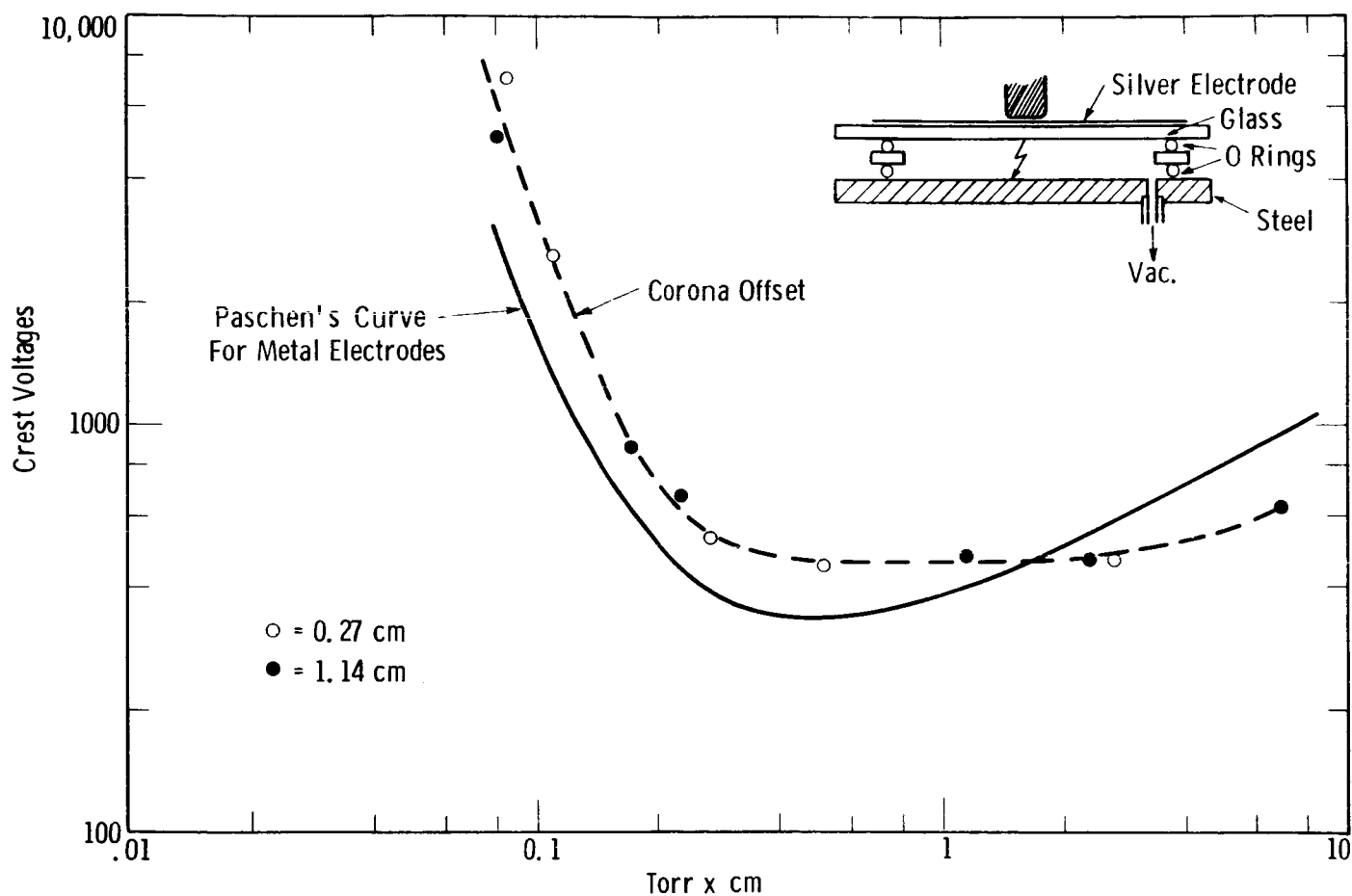
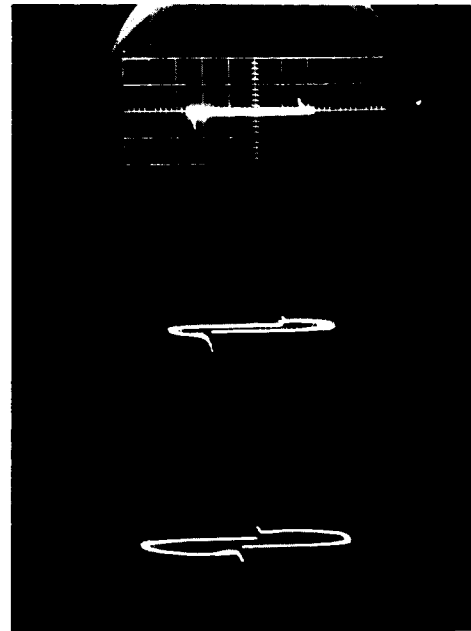


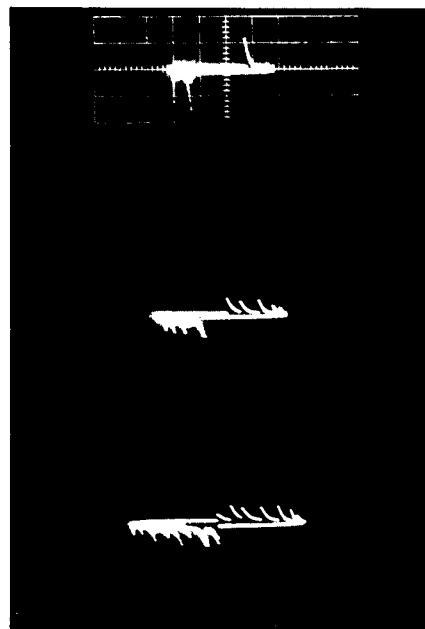
Fig. 30-1. Corona offset voltage between glass-steel surfaces at low pressures



$p \cdot d = 0.08 \text{ cm} \cdot \text{torr}; 5.6, 8.4, 11.2 \text{ KV}$   
 $\Delta Q \approx 40,000 \text{ pc}$



$p \cdot d = .23 \text{ cm} \cdot \text{torr}; 0.60, 0.81, 1.08 \text{ KV}$   
 $\Delta Q \approx 13,000, 24,000, 13,000 \text{ pc}$



$p \cdot d = 2.3 \text{ cm} \cdot \text{torr}; 0.42, 0.57, 0.76 \text{ KV}$   
 $\Delta Q \approx 12,000, 16,000, 16,000 \text{ pc}$

Fig. 30-2. AC discharge behavior at low pressures between metal and insulator surface, 1.13-cm gap in series with 0.92-cm pyrex (83% voltage on gas)

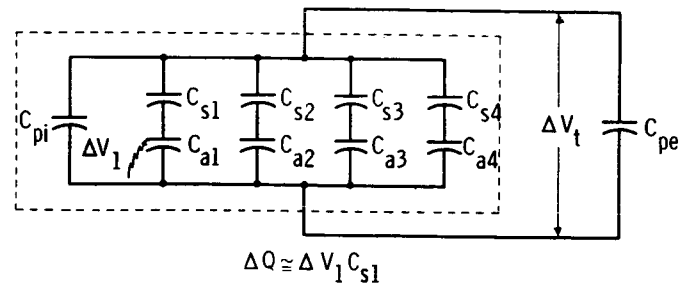
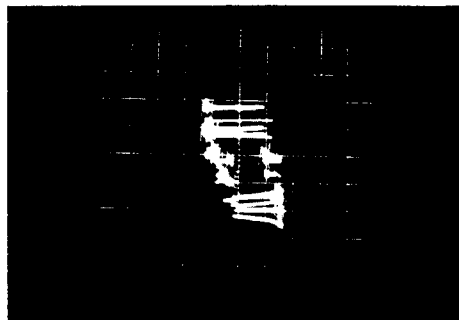
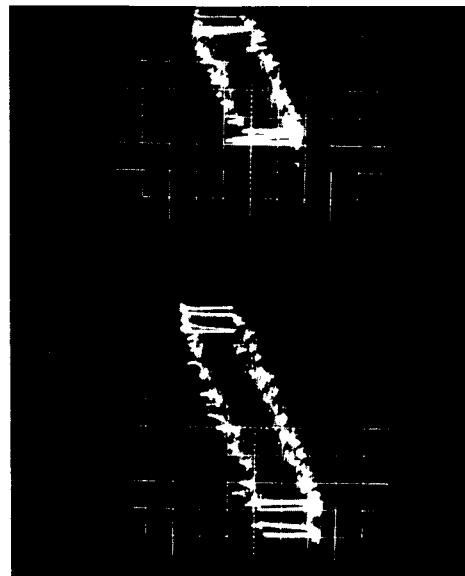


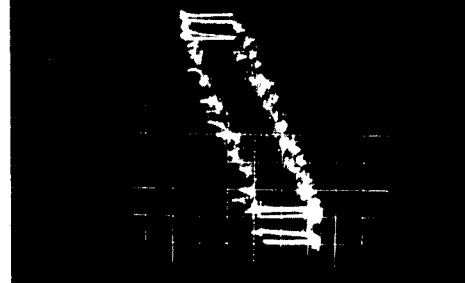
Fig. 30-3. Circuit analysis for a corona discharge in an insulation system



485 V(rms)  
 $Q_{\max} \approx 30,000 \text{ pc}$



660 V(rms)  
 $Q_{\max} \approx 40,000 \text{ pc}$



880 V(rms)  
 $Q_{\max} \approx 60,000 \text{ pc}$

Fig. 30-4. Integrated charge transfer per cycle across a 1.13-cm gap.  $p \cdot d = 2.3 \text{ cm-torr}$



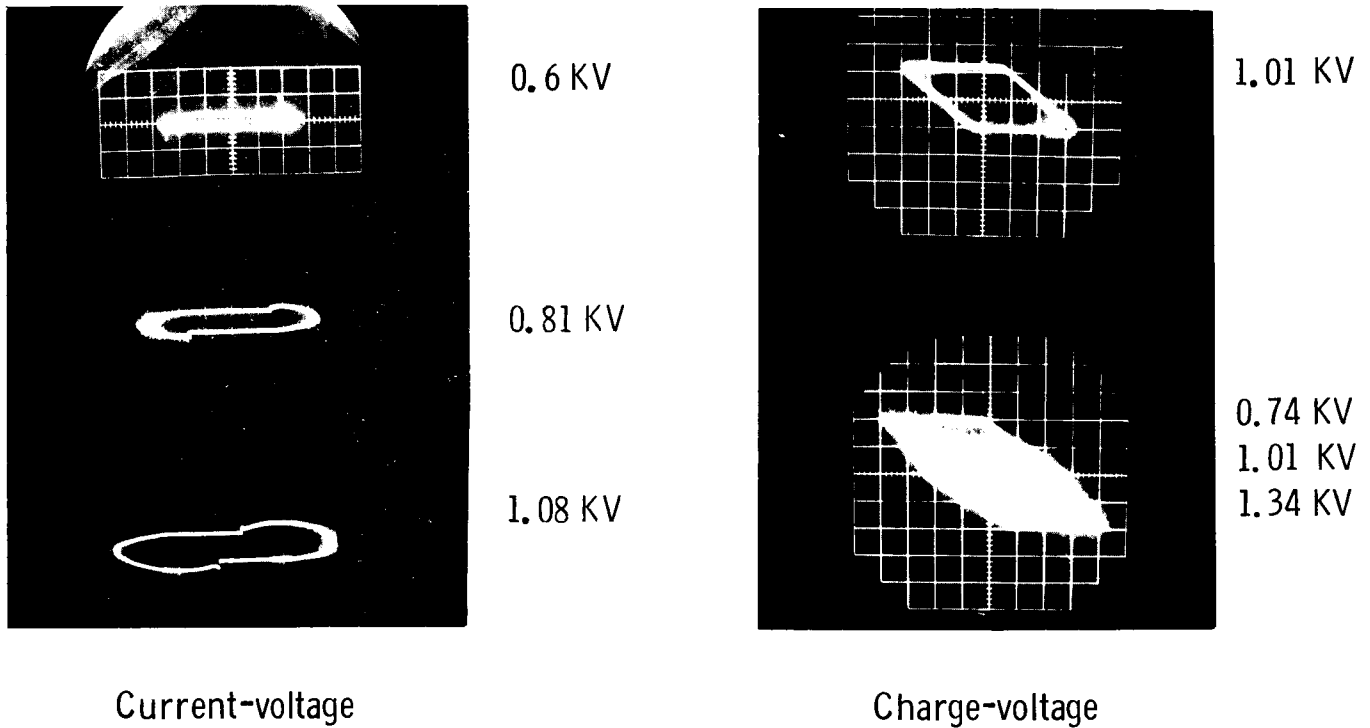


Fig. 30-5. AC discharge between metal and glass surfaces at 2 torr, 0-266-cm gap in series with 0.92-cm pyrex glass

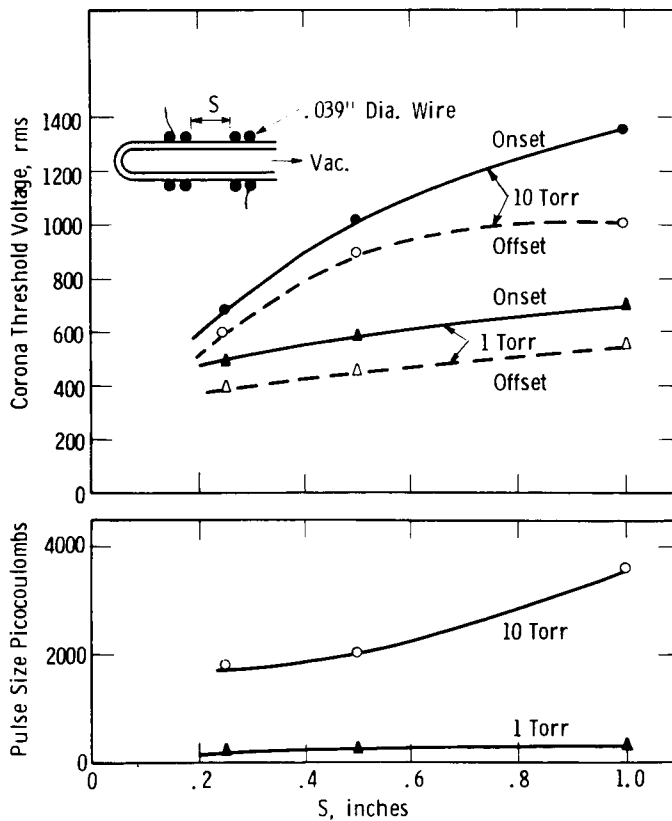


Fig. 30-6. Fringing field corona within a low pressure 5-mm-ID, 8-mm-OD glass tube

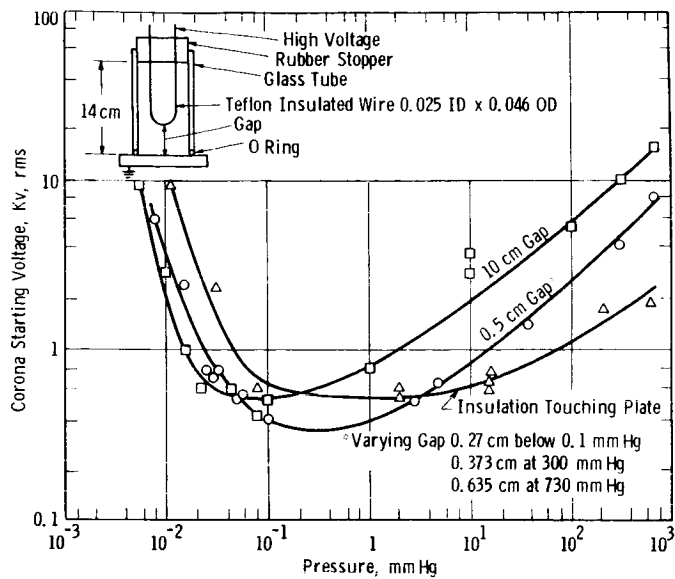


Fig. 30-7. Corona starting voltage from Teflon-insulated wire-to-metal plane

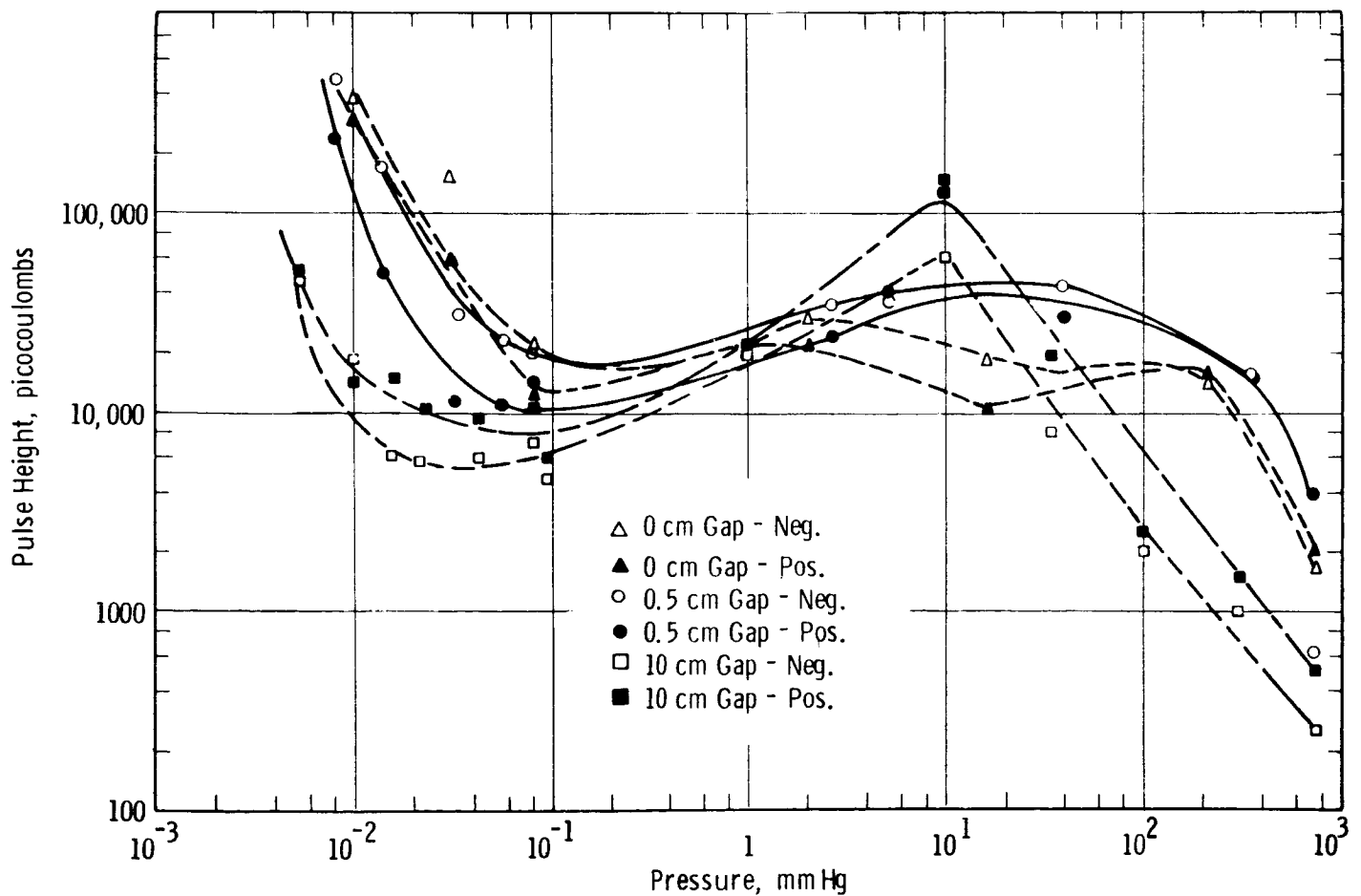


Fig. 30-8. Corona pulse height from Teflon-insulated wire-to-metal plane (see sketch on Fig. 30-7)

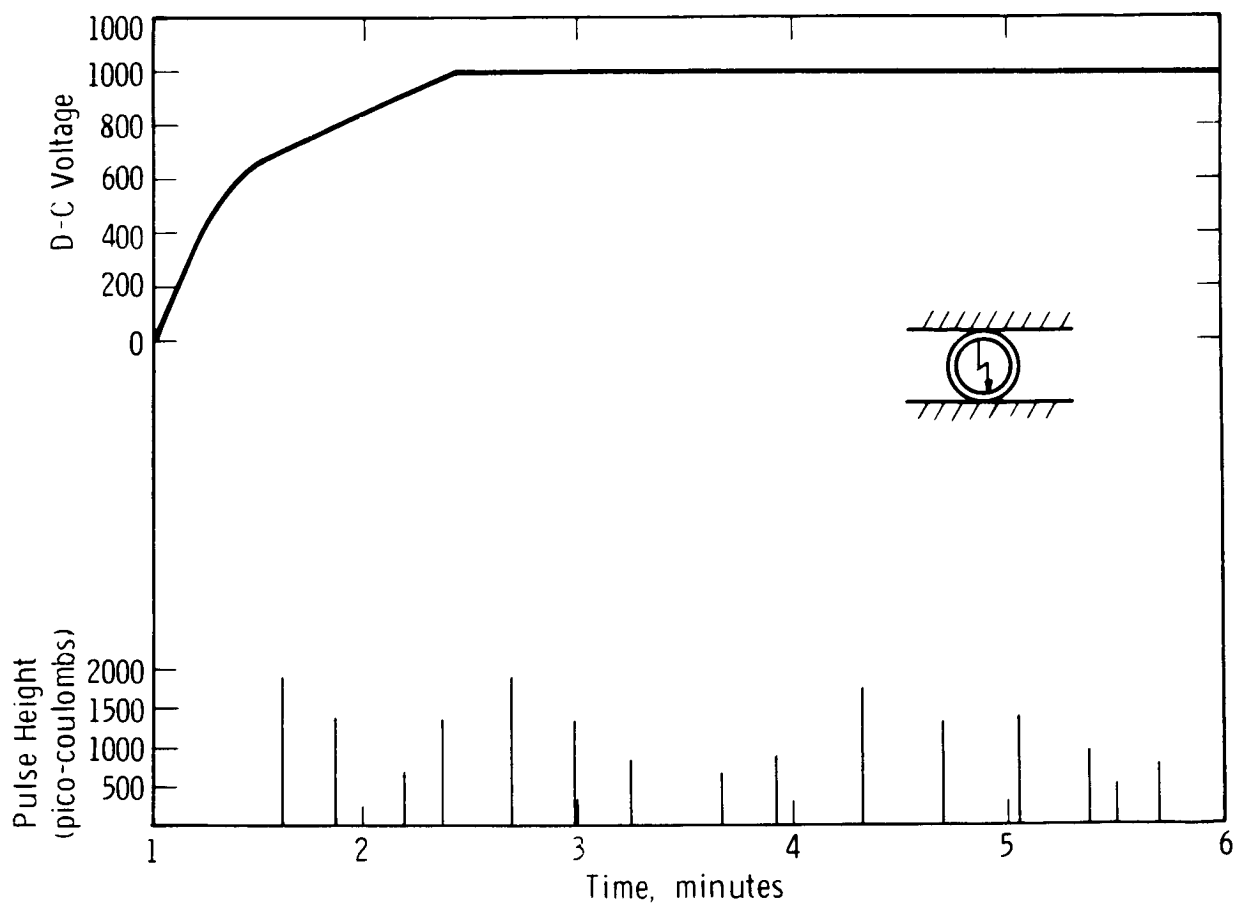


Fig. 30-9. Pulse behavior with direct voltage applied to a 5.1-cm length of 6-mm-ID glass tube ( $p = 500 \mu$ )

## REFERENCES

1. J. M. Meek and J. D. Craggs, Electrical Breakdown of Gases, Oxford University Press, London, England, 1953, p. 84.
2. R. Hawley, "Vacuum as an Insulator," Vacuum, Vol. 10, No. 4, 1960, pp. 310-318.
3. K. R. Allen and K. Phillips, Nature, Vol. 183, 174, 1959 (see also J. C. Devins and A. H. Sharbough, Electro-Technology, Vol. 67, 1961, p. 103).
4. H. Margenau, Physical Review, Vol. 73, 1948, p. 197 (see also "Gas Discharge II," Encyclopaedia of Physics, Vol. 22, Springer, Berlin, 1956).
5. T. W. Dakin and J. Lim, "Corona Measurement and Interpretation," Transactions, American Institute of Electrical Engineers, Vol. 76, Part III, Dec. 1957, pp. 1059-1065.
6. D. S. Rodbell, J. B. Whitehead, and C. F. Miller, Journal of the Electrochemical Society, Vol. 101, 1954, p. 91 (see also H. C. Hall and R. M. Russek, Proceedings of the Institute of Electrical Engineers, Vol. 101-2, 1954, pp. 47-55).
7. J. C. Devins, "Electrical Discharge Characteristics of the Plane Parallel Gap Bounded by Insulating Surfaces," American Institute of Electrical Engineers, Paper No. CP 57-83 (1957).
8. W. Boning, "Luftgehalt und Luftspaltverteilung geschichteter Dielektrika," Archiv. Für Electrotechnik, Vol. 48, 1963, pp. 7-22.
9. T. W. Dakin, P. J. Malinaric, "A Capacitance Bridge Method for Measuring Integrated Corona-Charge Transfer and Power Loss per Cycle," Transactions, American Institute of Electrical Engineers, Vol. 79, Part III (Power Apparatus and Systems), 1960, pp. 648-52.
10. A. Schwaiger, R. W. Sorensen, Theory of Dielectrics, John Wiley and Sons, Inc., N. Y., 1932, p. 60.
11. T. W. Dakin and C. N. Works, "Gas Discharges in Insulating Systems at Pressures Between Atmospheric and High Vacuum," Symposium on Dielectrics in Space, Westinghouse Research Laboratories, Pittsburgh, Pa., 1963, p. 2-1.
12. S. Whitehead, Dielectric Breakdown of Solids, Oxford University Press, London, 1951, p. 178.

## 31. PREVENTION OF DIELECTRIC FAILURES IN SPACECRAFT

E. C. McKannan  
Marshall Space Flight Center  
Huntsville, Alabama

At this Workshop we have heard about many voltage breakdown problems in electronic components. These problems have involved direct arcing between contact points, corona or glow discharge in the rarefied gas space between contacts, arcover or tracking along an insulator surface, and breakdown of foamed insulators. Many of these problems were not evident when equipment was tested at atmospheric pressure or even at very low pressures. They occurred when equipment was exposed to the pressure region of the Paschen Law, which describes a minimum in the function of breakdown voltage vs pressure and which has been thoroughly discussed in the preceding papers.

The subject pressure range from  $10^{+2}$  to  $10^{-2}$  mm Hg is associated with the standard environmental pressure at altitudes from 60,000 to 300,000 ft. However, much equipment has been subjected to pressures within the subject range while in spacecraft orbiting at much higher altitudes. It is important to note that the subject pressure range has been reached due to a variety of unexpected gas sources in relatively enclosed spaces. This occurred within equipment which was supposed to be operating at much lower pressures because of the higher altitude. Hence, there appears to be an even greater problem with equipment that operates for long times in orbit while exposed to gas sources than there is with equipment that traverses the critical altitude range during ascent. The unexpected gas sources involve:

1. Atmospheric gases: oxygen, nitrogen, and water vapor which are absorbed by polymeric materials prior to launch.
2. Volatilized fluids: oils, greases, hydraulic fluids, and sealants.
3. Outgassing of low-molecular-weight constituents of polymeric materials: plastics, elastomers, and paints.
4. Partially trapped gases which expand at lower pressures: screw threads, shaft clearances, sealed bearings, and hermetically sealed devices.

The problems which have been described in this Workshop have involved a wide variety of spacecraft and of manufacturers, but they have involved a relatively few specific electronics packaging techniques. A high-voltage discharge has bridged the open space between switch contacts or between tube socket pins. A high-voltage discharge has leaked across the surface of an uncoated printed circuit board or across the interface of a cable connector. A high-voltage surge in a circuit has shorted a transistor or a capacitor. A high-voltage discharge has broken down a foamed plastic potting compound. An electrostatic charge has accumulated on a surface and uncontrollably discharged along the wrong path. In every case the discharge resulted from combined high voltage and a critical pressure. It is a credit to the concept of all-systems testing that many of the problems were encountered, recognized, and fixed during evaluations in environmental simulation chambers. Many of those problems which occurred in flight did not impair the primary mission of the spacecraft. However, based on the experiences learned here, I think you will agree that many of these problems can be avoided in the future.

A summary of conservative design practices and packaging procedures may be given which would help to avoid the problems described.

1. Avoid high voltages wherever possible.
2. Avoid sharp points and close spacing to reduce field concentrations.
3. Encapsulate all portions of circuitry including tube pins and printed circuit boards to avoid exposure to gas space. This abandons the idea of using circuitry exposed to the space environment and of depending upon the vacuum of space to separate circuits.
4. Use electrical connectors with elastomeric faces and high-compression fittings to avoid gas spaces.
5. Eliminate gas by using large vent holes in boxes and enclosures. Use dry lubricated, open bearings. Provide open channels to screw threads, shaft clearances, and other tight spaces which trap gas.
6. Avoid hermetically sealed components unless the leak rate at low pressure is demonstrated to be negligible.
7. Use organic potting and insulating materials which have been thoroughly outgassed, dried, and purged of low-molecular-weight (volatile) constituents.

8. Use only solid potting compounds in place of foams, which allow diffusion of cell gases over a long period of time. The question of the corona resistance and breakdown strength of foams is not settled.
9. Use bleeder resistors to discharge capacitors, current limiters to protect power supplies, and external shielding to avoid electrostatic charge accumulation.

A flight experiment is planned to demonstrate the relative efficiency of these packaging techniques. It is expected that the experiment will be contained in a separate box on the instrument unit of a Saturn vehicle. The experiment will involve, mainly, a series of interdigitated, resistivity test patterns on printed circuit boards. Current flow and corona discharges will be measured at increasing voltages between two adjacent circuits on printed circuit boards under the following conditions:

1. Encapsulated in a solid, rigid compound.
2. Encapsulated in a solid, flexible compound.
3. Encapsulated in a low-density, foamed plastic compound.
4. Unprotected surface in a closed space in which pressure is measured.
5. Open to the space environment but screened from possible electrostatic fields.
6. Open to the space environment and unprotected from electrostatic fields.

A specimen in the form of a guarded plate capacitor with one open mesh screen electrode, employing the same dielectric material as the printed circuit board, will be used. It will provide information on dielectric constant or dissipation factor changes of the base materials during the experiment.

It is important to measure the environmental conditions as carefully as possible in order to interpret the results of the experiment. Therefore, we plan to measure the temperature, pressure, solar radiation, and electrical field intensity in the vicinity of each specimen. With this experiment we hope to duplicate under well defined conditions some of the problems which occurred and to compare the efficiency of the suggested solutions.

### 32. PROBLEMS ENCOUNTERED USING CONNECTOR SEPARATION FOR OPENING LOW VOLTAGE CIRCUITS

J. R. Goudy  
Electrical Systems Division  
Langley Research Center  
Hampton, Virginia

Some tests were run at Langley Research Center about a year ago, the results of which we found surprising and thought would be of interest to the attendees of this conference. The tests were run as a result of a review of the Scout vehicle ignition harness, which questioned the use of connector separation to open low-voltage circuits. The phenomenon encountered during the tests was not corona, but was in effect arcing and flashover, which was assisted by the critical air pressure region. The test consisted of opening circuits by separating connectors in a vacuum chamber. While corona is generally considered to be a problem in the 250- to 300-v range, the test uncovered a related problem in the 50-v range. Various pyrotechnic devices, such as igniters, explosive bolts, and cable cutters, used on vehicles occasionally short-circuit after activation. Since this effect can prevent the battery from performing its next function, the circuits usually incorporate some means of eliminating the problem, such as opening the circuit after the function has occurred or inserting a limiting resistor in the circuit.

Figure 32-1 essentially reflects the Scout second-stage ignition circuit as it was about a year ago. Tracing the circuit, we go from the battery positive through contacts controlled by the programmer, down through a connector at the third-to-second stage interface, down through connector PJ106 at the second-to-first stage interface, and then back up through to the second-stage igniter. The return route followed a similar path back to battery negative. Upon second-stage ignition, connector PJ106 separated and isolated the second-stage igniter from the battery.

If the second stage igniter had shorted on activation, connector PJ106 would have been opening a circuit carrying about 20 to 24 amp. You might note at this time the pin numbers, particularly the fact that after the separation, female pin 17 is referenced back to battery positive, while female pin 18 is referenced back to negative.

The particular concern expressed during the harness review was whether the initial arcing from the female to the male pin was ionizing the gases remaining at the face of the connector, thereby resulting in an arc or flashover from female to female pin.



To answer these questions, tests were run in which we tried as nearly as possible to simulate the actual vehicle conditions. They were run in a vacuum chamber, in which the vacuum ranged from 2.85 to 1.64 mm Hg or about 125,000 to 139,000 ft (a simulated attitude that was roughly that of second-stage ignition on the Scout). The pumpdown time for the chamber was 70 sec, which simulated first-stage burn time.

The connector being tested was a Deutsch DS-type connector; it was lanyard pull 27 pin. In the vacuum chamber a solenoid was used to pull the lanyard; the solenoid circuit is shown on the right of Fig. 32-2. Power supply 1 (feeding in plus and minus) was an unregulated power supply used to simulate the vehicle batteries. The circuit runs positive up through pin 17, down through pin 16 to the load, and then through pin 15, and back through pin 18 to negative (which was the same circuit and pins as used on second-stage ignition on the Scout). Three resistors shown on the figure were approximately 0.08 ohm and were put in strictly for instrumentation purposes. Power supply 2 (which is shown feeding in at the very bottom) was used strictly for control power.

The operation sequence went as follows: Switch 1 was closed energizing relay K-1, closing the contact, and putting power to the load. About 2 sec later, switch 2 was closed energizing relay K-2, which in turn energized the solenoid separating the connector. The second pole of switch 2 is used in this circuit with the 1.5-v battery in series with the galvanometer through the connector. This circuit was used to give us a time relationship on the connector separation between our various tests.

On one of the tests (No. 4), the voltage input at separation was 50 v; current in the circuit at separation was 15 amp. Less than 2 millisec after separation the current dropped to nearly 1 amp. It then started to rise rapidly and reached 46 amp about 1 millisec later. At this point started what I will refer to as the secondary arcing. As you see, pins 19, 8, 6, 2, and 1 were not originally conducting current when the connector was pulled. However, they are tied together and referenced back through a galvo to the positive of the supply.

Shortly after the main arc had reached 46 amp, pin 18, which had been arcing over the pin 17 during this time, suddenly started to arc over to pin 6 and possibly pin 19. But this secondary arcing rose rapidly and went up to about 30 amp, drawing off of the main arc from pin 18 to pin 17, which dropped down to 21 amp.

Shortly thereafter, this secondary arcing from pin 18 to pin 6 dropped off and went to zero, while the main arc increased a little bit in current, but generally remained about 20 to 30 amp for the duration of the arc (which was 770 millisec).

Figure 32-3 shows the key portion of the record of test 4 that I just described. We have extended the load current trace as can be seen on the figure; normally, it would have occurred earlier but this gives you a zero reference. Trace 4 shows the connector separation. You can also see the load current going back to nearly 1 amp, then rising sharply to 46 amp, at which point you get trace 1 the secondary arcing increasing to 30 amp drawing from the main arc, and it reduced about 21 amp. The secondary arcing then drops off, eventually going to zero while the main arc continues on for the 770 millisec.

We ran some tests prior to this one in which we used a little different pin arrangement. Figure 32-4 shows the face of the connector with the pin arrangement. As you remember, we were using pins 17 and 18 in the testing you just saw. We were wondering if this arcing could affect circuits on adjacent pins that might be using the same battery. To do this, instead of pins 17 and 18, we used pins 7 and 11, respectively. We jumpered the surrounding pins together and referenced them back to the opposite polarity; in this case, pins 6, 1, 2, 8, and 19 to negative, and the pins surrounding pin 11 back to positive.

A number of tests (at least ten or more) were run with this configuration. Of these tests, we received several arcs from pin 11 to one of its adjacent pins. These arcs were not of too long duration, relatively speaking, but they were still staying in the region of 5- to 10-millisec, and were of sufficient current to put a good transient on any line. The arcs would run anywhere from 20 to 35 amp depending on voltage.

Approximately 100 tests were run varying the parameters with the following results: The voltage was varied from 32 to 60 v. The lowest voltage at which an arc was obtained was 40 v. The frequency of arc occurrence increased with voltage, happening about 70% of the time at the 60-v level. The duration of the arc, however, was inversely proportional to the voltage, lasting about 30 millisec, generally at the 60-v level, while the arc obtained at 40 v lasted 1,026 millisec.

The current was varied over a range of 10 to 24 amp, and in this range did not seem to have much effect. In fact, the longest arc (1026-millisec) was triggered at 10 amp and 40 v. The vacuum ranged from 2.85 to 1.64 mm Hg in this range and did not seem to affect the results. The connector pull time was varied from 18 to 70

millisec and also did not affect the results a great deal. There was a slight increase in arc occurrence at the higher pull time.

A number of variables in these tests were not accurately controlled, and we were unable to make some measurements (particularly the pressure profile in the connector) that we would like to have made. These connectors were sealed, and the pressure profile would have contributed some valuable information. However, we are separating them in the critical range and perhaps the pressurized portion doesn't affect us a great deal; we don't know. If these tests had been run as part of a research project, we could have extended the current and the pressure (the tank pressure parameters) to where they could have become meaningful. As it was, they really have no meaning. We know we were at a level that was adequate, but we don't know what the extremes of this level are.

I feel sure that a much lower current level would trigger the same arc, and I think under the right conditions less than 40 v would trigger it. However, the tests were run to determine if the Scout had a possible ignition problem, and although we couldn't quite reach the Scout voltage levels and get an arc, it was still close enough to make us modify the circuit.

The one thing that I came out of this with was probably the inconsistency and the frustration of trying to do arc-testing of this type. I found that it's not predictable. You go to what you think are the worst cases and you may or may not get your arc. There are many variables to mating the connectors that just can't be accurately controlled. I do think that what we saw here might have some bearing on the Agena problem mentioned the other night during the discussion on connector separation, but I think it is an area that needs some more looking into.

#### OPEN DISCUSSION

DR. DAKIN: I don't pretend to be very knowledgeable about the behavior of arcs, but I asked some colleagues who talk about them frequently and one of the phenomena that occurs rather readily is the transfer of arcs to adjacent terminals. In fact, this transfer is utilized in the operation of power circuit breakers. They will have a contacting terminal and then as it is pulled away, the arc will transfer to an arcing terminal, which projects out a little bit further and is closer. It seems to me that this situation is comparable to that condition. In

other words, you have an arc starting out probably between the terminals that are being separated, and then as separation increases, the plasma is spread out enough so that it sees a closer terminal, and the arc transfers to it.

MR. GOUDY: In this connection, one of the things that I can't quite explain is why the secondary arc (as I referred to it) never sustained itself for any long period of time. In the test four you just saw, for example, for a while it was drawing 30 amp of arc when the main arc was down to 21 amp. The distance was about the same (as nearly as you get with a connector), and yet the secondary arc always drops out. Now I'm not quite sure why this happens.

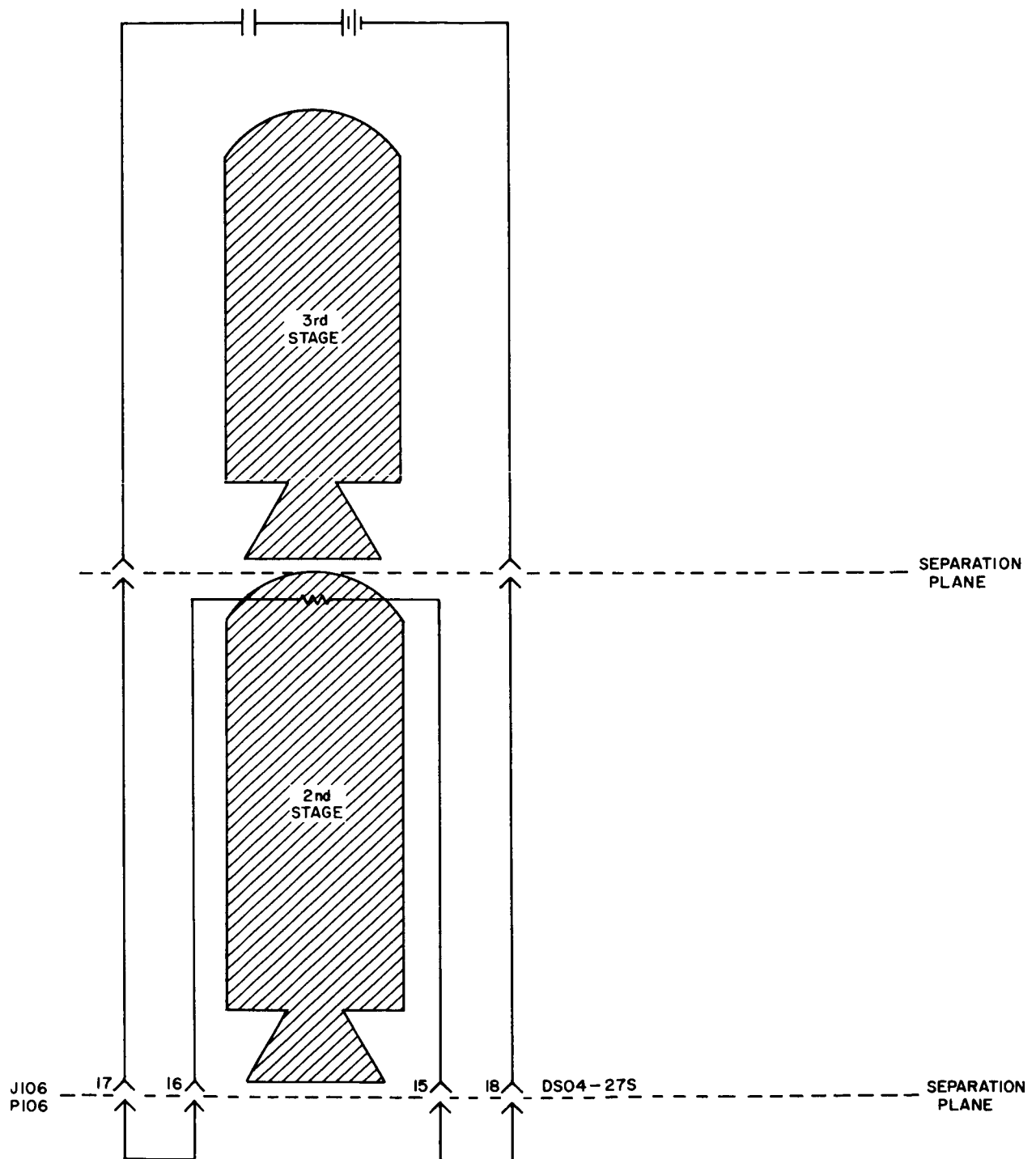


Fig. 32-1. Scout ignition circuit routing

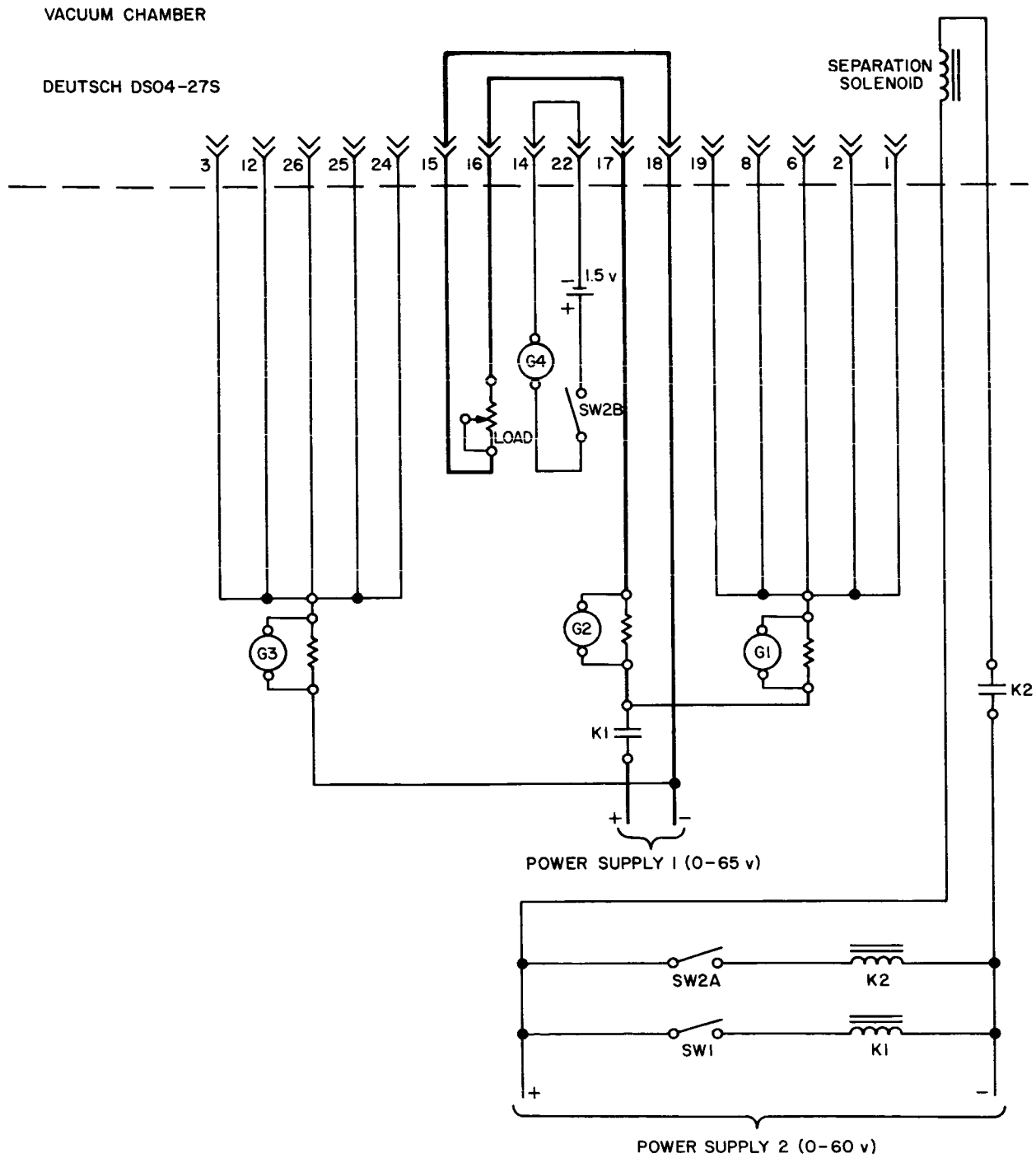


Fig. 32-2. Test circuitry

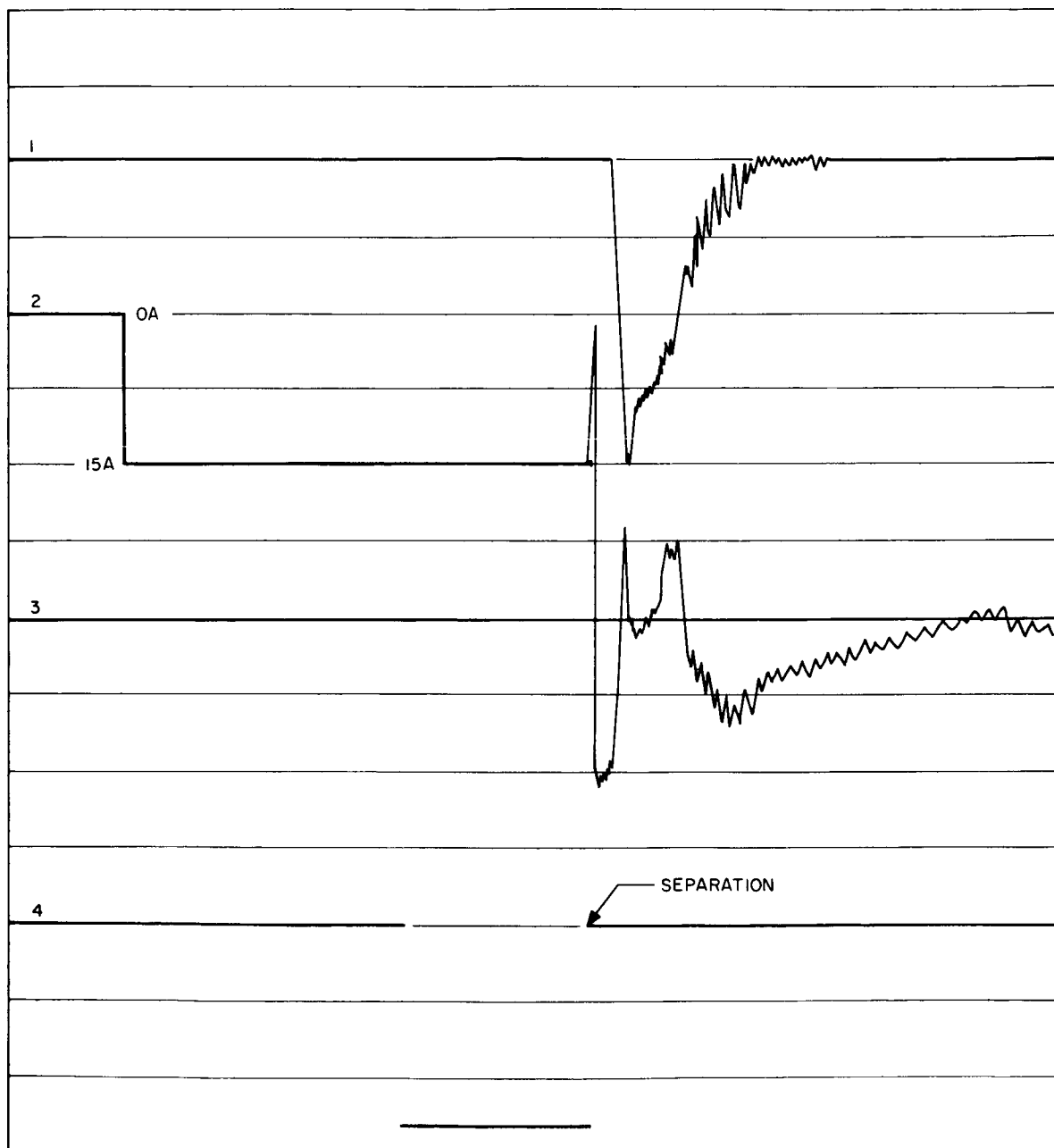


Fig. 32-3. Test No. 4 record





### 33. SAFETY CONTROL IN SPACE ENVIRONMENTAL CHAMBERS

E. A. Jackson  
Astro-Electronics Division  
Radio Corporation of America  
Princeton, New Jersey

I'm not going to talk about how to prevent electrical discharge in gases. My principal topic will be the idea of detecting the difficulty, preferably before it occurs.

We at RCA are well involved in the satellite area--the TIROS series, Ranger, RELAY, CERT, and subsystems for OAO, OGO, and many others. All these are tested in our vacuum chambers. I'm in a testing area, and occasionally trouble occurs in some subsystem with glow discharge or arc or both, and we lose quite a bit of time. So, I was told to do something about it.

The first topic of my discussion will be the protection inside the chambers themselves.

I broke up the safety circuits into three general areas. The first I call the specification safety. That's a safety dealing in the ionization-gage range. You have a specification to test to--such as  $10^{-4}$ ,  $10^{-5}$ ,  $10^{-6}$ --and if you go out of this level, you're no longer within the specs, and the test is invalid. To tell people when their spec has been exceeded, we have a simple circuit to attach to an ion-gage control (in this case the Veeco ion gage) in the vacuum chambers. It is simple but it is pretty effective, and it does take care of the first level. (The second level I call the live bird safety, and the third level I call the conflagration safety.)

Figure 33-1 shows the simple little circuit. The indicator is a bell. The trouble with the Veeco and other ion gages is that they have a power output, or a plug, that can be actuated by the gadgetry inside the ion gage control; but it works backwards. In other words, it turns off the power when the level is exceeded. I wanted just the opposite, so part of the circuitry is to turn this around in the right direction; when my vacuum level is degraded enough to go off the decade scale, the bell rings.

On the panel of the Veeco I attach a button, which is a spring-loaded switch that does nothing more than disable the bell so it doesn't keep ringing (the bell rings each time a technician sets the control). The bell doesn't bother anyone so long as it doesn't ring in the middle of a test. If it does, we act accordingly. My first safety

is only in the ion-gage level. It has nothing to do with gas discharge because it's not going to occur up there.

Figure 33-2 is a circuit that involves the two second levels of safety; the second that I call the live bird safety, and the third that I call the conflagration safety.

Live bird safety is meant to take care of operation in the danger region. The sensor is a discharge gage. I chose a discharge gage because it's most sensitive in the region that I want to operate in; namely, the micron and tenths-of-micron region,  $10^{-3}$  and  $10^{-4}$  torr. The other sensor in series with that sensor is an ordinary pneumatic switch. It's a Ross and Tiernan unit; it switches on during rise of pressure in the hundred-micron, or tenth-of-a-millimeter region. That's my conflagration device.

These two units are wired into the network as shown in the figure. The left side of the diagram shows a simple rectifying circuit--I don't want to use batteries--and a sensitive relay so that the Ross and Tiernan switch (which isn't supposed to take over 5 mil) is not overloaded. The other portions of the circuit are a motor starter (which is nothing more than a self-locking relay) and a mercury switch. Why mercury? Because it is the safest. I've never seen a mercury switch tie closed. The output of this last power relay (the mercury relay) is tied to the input lines around the chamber. We have five chambers varying in size from 4 to 24 ft.

Around each chamber is a series of outlets, into which is plugged the ground station equipment to actuate the actual test item inside the chamber. These outlets are all connected to the safety circuit so that when the pressure exceeds that set on the discharge gage (or for some reason the discharge gage doesn't work, then the pneumatic gage) prevents power from being supplied to the satellite.

If the satellite is self-powered (a complete satellite might well be self-powered because it would include the batteries) then it is plugged into an outlet that is a switch (another contact on that same motor-starter relay) that opens the battery power circuit when the pressure exceeds a certain minimum.

Figure 33-3 shows the circuit mounted in the panel (on which can be seen the bell to the Veeco alarm). It's a handy place to put the bell. I should also mention that the circuit contains a timer. The discharge gage was specially made by a vendor so as to be in the proper range. This range is calibrated by tenths of a micron from one micron to a tenth of a micron. It is a meter and a relay. Notice the set pointer

reading half scale. An optical circuit, which is fail safe, closes when the pointer goes past.

The jack shown is used for plugging in self-powered satellites. The outlets to the 110-v power supply to the chamber are not shown. Three lights are part of the panel: a red, a yellow, and a green one. The red lights as long as power supply and pressure to the unit is too high. When the pressure drops to a safe value, the yellow light goes on; the timer is now operating. Only after 4 hr of below-danger-area operation does the green light go on. When the green light goes on, you can have power. Power is switched on with the on-off switch, but this switch will do nothing so long as the green light isn't on. Therefore, engineers operating the satellite can only have power to their equipment when (1) the pressure is down to a safe level and (2) enough time has elapsed so that the boxes have been pumped out.

How do we know the boxes have been pumped out? I've tried to specify how much opening must be put into how large a box so it will pump down in the 4 hrs. This measurement is not easy to determine because the insides of the boxes are a variable. However, at the company we have only a certain number of items--a certain number of materials that have been approved by our chem labs for use in space hardware. The engineers use only the approved items for space hardware and they vent according to the procedure given, then the 4 hr are sufficient.

I use the discharge gage because it's very sensitive in just the region of pressure we want to work in. This level is below the sensitive level of the thermocouple gage and above the sensitive level of the ion gage. The discharge gage has several disadvantages, but overall it is useful and fairly consistent in its readings.

Figure 33-4 shows one of the chamber round flanges. It's about 8 in. in diameter, and on top are mounted two discharge gage sensors (the magnet is inside the box on the figure). One of the gages is in use, the other one is a spare. Occasionally, these gages get dirty after a test in which there's a lot of degassing. We may want to use the chamber right away and find out the gage won't light because it has gotten dirty. In such a case, we just switch to the other gage. We clean them up later. Gages aren't expensive, so that is no particular hardship.

The next job is to detect when pressure was in the danger region inside the black boxes, of which we have many. I was asked to develop a sensor that would tell us when the pressure was at the point where a glow discharge or an arc might occur. Several methods come to mind in doing this detecting; some of these methods have

been brought out at this conference. For instance, a sensitive photocell could be used, but I discarded this idea because I didn't want to see the glow; I want to prevent it from happening--when I have a glow, that's too late.

I thought of using an air gap--a little miniature spark gap. I checked out this idea and it didn't prove to be too satisfactory because it wasn't consistent.

I simply used an ion gage, about  $3/8$  in. in diameter and  $3/4$  in. long. It's not an inverted Baird-Alpert; it's a little triode and it does the job very nicely. It's been tested for shock to take 15 g random in any direction, so I can put it inside any package and leave it there. That's one of its advantages. It's cheap.

Figure 33-5 shows a blowup of the gage. It's nothing more or less than a triode, in a heavy glass envelope. The filament is the nonburnout iridium type, supported in the center so it will take 15-g shock. It has a light grid and the anode (or plate, if you use the triode designation) is a nickel sleeve just inside the inner face of the glass. To all intents and purposes, this gage resembles a tantalum capacitor they use on printed circuit boards. I felt it ought to be attached in the same way: just epoxy it on, wire the leads in, and make sure the open end is free (and preferably facing the direction of the high voltage supply). It weighs almost nothing. Mr. McKannan may be interested in this device. There's nothing wrong with flying it. It doesn't take any power and requires -45 at the anode, 175 or so in the grid, and a couple of volts in the filament. The only place you require any power is to keep the filament lit but even then you don't use it continuously.

The ideal way to use the gage: put it inside a black box when you manufacture the black box and you leave a little pigtail sticking out to connect to (or even a couple of extra pins will do, if you have them on the plugs leading out of the box). When we put the satellite, or the subassembly, inside one of the chambers, we connect the wires to the electronics and monitor the pressure inside. When the pressure reaches a safe level, the test is made. We turn off our gage and go on with the test. If, for some reason during the test, we feel that pressure might be building up, we turn on the gage again. But, normally, it's not used when the package (whatever is inside) is used. It's used only to determine when it's safe to turn the package on.

Ion gages have a bad reputation; they're not too very accurate. I appreciate this fact. All I want to know is the order of magnitude in which I'm working. Figure 33-6 shows the calibration of the miniature gage against the standard Baird-Alpert gage; we get a pretty straight line. These are experimental points, and you

notice that I chose the experimental points in the range that I wanted to operate in, between about  $1\mu$  and  $1/10\mu$ .

I checked my regular ion gages. I have crosschecks from one type of gage to another. I cross-checked the residual gas analyzer and when I have three or four gages of different types all agreeing within 3 or 4 points in an order of magnitude, I figure I'm doing about as good as I can. So, calibrating my miniature gage against one of these, I'm fairly sure the miniature gage is reading somewhere near where I want it to read.

Figure 33-7 shows an adaptation of a standard piece of equipment, a CVC ion gage control to use with the miniature gage. I changed the calibration; I have two scales. The lower one is to actually measure the pressure, and the upper one is in milliamps (as is usual in ion gages) to set emission currents. The little box off to the right of the figure is part of the assembly. Notice the switch in front. It switches one of six gages. I've six black boxes inside the vacuum chamber (this number is not unusual), and I've a gage in each one of them. By switching one gage on after another, I can see what the vacuum condition is inside each black box.

Inside this box also is a dropping resistor so I get proper filament current, because the big tube that's made to be used with this gage control is quite different from mine. However, I have no scale overlaid on the decade scale. The decade scale remains the same although I don't use all of it. My gage is only good to about  $10^{-6}$ . It's not made to go out any further.

Well, I've shown you the gage and its calibration, and the control that we use for it. Now came tests. We have to test it on a black box, so I looked for a black box that would be nice to test, and at this point I'd like to refer to Robert Boundy's presentation this morning. By sheer coincidence I happened to end up with the particular black box that he was interested in. I chose the Ranger power supply. That was given to me as a prototype box. I was told, "Here's a box for you to put your tube in. It's a high voltage supply. We'll put an external load on it, run it at about double what it should run, and you can check out your gage this way." I put it into a bell jar after attaching my gage (just cementing it with epoxy to the bottom surface of the inside of the box right across from one of the high voltage condensers). I wired up my gage, put the load circuit on the power supply, wired up the primary, turned it on and started pumping. I pumped my bell jar down to the  $10^{-6}$  level, and then applied power to the supply.

What happened can be seen in Fig. 33-8. Here the bell jar was pumped  $3 \times 10^{-6}$ . At the same time the miniature gage told me the box was pumped about  $1.5 \times 10^{-5}$ . The zero line in Fig. 33-8 is not the beginning of pumping. I'm pumped here, down to  $10^{-6}$ . My zero line signifies power on in the supply. The miniature gage goes up; (the scale is shown in hours, not minutes). The bell jar can't handle a load like that. There is quite a bit of electronics in there, and it's heating up pretty profusely. That bell jar has a 6-in. diffusion pump, so it goes up. It goes fairly high, but still not into the real danger area. However, the inside of the box, the separation of which from the outside was a little better than half a decade, has now separated way out, and is going up a lot faster and a lot higher. I might note this box was vented very well compared to most electronic boxes. Since it was a power supply, it didn't have any delicate rf circuits inside, so a lot of large holes were left in it. I would say that there was close to better than  $1/4$  in.<sup>2</sup> of opening between the inside and the outside of that box, and the box was a maximum of  $1/4$  ft<sup>3</sup>. When I turned power off in the power supply, the miniature gage went right down again, and, of course, the bell jar went down, too. Again, they tend to close up, come together again, much the same distance that they were at the start.

This convergence told me a number of things. First, it told me the miniature ion gage worked. Secondly, I was a little upset about the amount of gas generated by an electronic power supply, which was built to be operated in space; and still degassed quite badly. This power supply was not recently put together; it was not a brand new unit, but one that had been used for tests, in and out of thermal vacuum several times. It presumably had been thoroughly outgassed, and still the pressure showed up very significantly.

It goes to show that you can do a lot of calculation of what your gas load is going to be, what your vacuum level is going to be, and where you are in respect to the danger region, but when you try it you may find yourself somewhat surprised.

I felt that perhaps I ought to get a little bit more into this philosophy of the danger region and what to do about it. It has been expressed more than once here that we ought to build all our supplies in such a fashion that they can go sailing right through the danger region with no ill effects. Why? Because people make mistakes and turn things on at the wrong time. I don't think this is a good solution. I think we should separate our method of fabrication, depending on what the satellite is supposed to do.

If a satellite like CERT is simply supposed to go up, not orbit, stay up there for a few minutes, and come back down again after its test, that's one thing. If a satellite is supposed to go out into space as does TIROS and remain for 6 mo and never come down anywhere, probably burn up at the end of its life, that's another thing. If a satellite is supposed to go out like Surveyor and land in a more or less unknown atmosphere, which is more than likely in the dangerous region, then that's another story again.

I don't think we should try to build our VWs and our trucks all using one frame. I think that's expensive and not really necessary. Using our TIROS series as an example, a satellite can be built in which some components are exposed and some components are inside their own pressurized shells. After the satellite is launched and orbited, it floats around in orbit and degases nicely. Then you can turn it on and have no problems. On the other hand, if you have a satellite that has to operate in the danger region, then suitable precautions do have to be taken. But I don't think we should necessarily combine all these items and say everything has to survive. I think we're going to be spending a lot of money unnecessarily if we do. Also weight is still important; wasting a lot of weight, if nothing else, is wrong; also, of course, time.

The other comment I would like to make is this: People have mentioned here during various presentations about reinventing the wheel. I think it's worthwhile making that statement again. Let's not reinvent the wheel. People have been in the vacuum business for a good many years, ever since John Strong invented the idea of aluminum evaporation way back in the early part of the century. They have become gradually very skilled in vacuum technology. They know what can be put into a vacuum and how it will behave.

The people who make tubes are very skilled in vacuum work. A lot of what we are actually going over are things that they have known about for a good many years. I don't think we should do this unless we are first very careful to go over things that they have done. For example, the VR tubes; they've had a nice glow discharge regulator tube that works at 75 v for a good many years. They don't have any radioactive sources in there. They don't even have any special electrodes, just a simple little metal electrode. After all, what can you build for 75 cents and a few millimeters of argon? The tube operates very satisfactorily in the glow discharge region at 75 v, and regulates very beautifully between 5 and 30 mils. If you give it too much juice, you'll take the glow and make an arc out of it, but they know this.

The last thing I'd like to mention has perhaps been overdone already during this symposium--it is names. I don't think we should call these discharges "corona." Corona to me is practically another way of saying brush discharge. You can't have a brush discharge in the danger region between 50 mm and, say,  $0.5\mu$ . All you have is glow. You can have a glow discharge; you can have an arc; you can't have corona, really. Corona immediately involves high voltage, thousands of volts, or at least 300 or 500 v. Glow is perfectly nice and quite; all it does is very nicely short out everything in the vicinity; nothing more.

By the way, my little gage has not been manufactured for sale. We just made it for ourselves, and The Sarnoff Laboratory made a few of them for me. However, if there's call for it, I suppose it's not very difficult to make in production quantities.



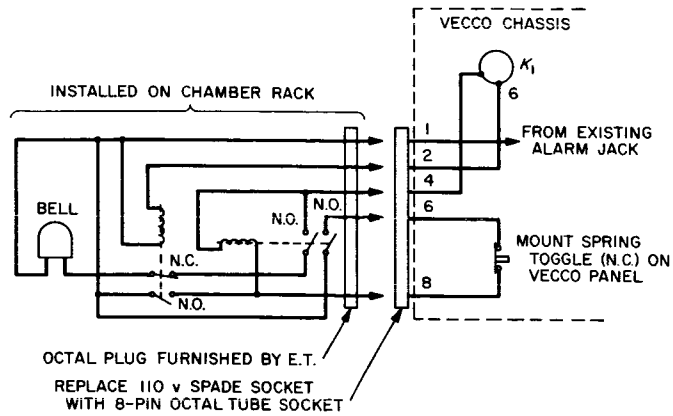


Fig. 33-1. Specification safety alarm circuit

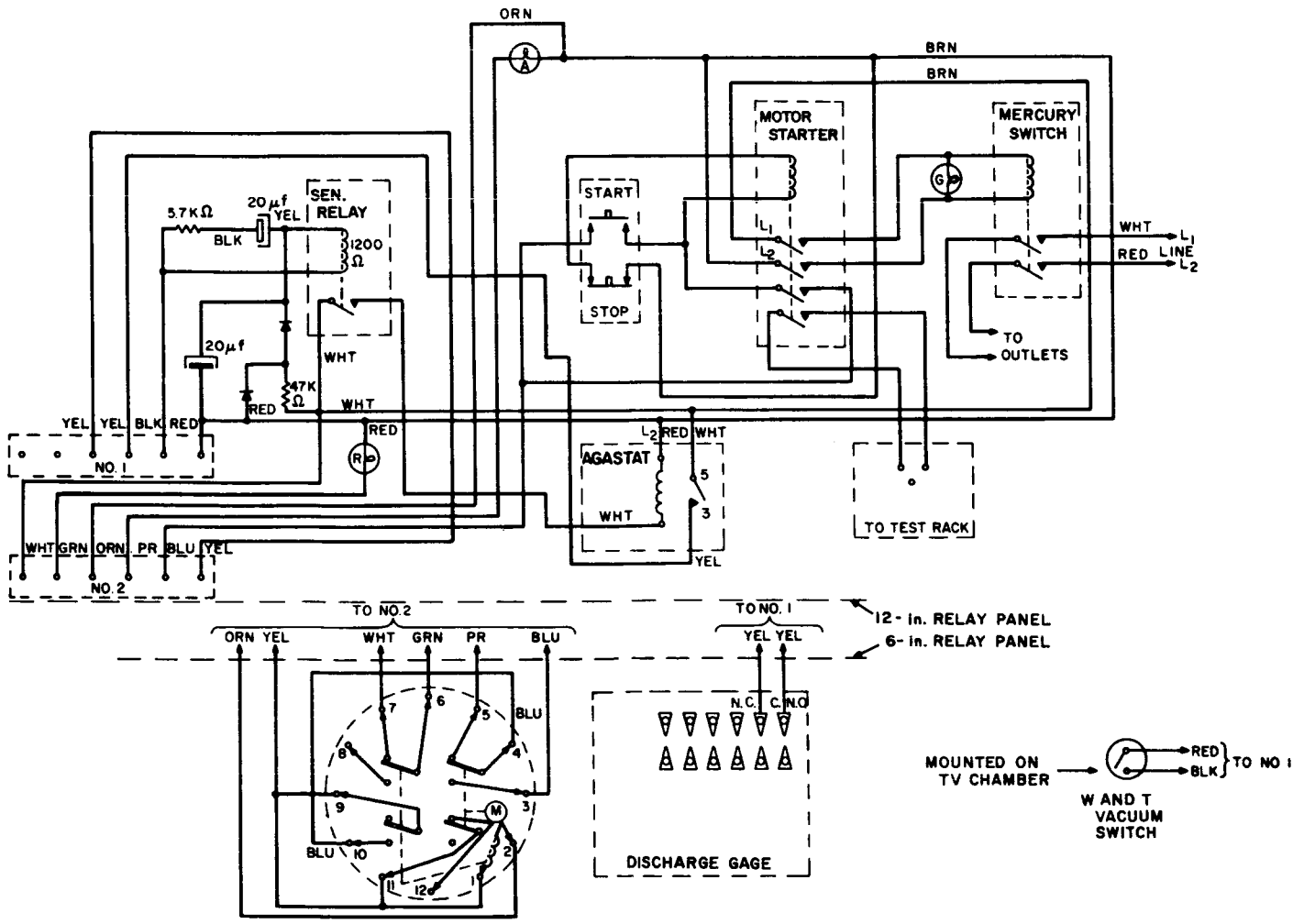


Fig. 33-2. Live bird and conflagration safety circuit

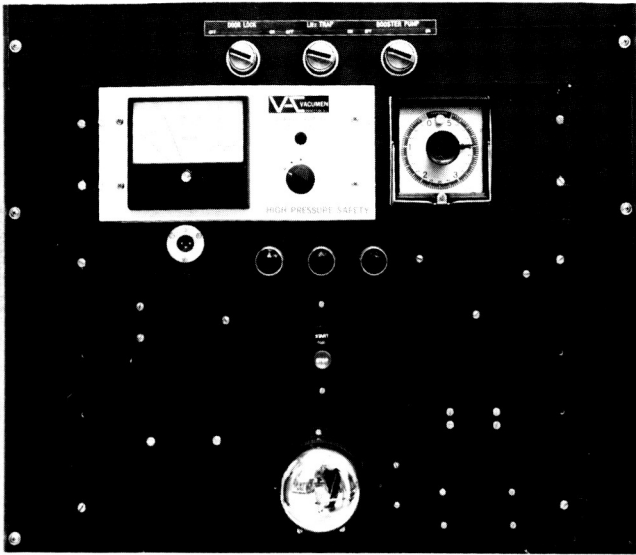


Fig. 33-3. Safety circuit control and indicator panel

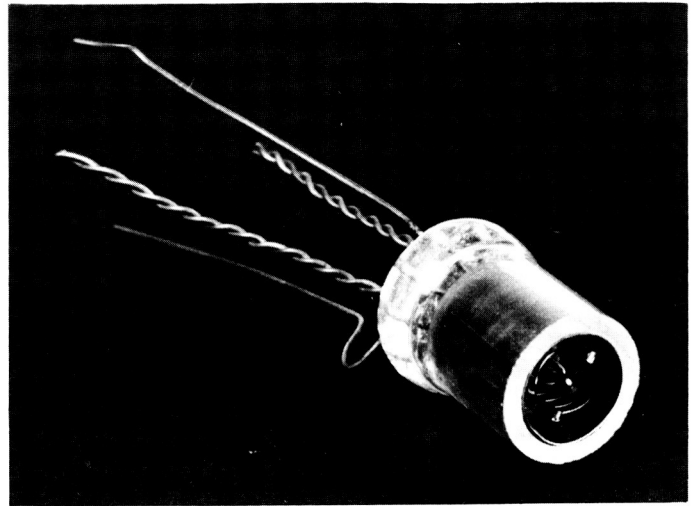


Fig. 33-5. Miniature ionization gage - glass envelope 3/4-in. long and 3/8-in.-dia

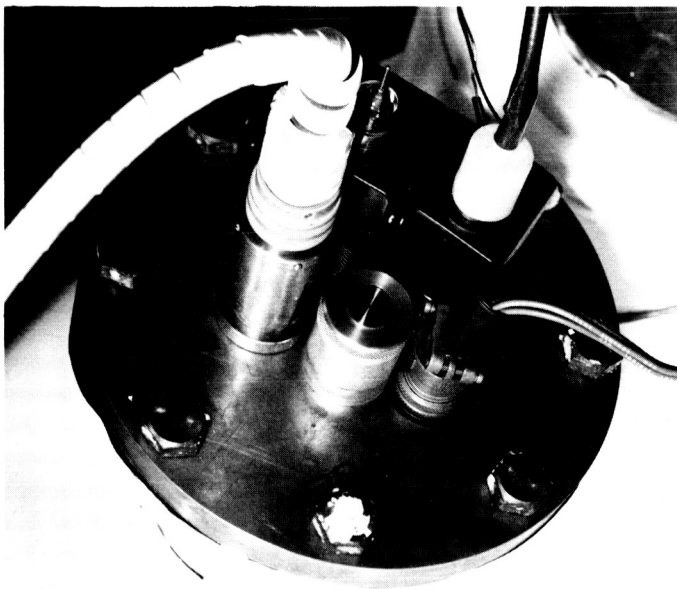


Fig. 33-4. Vacuum chamber flange showing to discharge gage sensors

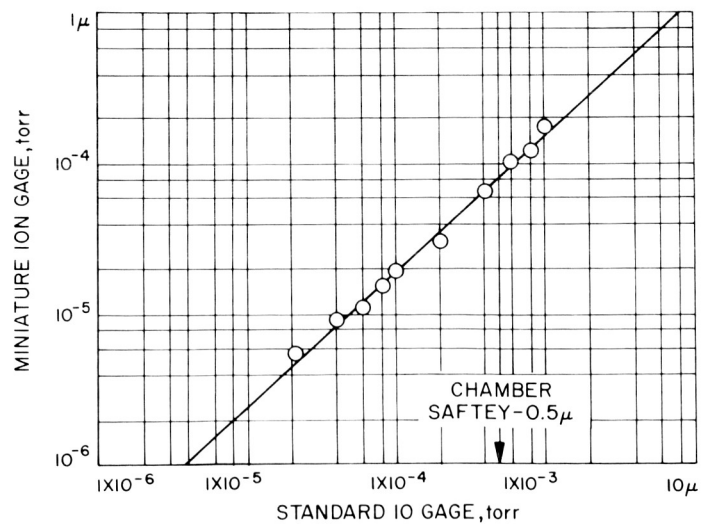


Fig. 33-6. Calibration of miniature ion gage using a standard ion gage



Fig. 33-7. Ion gage supply modified for use with miniature ionization gages

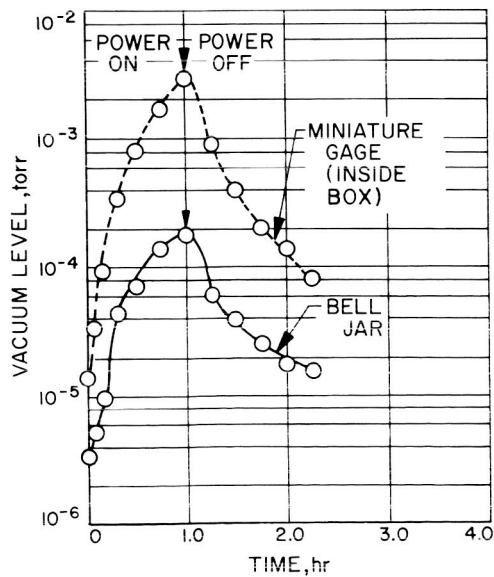


Fig. 33-8. Graph of vacuum level vs time showing gas buildup inside a "black box"

34. HIGH-VOLTAGE POWER SUPPLY DESIGN FOR OPERATION  
IN THE CRITICAL-GAS-PRESSURE REGIONS AND AT LOW  
TEMPERATURES ( $-55^{\circ}\text{C}$ )

Aldus C. Myers, Jr.  
Electronics Design Engineer  
Electro-Mechanical Research, Inc.  
Sarasota, Florida

INTRODUCTION

Electro-Mechanical Research, Inc. (EMR) is contractor to Smithsonian Institution Astrophysical Observatory for Project Telescope, one of the Orbiting Astronomical Observatories (OAO). The Telescope mission is to obtain star-catalog information in the ultraviolet portion of the spectrum for approximately 25,000 stars.

The Telescope experiment requires a -10 kv power supply for each of four ultraviolet camera tubes, called UVicon (a product of Westinghouse Electric Corp.). These supplies provide high voltage to an image intensifier section of the tube. The supplies are commanded on and off so that the high voltage serves as an electronic shutter for the ultraviolet camera tubes.

This paper summarizes the effort and results obtained by EMR in the development of a -10 kv power supply for Project Telescope. A review of past and present problem areas is given, and conclusions and recommendations for circumventing these problems are discussed. Improved packaging design concepts which have a higher probability of surviving in the critical-pressure and low-temperature environments are presented. Some desirable and undesirable characteristics of specific high-voltage electrical components (diodes, capacitors, resistors) required to operate in the critical-pressure environment and in the temperature range  $+50$  to  $-55^{\circ}\text{C}$  are discussed. Also, a discussion of high-voltage wire and interconnections of high-voltage wire that will survive the critical environment is presented. Dielectric media which may be used for operation in the critical environment are given consideration, and a simple but effective test fixture for passing high-voltage wire into (or out of) a vacuum chamber without breaking the wire or wire insulation is described.

CIRCUIT DESCRIPTION OF THE CELESCOPE HIGH-VOLTAGE  
POWER SUPPLY

The high-voltage power supply (HVPS) operates from a +28 v dc source by generating a 2000 v peak-to-peak square wave at approximately 10 kc. This wave is rectified and multiplied to approximately -10 kv (see Fig. 34-1). The supply is turned on by a +2 v command signal. A 100-megohm voltage divider across the output terminals allows selection of UVicon voltages F2 and F3. Rise and fall times of the voltage at F1 are 30 and 200 millisec, respectively, when commanded on and off. The supply circuitry is protected from accidental short circuiting of the -10 kv lead by the use of current limiters in the oscillator section. Additionally, the circuit is redundant where feasible in several critical areas.

## REVIEW OF PAST PROBLEMS

The first high-voltage power supplies we constructed were designed for mounting inside the UVicon case assembly. These units had a diameter of approximately 4 in. and a length of approximately 3.5 in. Installing the high-voltage power supply in the UVicon case assembly had the advantage of saving valuable space, and the lead lengths carrying high voltage to the UVicon were minimized. Disadvantages were a lack of versatility for repair of the UVicon assembly or replacement of any of the subassemblies. An additional disadvantage was that the environmental temperatures expected were such that qualification testing to -80° C was required. This was a severe requirement since most components are not rated at this temperature, and encapsulating materials could not be found which would perform as required at the extreme low temperature.

The circular high-voltage power supplies which were fabricated, and the encapsulating materials used are shown in Table 34-1.

Table 34-1. Encapsulating material for high-voltage supplies

Material	Units constructed
ERL 2795	1 Unit
RTV 601	1 Unit
Sylgard 182	3 Units
Fabricated but not encapsulated	2 Units

The experimental units using ERL 2795 and RTV 601 cracked and split when subjected to cold temperature ( $-80^{\circ}\text{C}$ ) testing. Use of these materials was therefore discontinued. Investigation of Sylgard 182 (a relatively new compound at that time, January 1963) revealed several desirable properties as follows:

1. The manufacturer's data sheet gave the brittle point as lower than  $-70^{\circ}\text{C}$ .
2. The compound is transparent, thus allowing visual examination for voids, lack of adhesion, and air bubbles in the cured assembly.
3. It is easily repairable.
4. It would give excellent damping to components when subjected to shock and vibration.
5. The compound is firm but flexible (Shore A scale hardness of 40).
6. Low cure temperature required ( $+65^{\circ}\text{C}$ ).
7. No exotherm.

Shortly after the selection of Sylgard 182 for use on the high-voltage power supply, it was also decided to use this material for encapsulating the UVicons in the UVicon case. This was an additional advantage in that there would be compatibility of the materials at the interface in the UVicon case. Thus, on the basis of the above considerations, three units were constructed in the circular configuration and encapsulated in Sylgard 182.

A component failure occurred with one of these units during thermal vacuum ( $-80^{\circ}\text{C}$ ) testing of the UVicon camera and high-voltage power supply assembly. The failed component was a hermetically sealed PT-60 resistor (manufactured by Pyrofilm Resistor Co., Inc., Parsippany, N.J.). Although the failure analysis did not determine the cause of failure, subsequent engineering test revealed that the

PT-60 and HV-100 resistors had arced over internally when subjected to vacuum tests with high voltage applied, presumably due to a failure of the hermetic seal. (It should be pointed out that these components were not intended for such severe environments.) This failure and the subsequent loss of an entire camera package prompted a relocation of the high-voltage power supply. The components already encapsulated in these units could not be salvaged and were scrapped. A total of seven units of the circular configuration were thus scrapped. Five had been encapsulated, and two were fabricated but not encapsulated.

In August 1963, it was decided to move the location of the high-voltage power supplies from the UVicon case to a position aft of the telescope. The supplies were the repackaged and relocated. Because of the repositioning, the lowest temperature for all testing was revised to  $-55^{\circ}\text{C}$ . The decision to relocate the high-voltage power supply was thus initiated by the failure of the Pyrofilm resistors and the attendant loss of an entire camera package. The camera tubes are very expensive and difficult to obtain. Loss of one due to a malfunction of some other unit could not be tolerated.

The repackaged supply is approximately  $4.25 \times 4.25 \times 4.75$  in. (see Fig. 34-2 and 34-3). Resistors (manufactured by International Resistor Company) were selected to replace the Pyrofilm resistors in the 100-megohm high-voltage divider. This selection was due in part to the fact that a sufficient quantity of these resistors (IRC-type MEF) to construct several supplies were already in inventory. A disadvantage in this selection was that 33 resistors were required to make up a 100-megohm divider (a consequence of the ohmic values and voltage ratings of the MEF resistors). Thus, a large number of soldered connections were required, and the package volume requirements were increased (each resistor is 0.375 in. in diameter by 1.125 in. long). Using a package design as shown in Fig. 34-2 and 34-3, a qualification unit and four prototype units were fabricated and encapsulated with Sylgard 182. These units survived environmental testing.

Since the qualification and prototype units were encapsulated with Sylgard 182, it was necessary to continue using this compound for the flight units, even though some evidence of undesirable and varying properties of the Sylgard 182 had already been noted. To change to another compound at that point would have caused a considerable delay in schedule, since qualification testing of a significantly different unit would have to be reperformed.

The second and current problem is that of maintaining a sufficient bond between the encapsulant, printed-circuit boards, and components, particularly at low temperatures ( $-55^{\circ}\text{C}$ ). The encapsulating material under the thermal stress contracts and breaks away from the circuit boards. The pressure in the void thus generated between encapsulant and exposed high-voltage points can be depended upon, at some time and temperature, to allow a high-voltage discharge to take place. In an effort to prevent discharges between lands and printed circuitry, a simple expedient of cutting slots in the printed-circuit boards between lands was tried, as can be seen in Fig. 34-2. Although this may have been of some aid, it was not sufficient to solve the problem.

Four units for the flight payload were fabricated (FHV-1, -2, -3, and -4). The second unit of this group (FHV-2) arced over during thermal vacuum testing. The EMR Reliability Department subsequently rejected all four units as reliability risks.

A design review was held at this time to consider an improved encapsulating material and/or process. It was decided to construct additional units by first conformal-coating the components with 3M-8 epoxy. The Sylgard 182 was then used as a filler over the 3M-8. Although this seemed at the time a good technique, a loss of adhesion of the Sylgard 182 to the 3M-8 and of the 3M-8 to the printed-circuit boards and components when temperature-tested caused this selection of materials to be discontinued. Of three units constructed in this manner (FHV-5, -6, and -7), the first two passed all environmental testing but the third unit failed. Further construction was then discontinued, and extensive efforts were made to resolve this problem area.

Since the most recent high-voltage power supply failure (March 1965), EMR has been pursuing every aspect of the high-voltage power supply problem, not only from a viewpoint of eliminating known problems, but also to anticipate some as yet uncovered problems.

To summarize the past problems, the first difficulty was the failure of the hermetically sealed high-voltage resistors. Although these units were totally encapsulated in Sylgard 182, the application of a vacuum and voltage caused the resistor to arc over on the inside of the glass body. When this discharge was allowed to take place for several minutes it removed enough of the resistive material to cause the resistor to become open-circuited. Upon release of the vacuum (before the resistor open circuited), the resistor performed normally with



applied voltage. Possibly this failure was related to, or caused by, the vacuum deaerating performed during encapsulation with Sylgard 182. The time element did not permit extensive tests on this problem, and a sound explanation is not available.

## DESIGN CONSIDERATIONS FOR HIGH-VOLTAGE POWER SUPPLY OPERATION IN THE CRITICAL ENVIRONMENT

### Packaging Concepts

Several high-voltage power supply failures have occurred during thermal vacuum testing. These have been caused by the loss of dielectric protection which allows a high-voltage discharge to occur with consequent erratic output voltage. Telescope high-voltage power supply components survive this stress and will survive short circuiting of the -10 kv output to ground. This loss of dielectric protection in the failed supplies has occurred at the interface of the encapsulating material to the printed-circuit boards (G-10 fiberglass).

Design reviews and failure analyses of the failure mechanisms involved have brought about significant revisions of the commonly employed circuit packaging concepts. Circuit packaging configurations which eliminate circuit boards (and thus eliminate the encapsulant-to-board interface problem) are currently being tested to determine how well this technique will survive in the critical environment and to determine if new problems will arise.

The cutting of slots in the printed-circuit boards was a first step toward relieving the encapsulant printed-circuit-board interface. The extrapolation of this technique would eliminate the use of printed-circuit boards or terminal boards and would result in component-to-component wiring which would be similar to an engineer's breadboard, where most components are simply tacked to one another and the circuit grows upward and outward without the benefit of a board or terminals connected to a board. Simple lapped solder joints present some obvious reliability and quality control problems, but connecting several components together in such a manner can be done reliably by using a sleeve over the leads and soldering as shown in Fig. 34-4. One possible quality control objection to this technique is that the solder joint cannot easily be inspected. If the sleeve is shortened to a mere ring, the leads can then be wrapped around the ring and can be inspected as in Fig. 34-5.

Fixtures for holding the components in place during assembly may be required and could remain around the body of the components as a holding fixture during

encapsulation. Or the network of components could be encapsulated as is with the necessary input/output wires already connected. It would be essential that the encapsulating material bond to the wire. Several holding fixtures are shown in Fig. 34-6, compared with a printed-circuit or terminal board.

Figure 34-7 shows a method of packaging that has very desirable characteristics in that a controlled amount of encapsulant may be applied to every point. It would also be easily assembled and very easy to inspect.

### High-Voltage Components

In addition to the usual reliability considerations of components, consideration must also be given to the surface and internal conditions of components used in the high-voltage power supply. The effects of component sorbed gases adversely affect the adhesion of the encapsulating materials. The component surface material must also be compatible with the encapsulating material to effect a good bond. Voids inside the components must be avoided since the gas pressure in the void changes with environmental conditions and this sets up a condition for a high-voltage discharge. The net coefficient of thermal expansion of the component should be related to the expansion coefficient of the encapsulating material, the flexibility and thickness of the encapsulant, the bond strength, and the temperature range over which the unit must perform.

Components with sharp edges and 90 deg angles are undesirable since maintaining a bond of the encapsulant at such points is difficult, particularly when temperature cycled. High-voltage components presently in use at EMR are as follows:

1. Capacitors. Erie, ceramic disc, 2700 pf, 4 kv. Purchased to EMR specification. Ten used per high-voltage power supply.
2. Diodes. PS1865, 3500 v piv. Ten used per high-voltage power supply.
3. Resistors. IRC type MEF and MDB (2.77 megohm). Thirty six MDB's used per high-voltage power supply ( $2.77 \text{ megohm} \times 36 = 100 \text{ megohm}$ ).

The reliability of all components, with the exception of the MDB resistor, has been established by tests at EMR. The reliability history of the MDB resistor has been established by the manufacturer (IRC), but not in this specific application.

However, all indications are that it will perform as satisfactorily as its predecessor (the MEF) in these supplies.

The 2700-pf capacitors have one disadvantage. The manufacturer's coating material (Durez) is very porous (see Ref. 1). To seal off the capacitors against moisture, they are wax impregnated by the manufacturer. Encapsulants will not adhere to the wax coating. Thus, EMR purchases these units to our specification without the wax impregnation. The capacitors are then vacuum dried and vacuum impregnated with Armstrong C-7, 40 parts resin to 60 parts activator W, and are cured at 65° C for 2 hr. Since the Durez bonds very well to the ceramic disc, it should be used as the initial coating material and then epoxy impregnated to seal out moisture and maintain the voltage rating.

The PS1865 diodes are manufactured by PSI (now TRW Semiconductors). These diodes are approximately 7/8 in. long and 3/8 in. in diameter. The reliability of these units has been established through extensive testing and use. Some disadvantages of these units are the sharp edges and large physical size. The diode is composed of a series string of six diodes of proven reliability.

The resistors used in the present high-voltage power supply design are IRC-type MEF. Thirty-three of these units were connected in series to total approximately 100 megohms. Again the component reliability has been excellent. Present plans are to discontinue use of the MEF resistor and to use the smaller MDB type. For the 100-megohm divider, 36 MDB resistors will be used. Some of these units have a hollow ceramic core but can be purchased with a solid core. EMR plans to use only solid-core resistors, even though the applied voltage on each resistor will be below 300 v. The minimum breakdown voltage for air is 327 v (see Ref. 2). It occurs at a pressure (p) and electrode spacing (d) product of approximately 5 ( $p \times d = 5$ ) for air where p is in mm Hg and d is in mm, for plane parallel electrodes in air at 20° C. Since the gas in voids inside components cannot be depended upon to be air and the electrodes are not parallel planes, it would be risky to use hollow-core resistors when the applied voltage is greater than perhaps 150 v. This area needs additional consideration. However, the use of solid cores avoids a possible problem.

## High-Voltage Wire and High-Voltage Connections

A prime consideration in the selection of high-voltage wire is that it be covered with an insulating material to which an encapsulating material will bond. The high-voltage leads may then be attached to, and encapsulated with, the components. The high-voltage leads from the high-voltage power supply may be left approximately 1 ft long.

The interconnection of the high-voltage power supply leads to other high-voltage leads is then totally encapsulated, thus giving continuity of insulation. Unencapsulated connectors are considered totally unreliable for the Telescope application. The high-voltage wire found most suitable, in that it is readily bonded with Armstrong C-7 40/60 w, is laboratory test lead wire. This wire is available in at least two sizes, 5 kv and 10 kv rated. The wire presently being tested is Belden. Type numbers are 8899 and 8898, respectively. The inner conductor is stranded wire, which may be a disadvantage since air is entrapped between strands. The test lead wire becomes quite rigid at  $-55^{\circ}\text{C}$  but does not break unless given a sharp snap when cold. EMR is presently obtaining additional data on this wire in order to determine its suitability for space applications. It is hoped that the wire can be used as is for the high-voltage power supply connection. Modifications to the wire may be necessary and investigation of those aspects are in progress. A conclusion concerning the effects of entrapped gas between strands of high-voltage wire has not yet been reached.

## Dielectric Media

There are several media which may be employed in a high-voltage power supply to obtain dielectric protection. Some of these methods are as follows:

1. Expose the high-voltage circuitry to the local vacuum.
2. Seal the high-voltage power supply circuitry in a fluid (oil, for example).
3. Seal the high-voltage power supply circuitry in a suitable gas, e. g.,  $\text{N}_2$ ,  $\text{SF}_6$  (see Ref. 3),  $\text{CCl}_2\text{F}_2$  (see Ref. 4).
4. Use an encapsulating material.

A high-voltage power supply vented to the local vacuum would not survive the critical-gas-pressure region. "Local" vacuum is used here in the sense that the vacuum inside and near the spacecraft is not the same as the space vacuum because

of outgassing in the spacecraft. For Project Telescope, the area in which the high-voltage power supply is mounted is not well vented to outer space, and pressures expected in that area are presently unknown.

If the local vacuum were used as the dielectric, the circuit components would have to be securely fastened to survive shock and vibration environmental testing and launch conditions. In addition, exposed high-voltage circuitry could become contaminated with dust, moisture, etc., during ground operation (this can be circumvented). Another very important consideration could be sublimation of metals on to the exposed circuitry, resulting in high leakage paths.

Sealing the high-voltage power supply in a fluid is not presently being considered for Project Telescope. Telescope is an optical experiment and the use of fluids presents possible optical contamination problems.

Sealing the high-voltage power supply in a suitable gas has some very interesting advantages over the other techniques. Use of a gas-filled high-voltage power supply would reduce or eliminate many of the electrical component problems such as internal voids, surface material of components, etc. A disadvantage is the reliability of the hermetic seal. Additionally, all components would have to be mounted securely in order to withstand shock and vibration environmental conditions.

At this time, the use of encapsulating materials is considered the best dielectric medium for use in the Telescope high-voltage power supply. The past problems with loss of adhesion to circuit boards during thermal vacuum testing are being reduced or eliminated with the improved package design. Also, the use of relatively new formulations of encapsulating materials is showing definite promise. From the previous experiences with encapsulating materials it is very clear that although Sylgard 182 has some very desirable properties, it also has some very undesirable properties, particularly when used in a rigid structure (see Fig. 34-8). The linear coefficient of thermal expansion (CTE) of Sylgard 182 (and of many other rubber-type materials) is approximately 320 ppm/°C. This very large CTE, coupled with poor adhesion properties (approximately 200-psi bond strength) and the low temperature levels (-55°C) at which the high-voltage power supply must perform, results in high-voltage power supply failure during thermal-vacuum testing.

Minimizing of interfaces in the repackaged high-voltage power supply and the application of a controlled amount of encapsulant around each component and wire will greatly improve the probability of constructing a successful high-voltage power supply.

Encapsulating materials presently under consideration and undergoing testing are Armstrong C-7, an epoxy resin adhesive, mixed 40 parts resin to 60 parts activator W, and Columbia Technical Corporation polyurethane 2A58. The linear coefficient of expansion of the 2A58 is 45 to 55 ppm/°C. The Armstrong C-7 is made more flexible by increasing the concentration of activator W. A flexible material is required so that crushing of components at low temperature is avoided.

### TEST FIXTURE

Problems frequently arise when high-voltage wires are fed into or out of a vacuum chamber. This is particularly true when testing is being performed in the critical-pressure region. An undesirable high-voltage discharge frequently occurs at the exposed high-voltage input connector. A usual procedure is to totally encapsulate the inside of the connector with a suitable compound. Unfortunately, this procedure is costly, cumbersome, time consuming, has marginal reliability, and has little or no versatility.

An improved technique for handling high-voltage leads in a vacuum would be to feed high-voltage rubber leads directly through the chamber wall in a new type connector, perhaps using O-rings to effect the vacuum seal (see Fig. 34-8). Using this method, the insulation on the high-voltage leads would not be cut. This would eliminate arcing problems, and leads could be slipped in or out of the connector without damage simply by loosening a compression nut on the O-ring. It may be possible to use a standard brass fitting with modifications for the major part of this assembly.

In addition to the bulkhead-type connector, another connector for internal connections in a vacuum chamber can be made from two of the bulkhead-type connectors placed back-to-back and holding atmospheric pressure internally. A cord grip (see Fig. 34-9), which uses a rubber bushing instead of O-rings, is available (John Remke, Inc., Chicago, Ill.). Although the cord grip is not intended for vacuum use, it works very well in this application.

## CONCLUSIONS

The efforts and ideas presented in this paper are pertinent primarily to the Telescope experiment and its expected environment. It should be emphasized that each high-voltage application should be considered as a separate problem and that there exists no single ideal solution. In other words, acceptable solutions are dependent upon the application and environment. However, for applications similar to that of the Telescope experiment, certain conclusions can be drawn. These are as follows:

1. Dielectric Medium. Use an encapsulant, or hermetically seal the high-voltage power supply in a suitable gas.
2. It is very important to eliminate all unnecessary interfaces between the encapsulating material and the package (no printed-circuit boards; no terminal boards).
3. High-voltage components should be free of internal voids, sorbed gas, and contaminants, before encapsulating. Voltages applied to resistors with a hollow ceramic core should be kept below the minimum breakdown potential for the particular gas entrapped. Resistors with solid ceramic cores are preferred.
4. High-voltage leads from the high-voltage power supply should be encapsulated in place at the high-voltage power supply. All high-voltage wire connections should be encapsulated (no connectors).
5. An encapsulant should be selected which has a linear coefficient of expansion compatible with that of the components and which exhibits good adhesion properties (epoxy such as Armstrong C-7 mixed with 40 parts resin to 60 parts activator W, Epon 828 made more flexible with Versamid 140, 3M-8, or a polyurethane such as 2A58).

Although some of the above considerations for packaging a high-voltage power supply reflect concepts presently in the testing stages, they are the result of several years effort and experience with high-voltage (-10 kv and 3 kv) power supplies and testing in thermal vacuum to as low as -80° C. In almost every case the direct cause of improper high-voltage power supply operation has been a loss of dielectric protection at the encapsulant to circuit-board interface during

thermal-vacuum testing. Thus, to maintain dielectric protection when encapsulants are used, interfaces should be minimized, and adhesion of the encapsulant to components and high-voltage wire should be very good to withstand thermal cycling to  $-55^{\circ}\text{C}$ . The thermal coefficient of expansion of the encapsulant should be related to the coefficient of expansion of the components, the temperature range of operation, the elasticity of the encapsulant, and the thickness of encapsulant on a particular component.



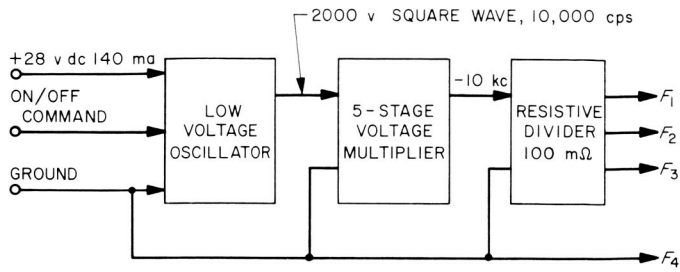


Fig. 34-1. High voltage power supply

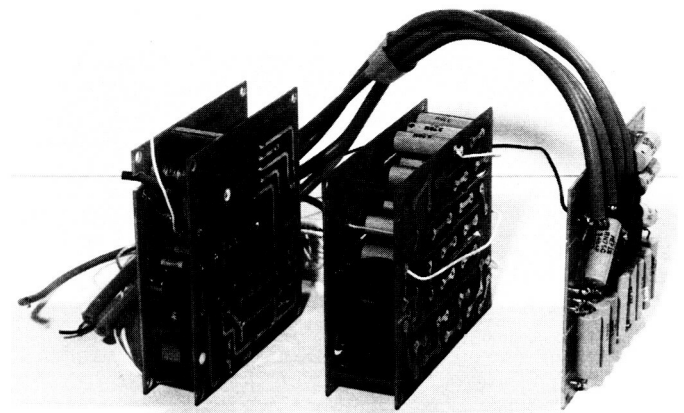


Fig. 34-2. Power supply

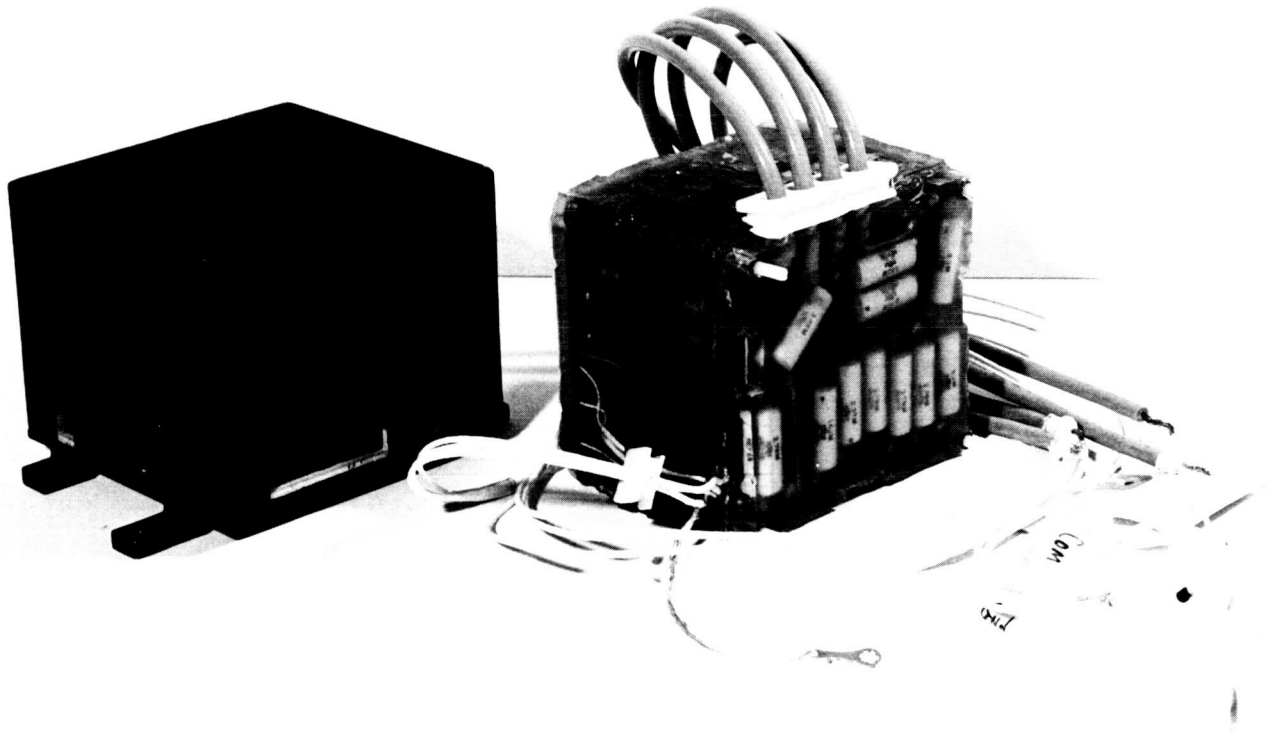


Fig. 34-3. Power supply

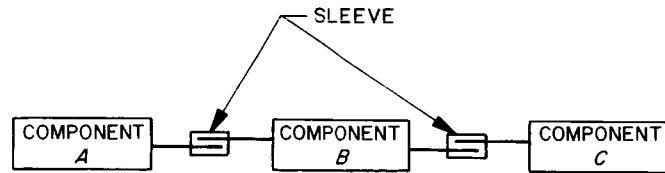


Fig. 34-4. Soldering technique using sleeve

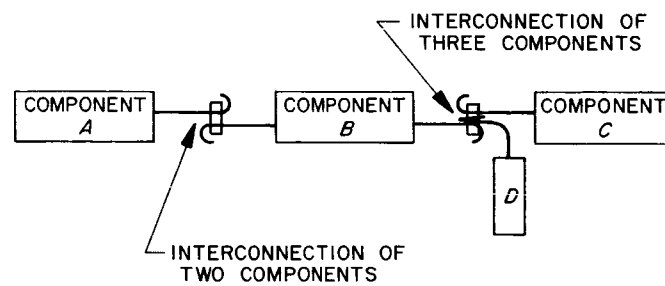


Fig. 34-5. Soldering technique using ring

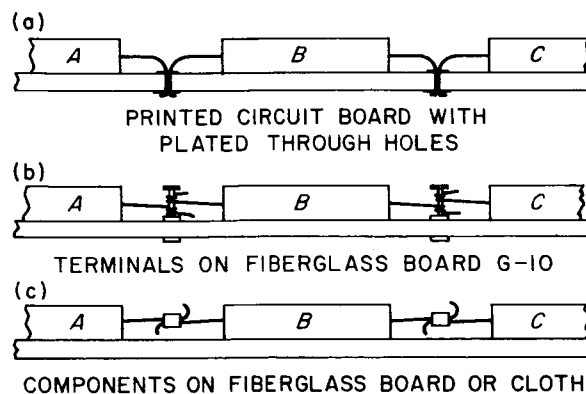


Fig. 34-6. Holding fixtures

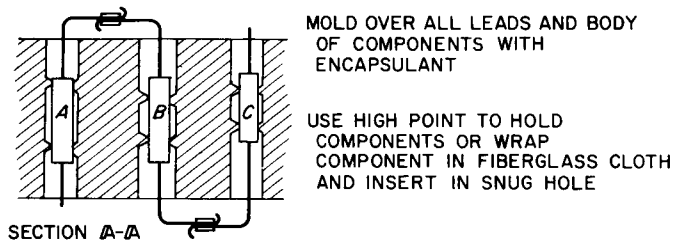
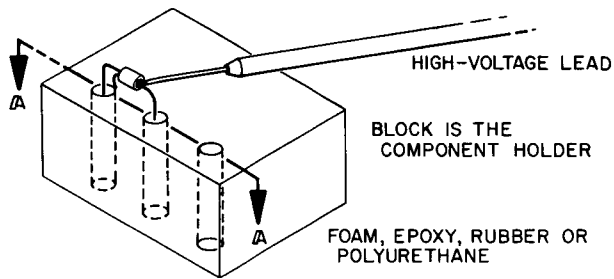


Fig. 34-7. Packaging methods

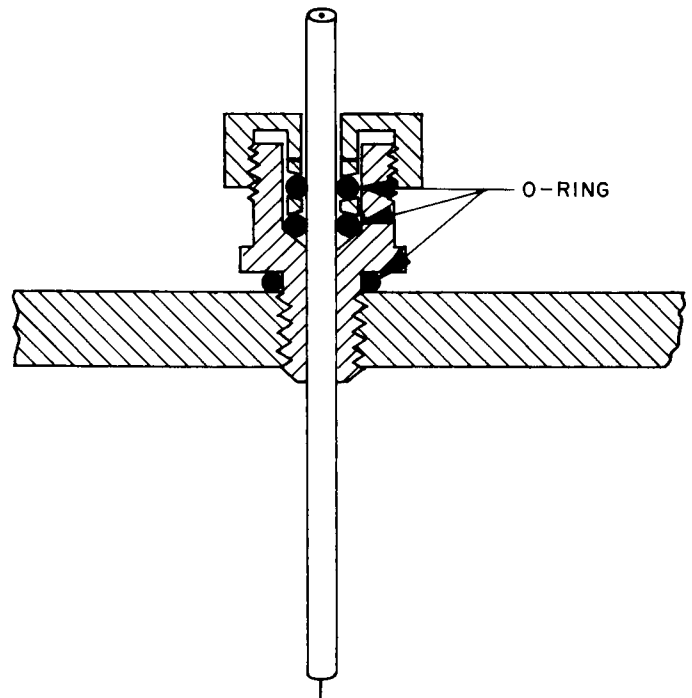


Fig. 34-8. Improved insulation method

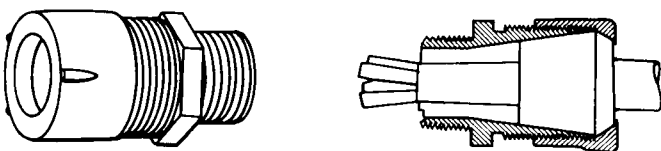


Fig. 34-9. Cord grip

REFERENCES

1. Handbook of Chemistry and Physics, 44th edition, p. 1545.
2. J. D. Cobine, Gaseous Conductors, McGraw-Hill Book Co., New York, N.Y.
3. N. J. Levenson and S. W. McClaren, "Sulfurhexafluoride Gas Cools Airborne Equipment," EDN, September 1964, p. 64.
4. E. E. Charlton and F. S. Cooper, General Electric Review, Vol. 40, No. 438, 1937.

**N 68-26910****35. A HIGH-VOLTAGE PROBLEM ENCOUNTERED IN THE DESIGN OF THE STAR TRACKER USED ON THE ORBITING ASTRONOMICAL OBSERVATORY\***

James J. Collins  
Kollsman Instrument Corp.  
Space Division  
Syosset, New York

Kollsman has encountered outgassing problems in the Orbiting Astronomical Observatory (OAO) program. In this system, a Sun-protect solenoid-operated shutter is used to prevent sunlight from damaging the photosensitive detector. This unit moves an opaque shutter into the front end of the tracker obscuring the optical system. During the final acceptance tests of the system, an identical group of failures were noticed. In each case, the unit failed, leaving the Sun shutter closed - a catastrophic condition.

At least four Sun-protect units failed under thermal vacuum test or immediately thereafter. Each of these units had undergone extensive testing at Kollsman in normal environment.

The recorded failures followed the same pattern. When power was initially applied, everything functioned normally. Energizing the Sun-protect circuit caused the solenoid to operate. However, when the circuit was dennergized, the solenoid did not release.

Detailed examination of the module revealed an excessive increase in leakage current in the two Darlington-connected output transistors, which prevented the solenoid from dropping out when the Sun-protect was de-energized. These units were 2N1613 transistors.

Initially, the circuit in question was separately analyzed by Kollsman, General Electric, and Fairchild. All reports were identical - no problem with the application of any components in the design.

Microscopic examination of the transistors in question by the manufacturer revealed a breakdown from collector to emitter caused by exceeding the breakdown limits of the units.

\*This paper was submitted but was not presented because of lack of time; it is included in the Proceedings because the information contained is pertinent to the subjects discussed at the workshop.

After the first failure an investigation of the component characteristics pointed out the fact that the  $BV_{CEO}$  rating of the 2N1613 was only rated at 29 v minimum. Since the  $B+$  was 28 v, this rating was considered to be critical, and a recommendation to use high reliability units with a minimum breakdown of 40 v  $BV_{CEO}$  was made.

The subsequent failures were identical to the initial failures except that now the high-reliability units failed. At this point a complete investigation of the problem rather than just the circuit was undertaken.

After talking to the engineers involved with all phases of test and evaluation of the sun-protect module several interesting points of information became obvious.

1. All failures occurred either during thermal-vacuum tests after some period of testing (1-2 days) or were noticed immediately after these tests were concluded. Testing was conducted at the G. E. facility.
2. Extensive life testing had been performed at Kollsman on prototype units and on each deliverable system. During these tests no degradation of transistors or failures were observed.
3. In all cases the failure was attributed to a Darlington-connected configuration containing transistors Q6 and Q7 in the Sun-protect circuit.
4. A total of 80% of the units failed (4 out of 5 systems). This proved that some were good with no deleterious effects.
5. In all failures a collector-to-emitter increase in leakage or short circuit was the culprit.
6. This was the only module in the system without a decoupling network off the  $B+$  supply.
7. A detailed examination of the module construction showed a number of high-voltage terminals (-900 v) in the module in question near transistor Q6 and Q7.
8. The previous prototype layout - identical transistors and circuitry but different packaging - had gone through the same tests without any failures. However, they were in a pressurized nitrogen environment during thermal-vacuum tests. This point of information (8) was not mentioned until the second week of the investigation.

From the data, items 1-6 pointed toward the possibility of transients appearing on the +28 v standby supply at the G. E. facility. Since the problem only occurred in

the thermal-vacuum area, it was suspected that radiated energy in that area might be picked up by the long power leads between the test console and the tracker.

Point 7 indicated that internal arcing might be the culprit but it was initially downgraded by the fact that the distances (40 mil, spacing between leads) were more than sufficient if the potting compound filled the area. The dielectric strength of the compound in question was greater than 400 v/mil.

After extensive testing lasting over 3 weeks both at Kollsman and G. E., the possibility of transients was downgraded as the source of trouble, and the focus of the investigation then shifted back to the internal arcover possibility. Examination of the layout of the module in question showed a spacing of 40 mil from the high voltage to the case of the transistor Q6. It was postulated that if arcover occurred to the case of Q6 it would burn out Q7. This is caused by the fact that the two collectors are common and the case is tied to the collector junction electrically.

Testing of this possibility was accomplished by charging an 0.1  $\mu$ f capacitor to -900 v and discharging it through the case of Q6, on the breadboard. This duplicated the exact failure mode observed on two of the units. Partial breakdown of Q6 and Q7 was noted with the operating characteristics as previously described.

Once this area of investigation opened up, it suggested the possibility that air spaces might be trapped under the surface of the Mylar in the dense packing area or that a film of air would exist because of poor bonding between the potting compound and the Mylar. Discussions with G. E. and Kollsman production experts indicated different views on these theories. These differences of opinion were not on a company basis since specialists in each company had conflicting opinions with their associates. Because of this, several tests were instituted to determine the feasibility of these theories.

High-Pot was determined to be the best method of detecting air paths. The initial High-Pot gave an arcover indication at 2.8 kv in the potted module. Then the potting compound was carefully removed from the high-voltage area, and the unit was again subjected to the same test. This time, the High-Pot again indicated 2.8 kv. From this test it was determined that in actuality, an air path did exist inside the module and that the potting compound had no effect. Cutting away the Mylar and potting the high-voltage section carefully raised the High-Pot to well over 5 kv.

Investigating the spacing in the module of 40 mil coupled with the dielectric constant of air of 75 v/mil yields a breakover of 3 kv at normal pressure. Since the

supply is 900 v, the safety factor under normal pressure was more than sufficient. To determine if arcover could occur at any pressure, a test was run using two wires with the correct spacing affixed on the surface of a test module. Then the unit was placed in an altitude chamber and high-potted at 10,000 ft intervals. The arcing was seen to vary from 3 kv at normal pressure to 300 v at 90,000 ft. This change of 10:1 for a given spacing was very enlightening.

In order for an air space inside the module to change pressure and go to a critical altitude equivalent, it was postulated that outgassing would have to occur through the potting compound. We recently obtained confirmation from G. E. that indeed outgassing does occur with this material.

Once this was verified, it explained why a unit could be tested for prolonged periods of time in normal atmosphere without trouble, while the same unit would fail in vacuum after 2 days of test.

It was further theorized that if an air pocket would decrease in pressure in a vacuum, it would, after being removed from vacuum, increase in pressure back toward normal pressure. Since in both cases it could pass through the critical pressure, a failure immediately after testing could occur. When this was mentioned, the G. E. representative recalled a unit that had operated satisfactorily in the vacuum chamber but failed the next day during a final checkout. In addition, B. Walker of Kollsman mentioned testing a unit that had failed in G. E. and observing that the collector voltage was deteriorating while he was examining it. The elapsed time between vacuum test and room test was approximately 1-2 days in both cases.

This theory explained why vacuum tests run at Kollsman did not indicate the problem - the period of testing was not of sufficient length. In addition, it explained why 20% of the units were satisfactory. If the potting compound did not leave a void, the arcover could not occur.

Another point of interest discovered at Kollsman and later verified at G. E. is the fact that the conformal coat does not form a good bond with the Mylar surface.

While testing a unit at Kollsman, an interesting effect was observed. During one High-Pot test, an arcover occurred between two points on the surface of the Mylar. When examined under a microscope, a tunnel was observed between the conformal coat and the Mylar. Arcing continued through this tunnel until it was cut open and recoated with conformal coating.



During the investigation, two cases of entrapped air were discovered in production modules. One occurred in a dynode resistance module immediately under the surface of the unit. The air pocket was on the side of the module under the surface of the Mylar. Discovery of this pocket was made when pressure of a fingernail was applied to a grey mark on the side of the module. The pressure caused the thin shell of potting compound to collapse, disclosing the cavity. The discoloration apparently indicated the small chamber under the potting surface.

The second cavity was discovered in a preamplifier module. Investigation was started when a failure occurred. When the module was opened an air bubble was found around the case of a transistor under the surface of the Mylar. In both of these cases, the existence of air bubbles would not cause any operating problem. However, both of these discoveries reinforced the theory on the sun-protect failures.

Because of the discovery of the air bubble in this particular module (production dynode module) and since radiation would not bother the resistors, this unit and another one of the same type were sent out for x-rays. When the x-rays were received, one unit indicated seven (7) separate air bubbles trapped under the surface of the Mylar, while the second had one (1). What was extremely interesting was that bubbles were under both Mylar surfaces in the one module. Under the top Mylar (the side where the leads project) the bubbles were in the component area, while under the bottom Mylar, the bubbles were in the welding area.

As a final test, an unpotted production unit was placed in an altitude chamber, where it could be observed visually. After energizing all circuits and coating all surface welds with double conformal coatings to limit surface arcing, the unit was taken up in altitude. At 40,000 ft, arcing was observed under the surface of the Mylar between the diode group and Q7 case. After approximately 10 sec, the unit was brought down in altitude and rechecked. The output had deteriorated in the same manner as in the units in the system with the same increase in leakage current. The second time the unit was taken up in altitude, arcing occurred to Q8 and caused the output to short to ground. This would also cause the solenoid to lock. These tests also reinforced the theory on the failures. On the basis of all these tests, a number of possible solutions were proposed:

1. Redesign the module.
2. Leave the high voltage area open to make use of the insulating properties of high altitude, since operation would not occur during critical altitude.
3. Drill holes through the potting compound and the surface of the Mylar to let the area breathe.
4. Use epoxy boards instead of Mylar to get a good bond. This would not help if entrapped air were the problem.
5. Use a potting compound which would outgas very rapidly.

The final solution adopted was to remove the nine components associated with the high voltage to a separate module. Since this was done, the problem has not occurred, and all units are operating satisfactorily.

An additional area for consideration when manufacturing a high-voltage supply is the problem with marking. Since most inks contain a carbon base, they are often conductive. Even if sufficient spacing exists between adjacent wires, the existence of an identification stamping in this area may reduce your safety factor to a critical level. If stamping is required, it should be done with a nonconductive marking solution.

N 68-26911

36. SOLUTIONS TO POISSON'S EQUATION AND THEIR APPLICATION  
TO VOLTAGE BREAKDOWN PROBLEMS\*

Glenn E. Hagen  
Chrysler Corporation  
Space Division  
New Orleans, Louisiana

The problem of electrical breakdown due to a low-pressure gaseous environment involves both the density of the gas in the region of a conductor and the strength of the electric field at that point. When the combination of electric intensity and mean free path is such that an ion can develop enough energy in one free path to create another ion pair upon collision with a gas molecule, a chain reaction spoken of generally as "secondary ionization" takes place and the gas breaks down and becomes relatively conductive. Not only will this pass current between exposed conductors, but bombardment by ions can lead to rapid failure of solid dielectrics. When we have reached a vacuum sufficiently hard that the mean free path of gas molecules is a large fraction of the physical dimensions of our electrical layout, secondary ionization is no longer self sustaining, and danger of breakdown disappears. This paper will concern itself with the situation prior to this point; that is, where the physical dimensions are still great in comparison with the molecular mean free path. The assumption is made throughout that the gas is a homogeneous fluid, and, if charged, has a charge density which varies as a continuous function of the coordinates.

Prior to the onset of corona discharge, the electric field in the vicinity of electric conductors charged with direct current is governed by the Laplace equation,  $\nabla^2 V = 0$ . The resulting distribution of potential and electric gradient is well known in the field of electrostatics for almost all simple geometries. Those who are familiar with the field have a clear mental picture of such distributions, to the point of being able to predict the approximate positions of equipotential surfaces and of high intensity electric fields. However, as soon as even the slightest ionizing discharge takes place in the vicinity, it will be shown in the development to follow that the picture is decisively and abruptly changed; so much so that points of high electrical intensity may not coincide at all with their former positions. Failure to appreciate the magnitude of such shifts in field pattern can lead to serious errors in the geometrical layout of electrical components and circuitry.

\*This paper was received too late for inclusion in the program but is included in the Proceedings because of its relevance to the material presented.

Let us assume that because of a corona discharge from an exposed conductor the region has become populated with ions to produce a space charge density of  $\rho$  esu/cm<sup>3</sup>. The electric field in such a region will be the negative gradient of the electric potential,

$$\bar{E} = -\bar{\nabla}V \quad (1)$$

where  $\bar{E}$  is the electric field vector and  $V$  is electric potential. If we assume all electric charges are positive, each particle becomes a source of electric flux, and from Gauss' law, the divergence of the electric field in the region is

$$\bar{\nabla} \cdot K\bar{E} = 4\pi\rho \quad (2)$$

where  $\rho$  is the charge density and  $K$  is the dielectric constant. From (1) and (2) we derive Poisson's equation

$$\nabla^2 KV = -4\pi\rho \quad (3)$$

which governs the potential distribution throughout the region.

Now, if a steady state has been reached, we know from the nature of an electric current that there will be no closed loops; that is, the curl of the current will be zero:

$$\bar{\nabla} \times \bar{I} = 0 \quad (4)$$

where  $\bar{I}$  is a vector representing current density, that is, current per unit area taken normal to the vector. This suggests that the current is derivable from a potential. Let us define a "current potential"  $\Phi$  (not to be confused with the electrical potential  $V$ ) such that

$$\bar{I} = -\bar{\nabla}\Phi \quad (5)$$

Now, the divergence of the electric current must be zero in any region not containing an electrode,

$$\bar{\nabla} \cdot \bar{I} = 0 \quad (6)$$

and from Eq. (5) and (6) we find that  $\Phi$  must be a solution of Laplace's equation:

$$\nabla^2 \Phi = 0 \quad (7)$$

If we assume that the region under study is in an atmosphere where the mean free path is short compared to physical dimensions of the region studied, it has been shown that the drift velocity of charged particles or ions is proportional to the applied electric field:

$$\bar{v} = M\bar{E} \quad (8)$$

where  $\bar{v}$  is the drift velocity and  $M$  is the mobility, a constant for a given size particle and density of medium. Furthermore, if all electric current is being carried by these particles, the current density is proportional to the particle velocity and charge density,

$$\bar{I} = \rho \bar{v} \quad (9)$$

and, thus, we derive

$$\bar{I} = \rho M \bar{E} \quad (10)$$

or

$$\bar{\nabla} \Phi = \rho M \bar{\nabla} V \quad (11)$$

This tells us that surfaces of equal  $\Phi$  are also surfaces of equal  $V$ ; although the two potential functions are not necessarily equal, they are at least the same family of surfaces. Furthermore, if we take the curl of both sides of Eq. (11),

$$\bar{\nabla} \rho \times \bar{\nabla} V = 0 \quad (12)$$

which clearly shows that unless, or except where one of the above gradients are zero, surfaces of equal potential must be surfaces of equal ion density.

To illustrate the effect of this, suppose we had a small needle point conductor close to a grounded wall at one end of the spacecraft undergoing corona discharge, the bulk of the current going into the wall. One would tend to say that the ions would be dense in between the conductor and the wall, in the path of the principal current, and be very rare at the other end of the spacecraft. Quite the contrary. Since the wall of the spacecraft is all one equipotential surface, there will be equal ion density around the entire wall, even at the opposite end of the craft. And, since it will be shown that the very presence of these ions can be the cause of electrical breakdown, a single small discharge can quickly spread throughout a large volume, and cause widespread breakdown of insulation.

To examine the behavior of ions released in a gaseous environment we must seek solutions of Eq. (11). Taking the divergence of both members of Eq. (11) we have,

$$\nabla^2 \Phi = M(\bar{\nabla} \rho \cdot \bar{\nabla} V + \rho \nabla^2 V) = 0 \quad (13)$$

or, using Eq. (3),

$$\bar{\nabla} \rho \cdot \bar{\nabla} V = \frac{4\pi}{K} \rho^2 \quad (14)$$

and, using Eq. (11),

$$\bar{\nabla} \rho \cdot \bar{\nabla} \Phi = \frac{4\pi M}{K} \rho^3 \quad (15)$$

Theoretically, this equation is solvable, since we know the Laplacian potential function  $\Phi$  as a function of the coordinates, for any given set of boundary conditions, and this leaves us with a differential equation involving only  $\rho$  and the coordinates of the system. Furthermore, we have already determined that the two vectors involved are parallel; therefore, if we can choose a coordinate system in which the direction of these vectors coincides with one of the axes, Eq. (15) reduces to an ordinary differential equation, the solution of which gives us the ion density along that axis.

One example is that of the region between two parallel planes of infinite extent, one of which is emitting ions and the other collecting them. Here we shall take  $z$

as the dimension normal to the planes.  $\nabla\Phi$  then reduces to  $\frac{d\rho}{dz}$  which is the current density  $I$ , a constant throughout the region. Thus, we have the ordinary differential equation

$$\frac{d\rho}{dz} = \frac{4\pi M}{KI} \rho^3 \quad (16)$$

which integrates to give

$$\rho = \frac{1}{\sqrt{A - \frac{8\pi Mz}{KI}}} \quad (17)$$

where  $A$  is an arbitrary constant.

Eliminating  $\rho$  between Eqs. (17) and (10) then gives

$$E = \frac{I}{M} \sqrt{A - \frac{8\pi Mz}{KI}} \quad (18)$$

Now, there will be some electric field  $E_1$  at the surface of the upper plane due to the charge residing upon it, and perhaps necessary to sustain the emission of ions. If the distance between the planes is  $h$ ,

$$E = \sqrt{E_1^2 + \frac{8\pi I}{KM} (h-z)} \quad (19)$$

disclosing that when ions are present the electric intensity increases as we move toward the lower plane, as opposed to holding constant in the case where no space charge is present. The ion density, on the other hand, falls off as we move toward the lower plane:

$$\rho = \frac{1}{\sqrt{E_1^2 + \frac{8\pi I}{KM} (h-z)}} \quad (20)$$

Integrating Eq. (20) from 0 to h gives us the potential difference between the planes,

$$V_a = \frac{2}{3} \frac{KM}{8\pi I} \left[ \left\{ E_1^2 + \frac{8\pi I h}{KM} \right\}^{3/2} - E_1^3 \right] \quad (21)$$

Returning to Eq. (19), if we may not exceed a given background field  $E_0$  at the bottom plane, we will be limited to a current density of

$$I = \frac{KM}{8\pi h} (E_0^2 - E_1^2) \quad (22)$$

Now, if we consider that ions are freely available at the upper plane, and, therefore,  $E_1$  is insignificant, Eqs. (21) and (22) reduce to

$$E_0 = \frac{3}{2} \frac{V_0}{h} \quad (23)$$

Had there been no ions present, the intensity at the lower plane would have been

$$E_0^1 = \frac{V_0}{h} \quad (24)$$

This shows rather clearly that with a given spacing and a given voltage, the presence of ions can cause a 50% increase in field strength adjacent to a flat surface.

An even more striking difference between solutions of Poisson and Laplace occurs in the cylindrical case. Consider two concentric cylinders, an inner one of radius  $a$  which is emitting positive ions, and an outer one of radius  $b$  which is collecting them. Since both the gradients in Eq. (15) can be expected to be radial, we can write it as the ordinary differential equation

$$\frac{d\rho}{dr} \frac{d\Phi}{dr} = \frac{4\pi M}{K} \rho^3 \quad (25)$$



The solution of Laplace's equation for the cylindrical boundary system is of the form

$$\Phi = A - B \log r \quad (26)$$

and we can easily deduce that the current density is of the form

$$\frac{d\Phi}{dr} = -I = -\frac{I_T}{2\pi r} \quad (27)$$

where  $I_T$  is the current per unit length of cylinder. Equation (25) can now be integrated to the form

$$\rho = \frac{1}{2\pi \sqrt{\frac{2M}{KI_T}} \sqrt{r^2 + C^2}} \quad (28)$$

$C$  being arbitrary. If the inner cylinder is a very fine wire, the constant  $C$  disappears, and the ion density falls off inversely with the radius. This results in a constant electric intensity,

$$E = \sqrt{\frac{2I_T}{KM}} \quad (29)$$

This is, of course, vastly different from the Laplacian field distribution which gives an intensity falling off inversely with the radius; it leads to electric fields many times stronger than expected, extending considerable distances from the wire.

Still another interesting solution is the electric field in the vicinity of a sharp point which has broken into corona discharge. Let us assume that the point undergoing discharge is a small sphere of radius  $a$ .

The applicable solution to Laplace's equation is of the form

$$\Phi = A - \frac{B}{r} \quad (30)$$

and, the current density is

$$\frac{d\Phi}{dr} = I = \frac{I_T}{4\pi r^2} \quad (31)$$

where, again,  $I_T$  is the total current. This gives for the intensity

$$E = \sqrt{\frac{2I_T}{3KM}} \frac{\sqrt{r^3 - C^3}}{r^2} \quad (32)$$

where  $C$  is a constant associated with the radius of the emitting sphere or needlepoint. When  $r$  is large compared with the emitter radius we have

$$E_0 = \frac{1}{2} \frac{V_a}{\sqrt{r}} \quad (33)$$

Thus, the electric intensity in the vicinity of a sharp point falls off inversely as the square root of the radius, rather than as the square of the radius as it would if there were no ions present. The effect, of course, is that electric fields produced at considerable distances from a point undergoing discharge are very much greater than they would be without the discharge.

Other geometries can be investigated as the application requires. More complex geometries will require the use of numerical integration; it should be remembered, however, that it is usually possible to obtain a closed form solution along an axis of symmetry wherever this coincides with the electric vector. Such solutions can then often be expanded through the use of various types of harmonics to give the complete solution.

An interesting and significant point about comparing solutions of Poisson's equation with those of Laplace for the same boundary conditions is that allowing the charge density to approach zero does not, generally, cause one solution to approach the other. In each case there is a discontinuity between the case of  $\rho$  zero and  $\rho$  not zero, no matter how small. Mathematically, it can be seen to be the dividing line between whether or not Eq. (11) holds. From a physical standpoint, it explains a number of interesting phenomena. One is the disruptive nature of the onset of corona,

in general, the discontinuous jump from no discharge to discharge, and resulting high frequency oscillation when there is insufficient current to maintain the discharge. Another is familiar to those who work with xerography or electro-photocopying; plates and papers often turn out to be uniformly charged except for "void" areas in which there was no charge whatsoever, the boundaries surrounding these areas being clear and sharp. This last effect has, in fact, suggested to the writer that there may be a field of "ion optics" wherein one deals with discrete pencils of ion current passing through regions where no other ions exist.

The effect of the presence of ions has been discussed in terms of exposed conductors. It should be pointed out, however, that very slight leakages of current through the insulation of insulated conductors can produce sufficient ionization to enforce the laws herein derived. It might also be pointed out that many very good insulators with high dielectric strengths will readily pass current when bombarded with ions, some of them ultimately breaking down as a result. It is well known, for example, in the field of potting high-voltage transformers, that any trace of corona discharge within the casing renders the transformer unsaleable because it will break down completely after a short time. It should be concluded, therefore, that from the standpoint of reliability, electrical circuitry which may be exposed to critical pressure should be designed with criteria of insulation and spacing consistent with intensities predicted by Poisson's equation rather than by those developed for the ordinary electrostatic stresses.

### CONCLUDING REMARKS

Earle Bunker

In conclusion, I would like to say that we are well pleased with the Workshop. One of the participants asked me what we learned from this, so I wrote down a few remarks, which will summarize at least what I've gotten from it.

First of all, problems have existed in the past and still exist in operation of high-voltage equipment in the critical region. Second, from the solutions shown here, the design and testing of equipment to operate in the critical pressure region does not seem to be insolvable. We should be able to do it. Third, it appears that the equipment should be designed to withstand the critical region, even though it is not intended to operate in that region. This would improve the reliability and tend to prevent failure caused by the effects of turnon or human error.

There will be an increasing demand for equipment to operate for extended periods of time in the critical region; e. g., the atmosphere of Mars is the same as 110,000 ft on Earth, and that is right in the critical region.

The problems of high-voltage design have been with us for a long time; only the people are new. Perhaps we can solve these problems so that the next generation of engineers won't have it to contend with.

And the last point, recognizing the controversy here over foam as a high voltage insulation, could be a paraphrase from Shakespeare, "To foam or not to foam, that is the question."

CLOSING REMARKS

Andrew Edwards

I think all of us here coming in at various levels of experience and knowhow in this field are going to come out of it with a heightened awareness of this whole area, and I think if that's what we've accomplished, it's certainly been well worth it.

There has been a good deal of specific data brought out, and to that end we'll try to get these proceedings out as quickly as possible.

I second Earle's thanks, and want to thank him particularly for putting this Workshop together. He's really made it possible. I want to thank all the speakers. I think everyone did a fine job. It's been an exceptionally good program in that respect, thanks to you attendees. I think you brought out a lot of good points. Thanks for coming.